Thèse n° d'ordre : 37-2012 Année 2012

PHD THESIS

Presented in
Claude Bernard University Lyon 1



for the degree of
Doctor of Philosophy in Neuroscience

SPECTRAL MODULATION OF MELANOPSIN RESPONSES

Role of Melanopsin Bistability in Pupillary Light Reflex

Presented and defended in public, Friday 2 March 2012

PETTERI TEIKARI

Supervisor of the thesis: Dr. Howard M. Cooper

Jury composition

PROF. ROBERT LUCAS Faculty of Life Sciences, University of Manchester, UK	Reporter
PROF. DOEKELE STAVENGA Computational Physics Group, University of Groningen, NL	Reporter
DR. DOMINIQUE DUMORTIER Housing Sciences Laboratory, ENTPE, Lyon, FR	Examiner
DR. HOWARD COOPER Department of Chronobiology, INSERM U846, Lyon, FR	Examiner, Supervisor of the thesis

Petteri Teikari: *Spectral Modulation of Melanopsin Responses,* Role of Melanopsin Bistability in Pupillary Light Reflex, © v. March 2012

ACKNOWLEDGEMENTS

I would like to thank my family for providing the support for this process. Also I would like to thank Krista and Stéphanie providing lovely balance for the scientific work, and special thanks for Stéphanie for giving the "final nudge" for the completion of this thesis. Special thanks are in place for an "external scientific advisor" Hemi being there. Special thanks also for Jean-David for providing inspirational non-conforming views on life outside the lab.

I like to thank for the inspirational impact of Prof. Domien Beersma and his laboratory (Marina, Marijke, Maan, Valeria and Marian among others) for providing me a way leading up to this moment. I also like to thank the Lighting Laboratory at Helsinki University of Technology (TKK, or currently known as Aalto University) under the supervision of Prof. Liisa Halonen and my former colleague Emmi Rautkylä who managed to defend before me.

The completion of the thesis would have been ultimately impossible without the unit 846 (U846) of INSERM. Thanks for the colleagues Marion, Mehdi, Raymond, Ludovic, Karim, Guy, Christine, Pierre, Xavier, Julio and the others. The additional thanks for foreign "social collaborators" go to Lloyd, Jorge, Céline, Marie, Véronique and Kat for being lovely. EUCLOCK Summer School 2008 gang was lovely as well.

Last but not least, I would like the thank the developers of Matlab, Linux Ubuntu distribution, Dropbox, Zotero and LyX for making my day-to-day scientific life a lot easier compared to the dark ages with MS Windows/Office and manual reference management. Also I would like to thank André Miede for providing *classicthesis* LyX stylesheet freely available for all.

ABSTRACTS

ABSTRACT OF THE THESIS

In addition to the canonical photoreceptors, rods and cones, a novel melanopsin-expressing retinal ganglion cell (mRGC) was recently discovered. The novel photopigment melanopsin in the human retina has been shown to express invertebrate-like bistable properties both *in vitro* and *in vivo*. In bistable photopigment systems, light elicits photosensory responses and drives photoregeneration of the chromophore to restore photic responsiveness. These studies have shown that prior light exposure can modulate the amplitude of subsequent photic responses of melanopsin.

In this thesis, the putative bistability of melanopin in humans is examined. The bistability was studied using 1) pupillary light reflex (PLR) as a tool, 2) developing a method for quantifying the effects of lens density for melanopsin-mediated photoreception, and 3) providing a quantitative mathematical framework for modeling bistable pigment systems and non-image forming (NIF) visual system.

Exploiting the bistable properties of melanopsin could allow for optimization of spectral light distribution in experimental, industrial, domestic and clinical phototherapy applications by appropriate use of the photoregenerative effects of long wavelength light.

Keywords: light; melanopsin; melanopsin bistability; modeling; lens density; photoreception

VÄITÖSKIRJAN TIIVISTELMÄ

Perinteisten fotoreseptorien, sauvasolujen ja tappisolujen, lisäksi verkkokalvolta on löydetty melanopsiinia sisältäviä gangliosoluja. Fotopigmentti melanopsiinin on huomattu käyttäytyvän ihmisen verkkokalvolla selkärangattomien eläimien bistabiilin näköjärjestelmän tavoin sekä *in vivo-* ja *in vitro-* olosuhteissa. Bistabiileissa fotopigmenttijärjestelmissä valo aiheuttaa sensoristen vasteiden lisäksi kromoforin fogeneraation vastevalmiisen tilaan. Nämä aiemmat tutki-mukset ovat osoittaneet, että aiempi valoaltistus voi moduloida siitä seuraavia melanopsiinivasteita.

Tässä väitöskirjassa melanopsiinin oletettua bistabiiliutta tutkittiin käyttäen 1) Pupillireaktiota työkaluna, 2) kehittämällä kvantitaviinen menetelmä mykiöntiheyden vaikutuksiin melanopsiini-fotoreseptiossa, ja 3) kehittäen kvantitatiivisen matemaattisen kehyksen bistabi-

ilien pigmenttijärjestelmien ja ei-visuaalisen näköjärjestelmän mallintamiseen.

Melanopsiinin bistabiileita ominaisuuksia on mahdollista optimoida valon spektrikoostumusta niin tieteellisissä, teollisissa, kotitalouksellisissa ja kliinisissä valoterapia sovelluksissa hyväksikäyttämällä punaisen aallonpituusalueen fotoregeneroivia vaikutuksia.

Avainsanat: valo; melanopsiini; melanopsiinin bistabiilisuus; mallintaminen; mykiöntiheys; fotoreseptio

RÉSUMÉ DE LA THÈSE

En plus des photorécepteurs canoniques traditionnels (bâtonnets et cônes), des cellules ganglionnaires contenant le photopigment mélanopsine ont récemment été découverts. Une étude récente de notre laboratoire a suggéré que, dans la rétine humaine, ce nouveau photopigment exprime des propriétés bistables similaires à celles notées chez les invertébrés tant in vitro qu'in vivo. Dans les systèmes de photopigments bistables, la lumière déclenche une réponse photosensorielle mais permet aussi la régénération du chromophore pour rétablir la réactivité lumineuse du photopigment. Cette dernière étude a montré qu'une exposition lumineuse antérieure peut moduler l'amplitude des réponses lumineuses de la mélanopsine.

L'objectif de ma thèse est d'étudier (1) la bistabilité présumée de la mélanopsine chez l'Homme en utilisant comme outil le réflexe photomoteur pupillaire. Ma thèse comporte aussi 2) le développement d'une technique d'évaluation quantitative des effets du brunissement du cristallin oculaire sur la photoréception impliquant la mélanopsine; 3) le développement d'un modèle mathématique portant sur le fonctionnement des photopigments bistables et du système photique non visuel.

L'exploitation des propriétés bistables de la mélanopsine et l'utilisation appropriée des effets photorégénérateurs des longueurs d'ondes lumineuses longues pourraient servir dans l'optimisation de la composition spectrale des applications photothérapeutiques (expérimentales, industrielles, domestiques et cliniques).

Mots Clefs: Mélanopsine; Bistabilité de la mélanopsine; Modèle; Densité du cristallin; Photoréception

CONTENTS

1 NON-IMAGE FORMING (NIF) VISUAL SYSTEM 1
- 1.1 Circadian rhythms 1
- 1.2 Non-image forming responses to light 3
  - 1.2.1 Locomotor activity 3
  - 1.2.2 Melatonin 3
  - 1.2.3 Sleep-Alertness 4
  - 1.2.4 Cognition & Emotions 5
  - 1.2.5 Adverse effects of light 6

2 VISUAL SYSTEM 7
- 2.1 Light 7
- 2.2 Ophthalmic optics 8
  - 2.2.1 Radiation transfer 8
  - 2.2.2 Stiles-Crawford effect 9
  - 2.2.3 Spectral transmittance of ocular media 10
- 2.3 Classical Visual Phototransduction 15
  - 2.3.1 Visual fields 16
  - 2.3.2 Spectral sensitivity 18
  - 2.3.3 Self-screening 21
  - 2.3.4 Spectral Opponency 24
  - 2.3.5 Irradiance ranges 25
  - 2.3.6 Ciliary kinetics 26
- 2.4 Non-Visual Phototransduction 29
  - 2.4.1 Retinal circuitry 29
  - 2.4.2 Spectral sensitivity 32
  - 2.4.3 Irradiance response characteristics 34
  - 2.4.4 Kinetics / Temporal characteristics 36
  - 2.4.5 Photoreceptor contributions 37
  - 2.4.6 Spatial sensitivity 39
  - 2.4.7 Retinal clocks 39
  - 2.4.8 Short-term adaptation 41
  - 2.4.9 Long-term adaptation 42
  - 2.4.10 Role in vision 43
  - 2.4.11 Aging 44

3 PUPILLARY LIGHT REFLEX - PLR 47
- 3.1 Anatomy 47
- 3.2 Pupil control circuitry 48
  - 3.2.1 Spatial sensitivity 50
  - 3.2.2 Pupillary light reflex waveform 53
  - 3.2.3 Eye movement control 57
  - 3.2.4 Pupil near response (PNR) 57
  - 3.2.5 Non-photic pupil responses 58
- 3.3 Photoreceptor contributions 60

3.3.1 Spectral sensitivity 60
3.3.2 Irradiance response characteristics 61
3.3.3 Chromatic interactions 63
3.3.4 Photoreceptor contributions 65
3.4 Pupil Noise 68
3.5 Instrumentation and analysis of PLR 68
3.5.1 Instrumentation 68
3.5.2 Data conditioning 71
3.5.3 Mathematical analysis of PLR waveform 71
3.6 Adaptation and circadian rhythmicity 73
3.6.1 Adaptation 75
3.7 Animal models of PLR 76
3.8 Modeling of PLR 77
3.9 Clinical and diagnostic use 80
3.9.1 PLR Diagnostics 81
3.9.2 Pupil noise 82
3.9.3 Pupil cycling time 83
3.9.4 Pupil perimetry 83
4 MELANOPSIN BISTABILITY 85
4.1 Invertebrate visual system 85
4.1.1 Insect optics 85
4.1.2 Phototransduction 87
4.1.3 Pseudopupil response 92
4.1.4 Screening pigments 92
4.2 Bistable system methodology 95
4.2.1 Definitions and equations 95
4.3 Bistable action spectra 101
4.3.1 Criterion Action Spectrum (CAS) 101
4.3.2 Difference spectrum 102
4.3.3 Equilibrium spectrum 103
4.3.4 Relaxation spectrum 103
4.3.5 Spectral sensitivities of the pigment states 104
4.4 Response types in bistable pigment systems 107
4.4.1 Early receptor potential (ERP) 107
4.4.2 M-potential 108
4.4.3 Late receptor potential (LRP) 109
4.4.4 Prolonged depolarization afterpotential (PDA) 110
4.5 Visual pigment states and kinetics 117
4.5.1 “Complete cycle” with intermediate states 117
4.5.2 Deactivation of the photoresponse 120
4.5.3 Measuring phototransduction kinetics 122
4.6 Visual-Pigment Arrestin Cycle 123
4.7 Melanopsin as a bistable photopigment 130
4.7.1 Bistability potentiation/Sensitization 131
5 RESEARCH PROJECTS 135
5.1 Background 135

5.1.1 PLR Setup 135
5.1.2 Individual PLR variability 138
5.2 Dark regeneration of melanopsin 141
5.2.1 Introduction 141
5.2.2 Material and Methods 141
5.2.3 Results 143
5.2.4 Discussion 148
5.3 Ocular media density measurement 153
5.3.1 Introduction 153
5.3.2 Material and Methods 156
5.3.3 Results 166
5.3.4 Discussion 169
5.4 Pupillary light reflex with aging 174
5.4.1 Introduction 174
5.4.2 Materials and methods 176
5.4.3 Results 178
5.4.4 Discussion 180
5.5 Model of bistable melanopsin 183
5.5.1 Introduction 183
5.5.2 Analytical Methods 183
5.5.3 Pigment kinetics 185
5.5.4 Transmitter gating model 189
5.5.5 Discussion 197
6 DISCUSSION 199
6.1 Melanopsin bistability interpretation 199
6.1.1 Melanopsin properties 199
6.1.2 Novel non-melanopsin photopigments 201
6.1.3 Photoreceptor contributions 204
6.1.4 Regeneration, melanopsin visual cycle 206
6.1.5 Intermediate photoproducts 210
6.1.6 Absolute versus relative pigment concentration 213
6.2 Paradigms to test the melanopsin bistability 215
6.2.1 Bistable response modulation 215
6.2.2 PDA Suppression 216
6.2.3 Anti-PDA 218
6.2.4 PDA Facilitation 218
6.3 Ecology and atmospheric modeling 222
6.3.1 SMARTS2 Simulation 224
6.3.2 Personal NIF dosimetry 225
6.4 Practical lighting implications 226
6.4.1 Implications of aging ocular media 227
6.4.2 Implications on architectural lighting design 232
6.5 Future methodology 234
6.5.1 Adaptive Optics 234
6.5.2 Genetic fluorescent tagging 237
A SCIENTIFIC PRODUCTION 239

A.1 Publications 239
A.2 Conference proceedings 239
A.3 Oral & Poster presentations 240
B TABLES AND CALCULATIONS 243
B.1 Light 243
B.1.1 Gaussian spectral power distribution 243
B.2 Ocular media corrections 243
B.2.1 Ocular media (crystalline lens) 243
B.2.2 Macular Pigment 244
B.2.3 Humors 246
B.3 Phototransduction 246
B.3.1 Nomogram 246
B.3.2 Irradiance response curve (IRC) 247
B.3.3 Photopigment density 247
B.4 Melanopsin phototransduction calculations 249
B.4.1 Visual pigment-arrestin cycle - parameter estimates 249
B.5 Daylight simulation 249
B.5.1 SMARTS2 Parameters 249
C SUPPLEMENTARY GRAPHS AND TABLES 253
C.1 Lens density measurement 253
C.2 Bistable photoreception simulations 253
C.2.1 Equilibrium spectrum 253
C.2.2 Relaxation spectrum 253
C.2.3 Effect of quantum efficiency on bistable spectra 253
C.2.4 Effect of pigment density 253
C.3 Pupil and aging 253
C.4 Photic memory 256
C.4.1 Individual PLR recordings 256
C.5 Bistability potentiation in human PLR 260
C.5.1 Individual PLR recordings 260

BIBLIOGRAPHY 265

LIST OF FIGURES

Figure 1 The human eye as an optical system 9
Figure 2 Spectral transmittance of the ocular media 11
Figure 3 Eyelid transmittance 13
Figure 4 Anatomy of the eye 14
Figure 5 Schematic illustration of the primate retina 17
Figure 6 Visual fields 18
Figure 7 Spectral sensitivities of human vision 20
Figure 8 Rhodopsin absorbance bands 21
Figure 9 Self-screening effect 23
Figure 10 Ambient illumination levels 27
Figure 11 mRGC subtype circuits 31
Figure 12 Characteristics of mRGC responses 1/2 35
Figure 13 Characteristics of mRGC responses 2/2 36
Figure 14 PLR Pathways 51
Figure 15 OPN firing and pupil response 51
Figure 16 OPN neuron receptive fields 52
Figure 17 PLR Circuitry and bilateral summation 54
Figure 18 Typical PLR Waveform 55
Figure 19 Mean PLR waveform for 480 nm light 55
Figure 20 PDA-like Pupil persistence 56
Figure 21 Near response triad (PNR) 58
Figure 22 Spectral sensitivity of the human PLR 61
Figure 23 Spectral sensitivity of the sustained PLR 62
Figure 24 Irradiance-response of the pupil 63
Figure 25 Photoreceptor contributions to PLR 67
Figure 26 PLR Setups 69
Figure 27 PLR Instrumentation schematics 70
Figure 28 Circadian rhythm of PLR 75
Figure 29 Matlab-Simulink model of PLR 81
Figure 30 Pupil perimetry with mfPOP 84
Figure 31 Comparison of monostable and bistable pigments 86
Figure 32 Fly compound eye 87
Figure 33 Illustration of bistable photoreception 88
Figure 34 (In)vertebrate visual cycle 89
Figure 35 Drosophila light responses 91
Figure 36 Fly screening pigments 94
Figure 37 Comparison of bistable action spectra 106
Figure 38 Vertebrate ERP 108
Figure 39 PDA dependence on stimulus amount 111
Figure 40 PDA Depression 113

Figure 41 Time course of anti-PDA 115
Figure 42 PDA-PDA Facilitation 116
Figure 43 Fly rhodopsin intermediates 118
Figure 44 Vertebrate rhodopsin intermediates 119
Figure 45 Photoreversal of human rhodopsin 121
Figure 46 Metarhodopsin fluorescence in *Drosophila* 124
Figure 47 Visual pigment-arrestin cycle 125
Figure 48 Photopotentiation of Zhu et al. (2007): IRC and duration 132
Figure 49 Pupil photopotentiation of Zhu et al. (2007) 133
Figure 50 Schematics of the PLR setup 136
Figure 51 Physical PLR setup 137
Figure 52 Luminance homogeneity of the PLR setup 137
Figure 53 Pupil image quality 138
Figure 54 Individual variability of PLR waveform 139
Figure 55 Individual variability of PLR components 140
Figure 56 Experimental protocol 144
Figure 57 Alteration of PLR response following pre-exposure of adapting light in short and long condition 146
Figure 58 "Photic memory" individual changes between short and long session 147
Figure 59 Robustness of potentiation in human PLR 148
Figure 60 Effect of LOWESS span on PLR results 149
Figure 61 Experimental difference spectra 151
Figure 62 LabView interface for lens density program 158
Figure 63 Physical lens density setup 159
Figure 64 Lens density luminance homogeneity 160
Figure 65 Lens density measurement protocol 162
Figure 66 Lens density index as a function of age 166
Figure 67 Left vs. Right eye 167
Figure 68 Lens density results for three age groups 167
Figure 69 Spectral attenuation of the three age groups 168
Figure 70 Behavior of CFF in the descending frequency condition 169
Figure 71 Aging in PLR, Experimental protocol 177
Figure 72 Absolute pupil sizes with three irradiances 179
Figure 73 Pupil light reflex in young and older individuals 180
Figure 74 Visual pigment-arrestin cycle 185
Figure 75 Intensity dependence of pigment kinetics 188
Figure 76 Wavelength dependence of pigment kinetics 189
Figure 77 Matlab GUI for pigment kinetic model 190
Figure 78 Block diagram of the transmitter model photo-transduction 190
Figure 79 Transmitter dynamics 192

Figure 80 Light drive (T) defined with an irradiance-response curve 194
Figure 81 Behavior of H as a function of H_0 195
Figure 82 Behavior of H as a function of u 196
Figure 83 Behavior of H as a function of $f(\cdot)$ 196
Figure 84 Bistability of mouse and human *Opn5* 203
Figure 85 melanopsin regeneration models 207
Figure 86 Melanopsin intermediates 208
Figure 87 Putative bistable intermediate cycle 213
Figure 88 Response modulation test paradigm 216
Figure 89 PDA suppression test paradigm 219
Figure 90 Anti-PDA test paradigm 220
Figure 91 PDA facilitation test paradigm 221
Figure 92 SMARTS2 atmospheric model simulation 225
Figure 93 Light source simulation with aging ocular media 229
Figure 94 Correlated color temperature simulation 231
Figure 95 Effect of ocular media for bistable action spectra 232
Figure 96 Schematic of an adaptive optics system 235
Figure 97 Layout of the adaptive optics retina camera 236
Figure 98 Sensitivity of the method for rhodopsin parameters, 1/2 254
Figure 99 Sensitivity of the method for rhodopsin parameters, 2/2 254
Figure 100 Effect of R/M peaks on equilibrium spectrum 255
Figure 101 Effect of R/M peaks on relaxation spectrum 256
Figure 102 Effect of relative quantum efficiency (ϕ) on bistable spectra 257
Figure 103 Effect of photopigment densityon bistable spectra 258
Figure 104 "Photic memory" individual PLR waveforms 261
Figure 105 "Photic memory" individual differences of reference and test stimuli 262
Figure 106 Bistable potentiation, individual PLR waveforms 263
Figure 107 Bistable potentiation, individual differences of reference and test stimuli 264

LIST OF TABLES

Table 1 Spectral sensitivities of NIF-responses 33
Table 2 Spatial sensitivity of NIF-responses 40
Table 3 Pupillary parameters and units 73

Table 4 Spectral sensitivities of rhodopsin intermediates 120
Table 5 Photopigment densities 248
Table 6 Parameter estimates for melanopsin model 1/2 250
Table 7 Parameter estimates for melanopsin model 2/2 251
Table 8 Detailed subjects characteristics 259
Table 9 The individual responses for the same three time bins 260

LIST OF ALGORITHMS

B.1 Light SPD as Gaussian 243
B.2 Ocular media model (Matlab) 244
B.3 Matlab implementation of ocular media model fitting . 245
B.4 Macular pigment absorption (Matlab) 245
B.5 Govardovskii's nomogram (Matlab) 247
B.6 Self-screening correction (Matlab) 247
B.7 Quantal→Energy sensitivity conversion (Matlab) . . . 247
B.8 Irradiance response curve (IRC) fit 248
B.9 Input text file for SMARTS2 simulation 249

NOMENCLATURE

AC	Alternating Current
AIC	Akaike Information Criterion
ANS	Autonomous Nervous System
BLH	Blue Light Hazard
CAS	Criterion Action Spectrum
CBT	Core Body Temperature
CCD	Charge-Coupled Device
CCT	Correlated Color Temperature
CFF	Critical Fusion Frequency
CIE	Commission internationale de l'éclairage
CMOS	Complementary Metal Oxide Semiconductor
CRI	Color Rendering Index
CTF	Contrast Transfer Function
DAP	Depolarizing After Potential
DC	Direct Current
DD	Dark-Dark cycle
DIN	Deutsches Institut für Normung, German Institute for Standardization
DMH	Dorsomedial Hypothalamic Nucleus
DOF	Depth-of-Field
ECG	Electrocardiography
ECoG	Electrocorticography
EEG	Electroencephalography
EMD	Empirical Mode Decomposition
ERG	Electroretinography

ERP	Early Receptor Potential
EW	Edinger-Westphal nucleus
FFT	Fast Fourier Transform
fMRI	functional Magnetic Resonance Imaging
FOV	Field-of-View
FWHM	Full-Width at Half Maximum
GCL	Ganglion Cell Layer
GPCR	G Protein Coupled Receptor
GPGPU	General-Purpose computation on Graphics Processing Units
HBW	Half-Bandwidth
ICA	Independent Component Analysis
IGL	Intrageniculate Leaflet, same as vLGN in primates
INL	Inner Nuclear Layer
IPL	Inner Plexiform Layer
ipRGC	instrinsically photosensitive Retinal Ganglion Cells
IRC	Irradiance Response Curve
IS	Inner Segment
LAN	Light-At-Night
LD	Light-Dark cycle
LDSF	Level Dependent Signal Flow
LED	Light Emitting Diode
LGN	Lateral Geniculate Nucleus
LL	Light-Light cycle
LRP	Late Receptor Potential
MEA	Multielectrode Array
mfPOP	multifocal Pupillographic Perimetry
mRGC	melanopsin-containing Retinal Ganglion Cells
mRNA	messenger Ribonucleic Acid
MTF	Modulation Transfer Function
NIF	Non-Image Forming
OD	Optical Density
ONL	Outer Nuclear Layer
OPL	Outer Plexiform Layer
OPN	Olivary Pretectal Nucleus, same as PON
OPN	Olivary Pretectal Nucleus
OS	Outer Segment
PCA	Principal Component Analysis
PCNA	Prolonged Corneal Negative Afterpotential
PCT	Pupil Cycling Time
PDA	Prolonged Depolarization Afterpotential
PIPR	Post-Illumination Pupil Response
PLR	Pupillary Light Reflex
PNR	Pupillary Near Reflex
PON	Pretectal Olivary Nucleus, same as OPN
pRGC	photosensitive Retinal Ganglion Cells
PSE	Pupil Size Effect
PSF	Point Spread Function
PUI	Pupillary Unrest Index
RAPD	Relative Afferent Pupil Disorder
RGC	Retinal Ganglion Cell
RPE	Retinal Pigment Epithelium
SAD	Seasonal Affective Disorder
SCE	Stiles-Crawford Effect
SCN	Suprachiasmatic nucleus
SI	The International System of Units (Système international d'unités)
SNR	Signal-to-Noise Ratio
SPD	Spectral power distribution
STFT	Short-Time Fourier Transform
SVD	Singular Value Decomposition
UV	Ultraviolet
vLGN	ventral Latern Geniculate Nucleus, same as IGL in non-primates
VLPO	Ventrolateral Preoptic nucleus
vSPVZ	ventral Subparaventricular Zone

PREFACE

AIM OF THE THESIS

The aim of the thesis is to investigate the putative bistability of melanopsin by three means: 1) with a PLR study on the dark regeneration of PLR sensitivity, 2) developing a method for measuring lens density, thus quantifying the retinal photon density, and 3) modeling quantitatively the putative bistable melanopsin system and providing a framework for predictions and validation of the bistability experimentally.

STRUCTURE OF THE REPORT

The report is structured to seven chapters, the first begin this introduction, the following four chapters reviewing the essential literature (1, 2, 3 and 4) needed for understanding the research projects (5). The final chapter summarizes the work and and discusses about future prospects (6).

Chapter 1 : NIF system

The basics of circadian rhythms, chronobiology and non-image forming (NIF) system are reviewed as a general background for the three following literature review chapters.

Chapter 2 : Visual system

The human visual system is reviewed in regard to three aspects: 1) the ophthalmic optics, 2) the canonical visual system employed in visual responses, and 3) the non-image forming (NIF) system with the characterization of the novel photopigment melanopsin.

Chapter 3 : Pupillary Light Reflex (PLR)

The human pupillary light reflex (PLR) is discussed in this chapter in depth as it was later used as the tool to study melanopsin-dependent photoreception. The literature analysis is extended beyond the typical scope used in melanopsin-related studies in an effort to provide a more complete idea of PLR as a tool.

Chapter 4 : Melanopsin bistability

In this chapter, the invertebrate bistable photopigment systems are reviewed first in regard to physiology and quantitative modeling.

Chapter 5 : Research projects

The research projects undertaken for the completion of this work are divided into five following subsections.

Introduction to PLR as a a tool

The first subsection describes the technical details of the pupillometric setup used in this work and in a previous study (Mure et al. 2009) from the same group, along with a pilot study done on individual PLR variability.

"Photic memory" PLR study

The second subsection investigates the existence of dark regeneration of photosensitivity in melanopsin photoreception using PLR in humans. This absence of dark renegeration in bistable flies were referred as "photic memory" by Hochstein et al. 1973.

Changes in PLR with aging

Third subsection studies the changes in PLR during aging. The study compares the pupil responses to monochromatic blue (480 nm) and green (560 nm) light between the control young group and healthy aged individuals.

Measuring ocular density in humans

In the fourth subsection, a psychophysical method developed for quantifying the human ocular media density is presented. With aging the ocular media density increases attenuating the light entering the retina, thus the quantitative knowledge of light filtering is essential for studying non-image forming (NIF) responses.

Model for melanopsin bistability

In the last subsection, a quantitative framework is provided for the putative melanopsin bistability allowing simulation of the bistable photoreception. The framework is implemented in Matlab and provided with a graphical user interface (GUI).

Chapter 6 : Conclusions and future directions

The last chapter sums up the work presented in this report and provides ideas for further research.

1

NON-IMAGE FORMING (NIF) VISUAL SYSTEM

Non-image forming (NIF) visual system refers to the processing of light information by the eyes and the brain with no resulting visual perception in contrast to normal definition of vision as a visual experience. The phenomenon of light responses without "classical visual photoreceptors" rods and cones (See Section 2.3) was first demonstrated in the 1920s by Keeler 1927 in mice with pupil constriction (as reviewed by Van Gelder 2008). The term *"non-image forming"* was first suggested by Gary Pickard in his study of circadian rhythm regulation in hamsters (Pickard 1982). Sometimes *"circadian visual system"* (Morin and Allen 2006; Foster and Hankins 2007) is used as a synonym for the functionally same visual system. The non-image forming (NIF) visual system can be seen as a broader definition with *"circadian vision"* only being one subsection the whole NIF system. In this chapter, the concept of circadian rhythms is introduced with an emphasis on the effects of light to physiology. More detailed analysis of human visual system is done in the next chapter (2).

1.1 CIRCADIAN RHYTHMS

Circadian rhythms (*'circa'* means about, and *'dies'* means day) refer to intrinsically generated rhythms in organisms varying from cyanobacteria (Williams and Poole 2006) to humans (Czeisler et al. 1999). The field of biology studying biological rhythms (including circadian) is chronobiology (chrono = time). Biological rhythms also range across a frequency spectrum, from ~100 Hz (neuronal firing rate) up to circa 10^{-9} Hz for very long population cycles (period τ~10 ms up to ~20 years). Periods (τ referring to intrinsic period of organism) of circadian rhythms range between 22 and 26 hours, and are then synchronized to the external period of exactly 24 hours (process referred as entrainment). Apart from circadian rhythms there are ultradian rhythms (τ << 24 h); infradian rhythms (τ >>24 h); circannual rhythm [τ ~1 year)]; circatidal rhythms (τ ~12.4 o 24.8 h) in anticipation of tides; and circalunar rhythms (τ ~ 29.5 days ~ 1 month, rotation of moon around earth).

Periodic leaf movements in plants were first discovered by Androsthenes Thasius 325 BC, followed by observation of De Mairan in 1729 that plants rhythms persisted in constant darkness and postulation of 'flower clock' by Linnaeus in 1751. First demonstration of intrinsically generated rhythms in primates was provided by Simpson and Galbrath 1906 in the core body temperature (CBT) of squirrel monkeys.

de Candolle 1832 noticed first the deviation of intrinsic period from 24 hours of day-night cycle in plants followed by the same observation in white-footed mice (Johnson 1926). de Candolle 1832 had seen the period length to be influenced by environmental light intensity, later formally coined as the "Aschoff's rule" byAschoff 1960.

Persistence of a free running rhythm in constant conditions demonstrates the existence of an oscillator in animal or plant (i.e. rhythm generation). An overt rhythm can be based on both exogenous and endogenous influences. The external timing cues like light that are capable of entraining organism, are referred as *zeitgebers* (German for time givers). Other common non-photic *zeitgebers* (e.g. Honma et al. 2003; Mistlberger and Skene 2005) are temperature (Miyasako et al. 2007), food intake (Fuller et al. 2008), social cues (Aschoff et al. 1971), and pharmaceutical administration (Burgess et al. 2008). In the extreme case of purely endogenous regulation, the rhythm will immediately cease upon turning off the *zeitgeber*, such as the light-dark cycle. In the other extreme of pure endogenous generation, the rhythm will appear to be self-sustained, and continue for ever without dampening of amplitude. How to study circadian rhythms are reviewed for example by Wirz-Justice 2007 and Hofstra and de Weerd 2008.

The master circadian clock in mammals is located in the suprachiasmatic nucleus (SCN), a small hypothalamic structure. SCN lesions abolish the circadian rhythmicity of physiological and behavioral functions (Moore and Eichler 1972; Stephan and Zucker 1972). The autonomous nature of the SCN has been elegantly demonstrated by Ralph et al. 1990 who showed that SCN transplants can restore circadian rhythms that display the period of the donor animal rather than that of the host. Circadian pacemaker can be functionally explained on the basis of harmonic oscillator by van der Pol 1934 obtained from studies with electrical discharge oscillations in fluorescent lamps. SCN in mammals connect to other accessory clock structures in the brain forming a clock network (see reviews by Herzog 2007; Baggs et al. 2009; Kyriacou and Hastings 2010; Colwell 2011) rather than a centralized master clock.

In popular literature, dysfunctions in human circadian system has been linked to the prevalence of Seasonal Affective Disorder (SAD, Partonen and Magnusson 2001; Wirz-Justice 2009) or as known also as 'winter depression'. The etiology of SAD is still unknown (for reviews, see for example Rosenthal et al. 1984 and Rohan et al. 2009) but the reduced light intensity has been suggested as a reason with psychological effects from changes in weather (Keller et al. 2005; Denissen et al. 2008). Light therapy has been used successfully for the treatment of SAD via assumed light-clock interaction.

1.2 NON-IMAGE FORMING RESPONSES TO LIGHT

In this section, the most important non-image forming responses to light in animals are reviewed briefly with the length needed for understanding this thesis (continuation of the Master's thesis of the author, Teikari 2006a). The three most used measures of the NIF-system are locomotor activity (mainly in rodents), sleep-activity cycles; and melatonin rhythm and melatonin suppression. In my work the measure have been pupillary light reflex (PLR) which is reviewed in more detail in chapter 3. In addition, there has been an increased interest for acute effects of light to human brain functioning with brain imaging techniques such as functional magnetic resonance imaging (fMRI).

1.2.1 *Locomotor activity*

Observing the locomotor activity [when the animals are active on a running-wheel or doing some other activity (Poirrier et al. 2006; Ou-Yang et al. 2011)] is very common in rodent studies. The regulation of circadian rhythms of locomotor activity appears to involve hypothalamic relays in the ventral subparaventricular zone (vSPVZ) and dorsomedial nucleus (DMH) as lesion of each of these structures can abolish the observed rhythm (Lu et al. 2001; Chou et al. 2003). The locomotor activity of rodents is also acutely inhibited when the animals are exposed to light during their activity period at night Redlin and Mrosovsky 1999. In nocturnal rodents an acute suppression of locomotion (negative masking, see review by Mrosovsky 1999) occurs in bright light (Aschoff and Goetz 1988) in an irradiance-dependent manner (Mrosovsky 1994). In dim light as opposed to darkness, an increase in locomotion (positive masking) is seen because visual guidance of movement enhances locomotion. In humans, the activity fluctuations do not seem to exhibit circadian rhythm (Ivanov et al. 2007), mainly due to environmental masking while it is still possible to see significantly altered activity fluctuations in specific conditions such as patients with Alzheimer's disease (Hu et al. 2009).

1.2.2 *Melatonin*

Melatonin is a hormone discovered in the late 1950s (Lerner et al. 1958) in bovine pineal tissue where it is secreted nocturnally (for an extensive review see Reiter et al. 2010). It was early on discovered that its secretion was connected to the environmental light-dark cycle (Snyder and Axelrod 1965). Besides the pineal gland, other organs may have the capability of producing melatonin (Hardeland 2009), such as in the retina (Gern and Ralph 1979). Melatonin production is driven by the master circadian clock SCN (for specific brain circuitry

see for example Hastings and Maywood 2008) as it was seen that the rhythm was abolished by SCN lesion (Moore and Klein 1974). Nocturnal melatonin cycle persists relatively unchanged until about middle age, after which the nighttime peak of melatonin start to be dampened both in humans (Sack et al. 1986) and in aged mammals (Reiter et al. 1981). The question, whether this dampening can be compensated in the elderly is still an open question (Brown et al. 2011a).

Melatonin was first discovered to be suppressed by light by Lewy et al. 1980 and the light-induced melatonin suppression has been used extensively to quantify the circadian responses (Brainard et al. 2001). It is considered to be more stable marker (Benloucif et al. 2005) for changes in circadian phase / entrainment than core body temperature (Cagnacci et al. 1992; Rajaratnam and Arendt 2001). In the context of phase changes, the dim light melatonin onset (DLMO) is used to track changes of experimental conditions imposed on intrinsic rhythms (Pandi-Perumal et al. 2007). There are various definitions for the time point for DLMO (Benloucif et al. 2008) but conceptually it is the time point when melatonin levels exceed some relative or absolute threshold defined for the given protocol. Melatonin can be combined with light therapy for optimized phase shifts (DJ-Skene 2003), for example for alleviating jet lag-related circadian problems (Dean et al. 2009).

1.2.3 *Sleep-Alertness*

The sleep is typically described with two-component model (Borbély 1982; Daan et al. 1984) consisting of an homeostatic component (process S) and a circadian component (process C). The homeostatic component describes the propensity of falling asleep correlating with the amount spent awake, whereas the circadian component (Saper et al. 2005b) reflects the 'internal wakefulness' signal that in certain extent tries to compensate for the sleepiness set by homeostatic component especially late in the evening (Strogatz et al. 1987). The two-process model can be extended into a three-process model, where the component of sleep inertia (Process W) is added (Åkerstedt and Folkard 1997; Åkerstedt et al. 2004). Sleep inertia is a transitional state of lowered arousal and impaired cognitive performance occurring immediately after awakening from sleep (Tassi and Muzet 2000), phenomenon not sufficiently described by the process S and process C.

All three processes can be theoretically manipulated with light exposure (see short review by Dijk and Archer 2009), for example by phase-shifting the alertness signal for process C (Duffy et al. 1996); acutely alerting the individual and acting against process S (Cajochen et al. 2000; Lockley et al. 2006; Vandewalle et al. 2006); and by dawn

simulation upon awakening for process W (Giménez et al. 2010). However, it should be noted that the three processes are not necessarily independent and the observed responses can be thought more as system response . The acute alerting effects (Effects to process S) of light (see reviews by Cajochen 2007 and Vandewalle et al. 2009) are probably the most studied of the these three components (Ali 1972; Badia et al. 1991; Daurat et al. 1996; Lockley et al. 2006) with recent interest to promote the productivity of workers manipulating general lighting (Juslén 2007; Viola et al. 2008; Vetter et al. 2011). The neuroimaging studies have shown that the thalamus is the structure most consistently recruited in response to light exposures during a cognitive task (Vandewalle et al. 2007a; 2006; 2007b) with the in activity in the thalamus directly relating to the improvement in subjective alertness induced by the light exposure (Vandewalle et al. 2006). The exact brain circuitry responsible for the light-induced alertness regulation is not well-known (see Vandewalle et al. 2009)

In rodents, light has shown to acutely promote alertness diurnal animals and sleepiness in nocturnal animals during darkness (Altimus et al. 2008; Lupi et al. 2008; Tsai et al. 2009), in addition to simply conteracting the sleepiness drive. In humans, light has shown to have wavelength-dependent effects on the sleep architecture as measured with electroencephalography (EEG; Kozaki et al. 2005; Münch et al. 2006). These results were further supported by a field study with environmental light recorded with wrist-worn actigraphs (accelerometer measuring motor activity, see review by Sadeh 2011 for use in sleep research), in which wavelength-dependent effects were found for sleep quality (Santhi et al. 2011).

1.2.4 *Cognition & Emotions*

Recently there have been studies suggesting the role of ambient light as a major modulator of brain function and cognition in humans (Vandewalle et al. 2009). Studies using memory tasks with fMRI showed improved cognitive performance both during biological night (Perrin et al. 2004) and during biological day (Vandewalle et al. 2007a; 2006; 2007b) with blue light over green and violet light (Vandewalle et al. 2007b); blue light over green light (Vandewalle et al. 2007a); and with bright 'white' light (Perrin et al. 2004; Vandewalle et al. 2006). Blue light (470 nm) was shown to elicit immediate responses after light onset in hippocampus and amygdala (Vandewalle et al. 2007b). According to the authors (reviewed in Vandewalle et al. 2009), this activation raises the possibility that blue light could favor an early affective and mnemonic arousal potentially participating in prompt behavioral adaptation to the environment. The amygdala (Aggleton 1992) activity would suggest therapeutic value for light treatment in mood disorders (Vandewalle et al. 2009; Rautkyä et al. 2011; Stephenson

et al. 2012). Furthermore, the same authors showed that light could wavelength-dependently modulate emotional response to vocal stimuli (Vandewalle et al. 2010), as well the strength of light modulation of cognitve responses depending on the circadian phase (Vandewalle et al. 2011).

1.2.5 *Adverse effects of light*

The increased trend to use blue light to promote "human health" (e.g. Viola et al. 2008; Vetter et al. 2011) and the emergence of a "24/7-society" (Kreitzman 1999; Williams 2011) have suggested to have adverse effects on human health. Recently a term "light-at-night" (LAN) has been introduced (Pauley 2004; Lyytimäki 2006; Kayumov et al. 2007; Stevens et al. 2007; Navara and Nelson 2007; Kantermann and Roenneberg 2009; Schernhammer and Stone 2011; Kloog et al. 2011) to describe the shown correlation between night exposure to light and prevalence of colorectal (Kloog et al. 2009), and especially breast cancer in women (Pukkala et al. 1995; Wu et al. 2011; Hansen and Stevens 2011). The prevalence of breast cancers have been linked to nocturnal melatonin suppression by light (Srinivasan et al. 2008), but no causal relation has yet been established.

The increased use of nocturnal artificial lighting is in general referred as "light pollution" (Teikari 2007b) due to the problems caused for astronomical observations (Kocifaj et al. 2010; Park 2011), wildlife (Rich and Longcore 2005; Hölker et al. 2010) and for economy (Gallaway et al. 2010). The light pollution from blue-enriched light sources, such as those from metal halide lamps and LEDs is stronger (Johnson and Shah 2011; Bierman 2012) mainly due to the Rayleigh-scatter in the atmosphere that scatters blue light more (Kocifaj 2011).

The use of blue light has been associated also with "blue light hazard" (BLH) which refers to the increased phototoxicity of blue light due to higher photon energy of short wavelength radiation (see reviews by Sliney 2006; Wu et al. 2006; van Norren and Gorgels 2011; Hunter et al. 2012) with an established human action spectrum peaking at ~320-400 nm similar to the one obtained for rodents (Knels et al. 2011). There is also evidence that the susceptibility to retinal damage has a circadian rhythm and can be modulated by the exogenous administration of an antioxidant (Vaughan et al. 2002).

2 VISUAL SYSTEM

2.1 LIGHT

In studies of phototransduction, the light-induced responses are strictly speaking quantized resulting from absorption of discrete number of photons, being in contrast of typical photometric macroscopic quantification of light responses (see e.g. Zwinkels et al. 2010). Thus it is typical to express light intensity either as total photon density or as photon density per wavelength (spectral irradiance). The energy of a photon E_{photon} is defined typically using either of the following three relations:

$$E_{photon} = \hbar\omega_{photon} = h\nu_{photon} = \frac{hc}{\lambda_{photon}} \tag{1}$$

where $\hbar$ is the reduced Planck constant ($h/2\pi$), ω is angular frequency ($2\pi\nu$), is the, h is the Planck constant ($\sim 6.625 \times 10^{-34}\, J \cdot s^{-1}$), ν is the frequency of the photon (in Hz), c is the speed of light ($\sim 3.0 \times 10^{8}\, m/s$), and λ_{photon} is the wavelength expressed typically in nanometers. In other words, monochromatic red light with a wavelength ~650 nm of the same optical power as of a monochromatic blue light (480 nm) will have ~1.3 times (=650/480) more photons.

The spectral content of the light depend on the type of the light source (see Elvidge et al. 2010 for review of light sources), ranging from polychromatic thermal radiators (sun, incandescent lamp, candle) spectrum corresponding to Planck blackbody radiation, spectrally "flat" Xenon arc sources, gas discharge lamps (fluorescent, metal halide lamps) exhibiting peaked spectral power distribution (SPD) corresponding to fluorescence peaks used in the lamp; to quasi-monochromatic light-emitting diodes (LEDs) and to monochromatic laser. The latter sources, LED and laser can be estimated conveniently as "Gaussian light sources" when knowing the peak wavelength and the half-bandwidth (HBW or full-width at half-maximum FWHM, describing the "broadness" of the spectral power distribution) of the light source, as following (Hecht 1988):

$$\sigma = (HBW/2) \times 2.355 \tag{2}$$

where σ is the standard deviation of the Gaussian pectral power distribution, see the Matlab implementation in B.1.1.

2.2 OPHTHALMIC OPTICS

2.2.1 *Radiation transfer*

From the optical parameters of the human eye (simplified optical model in Figure 1) and from the radiometric parameters of a light source, it is possible to calculate irradiance reaching the retina. Retinal irradiance E_r is directly related to source radiance L_s (brightness):

$$E_r = \frac{\pi d_p \tau}{4f^2} \cdot L_s = \frac{\tau E_c A_p}{A_r} \tag{3}$$

where, E_r is the retinal irradiance, d_p is the pupil diameter in mm, f is the focal length of the eye [estimated to be 1.67 cm (Gullstrand's model eye, Longhurst 1974; Land 1981) or 2.22 cm used in more recent literature (Vohnsen and Rativa 2011a)], L_S is source radiance,τ is the lens transmittance, E_c is corneal irradiance, A_p is the pupil are in mm², A_r is the area of the retinal image in mm². The corneal irradiance E_c (Sliney 2005; 1991) depends on the source geometry:

$$\begin{aligned} E_C &= L_s \cdot \Omega_s = L_s \cdot \frac{A_s}{r^2} = \frac{E_r 4f^2}{\tau \pi d} \cdot \frac{A_s}{r^2} \\ &= \frac{4}{\tau \pi d_p^2} \cdot \frac{f^2 A_s}{r^2} \cdot \frac{P_r}{A_r} = \frac{E_r A_r}{\tau A_p} \end{aligned} \tag{4}$$

where, E_c is corneal irradiance, L_S is source radiance, Ω_s is solid area in steradians, A_s is the source area in mm², r is the distance between the source and the lens, P_r is the retinal optical power, τ is the lens transmittance, d_p is the pupil diameter in mm, f is the focal length of the eye, E_r is the retinal irradiance, A_r is the area of the retinal image in mm², A_p is the pupil are in mm².

In practice the source radiance in this context refer to the light seen by the observer and not necessarily the light source itself, and the brightness therefore can refer to the surface radiance of a indirectly illuminated Ganzfeld (formless field of light without visual edges) dome for example. The image size (diameter) of the source at the retina can be calculated as following:

$$d_r = d_s \frac{f}{r} = \alpha f \tag{5}$$

where d_r is the size of the image at the retina, d_s is the size of the source, f is the focal length of the eye, r is the distance between the source and the lens, α is the angular subtense of the source.

The pupil diameter d_p along with lid closure (Sliney 1997) mechanically regulate the light entering the retina. The pupil diameter d_p varies from 1.5mm to 8mm on average (Reeves 1920) allowing maximal reduction in light intensity of $\log_{10}(1.5mm/8mm)^2 \sim 1.45$ log

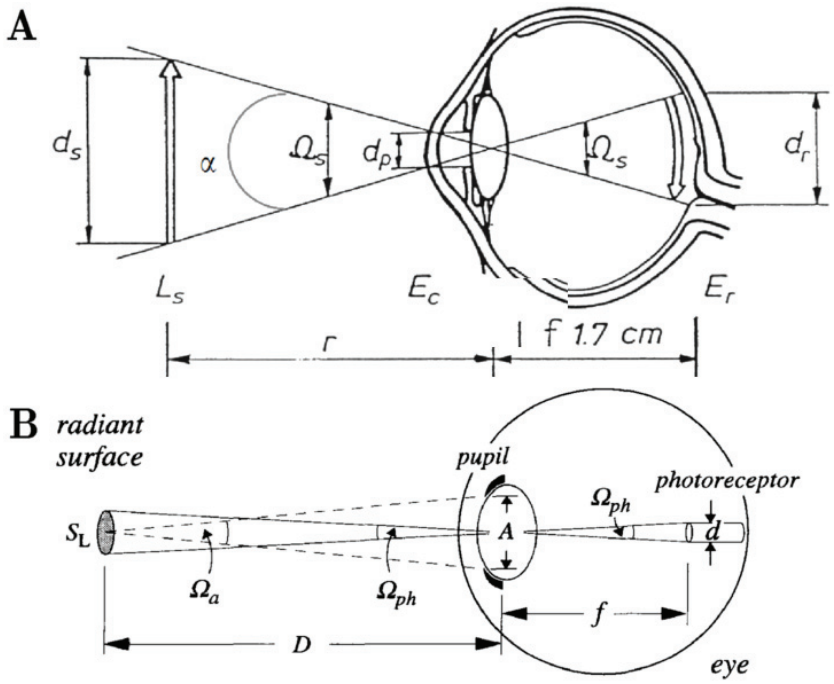

Figure 1: **A** The human eye as an optical system (Sliney 2005). **B** Photoreceptor optics (Warrant and Nilsson 1998)

units. The magnitude of lid opening (palpebral fissure constriction), thus its effect on field of view (FOV, see 2.3.1) can be estimated with the following empirical formula (Sliney 2008): $\varphi_{FOV} = 34°\text{-}0.0013L$, where φ_{FOV} is the upper field-of-view angle in degrees and L is the luminance in cd·m². The upper field-of-view angle of a group of subjects typically spans a range of about 25° (Deaver et al. 1996).

In regard to the NIF photoreception (see Section 2.4 below), the effect of pupil size on retinal irradiance and melatonin suppression is addressed by Takahashi et al. 2009, the ffect of angular subtense (visual field size) on the pupillary light reflex by Stanley and Davies 1995, the effect of light source geometry on retinal irradiance by Weber et al. 2004, the aging-related changes in radiative transfer reviewed by Charman 2003, and the problems of using human photometric quantities in animals is discussed by Bullough et al. 2006. In general radiative transfer issues are improperly addressed in NIF photoreception studies (Weber et al. 2004).

2.2.2 *Stiles-Crawford effect*

In previous purely geometric optics analysis of the human eye, the relation between pupil size and retinal irradiance is considered to be linear, but strictly speaking this is not true as it was shown by Stiles and Crawford 1933 that luminous efficiency of light varies as a function of the pupil location. In other words, the light hitting obliquely photore-

ceptors is less efficient eliciting a visual sensation compared to direct axial stimulation. This was shown originally for human cones *in vivo* (Stiles and Crawford 1933) and later *in vitro* (Enoch 1963) for human cones and for invertebrate photoreceptors (Snyder 1975). This was termed as Stiles-Crawford effect (SCE) of type I. Quantitatively, the phenomenon for cones is well characterized by the equation (Stiles and Crawford 1933; Vohnsen and Rativa 2011a):

$$\eta = 10^{-\rho r^2} \tag{6}$$

where η is the luminous visibility light beam entering, respectively, at the peak of the curve at a distance r millimeters from the peak luminous efficiency. The peak of sensitivity is usually thought to reside, though not invariably, close to the center of the pupil. It has been found sufficient to describe the shape of directional sensitivity with a single parameter ρ (~0.05 mm^{-2}). In other words, there is approximately a threefold reduction in luminous efficiency when a narrow beam is displaced from the center to the edge of a 6.5 mm diameter pupil.

The SCE have been shown to be more pronounced in cones responsible for photopic (daylight) vision, and originally thought to be insignificant for rods (Van Loo and Enoch 1975); which are responsible for scotopic (night) vision. However, it has been suggested by the results by Alpern et al. 1983 that a significant SCE could exist for rods while still less pronounced than for cones. The differential directional effect for rods and cones is most likely due to the microanatomical and molecular differences (Westheimer 2008). It has been suggested that the SCE has its origin most likely somewhere in the retinal receptor cells and the photon capture by the photopigment molecules. However, the exact mechanism is still unknown (Westheimer 2008; Enoch and Lakshminarayanan 2009), but it has been linked to the electromagnetic coupling of light wave to light-responsive outer segments of photoreceptors (see Section 2.3 and 4.1.1) as in radar waveguides (Toraldo di Francia 1949; Bernard and Miller 1970) and in optical fibers (Snitzer and Osterberg 1961; Vohnsen 2007). In melanopsin-mediated NIF photoreception (Section 2.4), the SCE (type I and II) can be expected to be insignificant, as there are no waveguiding or optical elements optimizing the photon catch of melanopsin-mRGCs (Do et al. 2009)

2.2.3 *Spectral transmittance of ocular media*

Knowledge of spectral transmission in the ocular media is of importance in vision research. In vivo determinations of various retinal visual sensitivities require as exact as possible knowledge of the ocular spectral filtration for the used light stimulus. The spectral characteristics of the ocular media is typically expressed in optical den-

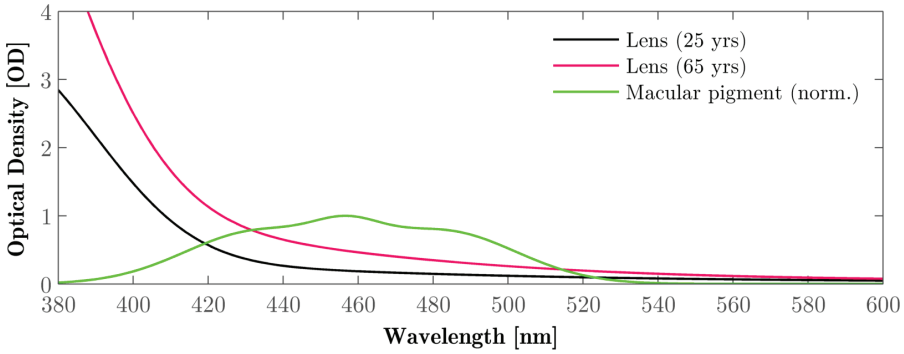

Figure 2: Ocular media with absorbance of the lens using two standard observers with ages 25 yr and 65 yr based on the model of van de Kraats and van Norren 2007a. The macular pigment density is normalized to unity density at peak based on the formulation of Walraven 2003.

sity ($OD(\lambda]$) units which define the absorption in log units and the transmittance is then defined by the Beer-Lambert law (e.g. Wind and Szymanski 2002; Sassaroli and Fantini 2004; Kocsis et al. 2006): $\tau(\lambda) = 10^{-OD(\lambda)}$, where $\tau(\lambda)$ is the transmittance in % as a function of wavelength. The ocular media consist of cornea, aqueous humor, crystalline lens, and vitreous humor (see Figure 2). The spectral absorption profile for visible light is dominated by the absorption of the crystalline lens (van de Kraats and van Norren 2007a). Additionally, the human lens is absorbing more light especially on the short wavelength range of visible light (van de Kraats and van Norren 2007a), compared to mouse (Jacobs and Williams 2007) and rat (Gorgels and Norren 1992) ocular media that starts filtering significantly at deeper blue and UV range.

The cornea is estimated to be of the order of 0.1 density units in the visible light range (van den Berg and Tan 1994; van de Kraats and van Norren 2008). The other media, e.g., the lens capsule (Murata 1987), the aqueous humor (Boettner and Wolter 1962) and the vitreous humor (Boettner and Wolter 1962) have negligible absorbance in visible range. The humors are mainly composed of water and start to absorb in deep-red/near-infrared range (Ma et al. 2011, Smith and Baker 1981). Below 320 nm, absorption by tryptophan residues becomes substantial (Kolozsvári et al. 2002; van de Kraats and van Norren 2007a) in the ocular media.

Light passing through the ocular media is also subject to light scatter which can be separated to scatter types: 1) Rayleigh-Gans scatter (Coppens et al. 2006), which is typically due to submicroscopic density fluctuations and thus can be found in all media with the resulting spectral shape being somewhere between being constant over wavelength and having the shape of the Rayleigh component ($\propto \lambda^4$). 2) Mie scattering (van de Hulst 1957) occurring on particles large in relation to the wavelength with the resulting spectral shape being con-

stant over wavelength, thus acting as a neutral density filter on top of retina.

On top of the central retina known as fovea there is a concentration of macular pigments that preferably absorb blue light (Walraven 2003). The density of the macular pigments decrease exponentially with eccentricity (Delori et al. 2001), but the peak density and the rate of decrease vary amongst individuals (Hammond et al. 1997a). There is evidence than with aging the macular pigment can gradually accumulate and spread out to the periphery of retina (Chen et al. 2001b), while others have found no significant age dependence (Berendschot and van Norren 2005). Macular pigment density has been traditionally measured with psychophysical methods (Ruddock 1963; Bone and Landrum 2004) or with reflectometer (Bone et al. 2007), but recently multispectral imaging solutions have emerged (Fawzi et al. 2011).

The early reference dataset used for ocular filtration was the spectral template provided by Wyszecki and Stiles 1967, followed by Stockman et al. 1999, and the current state of art model by van de Kraats and van Norren 2007a for human ocular media excluding macular pigment. The model consist of five age-dependent spectral templates with a sixth spectrally neutral "neutral density filter" as shown in Figure 2.

In special cases such as with intraocular straylight measuruments (Ijspeert et al. 1990; van den Berg et al. 2009b; Michael et al. 2009), the transmural (ocular wall) and iris transmittance need to be explicitly addressed in contrast of assuming them to be light-tight structures (van den Berg et al. 1990). The translucency of iris and the ocular wall are exploited by ophthalmologists when performing diaphanoscopy (cf Greenwood 1913), in which a light guide is positioned against the sclera and the pupil is seen to glow from within (La Hey et al. 1993). Additionally, the retinal veil resulting from transmural transmittance can degrade visual performance, the blue-eyed individuals sometimes experiencing a reddish veil over dark areas when a low sun shines on the side of their eyes (van den Berg et al. 1991). van den Berg et al. 1991 estimated the irises of blue-eyed individuals to attenuate the red light only 0.72 log units and the green for 1.48 log units, whereas the corresponding attenuation values were 2.27 for red and 2.64 log units for green light in brown-eyed individuals. In addition to the translucency of the iris and the surrounding ocular wall, fundal reflections (Vos 1963; van de Kraats and van Norren 2008) might contribute to the pigmentation-related differences. Furthermore, the iris pigmentation have been shown to correlate directly with choroidal pigmentation (Weiter et al. 1985) and to be reduced with aging (Schmidt and Peisch 1986).

Additionally, the closed human eyelid functions as a long-pass filter favoring the transmission of red light over blue light (Moseley

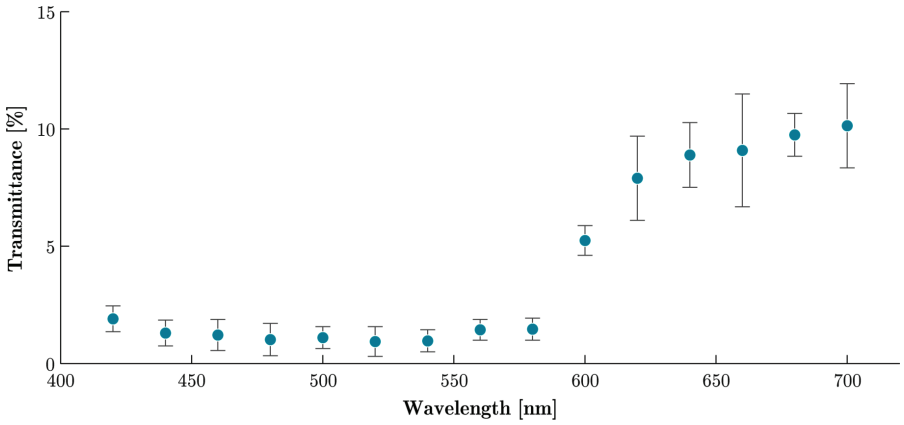

Figure 3: **Eyelid transmittance**. Redrawn from (Moseley et al. 1988).

et al. 1988; Robinson et al. 1991; Ando and Kripke 1996) as shown in Figure 3. The eyelid functions as a filter analog to the fly screening pigments (see sub 4.1.4 later) that favor the conversion of metarhodopsin to rhodopsin state. Bright light transmitted through eyelids can elicit physiological responses such as suppress melatonin secretion (Hätönen et al. 1999), but the light transmitted through eyelids at night when sleeping most likely won't have significant physiological responses (Kantermann and Roenneberg 2009) even though increased nocturnal artificial light have been linked to decreased sleep quality (Forejt et al. 2004). Additionally, even the dim red light could regenerate the "meta-melanopsin" back to the responsive "R state" partly explaining the positive responses from "dawn simulator" studies (Leppämäki et al. 2003; Van De Werken et al. 2010; Fromm et al. 2011), thus the melanopsin system (see Section 2.4 later) being the most responsive then upon dawn as suggested by Mure 2009.

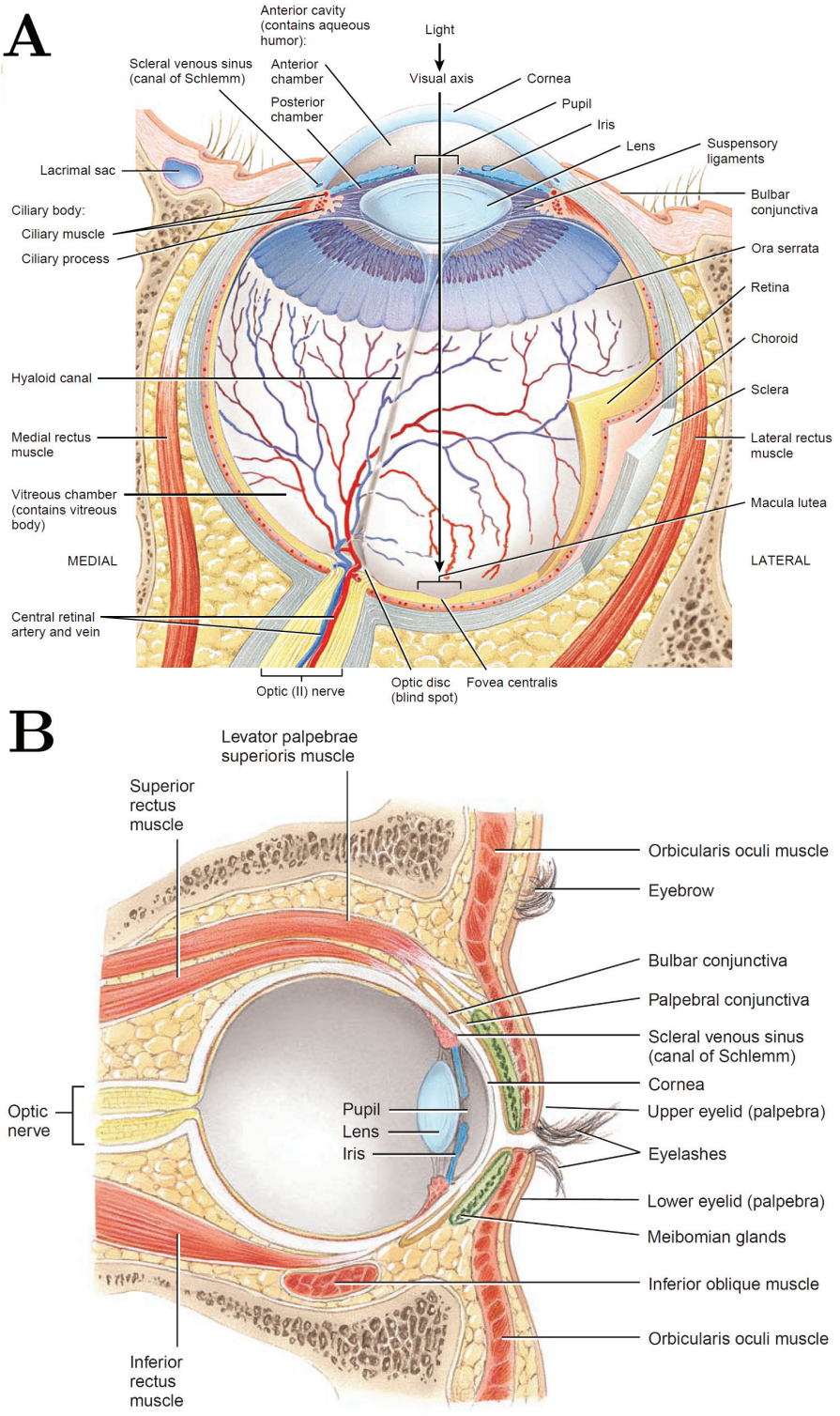

Figure 4: **Anatomy of the eye. (A)** Superior view of transverse section of right eyeball. **(B)** Sagittal view of the eye. (Tortora and Derrickson 2008)

2.3 CLASSICAL VISUAL PHOTOTRANSDUCTION

The spectrum of light that is visible to humans and most other mammals spans wavelengths of ~400–700 nm. Humans with normal color vision can distinguish many thousands of colors (Krauskopf and Karl 1992; Neitz and Neitz 2008) which is achieved by comparing signals from three types of cone photoreceptors. These are differentially sensitive (Merbs and Nathans 1992) to short (S, ~430 nm), medium (M, ~530 nm) and long (L, ~560 nm) wavelengths (much like Bayer array in modern digital cameras, Bayer 1976), but whose tuning is broad enough that each responds to light throughout much of the visible spectrum. The presence of three types of cone photoreceptor makes human color vision 'trichromatic'. Vision is dichromatic when there are two types of color sensitive detectors as in some color blind humans (see simulation in Wong 2011). The extreme example in animal kingdom are the mantis shrimps having up to 14 (check) different photopigments (Cronin et al. 2002). There are three kinds of human dichromacy: protanopia (lacking the L-cones), deuteranopia (lacking the M-cones), and tritanopia (lacking the S-cones). In addition to the cone photoreceptors, the human retina contains rod photoreceptors with the photopigment rhodopsin, that are mediating the vision in dim light (scotopic) conditions (Makous 2004). In older literature, the S-, M- and L-cone pigments have been referred as cyanolabe, chlorolabe and erythrolabe, respectively; and the rhodopsin as visual purple.

Cones are arranged to a triangular photoreceptor mosaic which is a seemingly randomly organized in regard to the different cone types (Curcio et al. 1990; Roorda and Williams 1999). The average human retina contains 4.6 million cones, and 92 million rods (Curcio et al. 1990), the mosaic being dominated by L- and M-cones with the S-cones being in a minority (5–10% of all cones, Calkins 2001). The central retina, fovea, contains the highest density of cones (Curcio et al. 1990), thus also corresponding to the region of highest visual acuity (Navarro et al. 1993; Rossi and Roorda 2010). In the fovea, there is additionally a small rod-free zone of a size ranging from 0.85 degrees (Ahnelt et al. 1987) to 1.25 degrees (Curcio et al. 1990), the rod densities increasing towards the peripheral retina. Recently, the cone packing density was shown to decrease with aging (Song et al. 2011). Amongst human individuals, the L:M-cone ratio varies between 1:4 and 15:1 without loss of normal color vision (Carroll et al. 2002), with the similar variation is seen in New World monkeys (Jacobs and Williams 2006). Despite this large variation, total information represented by the cone mosaic seem to remain relatively insensitive to changes in L/M cone ratio (Garrigan et al. 2010).

Human retina has a scotoma called *"blind spot"*, corresponding to patch (situated ~12–15° temporal and ~1.5° below the horizontal, of a

size ~7.5°× 5.5°) lacking of light-detecting photoreceptor cells on the optic disc of the retina where the optic nerve passes through it. This is compensated in practice filled-in by the visual system (Komatsu 2006; referred as inpainting in computer vision Bertalmio et al. 2000).

In turn, the photoreceptors are connected to a network of other retinal cell types with a recent estimate of the retinal network being composed of at least 50 clearly distinct cell types (Masland 2001; Gollisch and Meister 2010; Azeredo da Silveira and Roska 2011; Masland 2011). The simplified schematic of the retinal circuitry for perceptual vision is shown in Figure 5. The retinal circuit is composed of five major classes of neurons within a layered structure: outer nuclear layer (ONL); OPL, outer plexiform layer (OPL); inner nuclear layer (INL); inner plexiform layer (IPL); and ganglion cell layer (GCL). Additionally, there is pigment epithelium (RPE) that serves for providing nutrients for the retinal cells important in regeneration of visual sensitivity (Wang and Kefalov 2011).

Rod and cone photoreceptor cells transduce light into electrical signals and synapse onto bipolar and horizontal cells. Rod photoreceptors mediate night (scotopic) vision; cone photoreceptors mediate daylight (photopic) vision. Bipolar cells integrate and convey photoreceptor signals to retinal ganglion cells (RGCs) and amacrine cells. Horizontal cells perform lateral processing by interacting with bipolar and photoreceptor cells; amacrine cells perform lateral processing by interacting with bipolar cells and RGCs. RGCs transmit visual information, in the form of spatiotemporal patterns of action potentials brain.

Each major retinal cell class consists of multiple cell types distinguished by morphology, connectivity, and light response properties. Thus the "retinal circuit"' can be be considered to consist of many "microcircuits" instead of one big circuit (Dacey 1999). For example, by anatomical and molecular criteria ganglion cell types number about 15-17 in mammalian retina (Wässle 2004; Field and Chichilnisky 2007; Berson 2008; Masland 2011), whereas the functional studies typically reveal around 5 (Carcieri et al. 2003). The anatomical diversity suggests that there is much function left to be discovered in the human retina (Gollisch and Meister 2010) as the discovery of intrinsically photosensitive retinal ganglion cells (mRGCs) demonstrated (Berson et al. 2002, see Section 2.4).

2.3.1 *Visual fields*

Human visual field is typically divided into four areas which are superior (upper), inferior (lower), nasal (closer to the nose) and temporal fields (away from nose, peripheral), which correspond to lower, superior, temporal and nasal parts of retina, respectively as the exter-

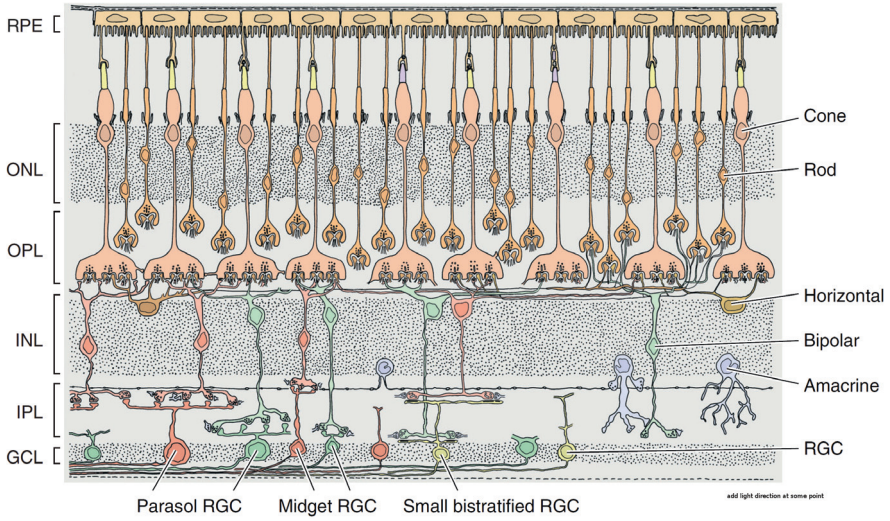

Figure 5: **Schematic illustration of the primate retina in cross-section.** In general, the processes of on bipolars terminate in the inner layers of the IPL and synapse on to on RGCs (green); similarly, off bipolars stratify in the outer layers and synapse on to off RGCs (red). Some RGCs stratify in more than one layer of the IPL and receive input from both on and off bipolars (yellow). Bipolar cells, amacrine cells, and RGCs make cell-type specific contacts in different sublayers of the IPL, which contribute to shaping RGC light responses. Five major circuits, including on and off midget bipolars synapsing on midget RGCs, on and off diffuse bipolars synapsing on parasol RGCs, and S cone bipolars synapsing on small bistratified cells are shown in detail (left). (Right) Shown are two elements of rod pathway circuitry (Arshavsky 2002): the synaptically connected A2 amacrine cell and rod bipolar cell. Several bipolars, amacrines, and RGCs are shown with truncated and/or disconnected processes to indicate uncertainty about their morphology and connectivity.

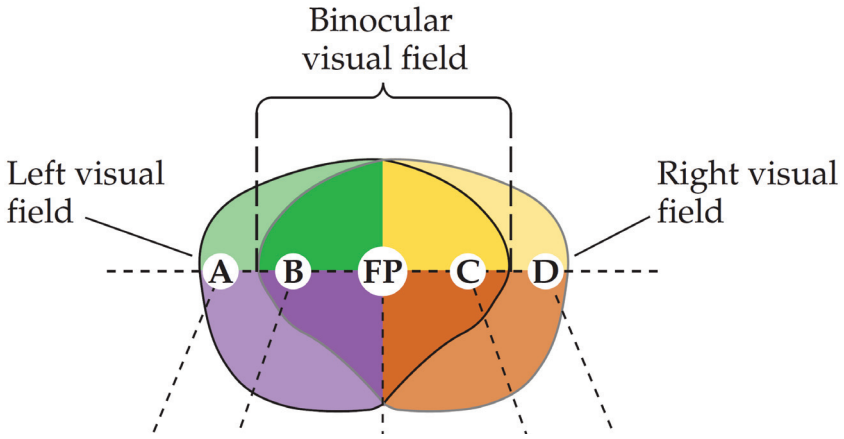

Figure 6: Projection of the binocular field of view onto the two retinas. (Purves 2008)

nal image is inversed on the retina. These four areas these then form four quadrants termed upper temporal, upper nasal, lower temporal and lower nasal quadrants. Binocular visual field is larger than either of the monocular visual fields alone. Forehead, nose and cheeks limit visual field so that it is larger horizontally than vertically. Binocular visual field is horizontally about 190°, and below the horizontal level about 70-80° and above 50-60° (Purves 2008). However, visual processing is not uniform across the visual field: 25% of cortex is devoted to the central five degrees of the field of view. There is evidence pointing differential function for the lower and upper fields (Previc 1990; Corbett and Carrasco 2011), as also seen in NIF-responses such as melatonin suppression (2.4.6) and pupillary light reflex (3.2.1).

2.3.2 *Spectral sensitivity*

The spectral sensitivity of human vision was first measured through psychophysical experiments in the early part of this century (for early references see e.g. Hecht et al. 1942; Crawford 1949; and for recent overview Stockman et al. 2008). The recent studies in animals have used microspectrophotometry (Govardovskii et al. 2000) as the technique of choice. Microspectrophotometry allows high-resolution spectral sensitivity functions to be derived from measurements, in comparison to psychophysical methods in humans yielding coarser spectral resolution. The derived spectral sensitivity spectra are referred also as action spectra emphasizing the "task-dependency" of the spectral sensitivity, for example how bright does a surface look as a function of light wavelength as with photopic luminosity efficiency function $V(\lambda)$ (Sharpe and Stockman 2008).

The spectral sensitivity of a mammalian photoreceptor is determined by a protein coined as opsin that the photoreceptor expresses. Opsins are located in the outer segments (OS) of rods and cones (see

Figure 5) bound to a molecule called chromophore (Wald 1964) that changes its conformation upon absorbing light. The chromophore in human rods and cones is 11-cis-retinal which is an aldehyde of Vitamin A1. After absorbing a photon, the photopigment undergoes photoactivation and "bleaches" to opsin and all-trans-retinal (Wald 1968), in other words the photopigment optically decolorizes with a reduced optical density (see 2.3.3). The classical equation used to describe the steady-state bleaching relation was the rectangular hyperbola derived by Stiles and Crawford 1932 for rhodopsin. This was later shown to provide a poor fit for the cone bleaching data (Valeton and van Norren 1983), and subsequently improved by Reeves et al. 1998 and Mahroo and Lamb 2004.

The spectral sensitivity of this compound is determined by the sequence of amino acids that make up the opsin protein. The peak wavelength sensitivity of the given pigment is the most sensitive to, is referred as the λ_{max} value of the pigment. There are no known rhodopsin polymorphisms (Sung et al. 1991) effecting its peak spectral sensitivity. This is contrast to the cones, with an evidence for a long-wavelength cone polymorphism (Neitz and Jacobs 1986; Deeb 2006; Neitz and Neitz 2011) in human observers with normal visual function. Dartnall et al. 1983 additionally found bimodal distributions for the peak spectral sensitivities for both M-cones (~533.7 nm and ~527.8 nm) and L-cones (~563.2 nm and ~554.2 nm), while distributions were found to be unimodal for rods (~496.3 nm) and S-cones (~419.0 nm) using microspectrophotometry for removed human retinas due to malignant growths.

The shape of the spectral absorption of all opsins with different λ_{max} can be expressed using a specific spectral template referred commonly as a "nomogram". The earliest nomogram was defined by Dartnall 1953 later found only suitable for visual pigments with a $\lambda_{max} \approx 500$ nm (Stavenga et al. 1993). Later modifications were made by MacNichol 1986, Baylor et al. 1987 and Lamb 1995 among others, the current "state-of-the-art" nomogram being defined in analytical form by Govardovskii et al. 2000. To date however, no comprehensive physical theory exists for the relation between molecular structure and absorbance characteristics, and the nomogram depend wholly on empirical curve-fitting to the recorded data. The shape of the nomogram is not strictly speaking invariant either, but depend on the temperature (Koskelainen et al. 2000) and the density of the visual pigment referred as the self-screening effect (Packer and Williams 2003) analyzed more thoroughly in 2.3.3.

In practice, there is no way of identifying a "true" peak in noisy data without assumptions on the shape of the underlying function. Thus, the "wavelength of maximum absorbance" λ_{max} is always a parameter of fitting data with a certain predetermined template, and, as such, depends of what template is used (cf. Levine and MacNi-

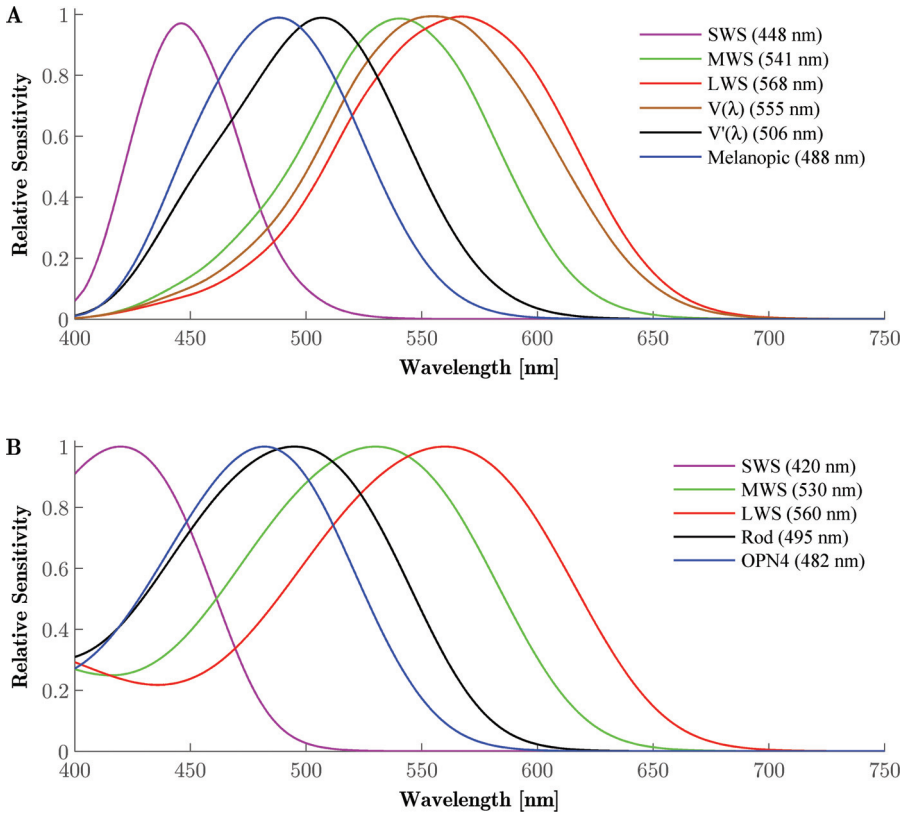

Figure 7: Spectral sensitivities of human vision **(A)** Corneal spectral sensitivities with the cone sensitivities, $V(\lambda)$ and $V'(\lambda)$ from the tabulated values of Stockmann and Sharpe. The "melanopic sensitivity" is given by Enezi et al. 2011. **(B)** Retinal spectral sensitivities generated using the nomogram of Govardovskii et al. 2000, with the peak spectral sensitivities given in legend.

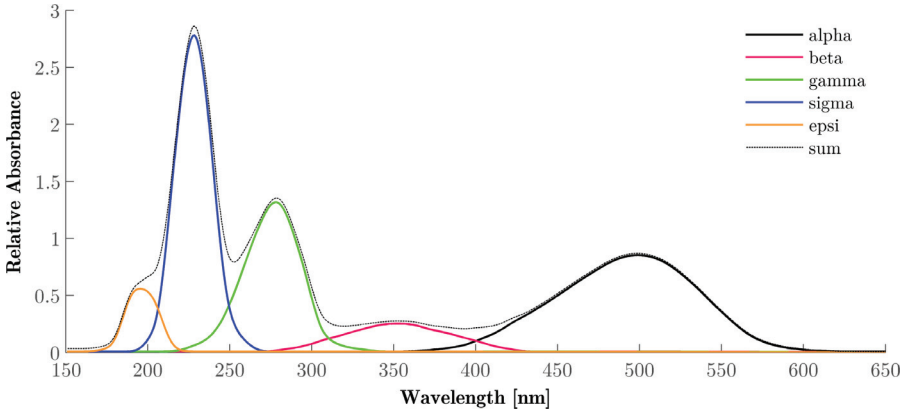

Figure 8: The absorbance spectrum of an exemplary vertebrate rhodopsin (λ_{max}~ 500 nm), considered as a sum of absorbance bands, indicated by alpha (α), beta (β), gamma (γ), sigma (σ) and epsilon (ϵ) normalized to the peak absorbance of the alpha-band (after Stavenga and van Barneveld 1975). (Stavenga 2010).

chol 1985). For this reason, different authors may give significantly different λ_{max} values for the same visual pigment and this need not indicate any real differences (e.g. genetic polymorphism) or inaccuracy of data. In general, the high accuracy in knowing the location of a "true" maximum is unimportant as such, since the peak is so broad that curves may be significantly shifted without experimentally measurable changes in absorbance at this spectral location (Govardovskii et al. 2000).

In addition to the "main band" of the nomogram (α-band), there are sidelobes in shorter wavelengths as illustrated in Figure 8 of which the β-band was included with the main band in the original formulation of Dartnall 1953 and later separated to analytical formulations of α-band and β-band in Govardovskii et al. 2000. The effect of β-band in human photoreception is limited due to ocular media filtration as shown in 2.2.3, but it has been shown to contribute to visual perception in humans without crystalline lens [aphakic or pseudophakic subjects, (Griswold and Stark 1992; Tan 1971; Goodeve et al. 1942)]. Due to the uncertainty in the short-wavelength range caused by the β-band and the pre-receptoral filtering, the nomogram has been traditionally fitted (proposed first by Dartnall and Lythgoe 1965) to the long-wavelength limb ("$\lambda_{0.5}$ equation"), which has a near-linear slope when plotting the sensitivity in logarithmic units (MacNichol 1986; Govardovskii et al. 2000).

2.3.3 *Self-screening*

The dependence of the photopigment spectrum on optical density (OD) is known as self-screening. As photons of many wavelengths pass axially through the photoreceptor, those of wavelength close to

the peak sensitivity of the photopigment are absorbed more superficially leading to broadening of the photopigment spectral sensitivity as light passes deeper in photoreceptor (Figure 9A). In other words, the wavelengths outside the peak wavelength are over-represented as photons deeper in the photoreceptors [see Figure 9B (Warrant and Nilsson 1998)]. The spectrum of the photopigment contained in an outer segment of a particular length can be calculated from the Beer–-Lambert law (e.g. Sassaroli and Fantini 2004):

$$t(\lambda) = 10^{-dce(\lambda)} \tag{7}$$

where t is the proportion of incident light transmitted (transmittance) as a function of wavelength (λ), d is the path length through the pigment, c is pigment concentration and e is the absorbance (absorptivity the original word) of the pigment as a function of wavelength (λ). Alternatively the effect can be expressed as a function of the spectral sensitivity (Lamb 1995):

$$S(\lambda)_{ss} = log_{10}\left\{\frac{1-\left[S(\lambda)\cdot\left(1-10^{-D}\right)\right]}{-D}\right\} \tag{8}$$

where $S(\lambda)_{ss}$is the spectral sensitivity corrected for self-screening, $S(\lambda)$is the normalized spectral sensitivity of the visual pigment obtained for example using the analytical nomogram by Govardovskii et al. 2000, D is the density of the pigment in logarithmic units (OD, optical density), Table 5 listing the values from the literature for dark-adapted human visual pigments.

In practice, differential pigment densities for example in two cones expressing the same photopigment will lead to the photoreceptors having different spectral sensitivities. This has been suggested to be the case in anomalous trichromats (having all three different cones, but with the M and L cone sensitivities overlapping) with the ability for trichromatic color discrimination due to higher L cone pigment density than the M cone pigment density (termed L′ in deuteranomalous observer). Depending on the photoreceptor optics, the final spectral sensitivity of the photoreceptor can be different than for the photopigment, as suggested in humans with high illuminance affecting the spectral waveguide properties (Alpern et al. 1987; Fuld et al. 1979) of the cones. The effect of self-screening on spectral sensitivity have been the most studied in color matching experiments, in which a "color-match illuminance effect" has been shown (Wright 1936; Burns and Elsner 1985) due to the bleaching of the photopigment (reduced optical density) in response to the experimental light stimulus (Burns and Elsner 1993). Thus, the effect of optical density becomes more significant with increased light intensity and should be taken into account when fitting nomogram models to experimental data with assumed contribution from multiple photoreceptors.

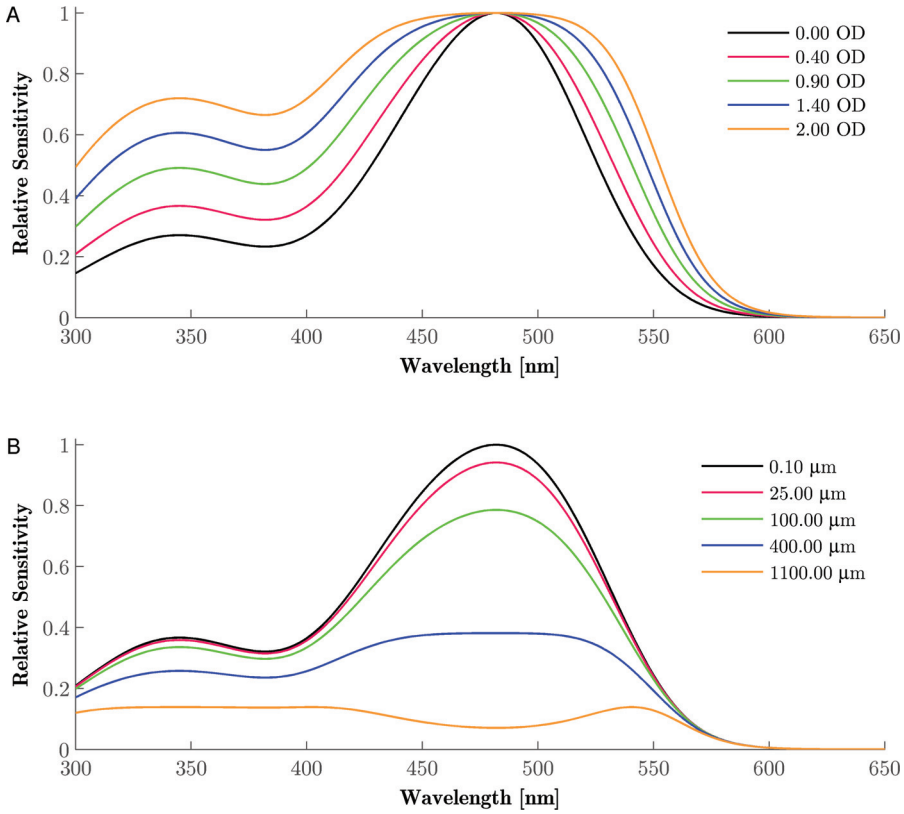

Figure 9: **Self-screening effect. (A)** Percentage absorption spectra of various concentrations of photopigment with both alpha and beta-bands included (Govardovskii et al. 2000). For convenience in comparing the shapes of the curves, their maxima have all been equated to 1 and superimposed. The actual fraction absorbed at the maximum is shown for each curve. It is apparent that with increasing concentration the absorption curve steadily increases in width (**B**) An illustration of self-screening in a photoreceptor 800 µm long. The absorbance peak wavelength (λ_{max}) of the resident visual pigment is taken as 500 µm. In the distalmost 100 µm, the absorption spectrum resembles the absorbance spectrum. In successively more proximal 100 µm segments (as indicated at right), the absorption spectrum becomes more bi-lobed in appearance, the lobes displacing further from λ_{max} with increasing depth. The wavelengths within the lobes are the only wavelengths remaining which can still be absorbed, with wavelengths around λ_{max} having already been strongly attenuated. This self-screening significantly widens the spectral sensitivity of the photoreceptor (Warrant and Nilsson 1998). Note that the 800 µm is very exaggerated example for photoreceptor length, the human rod photoreceptor being ~25 µm (Pugh and Lamb 2000) and the cone photoreceptor ~13 µm (Baylor et al. 1984). The longest known photoreceptor has been found in dragonfly being ~1,100 µm (Labhart and Nilsson 1995).

2.3.4 *Spectral Opponency*

Counterintuitive to the existence three spectral classes of cone photoreceptor (2.3.2), there seems to be four unique color hues in human vision - blue, green, yellow, and red (Bornstein 1973). The four unique hues arise from opponent pairs formed in the post-processing pathway between the photoreceptors and the brain, termed blue/yellow (B/Y) and red/green (R/G) channels (Chatterjee and Callaway 2003; Stockman et al. 2005; Solomon and Lennie 2007). The opponency (or mutual exclusivity) refers to the inability to simultaenously perceive blue and yellow, or red and green. In a simplified model of color opponency, the signal from blue-yellow channel is expressed as $B/Y = k_s S - (k_M M + k_L L)$, an antagonistic combination of S-cone signal (S) with the additive signal from R/G-channel ($M + L$), the k being the scaling constant for magnitude of the spectral sensitivities. For the red-green channel, the combination can be expressed as $R/G = (k_L L + k_S S) - k_M M$, an antagonistic combination of additive signal of L and S-cones ($L + S$) and M-cone signal (M) (Calkins 2003). The peak of spectral sensitive of the yellow signal of the B/Y-channel is "formed" at ~570-580 nm (unique yellow) due to cancellation L- and M-cone terms in the L/M-pathway. Another neutral point is formed similarly near 500 nm when B- and Y-signal terms cancel each other. Despite of individual and spatial variations in relative S/M/L-cone numbers, the neutral points have been shown to be remarkably invariant as a function of retinal eccentricity (Hibino 1992), color discrimination functioning similarly in fovea and in peripheral retina (Webster et al. 2010). The color perception of different hues appear to depend on statistical sampling of the mosaic (Brainard et al. 2008a; Garrigan et al. 2010) instead of linear combination of different channels as in RGB color systems (*Gonzalez and Woods 2002*).

In previous section (2.3.2), the cone signals were considered to be summed linearly to produce a "apparent brightness" sensation as formulated by the photopic luminous sensitivity $V(\lambda)$. This linear assumption termed univariance (Naka and Rushton 1966; Mitchell and Rushton 1971; Rushton and Powell 1972) holds for rod photoreception [defined by scotopic luminous sensitivity $V'(\lambda)$] which fulfills the requirement of any system of photometry, which is that the luminous efficiency of any mixture of lights is the sum of the efficiencies of the components of the mixture; otherwise known as Abney's Law (Abney and Festing 1886; Abney 1913). The original CIE photopic 1924 $V(\lambda)$ was seriously in error, underestimating the short-wavelength sensitivity and being limited only to certain tasks (see Stockman et al. 2008 for discussion). New improved photopic spectral sensitivities for normal observers [$V^*(\lambda)$, Sharpe et al. 2005; 2010] and for aged observers (Sagawa and Takahashi 2001; Sarkar et al. 2011)

have been proposed to reduce the errors in spectral sensitivity, while not being able to predict the non-additive chromatic interactions.

In specific responses [see 3.3.4 for pupillary light reflex (PLR)], the non-additive nature of cone-pathways can be shown, in practice broadening the spectral sensitivity with possible added notches and humps of spectral sensitivity (Stiles and Crawford 1933; Thornton and Pugh 1983; Kurtenbach et al. 1999). The so-called Sloan's notch (Sloan 1928; Kimura and Young 1995 in PLR) occurs when the "target" (stimulus) wavelength produces the same chromatic signal as the "background light" used for adapting the observer, so the stimulus is detected by less sensitive achromatic pathway. In contrast, the humps occur when the target stimulus produces a large chromatic signal with respect to the background. Common way to quantify the chromatic signal strength, is to to use cone contrast space (Smith and Pokorny 1996) as used for example with PLR (Tsujimura et al. 2006; Kimura and Young 2010), which simply relates the change in chromatic signal between target and the background cone excitation ($\triangle L_{target} / L_{adapt}$, L referring to L-cones).

Similar chromatic mechanisms are found in lower vertebrates (Jacobs 1993), with the most extreme example occurring in the parietal eye of lizards, in which two visual pigments are co-expressed in the same photoreceptor requiring no post-receptoral cells for the opponent mechanism (Solessio and Engbretson 1993). This organization of "internal opponency" has been functionally linked to mediating the organism's responses to dawn and dusk (Solessio and Engbretson 1993; Su et al. 2006). Finally, chromatic opponency has been linked to non-image forming (NIF) responses (see below Section 2.4) in anatomical studies (Dacey et al. 2005), in melatonin suppression studies (see 1.2.2, Figueiro et al. 2005; 2004; 2008; Revell et al. 2010), and in PLR studies (see 3.3.3, Kimura and Young 1996; 2010).

2.3.5 *Irradiance ranges*

The visual system is able to operate from starlight to bright sunlight; over a change in illumination by more than a factor of 10^{11}, despite the limited (approximately 10^2) dynamic range of the retinal ganglion cells (Fain et al. 2001). Figure 10 illustrates the range of illumination levels to which the human eye is exposed, from absolute rod threshold and the detection of a few photons to levels that bleach almost all of the photopigment. The range is divided into three regions (scotopic, mesopic, photopic) according to which types of photoreceptor are functioning. The boundaries between different irradiance ranges are loosely defined as there are contradictions in the literature of how high light levels rod still function (Makous 2004). Spectral sensitivity measurements in man have shown pronounced rod activity up to high luminances in the retinal periphery (Stabell and Stabell 1981),

significant rod input up to 1000 (Kurtenbach et al. 1999) trolands extrafoveally Yeh et al. 1995, rod input to both parvocellular and magnocellular cells up to 600 td at eccentricities larger than 18 degrees Weiss et al. 1998 with the rod input increasing with eccentricity. Lee et al. 1997 found that macaque parvocellular cells between 3 and 15 deg eccentricity show rod input up to 2 td, whereas magnocellular cells are rod dominated up to 20 td with some cells even show rod input up to 2000 td. The similar behavior of cone-rod weights as a function of retinal eccentricity was found with humans using psychophysical tools (Raphael and MacLeod 2011).

Furthermore, the duplicity theory proposed in early studies (Hecht et al. 1935) of independent function of rods and cones act independently has been shown to be incorrect in recent. Dark-adapted rods have shown to suppress the cone activity (Goldberg et al. 1983; Heikkinen et al. 2011), and the signals from rods and cones being shown to summate especially in mesopic vision conditions (Naarendorp et al. 1996). Alexander and Kelly 1984 have reported that excitation of cones moves rod saturation to lower values, this being hypothesized to be due to the leakage of cone signals into the rods through the gap junctions (Schneeweis and Schnapf 1995). This increased rod saturation was shown to be even stronger when flashing the background instead of a steady background adapting field (Adelson 1982).

2.3.6 *Ciliary kinetics*

In addition to spectral tuning differences of rods and cones, their response speed (i.e. kinetics of the response) differ significantly. In cones, a rapid response is crucial in detecting fast events in daylight, whereas rods need to provide visual information in dim light conditions with longer integration times. In cones, the light response signalled via transducin molecule (Govardovskii and Firsov 2011) is rapidly terminated resulting an improved temporal resolution. The shut-off of activated photopigment/transducin in mammalian cones is 400-fold faster than that in mammalian rods (approx. 40 ms; cf. 14,000 ms), and this rapid shut-off has been suggested to account for the ability of mammalian cones to avoid saturation, no matter how intense the steady light becomes (Lamb and Pugh 2006; Lobanova et al. 2010; Reuter 2011).

Furthermore, a rod recovers from intense bleaching light exposures far more slowly than does a cone . Indeed, upon extinction of steady illumination bleaching 90 per cent of the visual pigment, the time for complete recovery of circulating current in mammalian photoreceptors is around 20 min in a rod (Thomas and Lamb 1999) , but only 20 ms in a cone (Kenkre et al. 2005). This difference, a factor of 60 000-fold, is the greatest known difference in properties between mammalian rod and cone photoreceptors (Lamb 2009). Additionally,

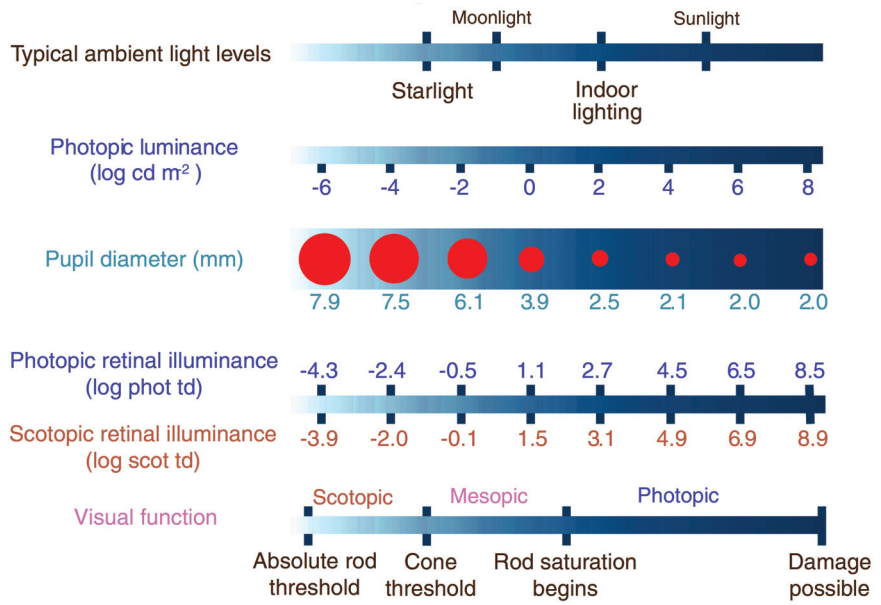

Figure 10: **Illumination levels.** Typical ambient light levels are compared with photopic luminance (log cd m)2), pupil diameter (mm), photopic and scotopic retinal illuminance (log photopic and scotopic trolands respectively) and visual function. The scotopic, mesopic and photopic regions are defined according to whether rods alone, rods and cones, or cones alone operate. The conversion from photopic to scotopic values assumed a white standard CIE D65 illumination. (Stockman and Sharpe 2006)

the half-recovery of the cone current occurs at least 5000-fold (100 s/20 ms) faster than half-regeneration of cone pigment (Mahroo and Lamb 2004), indicating the immunity of cone's circulating current level to presence of bleached pigment (opsin) and to intermediate photoproducts (Schnapf et al. 1990; Wang and Kefalov 2011; see 4.5.1 for significance of intermediate photoproducts).

Although pigment regeneration has generally been assumed to proceed as a first order process (Mahroo and Lamb 2004), the finding of a shorter time constant after smaller bleaches is not consistent with this assumption, and Paupoo et al. 2000 suggested that recovery may instead be 'rate-limited', so that after a large bleach regeneration proceeds approximately linearly with time. Mahroo and Lamb 2004 defined the recovery for both rod and cone photoreceptors using the following rate-limited expression:

$$P(t) = 1 - K_m W\left\{\frac{B}{K_m} exp\left(\frac{B}{K_m}\right) exp\left(\frac{1+K_m}{K_m} vt\right)\right\} \qquad (9)$$

where the K_m is the Michaelis constant, $W(t)$ denotes the Lambert W function (e.g. Corless et al. 1996, Matlab code given in Mahroo and Lamb 2004) as the function that satisfies $W(t)e^{W(t)}W(t) = t$, and where B is the initial value of P, B is the initial bleaching level, t is the time, v denotes the initial rate of recovery following a total

bleach. The parameter values are different naturally for cone and rod phototransduction, see Mahroo and Lamb 2004 and Lamb and Pugh 2004 for parameter estimates, detailed discussion and mathematical expression for bleaching kinetics.

2.4 NON-VISUAL PHOTOTRANSDUCTION

While the role of the mammalian eye in detecting light for vision has long been known, it has only recently emerged that the eye performs a dual role in detecting light also for a range of behavioral and physiological responses that are distinct from sight (reviewed for example by Lockley and Gooley 2006; Van Gelder 2008; Hatori and Panda 2010; Benarroch 2011; Pickard and Sollars; Provencio and Warthen 2012). Light-dependent phenomena were shown to be preserved in blind mice lacking rods and cones, including synchronization of the circadian clock to light–dark cycles and suppression of production of melatonin from the pineal gland by light observed at night (Lucas and Foster 1999, Lucas et al. 1999). In humans, light remained effective in suppressing pineal melatonin secretion and entraining the circadian clock in some people who were blind from severe loss of rods and cones, without impinging on conscious perception (Czeisler et al. 1995), or with "conscious perception" similar to *'blindsight'* reported by Zaidi et al. 2007.

Screening the photosensitive dermal melanophores of *Xenopus laevis*, Provencio et al. 1998 discovered an opsin that they named melanopsin (referred also as opn4). Soon after its discovery, melanopsin was localized to a small subset (1–2%) of retinal ganglion cells (RGCs) in the rodent eye (Gooley et al. 2001; Hattar et al. 2002; Provencio et al. 2000; 2002). The novel photosensitive cells were referred as intrinsically photoreceptive retinal ganglion cells (ipRGCs) (Berson et al. 2002) which is still used along with melanopsin-containing RGCs (mRGCs) and photosensitive RGCs (pRGC) meaning the same thing. To avoid confusion with possibly other photosensitive RGCs (opn5, Nieto et al. 2011), the cells are from now on referred as mRGCs in this work. In the macaque-monkey retina (Dacey et al. 2005), there are 3,000 mRGCs, constituting even smaller subset 0.2% of the total RGC population (~1.5 million in humans) compared to rodents, with an estimate of 0.2% to 0.8% of all ganglion cells in the human retina (Hannibal and Fahrenkrug 2004; Dacey et al. 2005). The spectral sensitivity of the newly light sensitive cells (e.g.Koyanagi et al. 2005; Qiu et al. 2005; Panda et al. 2005, and an excellent review on mRGCs by Do and Yau 2010), was to found to be around 480 nm, closely matches that of the different melanopsin dependent responses studied as reviewed more closely in 2.4.2.

2.4.1 *Retinal circuitry*

Opposed of being one homogeneous group of mRGC as thought initially (Berson et al. 2002; Hattar et al. 2002), recent research indicates that mRGCs consist of several subtypes that are morphologically and physiologically distinct as reviewed by Schmidt et al. 2011.

Current knowledge (Schmidt et al. 2011) suggests the existence of six distinct mRGC subtypes referred as $M1_{Brn3b+}$, $M1_{Brn3b-}$ M2, M3, M4 and M5 with the suffix M referring to melanopsin . The subtypes can be for example classified either by their morphology and projections (illustrated in Figure 11); or by their physiology. The most well-characterized subtypes are the M1 mRGCs and the M2 mRGCs. M1 mRGCs were the types originally characterized (Berson et al. 2002), stratifying the outermost sublamina of the IPL and recently further sub-categorized to $M1_{Brn3b+}$and $M1_{Brn3b-}$ (based on *Brn3b* marker expression) with differential brain projections (Chen et al. 2011). The M2 mRGCs which stratify in the innermost sublamina of the IPL (Baver et al. 2008, Berson et al. 2010, Schmidt and Kofuji 2009, Schmidt et al. 2008). The bistratified M3 mRGCs, with dendrites in both inner and outer sublaminae, have been only recently characterized (Schmidt and Kofuji 2011b). M4 cells have the largest soma of any described mRGC subtype, as well as larger and even more complex dendritic arbors than M2 cells (Ecker et al. 2010). By contrast, M5 mRGCs have small, highly branched arbors arrayed uniformly around the soma (Ecker et al. 2010). In overall, the characteristics of these M4 and M5 are poorly understood compared to other subtypes (Ecker et al. 2010; Schmidt et al. 2011). The photoresponse characteristics of different subtypes are further reviewed in 2.4.3.

Based on the stratification patterns of the mRGC subtypes (M1, OFF; M2, M4 and M5, ON; M3, ON/OFF), the prediction is that M1 cells would receive synaptic inputs from the OFF pathway, M2, M4, and M5 cells would receive input from the ON pathway, and M3 cells would receive input from both the ON and OFF pathways. Contrary to this expectation, both ON (i.e. M2), OFF (i.e. M1), and ON-OFF-stratifying (i.e. M3) mRGC subtypes receive predominantly ON-input (Pickard et al. 2009, Schmidt and Kofuji 2010), although, a very weak OFF input to M1 cells has been reported, but only under pharmacological blockade of amacrine cell inputs (Wong et al. 2007). Anatomical studies have revealed the source of this unusual synaptic input: ON bipolar cells make *en passant* synapses with M1 mRGC dendrites that stratify within the OFF sublamina of the IPL (Dumitrescu et al. 2009, Grünert et al. 2010, Hoshi et al. 2009). M1 mRGC dendrites also colocalize with dopaminergic amacrine cells (Dumitrescu et al. 2009,Vugler et al. 2007). Dopaminergic amacrine cells were recently implicated in guiding M1 cell dendrites to the OFF layer of the IPL (Matsuoka et al. 2011). Previous observations have also suggested that mRGCs signal back to dopaminergic amacrine cells in the opposite direction of classical retinal circuits. The function of this unusual reverse signaling between M1 mRGCs and dopaminergic amacrine cells is unknown. The unexpected findings concerning M1 connectivity indicate that mRGC circuitry in the retina is far more complex than previously appreciated (Schmidt et al. 2011).

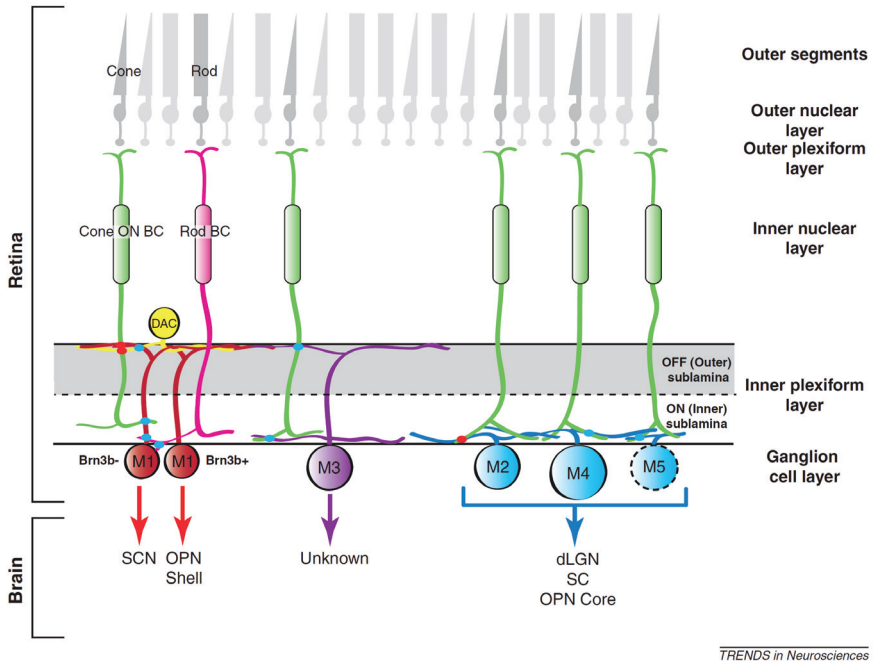

Figure 11: **Schematic diagram** illustrating the connectivity and location of the five distinct morphological subtypes (M1-M5) of mRGCs and projections to their predominant targets in the brain. For simplicity, M1 mRGCs displaced to the INL Hattar et al. 2002] are not depicted in this diagram. M1 mRGCs stratify in the OFF sublamina (red); M2, M4, M5, stratify in the ON sublamina (blue); and M3, stratify in the ON and OFF sublamina (purple) of the IPL of the retina. M4 mRGCs have the largest cell body size, and M1 cells have smaller body size than M2-M4 cells [Schmidt and Kofuji 2009,Ecker et al. 2010,Schmidt and Kofuji 2011b]. The cell body size of M5 is not known (dotted line). The proportion of ON and OFF stratification in M3 mRGCs varies considerably between cells Schmidt and Kofuji 2011b. Recent findings suggest that the M1 subtype consists of two distinct subpopulations that are molecularly defined by the expression of the Brn3b transcription factor Chen et al. 2011. Red dots indicate synaptic connections for which both functional and anatomical evidence exists (Viney et al. 2007; Belenky et al. 2003; Schmidt and Kofuji 2010; Dumitrescu et al. 2009; Hoshi et al. 2009). Blue dots indicate synaptic connections for which either functional or anatomical evidence exists [Ecker et al. 2010; Schmidt and Kofuji 2011b; Zhang et al. 2008; Ostergaard et al. 2007]. mRGC subtypes project to distinct non-image and image-forming nuclei in the brain [Hattar et al. 2006; Ecker et al. 2010]. M1 cells predominantly project to non-image forming centers such as the suprachiasmatic nucleus (SCN) to control circadian photoentrainment and the shell of the olivary pretectal nucleus (OPN) to control the pupillary light reflex. M3 brain targets are completely unknown at this time. M2, M4 and M5 are included together because no specific genetic marker exists for a single subtype. Collectively, they project to image forming areas in the brain such as the lateral geniculate nucleus (LGN) and the superior colliculus (SC), but also to the core of the OPN of which no specific function is assigned to this brain region [Ecker et al. 2010; Brown et al. 2010]. Retrograde analysis confirms that M2 cells project minimally to the SCN and strongly to the OPN Baver et al. 2008. Figure from Schmidt et al. 2011

The mRGCs send their axons to well over a dozen regions in the brain (see for example reviews by Saper et al. 2005a; Lockley and Gooley 2006; Vandewalle et al. 2009 and Do and Yau 2010). Most notable among these are the SCN (the master circadian clock (Moore and Eichler 1972, Colwell 2011)), the intergeniculate leaflet [IGL, a center for circadian entrainment in rodents (Muscat and Morin 2006); corresponding structure in humans (Vandewalle et al. 2009) is ventral lateral geniculate nucleus (vLGN)], the olivary pretectal nucleus (OPN, a control center for the pupillary light reflex (Clarke et al. 2003a)], the ventral subparaventricular zone [vSPZ, implicated in "negative masking" , or acute arrest of locomotor activity by light in nocturnal animals (Mrosovsky 1999, Thompson et al. 2008)), and the ventrolateral preoptic nucleus [VLPO, a control center for sleep (Saper et al. 2005a)]. Other projections that are more enigmatic in function include those to the lateral habenula and amygdala (Hattar et al. 2006). Interestingly, the axon of a single melanopsin cell in hamster can branch and innervate at least two different brain regions, suggesting some common information being transmitted for different behaviors (Morin et al. 2003).

2.4.2 *Spectral sensitivity*

Studies of the spectral sensitivity of the novel photopigment point to a retinal peak spectral sensitivity (λ_{max}) at the blue region of visible light around ~480 nm (see Table 1). The two exceptions by Newman et al. 2003 and Melyan et al. 2005 with shorter wavelength peaks. There is consierable amount of literature on the quest for spectral sensitivity of melanopsin, and interested reader is recommended for example the reviews by Brainard and Hanifin 2005, and Do and Yau 2010. There have been efforts for creating a standardized "circadian / NIF" sensitivity function for non-image forming visual responses (e.g. Gall and Bieske 2004; Weber et al. 2004; Rea et al. 2005; TC6-62; Rea 2011b; Kozakov and Schoepp 2011). In 2011, in Germany an efficiency function $C(\lambda)$, first introduced by Gall 2004, Gall and Bieske 2004, was standardized by DIN as the unit to measure "circadian" efficiency of light source (Lang 2011) based on the melatonin suppression action spectra by Thapan et al. 2001 and Brainard et al. 2001. Recently, Enezi et al. 2011 introduced a "melanopic action spectrum" based on the λ_{max}~ 480 nm peak sensitivity and a nomogram by Govardovskii et al. 2000. The obtained spectral sensitivities from recent studies are summarized in Table 1.

Table 1: Summary of obtained spectral sensitivities for NIF-responses. Modified from Brainard and Hanifin 2005 and Mure 2009.

Species	**Measure**	λ_{max}	**References**
Mouse *rd cl*	PLR	479	Lucas et al. 2001
Mouse *rd cl*	Phase shift	481	Hattar et al. 2003
Rat WT	mRGC light response	484	Berson et al. 2002
Macaque	mRGC light response	482	Dacey et al. 2005
Macaque	PLR	482	Gamlin et al. 2007
Human	Melatonin suppression	460, ~477*	Brainard et al. 2001
Human	Melatonin suppression	460, ~480*	Thapan et al. 2001
Human	Cone ERG regulation	483	Hankins and Lucas 2002
Human	Heterologous expression	420-440	Melyan et al. 2005
Mouse	Heterologous expression	420	Newman et al. 2003
Mouse	Heterologous expression	479	Qiu et al. 2005
Mouse	Heterologous expression	480	Panda et al. 2005
Human *rd cl*	PLR	480	Zaidi et al. 2007
Amphioxus	Heterologous expression	?	Koyanagi et al. 2005
Chicken	Heterologous expression	476 and 484	Torii et al. 2007
Human	PLR	~490	Bouma 1962

* *data points refitted in logarithmic domain with Govardovskii (2000) nomogram*

2.4.3 *Irradiance response characteristics*

In vision research irradiance-response curves (IRC) are used to define the relationship between the intensity of the light stimulus and the elicited response, being conceptually similar to the Weber's law in psychophysics (Krueger 1989) and dose-response curves in pharmacological studies (Meddings et al. 1989; Gottschalk and Dunn 2005). Irradiance-response curves have typically a sigmoidal shape [e.g. Naka-Rushton for visual responses (Naka and Rushton 1966), Michaelis equation for enzyme kinetics (Cornish-Bowden 1995), Hill equation for thermodynamics (Hill 1938)] with typically three (e.g. Gamlin et al. 2007) or four parameters (e.g. Brainard et al. 2001) used to describe the irradiance-dependence of the response. Often the half-saturation response (denoted typically with IR_{50}or with X_{50}) is selected as the experiment irradiance reducing response saturation or compression, and allowing proper study of possible response modifying aspects of preceding stimulus (as done e.g. in Zhu et al. 2007 and in Mure et al. 2009). Half-saturation defines the point where the elicited response is half of the maximum possible. In other words if the maximum pupillary diameter constriction is 6 mm (pupil area = $(8^2 - 2^2)\pi = 60\pi$ mm^2) from the dark-adapted 8 mm-diameter pupil to the light-adapted 2 mm-diameter pupil, then the half-saturation constriction would occur at an irradiance that is constricting the pupil 30π mm^2, resulting in a ~5.83 mm-diameter pupil (pupil area 34π mm^2).

Flashes of light are a standard method for studying rods and cones because the resulting "impulse responses" (Baylor et al. 1974b) allow more straightforward quantitative analysis. In principle, the flash response can predict the responses to more complex light stimuli if the superposition of quantal responses is linear (Do et al. 2009; Luo et al. 2008). In other words, the Bloch law [Bloch 1885, known also as Bunsen-Roscoe law (Brindley 1952)] holds when light intensity and duration can be proportionally interchanged without affecting the response amplitude or kinetics (Luo et al. 2008). Half-saturation of the mRGC flash (subtype M1) response requires 10^7 photons/μm^2 (10^{15} photons/cm^2) at the optimal wavelength (λ_{max}), 10^6-fold higher than for rods and 10^4-fold higher than for cones at their corresponding λ_{max} values (Figure 12B, Do and Yau 2010). Thus mRGCs are significantly less sensitive than rods and cones (also see Dacey et al. 2005; Wong et al. 2007), explaining why melanopsin-knockout mice show behavioral deficits primarily in bright light (e.g. Hattar et al. 2003; Lucas et al. 2003).

Other way of quantifying elementary responses of the photoreceptor, is to employ single-photon response technique allowing the study of a response elicited by a single absorbed photon as the name implies (Rieke and Baylor 1998). In contrast to the weak flash response

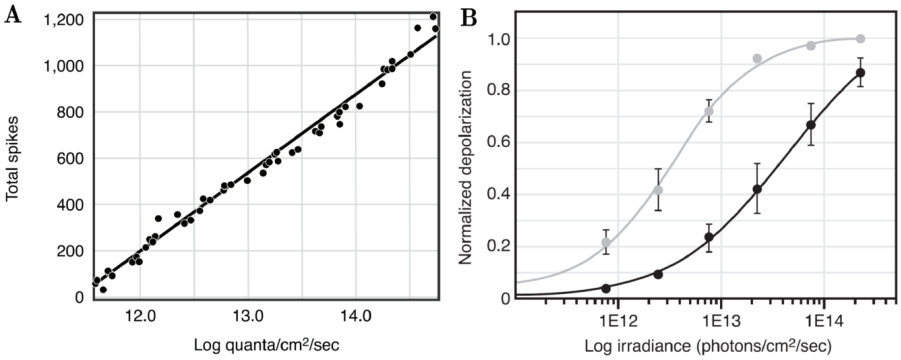

Figure 12: **Characteristics of mRGC responses 1/2 (A)** total number of spikes elicited by a 10-s light stimulus rising monotonically with light intensity for a macaque mRGC recorded with synaptic transmission blocked (Dacey et al. 2005). **(B)** light-evoked depolarization (recorded in current clamp) in the two mRGC subtypes as a function of light intensity. M1 cells (gray curve) are roughly 10-fold more sensitive than M2 cells (black curve) at 32–34°C. [A and B modified from Schmidt and Kofuji 2009). Figures adapted from Do and Yau 2010.

of mRGCs, the single-photon response of mouse M1 mRGCs has been shown to be large, electrical current of >1 pA at roughly body temperature, being larger than that of rods and 100 times that of cones (Do et al. 2009). Its waveform in mRGCs follows the convolution of two single-exponential decays (described by two time constants; Figure 13B), unlike the rod response, which require four (Baylor et al. 1979) and the cone response that require five (Kraft 1988) time constants. Two time constants suggest that there are two particularly slow steps in mRGC phototransduction . In comparison, invertebrate single-photon responses (called quantum bumps, reviewed later in **4.1.2**) also have a more complex waveform (Hardie and Postma 2008).

A flash of light is an instantaneous pulse of photons, while a step of light is a continuous shower of photons, the latter being the most frequent form to study the melanopsin characteristics especially on a behavioral level. The waveform of the response and the irradiance-response characteristics change from studies using flash response compared to the single-photon response The waveform of the step response is more complex (Do et al. 2009; Wong et al. 2005), for example due to adaptation of the mRGCs (see 2.4.8). When stimulated by a long, bright step of light, the mRGC voltage response rises to a transient peak and then relaxes to a lower level (Dacey et al. 2005; Warren et al. 2003; Wong et al. 2005; see the response returning to dark baseline levels towards the end of the light pulse inFigure 13A).

Immunohistochemical studies (Hattar et al. 2006; Baver et al. 2008) have indicated that M1 mRGC cells may express more melanopsin pigment than other subtypes, based on the higher levels of anti-melanopsin antibody staining. Consistent with this hypothesis, Schmidt

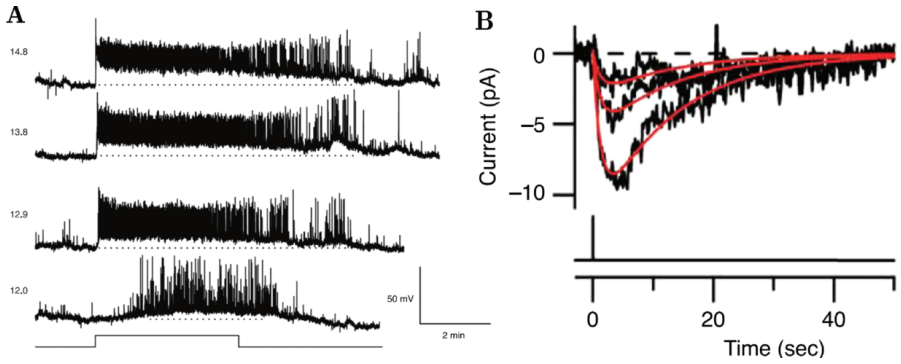

Figure 13: **Characteristics of mRGC responses 2/2 (A)** Step response and adaptation of mRGCs. A: an mRGC recorded in the flat-mount rat retina under current clamp, showing sustained firing during long steps of light. Numbers to the left of each trace represent the log irradiance (500 nm photons·cm^{-2}·s^{-1}). [Modified from Berson et al. 2002] **(B)** Three smallest responses from *Fig 7A* of Do and Yau 2010, elicited by successive approximate doublings of flash intensity, on expanded ordinate and longer time base, to demonstrate linearity. Responses fit with the same convolution of two single-exponential decays but scaled by the relative flash intensities (red). Figures adapted from Do and Yau 2010.

and Kofuji 2009 showed for M1 mRGCs a tenfold higher sensitivity to 480 nm light than for M2 mRGC cells assessed in irradiance-response experiments. Light responses in M2 cells, on the other hand were seem to be driven primarily by the ON pathway via synaptic transmission at photopic light intensities. The responses of M2 cells were noticed to be largely preserved in the melanopsin-null mice (Schmidt and Kofuji 2009) indicating a modulation of the mRGC response from the classical photoreceptors (Section 2.3), allowing mRGCs to detect and respond to light stimuli of lower irradiance than the intrinsically driven mRGC sensitivity alone (Wong et al. 2007; see below 2.4.5).

2.4.4 *Kinetics / Temporal characteristics*

In addition to evaluating the response magnitude, photoreception can be characterized by the temporal characteristics of the response. The mRGC response can be slow, taking several seconds to reach peak under dim light intensities (Berson et al. 2002), higher light intensity reducing the response latency (Do et al. 2009; Graham et al. 2008). The mRGC response is also sluggish to cease responding at light offset, the mRGC firing rate not instantaneously returning to the baseline level (Figure 13A), showing a progressive decrease duration being dependent on the stimulus irradiance (Drouyer et al. 2007). The higher the irradiance the longer the time for return in mRGCs to the baseline level, similar to the prolonged depolarizing after-potential (PDA) seen in invertebrate photoreceptors (Berson 2007; see 4.4.4). Studies on melanopsin-only (*rd cl*) mice suggests that even at the highest ir-

radiances, the melanopsin-mediated response in PLR is delayed by ~300 ms compared to that of the classical photoreceptors (Lucas et al. 2001). With *in vitro* cells, the response latency shortens from ~3 second of the single-photon response to 200 ms for the saturated response, reflecting light adaptation according to the authors (Do et al. 2009) due to the speeding of the response deactivation (Wong et al. 2005). The response was found to be also approximately threefold larger in amplitude and about threefold faster in kinetics near 37°C compared with room temperature (23°C) (Do et al. 2009) consistent with known temperature-dependency of phototransduction.

Compared to cones and rods, the single-photon response of the mRGCs is very slow despite the large photocurrent. A useful metric for the comparison is of the time courses of responses with different waveforms is the "integration time" as employed by Do et al. 2009, being defined as the area under the response divided by the response peak (Luo et al. 2008). The mouse mRGC single-photon response has an integration time of 8 s at 37°C (Do et al. 2009). This is 20 times that of rods and over 100 times that of cones. It is also much slower than the typical light response of invertebrate photoreceptors (Hardie and Postma 2008). A long integration time allows summation of photons arriving many seconds apart while making the cell insensitive to rapid fluctuations in light intensity. In contrast, it is beneficial for rods and especially for cones to be deactivated rapidly (Burns and Baylor 2001), in other words to have a shorter integration time, allowing the visual system to remain responsive for fast events.

2.4.5 *Photoreceptor contributions*

It is tempting to predict that the only partly overlapping irradiance-response curves (Figure 13C) and spectral sensitivities (Figure 5), would expand both the dynamic range and the spectral window of the NIF system as a whole, if the different photoreceptor systems were coupled. Indeed, it has been shown that mRGCs receive rod and cone inputs (e.g.Dacey et al. 2005; Wong et al. 2007; Jusuf et al. 2007; Güler et al. 2008; Schmidt and Kofuji 2010). Güler et al. 2008 showed in melanopsin-ablated mice (functional mRGCs without the photopigment melanopsin), that although the melanopsin pigment is not required for PLR induction at low light intensity, the rod–cone drive for PLR still requires the mRGCs to relay the response to olivary pretectal nucleus (OPN). This connection would allow light detection at lower intensities via synaptic input from more sensitive rod-cone system extending the dynamic range of the whole NIF-system. Schmidt and Kofuji 2010 showed differential outer retinal modulation for M1 and M2 subtypes (see 2.4.1) with robust synaptic inputs to M2 cells at low light intensities at least a log unit lower than the threshold for individual M2 mRGC cells.

Studies with different NIF-responses have suggested distinct modulatory roles for rods and cones. Studies with melatonin suppression have suggested a significant cone moduation to the melatonin suppression, without significant rod modulation (Gooley et al. 2010). Studies with PLR however have suggested a role for rods even at relatively high intensities in addition to the mRGCs drive [McDougal and Gamlin 2010; Lall et al. 2010; but see Tsujimura et al. 2010 for M/L cone contribution, and Allen 2011 for S cone contribution in mice]. Rods have been also found to be sufficient in mediating circadian entrainment in dim light conditions in rodents (Altimus et al. 2010; Lall et al. 2010; Butler and Silver 2010). Lall et al. 2010 found no cone modulation for entrainment with the same irradiance used previously by (Dkhissi-Benyahya et al. 2007), while the study by Freedman et al. 1999 in cone degenerated mice supported the findings of Lall et al. 2010. Results revealed however, that cone-dependent phase shifts can be induced using intermittent light exposure, consistent with the mainly phasic and "edge detecting" responses of cones (2.3.6). Recently it has been suggested that cones can inhibit melanopsin contribution in the absence of rods (Rupp et al. 2011) at low light levels questioning the validity of results obtained from rodless animal models. These studies demonstrating differential classical photoreceptor modulation for different NIF responses, combined with the existence of distinct mRGC subtypes (Schmidt et al. 2011), highlight the likely specificity of certain NIF-response pathways. In other words, it may be difficult to generalize the results from PLR studies for example winter depression light treatment or circadian entrainment.

Furthermore it has been shown that photoreceptor contribution is not simply dependent on irradiance and spectral sensitivity, but also on the duration of the light stimulus. Gooley et al. 2010 suggested that the light-induced melatonin suppression is initially driven by cones and then taken over by the melanopsin-system with increasing light exposure duration. It has proposed that using pulsed light, the "average cone-drive" can be significantly increased as the cones adapt very quickly and seem to provide only phasic input to mRGCs (Morin and Studholme 2009; Lall et al. 2010; Zeitzer et al. 2011). Although cones are known to show rapid light-adaptation under extended illumination, they do not saturate completely but attain a steady-state polarization with an intensity-dependent magnitude (Burkhardt 1994; Normann and Perlman 1979; Valeton and van Norren 1983;). Lall et al. 2010 suggested that prior light exposure over timescales ranging from tens of seconds to tens of minutes reduces the ability of cones to regulate pupil size (see later discussion about adaptation: 2.4.8 and 2.4.9).

This is further supported by lack of integrating capacity of the assumed melanopsin-driven steady-state of PLR in the study by McDougal and Gamlin 2010, in contrast to results from the previous

studies (Berson et al. 2002; Dacey et al. 2005; Gamlin et al. 2007; Wong et al. 2007). Authors (McDougal and Gamlin 2010) suggested that the melanopsin photoresponse may act as a leaky integrator (see Bressloff et al. 1996 for PLR, and Pillow et al. 2005 for primate RGC firing) during steady-state light exposure. Alternatively, the integrative function of the melanopsin photoresponse may be intensity dependent as the stimuli irradiances were lower (McDougal and Gamlin 2010) than those that produced a significant integration in previous studies of both the PLR (Gamlin et al. 2007), and in vitro cellular recordings (Berson et al. 2002; Dacey et al. 2003; Wong et al. 2007). An intriguing suggestion of study by McDougal and Gamlin 2010 was that the three distinct photoresponses (rods, cones, melanopsin-mRGCs) driving the PLR in humans do not appear to linearly combine at the level of mRGCs, but rather the outer and inner retinal signals act in a ''winner take all" fashion, with only one photoreceptor class in the end driving the NIF response. This finding is supported by the found outer retinal shunting of melanopsin photoresponse in mice PLR (Sekaran et al. 2007). Although the shunting does not seem to be complete, and the sustained response seem to be also augmented by outer receptor inputs in response to long wavelength lights.

2.4.6 *Spatial sensitivity*

As with traditional visual system (2.3.1) there is evidence for differential visual field responses also in NIF photoreception as shown for melatonin suppression in Table 2. The preference for upper temporal visual field (nasal and lower retina) corresponds roughly to bright sky in real-life evolutionary settings the nasal visual field being attenuated by shadowing nose. Additionally, this suggested preference seems to be in contrast with the spatially uniform distribution ("photoreceptive net", Provencio et al. 2002) of mRGCs in retina. This could be interpreted differences either in post-receptoral processing after mRGCs, non-homogenous distribution of mRGC suptypes (see for 2.4.1 for M3 subtype for example), and/or significant contribution from rod and cone photoreceptors. Similar differential responses on different visual field can be seen with pupillary light reflex (PLR, 3.2.1)

2.4.7 *Retinal clocks*

In invertebrate *Limulus* the circadian rhythms control the photoreceptor gain (Kass and Renninger 1988), temporal-frequency response (Batra and Barlow 1990), photoreceptor noise (Kaplan and Barlow 1980), quantum bumps (Kaplan et al. 1990), screening pigment movement (Kier and Chamberlain 1990), and opsin co-expression (Katti et al. 2010); in combination resulting a varying circadian retinal sen-

Table 2: Comparison of studies for spatial sensitivities in NIF-responses focusing on visual field diffrences in melatonin suppression. See 3.2.1 for spatial sensitivity in pupillary light reflex (PLR).

Reference	Measure	Results
Adler et al. 1992	Melatonin suppression	No difference in melatonin suppression between central and peripheral visual field
Gaddy et al. 1992	Melatonin suppression	More light required for lower retinal illumination compared to full retinal exposure
Brainard et al. 1997	Melatonin suppression	Binocular light exposure was more effective than monocular light
Visser et al. 1999	Melatonin suppression	Difference between nasal and lateral areas, but not between the upper and lower areas.
Lasko et al. 1999	Melatonin suppression	Lower half of the human retina (upper visual field) more sensitive)
Smith et al. 2002	Melatonin suppression	No difference between lower and upper visual field in the elderly
Glickman et al. 2003	Melatonin suppression	Lower retina (upper visual field) being more sensitive for melatonin suppression.
Rüger et al. 2005	Melatonin suppression	Nasal retina more sensitive than temporal for melatonin suppression
	CBT	No difference between nasal and temporal retina
	Subjective sleepiness (KSS)	No difference between nasal and temporal retina

sitivity over 5 log units during day (Barlow et al. 1985; Chamberlain and Barlow 1987; Battelle 2002) with additional adaptive mechanisms (Pieprzyk et al. 2003). There is extensive evidence also clock-driven rhythms in the mammalian retina (for a review see e.g. Barlow and Helga Kolb 2001) with the neurotransmitter dopamine being central in this circadian regulation (Pozdeyev et al. 2008, Doyle et al. 2009). It has been suggested that the circadian control of rod-cone electrical coupling functions as a synaptic switch allowing cones to receive very dim light signals from rods at night, but not during the day (Ribelayga et al. 2008).

In a study by Hannibal et al. 2005, it was noticed that both melanopsin mRNA and protein showed a diurnal variation during a 24-h LD cycle (12/12) with the highest level of melanopsin mRNA observed at early night, whereas the protein peaked at late subjective day (~20 h lag between the mRNA and protein peak level). These findings according to the author, together with the reported rhythmic melanopsin expression in pigmented animals (Sakamoto et al. 2004), favor the possibility that the short-term diurnal changes in melanopsin expression are primarily controlled by the retinal clock system.

2.4.8 *Short-term adaptation*

The ambient light level varies over 9-10 orders of magnitude in the course of a day, while the post-receptoral spiking neurons have a dynamic range of only 2 log units, the visual system must adjust its sensitivity to the ambient light intensities. Rods and cones can gradually reduce their sensitivity for constant illumination allowing the photoreceptor to respond to further increments in light intensity. This process, termed light adaptation (Thomas and Lamb 1999, Dunn et al. 2007), extends the dynamic range of these receptors by normalizing their sensitivity to the given background light level. The process is complete before spiking neurons get involved. As a result, the ganglion cell signals are more or less independent of the illuminating intensity, but encode the reflectances of objects within the scene (Gollisch and Meister 2010).

The opposite process , when in darkness after prolonged exposure to bright light, the photoreceptors gradually recover from light adaptation by regaining sensitivity in a process called dark adaptation (Dowling 1987; Lamb and Pugh 2004). Both in the case of light and dark adaptation, the cones adapt more rapidly than rods, due to their ability either to regenerate the pigment more rapidly for dark adaptation (Hecht 1937; Lamb and Pugh 2004), or to use more elaborative light adaptive schemes (see Pugh et al. 1999; Fain et al. 2001) avoiding electrical saturation at any steady light intensity (Barlow 1972; Lobanova et al. 2010). In addition to simple light intensity adaptation, both vertebrate rods and cones and invertebrate photoreceptors accelerate the responses to dim flashes, enhancing temporal resolution. The time to response peak is shortened in light-adapted photoreceptors and post-stimulus recovery is more rapid and the inverse for dark adaptation (Fuortes and Hodgkin 1964; Baylor and Hodgkin 1974; Fain et al. 2001).

It is unknown whether similar adaptational processes occur in the mRGCs. The operational requirement for non-image forming system differ from those imposed on classical visual system. The classical visual system must be able to respond rapid changes in scene information, in other words detect significant edges and contours for visual perception (Marr and Hildreth 1980; Simoncelli and Olshausen 2001). In contrast, the non-image-forming system requires a stable representation of absolute light intensity. The first evidence to support the existence of both light and dark adaptation in mRGCs came from the study by Wong et al. 2005 done with intact *in vitro* rat retinas under blockade of glutamatergic synaptic transmission (Dolan and Schiller 1994). The kinetics of rat mRGC light adaptation (with a time constant of ~1 min and completion within ~5 min) was found to be somewhat slower than that for rods and cones of various vertebrate species, reported of fully light adapting within anywhere from 1 s to

3 min (Normann and Perlman 1979; Cervetto et al. 1985; Silva et al. 2001; Calvert and Makino 2002). The time constant for dark adaptation was ~3 hr. This is slower than for example the complete dark adaptation of albino rat cone occurring within about 30 min, and the time constant of ~40 min and the steady state full adaptation occurrin in about 3 hour for rods of the same animals dark adapted (Perlman 1978; Behn et al. 2003). The same authors extended these findings providing preliminary evidence for light adaptation in mRGCs during a prolonged light exposure of 1 hour (Wong et al. 2011).

Behavioral correlates of the mRGC adaptation (Wong et al. 2005) can be found for example from PLR studies, where the PLR gradually regains sensitivity as the duration of dark adaptation after prior exposure to adapting light increases (Ohba and Alpern 1972; Trejo and Cicerone 1982). Increased firing rates evoked by light in SCN cells often decay during steady illumination in a manner suggestive of light adaptation (Aggelopoulos and Meissl 2000). Light adaptation in conventional photoreceptors has been shown to make their intensity-response curves (IRC) shallower, compared to absent light adaptation, thus broadening dynamic ranges of their responses (Baylor and Hodgkin 1974; Matthews et al. 1988). It is plausible that light adaptation in mRGCs likewise serves to enable them to discriminate a wider range of light intensities, e.g., from dawn light to noon light or in longer term (see 2.4.9), between summer and winter. Furthermore, there has been some evidence suggesting a role for mRGCs in intraretinal processing (Van Gelder 2001; Hankins and Lucas 2002), and the adaptational properties of mRGCs might therefore modulate the adaptational states of other retinal cells.

2.4.9 *Long-term adaptation*

The human behavioral sensitivity of the non-image forming (NIF) visual system seem to be modulated by not only the ambient light but also by the light history preceding the ambient lights even up to periods of several days (Hébert and Stacia 2002; Smith et al. 2004; Jasser et al. 2006; Rufiange et al. 2007; Beaulieu et al. 2009; Danilenko et al. 2009; Danilenko et al. 2011; and Chang et al. 2011), or by the season (Mathes et al. 2007; Higuchi et al. 2007). It is however unclear at the moment where the observed phenomena originate from.

Study by Hannibal et al. 2002 in albino Wistar rats showed an amount of melanopsin protein varying over 24 h cycle, suggesting either an oscillator or adaptive mechanism driving the amount of melanopsin pigment. Follow-up study by the same group (Hannibal et al. 2005) further supported the findings that the expression of melanopsin protein in the retina of the albino Wistar rat is strongly regulated by light and darkness (10-fold suppression in constant light condition (LL) and a 7.5-fold increase in constant darkness (DD) after

5 d of LL). The up-regulation in DD seemed to be faster and more pronounced than the down-regulation in LL. It was suggested by the authors (Hannibal et al. 2005) that the observed phenomenon reflect a functional adaptation. Adaptation was shown to be morphological in addition to mere regulation of the protein, melanopsin immunoreactive dendrites form an extensive network during DD, whereas during LL, melanopsin immunoreactivity was limited to the soma and proximal dendrites. The source for the observed adaptation was suggested to be cone-rod driven (Sakamoto et al. 2004; Mathes et al. 2007) more specifically via rod-cone driven dopamine synthesis, dopamine finally regulating melanopsin expression (Sakamoto et al. 2005).

The findings were further supported in a study with three diurnal and 4 nocturnal rodent species (Refinetti 2007), where in four of the species tested (diurnal rodent: degus; and nocturnal rodents: CD-1 mice, Wistar rat and Syrian hamster) phase delays of the running-wheel activity rhythm evoked by 1-h light pulses were several-fold larger after 3 to 4 weeks of exposure to darkness than after a single day. This finding was consistent with previous estimate of full adaptation in the circadian system of rodents taking up to 3 or 4 weeks (Daymude and Refinetti 1999; Refinetti 2001; Refinetti 2003). Counter-intuitively, dim nighttime illumination have been found to enhance the phase-shifting abilities of following bright light exposure in hamsters (Evans et al. 2009; 2011, Frank et al. 2010) and in humans (Chang et al. 2011). It has been suggested (Mure 2009) that the observed potentiation of the observed response could be due to melanopsin bistability (see 4), the dim light penetrating the selectively red-transmitting eyelids (Moseley et al. 1988; Robinson et al. 1991; Ando and Kripke 1996) favoring photoconversion from the M state to the R state (4) and ensuring maximum pool of photoresponsive melanopsin.

2.4.10 *Role in vision*

There is increasing evidence that in addition to non-image forming visual system, the mRGCs are also contributing to classical visual perception. In primates, the projections of the mRGCs to the LGN (Dacey et al. 2005) have been shown to be similar to the "luminance units" found 40 years ago by Barlow and Levick 1969 in the cat retina, as also found in macaque LGN (Marrocco 1975) and in macaque primary visual cortex (Kayama et al. 1979. It was suggested, that the LGN projections could be involved in brightness perception explaining why mice lacking rods and cones (*rd/rd cl*) are capable of employing light as a conditioning stimulus (Mrosovsky and Salmon 2002). In a recent study by Ecker et al. 2010 in mice suggested that the mRGCs projecting to visual structures were non-M1 cells (see 2.4.1).

Supporting evidence for mRGC involvement in brightness perception are obtained from lighting research (see overviews by Berman 2008, Berman and Clear 2008), where high color temperature (CCT) lighting was observed to appear brighter compared to illuminance-matched low color temperature lighting by (Harrington 1954 and Berman et al. 1990, however this difference found to be negligible in the study by Kanaya et al. 1979. Recently in a study with Kruithof's rule (Kruithof 1941) for LEDs (Viénot et al. 2009) it was suggested that melanopsin-drive could explain brightness perception unexplainable by rod/cone spectral sensitivities.

The mRGCs were shown to be involved in rudimentary pattern vision and visual acuity in a study by Zaidi et al. 2007 where a human patient lacking rods and cones showed a visual awareness (analogous to cortical "blind sight", Overgaard 2011) to the wavelength of light (~480 nm) most effective at activating melanopsin. Brown et al. 2010 were able to show light responses in the thalamus and the cortex of *rd/rd cl mice* supporting the hypothesis of primary visual centers being modulated by mRGC responses. The results of Brown et al. 2010 revealed that mRGCs sets the sustained firing rate under steady illumination of around 40% of all light responsive units in the LGN with a major source of light information for accessory visual centers in the hypothalamus and pretectum (Güler et al. 2008; Göz et al. 2008; Hatori et al. 2008). These findings supported the capability of melanopsin system to provide accessory pathway for mammalian for an accurate assessment of luminance/illuminance over extended light intensity range. Recent study from the same group (Brown et al. 2011b) provided support for the role of melanopsin in pattern vision, furthermore classifying four distinct response types from the hypothalamic neurons: transient cells, sustained cells, delayed cells and suppressed cells.

2.4.11 *Aging*

It has been well documented that with age the vision undergoes significant changes with aging (see review by Owsley 2011). However, age-related changes in visual functions, including pre-retinal factors, may to some extent be compensated by the plasticity of the adult visual system (Coombs and Chalupa 2011). Less is known about the age-related changes to the melanopsin system, but it could be assumed that the plasticity is present also in the non-image forming visual system. As reviewed in 2.4.9, the melanopsin protein levels could be simply up-regulated in response to reduced retinal light exposure due to pre-retinal filtering (see 2.2.3 and Charman 2003) in majority of the human population. There is recent evidence that there are morphological changes in the aging retina such as increased rod bipolar dendrite sprouting in mouse (Liets et al. 2006); and dendritic

reorganization in human rod / ON-cone bipolar cells and horizontal cells (Eliasieh et al. 2007).

There is contradictory evidence from behavioral studies in regard to plasticity in aging non-image forming system (see reviews by Revell and Skene 2010; Turner et al. 2010; Brown et al. 2011a) . Decreased sensitivity in the elderly was found for phase-shifting (Duffy et al. 2007), short-wavelength light for melatonin suppression (Herljevic et al. 2005). No significant changes were found for phase delay in two other studies (Benloucif et al. 2006, Sletten et al. 2009). Studies with cataract surgeries (see Gimenez et al. 2010 for discussion on the approach in circadian studies) indicate that there is an acute effect for the increased blue light transmission (Kitakawa et al. 2009; Schmoll et al. 2011.)

3

PUPILLARY LIGHT REFLEX - PLR

3.1 ANATOMY

Normal human pupil diameter varies on average from 1.5 mm to 8 mm (Reeves 1920) corresponding to light regulation capability of ~1.5 log units ($log_{10}[(8mm/1.5mm)^2]$. This ~1.5 log unit range is negligible compared to the ~10 log unit variation of ambient light intensity (2.3.5) thus the pupil size regulation mainly serves to dampen the rapid changes in ambient light intensity (Woodhouse and Campbell 1975). The human pupil is roughly circular in shape getting more elliptic with aging (Loewenfeld 1979; Wyatt 1995). Average pupillary size is maximal between the ages of 15 and 20 years showing a continuous decrease of 0.4 mm per decade known as senile miosis (Loewenfeld and Lowenstein 1993). Additionally the minimal pupil size (maximal constriction) increases (Bitsios et al. 1996a).

Iris is a muscular structure (Bron et al. 1997) with an average diameter of 12 mm controlling the size of the pupil (Trevor-Roper 1984). Pupil center may deviate from the center of the iris by an offset of up to 20%, thus not being necessarily concentric with the iris (Kristek 1965; Trevor-Roper 1984; Walsh 1988). This deviation has been shown to be larger with pharmacologically dilated pupils, with estimates for off-center offset ranging from 0.4-0.5 mm (Walsh 1988; Wilson et al. 1992) to offsets as large as 0.7 mm (Fay et al. 1992).

The human iris is divided in two zones by the collarette, a delicate zig-zag line also known as the iris frill. The pupillary zone is bounded by the pupil, while the ciliary zone extends to the outer border of the iris. Each zone is characterized by a muscle. The sphincter, located in the pupillary zone, is a concentric muscle that constricts to decrease the pupil size. The dilator, found in the ciliary zone, is a radial muscle that constricts to increase the pupil size. These two muscles overlap at the collarette (Pamplona et al. 2009).

The sphincter and dilator muscles are independently connected to the autonomous nervous system (ANS, see Section 3.2) (Tilmant et al. 2003) and the resulting pupil size depends on the balance of the separately incoming neural stimuli to the two muscles (Bergamin et al. 1998). In practice the constriction of pupil in response to light is constrained by the inherent slowness in the iris muscle, in contrast to the faster neural signal processing (see discussion in Bergamin and Kardon 2003) with an estimate for maximal constriction of ~ 0.0075 mm/ms (Myers and Stark 1993), and a practical threshold used for data rejection of 0.1 mm/ms . Additionally, the kinetics of the pupil

constriction and dilation seem to depend on the iris color [(Bergamin et al. 1998), i.e. on the amount of melanin pigment (Wakamatsu et al. 2008; Medina et al. 2011)] whereas absolute pupil diameter and response latency time does not seem to be effected by iris color (Winn et al. 1994; Bergamin et al. 1998; Bradley et al. 2010).

In addition to regulating the retinal irradiance, the pupil also affects the retinal image quality (Westheimer 2009) as aperture size in non-biological imaging systems (Freeman 1990). The diffraction of light rays by an aperture (iris in an eye) is a major limiting factor in the resolution of an image quality in imaging in general (Fang et al. 2005). As the pupil size increase, diffraction-degradation decrease (Campbell and Green 1965; Charman 1995) while optical aberrations increase (Liang and Williams 1997; Schwiegerling 2000). There is thus a trade-off between image quality degradation due to diffraction and ocular aberration, the optimal pupil size approximately being between 2 and 4 mm for the human eye (Westheimer 1964; Campbell and Gubisch 1966). In any optical system, the image quality is typically quantified by modulation transfer function (MTF, Van Nes and Bouman 1967) which is closely related to the point-spread function (PSF, Santamaria et al. 1987) and a contrast transfer function (CTF, Schober and Hilz 1965), all these three functions describing "the sharpness" of the optical system. . At typical daylight intensities, the visual information is on average maximized (Snyder et al. 1977; Hirata et al. 2003), and the retina is found to be adapted to the imperfections of the ocular optics (Garrigan et al. 2010).

Third major effect of pupil size to retinal image quality, in addition to ocular aberrations and diffraction, is its effect on the depth-of-field (DOF), that define the range of distance in depth that appears to be in focus (Potmesil and Chakravarty 1981). The depth-of-field depends both on viewing distance and the aperture size (for photographic exploitation of the effect see Kim et al. 2011), so that for the objects close to the eye the depth-of-field is shallow and for objects in distance deeper. When the distance is kept constant, the decrease in pupil diameter results in deeper depth-of-field (Marcos et al. 1999; Wang and Ciuffreda 2006).

With aging, the reduction of maximal pupil size can serve to reduce light scatter (van den Berg et al. 2009a), counteract the expected decline in visual performance due to retinal cell loss (Woodhouse 1975; Sloane et al. 1988; Elliott et al. 1990), and protect the aged retina from phototoxic damage (Winn et al. 1994; Wu et al. 2006)

3.2 PUPIL CONTROL CIRCUITRY

A summary diagram of the pathways controlling pupil diameter is shown in Figure 15A. The parasympathetic component of the autonomic nervous system (ANS) innervates the sphincter pupillae mus-

cle of the iris, and the sympathetic component of the ANS innervate the dilator pupillae muscle (for review see McDougal and Gamlin 2008). Pupillary light reflex (PLR) is a constriction of the iris muscles in response to light stimulus. The direct PLR, is the constriction of the pupil in the same eye as the eye simulated with light. The consensual PLR is the the constriction of the pupil in the eye opposite to the eye simulated with light. In primates including humans the direct and consensual PLR are almost equal in strength (Lowenstein 1954, Lowenstein and Friedman 1942) with certain degree of asymmetry (anisocoria) between direct and consensual response being normal even in human with no ocular pathologies (Smith et al. 1979). In species with more lateral eyes like rats and rabbits, the direct PLR is more pronounced (Loewenfeld and Lowenstein 1993). In binocular stimulation (both eyes stimulated), pupil constriction is shown to be larger (ten Doesschate and Alpern 1967; Thomson 1947) opposed to monocular stimulation.

The PLR pathway, traditionally consists only of the parasympathetic component of the pupil diameter control pathway. The PLR pathway can be separated into afferent and efferent pathways. The afferent pathway is composed of both the retinal cells (including mRGCs) that project to the pretectum and their recipient neurons that project bilaterally to the Edinger-Westphal (EW) nucleus (Edinger 1885; Westphal 1887). The efferent pathway is composed of the EW nucleus and ciliary ganglion, the latter projecting to the sphincter muscle of the iris.

In the afferent leg of the the PLR pathway, the first neurons are the photoreceptors (reviewed earlier in Section 2.3 and Section 2.4) of which the cones and rods are believed to mediate the transient (phasic) response to light and the mRGCs the sustained (tonic) response to light stimulus (Gamlin et al. 2007). There is however recent evidence suggesting that the situation might be more complex e.g., McDougal and Gamlin 2010; Kimura and Young 2010; Thompson et al. 2011; Allen et al. 2011), this differential photoreceptor contribution further reviewed in Section 3.3 and 3.3.1. The secondary neurons in the afferent pathway are luminance neurons in olivary pretectal nucleus (OPN) that show a transient burst of firing followed by steady tonic activity in response to light (15B-C).

In the efferent leg of the PLR pathway, the first neurons are the pre-ganglionic pupilloconstriction fibers of the EW nucleus. EW is a distinct nucleus of the midbrain, lying immediately dorsal to the oculomotor complex. In the 1930s it was shown that electrical simulation of EW can elicit a pupilloconstriction (Ranson and Magoun 1933), and bilateral lesions of the monkey OPN abolish the pupillary light reflex (Carpenter and Pierson 1973). However, the neurophysiology of EW pupilloconstriction neurons still have not been studied extensively (McDougal and Gamlin 2008). This is due to the small

size of EW and the small number of pupilloconstriction neurons in EW, reported to be as few as 10% of the total number of cells in EW (Gamlin 2000; McDougal and Gamlin 2008). The firing pattern has been shown to be similar in EW than in mRGCs (Berson et al. 2002) and in OPN (Gamlin et al. 1995) with a transient firing followed by a sustained firing in a range from 10 to 25 spikes s^{-1}(Gamlin 2000). This initial burst of EW neurons has been suggested to overcome the sluggish nature of the iris musculature (Bron et al. 1997). The second neuron layer in the efferent leg is in the ciliary ganglion, which is approximately 3 mm in size and 2-3 mm posterior to the globe and lateral to the optic nerve. Traditionally these neurons in the ciliary ganglion have thought to receive input only from EW, but there is evidence suggesting additional modulatory signals (May and Warren 1993), the ciliary ganglion serving as a potential location for neural integration (Gamlin 2000).

The sympathetic component of pupil size control, originate from the C8-T1 segments of the spinal cord, a region termed the ciliospinal center of Budge (and Waller). The axons of these pre-ganglionic neurons project to the sympathetic chain and travel in the sympathetic trunk to the superior cervical ganglion (Kardon 2005) continuing to the eye via short and long ciliary nerves and travel to the iris (Figure 15A). In addition to the parasympathetic path for PLR, the light may cause a reduction in the tone of dilator muscle via sympathetic pathway enhancing PLR. The light intensity-dependent inhibition of pupillodilation fibers have been shown in cats (Nisida et al. 1960; Passatore and Pettorossi 1976) mediated presumably via "darkness detector" cells as shown in pretectum of rats (Clarke and Ikeda 1985). However, this has not been found in primates (Clarke et al. 2003b), implying the possibility of sympathetic pathway only having a tonic role in the primate PLR (Clarke et al. 2003a).

3.2.1 *Spatial sensitivity*

Clarke et al. 2003b studied the receptive fields, luminance sensitivities, spatial summation, and ocular dominance properties of the olivary pretectal [(OPN), in some contexts referred as pretectal olivary nucleus (PON)] neurons (121 pretectal ON luminance neurons) for the first time in alert primates. The authors found OPN luminance neurons possessing large receptive fields with three major classes (Figure 16). Figure 16A shows a neuron responding equally well to the stimulus irrespective of where it is presented in the visual field ("bilateral" cells). Figure 16B neurons give a maximal responses for stimuli presented less than 10° from the fixation point. The response of these neurons was much reduced when the stimulus was presented in the periphery ("macular" cells). Figure 16C shows a receptive field of a neuron that responded best to stimuli placed in the visual field con-

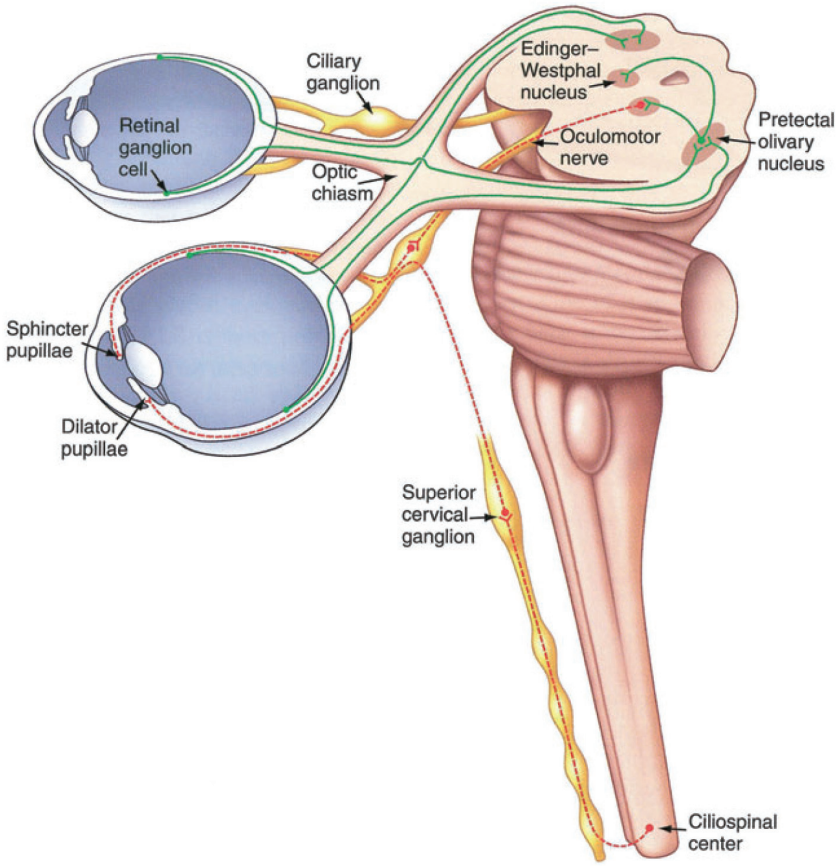

Figure 14: **PLR Pathways.** Anatomical drawing showing the direct and consensual pupillary light reflex pathways and the parasympathetic and sympathetic innervation of the iris in primates. (McDougal and Gamlin 2008). Luminance neurons in the olivary pretectal nucleus (OPN) drive the pupillary light reflex.

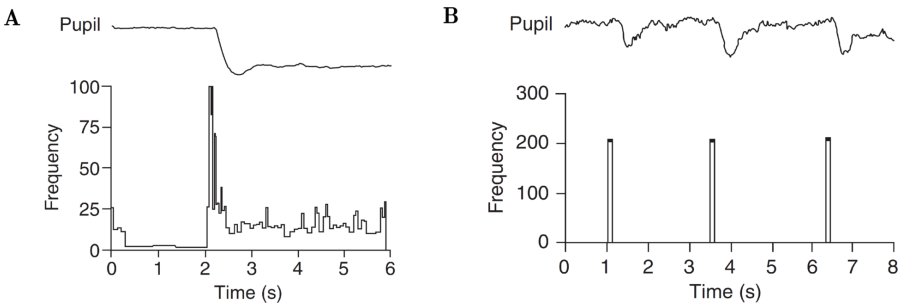

Figure 15: **OPN firing pattern and pupil response. (A)** The response of a single neuron is the OPN in response to a 100-troland light stimulus. The pupillary response to the same light stimulus is shown in the trace above. **(B)** Electrical microstimulation at the level of the OPN produces pupillary constriction, even in the absence of a light stimulus. (McDougal and Gamlin 2008)

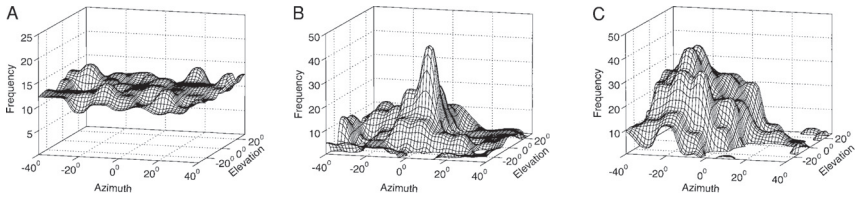

Figure 16: Examples of the 3 types of receptive fields that characterize OPN luminance neurons. **A:** bilateral; **B:** macular; **C:** contralateral. The 3-dimensional plots were constructed from averages of the mean neuronal firing rate recorded in response to stationary 35 cd/m², 5° stimuli presented at specific locations in the visual field during steady fixation at primary position. Upper and ipsilateral visual fields are denoted respectively by positive values. (Clarke et al. 2003b)

tralateral. Neurons belonging to each of these receptive field classes were encountered throughout the recording area, with no evidence of clustering or topography.

OPN luminance neurons of the bilateral and contralateral classes possessed very large receptive fields, exceeding 4,800°² for the bilateral class and 2,500°² for the contralateral class. The receptive fields of the luminance RGCs that project to the OPN were estimated to be approximately 7°² centrally and 20°² peripherally (Gamlin et al. 2001). Thus input from hundreds of luminance RGCs would be required to generate the receptive fields possessed by bilateral and contralateral neurons. In contrast, the receptive fields (approximately 100–900°²) of macular OPN neurons could be constructed from approximately 50 (range 20–100) centrally located luminance RGCs (Clarke et al. 2003b).

None of the individual receptive fields of OPN neurons matched the overall pupillomotor response fields obtained in Clarke et al. 2003a suggesting that all the three receptive field type classes project to the EW nucleus. The combined response resemble the profile of the pupillomotor response field as shown in Figure 17A further suggesting the integration of the OPN neuronal receptive field properties in the EW nucleus. Under normal circumstances, signals from neurons in the left and right OPN combine directly at the EW nucleus, therefore a signal such as shown in Figure 17A for the unilateral OPN output stage would not be observed. However, authors predicted that unilateral inactivation of the OPN would reveal such a signal. This model is similar to the cybernetic binocular summation model by Krenz et al. 1985 explaining roughly equal direct and consensual pupillary responses.

There is some evidence for similar visual field preference in PLR as noted for melatonin suppression (see 2). Wyatt and Musselman 1981 noticed that when a stimulus fell on nasal retina, the response was greater in the stimulated eye. The difference between responses was much less sensitive to stimulus timing than was the average response size. Schmid et al. 2000 found nearly equal direct and con-

sensual when stimulating the temporal retina. Xu and van Bommel 2011found inferior retina exposure (superior visual field) to constrict pupil more than the superior retina exposure. Carle et al. 2011c proposed a simple model mainly for clinical applications (e.g. Chen et al. 2005) describing the segregation and summation of signals from the olivary pretectal nucleus (OPN) to each Edinger-Westphal (EW) nucleus depending on the visual field being simulated.

3.2.2 *Pupillary light reflex waveform*

The shape of the human dark-adapted pupil response (i.e. the waveform of PLR) to light can be roughly generalized having three distinct components, phasic, sustained and post-illumination persistence (see Figure 19). Phasic component (TA_{min} in Figure 18A) is the rapid initial constriction, that is followed by a slight dilation to a larger steady-state (tonic) pupil diameter ($TA_{75\%}$ in Figure 18A) also referred as a pupillary escape (Lowenstein and Loewenfeld 1959; Levatin 1959; Hung and Stark 1979; Sun and Stark 1983). With higher light intensities the steady-state pupil size is more or less equal to the initial phasic size (see for example Fig. 2A in Mure et al. 2009) and this maintenance of initial pupil size is referred as pupillary capture (Usui and Stark 1978; Sun and Stark 1983). The phasic and sustained components have rough correspondences at the level of olivary pretectal nucleus (OPN), where two types of neurons were found in macaques based on their firing patterns, burst-sustained ("phasic-sustained") neurons and transient neurons that responded both to lights-ON and lights-OFF (Pong and Fuchs 2000a).

After light offset, the pupil does not immediately return to its dark-adapted diameter, and this sluggish return to baseline is referred as the post-illumination persistence (PIPR). At light offset there might be an initial dilation followed by reconstriction as shown first by Alpern and Campbell 1963. It was further shown (Newsome 1971) that after extremely bright light (3.5 x 10^6 Td) the pupil remained constricted in darkness as long as ~5-6 minutes reaching full pupil size after 15-18 minutes of light offset as seen in Figure 20A. The re-contraction and initial dilation was shown to depend on the light intensity (Figure 20B). The pupil reconstriction was shown to disappear with light stimuli shorter than 1 sec (Figure 20C) presumably corresponding to sluggish response of the yet undiscovered mRGCs. Similar results were obtained in a study by Alpern and Ohba 1972 with recordings of post-stimulation pupil size extending up to 30-40 minutes in the darkness.

The post-illumination response was linked to mRGCs (Gamlin et al. 2007), eliciting interest for the use of this response as a diagnostic tool (Kankipati et al. 2010; Park et al. 2011) for several retinal pathologies

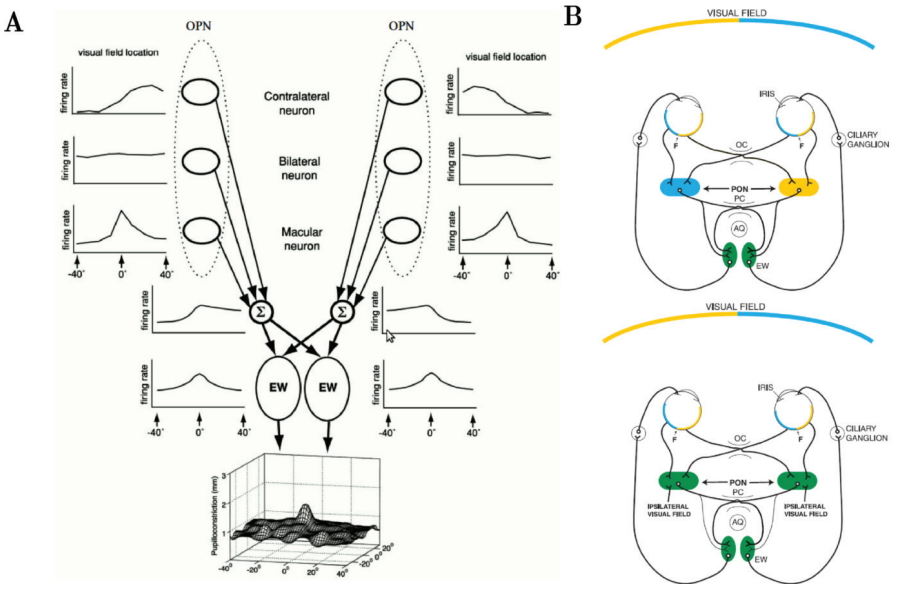

Figure 17: **PLR Circuitry and bilateral summation (A)** This schematic diagram shows bilateral OPN stages each with 3 neurons possessing the receptive fields characteristics of the 3 classes of OPN neurons. Output from the OPN is combined bilaterally at the Edinger-Westphal nucleus (EW) to produce the output of this nucleus. This output then produces the observed pupillary responses as shown in the bottom In this schematic diagram, before the OPN signals converge on the EW nucleus, a summing junction is shown as combining unilaterally the signals from each class of OPN neuron as a weighted sum based on their prevalence (bilateral = 0.4; macular = 0.3; contralateral = 0.3). However, because the OPN has direct, bilateral projections to the EW nucleus, the response shown at the summing junction would not normally be seen and is presented only as a diagrammatic convenience (Clarke et al. 2003b). **(B)** Schematic diagrams showing the representation of the visual field at different points along the pupillary light reflex pathway. The left and right hemifields and their central representations are color-coded yellow and blue, respectively. Points at which the entire visual field is represented are color-coded green. A: the currently held view that the contralateral visual field is represented in each PON and that bilateral projections to the EW result in a bilateral visual field representation in this nucleus. B: a revised version based on the results of the present study showing bilateral visual fields in the PON. The source of the ipsilateral visual field in PON is currently unknown. This figure also shows that the projection from the PON to the EW predominantly crosses in the posterior commissure (Clarke et al. 2003b).

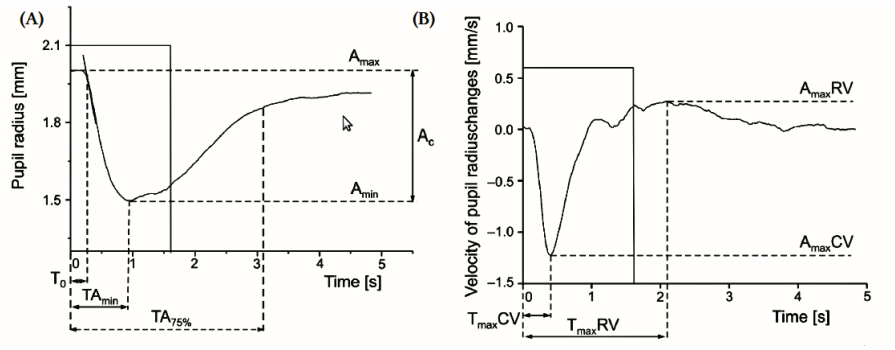

Figure 18: **(A)** Time course of a typical pupillary light response. **(B)** Velocity of pupil radius change to light stimulus, i.e. the derivative of a typical PLRSzczepanowska-Nowak et al. 2004. T_0, time delay to reach minimum diameter; A_{max}, maximum pupil diameter; A_{min}, minimum pupil diameter; TA_{min}, time to reach minimum diameter; $TA_{75\%}$, time to which pupil has redilated to 75% of the reflex amplitude; A_c, response amplitude; $T_{max}CV$, time to maximum constriction velocity; $T_{max}RV$, time to maximum redilation velocity; $A_{max}RV$, maximum redilation velocity; $A_{max}CV$, maximum constriction velocity.Szczepanowska-Nowak et al. 2004.

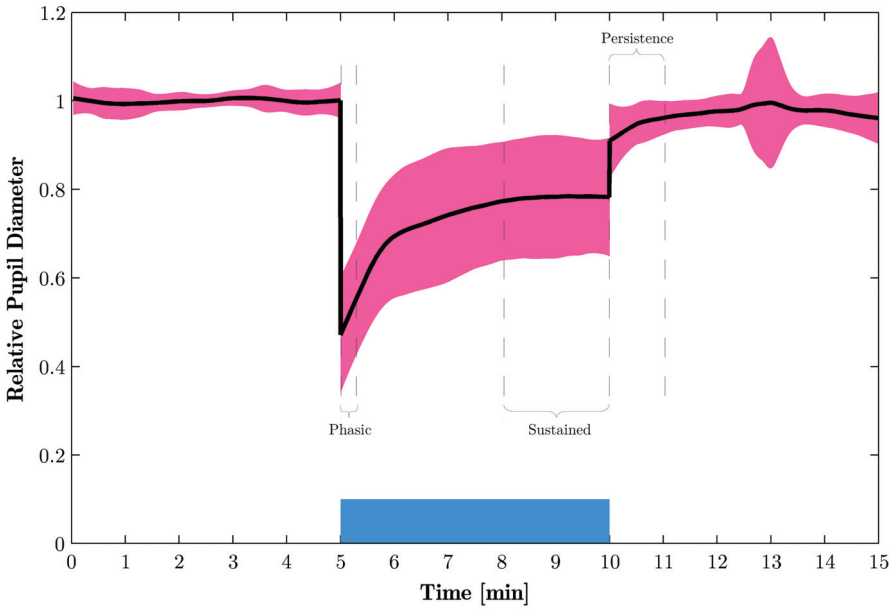

Figure 19: Mean PLR diameter waveform (black line) with the standard deviation (red) in response to 480 nm light with a photon density of 12 log photons·cm^{-2}·s^{-1} constructed from 24 individuals recorded with the study later discussed in 5.2.3.1, with the individual PLR waveforms shown in Figure 106. The three time bins (phasic, sustained and persistence) are shown schematically with the PLR waveform.

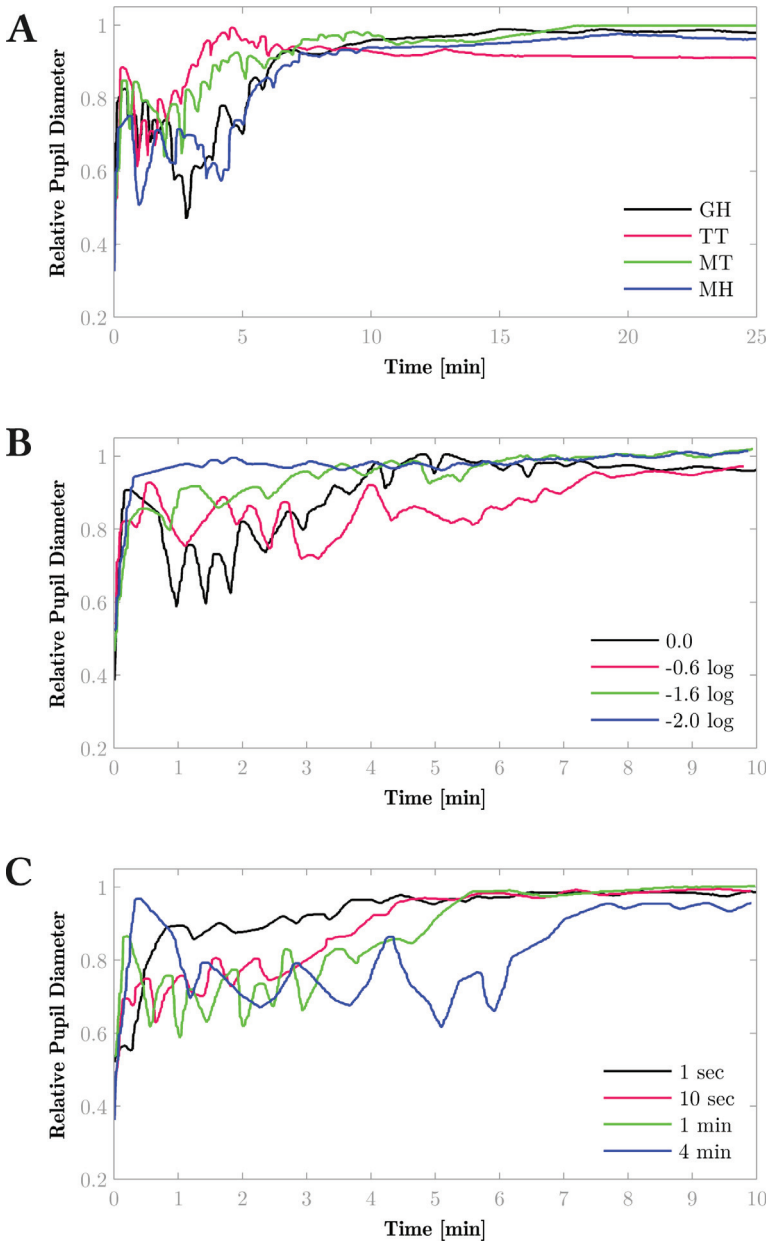

Figure 20: **Pupil persistence. A** Four subjects' pupil activity in darkness after 2 min full-intensity light. These curves show inter-personal variations in (1) average amplitude of recontraction, (2) duration and amplitude of unrest. **(B)** Effect of decreasing intensity of light stimuli. The same subject was given four 2-min light stimuli, with the brightness progressively diminished from full intensity. The period of pupillary recontraction with unrest was progressively diminished when the light was reduced by 0.6 log units, and 1.6 log units; it was absent when a 2.0 log filter was interposed. With the weakest light them was no latent period for the positive afterimage. **(C)** Effect of decreasing duration of the light stimulus. The same subject was given the full intensity light stimulus for exposures up to 4 min. Decreasing the duration of exposure to 1 min and then to 10 set shortened the length of the afterimage latent period, lowered the peak of the initial pupil dilation, and diminished the extent and duration of the recontraction with unrest. When the exposure was for only 1 sec, the afterimage was seen immediately, and pupillary recontraction was absent. (Newsome 1971)

such as diabetic retinopathy (Feigl et al. 2011), glaucoma (Kankipati et al. 2011), retinitis pigmentosa (Kardon et al. 2011) and outer retinal diseases (Léon et al. 2011), as later reviewed in Section 3.9.

3.2.3 *Eye movement control*

Typically PLR studies are done with systems meant to study eye movements (cf Hussain et al. 2009), thus a short introduction of eye movements are presented here. The eye movements can be roughly categorized (see for example Yarbus 1967; Rayner 1998; Krauzlis 2005) into fixational eye movements (Martinez-Conde et al. 2004; Mould et al. 2012), gaze-stabilizing mechanisms [vestibulo-ocular reflex (Fetter 2007) and optokinetic reflex (Cahill and Nathans 2008, as used in melanopsin studies Thompson et al. 2011; Altimus et al. 2010)] and gaze shifting mechanisms (saccades (Findlay and Walker 1999), microsaccades (Martinez-Conde et al. 2009), smooth pursuit eye movements (Lisberger 2010) and vergence movements (Erkelens 2011)). The eye movement dynamics are described by Listing's Law and Donder's Law (Villanueva et al. 2006). Saccade studies may require recording systems with significantly higher frame rates [even up to 6-12 kHz with custom electronics (Talukder et al. 2005; Yang et al. 2010)] than PLR studies (50-60 Hz), as angular velocities of saccades can be as high as 500°/s (Clarke 1994).

3.2.4 *Pupil near response (PNR)*

In addition to responding to light, the pupil constricts when viewing distance changes from far to near, referred as the pupillary near response (PNR, Marg and Morgan 1949). The PNR is characterized by three simultaneous oculomotor responses on far-to-near transition, commonly referred as the near triad (see review in McDougal and Gamlin 2008). In near triad, the eyes first converge to bring the image of the object onto similar regions of each retina, second the refraction of crystalline lens is adjusted to bring the image into focus, and thirdly the pupil constricts. Traditionally the PNR has been thought to be driven exclusively via the parasympathetic pathway increasing the drive to the sphincter muscle (Kasthurirangan and Glasser 2005) sharing common pathways with the PLR. However, in certain neurological clinical conditions such as Adie syndrome and of neuropathic tonic pupils (Lowenstein 1956; Thompson and Kardon 2006) an intact PNR has been demonstrated with an absence of PLR implying more complex pathways.

Figure 21 shows the current dual-integration model for PNR (McDougal and Gamlin 2008), where two neural controller operate in the PNR: one that integrates stimuli for accommodation such as blur (Burge and Geisler 2011), and the other that integrates stimuli driving

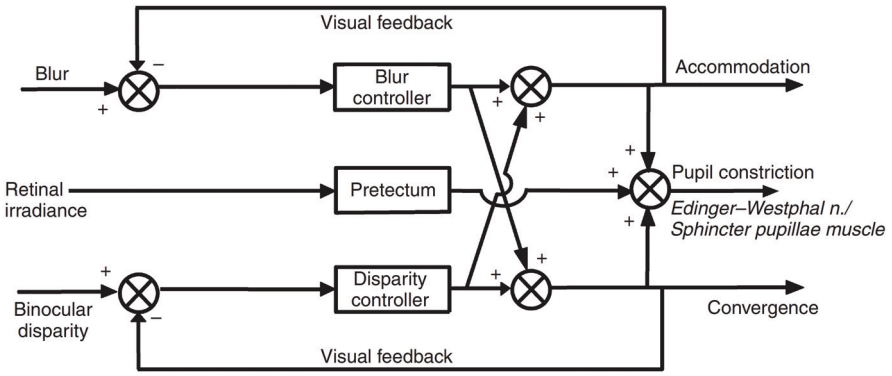

Figure 21: **Near response triad.** Schematic of the modified dual-interaction model that accounts for the pupillary near response component of the near response triad. This model indicates that the combined output of the accommodation controller and the convergence controller drives the pupillary near response. (McDougal and Gamlin 2008)

convergence. The model emphasizes the notion that PNR is not drives by either convergence or accommodation alone, but by an interaction of the two controllers (Myers and Stark 1990). It seems likely that the supraoculomotor area of the midbrain is projecting to medial rectus motor neurons and to EW nucleus being responsible for carrying the accommodation and convergence signals to the pre-ganglionic pupilloconstriction neurons (Gamlin 2002).

3.2.5 *Non-photic pupil responses*

It is known that pupillary responses to light stimuli of similar intensities can fluctuate from day to day in the same individual (Tryon 1975; Semmlow et al. 1975; Loewenfeld and Lowenstein 1993; Winn et al. 1994; see 5.1.2 below) for various reasons briefly reviewed here. In the context of pupillary light reflex (PLR) experiments, the non-photic are considered as artifacts that need to be minimized in order to derive the light-dependent drive of pupil diameter. The pupil size being controlled by the autonomous nervous system (ANS, see Section 3.2 above), all stimuli affects ANS activity might potentially have an effect on pupil behavior.

The most studied non-photic influences for pupil diameter in addition are changes in accommodative state (Phillips et al. 1992; Ishikawa et al. 2004; Kasthurirangan and Glasser 2005; Kasthurirangan and Glasser 2006; and see 3.2.4 above) are changes in state of arousal (Lowenstein and Friedman 1942; Lowenstein et al. 1963; Morad et al. 2000; Wilhelm et al. 2001; McLaren et al. 2002; Aston-Jones and Cohen 2005; Wilhelm et al. 2011), or in cognitive activity (Beatty and Wagoner 1978; Beatty 1982). The cognitive response are also referred as task-evoked pupillary responses (TEPRs) and have become a well-

established tool of cognitive psychology (Beatty and Lucero-Wagoner 2000).

These pupillary responses are generally reported to vary in magnitude from 0.2 to 0.7mm (McDougal and Gamlin 2008), and have been shown to be an accurate reporter of cognitive load across such diverse functions as pain perception (Höfle et al. 2008), fear of pain (Bitsios et al. 1996b), sexual arousal (Zuckerman 1971), cognitive load (Cabestrero et al. 2009), emotional processing (Demos et al. 2008; Steidtmann et al. 2010), in movement preparation (Richer and Beatty 1985), anticipation of an event (Reinhard and Lachnit 2002), sound and noise perception (Kumnick 1956; Jones et al. 1977; O'Neill and Zimmerman 2000), social signaling (Niedenthal and Cantor 1986), and interest and attention (Hess and Polt 1960; Hess and Polt 1964; Hess 1965; Hess et al. 1965; Steinhauer et al. 2004; Laeng et al. 2012). Phasic pupil size found to be more sensitive indicator for cognitive and attentional changes than the tonic pupil size (Beatty 1982; Deijen et al. 1995).

Common psychoactive substances such as alcohol (Bender 1933; Skoglund 1943), tobacco (Lie and Domino 1999; Morte et al. 2005) and caffeine (Minzhong et al. 2004; Michael et al. 2008) have noticed to have an influence on pupil. Additionally, a variety of pharmacological have an influence of pupil behavior including sedatives (Sigg and Sigg 1973), beta blockers (Koudas et al. 2009), antidepressants (Bär et al. 2004), anesthetics (Larson et al. 1991; Belani et al. 1993), and alerting agents such as modafinil and diphenhydramine (Hou et al. 2007).

Typically the other pupil for PLR studies is pharmacologically dilated (dilated eye stimulated with eye, and non-dilated eye recorded) using a mydriatic drug (Gambill et al. 1967; Smith 1976) such as tropicamide (Elibol et al. 1997) which might not induce an ideal dilatation (Granholm et al. 2003; Hammond et al. 2000). In a non-dilated pupil, eye blinks induce rapid dilatations of the pupil due to reduced retinal illuminance (Loewenfeld 1999; Hupé et al. 2009) that might require special care in data analysis. Furthermore, there might be significant inter-eye asymmetry in pupil responsiveness in healthy subjects known as anisocoria (Bär et al. 2005; see 3.2.1), with an evidence for increased asymmetry in males (Fan et al. 2009b).

Physiological artifacts can be caused by respiratory fluctuations (Ohtsuka et al. 1988; Yoshida et al. 1994; Calcagnini et al. 2000), heart rate fluctuations (Calcagnini et al. 2000), sleep deprivation (Franzen et al. 2009), depression (Siegle et al. 2001; Siegle et al. 2004), hypothermia (Huet 1989), high altitude (Wilson et al. 2008). Pupil behavior have been also used concurrently with fMRI recording to aid the interpretation of event-specificity of fMRI responses (Siegle et al. 2003), and shown to be effected by transcranial magnetic stimulation (TMS; Niehaus et al. 2001).

3.3 PHOTORECEPTOR CONTRIBUTIONS

3.3.1 *Spectral sensitivity*

Laurens 1923 was the first to study the spectral sensitivity of PLR in humans demonstrating λ_{max} ~ 554 nm for light-adapted eye (photopic sensitivity) and λ_{max} ~ 514 nm for the the dark-adapted eye (scotopic sensitivity). From early on, the spectral response was found to be a combination of cone and rod inputs (Wagman and Gullberg 1942; Spring and Stiles 1948; De Launay 1949; Bouma 1962), with mixed interpretations of the results. For example, Spring and Stiles 1948 studied the directional sensitivity (i.e. Stiles-Crawford effect, see 2.2.2) of PLR and concluded that due to the lack of directionality for large fields (53°), the rod input was significant to the PLR. Furthermore, directionality for PLR was shown (Alpern and Benson 1953) with small <1° fields supporting this reasoning. Given the lack of light-guiding structures in human mRGCs, the non-directional sensitivity results of Spring and Stiles 1948 could be interpreted originating from the mRGCs. Similarly in a study of Hess 1908 blind spot illumination was shown to produce an observable pupillary constriction which was at the time attributed to the non-directional sensitivity of rods to scattered light.

Bouma 1962 found a λ_{max} ~ 490 nm (Figure 22C) corresponding closely to the melanopsin of λ_{max} ~ 482 nm with crystalline lens correction (van de Kraats and van Norren 2007a), while Alpern and Campbell 1962 found λ_{max} ~ 530-540 nm both for transient and steady-state pupil sizes. The steady-state peak sensitivity differed from the λ_{max} ~ 511 nm of Wagman and Gullberg 1942, probably due to the lower light intensity (criterion pupil constrictions of 0.5 - 1.0 mm) used by Alpern and Campbell 1962.

After the discovery of mRGCs, the spectral sensitivity of the PLR has been re-assessed, see discussion for example in Berman 2008; Gamlin et al. 2007; Young and Kimura 2008; Kimura and Young 2010 for human PLR. Gamlin et al. 2007 showed that the post-illumination persistence response seem to be completely driven by mRGCs (22C) whereas the sustained component (10 sec light exposure) had a significant contribution from rods and cones demonstrated by pharmacologically blocking (Dolan and Schiller 1994) the signals from them (Figure 18). Mure et al. 2009 used a longer 5 minute light exposure arguing that the 10 second light exposure would not be enough to set the pupil response to steady-state. Mure et al. 2009 showed similar spectral sensitivity for both the sustained (3-5 min of the light pulse) and the persistent (0-60 seconds after light offset) response with λ_{max} between 460-480 nm. This result was suggested to demonstrate the mRGC-mediated sustained response and saturation of the classical photoreceptors. Study in blind human lacking visual perception re-

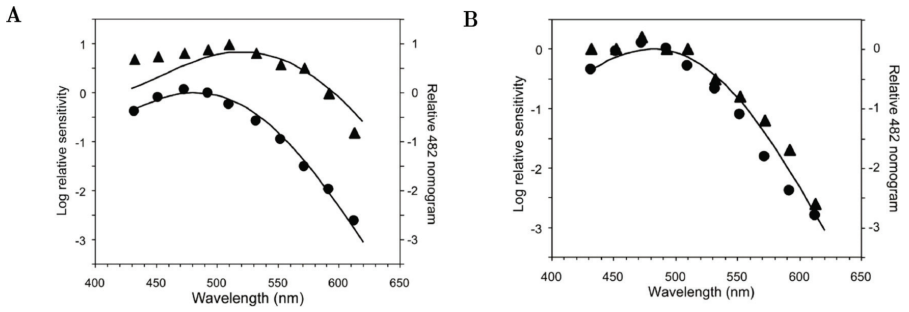

Figure 22: **(A)** Spectral sensitivity data in macaques derived for the sustained part of the 10 sec light exposure for the half-saturation response derived from irradiance-response curves. The data in the normal condition (▲) is poorly fit (R^2 ~ 0.77) by a best fit, vitamin A1 pigment nomogram (λ_{max}~ 522 nm). The data obtained during pharmacological blockade of rod/cone signals (●) is well fit (R^2 ~ 0.99) by a vitamin A_1 pigment nomogram with peak λ_{max}~ 482 nm (Gamlin et al. 2007). **(B)** Post-stimulus, sustained pupillary responses in macaques. The solid curve, a vitamin A_1 pigment nomogram with λ_{max}~ 482 nm, closely matches the data obtained both under normal conditions (▲, R^2 ~ 0.98) (best fit λ_{max}~ 483 nm) and during pharmacological blockade (●, R^2 ~ 0.97) (best fit: λ_{max}~ 476 nm). The human sensitivity for persistence matched closely (not shown) to the macaque with a λ_{max}~ 482 nm (Gamlin et al. 2007).

sulted an estimate of λ_{max} ~ 476 nm for the peak sensitivity of PLR (Zaidi et al. 2007). Furthermore, studies in melanopsin-knockout mice demonstrated that without melanopsin-mRGC, the pupil cannot hold its sustained response dilating back to baseline (Zhu et al. 2007) and failing to constrict maximally (Lucas et al. 2003).

3.3.2 *Irradiance response characteristics*

The steady-state pupil diameter as a function of light intensity (white light) was evaluated as early as in the 1920s by (Reeves 1920, follow-up by Wagman and Nathanson 1942 with more rigorous methodology) showing a sigmoid-shape curve of the pupil size (Figure 24A, see later Section 3.8 for more detailed analysis). Early studies had contradictory results whether the sensitivity of the PLR pathway was higher or lower than the perceptual visual response. Results from Schweitzer 1956, Schweitzer and Bouman 1958 suggested that PLR is less sensitive than the perceptual scotopic response, whereas later study by Stewart and Young 1989 came to the opposite conclusion that the PLR pathway must be equally sensitive or more sensitive than the visual pathway. It was suggested (Alpern and Campbell 1962) that the discrepancy could have been due to small test fields used by Schweitzer 1956, Schweitzer and Bouman 1958 with entire

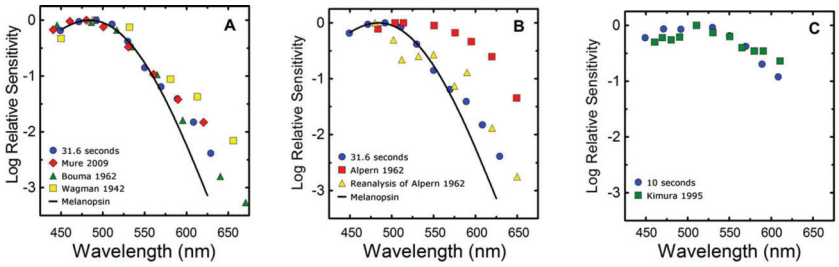

Figure 23: **Comparison of the steady-state spectral sensitivities**. **(A)** The data (●) from McDougal and Gamlin 2010 shows good concordance with previous reports by Mure et al. 2009 (⧫), Bouma 1962 (▲), and Wagman and Gullberg 1942 (■) of the spectral sensitivity of the human PLR in response to steady-state light stimuli. Conversely, **(B)** The data (●) from McDougal and Gamlin 2010 is not in agreement with the report by Alpern and Campbell 1962 (■) of the spectral sensitivity of steady-state PLR. However, when the data of Alpern and Campbell 1962 is reanalyzed to correct for possible errors produced by incorrect baseline measurements (▲), the results are similar to the results of the current study. **(C)** Measured spectral sensitivity of the PLR (McDougal and Gamlin 2010) for shorter stimulus durations (●) is also in good concordance with the spectral sensitivity measured by Kimura and Young 1995 (■) for similar stimulus durations. All previously reported data were converted from corneal illuminance to retinal irradiance when necessary in order to facilitate the comparisons between studies. In panels A and B, the absorbance spectrum of melanopsin is represented by a Baylor nomogram (Baylor et al. 1987) with a λ_{max} at 483 nm. (McDougal and Gamlin 2010)

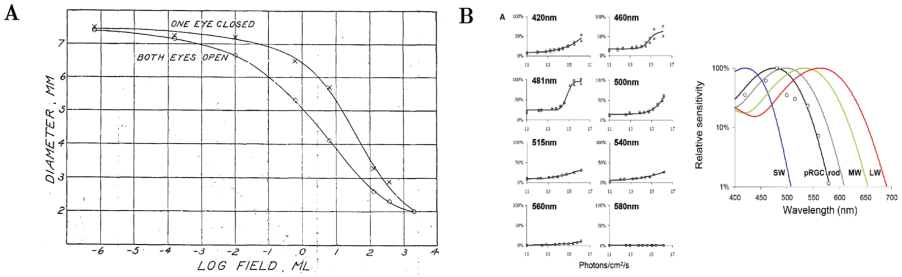

Figure 24: **Irradiance-response characteristics of the human pupil. (A)** Pupil size as a function of light intensity (Reeves 1920). **(B)** Irradiance-response curves (IRCs) were conducted at eight wavelengths for both eyes (squares indicate left eye, triangles indicate right eye. Responses are plotted as percentage of maximum response obtained. The resulting action spectrum of pupil responses provided a poor fit to rod and cone. An optimum fit to the pupil response to light was provided by an opsin/vitamin A-based template withλ_{max}~ 476 nm corresponding closely to the mRGC system. (Zaidi et al. 2007)

visual fields corresponding to the results obtained by Stewart and Young 1989.

In rodent studies, it has been shown that the irradiance response range of different photoreceptors are overlapping with the differential responses shown in genetically modified animals. It has been shown that melanopsin photopigment is required for the full constriction at high irradiances in mice (Lucas et al. 2003), and that the mRGCs are needed for fully function PLR in mice (Hatori et al. 2008; Güler et al. 2008). Study by Thompson et al. 2011 demonstrated that in mice, rod and cone systems are needed for fully functional PLR even at high intensities. Do et al. 2009 estimated corneal threshold (4% of maximal constriction) for pupil constriction to be ~3×10^{12} photons cm^{-2} corresponding to roughly ~500 single-photon responses over all mRGCs. Furthermore, recent studies with hamsters (Hut et al. 2008) and with mice (Butler and Silver 2010) showed that PLR thresholds were higher than for the circadian entrainment. This contrasts the early human studies but the discrepancy most likely raises from different definitions of criterion response. Only comparable human study so far showed that PLR in a blind human lacking conscious vision (Zaidi et al. 2007), the spectral sensitivity of the PLR corresponded to the putative λ_{max} ~ 480 nm of the melanopsin photopigment (Figure 24B).

3.3.3 *Chromatic interactions*

Previous sections (3.3.1 and 3.3.2) dealt simple experimental settings, whereas there is evidence for cone-specific chromatic modulation for PLR. Kohn and Clynes 1969 were first to show that pupil constricted to the color change from red to green and vice versa without any

change in luminance. Pupil constriction was also seen with a removal of one primary color (red, green, blue) from the light spectrum. These results were further validated (Saini and Cohen 1979; Young and Alpern 1980), suggesting a functional spectral opponent system in PLR (see 2.3.4). Krastel et al. 1985 were the first to provide quantitative evidence with a chromatic-flash-on-white-background paradigm. This paradigm isolates the response of the chromatic (color-opponent) from that of the achromatic (luminance) channels, and the noticed Sloan notch (2.3.4) in three-lobe action spectrum reflects the subtractive interaction of the underlying cone-opponent mechanism as in psychophysics (Sperling and Harwerth 1971; Kalloniatis and Harwerth 1990). These findings were again supported by Kimura and Young 1995, with the PLR being non-exclusively luminance-driven. The previous findings were extended with a pronounced Sloan notch in the OFF-response but not in the steady-state PLR (Figure 22A) , and the ON response had varying shapes depending on the intensity level lending support to previous observations on the action spectra shapes (Young et al. 1993; Young and Kennish 1993).

This was followed by another study from the same group providing direct evidence for chromatic cancellation and the existence of a neutral point (i.e., the signal from the visual process could be nulled by selecting a light of some wavelength composition) in the human PLR (Kimura and Young 1996). Sensitivity of the pupil for 6 sec light flashes seemed to be higher when the photons were absorbed by only L or M cones than when the same number of quanta is absorbed by both L and M cones (later reproduced also by Tsujimura et al. 2001). However, chromatic cancellation was shown only to occur across a narrow range of flash intensities near the pupillary threshold, raising questions about whether this intensity-dependent property was consistent with the proposed L- and M-opponent model. Authors suggested L and M cones being the most sensitive photoreceptors in the used protocol explaining the observed nonlinearity, with additional weak S cone input supporting previous study by Verdon and Howarth 1988. These results were in accordance with the studies of Barbur et al. 1998; 1992 where chromatic mechanisms were demonstrated along with pupillary responses to structure and movement, and in the study of chromatic pupillary responses linked to photosensitive seizures (Drew et al. 2001).

Furthermore, short-wavelength lobe (λ_{max} ~ 440 nm) for OFF was demonstrated (Kimura and Young 1999) for long-wavelength backgrounds. The anatomical site of such observed antagonistic interaction still remained unclear, even with the possibility of "inverted sign" S-cone input to M and L cone signals as with perceptual luminance (Lee and Stromeyer 1989; Stockman et al. 1991). However, during the time of the study the OFF response of S-cones to the melanopsin-mRGCs was not yet characterized (Dacey et al. 2005).

The next studies on chromatic interactions were done after the discovery of melanopsin. Young and Kimura 2008 employed the *light-onset* method (in contrast to *light-offset* of Gamlin et al. 2007 referring to the persistence analysis) inspired by the finding of late contraction (sluggish response) in rabbits (Knapp 1986). To re-evaluate their old findings (Kimura and Young 1995; Kimura and Young 1999) in regard to melanopsin. Knapp's observation suggested that the onset of light could generate a melanopsin-induced effect on the pupil and that the effect could be differentiated from those of rods and cones by its very late time-to-peak. The outcome of re-evaluation was that with melanopsin-mRGCs, the need to postulate separate effects occurring during the ON-sustained, OFF-transient, and OFF-sustained periods could be obviated . Instead, the entire set of results could be accounted for by a single (melanopsin-mediated) process that has a relatively long time-to-peak and a slow offset recovery. These re-evaluated finds were contrasted by a follow-study with new subjects (n=2) to study the chromatic interactions for the sustained portion (for 3 s step-change in chromatic and luminance contrast from the white background) of PLR (Kimura and Young 2010), where a significant chromatic cone drive was found with no the intrusion from rod or melanopsin signals.

3.3.4 *Photoreceptor contributions*

In early pre-melanopsin PLR studies, the observed responses were modeled as rod-cone interactions (e.g. Alpern and Campbell 1962) inspired either by mesopic modeling by Donner and Rushton 1959a, Rushton 1959, or by trying to isolate the photoreceptor systems exploiting different directional sensitivity (Stiles-Crawford effect, see 2.2.2) of rod and cone photoreceptors (Donner and Rushton 1959b). The differential directional sensitivity as an approach was related to the studies with blind spot simulation (Hess 1908; Campbell and Alpern 1962) in which PLR was noticed. This PLR was attributed to the fundus scatter, detected by rods which in retrospect could have been mediated also by non-directional mRGCs with or without rod input.

After the discovery of melanopsin, several PLR studies were conducted using a silent substitution technique (Ishihara 1906; Estévez and Spekreijse 1982; Klee et al. 2011). The technique is based on the assumption that photoreceptor classess can be isolated by modulating the intensities of spectrally different experimental light sources, while knowing the spectral sensitivities of the underlying photoreceptors (see Estévez and Spekreijse 1982 for discussion). In practice for example for cone contribution analysis, the lights could modulated in such way that luminance is kept constant, individually varying M and L cone stimulation and observing differential M and L cone

responses. This approach can be in theory extended into more photoreceptors including melanopsin (Viénot et al. 2010; Tsujimura et al. 2010; Tsujimura and Tokuda 2011).

The constant-luminance was the approach in the study by Viénot et al. 2010 for steady-state PLR (1 minute after light onset), based on a five-channel LED light setup (see Pokorny et al. 2004 for instrumentation). The authors found no change in steady-state pupillary response with a variation of rod, S-cone, or melanopsin excitation alone. Differential steady-state pupillary response could only be obtained with an higher-contrast variation of the melanopsin stimulus either with or without associated variation of rod excitation. Tsujimura et al. 2010 studied the steady-state (2 sec at the end of 20 sec light exposure) PLR with four-channel LED system modulating either luminance, or the melanopsin excitation while keeping the luminance constant. Their results indicated ~3-fold more contribution from mRGC signals than from cones to steady-state PLR while the exact mechanisms remained unknown.

In the follow-up study (Tsujimura and Tokuda 2011), the number of LED channels were doubled (four for background and four for target) for studying of transient PLR (2 sec light pulse). In addition to intensity and spectral modulations of light for isolation, the waveform of the light stimulus was sinusoidal for melanopsin and square-wave for cones, in belief that sluggish mRGCs could not follow such rapid light level changes as well as cones (De Lange DZN 1954). The authors demonstrated longer latency (time to peak difference ~130 ms) for the mRGC condition which was attributed to a putative difference between signals from post-receptoral mechanisms and mRGCs.

McDougal and Gamlin 2010 employed a model, termed the Quick pooling model (Quick 1974; see Graham 2001 for details) . Quick pooling model has been successfully used to model the spectral sensitivity of a variety of visual functions, such as contrast sensitivity (Robson and Graham 1981), mesopic spectral sensitivity (Kurtenbach et al. 1999) and increment threshold spectral sensitivity (Miyahara et al. 1996). The model can be used to get estimates of the relative weights of different photoreceptors by fitting the following equation (Eq. (10)) to the experimental data, further allowing also the temporal analysis of spectral sensitivity:.

$$S(\lambda) = \left\{ \{m[S_m(\lambda)]\}^{k_2} + \left[\left(\{c[S_c(\lambda)]\}^{k_1} + \{r[S_r(\lambda)]\}^{k_1} \right)^{\frac{1}{k_1}} \right]^{k_2} \right\}^{\frac{1}{k_2}} \tag{10}$$

Where m, c and r are the weights for melanopsin, cone and rod contributions respectively; S_m and S_r are the spectral sensitivities for melanopsin (482 nm nomogram) and rod ($V'(\lambda)$ contributions respectively; , $S_c = \{p\,[S_L(\lambda)] + (1-p)\,[S_M(\lambda)]\}$ is the cone sensitiv-

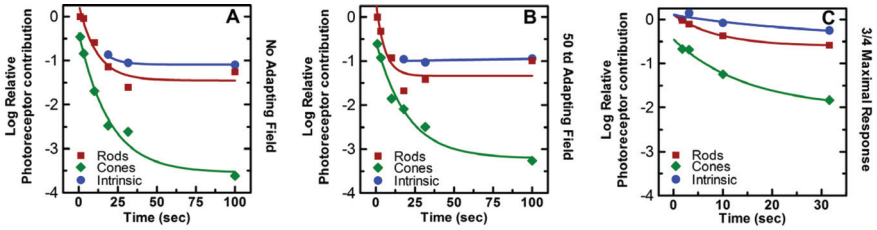

Figure 25: Relative contribution of the rod, cone, and melanopsin photoresponse to the spectral sensitivity of the PLR over time. The time course of light adaptation of the rod (■), cone (♦), and melanopsin (●) photoresponses while maintaining a half maximal PLR with **(A)** no background present, **(B)** a 50 td adapting background, and **(C)** a three-quarter maximal PLR with a 50 td adapting background. (McDougal and Gamlin 2010)

ity composed as a weighed sum of M and L cone sensitivities, with $p = \frac{1}{ratio(L/M)} = \frac{1}{1.625} = 0.67$ for the standard observer (Pokorny et al. 1993); $k_1$and $k_2$are the scaling exponent, k_1 (fixed at 1 by the authors) reflects the combination rule for the outer retinal sensitivities and k_2 (fixed at 10 by the authors) reflects the combination of the outer retinal signals with the melanopsin photoresponse. As k_i increases to values greater than 1, a nonlinear addition of the individual sensitivities occurs. Furthermore, as k_i is increased towards infinity, the sensitivity of the array approaches a situation of ''winner take all'', where the most sensitive element in an array at a particular wavelength defines the total sensitivity of the array at that wavelength.

The major findings of the study was that the melanopsin photoresponse of mRGCs contributes not only to pupillary constriction at high irradiances, but also acts to maintain pupillary diameter in steady-state photopic lighting conditions. Cones contributed minimally to the maintenance of steady-state pupillary diameter at low and high photopic irradiances, whereas rods kept surprisingly responding even in steady-state photopic conditions as found also by Bi et al. 2011. The three photoresponses driving the PLR in humans did not seem to be combining linearly at the level of mRGCs, but rather the outer and inner retinal signals act in a ''winner take all'' fashion. The determination of which photoreceptors would drive the response would be solely dependent on whether the illumination was sub- or suprathreshold for the shunting of outer retinal photoresponses by sufficient activation of the melanopsin photoresponse. Furthermore, it could be argued that this threshold would be highly dynamic depending for example on the time of the day (Zele et al. 2011) and recent light history (Chang et al. 2011 for circadian system).

3.4 PUPIL NOISE

The pupil diameter has been demonstrated to exhibit fluctuations usually referred as hippus (Bouma and Baghuis 1971; Müller-Jensen and Hagenah 1978), also known as pupil noise (Stark 1959; Longtin and Milton 1989; Longtin et al. 1990), spontaneous pupil fluctuations (Nowak et al. 2008) and pupil unrest (Stark et al. 1958). The noise is almost completely correlated between the two eyes (Stark and Cornsweet 1958) indicating that the noise is inserted in the system before the efferent oculomotor bifurcation. The noise controlling signal seems to be common for both accommodation and PLR suggesting that the Edinger-Westphal (EW) nucleus (see 3.2) as the point of noise injection (Stanten and Stark 1966). The pupil noise seem to of a stochastic origin (Longtin et al. 1990) even though chaos cannot be excluded (Rosenberg and Kroll 1999). Additionally, single midbrain neurons of irregular pulse sequence were found to be highly correlated to pupil noise (Smith et al. 1968).

Hippus is characterized as a random noise on top of the "mean pupil size"-signal in the frequency range of 0.05-0.3 Hz (Stark 1959; Usui and Stark 1982). Experiments have indicated skewing of the pupil noise spectrum from Gaussian white noise at high and low pupil areas. This skewing has been attributed the multiplier gain dependence on the expansive range nonlinearity and length-tension relationship of iris muscles (Usui and Stark 1978; Usui and Stark 1982) . In practice, pupil neuromuscular dynamics shape the high frequency cutoff for noise pulses and large and small sinusoids, whereas retinal adaptation accounts for the low-frequency asymptotes (Stanten and Stark 1966; Stark 1984).

In practice, the pupil noise has to be taken into account when analyzing PLR recordings as no "true pupil value" can be estimated from just one image of pupil. Average successive frames in a video for more robust estimate of the "true pupil value". Additionally, the pupil noise has been shown to have clinical diagnostic value as reviewed later in 3.9.2.

3.5 INSTRUMENTATION AND ANALYSIS OF PLR

3.5.1 *Instrumentation*

In typical chronobiological papers, the instrumentation side of pupil light reflex quantification receives very little or practically no attention, thus a brief overview of the available literature is presented here to compensate for the lack of instrumentation information. In general the literature on pupillometry-specific instrumention is scant in opposite to eye tracking-specific methodology (see for example reviews by Böhme et al. 2008; Hansen and Ji 2010) which are in however most as-



Figure 26: **Physical PLR setups. (left)** Early implementation of PLR recording system with custom-made dental bite bars to ensure stability of the subject throughout the experiment (Stark 1959). **(right)** Modern low-cost implementation using welder's goggles and webcam to monitor to pupil responses of the subject, goggles ensuring fixed distance between the camera and the eye (Mirtaheri 2010).

pects applicable to pupillometry. Example of a schematic for modern infrared video pupillometric setup for the recording of consensual pupil light reflex is shown in Figure 27, and Figure 51 illustrating possible physical implementations. The left eye in the schematics is stimulated by the excitation diode or with any light source with a fixation diode for either left or right eye ensuring proper fixation. The right eye is then monitored with a CCD/CMOS camera or with linear sensors (see for example Talukder et al. 2005), an industrial CCD camera being the typical choice. The eye is either illuminated off-axis (dark pupil technique), on-axis (bright pupil technique) or by multiplexing both light source types (Morimoto et al. 2000). To further reduce subject motion artifacts (subject movement in z-dimension in relation to the camera), the CCD camera can be placed further from the eye equipped either with a normal telephoto lens (smaller field of view and larger focal length) or with a telecentric (cf Watanabe and Nayar 1996) telephoto lens to further reduce motion artifacts as used in the study by Zele et al. 2011.

Ultimately the quality of the pupil recording depend on the image quality of the PLR setup, thus it is very important that the pupil data is obtained by a proper illumination and an accurate set up of the instrumentation (De Santis and Iacoviello 2006). Pupil image segmentation errors due to poor image quality further makes the physiological interpretation of the results more difficult (Proenca and Alexandre 2006). Proper infrared illumination will accentuate the edge between the iris and the pupil making the image segmentation (image processing to delineate parts of the image, see for example Pal and Pal 1993; Teikari 2007a; Udupa et al. 2006) algorithms perform as robust as possible. In practice pupil recordings with brown irises yield the best quality due to the higher reflectance of brown irises (Medina et al. 2011) on the typically used near- infrared range (NIR, ~850-950 nm) in pupillometry.

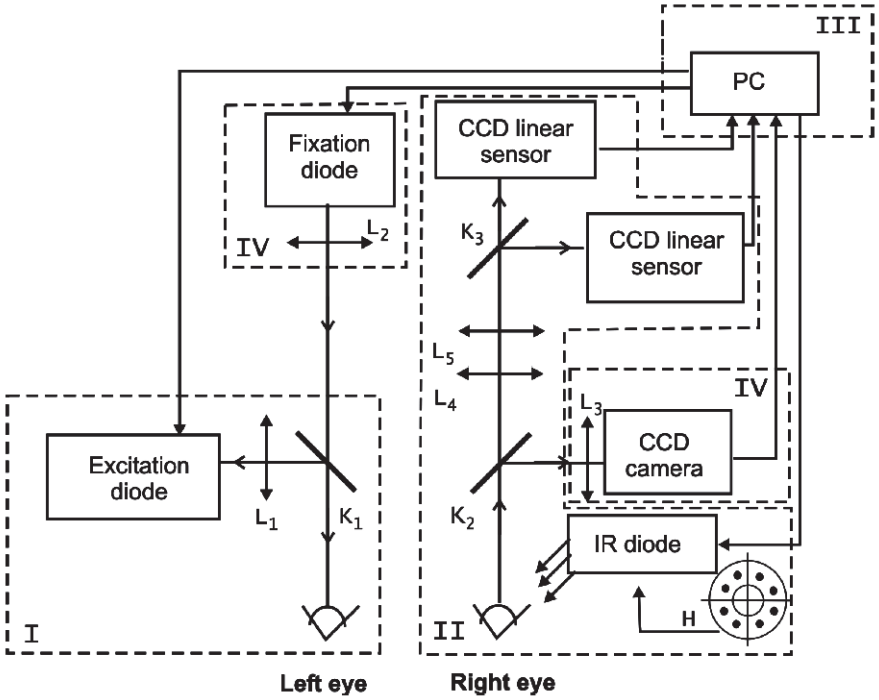

Figure 27: Example of an experimental set-up for the measurement of consensual PLR. I - stimulation module, II - recording module, III - control module, IV - calibration module. K_i are beamsplitters and L_i are lenses. (Szczepanowska-Nowak et al. 2004).

The simplest of image segmentation techniques is thresholding (Sezgin and Sankur 2004) which in essence separates the raw pupil image to parts belonging to the pupil and those not using the pixel intensity values. This approach is computationally light and used often in real-time eye tracking, while being the least robust in general of possible segmentation approaches. Another common approach is to use edge detection algorithms (Iacoviello and Lucchetti 2005) to find the gradients corresponding to the pupil-iris transition, being computationally feasible with the possibility of general-purpose graphical processor unit (GPGPU) hardware acceleration (Ogawa et al. 2010). Recent open-source eye tracker project openEyes employed an algorith called Starburst (Li et al. 2005)based on statistical method RANSAC (RANdom SAmple Consensus; Fischler and Bolles 1981) offering more robust segmentation compared to previous approaches, with feasible computational cost being suitable for also real-time analysis [see also other projects open-source such as Opengazer (Zieliński 2007) and ITU Gaze Tracker (San Agustin et al. 2009; 2010)]. Further studies have used even more robust techniques, such as level set segmentation (De Santis and Iacoviello 2006; Roy et al. 2011) and active/-geodesic contours (Shah and Ross 2009) more suitable for offline analysis allowing the most robust analysis not having to compute the pupil contours in real time..

One of the future trends, especially in clinical applications, is the use of perimetric pupillometry allowing differentiation of pupillometric responses between different retinal areas. For example, dichoptic multifocal pupillographic objective perimetry (mfPOP, Maddess et al. 2009; Bell et al. 2010) was shown to provide high-resolution mapping of local regional differences between direct and consensual responses in a study by Carle et al. 2011c. Additionally for better artifact management, the accommodative state of the lens could be measured as done for 3D eye tracking (Morimoto and Mimica 2005) and with photorefractive systems (Suryakumar et al. 2009).

3.5.2 *Data conditioning*

Raw pupil recordings are inherently noisy and variable in human subjects requiring further data conditioning before the physiological analysis. Very little literature (see for example Merritt et al. 1994; Bergamin and Kardon 2003; Teikari 2007a; Canver et al. 2010), thus one can use the literature from the domain of biomedical signal processing (see for example Semmlow 2008; iii; Cerutti et al. 2011). The two most common artifacts are eye blinks and spontaneous pupil fluctuations ("noise signal") on top of "mean pupil size" signal.

Eye blinks can be excluded from the raw data heuristically using for example the maximum known constriction velocity (Bergamin and Kardon 2003) or using a circularity coefficient of the found pupil contours (Mure et al. 2009) to eliminate false pupil detections during blinks. The noise signal is typically treated with smoothing filters (Dokuchaev 2012) such as negative exponential smoothing (Savitzky and Golay 1964; used in Wyatt 2010), binomial smoothing filter (Marchand and Marmet 1983; used in Clarke et al. 2003a), Savitzky-Golay (Savitzky and Golay 1964; used in Bergamin and Kardon 2003) or locally weighted scatterplot smoothing (LOWESS, Cleveland 1979; used in Mure et al. 2009). However, in some paradigms the eye blinks (Michael et al. 2008) or the pupillary noise (Warga et al. 2009) can be the main interest imposing different requirements for the data conditioning. Advanced adaptive filtering schemes (see for example Douglas and Losada 2002 and He et al. 2007) have not been used in pupillometry studies to my knowledge. Furthermore, depending on the paradigm individual PLR recordings can be averaged (Stewart and Young 1989) to increase the signal-to-noise-ratio (SNR) as for example with evoked potentials in electroencephalography (Coppola et al. 1978).

3.5.3 *Mathematical analysis of PLR waveform*

Various parameters can be extracted from the conditioned data (some of the common parameters are listed in Table 3). In melanopsin stud-

ies, typically only the pupillary area is examined with occasional inclusion of latency analysis. As the pupil size undergoes spontaneous fluctuations, the analysis of pupil size is the more robust by combining successive estimates of pupil size to time bins in order to extract true mean size. With the time binning approach, the smoothing of the raw data (see previous 3.5.2) can be skipped allowing less information to be lost during conditioning and analysis. Additionally, the pupil size can be decomposed statistically for differential study of different components, as done by Kimura and Young 1995 for transient and sustained component using principal component analysis (PCA (Jolliffe 2005); and for tutorial see Smith 2002). Alternatively other decomposition techniques such as independent component analysis (ICA, Hyvärinen et al. 2001), non-negative matrix factorization (NMF, Lee and Seung 1999), empirical mode decomposition (EMD, Huang et al. 1998) and Hilbert-Huang transform (Huang and Shen 2005) could be used among other techniques.

For latency analysis of the PLR (for an old review see Bos 1991), either the first derivative (Link and Stark 1988) or the second derivative (Bergamin and Kardon 2003) of the pupil size can be used to detect the maximum constriction of the pupil and compare it to the light onset timing. Link and Stark 1988 used the Akaike information criterion [AIC, Akaike 1974; used in smoothing by Hurvich et al. 1998] to fit a polynomial to the latency of light-pupil reflex as a function of both stimulus repetition rate and brightness. Bergamin and Kardon 2003 upsampled the original 60 Hz data with Savitzky-Golay smoothing (Savitzky and Golay 1964) and Nyquist interpolation (Pierce 1980; Blanche and Swindale 2006) up to 300 Hz demonstrating that this could improve the temporal resolution in latency estimation compared to the original sampling rate (60Hz). Barbur et al. 1998 had developed a normalization technique (used by Tsujimura et al. 2001) based on the notion that, to a particular class of stimulus, all pupil responses have the same time-course to peak, and match perfectly when scaled to the same peak amplitude.

In a study of Straub et al. 1994, pupil noise (Section 3.4) was studied by first smoothing the signal with a Hanning moving average filter (Brockwell and Davis 2002), followed by detrending (Wu et al. 2007) via subtraction of a polynomial trend of the sixth order to stationarize the data (for stationary requirement see Kwiatkowski et al. 1992and Ijima et al. 2007). Finally autocorrelation analysis was applied to find the regular oscillation of the pupillary area (Matthews et al. 1983). The process for finding periodicities was thus similar as analyzing circadian rhythm periods (Levine et al. 2002; Refinetti et al. 2007) allowing more advanced alternatives for autocorrelation such as wavelet analysis (Benedetto and Pfander 2002; Zhang 2009) and singular value decomposition (SVD, Kanjilal et al. 1999). Furthermore, time-frequency analysis (for review see Addison et al. 2009) of

Table 3: Pupillary parameters and units, adapted from Straub et al. 1994

Meaning	Unit
Static and simple dynamic parameters	
Maximal pupillary area or diameter	mm^2or mm
Contraction velocity	mm^2/s
Dilation velocity	mm^2/s
Minimal pupillary area/diameter	mm^2or mm
Parameters of pupillary unrest	
Amplitude of pupillary unrest after detrending the data set	$mm^2 \cdot s$
Area under the detrended non-smoothed curve of pupillary unrest (AUC)	$mm^2 \cdot s$
Period of pupillary unrest derived from the first nadir of autocorrelation	ms
Second order dynamic parameters	
Latency time of pupillary light reflex	ms
Fusion frequency of pupillary response following flicker stimuli	Hz

the pupil noise can be done either with short-time Fourier transform (STFT, Cohen 1989) as done by Nowak et al. 2008 or with wavelet analysis (Guido et al. 2009) as in the study by Leal et al. 2011.

3.6 ADAPTATION AND CIRCADIAN RHYTHMICITY

Despite the widespread use of pupillographic measures in various experimental and clinical conditions, little is known about the circadian rhythmicity of pupillary responses. There is evidence for circadian rhythmicity for visual threshold (Bassi and Powers 1986; Roenneberg et al. 1992; O'Keefe and Baker 1987; Tassi et al. 2000a), visual acuity (Tassi et al. 2000b), electroretinography (ERG, Anderson and Purple 1980; Tuunainen et al. 2001) among other retinal rhythms (see for example Tosini and Fukuhara 2002), thus suggesting the possibility of a rhythm in PLR as well. Contradictory results have been reported for the resting pupil diameter (Doring and Schaffers 1950; Tiedt 1963; Borgmann 1966; Lavie 1979) with contradictions most likely arising from the methodological differences (Wilhelm et al. 2001). A recent study (Loving et al. 1996) concluded that there was no diurnal rhythm in pupil size, while Wilhelm et al. 2001 found daytime variation in pupil size corresponding to the results of Doring and Schaffers 1950).

Maximum in baseline pupil size was found in the morning (08h) accompanied with a afternoon minimum (15h) being in accordance with previous reports (Doring and Schaffers 1950; Borgmann 1966). Diurnal variation of constriction amplitude and latency was also found by Wilson et al. 2008 with no changes observed in pupil constriction or dilation velocities, further extended by the results of Yu et al. 2007 with no diurnal variation in constriction latency. A recent study by Nikolaou et al. 2008 showed that a novel alertness-promoting drug modafinil (Minzenberg and Carter 2007) was able to abolish circadian rhythm in reduction of pupil size in patients suffering from obstructive sleep apnea (Shamsuzzaman et al. 2003). This effect was thought to be modulated by modafinil-activation of the hypoxia-sensitive nucleus locus coeruleus (LC) which is has been suggested to play a role in PLR control also (Aston-Jones and Cohen 2005).

Recently, Zele et al. 2011 were the first to study systemically the diurnal variations of PLR in regard to mRGCs. The individual PLR was measured by four consensual pupil recordings of 55 seconds (10 seconds pre-stimulus, 10 seconds stimulus and 35 seconds post-stimulus) repeated every hour during a 20–24 h laboratory test period, during which the participant remained awake. The short wavelength stimulus (488 nm) was chosen to maximize mRGC contributions to the post-illumination pupil response (PIPR) (Markwell et al. 2010; Gamlin et al. 2007), and the long wavelength stimulus (610 nm) for determining outer retina cone contributions to the PIPR and as a control of nonspecific factors such as fatigue on the PIPR (Markwell et al. 2010; Gamlin et al. 2007; Kankipati et al. 2010). Figure 28A shows the rhythm of baseline pupil diameter, Figure 28B,C the rhythm of transient PLR to 488 nm (Figure 28B) and to 610 nm (Figure 28). Figure 28D,E shows the average redilation kinetics of the PIPR (exponential time-constant) with the 488 nm and the 610 nm lights as a function of circadian time and modeled over 24 hours with the skewed baseline cosine function (Van Someren and Nagtegaal 2007).

In conclusion, the results suggested that the change in mRGC controlled post-illumination pupil response is on average, 2:40 h in advance of the onset of melatonin secretion, and the minimum post-illumination pupil response occurs on average, 1.31 h after melatonin onset. It has been shown in mice that rod photoreceptors drive photoentrainment at scotopic and photopic light levels via mRGC retinal circuitry (Altimus et al. 2010) and contribute significantly to the steady-state pupillary diameter in humans (McDougal and Gamlin 2010). There is evidence suggesting that baseline pupil diameter shows diurnal variation only when rods are active (Fosnaugh et al. 1992). The shown diurnal variation of mRGC-mediated PLR responses *in vivo* is in contrast with the *in vitro* electrophysiological data in rat retinal preparations (Weng et al. 2009), in which only a modest increase for melanopsin modulation during subjective night was

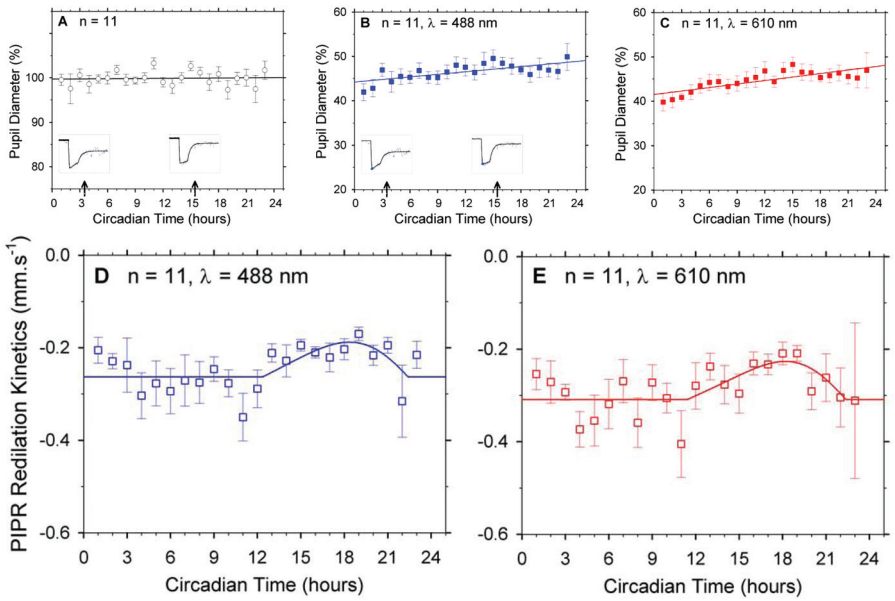

Figure 28: Diurnal cone photoreceptor contributions to the human pupil light reflex. **(A)** Baseline pupil diameter of 11 participants (mean ± SEM) viewing a uniform photopic screen, recorded over 20–24 hours **(B)** Average maximum pupil constriction (488 nm) for 11 participants (± SEM). Insets; Coloured lines show baseline pupil diameter (Fig. 1A) and maximum constriction of one participant (19,F) at circadian times of 3.5 h and 15.4 h. **(C)** Average maximum pupil constriction (610 nm) for 11 participants (± SEM). **(D)** Redilation kinetics ($mm{\cdot}s^{-1}$) derived from the time-constant of the best-fitting exponential functions to the 488 nm PIPR. **(E)** Re-dilation kinetics ($mm{\cdot}s^{-1}$) for the 610 nm PIPR. Change in post-illumination pupil response amplitude and kinetics independent of the constant external illumination demonstrates circadian control of mRGC activity. (Zele et al. 2011)

found. Putative SCN-mediated negative feedback mechanism gating mRGC activity was suggested for the observed phenomenon based on the data on gene feedback loops (Hastings et al. 2003; Garcia-Ojalvo 2011), and circadian variation in melanopsin mRNA and protein synthesis (Hannibal et al. 2005; Mathes et al. 2007).

3.6.1 *Adaptation*

Adaptation of PLR response like the circadian rhythmicity is not well understood and extensively studied either (for comparison, see sections 2.4.8and 2.4.9 for melanopsin adaptation). Early studies have found that the threshold for a criterion response for PLR varies in analogous to the visual threshold both with bleaching backgrounds (Alpern et al. 1959; Alpern and Ohba 1972) as with real backgrounds (Schweitzer and Bouman 1958; Alexandridis and Dodt 1967, Alexandridis and Koeppe 1969; Schubert and Thoss 1967; Webster 1971,

Webster et al. 1968). However, some of the results were criticized for experimental conditions (Brecher 1959) leading Ohba and Alpern 1972 to conduct a study on adaption of PLR for light onset (positive pulse), using the criterion response (0.5-1 mm constriction depending on the condition) protocol (Webster et al. 1968). The obtained results were in line with the results for visual threshold studies (Burke and Ogle 1964) suggesting a common neural pathway for both responses. The possibility of parallel channels undergoing identical adaptations could not be excluded, with the use of short flashes not revealing mRGCs responses.

Study by Stark 1962 examined the dark adaptation effect on transient pupil constriction in response to light offset (negative pulse). Author varied the period of time in the dark (varying pulse width of the negative pulse) and exposing the retina to light. The light level was being controlled by the experimenter and adjusted to give a constant amplitude response. It was shown that the dark adaptation process for the negative pulse was significantly faster (order of couple of seconds, compared to the time constant 120 sec for light onset for the same condition) than for the light onset. It was suggested, that the retinal sensitivity is not a direct function of the instantaneous states of pupil area or stimulus intensity, but a function of the past history of these states. These results were supported of earlier findings by Boynton 1961.

3.7 ANIMAL MODELS OF PLR

The detailed analysis of pupillary light reflex in various animals is beyond the scope of this work and interested readers are referred to reviews on pupil function for example in terrestrial vertebrates (Malmström and Kröger 2006), flies (Roebroek and Stavenga 1990a), rhesus monkeys (Clarke et al. 2003a;b), macaques (Pong and Fuchs 2000a;b), and in rats (Young and Lund 1994). For animal optical system, there are schematic eye models are available for example for macaques (Lapuerta and Schein 1995), rat (Hughes 1979), mouse (Remtulla and Hallett 1985), rabbit (Hughes 1972), pigeon (Marshall et al. 1973), cat (Vakkur and Bishop 1963); and see Martin 1983 for general overview of vertebrate eye models. For visual system of mice, see Jacobs and Williams 2007 for ocular media and Schaeffel 2008 for visual function in mice. A method to measure ocular media transmission in animals *in vivo* is described by Dillon et al. 2000, being also possible with Scheimpflug technique (Wegener and Laser-Junga 2009) as demonstrated for salmon ocular media for example (Wegener et al. 2001) .

Typically rodents are anesthetized for pupillary recordings (Hussain et al. 2009), and this itself can have an effect on the recorded pupillary response. For example, light ketamine-xylazine sedation

method has been validated in some recent animal studies (Aleman et al. 2004; Mukherjee and Vernino 2007; Hussain et al. 2009) and is considered not to effect the pupillary response. Anxiety, in case without anesthesia, can also result in recordings with artifacts (Bitsios et al. 1996b; Pollak et al. 2010), being even more pronounced in mice with retinal degeneration (Cook et al. 2001).

The closest animal model for human PLR is the primate model with macaques (Pong and Fuchs 2000a;b) and rhesus monkeys (Clarke et al. 2003a;b) characterized. In primates, it is possible to use alert animals without anesthesia eliminating their possibly compromising effects on PLR. Clarke et al. 2003b found the rhesus monkey providing an excellent model for experimental studies of the neural control of the pupil. Major differences with rhesus monkeys and humans were, the more variable PLR of the monkey and significantly shorter minimum latency for pupil constriction, [~140 ms compared to human ~200 ms (Feinberg and Podolak 1965; Lee et al. 1969; Müller-Jensen and Hagenah 1976)].

3.8 MODELING OF PLR

For quantitative synthesis of the complex phenomena for human pupillary light reflex (PLR) various mathematical modeling approaches have been used (see review by Stark 1984 of early models). Early pioneering model by Stark and Sherman 1957 was based on a third-order linear control system related on the cybernetic framework (Wiener 1947). Later the linear models have been modified to incorporate the observed non-linearities in pupil response. Biomechanical iris muscle models such as presented by Usui and Hirata 1995 and Yamaji et al. 2001; 2007 are beyond the scope of this chapter.

The first of the non-linearities in PLR, is the approximate linear relationship between steady state pupil size and the log of light level excluding the saturation at both extreme values first shown by Reeves 1920. Among the most popular of the early models for the relationship for pupil size and light intensity is the one by Moon and Spencer 1944 described as:

$$D = 4.9 - 3tanh\left[0.4\left(log_{10}(L_b) - 0.5\right)\right] \tag{11}$$

where the pupil diameter D varies from 2 to 8 mm, and L_b is the background luminance level expressed in blondels, varying from 10^5 blondels in sunny days to 10^{-5} blondels in dark nights. Link and Stark 1988 extended the relation for the pupil response latency with constant background as following

$$\tau(R, L_{fL}) = 253 - 14ln(L_{fL}) + 70R - 29Rln(L_{fL}) \tag{12}$$

where τ is the latency in milliseconds, L_{fL} is the luminance measured in foot-Lamberts (fL; mostly obsolete non-SI US unit, 1 fL $\approx$ 3.43 cd/m^2), and R is the light frequency measured in Hz. Recently, Pamplona et al. 2009 proposed a synthesized physiology-based model based on the work of Moon and Spencer 1944 and Longtin and Milton 1989. The dynamic behavior of pupil size is modeled using a delay differential equation (Erneux 2009) as following:

$$\frac{dM}{dD}\frac{dD}{dt} + 2.3026 atanh\left(\frac{D-4.9}{3}\right) = 5.2 - 0.45 ln\left[\frac{\phi(t-\tau)}{\phi}\right] \quad (13)$$

where M is iris muscle activity in scaled arbitrary units, D is the pupil diameter in mm, light flux ϕ is expressed in lumens, latency τ is calculated from Eq. (12) noting that 1 blondel = 0.0929 fL = 0.3183 cd/m^2. Pupil constriction velocity is approximately 3× faster than (re)dilation velocity (Ellis 1981; Bergamin et al. 1998). Differential time steps for constriction (dt_c) and dilation (dt_d) can be solved numerically from the following:

$$dt_c = \frac{T_c - T_p}{S} dt_d = \frac{T_c - T_p}{3S} \quad (14)$$

where T_c and T_p are respectively the current and previous simulation times (times since the simulation started) measured in milliseconds, S is a constant that affects the constriction/dilation velocity and varies among individuals. The higher the S value, the smaller the time step used in the simulation and, consequently, the smaller the pupil constriction/dilation velocity. The model was designed to handle individual variations in PLR (Tryon 1975; Semmlow et al. 1975) as shown for differences in pupil diameter (Crawford 1936 ; Moon and Spencer 1944; De Groot and Gebhard 1952; Ellis 1981; Winn et al. 1994), latency, and constriction and re-dilation velocities (Ellis 1981; Bergamin et al. 1998).

The second nonlinearity in PLR, the pupil-size effect (PSE; Sun et al. 1983; Sun and Stark 1983; Krenz and Stark 1984) describes the dependency of the earlier described (3.2.2) phenomena pupillary escape (as named by Lowenstein and Loewenfeld 1969) and pupillary capture (Usui 1974) on the operational range of the pupil size and not solely on light intensity. When the pupil operating level is large (e.g. constriction from dark-adapted pupil to light pulse) pupillary escape occurs; if the operational range is small (e.g. light-adapted pupil and light pulse), pupillary capture occurs. Functionally, in case of initially large pupils (scotopic conditions) it is less important for the pupil to regulate the long-term light flux onto the retina via the pupil, thus causing pupillary escape in the large pupil. Conversely, with a small pupil (photopic conditions) regulation of light flux into the eye be-

comes more important causing pupillary capture to occur (Sun et al. 1983).

The third nonlinear phenomenon in PLR, is the "AC rectifier effect" (Sun et al. 1979; 1981; Privitera and Stark 2006) in which pupil response is smaller and slower for light decrements than to light increments. This phenomenon has been attributed to the ganglion Y cell, (see for example Gaudiano 1994) and was represented as a rectifier element in the "AC pathway" in the control engineering inspired Matlab-Simulink model of Privitera and Stark 2006, analogous to the rectifier block in electrical engineering (Pires and Silva 2002). The observed phenomenon is closely related to the pupillary Varju-Troelstra effect (Varjú 1964; Troelstra 1968) in which average pupil area is reduced as modulation coefficient (m, amplitude of oscillation) increases with average light level held constant. Psychophysical equivalent to this is the Bezold-Brücke effect (cf Bimler and Paramei 2005) describing the nonlinear increase in perceived brightness as modulation coefficient is increased.

The fourth PLR non-linearity is the level-dependent latency, in which the latency depends both on the adaptation light level (before light pulse) and the light pulse intensity (Myers and Stark 1993, Myers et al. 1993). First evidence of the level-dependent latency came from the studies of Sandberg and Stark 1968 with sinusoidal light stimuli for PLR and ofMiller and Thompson 1978a for pupil cycle time (PCT). The effect was modeled by Myers and Stark 1993, Myers et al. 1993 as a Level Dependent Signal Flow (LDSF) operator (called also "bucket brigade" (Janssen 1952)) which presents pupil response as a high-pass lossy transmission line. In practice the "LDSF block" results in an antilog operator, transient signal response becoming more proportional to the linear light intensity rather than its logarithm as shown with *Limulus* ommatidia (Fuortes and Hodgkin 1964; Section 4.1). Similar observations were made by Lennie 1981, transient signals (large high frequency content) exhibiting the shortest latency and the least LDSF.

The fifth PLR nonlinearity arises from the iris length-tension curve which is analogous to Huxley sliding filament model (Huxley 2004) for striated muscles, contributing to the observed asymmetry between dilatation and contraction kinetics (Reeves 1918; Clynes 1961; Stark 1959). As this non-linearity characterizes a wide portion of the pupillary range, it has further been named "expansive range non-linearity" (Semmlow et al. 1975). This nonlinearity has been modeled for example with a sigmoid function (Privitera and Stark 2006).

In addition to the above-mentioned phenomena, there is the need to include the effect of pupil noise (see Section 3.4) to the model of PLR. While the exact physiological origin of the noise is unknown (Ukai et al. 1997, Usui and Stark 1982), it has been modeled with added noise block (Stanten and Stark 1966, Stark and Cornsweet 1958, Stark 1959, Stark et al. 1958). Pamplona et al. 2009 approximated the

pupil noise by adding small random variations (standard deviation of the noise corresponding ~10% of the pupil diameter (Usui and Stark 1982)) to the light intensity (between $-10^{0.3}$ and $10^{0.3}$ blondels), to induce small variations in the pupil diameter (of the order of 0.2 mm, Hachol et al. 2007), in the frequency range of 0.05Hz to 0.3Hz. Additionally, the Gaussian distribution of pupil noise can be skewed at large and small pupil ares (Stark 1984) to reflect the length-tension relationship of the iris muscles (Usui and Stark 1978; 1982). Pupil noise can thus be simply considered as cross-talk additive Gaussian noise injected into the pupil system at midbrain level (Usui and Stark 1982).

The Matlab-Simulink model for binocular pupil responses of Privitera and Stark 2006 is shown in Figure 29 represented as blocks typical for control engineering (Dorf and Bishop 2010). The pupil model is divided in three main compartments: the two afferent retinal pathways are separated (left and lower-left inset) and they both implement logarithmic response to light and "AC rectifier effect", as well as the DC and AC modules. Light stimuli can be applied to both pathways simultaneously or in alternating fashion. The midbrain ocular motor complex (Brain module in the center lower-middle inset) implements the pupil size effect and combines together the AC and DC dynamic components. The pupil noise is inserted to the system before the efferent oculomotor bifurcation. The oculomotor III nerve efferent pathway, one for each eye, has the second-order lag block and transport delay modules (Verbeek 2000; Dorf and Bishop 2010) and continues to the final length–tension non-linearity. Specific melanopsin block has been excluded from the model, and the authors hypothesize that the description of melanopsin dynamics could lead to a different or more elaborated definition of the PSE mechanism. Furthermore, the gain control operator is thought to be defined in the Brain block generally enough, and it could be functionally extended to interpret different retinal contributions to the PSE non-linearity. Alternatively, a third melanopsin input could for example be added in parallel to the AC and DC channels (Privitera and Stark 2006).

3.9 CLINICAL AND DIAGNOSTIC USE

Pupillary light reflex (PLR) and the accompanying pupil phenomena hippus and pupil cycle time have been used successfully for diagnostics and monitoring of various ocular and non-ocular pathologies, thus the clinical applications are briefly reviewed here. The clinical use of pupillary near reflex (PNR) is beyond the scope of this chapter, but interested readers are referred to Digre 2005 and McDougal and Gamlin 2008.

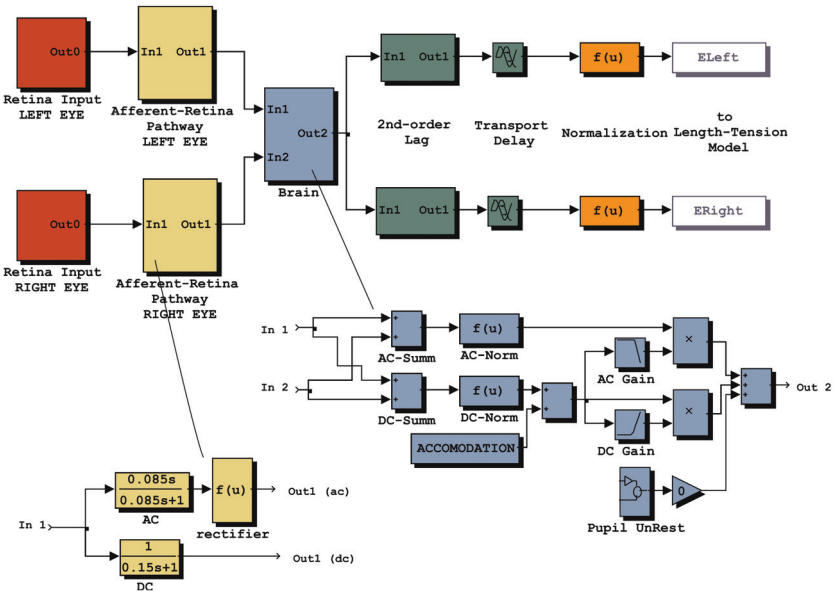

Figure 29: The binocular Matlab-Simulink pupil model divided into three main compartments: the two afferent retinal pathways, (left and lower-left inset), the mesencephalic ocular motor complex, (brain module and the attached lower-middle inset), and the two oculomotor III nerve efferent pathways (right). (Privitera and Stark 2006)

3.9.1 *PLR Diagnostics*

Variety of disorders effecting retinal, midbrain, and autonomic functions concurrently can be easily assessed non-invasively measuring pupillary light reflex (see Kardon 1995; Kawasaki 2005 and McDougal and Gamlin 2008 for a more comprehensive reviews). For diagnostic purposes, abnormalities of the pupil are traditionally classified as afferent or efferent defects (see Figure 15). PLR has been used as a diagnostic tool in pathologies such as multiple sclerosis (Surakka et al. 2008), autism (Fan et al. 2009a), retinitis pigmentosa (Skorkovská et al. 2008), Alzheimer's disease (Fotiou et al. 2007), diabetic retinopathy (Straub et al. 1994;Long et al. 2007), optic nerve diseases (Bremner 2004) and glaucoma (Carle et al. 2011b; Asakawa et al. 2010; James et al. 2011). PLR has been used in clinical monitoring of the response to analgesics (Knaggs et al. 2004), visual field loss (Bergamin and Kardon 2002) and autonomous nervous system (Yamaji et al. 2002)

Afferent defects in the PLR are characterized by an asymmetry in the PLR between the eyes in response to a light (Thompson 1992; Digre 2005), referred as relative afferent pupillary defect (RAPD) reflecting differential light sensitivity of the two eyes. Various midbrain lesions can produce abnormalities in the PLR, which are characterized by an absence or attenuation of the light reflex in one or both eyes. Efferent defects of the PLR are most often characterized by a dissymmetry in the size of the two pupils under steady-state illumi-

nation, referred as anisocoria. More commonly, anisocoria is caused by a unilateral global dysfunction in either the sympathetic or the parasympathetic branch of the ANS.

Early study by Straub et al. 1994 examined the valid clinical parameters of PLR suggesting maximal pupil area and pupil response time being the most relevant in clinical settings with pupillary fusion frequency [analog to critical flicker fusion (CFF) frequency in vision, see for example Ives 1922; Brown 1965a; Bowles and Kraft 2012) found to be too time-consuming for practical purposes. Bergamin et al. 2003 found the peak contraction (pupillary escape, see 3.2.2) carrying the most diagnostic value with highly variable irradiance response. The inter-eye asymmetries in latency was suggested to be clinically useful in a study by Bergamin and Kardon 2003. In some patients, the diagnostic difference was the most pronounced at lower intensities, in some at midrange intensity, yet others showed the greatest diagnostic power at the brightest intensities. In addition to light flux increments, the measurement of pupil responses to the onset of stimulus structure, color and movement was suggested to provide clinical information on the optic nerve fiber functionality (Barbur et al. 2004; Moro et al. 2007). These results highlight the need to consider various parameters of PLR both in clinical and research settings.

There has been increased interest after the discovery of melanopsin, using post-illumination pupil response (PIPR, see e.g. Markwell 2011, the PIPR being the same as persistence described in 3.2.2) as a diagnostic tool for pathologies such as diabetic retinopathy (Feigl et al. 2011), retinitis pigmentosa (Kardon et al. 2011), Leber hereditary optic neuropathy (Kawasaki et al. 2010) and with glaucoma (Kankipati et al. 2011). In practice, the melanopsin-mediated PIPR is studied using a pair of light wavelength (termed also as chromatic pupillometry, (Herbst et al. 2011; Kardon et al. 2011)) of which the other preferentially stimulates the melanopsin system (blue light) whereas the other does not (red light). For example, in a study of Kardon et al. 2011 chromatic pupillometry was shown to provide a suitable clinical tool, particularly in patients with severe retinitis pigmentosa and non-recordable electroretinography (ERG).

3.9.2 *Pupil noise*

In addition to PLR, the pupil noise (i.e. hippus, see Section 3.4) has been used in various experiments. Pupil noise has been used for example to study the changes in arousal levels in patients with narcolepsy (O'Neill and Trick 2001; Prasad et al. 2011), in bright light treatment studies (Szabo et al. 2004; Warga et al. 2009; Rautkylä 2011), in studying workplace lighting (Wilhelm et al. 2011), in drowsiness monitoring (Morad et al. 2000; Nishiyama et al. 2007), and in quantifying the progression of Parkinson's disease (Jain et al. 2011). The

pupil noise is characterized typically as either cumulative changes of pupil diameter (Pupil Unrest Index (PUI), e.g. Lüdtke et al. 1998) or by the power spectrum of the noise using for example traditional Fourier (Grünberger et al. 1996), short-time Fourier (STFT, Nowak et al. 2008) or wavelet analysis (Leal et al. 2011).

3.9.3 *Pupil cycling time*

When a narrow beam of light is placed at the iris margin, some light entering the eye, the pupil contracts. The iris margin moves towards the center of the pupil, thereby preventing the light beam from entering the eye, and the pupil dilates back. This allows the light to enter the eye again, the pupil to contract, and the cycle of pupil contraction and dilation is established. This repetitive change in pupil size is known as pupil cycling (for modeling see Bressloff et al. 1996; Bressloff and Wood 1998), and the time taken to complete one cycle, the period, is termed the "edge-light pupil time" or pupil cycling time (PCT) (Miller and Thompson 1978a). The period of the cycle will depend upon the time delays in the pupillary reflex arc and the mechanical properties of the iris musculature. Hence pupil cycling has been used in studies on the dynamic properties of pupillary movement (Milton and Longtin 1990; Howarth et al. 2000). The pupil cycling can be induced electronically modulating the light rather than by mechanical moving of the light simplifying the experimental setup (Milton and Longtin 1990; Howarth et al. 2000).

The clinical use of pupil cycling has been extensive, and abnormal PCTs have been reported in various conditions where neurological changes might be expected. These include (Miller and Thompson 1978b), myasthenia gravis (Lepore et al. 1979), HIV infection (Maclean and Dhillon 1993), optic nerve compression (Weinstein et al. 1980), space-occupying lesions (Manor et al. 1982), central depressant drugs (Safran et al. 1981), multiple sclerosis (Wybar 1952), optic neuropathy (Milton et al. 1988), primary closed-angle (Clark and Mapstone 1986) and open-angle (Niles and Bartiss 1991) glaucoma, ocular hypertension (Clark and Mapstone 1987), diabetes (Clark 1988; Zangemeister et al. 2009; Lee et al. 2011), progressive autonomic failure (Clark and Ewing 1988), Horner's syndrome (Blumen et al. 1986), leprosy (Karaçorlu et al. 1991), gastrooesophageal reflux (Chakraborty et al. 1989) and familial dysautonomia (Gadoth et al. 1983). So far, pupil cycling time has not been linked to melanopsin system as a diagnostic or research tool.

3.9.4 *Pupil perimetry*

Recently Carle et al. 2011c proposed a model for assessing asymmetries in pupillary response components for clinical applications

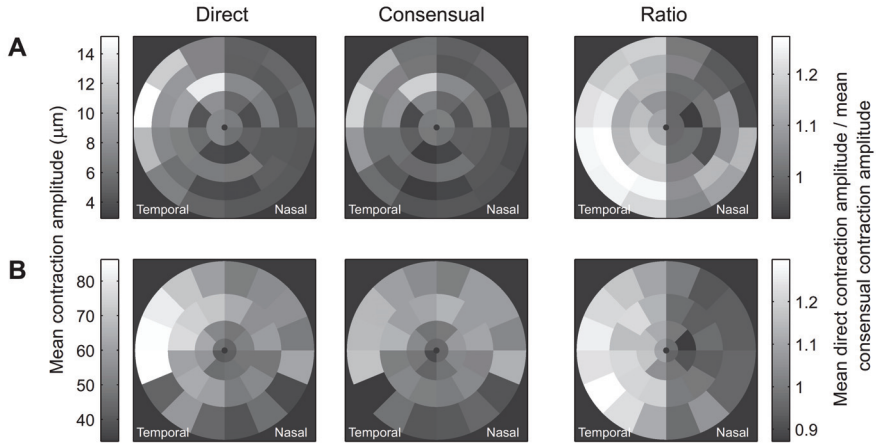

Figure 30: **Asymmetries in pupil contraction.** Mean pupillary contraction amplitudes and direct/consensual ratios for two representative stimulus protocols (see Carle et al. 2011c). Larger values are plotted in lighter shades. Mean amplitudes of subjects' direct responses (left) exhibit a gradient of sensitivity across the visual field. (B). A similar pattern is seen in the means of consensual responses (center). In contrast, ratios between direct and consensual responses in corresponding test regions exhibit a different pattern: relatively homogeneous values were produced within each hemifield, these being consistently larger to stimulation in the temporal field (right) (Carle et al. 2011c).

using multifocal pupillographic objective perimetry (mfPOP, True-Field Analyzer®, Seeing Machines Inc., the authors representing the company as well), allowing the stimulation of specific parts of the visual field (see Figure 30). The proposed model suggested clinical utility of the method for the assessment of neural dysfunction using pupillary responses. The method was extended to quantify melanopsin-mediated pupillary responses in glaucoma diagnostics (Carle et al. 2011b), the preliminary evidence not demonstrating a significant melanopsin-mediated clinical diagnostic value (Carle et al. 2011a). However even the 750 ms light blue pulse (75 cd/m², wavelength not specified in the poster) protocol showed according to the authors significant melanopsin contribution not fitting the spectral sensitivity of S-cones.

4

MELANOPSIN BISTABILITY

Bistability – the capacity of a system to exist in either of the two stable states when at equilibrium - is a general property of many biological (Ferrell 2002; Rietkerk et al. 2004; Samoilov et al. 2005; Shoemaker 2011), physical (Sessoli et al. 1993; Itkis et al. 2002) and engineered systems (Gibbs 1985; Epstein 2007; Kuo et al. 2011). The observed bistability can either be an emerging property of the system macroscopically (Bhalla and Ravi Iyengar 1999; To and Maheshri 2010) or to be observed in the individual components (Korogod and Kulagina 2000; Loewenstein et al. 2005), the latter being the case with putative melanopsin pigment bistability (Rollag 2008; Section 5.5.1). If the bistability is light-controlled, the system can be referred as photochromic [photochromic chemicals used in optoelectronics (Dulić et al. 2003)] or as photoreversible [e.g. Dronpa (Donnert et al. 2007), fluorescent protein derived from *Pectininiidae* coral reviewed in Newman et al. 2011] system also.

Rhodopsin and related pigments possess 11-*cis*-retinal in the dark, and light (with a frequency of ν_1 in Figure 31A) isomerizes the retinal to the all-*trans* form (see Section 2.3). The photoproduct *all-trans* of vertebrate cones/rods is thermally unstable and eventually releases all-trans-retinal chromophore (i.e. it "bleaches") to become a colorless opsin (Wald 1968, Figure 31A). In contrast, in invertebrate systems (see extensive review by Hillman et al. 1983) the active photoproduct (metarhodopsin) has a much higher thermal stability; the stable photoproduct (*all*-trans*)* is stable and can be reverted to the original dark state by subsequent light absorption (with a frequency of ν_2 inFigure 31B), showing photoregeneration ability (Hubbard and St. George 1958). The ability of bistable pigments to bind to 11-*cis* and all-*trans* retinals is similar to the characteristics of typical G-protein coupled receptors (GPCRs) when they bind to antagonist and agonist (Figure 31C) making rhodopsin a suitable model for various GPCRs (Palczewski et al. 2000; Hofmann et al. 2009).

4.1 INVERTEBRATE VISUAL SYSTEM

4.1.1 *Insect optics*

In flies, the eight photoreceptors (peripheral R1-6 and central R7 and R8) of an ommatidium form an open rhabdom (the rhabdomeres remain separate), and each fly rhabdomere acts as an optical waveguide

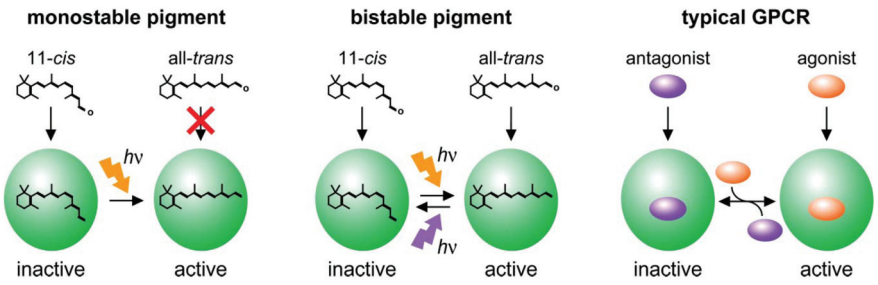

Figure 31: **Comparison of activation scheme among monostable and bistable pigments and typical GPCRs**. Monostable pigments can bind to 11-cis-retinal but not all-trans-retinal directly. Bistable pigments can bind both to 11-cis and all-trans retinals directly, and 11-cis-retinal and all-trans-retinal binding states are interconvertible upon light absorption. The ability of bistable pigments to bind to 11-cis and all-trans retinals is similar to the characteristics of typical GPCRs when they bind to antagonist and agonist. The inactive and active states of typical GPCRs are stabilized by binding of antagonist and agonist, respectively. In general, addition of excess antagonist or agonist can exchange ligand bound to typical GPCRs, because there are not covalent bonds to ligands in typical GPCRs, unlike in monostable and bistable pigments. Tsukamoto and Terakita 2010 add subscripts 1 and 2 to ν's

(Hardie 1986). In bees and butterflies, the nine photoreceptors of an ommatidium have their rhabdomeres joined into a fused rhabdom, which acts as one, efficient optical waveguide (review by van Hateren 1989). Each ommatidium consists of a light-diffracting facet lens, a crystalline cone, and photoreceptor cells with a wave-guiding rhabdom (Beersma et al. 1982; Stavenga 2003, Stavenga and van Hateren 1991; and see Figure 32A,B).

The rhadbomeres of *Drosophila* consist of roughly 30-50,000 microvilli (Hardie and Postma 2008), each 1,2 μm long and 60 nm in diameter. Each microvillus contains ~1,000 rhodopsin molecules close packed at a density of ~4,000 μm^{-2} (Hardie and Postma 2008), compared to a higher rhodopsin density of ~25,000 μm^{-2} in mouse rod outer segments (Liebman et al. 1987). The parallel arrays of microvilli also provide rhabdomeric an intrinsic dichroism (Snyder and Laughlin 1975) allowing Drosophila, *arthropods* and mollusk to detect and discriminate polarized light (Marshall and Cronin 2011; Hardie 2012), ability being largely absent in humans (Le Floch et al. 2010). Rhabdomeres form a precise hexagonal in cross section with six peripheral rhabdomeres (R1-6) all containing the same rhodopsin (Rh1, λ_{max}~ 480 nm), with the central tiered rhabdomere (R7, R8) containing variety of visual pigments (Rh3-6,λ_{max}~ 340, 370, 440, and 510 nm) utilized in color vision (Yamaguchi et al. 2010) analog to the human fovea (Section 2.3). In most physiological studies, the R1-6 cells dom-

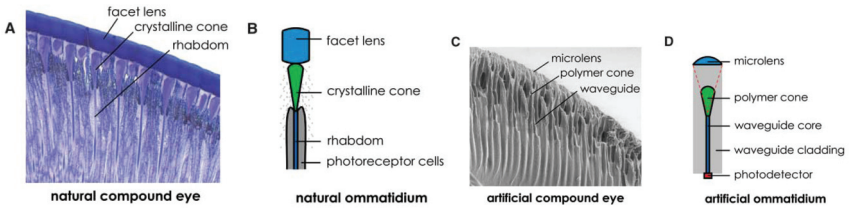

Figure 32: Anatomical comparisons between a natural compound eye and an artificial compound eye described from the cross sections. **(A)** An optical micrograph of a honeybee's apposition compound eye (courtesy of B. Greiner). As an individual optical unit, **(B)** a natural ommatidium consists of a facet lens, a crystalline cone, and photoreceptor cells with a wave-guiding rhabdom. **(C)** A scanning electron micrograph of an artificial compound eye and **(D)** an artificial ommatidium comprising a microlens, a polymer cone, and an optical waveguide that has a higher index core surrounded by a lower index cladding in a polymer resin. Light impinging onto a microlens is coupled with polymer cones and waveguides and then guided to the end of the waveguide. (A-D from Jeong et al. 2006))

inate the response, and special study design is needed to isolate the R7 and R8 responses (Minke et al. 1975).

The omnidirectionally arranged ommatidium collects incident light with a narrow range of angular acceptance independently contributing to the capability of wide field-of-view (FOV) detection [Hardie et al. 1989, conceptually similar to plenoptic (light field) imaging (Ng et al. 2005; Ihrke et al. 2010)]. The whole optical system is typically referred as the compound eye, containing ~750 facets in *Drosophila*. The ommatidia has inspired a fabrication of several engineered optical systems (Jeong et al. 2006). These biomimetic compound eyes are anatomically as well as functionally close to natural compound eyes (Figure 32C). The artificial ommatidium consists of a honeycomb-packed hexagonal microlens, a cuvette-shaped polymer cone, and a polymer waveguide (Figure 32D).

Besides the compound eye, the fly employ a second visual system, the ocelli containing Rh2 rhodopsin photopigment (Srinivasan and Zhang 2004). The ocelli system is low-spatial frequency system capable of responding even faster than the compound eye (Nässel and Hagberg 1985). It has been shown to play a role in sensing rotations crucial for gaze stabilization (Hengstenberg 1993), but in regard to the scope of bistable photopigment system it has not been shown to play any role (Krapp and Wicklein 2008).

4.1.2 *Phototransduction*

Phototransduction can be roughly divided to ciliary (vertebrate, introduction in Section 2.3) and to rhabdomeric (invertebrate) transduction (see reviews by Hardie and Raghu 2001 and Yau and Hardie

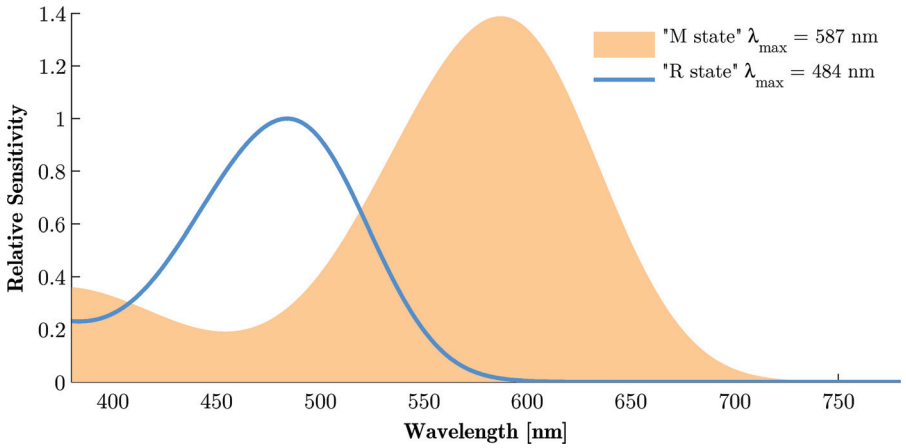

Figure 33: **Illustration of bistable photoreception.** Illustration of the light-driven "R state" (corresponding to rhodopsin) and "M state" (corresponding to the metarhodopsin) isoforms of the visual pigment. The peak spectal sensitivities correspond to the putative peaks obtained by Mure et al. 2009 for human melanopsin *in vivo*. The "M state" restoring visual sensitivity (renegerating the pigment back to the "R state") has a spectral sensitivity extending throughout the visible light spectrum, thus in practice it is not possible to drive all pigment population to the "M state".

2009). Some organisms exhibit photopigments of both type (Arendt 2003), invertebrate characteristics of vertebrate melanopsin being the most obvious example (Graham 2008). The most significant between the invertebrate and vertebrate systems in regard to this work is the ability to regenerate the "inactivated" visual pigment back to "responding state" employing another wavelength of another wavelength (Figure 33A; however see Section 4.5for photoregeneration in vertebrate vision). The photoisomerase spectral sensitivity (M state) can be either red-shifted (bathochromic shift, as in Figure 33A), blue-shifted (hypsochromic) or overlapping with each other (see Table 1 of Hillman et al. 1983). The hypsochromic is the dominant arrangement in invertebrate species (Stavenga 1992; Stavenga and Hardie 2010) making only handful of invertebrate suitable as models for putative bathochromic bistable melanopsin photopigment. Functionally the red and blue-shifted pigment system differ significantly in regard to their exploitation of screening pigments (4.1.4) and in their dark regeneration kinetics (see below). In *Drosophila*, both arrangements are found with the most studied rhodopsin Rh1 of R1-6 having a $\lambda_{R,max}$~ 470 nm and $\lambda_{M,max}$~ 570 nm, whereas in rhodopsin Rh6 of R8, the M state is blue-shifted to $\lambda_{M,max}$~ 468 nm with the R state sensitivity peaking at $\lambda_{R,max}$~ 508 nm (Salcedo et al. 1999).

The process from light activation until regenerated visual pigment is referred as the visual cycle (Ala-Laurila et al. 2006; Kusakabe et al. 2009), which in vertebrates is different (Figure 34A) for the cones (Wang and Kefalov 2011) and for the rods (Mata et al. 2002). Simi-

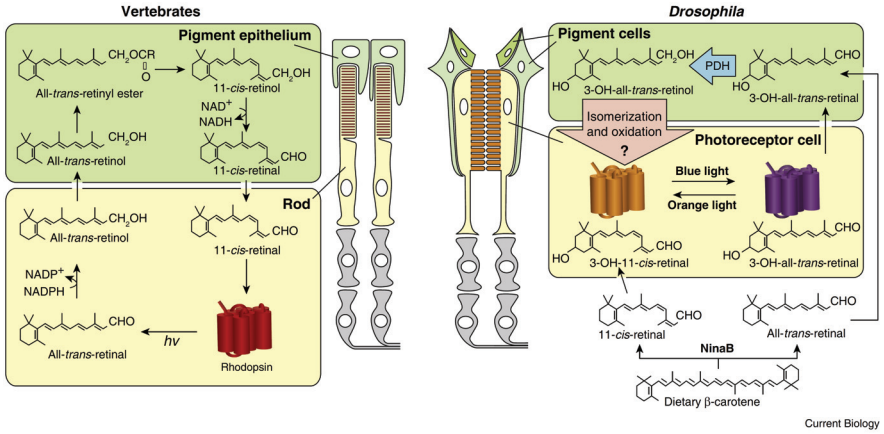

Figure 34: The vertebrate visual cycle (left) and the putative visual cycle in Drosophila (right). See text for full details. The enzymatic activity of PDH described by Wang et al. 2010 is illustrated by a block blue arrow; hypothetical steps of this cycle, for which molecular identities of underlying enzymes and their cellular localization are unknown, are illustrated by a block pink arrow. Visual pigments are shown as seven-helical structures in colors imitating their actual appearance. Parts of the drawing are modified from (Arshavsky 2002; Wang et al. 2010), adapted from Arshavsky 2010

larly, dark regeneration pathway exists for invertebrate pigments as recently shown by Wang et al. 2010 (see also reviews by Arshavsky 2010 and von Lintig et al. 2010). The relative stability of the inactivated M-state (all-*trans*-retinol state in Figure 34) has been taken as the basis for the term "bistable photopigment" as regeneration to the R-state (11-*cis*-retinol) is not immediately followed, the time course of regeneration depending on the species.

Strictly speaking neither rhodopsin nor metarhodopsin is stable in invertebrates. Thermal isomerization of rhodopsin occurs at an extremely low rate, i.e., half-time is several years (Lisman and Bering 1977), whereas metarhodopsin conversion in the dark varies hugely depending on the species. In bathochromic fly, enzymatic visual pigment turnover is slow, taking several hours (Pak and Lidington 1974; Stavenga 1975; Bruno et al. 1977; Schwemer 1989), whereas in hypsochromic butterflies, the time-course of same process is reduced to several minutes (Bernard 1983). In contrast, the thermal decay half-life of vertebrate tod rhodopsin was estimated to be 2,000 years (Burns and Baylor 2001), and for primate rod to be up to 420 years (Baylor 1987), this thermal stability ensuring reliable detection of very dim light. Furthermore, there is an evidence for diurnal modulation of the turnover rates of invertebrate pigments (Stowe 1980; Toh and Waterman 1982).

The response kinetics of the vertebrate and invertebrate photoreception differ (see Section 4.5). Fly photoreceptors possess the fastest

known G-protein-signalling pathways (for review see Hardie and Raghu 2001), responding around 10 times more quickly than mammalian rods and ~100 times faster than toad rods recorded at similar temperatures. By contrast, despite their exquisite sensitivity to single photons (Wu and Pak 1978; Howard et al. 1987; Pumir et al. 2008), fly photoreceptors successfully light adapt over the entire environmental range, up to ~10^6 effectively absorbed photons per second (Juusola and Hardie 2001a). For example, in light adapted flies, photoreceptors can respond to visual stimuli at a rate of up to 100 Hz in *Drosophila* [an information capacity of 200 bits per second at 25°C (Juusola and Hardie 2001a; Takalo et al. 2011), and up to 300 Hz in rapidly flying *Calliphora* (Weckström et al. 1991).

The single-photon absorption in *Drosophila* photoreceptors lead to the opening of ~15 cation channels depolarizing the photoreceptor, in contrast to vertebrate hyperpolarization requiring roughly closing of ~200 cation channels (Henderson et al. 2000; Hardie and Postma 2008) during a so-called "quantum bump" . The quantum bumps n *Drosophila* have a duration of ~20 ms (Figure 35A), with a characteristically highly variable latency of between ~20-100 ms (Schnakenberg 1989; Scott and Zuker 1998; Pumir et al. 2008), in contrast to rather invariant latencies of invertebrates (Hardie and Postma 2008). The waveform of the of the macroscopic response (Figure 35B) in *Drosophila* is a linear superposition of the individual quantum bumps, over a large range of the quantum bump waveform and its latency dispersion. The complexity of the waveform is similar to the dim-flash responses in vertebrates with rod response being described by convolution of four (Baylor et al. 1979), and cones by five single-exponential decays (Kraft 1988), contrasting the only 2 stage waveform of mouse mRGCs (Do et al. 2009).

Addition to the intracellular whole-cell recordings (Dolph et al. 2011b), extracellular electroretinography (ERG) is possible in *Drosophila* by placing an electrode on the surface of the cornea (Dolph et al. 2011a; Belušič 2011). The recorded ERG represents the summed activity of all the photoreceptors with contributions from higher-order neurons and glial cells. Thus, the recorded ERG is an "indirect estimate" of the photoreceptor responses, but due to its ease of use it has been widely used in bistability studies (cf. Belušič et al. 2010) . Figure 35C shows a simplified recording demonstrating both rapid ON (light onset) and OFF (light offset) response rising from second-order interneuron activity [similar to motion ON and OFF channels in *Drosophila* (Joesch et al. 2010)] *as* well the prolonged depolarization afterpotential (PDA) induced by "strong" blue light (see later 4.4.4).

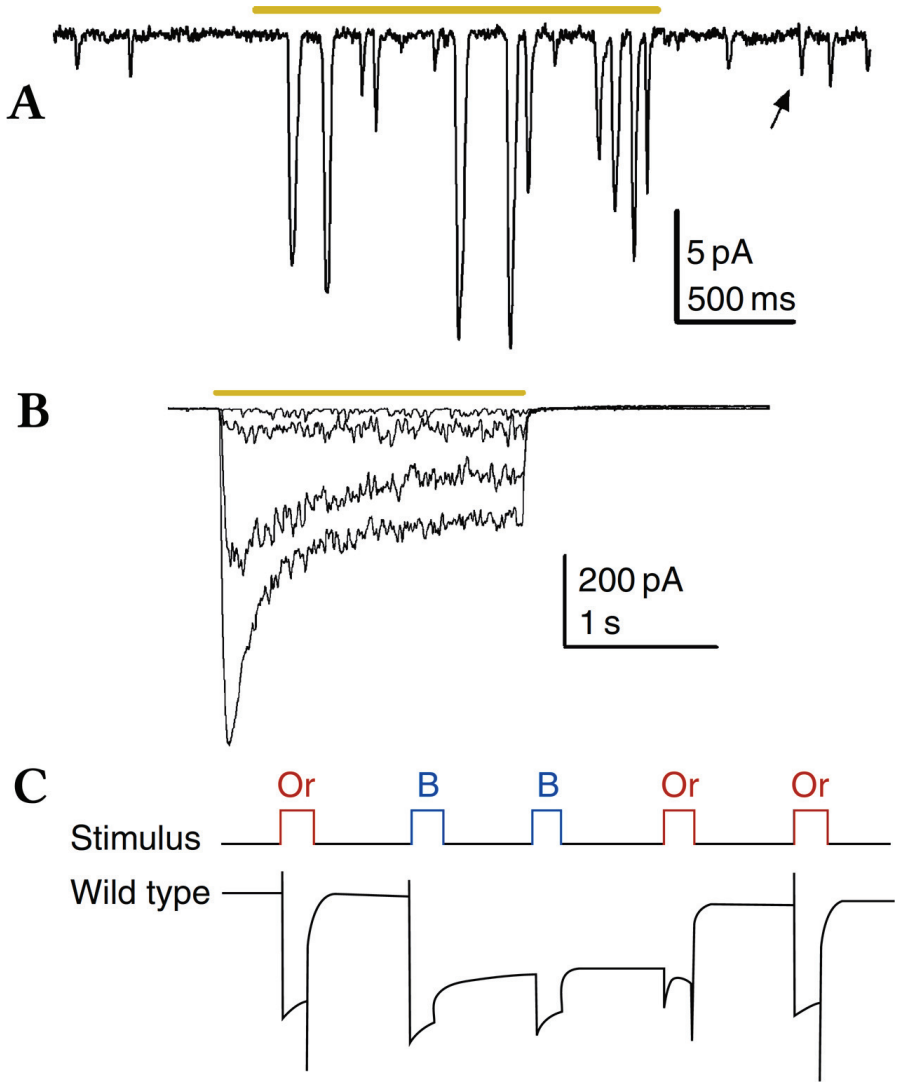

Figure 35: **Illustration of Drosophila light responses (A)** Response of a whole-cell voltage-clamped photoreceptor to 2 s of dim illumination (2 effectively absorbed photons per second, bar). In the dark, small 2 pA events (e.g., arrow) are likely to represent spontaneous activation of single G proteins. Light induces a train of 10 pA quantum bumps. **(B)** Responses to 2 s steps of light of increasing intensity: bumps fuse to form noisy inward currents, which then show an increasingly rapid peak–plateau transition as intensity increases (30, 300, 3000, and 18 000 photons per second). This transition is a direct manifestation of light adaptation. **(C)** Electroretinogram (ERG) recordings. In a wild-type (WT) fly a 5 s pulse of orange light elicits a typical ERG with on and off transients and a maintained corneal negative component. At light off, the potential returns rapidly to baseline; however, a blue stimulus which converts >50% of R to M, creates a prolonged depolarizing afterpotential (PDA), whilst a second blue test flash elicits a much reduced (inactivated) response lacking the transients, and which is primarily mediated by the R7 cells. A subsequent orange stimulus, which reconverts M to R, terminates the PDA and restores sensitivity. Figures adapted from Hardie and Postma 2008.

4.1.3 *Pseudopupil response*

Flies employ a highly active pupil mechanism (termed as the pseudopupil response), mediated by yellow-coloured pigment granules located in the photoreceptor cell soma, which accumulate near the rhabdomere upon light adaptation. The functions of the pupil in the fly extend those of in humans (see 3). Firstly, the pupil serves to control the light flux along the rhabdomere expanding the dynamic range of the photoreceptor (Howard et al. 1987). Secondly it narrows the angular sensitivity of the photoreceptors by absorbing preferentially from higher order waveguide modes (Vogt et al. 1982; Smakman et al. 1984; as the Stiles-Crawford effect in humans, 2.2.2). Thirdly, unlike the human pupil which is rather light tight especially in brown-eyed individuals (van den Berg et al. 1991), the fly pupil absorbs blue-green light (Roebroek and Stavenga 1990a) transmitting yellow favoring the photoreconversion from metarhodopsin to rhodopsin (Stavenga 2002), similar to the red screening pigment (Stavenga 1980, see 4.1.4 below).

The effective optical density of the pupil can be above 2 log units at the absorption peak wavelength, but in the yellow it is only 1 log unit (Roebroek and Stavenga 1990b). The pupil selectively suppresses light of the rhodopsin-converting ($R \rightarrow M$) wavelengths and transmits light of the metarhodopsin-reconverting ($M \rightarrow R$) wavelengths to maximize f_R. The rhodopsin fraction (f_R) of about 65%, resulting from white light entering on-axis with an open pupil, consequently increases to about 85% with a closed pupil (Stavenga 1980). The rhodopsin fraction can be increased further to about 95% or more with the assistance of red stray light, which has passed the red screening pigment.

As in human photoreception studies, there is a need to "open the loop" (see 3.5.1) of the pupil mechanism also in insect. In practice, this is achieved by recording sufficiently long ($\geqq$1 min in flies) after light irradiation allowing pseudopupil to reach steady-state response before the actual experimental stimulus (cf Stavenga 1976) . Half-time of the pupil closure in flies have estimated to be ~1-3 s (Franceschini and Kirschfeld 1976; Stavenga 1979), increasing to 10-20 seconds in *hymenopterans* (Stavenga and Kuiper 1977).

4.1.4 *Screening pigments*

Analogous to the human eye (see 2.2.3) and oil droplet in birds, reptiles and in fish (cf Hart 2001 for birds), most of the insect eyes contain screening pigments filtering the incoming light (see review by Stavenga 2002). Most insect eyes contain black screening pigments preventing retinal straylight in similar fashion as fundus in humans (Delori and Pflibsen 1989), thus making the pupil appear black. In addition to the yellow pigments of pseudopupil response, flies contain

red screening pigment that allow straylight to be used to reconvert M state back to R state (Figure 36).

In natural environment, fly eyes receive broadband polychromatic sky and sun light from various directions. Light entering the facet lens on-axis is focused into the rhabdomeres, but off-axis light hits the screening pigments (Figure 36, inset). The long-wavelength part of it will pass the red screening pigment and penetrate the eye. The red stray light thus can reach the rhabdomeres from oblique directions and thus can convert metarhodopsin molecules to their native rhodopsin state (review by Stavenga 1992). This filtering mechanism is however only employed in insects with bathochromically (red-shifted) shifted M absorption peak, whereas in insects with hypsochromically (blue shifted) M absorption, the screening pigment cells are packed with massive amounts of black pigment granules to protect the R state (Stavenga 2002). In most cases, fly photoreception studies are done in white-eyed mutants referred as *chalky* (Lindsley and Grell 1967; Gribakin and Ukhanov 1990), which do not contain the red screening pigment at all allowing higher possible f_M concentrations (Hardie and Postma 2008) and PDA induction (see later 4.4.4) that could be difficult to achieve in wild-type flies.

The above-described screening pigments function as color filters simply filtering the "unwanted" spectral range of light. Additionally there are pigments that "sensitize" the visual sensitivity transferring energy from one photon frequency to another frequency, in flies the transfer occurring from UV (double peaks at ~350 nm in Figure 36) to blue range both in rhodopsin and metarhodopsin (Minke and Kirschfeld 1979). This is analogous to photosynthesis in plants, in which carotene absorb "blue photons" and transfer the energy to the green-absorbing chlorophyll (Platt 1959). The mechanism appear to be mediated via dipole-dipole "direct" energy transfer [Vogt and Kirschfeld 1983; commonly referred as fluorescence resonance energy transfer (FRET), Selvin 2000]

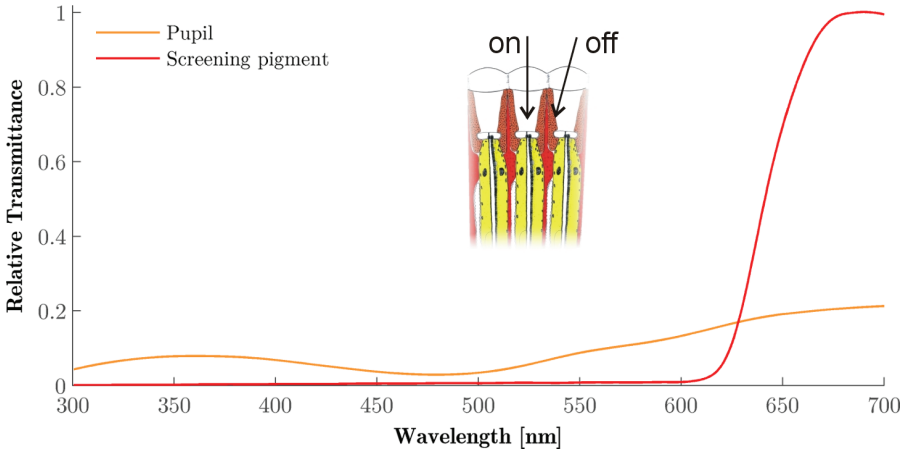

Figure 36: (inset, red). The visual pigment, contained in the rhabdomeres of the main photoreceptors, R1–6, is a rhodopsin (R) absorbing maximally at about 490 nm. Its photoproduct, metarhodopsin (M), peaks at about 570 nm. A UV-absorbing-sensitizing pigment enhances the photosensitivity of both visual pigment states (Minke and Kirschfeld 1979; Hardie 1986). The photoreceptor cells (nset, yellow) contain pupillary pigment granules, which absorb predominantly in the blue and less in the yellow and red wavelength ranges. Accordingly, the transmission is higher in the yellow and red; the degree of pupil closure, which depends on the state of light adaptation, determines the actual magnitude of the transmission. The transmission of the red- screening pigment is negligible at wavelengths up to 600 nm, but rises rapidly above this value. Whereas the pupillary pigment filters light which has entered the facet lens on-axis and propagates along the rhabdomeres, the screening pigment filters light entering the facet lenses off-axis (inset). Yellow and red light, remaining from white light filtered by the pupillary and the screening pigments, preferentially converts metarhodopsin into rhodopsin. Stavenga 2002

4.2 BISTABLE SYSTEM METHODOLOGY

4.2.1 *Definitions and equations*

The concepts involved in "bistable photoreception" differ in some aspects from those used in vertebrate "monostable photoreception", thus the review and and clarification of the essential concepts is undertaken here (adapted mainly from Hillman et al. 1983)

A. Closed system. In invertebrate visual pigment systems, it is generally considered to be closed systems, i.e. the total amount of pigment in the system is conserved without destruction or creating of visual pigment. This can formally expressed as $f_M(\lambda, \infty) + f_R(\lambda, \infty) = 1$, where $f_M(\lambda, \infty)$ and $f_R(\lambda, \infty)$ are the fractional concentrations of R and M pigment states, respectively, in equilibrium. However, it should be noted that this is not valid necessarily for experiments of long durations considering the possible of circadian and environmental influence on melanopsin pigment concentrations (Sakamoto et al. 2004; Hannibal et al. 2005)

B. Molecular absorbance coefficient. The molecular absorbance (or extinction) coefficient [$\alpha_i(\lambda)$, i = R, M, in cm² or in μm²] is a measure of the efficiency with which light is absorbed by a pigment molecule (Dartnall 1972). Its shape can be described as a nomogram as is the case with monostable ciliary photoreception, the shape slightly varying between the invertebrate nomogram (Stavenga 2010) and the vertebrate nomogram (Govardovskii et al. 2000). It can be derived for absolute units with the knowledge of peak molar absorbance (or extinction) coefficient ($\epsilon(\lambda)$ in liters · mol^{-1}· cm^{-1}) that is ~33,000-35,000 liters · mol^{-1}· cm^{-1} for *Drosophila* (Harris et al. 1976; Ostroy 1978) and ~40,600 liters · mol^{-1}· cm^{-1} for vertebrate rods (Wald and Brown 1953). *human estimate*

C. Quantum efficiency. The quantum efficiency (γ_i) is the efficiency with which an absorbed photon causes conversion of a pigment molecule. In invertebrates, it is assumed to be wavelength independent [use of scalar γ instead of a wavelength-dependent $\gamma(\lambda)$] without theoretical or experimental justification (Hillman et al. 1983). In crayfish values of γ_R = 0.69 and γ_R = 0.49 were found (Cronin and Goldsmith 1982b), with similar γ_R = 0.67 found for bovine rhodopsin (Dartnall 1972). The relative quantum efficiency ($\varphi = \gamma_M/\gamma_R$) describes the relative quantum efficiencies of the conversion of the two pigment states (Stavenga et al. 2000; Stavenga and Hardie 2010), with values ranging from 0.93 in *Calliphora* (Hamdorf 1979), to 0.71 in *Drosophila* (Stark and Johnson 1980).

D. Photosensitivity. The photosensitivity [$\beta(\lambda)$, in older literature $K(\lambda)$ (Hillman et al. 1983)] is the product of molecular absorbance coefficient [$\alpha_i(\lambda)$] and quantum efficiency (γ): $\beta_i(\lambda) = \gamma\alpha_i(\lambda)$. Peak photosensitivity (β_{max}, in cm^2 or in μm^2) for either of the states can be derived as (for R below, for the simplicity (Stavenga and Hardie 2010)):

$$\begin{aligned} \beta_{R,max} &= \gamma_R \cdot \alpha_{R,max} \\ &= \gamma_R \cdot \frac{\kappa_{max}}{C} \end{aligned} \tag{15}$$

where $\kappa_{max}$is the absorbance coefficient (in μm^{-1}) at the peak wavelength (Stavenga and Hardie 2010), estimated to be 5.0 $\times$ 10$^{-3}\mu$m^{-1} of the rhabdomere medium in *Drosophila* (Warrant and Nilsson 1998) and 3 $\times$10$^{-6}\mu$m^{-1} for mouse melanopsin (see B for derivation); and the C is concentration (in μm^{-3}) of the visual pigment molecules, estimated to be 2.5 $\cdot$ 10$^{-5}\mu$m^{-3}in a rhabdomere volume of *Drosophila* (Hardie and Postma 2008) and 1,560 μm^{-3} for mouse melanopsin (see B for derivation).

E. Phototransition rate constant. The rate constant (k_R or k_M) for the transition from state to the another state (k_R for $R \rightarrow M$ transition, and k_M for $M \rightarrow R$ transition) is a product of the photosensitivity [$\beta(\lambda)$] and the light intensity [$I(\lambda)$] having a dimension of reaction rate of the first order (s^{-1}) (i=R,M):

$$\begin{aligned} k_i &= \int \beta_i(\lambda) I(\lambda) d\lambda \\ &= \int \gamma_i \alpha_i(\lambda) I(\lambda) d\lambda \end{aligned} \tag{16}$$

F. Weighting factor. The weighting factor (W) is a parameter that determines the probability that a molecule isomerized from one stable state will reach the second stable state (Hochstein et al. 1978). It is assumed to be independent of λ. It is not typically used for systems without significant intermediate photoproducts like in *Drosophila*, but are needed for more complex phototransduction schemes as in barnacle with multiple thermal transitions and intermediate photoproducts (Minke et al. 1974).

G. Criterion Action Spectrum (CAS). The criterion action spectrum (CAS) is a plot of the reciprocal of the number of incident photons required to produce a given effect as a function of λ. The CAS is commonly used to assign a particular response (see 4.4) to a pigment state by finding that the CAS for that response to the spectral sensitivity $\beta(\lambda)$ of that state (Goldsmith 1972). For to be possible to derive a CAS, following conditions need to be met (Hillman et al. 1983):
1) All the pigment should be possible to be shifted to only one

state [as in *Drosophila*, intense red light adaptation shifting all the pigment to R state (Minke and Kirschfeld 1978; Stavenga 1976)], the R and M state photosensitivities not overlapping "too much".

2) If response arises selectively from activation of one state only, as it is the case in *Drosophila* for late receptor potential (LRP, see 4.4) arising only from R activation (Järvilehto 1979), and M-potential arising from activation of the M only (Pak and Lidington 1974). In contrary, this is not that case in more complex barnacle (Minke et al. 1973; 1974). The criterion chosen to measure the CAS is arbitrary, thus the CAS is a relative measure and only the shape and λ location of the spectrum are significant. The CAS gives information about particular pigment states but not of the system as a whole, and its shape can be distorted by ocular pigments functioning as color filters (Hardie et al. 1979; Kirschfeld et al. 1978a) or as sensitizing pigments (Kirschfeld et al. 1988; Stavenga 2002).

H. Difference spectrum. $D(\lambda)$ is the absorbance difference of a pigment system in two different conditions, and unlike CAS, it is a measure of a pigment system and not a single state. The existence of a single isosbestic point (λ_{iso}) in the difference spectrum at various test wavelengths (λ_{test} for example in Figs. 1,5 of Stavenga 1976), can be thought to provide strong evidence for a single bistable pigment system (Hillman et al. 1983). With melanopsin, this has not been done yet as Mure et al. 2009 only used one stimulus wavelength at 480 nm. For the bistable pigment systems of invertebrates, the difference spectrum [$D(\lambda)$] was given as the following (Stavenga 1975):

$$D(\lambda) = g\left[\alpha_R(\lambda) - \alpha_M(\lambda)\right] \int_0^L \left[f_{R1}(x) - f_{R0}(x)\right] C_p(x)dx \quad (17)$$

where g is a constant equal to $log_{10}e$; C_p is the total number of pigment molecules in the system per unit of volume; $\alpha_R(\lambda)$ and $\alpha_M(\lambda)$ are the molecular absorbance coefficients of R and M, respectively; f_{R1} and f_{R0} are the fractions of R after color adaptation of wavelengths λ_1 and λ_0, respectively; x is a position in the medium; and L is the total length of the medium. In other words, the difference spectrum [$D(\lambda)$] in bistable pigments is always proportional to the difference in molecular absorbance coefficients [$\alpha_R(\lambda) - \alpha_M(\lambda)$], irrespective of distribution of R and M states after various color adaptations. In practice, the derivation of difference spectrum becomes more difficult if there is a considerable overlap between the R and M spectra (Hillman et al. 1983).

I. Isosbestic point. General term referring to the wavelength λ_{iso} at which the interconvertible states of a pigment system have equal α values, i.e. the crossing point of spectral sensitivities of R and M spectral sensitivities ($\alpha_i$or β_i).

J. Photoequilibrium, spectrum. For a stimulus duration "long" enough (time defined by the time constant τ, Eq. (20)) of monochromatic light, a photoequilibrium is eventually reached. The fractional concentration of M state (in similar fashion for R state) in photoequilibrium [$f_M(\lambda,\infty)$ or $f_{Me}(\lambda)$, e denoting equilibrium] can be expressed as (older literature use also saturation spectrum):

$$\begin{aligned} f_{Me}(\lambda) &= \frac{\beta_M(\lambda)}{\beta_M(\lambda)+\beta_R(\lambda)} \\ &= \frac{1}{1+\varphi\frac{\alpha_M(\lambda)}{\alpha_R(\lambda)}} \end{aligned} \tag{18}$$

These fractions (f_{Me}or f_{Re}) are independent of the initial distribution between R and M states and of the intensity of light I and depend only on the light driving the system to equilibrium (Hamdorf and Razmjoo 1979). The fractional concentration can be also expressed using the rate constants $k_R$and k_M (Stavenga and Hardie 2010) defined in Eq. (16):

$$f_{Me} = \frac{1}{1+(k_M/k_R)} \tag{19}$$

The approach to equilibrium follows an exponential time course, and the time constant τ can be also expressed using the time constants $k_R$and k_M (Stavenga and Hardie 2010):

$$\tau = \frac{1}{k_M+k_R} \tag{20}$$

The photoequilibrium spectrum is not typically normalized in invertebrate studies in contrast to the approach by Mure et al. 2009. The M-state fraction f_M in *Drosophila* cannot exceed 0.8 due to the overlapping spectral sensitivities of R and M states (β_i), and more exactly due to the β-band of M-state (Hardie and Postma 2008). This value of 0.8 is in practice further reduced to values under 0.2 in real-world lighting conditions due to the red screening pigment employed by *Drosophila* (Stavenga 2002) favoring M state absorption, and the extreme value of 0.8 is obtained in white-eyed mutants (chalky) lacking screening pigments. Strictly speaking, photoequilibrium spectrum cannot be use analogously to an action spectrum, as the photoequilibrium spectrum contain the assumption that the studied re-

sponse must be linearly (*or known relation)* related to the pigment concentration. In other words, the photoequilibrium can be reached with a dim light stimulus for long duration, and a subsequent stimulus of the same wavelength with high intensity would not change to photoequilibrium.

K. Q-Spectrum Q-spectrum is obtained from photoequilibrium spectrum f_{Me} by normalizing the value at isosbestic wavelength to unity (Stavenga 1975) using a test stimulus of λ_{test}:

$$Q(\lambda_{test}) = \frac{f_{Me}(\lambda_{test})}{f_{Me}(\lambda_{iso})} \tag{21}$$

where the λ_{test} is the wavelength used to establish a photoequilibrium as set to 480 nm by Mure et al. 2009. To avoid confusion in nomenclature and ensure compatibility with older literature, Q-spectrum ($Q(\lambda_{test})$) and photoequilibrium spectrum ($f_{Me}(\lambda)$) are referred with different symbols, whereas Mure et al. 2009 use term "equilibrium" interchangeably for both Q-spectrum (Fig. 4C) and to normalized photoequilibrium spectrum (Fig 4B).

L. Relaxation spectrum The approach to photoequilibrium of a simple bistable pigment system (like that of *Drosophila*, but not of a barnacle) as a function of the duration t of a monochromatic light of intensity I (in regard to the melanopsin system this could be approximated by the product of spectral irradiance and an action spectrum for the response of interest) is given for the fraction of M (f_M) by:

$$\begin{aligned} f_M(I(\lambda)\cdot t) &= f_M(\infty) \\ &= +[f_M(0) - f_M(\infty)]\, exp\,[-(\beta_R + \beta_M)\cdot I(\lambda)\cdot t] \end{aligned} \tag{22}$$

M. where t is the time, $f_M(\infty)$ is the fraction of M at infinity, and $f_M(0)$ is the fraction of M at the beginning of illumination. A similar equation could be derived also for R state (f_R). The approach to equilibrium is typically referred as the relaxation spectrum [$\Lambda(\lambda)$] or relaxation constant [$\Lambda(\lambda)$] (Hillman et al. 1983; Belušič et al. 2010):

$$\begin{aligned} \Lambda(\lambda) &\equiv \beta_R(\lambda) + \beta_M(\lambda) \\ &\equiv W_R\beta_R(\lambda) + W_M\beta_M(\lambda) \end{aligned} \tag{23}$$

which is the same for f_M as for f_R. In bistable pigment systems with multiple thermal transitions (as in barnacle (Hochstein et al. 1978)), the weighting factors W_R and W_M need to be added, and in simple systems (such as in *Drosophila*) they can be set to

unity.

The important difference between relaxation $\Lambda(\lambda)$ and equilibrium spectrum is that the relaxation spectrum can be derived from the various responses that are linear with pigment change on an absolute scale. Relaxation spectrum is measured for *Calliphora* for the M-potential (Minke and Kirschfeld 1979), microspectrophotometrically and for the M-potential in *Musca* (Minke and Kirschfeld 1979), microspectrophotometrically for *Drosophila* (Stark and Johnson 1980), for the ERP and prolonged depolarization afterpotential (PDA) in barnacle (Minke et al. 1978), and using the autofluorescence of the M state in crayfish (Cronin and Goldsmith 1982a). As the relaxation spectrum is the sum (Eq. (23)) of the photosensitivity spectra of the two stable states of a pigment system, it may also sometimes be used to determine the photosensitivity spectrum of one of the two states if only the other may be measured [the first might be "silent", for instance as in the Drosophila "M-potential" (Pak and Lidington 1974)]. Another important feature of relaxation spectrum is that it does not include the spectrum of the sensitizing pigment in invertebrates, the measure reflecting more the underlying spectral sensitivities of the R and M states (Minke and Kirschfeld 1979).

4.3 BISTABLE ACTION SPECTRA

There are typically five different action spectra types used in characterizing the behavior of a bistable pigment system, which are criterion action spectrum (CAS), difference spectrum [$D(\lambda)$], equilibrium spectrum [$f_{Me}(\lambda)$, $f_M(\lambda)$ or $Q(\lambda)$], relaxation spectrum [$\Lambda(\lambda)$] and the spectral sensitivities of the R an M pigment states [$\beta_R(\lambda)$ and $\beta_M(\lambda)$]. The three spectra: difference, equilibrium and relaxation spectrum, can be calculated from the spectral sensitivities of the visual pigments. In practice however the spectral sensitivities are unknown and the mentioned three spectra need to be measured, and the spectral sensitivities derived from measurements. The use of criterion action spectrum (CAS) is the classical method of deciding whether two responses come from the same pigment state (Hochstein et al. 1978). If two CAS's agree, it is very likely that both responses come from the same pigment state. If they disagree, the responses must come from different pigment states, but these states may or may not be of the same pigment system.

In some cases, the spectral sensitivities of the R and M states may overlap (see Table 1 of Hillman et al. 1983) making the differentiation of pigment states difficult with spectral modulation. In those cases it is possible to study the differential electric dipole moments of the pigments (Petersen and Cone 1975) or their dichroic absorptions properties (Hárosi and Malerba 1975; Thomas et al. 2009). Example of the latter was provided in the study by Kolesnikov et al. 2003, where it was possible to distinguish various intermediate photoproducts with overlapping spectra (isochromic pigments) from each other comparing their differential dichroic absorption ratios (longitudinal vs. transversal plarization) using a fast-scanning dichroic microspectrophotometer (Firsov et al. 2002). Lisman and Sheline 1976 demonstrated also that by increasing pH of the *in vitro* solution of *Limulus* rhodopsin it was possible to red-shift the metarhodopsin (M) absorption maximum the peak of rhodopsin (R) absorption being unaffecteds, thus making easier to study differential activation of the rhodopsin (R) and metarhodopsin (M) states.

4.3.1 *Criterion Action Spectrum (CAS)*

The criterion action spectrum (CAS) is a plot of the reciprocal of the number of incident photons required to produce a given effect as a function of λ as with the use of criterion responses in ERG () and in PLR () for example. The CAS is commonly used to assign a particular response (see 4.4) such as early receptor potential (ERP), late receptor potential (LRP) or behavioral response to a pigment state by finding that the CAS for that response to the spectral sensitivity $\beta(\lambda)$ of that state (Goldsmith 1972), being valid only under certain conditions

(Hochstein et al. 1978). For CAS to be possible to be derived: 1) All the pigment should be possible to be shifted to only one state [such as in *Drosophila*, intense red light adaptation shifting all the pigment to R state (*Minke and Kirschfeld 1978*; Stavenga 1976)], requiring that the R and M state photosensitivities are not overlapping "too much", in other words if equilibrium has values of 0 and 1. 2) If response arises selectively from activation of one state only, as it is the case in *Drosophila* for late receptor potential (LRP, see 4.4) that arise only from R activation (Järvilehto 1979), and M-potential that arise from activation of the M only (Pak and Lidington 1974). In contrary, this is not the case in more complex bistable phototransduction scheme of barnacle (Minke et al. 1973; 1974). The criterion chosen to measure the CAS is arbitrary, thus the CAS is a relative measure and only the shape and λ location of the spectrum are significant. The CAS gives information about particular pigment states but not of the system as a whole, and its shape can be distorted by ocular pigments functioning as color filters (Hardie et al. 1979; Kirschfeld et al. 1978a) or as sensitizing pigments (Kirschfeld et al. 1988; Stavenga 2002).

4.3.2 *Difference spectrum*

The difference spectrum $D(\lambda)$ is the absorbance difference of a pigment system in two different conditions and unlike CAS, it is a measure of a pigment system and not a state. The existence of a single isosbestic point (λ_{iso}) in the difference spectrum at various stimulus wavelengths (λ_s for example in Figs. 1,5 of Stavenga 1976), can be thought to provide strong evidence for a single bistable pigment system (Hillman et al. 1983). In melanopsin, this has not been done yet as Mure et al. 2009 only used one stimulus wavelength at 480 nm. For the bistable pigment systems of invertebrates, the difference spectrum $[D(\lambda)]$ was given as the following (Stavenga 1975):

$$D(\lambda) = g\,[\alpha_R(\lambda) - \alpha_M(\lambda)] \int_0^L [f_{R1}(x) - f_{R0}(x)]\, C_p(x)dx \qquad (24)$$

where g is a constant equal to $log_{10}e$; C_p is the total number of pigment molecules in the system per unit of volume; $\alpha_R(\lambda)$ and $\alpha_M(\lambda)$ are the molecular absorbance coefficients of R and M, respectively; f_{R1} and f_{R0} are the fractions of R after color adaptation of wavelengths λ_1 and λ_0, respectively; x is a position in the medium; and L is the total length of the medium. In other words, the difference spectrum $[D(\lambda)]$ in bistable pigments is always proportional to the difference in molecular absorbance coefficients $[\alpha_R(\lambda) - \alpha_M(\lambda)]$, irrespective of distribution of R and M states after various color adaptations. In practice, the derivation of difference spectrum becomes more difficult if there is a considerable overlap between the R and M spectra (Hillman

et al. 1983). For examples of the use of difference spectra in vertebrate phototransduction can be seen for example in Rushton 1956 and Einterz et al. 1987.

4.3.3 *Equilibrium spectrum*

The equilibrium spectrum (typically $f_{Me}(\lambda)$ expressing the fraction of pigment in M state as a function of the wavelength λ) is also a measure of the pigment system, always being proportional to the ratio of the photosensitivities of the R and M states (see Eq. (18) and Eq. (19)). The equilibrium spectrum can be calculated from known (Hamdorf et al. 1973a) or simulated spectral sensitivities using a nomogram (see 2.3.2). In practice as the spectral sensitivities are not known, the equilibrium spectrum has to be derived from experimental data. In fly and crayfish, the equilibrium on a relative scale can be derived by only measuring the difference spectrum in various equilibrium states (Stavenga 1975; 1976) with the knowledge of relative quantum efficiency(φ) needed . The φ was estimated in a drone fly electrophysiologically exploiting the linear dependence of late receptor potential (LRP) sensitivity on R concentration (Tsukahara and Horridge 1977). The derivation is more complicated again in barnacle, where pigment molecules leaving each stable state may return to the same state, the derivation being only possible when the light intensity is not too high and with the inclusion of weighting factors W_R and W_M to Eq. (18) resulting the following:

$$f_{Me}(\lambda) = \frac{W_M \cdot \beta_M(\lambda)}{W_M \cdot \beta_M(\lambda) + W_R \cdot \beta_R(\lambda)} = \frac{1}{1 + \frac{\varphi \cdot W_M \cdot \alpha_M(\lambda)}{\cdot W_M \cdot \alpha_R(\lambda)}} \tag{25}$$

4.3.4 *Relaxation spectrum*

The relaxation spectrum defines the dependence of the rate of approach of the pigment-state population to the equilibrium on the λ of the adapting (environmental) light, and the Eq. (22) and Eq. (23) can be changed to more compact form (Hillman et al. 1983):

$$\Lambda(\lambda) = \frac{1}{I \cdot t} \cdot ln \left[\frac{f_M(\lambda, \infty) - f_M(\lambda, I \cdot t)}{f_M(\lambda, \infty) - f_M(\lambda, 0)} \right] \tag{26}$$

where t is the stimulus duration, and I the intensity of the light, and the product $I \cdot t$ is referred as the amount of light. The important difference between relaxation $\Lambda(\lambda)$ and equilibrium spectrum is that the relaxation spectrum can be derived from the various responses that are linear with pigment change on an absolute scale. Relaxation spectrum has been measured for example in *Calliphora* for the M-potential (Minke and Kirschfeld 1979), microspectrophotomet-

rically and for M-potential in *Musca* (Minke and Kirschfeld 1979), microspectrophotometrically in *Drosophila* (Stark and Johnson 1980), for the ERP and prolonged depolarization afterpotential (PDA) in barnacle (Minke et al. 1978), and using the autofluorescence of the M state in crayfish (Cronin and Goldsmith 1982a).

As the relaxation spectrum is the sum (Eq. (23)) of the photosensitivity spectra of the two stable states of a pigment system, it may also sometimes be used to determine the photosensitivity spectrum of one of the two states if only the other may be measured [the first might be "silent", for instance as in the Drosophila "M-potential" (Pak and Lidington 1974)]. Another important feature of relaxation spectrum is that it does not include the spectrum of the sensitizing pigment in invertebrates, the measure reflecting more the underlying spectral sensitivities of the R and M states (Minke and Kirschfeld 1979). A rough vertebrate analog of relaxation spectrum is used in the human study of Dartnall et al. 1936.

4.3.5 *Spectral sensitivities of the pigment states*

In conclusion, the typical use of different action spectra is the derivation of the underlying pigment spectral sensitivities, and that derivation can be done In three ways. First, it is possible to derive the spectral sensitivities directly from the measured difference spectrum assuming nomogram shapes for the pigment spectral sensitivities (Hamdorf et al. 1973b, Hamdorf 1979, Hamdorf et al. 1973a) and numerically fitting the spectral sensitivities to the experimental data. Second possibility is to derive the sensitivities jointly from the measured equilibrium and difference spectrum as done by Mure et al. 2009 based on the formulation of Stavenga 1975; 1976, where the difference spectrum in equilibrium $D_\infty(\lambda_t, \lambda_s)$ was defined as:

$$D_\infty(\lambda_t, \lambda_s) = f_{Me}(\lambda_s, \infty) N(\lambda_t) \left[\alpha_M(\lambda_t) - \alpha_R(\lambda_t)\right] \tag{27}$$

where $N(\lambda_t)$ is the expressed the total amount of molecules of the pigment in the sample and it is typically unknown (Stavenga 1975), and is defined as:

$$N(\lambda_t) = g \int_0^L C_p(x) dx \tag{28}$$

where the variables are the same as in Eq. (24). The $N(\lambda_t)$ can be set to unity as in Mure et al. 2009 (constant k) with little error in calculations (see the discussion in Stavenga 1976), especially if the photoreceptors do not have waveguiding effects as seems likely for melanopsin (see 2.2.2), but not for fly rhabdomere (cf Hao et al. 2009). The difference spectrum using the monochromatic light of isosbestic wavelength λ_{iso} as the test light:

$$\begin{aligned} D_{iso}(\lambda_t) &\equiv D_\infty(\lambda_t, \lambda_{iso}) \\ &= (1+\varphi)^{-1} N(\lambda_t) \left[\alpha_M(\lambda_t) - \alpha_R(\lambda_t)\right] \end{aligned} \tag{29}$$

The Q function is obtained from the equilibrium spectrum $f_{Me}(\lambda)$ normalizing the responses at different spectral light (λ_s) to be unity at the isosbestic point (λ_{iso}) obtained from difference spectrum (Stavenga 1975), or using the stimulus wavelength as close as possible to the isosbestic point as done by Mure et al. 2009. The relation can be expressed as following:

$$Q(\lambda_s) \equiv \frac{D_\infty(\lambda_t, \lambda_s)}{D_\infty(\lambda_t, \lambda_{iso})} = (1+\varphi) f_{Me}(\lambda_s, \infty) \tag{30}$$

By dropping the subscripts in these equations and using the Eq. (18) for f_{Me},expressions for $\alpha_R(\lambda)$ and $\alpha_M(\lambda)$ can be derived (Stavenga 1975):

$$\alpha_M(\lambda) = \frac{D_{iso}(\lambda)\left[1+\varphi+-Q(\lambda)\right]}{N(\lambda)\left[1-Q(\lambda\right]} \tag{31}$$

$$\alpha_R(\lambda) = \frac{D_{iso}(\lambda)\varphi Q(\lambda)}{N(\lambda)\left[1-Q(\lambda\right]} \tag{32}$$

This method was designed for photometric measurements, but in special cases can be used in drone fly electrophysiology (Tsukahara and Horridge 1977), and with human PLR (Mure et al. 2009). Finally it is possible to derive the spectral sensitivities using relaxation and equilibrium spectrum as following (Hochstein et al. 1978; Minke and Kirschfeld 1979):

$$\beta_R(\lambda) = \frac{1}{W_R}\Lambda(\lambda) f_{Me}(\lambda, \infty) \tag{33}$$

$$\beta_M(\lambda) = \frac{1}{W_M}\Lambda(\lambda)\left[1 - f_{Me}(\lambda, \infty)\right] \tag{34}$$

In practice this approach is problematic as the weighting factors W_R and W_M are typically unknown (see Minke and Kirschfeld 1979; Stark and Johnson 1980; Cronin and Goldsmith 1982a and Hillman et al. 1983). In studies by (Stark et al. 1977; Stark and Zitzmann 1976) the spectral sensitivity of the M state was derived while knowing the spectral sensitivity of the R state, with the "unknowns" φ and W values simply set to unity. This approach required the need for accurate data of both the equilibrium spectrum $f_{Me}(\lambda)$ and spectral sensitivity of R $\alpha_R(\lambda)$ in the orange-red spectral range, where both spectra have small values (note similar situation in the study by Mure et al. 2009). This resulted in significantly different estimates for the M spectrum compared to previous studies with more accurate raw data (Minke and Kirschfeld 1979; 1980; Stavenga 1976).

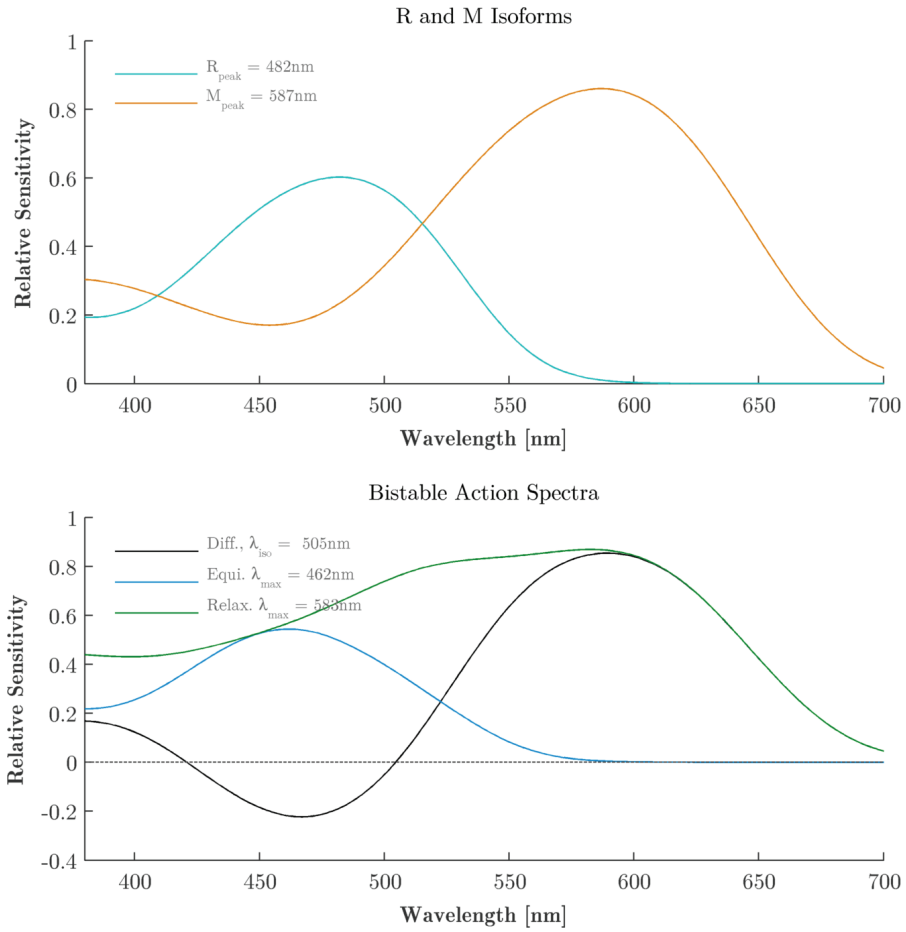

Figure 37: **Comparison of bistable action spectra.** (Above) Spectral sensitivites obtained for melanopsin by Mure et al. 2009. (below) The corresponding simulated bistable action spectrum with the isosbestic wavelength λ_{iso} ~505 nm in difference spectrum, equilibrium spectrum with λ_{max}~ 462 nm, relaxation spectrum with λ_{max}~ 583 nm.

4.4 RESPONSE TYPES IN BISTABLE PIGMENT SYSTEMS

In this chapter, the observed phenomena of bistable pigment systems are reviewed. In ideal case the constructed model (see Section 4.6) should be able to predict all the observed phenomena, but in practice the existing models have not been able to produce all the phenomena (see review by Hillman et al. 1983). The following responses are analyzed using invertebrate models, and one of the fundamental difference to vertebrate photoreception in general is the linear relationship between sensitivity and photopigment concentrations (e.g. Hamdorf and Schwemer 1975; Rosner 1975) whereas in vertebrates most of the visual responses exhibit nonlinear response (e.g. Rushton et al. 1955; Dowling 1960; Dowling 1963; Reuter 2011; Wang and Kefalov 2011)

4.4.1 *Early receptor potential (ERP)*

Absorption changes in the the photopigment molecules are followed by a redistribution of charges in pigment molecules (Cone 1967; Hagins and McGaughy 1967; Minke and Kirschfeld 1979), which can be measured either intracellularly (Hillman et al. 1972; Lisman and Sheline 1976) or extracellularly (Brown and Murakami 1964; Hagins and McGaughy 1967). This recorded electrophysiological response is called the fast photovoltage or the early receptor potential (ERP). When light is absorbed by R and M, the intracellular ERP is negative and positive, respectively [in invertebrates (Hillman et al. 1972; Minke et al. 1973; Lisman and Sheline 1976) and in vertebrates (Murakami and Pak 1970; Zanen and Debecker 1975)].

In albino rats (Cone 1964), non-human primates (Brown and Murakami 1964) and in humans (Carr and Siegel 1970) the ERP is also thought to arise from conformational changes of photopigment molecules. The ERP in vertebrates is a biphasic response consisting of an initial corneal positive phase [R1, (Trissl 1982)], followed by a slower corneal negative phase (R2) lasting few milliseconds after the flash (Brown and Murakami 1964). The amplitude of the ERP in monkey is low compared to more commonly recorded a-wave (Breton et al. 1994; Cameron et al. 2008), and sometimes the R2 component can not be clearly recorded as it is the case in Figure 38A. The spectral sensitivity of the human ERP seems to be mainly cone-dominated (Goldstein and Berson 1969; 1970; Carr and Siegel 1970), with Zanen and Debecker 1975 suggesting the R1 component to be originating completely and R2 having a rod contribution. Due to the linear dependence of ERP amplitude to pigment concentration (Debecker and Zanen 1975) it has been used to study pigment regeneration in humans (Sieving 1981), but it has not been recently studied nor really used in clinical practice for some reason (Müller et al. 1982; Walther

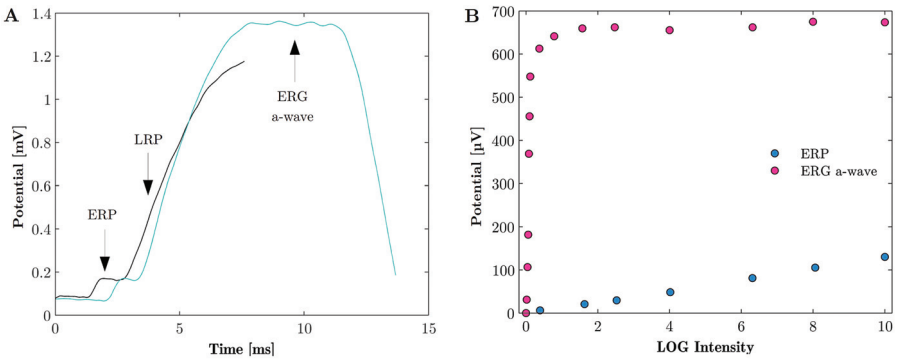

Figure 38: **(A)** Time course of the ERP and LRP (4.4.3) in monkey retina recorded with two different time resolutions (black and blue trace, thus due to recording imprecisions the ERPs of black and blue do not match timing-wise). The ERP and LRP, thus preceded the a-wave commonly used in clinical and experimental electroretinography (ERG) (redrawn from Brown and Murakami 1964). Intensity-dependence of human ERP **(B)**. Abscissae: attenuation of the flashes by neutral filters. Ordinates: amplitude of the R_2 wave of the ERP (blue circles) and of the a-wave of the ERG (red circles). (redrawn from Debecker and Zanen 1975)

and Hellner 1986: Fioretto et al. 1992). In theory, it could be hypothesized that in retinitis pigmentosa (e.g. Esquiva et al. 2010; Busskamp and Roska 2011) with no functional rod and cone photoreceptors, human melanopsin ERP could be recorded however the low pigment amount (Do et al. 2009) and the accompanying weak potential most likely being masked by instrumentation noise.

4.4.2 *M-potential*

In the fly, a fast potential was found arising from light absorption by the M state (Minke and Kirschfeld 1979; Pak and Lidington 1974). The dominant component of the *Drosophila* M-potential is corneal positive, however, the M-potential is typically preceded by a small corneal negative wave (Pak and Lidington 1974). Intracellular recordings have suggested that the M-potential is predominantly a response of the second-order neurons (Minke and Kirschfeld 1980; Stephenson and Pak 1980). The M-potential in the second-order neurons (M_2 phase) is induced by the positive ERP (M_1 phase), which arises from selective absorption by the M state. The observed M-potential have shown to roughly have a linear relationship with pigment concentration, the second order neuron contribution slightly compressing the response. The M potential sometimes saturates before the maximal amount of pigment has been shifted to metarhodopsin, a phenomenon which never occurs with the ERP (Minke and Kirschfeld 1979. The specific responses arising from both R (ERP) and M state (M-potential) activations facilitate the study of the two pigment states (see 4.3.1).

It has been traditionally thought (see review by Hillman et al. 1983) that the M state activation would have no physiological consequence with one exception shown in barnacle with high light intensity. Hanani and Hillman 1979 showed that light absorption of M state resulted in decreased sensitivity as measured by LRP amplitude (see below), the effect being restricted only for high light intensities (Hillman et al. 1983). This observed contribution from the M state in invertebrates could partly explain (Mure 2009) the anomaly in human vision referred as the transient tritanopia (Stiles 1949a;b), in which after the extinction of a an intense long-wavelength adapting field (for action spectrum see Alpern and Zwas 1979 and Wisowaty 1983), the sensitivity for short-wavelength stimulus is greatly reduced for a short period of time. The anomaly has been furthermore shown to abolish at high intensities (Reeves 1981), and being persistent in aging via adaptational mechanisms (Werner et al. 2010). Valeton and Norren 1979 suggested the transient tritanopia originates between the photoreceptors and the bipolar cells, probably at the horizontal cells as already earlier hypothesized by Augenstein and Pugh 1977. Alternative or additionally in theory, the M state activation could reduce either the luminance drive of the melanopsin system (2.4.10), affect classical photoreceptors, or both melanopsin and classical photoreceptors.

4.4.3 *Late receptor potential (LRP)*

Late receptor potential (LRP) is stimulus-coincident response (like ERP and M-potential) produced by a sum of discrete voltage fluctuations, called quantum bumps (Fuortes and Yeandle 1964; Dodge et al. 1968). LRP depends on the activation of the R state (Stratten and Ogden 1971), however unlike with ERP and M-potential, no net pigment shift is not necessarily required. (see below, 4.4.4). The criterion action spectrum (CAS) for "weak stimulus" of the LRP has been shown to match the R spectral photosensitivity, and being independent of M activation (Barnes and Goldsmith 1977; Atzmon et al. 1978; 1979; Strong and Lisman 1978). With increased stimulus strength the influence of M activation can be seen in the CAS (Hanani and Hillman 1979). In *Drosophila* (Hamdorf et al. 1973b; Razmjoo and Hamdorf 1976; Harris et al. 1977) and in several other preparations the LRP sensitivity has been shown to depend linearly on R population. With prior adaptation to monochromatic light (cf Hochstein et al. 1973 for methodology), some flies were shown to have greater than linear dependence on R population (Razmjoo and Hamdorf 1976), and barnacles a less than linear dependence (Minke et al. 1974).

4.4.4 *Prolonged depolarization afterpotential (PDA)*

In contrast to ERP, M-potential and LRP that arise from the pigment activation as in vertebrate transduction, the prolonged depolarization afterpotential (PDA) [also referred as the "tail" (Hochstein et al. 1973), depolarizing after potential DAP (Baumann and Hadjilazaro 1972), "latchup" (Brown and Cornwall 1975), "glueing effect" (Stavenga et al. 1975), and prolonged corneal negative afterpotential PCNA (Wright and Cosens 1977)] is caused by a net pigment shift R to the M state. PDA is characterized as a slowed-down decay of LRP back to pre-stimulus ("baseline") conditions similar as the persistent response of human pupillary light reflex (see 5.5.2, Newsome 1971), melanopsin-ipRGC firing rate (Berson et al. 2002). PDA was first demonstrated in an invertebrate surf clam (Kennedy 1960), and in *Drosophila*, the longest PDA measured was shown to last up to 6 hours (Wright and Cosens 1977).

The PDA is the most studied response of bistable systems, and can be elegantly measured photometrically (metarhodopsin fluorescence) simultaenously with electroretinography (Belušič et al. 2010). Albani et al. 1980 reported that R bleach induces an extended period of suppression in rat retinal rods and that R regeneration hastens the recovery, appearing to be a vertebrate analogue of the PDA. Conceptually similar phenomenon is found in vertebrate rod dark adaptation Firsov et al. 2005, very dim light pulses were found to be followed by an immediate sensitivity recovery with an existence of "switch-like" intensity threshold. When the light flash intensity increased to 1.9×10^7 activated molecules (about 1% of the total rhodopsin content), the rod stayed in saturation for prolonged time, in other corresponded the classical dark adaptation behavior (Reuter 2011).

PDA induction

In invertebrates, the PDA has been shown to depend mainly on the net pigment shift, in other word how much is the R pigment shifted to the M-state, thus the spectral sensitivity of the PDA should match the spectral sensitivity of the R state. Furthermore, the PDA amplitude in invertebrates have seemed to depend only on the amount of stimulation ($I \cdot t$) and not on either stimulus duration t or intensity I alone (Stark 1975; Wright and Cosens 1977), following the Bunsen-Roscoe / Bloch's law (Brindley 1952). This was not shown to be the case for LRP which depended only on the I of the stimulation for t values above a few hundred milliseconds. The shape of the PDA is not invariant with an observed dependence of stimulation amount on both the height and decay time of the PDA with contradictory reports. Nolte and Brown 1972 reported the return to resting potential always to be monotonic, whereas Hillman et al. 1983 had noticed occasional fast dips followed by a rise in potential on the initial portion of

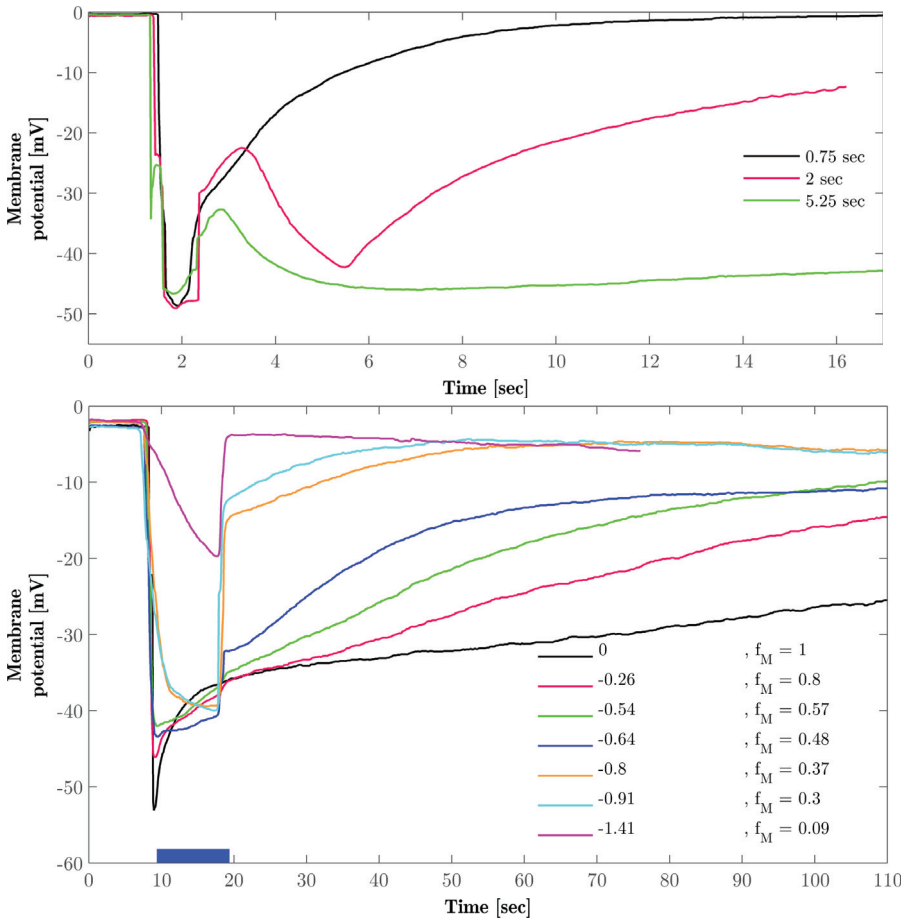

Figure 39: Dependence of PDA on stimulus amount ($I \cdot t$) in *Limulus* median eye (Nolte and Brown 1972), **(A)** on stimulus duration t with a fixed intensity I, and **(B)** on stimulus intensity I for fixed duration t. (A,B adapted from Hillman et al. 1983).

the PDA (see Figure 20 for comparison of the PLR persistence). Given that the PDA time course is not fixed, the analysis is not as straightforward as pointed out by Hillman et al. 1983. Typically, PDA induction in invertebrates is studied with monochromatic lights, Hamdorf and Razmjoo 1977 being one of the few exceptions using white light for PDA induction.

PDA refractoriness

It has been shown that during a maximal PDA, there is little or no response for neutral stimulus (no induced net pigment change) that would normally induce a LRP, this being referred as PDA-dependent "refractoriness". This refractoriness was one of the first wavelength-dependent after-effects discovered (Cosens and Briscoe 1972), and it has been used a sensitive measure of PDA amplitude in non-mutant

flies (Stark 1975), and in vitamin A deprived *Drosophila* (Stark et al. 1975).

PDA depression

Stimulus during PDA that causes a large net $M \rightarrow R$ pigment-state shift (in the case of melanopsin system, long wavelength light during the persistent response) during a PDA results in speeding up of the decay of the afterpotential towards baseline. This phenomenon is typically referred as PDA depression [also "tail-kill" (Hochstein et al. 1973), "repolarizing response" (Nolte and Brown 1972), "knock-down" (Brown and Cornwall 1975)]. The spectral sensitivity of PDA depression corresponds to the spectral sensitivity of the M state making it an ideal phenomenon to study melanopsin bistability in vivo as done by Qiu and Berson 2007 (unpublished data) in mice and suggested by Do and Yau 2010. As with PDA, the invertebrate PDA depression also depend on the stimulus amount [$(I \cdot t)$, see Figure 40. Stark 1975; Wright and Cosens 1977]. Minke 1979 showed that PDA declined back to baseline during a continuous 6 h blue in *Drosophila*. This result was taken as an evidence for dark thermal regeneration to have the same effect on PDA induction and depression as light-driven $M \rightarrow R$ pigment shift.

Anti-PDA

In addition to PDA depression phenomenon, closely related phenomenon termed "anti-PDA" (Hochstein et al. 1973; Minke 1979) is found in which after a saturating $R \rightarrow M$ stimulus (e.g. intense 480 nm light for melanopsin), additional PDA cannot be induced without an intervening M R stimulus (e.g. 590 nm light in melanopsin). Like PDA depression, the action spectrum of anti-PDA has been shown to match the M-state spectral sensitivity (Minke et al. 1978). Additionally, following the decay of the PDA and $M \rightarrow R$ stimulus, a further PDA ($R \rightarrow M$ stimulus) can only be elicited if the photoreceptor is first left for some time (~10 s) in the dark in *Drosophila*. Stavenga and Hardie 2010 suggested that this refractory 10 s arises from rhabdomeres being fully loaded with arrestin following translocation (Satoh et al. 2010), the time course depending of the reverse translocation of arrestin out of the rhabdomere. There seems to be at least two different R states, the other R_i (see Figure 47) not being dependent on light stimulus and requiring the "dark" refraction period (**Hamdorf and Razmjoo 1977**; Levine et al. 1987; Kiselev and Subramaniam 1994; Stavenga and Hardie 2010). $M \rightarrow R$ stimulus induces first an inactive form (R_i) followed by the active form (R_a) after a light-independent fixed time (see Section 4.6 below).

Given that the anti-PDA is an "invisible phenomenon" without direct photoreceptor membrane conductance or potential changes.

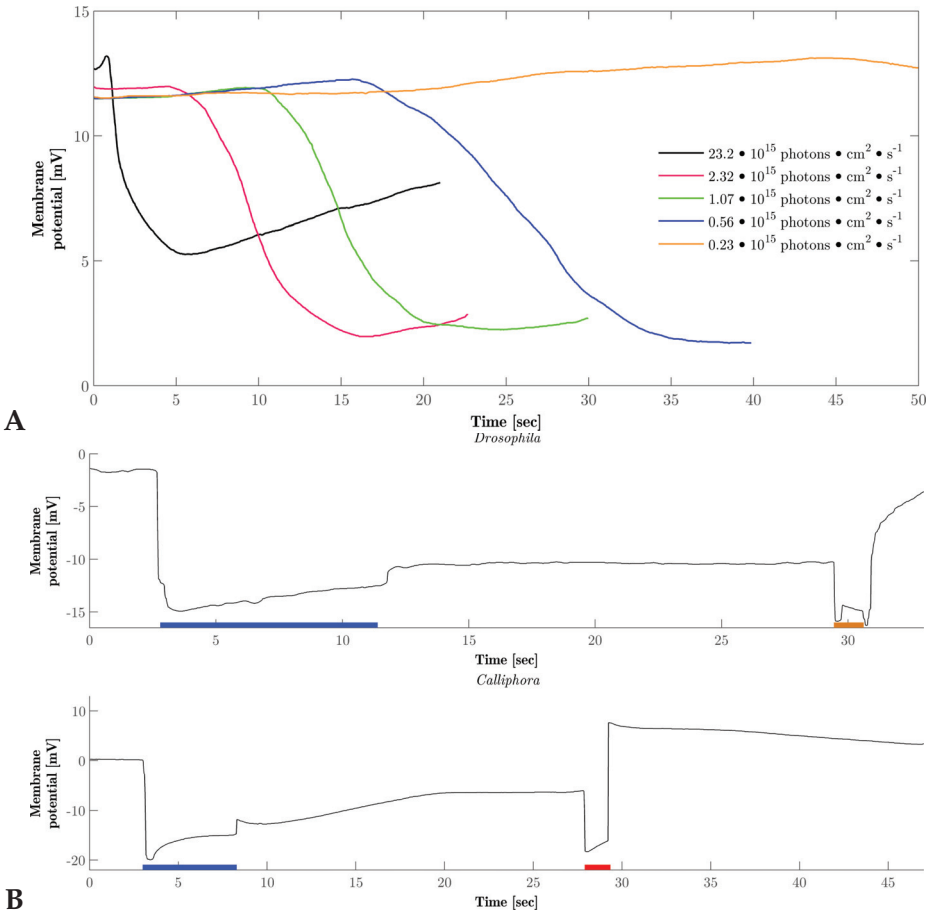

Figure 40: **(A)** Dependence of PDA depression in barnacle on stimulation amount with R-state activating light (pigment shift $R \rightarrow M$) followed by M-activating ($M \rightarrow R$) light of fixed duration t but variable intensity I (Hochstein 1972). **(B)** PDA depression. Light stimulus that induces a large net $R \rightarrow M$ shift (blue light) is followed by $M \rightarrow R$ resulting a rapid decay of that PDA. (top) *Drosophila*, white after blue (Cosens and Briscoe 1972); (bottom) *Calliphora*, red after blue (Muijser et al. 1975).

Minke 1979 demonstrated the time course of anti-PDA in *Calliphora* (Figure 41B) by 1) giving an $R \rightarrow M$ stimulus, 2) dark-adapting the cell and let the possible PDA decline, 3) present the anti-PDA-inducing $M \rightarrow R$ stimulus, 4) varying the dark period (3 different periods in Figure 41B), and 5) test the cell with a fixed$R \rightarrow M$ stimulus. In *Calliphora* the PDA was shown to be completed recovered after a dark period of ~50 s. Anti-PDA effect is directly proportional to the degree to which the PDA had declined at the time of anti-PDA induction. When a closely following pair of saturating stimuli, one $M \rightarrow R$ and one $R \rightarrow M$, is presented during a partially declined maximal PDA, the first suppresses the PDA and induces a partial anti-PDA and the second re-induces a partial PDA whose level is close to that preceding the stimulus pair. This is as one would expect-the pair of stimuli together are a "neutral stimulus" in that no net pigment is shifted between R and M, and thus no residual effect on the PDA should result.

Figure 41B demonstrates the dependence of I of the first $R \rightarrow M$ stimulus (and thus on the amount of pigment transferred by the second $M \rightarrow R$ stimulus) is the opposite of the dependence on the I of $R \rightarrow M$ stimulation (see Figure 40A). This suggests a one–to-one relationship between pigment included in the anti-PDA induction and that excluded from the PDA induction.

In conclusion for PDA induction and anti-PDA, the response after any stimulus series of duration short compared with those of the PDA and anti-PDA depends only on the initial and final states of adaptation (Hochstein et al. 1978). For instance, a final saturating $R \rightarrow M$ stimulus always induces a PDA if all the pigments were in R state, or never induces a PDA in an initially "M-adapted state" ($R \rightarrow M$ stimulus adapted), no matter what other stimuli intervened during a time, preceding the $R \rightarrow M$ stimulus, short compared with the PDA and anti-PDA durations.

PDA non-localities

In invertebrates, the PDA phenomenon is shown to spread spatially from its point of initiation referred as the nonlocality of PDA (Hillman et al. 1976). A local phenomenon should depend linearly on the number of transitions, because the response of each transition is unaware of the number of other transitions taking place. Almagor et al. 1979 showed using a microspot stimulation that the spread was at least to the next-nearest-neighbor, but not necessarily throughout the cell.

PDA facilitation

The observed non-localities in PDA phenomena are possibly related to another mechanism referred as "PDA facilitation" (Hillman et al.

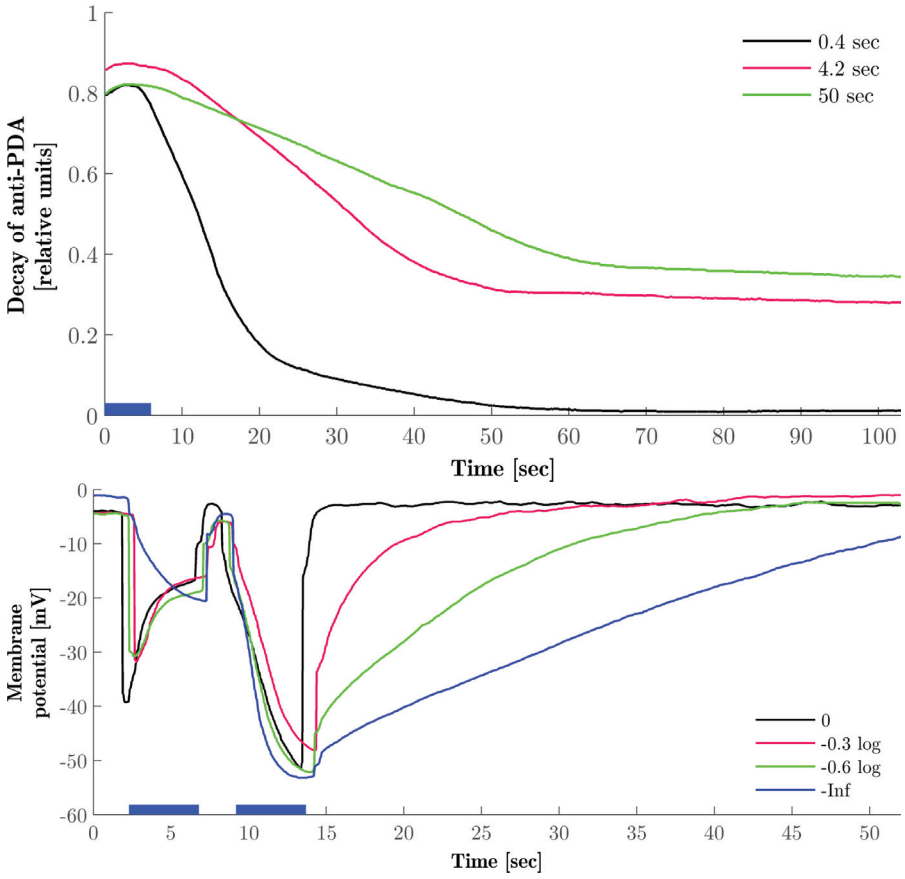

Figure 41: **(Top)** Time course of anti-PDA in *Calliphora*. Decay of anti-PDA is shown by decline of its effect on PDA, with increase of interval between anti-PDA induction and the following $R \rightarrow M$. Superimposed tracings of responses to identical $R \rightarrow M$ corresponding to various inter-stimulus intervals. Data from Minke 1979. **(Below)** Anti-PDA dependence on amount of pigment transfer. The cell is prepared with varying M/R ratios so that saturating stimulus (always bringing pigment to the same final distribution) induces varying amounts of f_M by varying PDAs induced by subsequent $R \rightarrow M$. Traces are for intracellular recordings in barnacle. Numbers at left are log attenuation of intensities of $R \rightarrow M$ stimulation that prepared varying M/R ratios (Hochstein 1972). Graphs replotted from Hillman et al. 1983.

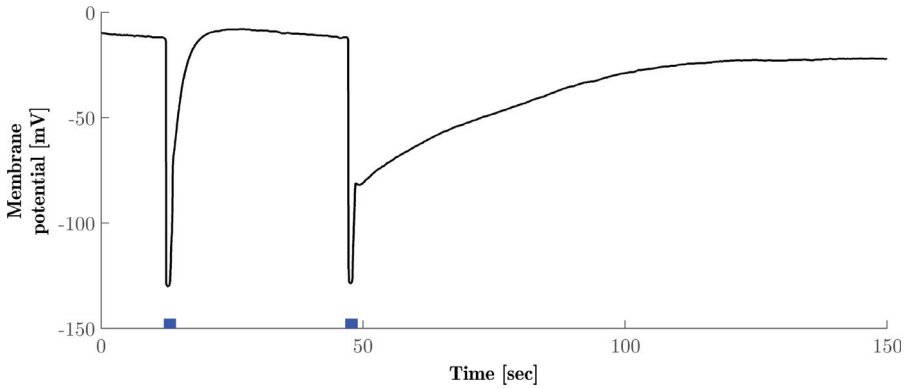

Figure 42: PDA-PDA facilitation. Weak $R \rightarrow M$ stimulus (transferring 14% of the pigment to the M state). Long after this PDA has declined to base line, and a second equal $R \rightarrow M$ induces a much larger PDA. This facilitatory effect declines with time interval between the two stimuli. Existence of facilitatory effect indicates an underlying latent nonlocal process. (Data from Hillman et al. 1976, graph replotted from Hillman et al. 1983)

1976). In PDA facilitation, prior PDA is shown to enhance the following PDA as shown in Figure 42. PDA Facilitation was modeled in Öğmen and Gagné 1987 to arise from the antagonistic component to the "light drive" that decays at a different rate than the actual pigment states.

4.5 VISUAL PIGMENT STATES AND KINETICS

In this chapter the intermediate photoproducts of the *Drosophila* visual phototransduction are reviewed serving as a physiological primer for the following modeling chapters (Section 4.6 and Section 5.5)

4.5.1 *"Complete cycle" with intermediate states*

In 4.1.2, the basic scheme of the invertebrate phototransduction was discussed omitting the details needed for quantitative understanding of the phototransduction process. Both vertebrate and invertebrate phototransduction consist of various steps of which many occur in picoseconds making the measurement them difficult in room temperatures and *in vivo* conditions. The phototransduction is highly temperature dependent (Thorgeirsson et al. 1993; Szundi et al. 2010), thus the kinetics can be slowed down significantly *in vitro* conditions, even down to ~ -195°C using liquid nitrogen. The obtained results can be then temperature corrected for physiological conditions.

A simplified schematic of the visual cycle (4.1.2) with only the distinct conformational forms is shown in Figure 87 (Kruizinga et al. 1983). The activation of the "response-ready" R-state by light absorption ($h\nu_1$) converts the R to bathorhodopsin B, which then thermally decays to lumirhodopsin L, metarhodopsin M following. The M-state now corresponds to the bistable state referred in 4.1.2), and the M-state can be regenerated back to the R via an intermediate photoproduct K. The time constants (τ) of the steps are shown at room temperate (≈22°C). Additionally, in temperatures below 0°C, bathorhodopsin have been shown to convert to isorhodopsin (Suzuki et al. 1976), making it under physiological temperatures insignificant (Kruizinga et al. 1983). The intermediate K was seen in the study by Kruizinga et al. 1983, while previous study had failed to see an intermediate (Kirschfeld et al. 1978b), and another study found an additional intermediate N in the regeneration pathway.

Additionally, exploiting the fluorescence of the M state (Stark et al. 1977), it has been suggested that there is an additional intermediate photoproduct in *Drosophila* termed as M' (Franceschini et al. 1981), being suggested to be converted from lumirhodopsin L. The putative M' state was shown to fluoresce > 3 times more stronger than the M state with the photosensitivity of M' being significantly smaller. The excitation and emission spectra λ_{max} of M' was shown to be redshifted to ≈ 660 nm from the λ_{max} ≈ 570-580 nm of the M state. Furthermore, the photoproduct M' was seen to build up only at extreme light intensities. From physiological viewpoint the M' was considered to be completely unimportant and artificially produced state (Stavenga 1983). However, if one considers the possibility that similar "high intensity-only" intermediate exists for melanopsin and it

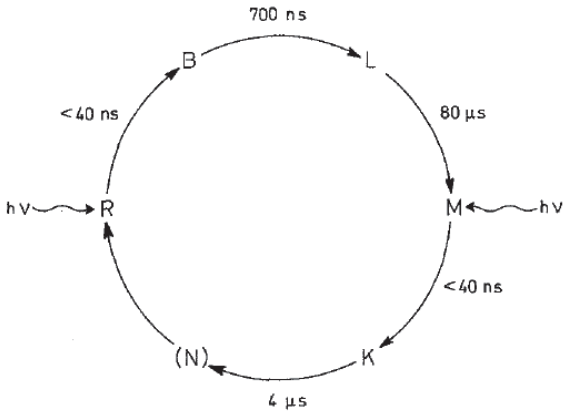

Figure 43: Schematic representation of the photochemical cycle of blowfly (*Calliphora*) rhodopsin. rhodopsin R excited by light absorption converts to bathorhodopsin B. Thermal decay via lumirhodopsin L to metarhodopsin M follows. The back reaction proceeds via putative intermediates K and possibly N. Time constants of the conversion steps are indicated (Kruizinga et al. 1983).

would be capable of signaling, it could offer an explanation for the "paradoxical" photopotentiation seen in mouse PLR (Zhu et al. 2007, later reviewed in 4.7.1).

The similar scheme seem to exist for the vertebrate rhodopsin (first shown by Matthews et al. 1963) as shown in Figure 44 (Bartl and Vogel 2007) with the lumi- and bathorhodopsins excluded from the scheme. Activation of rhodopsin ("dark state") by light leads to a conformational equilibrium of inactive Meta I and active Meta II state (Figure 44A for Meta II), absorbing at 480 and 380 nm, respectively. In addition to the transduction cascade progressing "normally" towards the all-*trans* state, Meta III [in early literature (Matthews et al. 1963) also referred as 465 nm compound, transient orange, pararhodopsin, P470 and metarhodopsin$_{465}$] can be formed that is maximally absorbing at 470 nm (Figure 44B). The Meta III was shown to be light sensitive (Matthews et al. 1963), using a second illumination with light >475 nm after the initial activation ("first illumination" in Figure 44A) efficiently converting Meta III back to Meta II/I (Figure 44B). Other decay products such as opsin, released all-*trans*, and Schiff base being insensitive for this light step (Heck et al. 2003; Vogel et al. 2003; Bartl and Vogel 2007). Additionally, previous study had shown illumination of Meta III resulting in photoregeneration of rhodopsin and isorhodopsin (Donner and Reuter 1969).

The Meta III is a relatively stable state thermally (at 30°C, time constant is in the range of hours). It has been suggested to functions as a storage for all-*trans* retinal and remove it temporally from the biochemical reactions of the visual cycle (Heck et al. 2003). Recent studies have shown that excess all-trans retinal in the outer segment of photoreceptor cells may form deleterious adducts to rhodopsin, which

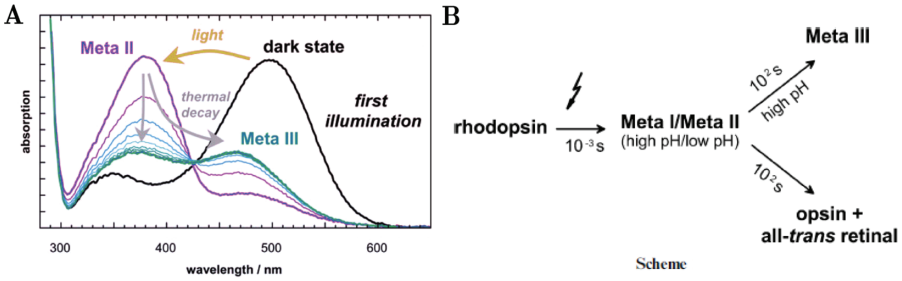

Figure 44: **Vertebrate** rhodopsin **intermediates.** (**A**) Decay of the activated Meta II state to Meta III. Illumination of rhodopsin's dark state (λ_{max} = 500 nm**)** produces the Meta I/Meta II photoproduct equilibrium, which consists mostly of active Meta II at 30 1C and pH 8.0, absorbing at 380 nm (A). This equilibrium then decays thermally on the time scale of minutes via two pathways to (i) opsin and all-trans retinal via hydrolysis of the retinal Schiff base, leading to an absorption loss at 380 nm, and (ii) Meta III, giving rise to an absorption increase at 470 nm (spectra were recorded immediately after illumination and subsequently at 2 min intervals up to 20 min after illumination). By applying a second illumination, the decay product Meta III of the second pathway can be converted back to Meta I/Meta II (again consisting mostly of Meta II), while the decay products of the first pathway, opsin and all-trans retinal, remain largely unreactive. **(B)** (Bovine) rhodopsin transduction. Activation of rhodopsin is achieved by light-dependent isomerization of the chromophore and subsequent thermal relaxation of the receptor on the millisecond time scale to the active receptor conformation. This relaxation of the receptor proceeds via several, spectroscopically resolvable intermediates and involves as a key event the transition from the still inactive Meta I to the active Meta II state, absorbing at 480 and 380 nm, respectively. These two photoproduct states form a conformational equilibrium that can be shifted from Meta I to Meta II by decreasing pH or increasing temperature. (Bartl and Vogel 2007)

Table 4: Spectral parameters of rhodopsin and products of its photolysis in *B. bufo* (first row) and *R. temporaria* rods (second row)[a] (Kolesnikov et al. 2003).

	Rh	Meta I	Meta II	Meta III	Retinal	P440	Retinol
λ_{max}	502	489	379	479	381	440	325
nm	503	470	382	478	381	449	325
ϵ	1	1.09	1.16	1.0	1.05	0.9	1.29
	1	1.09	1.16	1.0	1.05	0.9	1.29
DR	6.4	6.4	12.5	12.5	0.49	0.36	0.41
	5.7	5.7	14.6	14.6	0.5	0.7	0.5

[a] λ_{max}, wavelength of maximum absorbance; ϵ molar extinction at λ_{max}, with respect to rhodopsin; DR, dichroic ratio Transversal polarization/Longitudinal polarization. In each row, the upper line corresponds to *B. bufo*, and the lower, to *R. temporaria*. λ_{max} for retinal and retinol and ϵ for retinol are taken from Knowles et al. 1977.

are involved in age-related macular degeneration and other retinal diseases (Fishkin et al. 2003, Różanowska and Sarna 2005). Under intense light with higher bleaching, a delayed release of all-trans retinal during Meta II decay by formation of a Meta III storage, thus might be physiologically advantageous for retinal protection (Bartl and Vogel 2007). The spectral sensitivity and dichroic ratios of intermediate photoproducts are summarized in Table 4 (Kolesnikov et al. 2003).

Hubbard and Kropf 1958 was first to show that normal photobleaching could be prevented if additional light was absorbed by the bleaching intermediates, referred as the "photoreversal" of bleaching (Williams 1964). Similar phenomenon was observed in early receptor potential (ERP) recordings of a rat, with complete bleaching of rhodopsin abolishing early receptor potential, but being recordable again after a blue light flash (Figure 45B, Cone 1967). The most likely intermediate photoproduct being photoreversed was suggested to be metarhodopsin II, that has a peak absorbance at ~380 nm with a 1.2 times higher excinction coefficient than rhodopsin (Weale 1967; Bartl and Vogel 2007). Further rat study *in vivo* by Grimm et al. 2000 estimated the quantum efficiency of photoisomerization to be roughly ~0.3 (Figure 45A,inset), while demonstrating that light at 550 nm was able to fully bleach the rhodopsin, in contrast to the "rhodopsin-equal" exposure at 403 nm that left significant portion of rhodopsin to the unbleached state (Figure 45A). This blue-enhanced photoreversal was linked to the increased susceptibility for blue-light damage (Grimm et al. 2001).

4.5.2 *Deactivation of the photoresponse*

The temporal resolution of the visual process depends on the speed of the biochemical chain and on the lifetime of the active metarhodopsin state (M_a), the trigger of the phototransduction chain (Burns and Arshavsky 2005, Burns and Baylor 2001). Inactivation of the metarho-

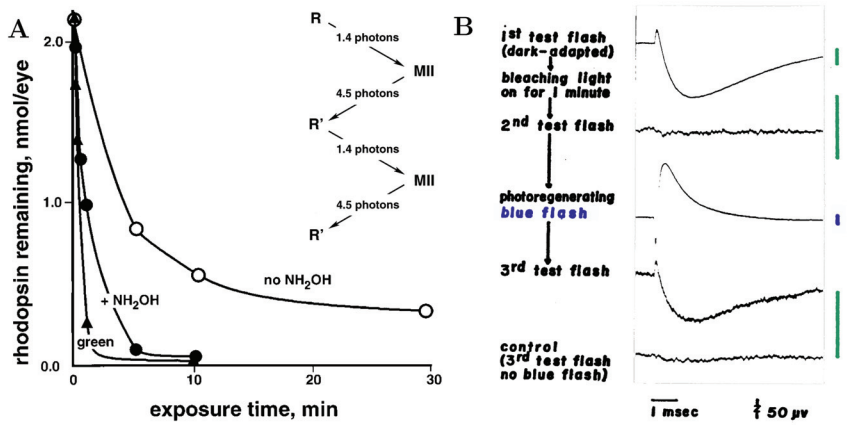

Figure 45: **Photoreversal of human** rhodopsin**. A)** Bleaching of rhodopsin *in vivo* by blue and green light. Eyes of anesthetized rats were exposed to green light (▲, 550 nm), to blue light (○; 403 nm), or to blue light in the presence of NH2OH to inhibit potential photoreversal of bleaching (●; 403 nm). rhodopsin disappeared rapidly in green light and in blue light with NH2OH, conditions with minimized photoreversal of bleaching. However, in blue light without NH2OH, rhodopsin disappeared slowly, despite irradiation with the same photon fluxes as in the other two conditions. **Inset:** Scheme for calculating the total number of photons absorbed by rhodopsin (R) and the photoreversible intermediate, assuming it is metarhodopsin-II (MII). Photoregenerated rhodopsin is shown as R′. The numbers on the arrows indicate the average numbers of photons needed to cause the reactions and reflect the fact that the quantum efficiencies of bleaching and photoreversal are not unity (Grimm et al. 2000). **(B)** Photoregeneration of the ERP in the eye of the albino rat. Both the test flash and the bleaching light consisted of long wavelengths primarily absorbed by rhodopsin. The blue, photoregenerating flash contained wavelengths absorbed by the longer-lived intermediates of the bleaching process. The control trace was obtained from a second eye subjected to the same bleaching exposure and test flashes, but without the blue flash. Temperature, 27°C (Cone 1967).

dopsin state occurs on binding of an arrestin molecule [cf Nair et al. 2005 in vertebrates, and Belušič et al. 2010 in invertebrates], allowing the visual system to respond to subsequent stimuli (Hardie 2001). Photoconversion of the metarhodopsin (M_i) back to rhodopsin ($R_i \rightarrow R_a$ transition) is followed by arrestin release, after which the resulting native rhodopsin (R_a) is ready for another round of phototransduction (Byk et al. 1993; Hardie and Postma 2008). Similar role of arrestin in the deactivation of the melanopsin photoresponse was shown by Hatori and Panda 2009 as suggested earlier in Panda et al. 2005, thus being included to the quantitative model of melanopsin phototransduction later (Section 4.6).

In *Drosophila*, which has been extensively studied, there are two arrestin forms, arrestin1 (*Arr1*) and arrestin2 (*Arr2*), originally identified as phosrestin 2 and 1, respectively (Matsumoto and Yamada 1991). *Arr2* is approximately sevenfold more abundantly expressed than *Arr1* in the wild type fly. *Arr2* is the functionally more important form for the inactivation of metarhodopsin (Dolph et al. 1993), *Arr2* mutants ($w-;arr2^3$) having a log unit lower threshold for entering the PDA state compared to the wild-type flies (Dolph et al. 1993; Vinós et al. 1997; Belušič et al. 2010). The residual arrestin in *Arr2*-mutants is mostly *Arr1*, still being able to inactivate metarhodopsin, while less effectively resulting in a slow course of inactivation in the *Arr2* mutant (Ranganathan and Stevens 1995). At low light intensities, the photoreceptor sensitivity was shown to be arrestin independent (Liu et al. 2008; Belušič et al. 2010).

In vertebrates, the rhodopsin is multiply phosphorylated by rhodopsin kinase, and phosphorylation is essential for the inactivation (Benovic et al. 1986; Chen et al. 1995). In contrast, in a mutant with the phosphorylation sites deleted, showed no defects in electrical responses or in the ability of arrestin to bind to rhodopsin (Vinós et al. 1997), implying that the phosphorylation plays no direct role in the fly phototransduction (Hardie 2001; Liu et al. 2008). Light-dependent phosphorylation have been suggested to be involved in melanopsin photoresponse deactivation (Robinson et al. 2009; Blasic et al. 2011).

Additionally, upon illumination arrestin translocates from photoreceptor cell bodies to rhodopsin and membrane-rich photosensory compartments, vertebrate outer segments (Calvert et al. 2006) and invertebrate rhabdomeres (Satoh et al. 2010). This physical translocation of the arrestin molecules has suggested to play a role of adapting arresting levels to the prevailing f_{Me} levels determined by the ambient illumination (Satoh et al. 2010).

4.5.3 *Measuring phototransduction kinetics*

In invertebrates, the simultaneous study of electrical responses (ERG) and pigment state can be conveniently studied via fluorescence mea-

surements (Figure 46B). The fluorescence of *Drosophila* rhodopsin has been shown to be negligible, while the metarhodopsin states M and M' (4.5.1) exhibit a strong fluorescence (Figure 46A), with a high emission in the red wavelength range (Stavenga et al. 1984, Stavenga 1983). The fluorescence measurements are preferably applied in white-eyed mutants and are performed with a microspectrophotometer, the instrument diaphragm isolating the fluorescence from the deep pseudopupil (Lee et al. 1996; Stark and Thomas 2004). Figure 46C shows the relation of the measured ERG and PDA responses as a function of light intensity in both the wild type ($w-$) and the arrestin mutant ($w-;arr2^3$) fly demonstrating pronounced PDA in arrestin-deficient mutant flies as expected (4.5.3).

In vertebrates, the kinetics of phototransduction have been studied *in vivo* for example, measuring the changes in near-infrared light scattering (Uhl et al. 1990) following the photoactivation of rhodopsin (Vuong et al. 1984). Recently, adaptive optics system (for reviews see Porter et al. 2006; Hampson 2008; Roorda 2011) have been added allowing measurements of phototransduction in humans *in vivo* (Grieve and Roorda 2008; Jonnal et al. 2010; Hunter et al. 2011). There are no reports describing the fluorescence of melanopsin intermediate photoproducts. In theory the fluorescence of melanopsin could be measured with adaptive optics systems (Gray et al. 2006; see also Section 6.5) *in vivo* to determine the relative concentration of R and M states if similar fluorescence were found for the melanopsin M state, and other ocular fluorescent sources would not have spectrally overlapping fluorescence.

4.6 VISUAL-PIGMENT ARRESTIN CYCLE

Simplified visual pigment-arrestin cycle is shown in Figure 47 providing a quantitative framework for pigment-level kinetics in a fly bistable pigment system. Photoconversion of the native, active rhodopsin (R_a) creates the active metarhodopsin state (M_a, at a rate of k_R) , this M_a state triggers the phototransduction. Upon binding arrestin (A) the photoresponse is quenched and M_a converts into inactive metarhodopsin (M_i, at a rate of k_b) . Photoconversion of M_i creates inactive rhodopsin (R_i, at a rate of k_M), which upon arrestin release return to the active rhodopsin state R_a (at a rate of k_d). Inactive metarhodopsin (M_i) is phosphorylated when photoconverted from M_a, dephosphorylation occurring upon photoconversion from R_i to R_a (Kiselev and Subramaniam 1994). However, available data in flies indicate that the phosphorylation state does not influence its activity or its activity to bind to arrestin (4.5.2), making it possible to exclude it from the quantitative modeling. Additionally, the arrestin-bound states M_i and R_i are subject to spontaneous degradation with a rate of k_f, with R_a regenerating in the dark at the rate of k_g.

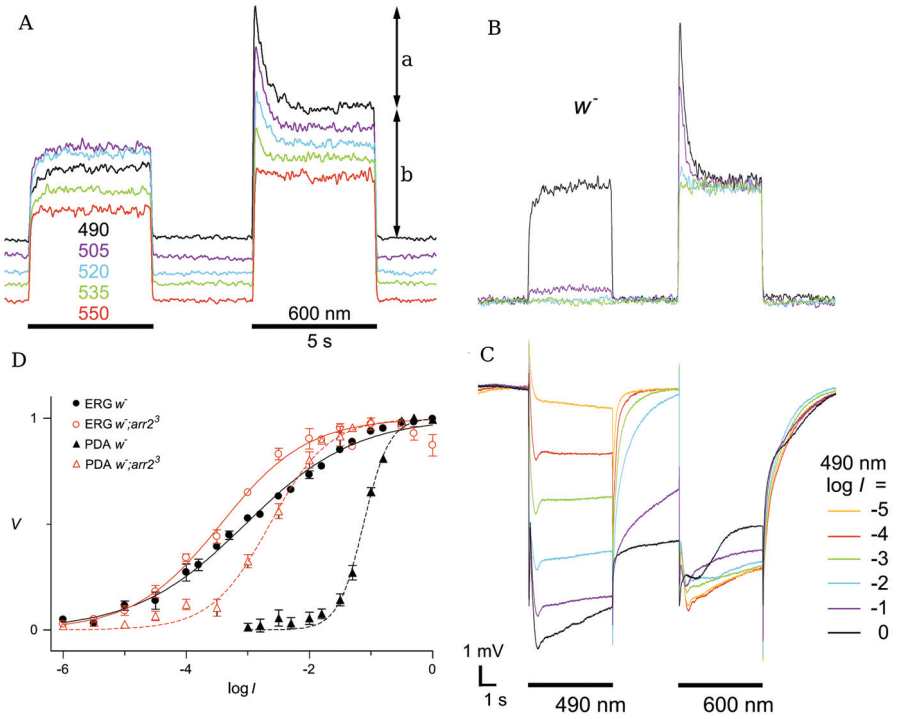

Figure 46: **(A)** Metarhodopsin fluorescence as a function of wavelength. a Fluorescence signals induced by a number of monochromatic light pulses (wavelengths 490–550 nm) followed by a red (600 nm) light pulse (*Drosophila*). The values of the initial red-induced emission due to the metarhodopsin, **a**, and the background value, **b**, were measured. Simultaneous measurements of the metarhodopsin fluorescence **(B)** and electroretinogram **(C)** from the eyes of a wild-type *Drosophila*, elicited by monochromatic blue pulses of 490 nm followed by red pulses (600 nm). Blue pulses with intensities log I > -3 created a measurable metarhodopsin fraction as witnessed by the red-induced fluorescence signal (fluorescence decay induced by the 600 nm pulse). **(D)** Amplitudes V of ERG responses (ERG) and afterpotentials (PDA) elicited by the blue light (490 nm) pulses of **(B)**, for both the wild type ($w-$) and the arrestin mutant ($w-;arr2^3$); error bars, SEM. The ERG responses and PDA functions are fitted with sigmoidal Hill functions. Adapted from Belušič et al. 2010

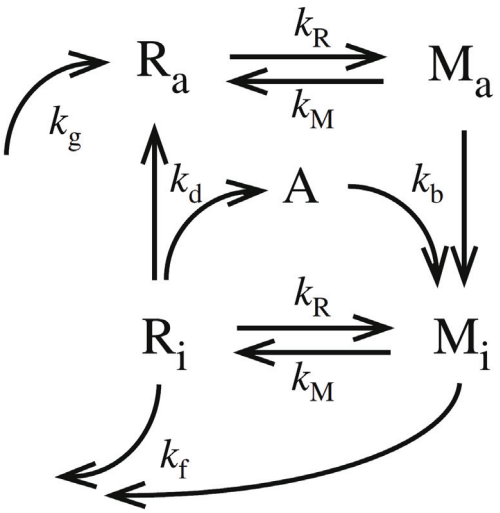

Figure 47: **Visual pigment-arrestin cycle.** Photoconversion of active rhodopsin, R_a, creates active metarhodopsin, M_a, which upon binding arrestin, A, becomes inactive metarhodopsin, M_i. Photoconversion of M_i creates inactive rhodopsin, R_i, which upon arrestin release converts into the native rhodopsin, R_a. The light-induced conversion processes have rate constants k_R and k_M, the rate constants of arrestin binding and dissociation are k_b and k_d. R_i and M_i are degraded with rate constant k_f, and R_a is regenerated with rate constant k_g. (Stavenga and Hardie 2010).

To simplify the quantitative analysis of the pigment-arrestin cycle, the cycle can be assumed to be a "closed system" (4.2.1) so that the total number of pigment molecules does not change:

$$R_0 = R_a + M_a + R_i + M_i \tag{35}$$

The microvillus might not be completely filled with the maximal number of molecules R_{max} then the number of missing visual pigment molecules is $R_m = R_{max} - R_0$. When A_0 is the total number of arrestin molecules and A the number of unbound arrestin molecules, then:

$$A_0 = R_i + A + M_i \tag{36}$$

The pigment-arrestin cycle can be described by a set of linear differential equations (Stavenga and Hardie 2010, note that the $+k_d R_a$ term from was missing from the original publication):

$$
\begin{aligned}
dR_a/dt &= -k_R R_a + k_M M_a + k_g R_m && (37)\\
dM_a/dt &= -k_M M_a + k_R R_a - k_b A M_a && (38)\\
dM_i/dt &= -k_M M_i + k_R R_i + k_B A M_a - k_f M_i && (39)\\
dR_i/dt &= -k_R R_i + k_M M_i - k_d R_i - k_f R_i && (40)\\
dA/dt &= -k_b A M_a + k_d R_i + k_f M_i + k_f R_i && (41)
\end{aligned}
$$

The steady-state (photoequilibrium) is when the net pigment transitions equal zero: $dR_a/dt = dM_a/dt = dM_i/dt = dR_i/dt = dA/dt = 0$, thus the fraction in equilibrium is:

$$f_{Me} = (M_a + M_i)/R_0 \quad (42)$$

The rate constants k_R and k_M (s^{-1}, Eq. (16)) depend on the light intensity, increasing intensity driving the pigment-arrestin system more quickly to photoequilibrium (smaller rate constants), following an exponential time course with time constant $\tau_c = 1/(k_R + k_M)$ (Eq. (20)). The behavior of the system (i.e. rate constants for the $R \rightleftharpoons M$ transitions) depends furthermore on the values of quantum efficiency (γ_i), the molecular absorbance coefficient (α_{max}), concentration (C) of the photopigment, and on the absorbance coefficient of the rhabdomere / outer segment medium (κ_{max}). Typical values for these value from the literature are listed in Table 6 in B). The rate constants k_R and k_M can be expressed for monochromatic light stimulus as following combining Eq. (15) and Eq. (16):

$$k_R = \int_{380}^{780} \left[\left(\gamma_R \frac{\kappa_{max}}{C} \alpha_{R,norm}(\lambda) \right) \times (I(\lambda) h(\lambda))\, d\lambda \right] \quad (43)$$

$$k_M = \int_{380}^{780} \left[\left(\gamma_M \frac{\kappa_{max}}{C} \alpha_{M,norm}(\lambda) \right) \times (I(\lambda) h(\lambda))\, d\lambda \right] \quad (44)$$

where the $I(\lambda)$ is the corneal spectral irradiance, $h(\lambda)$ is the ocular media transmittance [to avoid confusion with time constant τ_c the typically used $\tau(\lambda)$ was changed (2.2.3)], and the $\alpha_{i,norm}$ is the spectral shape of the photon absorption as defined by a nomogram (Govardovskii et al. 2000; Stavenga 2010). The parameters for melanopsin system were estimated to be (see also Section B.4) 1.0 for relative quantum efficiency ($\varphi = \gamma_M/\gamma_R$), $5.5 \times 10^{-5}\mu m^2$ for molecular absorbance coefficient (α_{max}), 1,560 μm^{-3} for melanopsin concentration (C), and $3.5 \times 10^{-2}\mu m^{-1}$for the melanopsin "medium" coefficient (κ_{max}). This model of Stavenga and Hardie 2010, allows the evaluation of relative distribution of the four pigment states and arrestin dynamically as a function of time and light intensity.

This proposed model can be further elaborated for melanopsin system, incorporating the melanopsin photoreceptor geometry to the model as outlined by Warrant and Nilsson 1998 for general photoreception. The above-defined equations are valid for infinitesimal photoreceptors, which is not the case for real-world photoreceptors. The self-screening effect (2.3.3) of the photoreceptors thus has to be taken into account for the path length of the traveled light through photoreceptors, extreme case being dragonfly which has the longest photoreceptors known (>1.1 mm) in nature (Labhart and Nilsson 1995). The absorption coefficient κ_{max} (in older literature k) relates the medium properties (i.e. pigment density) to the fraction $F(l)$ absorbed in the total medium as a function of photoreceptor length l in simple case (Warrant and Nilsson 1998):

$$F(l) = 1 - e^{-\kappa_{max} l} \tag{45}$$

This fraction $F(l)$ is known as *absorptance* (Knowles et al. 1977), the larger the value being the more light incident on the photoreceptor is absorbed by it. Small $F(l)$ indicate that self-screening has no significant effect on the spectral sensitivity of the given pigment, due to short path length or low pigment concentration ($C = \kappa_{max}/\alpha_{max}$). The Eq. (45) is however only valid for monochromatic light, and not valid for polychromatic white light, and the wavelength dependence of parameter κ has to be added for $F(l)$ knowing that $k(\lambda) = k\alpha_{norm}(\lambda)$ as following:

$$F(l, \lambda) = 1 - e^{-\kappa\alpha_{norm}(\lambda) l} \tag{46}$$

Eq. (46) describes the *absorptance spectrum*, with absorbance spectrum $\alpha(\lambda)$ having values between 0 and 1 with a nomogram shape, $\kappa(\lambda)$ varying between 0 and κ_{max}. This equation can now be used to calculate the spectral absorbance as a function of path length, i.e. how the spectral sensitivity changes as light is absorbed in the deeper layers of the photoreceptors (see Figure 9). This effect can be expressed as the fraction $F_w(\kappa, l)$ of total number of photons Q_T available to the photoreceptor from environmental light $I(\lambda)$ in wavelength range between λ_1 and λ_2:

$$Q_T = \int_{\lambda_1}^{\lambda_2} I(\lambda) d\lambda \tag{47}$$

and the total number of photons absorbed Q_A by the photoreceptor of a given length l with an absorptance spectrum $\alpha(\lambda)$:

$$Q_A = \int_{\lambda_1}^{\lambda_2} I(\lambda) F(l, \lambda) d\lambda = \int_{\lambda_1}^{\lambda_2} I(\lambda) \left(1 - e^{-\kappa\alpha_{norm}(\lambda) l}\right) d\lambda \tag{48}$$

The fraction $F_w(\kappa, l)$, thus becomes (Warrant and Nilsson 1998):

$$F_w(\kappa, l) = \frac{Q_A}{Q_T} = \frac{\int_{\lambda_1}^{\lambda_2} I(\lambda)\left(1 - e^{-\kappa\alpha_{norm}(\lambda)l}\right) d\lambda}{\int_{\lambda_1}^{\lambda_2} I(\lambda) d\lambda} \tag{49}$$

where the subscript w denotes "white" light absorption. The obtained $F_w(\kappa, l)$ can now be combined with commonly used Land equation (Land 1981; Kirschfeld 1974) for determining the optical sensitivity S_w of an eye (as used by Stavenga and Hardie 2010 for *Drosophila*) that is given as:

$$S = \left(\frac{\pi}{4}\right)^2 A^2 \left(\frac{d}{f}\right)^2 \left(1 - e^{-\kappa l}\right) \tag{50}$$

where A is the diameter of the (circular) aperture through which light enters the eye (pupil in humans, Section 3.1), f is the focal length of the eye (~1.67 cm in humans, 2.2.1), and d the diameter of each photoreceptor (~10 μm for mouse ipRGC, B.4.1). Now by replacing the Eq. (46) in Eq. (50), we obtain the following for optical sensitivity $S_w(\kappa, l)$ of the human eye to white light as a function of absorbance coefficient $\kappa(\lambda)$ and path length l (Warrant and Nilsson 1998):

$$\begin{aligned} S_w(\kappa, l) &= \left(\frac{\pi}{4}\right)^2 A^2 \left(\frac{d}{f}\right)^2 F_w(\kappa, l) \\ &= \left(\frac{\pi}{4}\right)^2 A^2 \left(\frac{d}{f}\right)^2 \left(\frac{\int_{\lambda_1}^{\lambda_2} I(\lambda)\left(1 - e^{-\kappa\alpha_{norm}(\lambda)l}\right) d\lambda}{\int_{\lambda_1}^{\lambda_2} I(\lambda) d\lambda}\right) \end{aligned} \tag{51}$$

The optical sensitivity $S_w(\kappa, l)$ is the ratio of the number of photons (at λ_{max}) absorbed by a photoreceptor to the number (at λ_{max}) emitted per steradian of solid angle from a unit area of an extended source. In other words, it is a measure of a photoreceptor's ability to capture photons when viewing an extended light source of given radiant intensity. This ability depends partly on the design of the eye, and partly on the design of the photoreceptor: photoreceptors absorb more photons when they view larger solid angles of visual space [proportional to $((d/f)^2$] through larger pupils [proportional to A^2]. $S_w(\kappa, l)$ therefore has units of $\mu m^2 \cdot steradian^{-1}$ (Warrant and Nilsson 1998).

Strictly speaking in the above equation, it is assumed that the parameter $\kappa(\lambda)$ is constant over time, while in reality is the effected by the "bleaching state" of the pigment (2.3.3) being effectively smaller in light-adapted retina for cones and rods. Given the uncertainty whether melanopsin bleaches optically (i.e. does its transmission characteristics significantly change), with its very low pigment density (~4 log units less, Do et al. 2009), the added complexity of estimating bleaching state as a function of light intensity and duration (for

calculation see Mahroo and Lamb 2004) can be avoided. Now the optical sensitivity $S_w(\kappa, l)$ can be combined with the rate constant (k_R and k_M) equations Eq. (16) to obtain more complete descriptions for polychromatic light than defined previously for monochromatic light in Eq. (43) and Eq. (44). The ratio can be dropped, retaining only the absorbed photons Q_A as illustrated in Fig. 3 of Warrant and Nilsson 1998:

$$k_R = \left(\frac{\pi}{4}\right)^2 A^2 \left(\frac{d}{f}\right)^2 \int_{380}^{780} I(\lambda) h(\lambda) \left(1 - e^{-\kappa \gamma_R \alpha_{R,norm}(\lambda) l}\right) d\lambda \tag{52}$$

$$k_M = \left(\frac{\pi}{4}\right)^2 A^2 \left(\frac{d}{f}\right)^2 \int_{380}^{780} I(\lambda) h(\lambda) \left(1 - e^{-\kappa \gamma_M \alpha_{M,norm}(\lambda) l}\right) d\lambda \tag{53}$$

The obtained expressions can be numerically evaluated, in contrast to the approximated and tabulated values proposed by Warrant and Nilsson 1998.

4.7 MELANOPSIN AS A BISTABLE PHOTOPIGMENT

There is evidence suggesting that mammalian melanopsin functions like an invertebrate bistable rhodopsin. Evidence from studies employing heterologous expression of melanopsin suggest that melanopsin could act as both a sensory photopigment and a photoisomerase allowing regeneration of the activated photopigment (Melyan et al. 2005; Panda et al. 2005), while in contrast Qiu et al. 2005 found no support for this. Studies by Doyle et al. 2006 and Fu et al. 2005 suggest that melanopsin could work independently of the the visual retinoid cycle implying bistable capability of the photopigment indirectly. Studies on mice have provided contradictory results, two studies are in favor of bistability *in vivo* (Mure et al. 2007; Qiu and Berson 2007), whereas Mawad and Van Gelder 2008 found no evidence for either *in vivo* nor *in vitro* melanopsin bistability. The discrepancy between the results may rise from the high irradiance used by Mawad and Van Gelder 2008 close to melanopsin response saturation making the assessment of bistability more difficult (Cooper and Mure 2008).

The question of melanopsin bistability was suggested to be solved via biochemical (Van Gelder and Mawad 2008) or spectrophotometric means, with suitable light stimuli driving the pigment back and forth between the thermostable inactive and active states each with its characteristic absorption spectrum. The hypothesis of melanopsin bistability was supported by the spectrophotometric results of Koyanagi et al. 2005 for *Amphioxus* melanopsin (inactive "R-state" λ_{max}~ 485 nm, and an active Meta-state with a red-shifted λ_{max}~ 520 nm). However it should be noted, the *Amphioxus* is an invertebrate (Koyanagi et al. 2005; Gomez et al. 2009), and mammalian melanopsin may be functioning differently (Bellingham et al. 2006, Koyanagi et al. 2005). Walker et al. 2008 found that for purified mouse mRGCs, following 480-nm stimulation, both *cis*- and *trans*- forms were observed suggesting additional light-independent pathway ("dark regeneration" as for rods and cones) while not excluding bistable hypothesis.

In humans, the evidence for melanopsin bistability is still very limited. The study of Mure et al. 2009 used PLR as a tool in humans with a classical strategy of successive monochromatic stimulations used first by Lisman and Sheline 1976 with *Limulus* to demonstrate the "bistable hypothesis" using early receptor potential (ERP). In this strategy, two equal "test" light pulses are presented (480 nm light in Mure et al. 2009) with an adapting light stimulus between these two [for example $M \rightarrow R$ (red light) and $R \rightarrow M$ stimuli (blue light)], and then the modulating effect of this light pulse is quantified using the action spectra described in Section 4.3. Additionally, several different "test" light pulses could have been used [see Fig. 1 of Stavenga 1976] to provide stronger evidence of the existence of bistable pigment system with a single isosbestic point (4.3.2). Mure et al. 2009 found the

preceding $M \rightarrow R$ stimulus (620 nm) potentiating the following sustained PLR component in response to the "test" $R \rightarrow M$ stimulus (480 nm), and the preceding "adapting" $R \rightarrow M$ stimulus (460 nm) depressing the following sustained PLR component, as predicted by the bistability hypothesis.

Similar protocol was used by Hansen et al. 2011 reducing the time between pulses to 30 secs compared to the 40 minutes of Mure et al. 2009 between adapting and the second "test light". In this temporally compressed protocol, both preceding blue (470 nm) and red (660 nm) light was found to potentiate the following PLR response. The authors themselves provided little explanation for the found discrepancy with previous data, but an invertebrate analog for the observed phenomenon could be the "PDA facilitation" (4.4.4) in which subsequent identical stimulus can be potentiated if the preceding stimulus has not transferred "too much" of the pigment from the R to the M state. Fontaine and Hébert 2011 found preliminary evidence for potentiating effect of red (620 nm) light alternated very rapidly with blue (460 nm) light (3 ms of blue, 11 ms of red) for mean heart rate.

4.7.1 *Bistability potentiation/Sensitization*

An observed phenomenon closely related to "bistability–potentiation", is the photopotentiation demonstrated by Zhu et al. 2007 in mice. After "supersaturating" light stimulus (1 minute of 18 W/m², white light from an unspecified halogen light source) the following 1 minute blue "probe" light (470 nm) pulse, either at half-saturating irradiance IR_{50} or at 70%-saturating irradiance IR_{70}, was shown to elicit a potentiated PLR rather than a depressed PLR. The photopotentiation was shown to originate from melanopsin despite the unique action spectrum (Figure 48B) as mice ($opn4^{-/-}$) lacking melanopsin showed no photopotentiation. The shown photopotentiation was shown to depend strongly on the dark period after the supersaturating stimulus (Figure 48A) with the photopotentiation effect quickly dissipating with increased dark period. Secondly, the photopotentiation exhibited very non-linear even switch-like dependence on irradiance (Figure 48B) occurring approximately at 2 log units higher light intensity than required to drive the PLR itself. Thirdly, the spectral sensitivity was measured (Figure 48C) with photopotentiation occurring nearly equally at all blue-light wavelengths, but falling off at wavelengths longer than 500 nm.

Underlying photosensitive structure was not identified by the authors, but visually comparing the results (Figure 48B) to the absorbance spectrum of the Metarhodopsin II/III (Figure 44A) in vertebrates, the shape could be in theory explained by photosensitive melanopsin intermediate photoproducts. Similar unexplained "third photosensitive" state was found in the study of Cronin and Goldsmith 1984

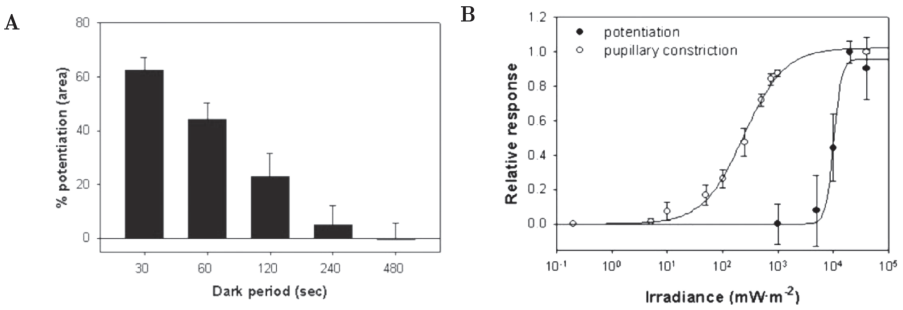

Figure 48: **(A)** Time-course of decay of photopotentiation in *rd/rd* mice. A dark period of variable length was interposed between the saturating white-light pulse and the subsequent 470-nm probe-light stimulus. Percentage of potentiation was calculated by comparing dark-adapted and post-saturated PLRs during probe-light stimulation. Data plotted as the mean ± SE (n = 5). **(B)** Intensity dependence of photopotentiation in *rd/rd* mice. Data are plotted as the mean SE (n = 7). Energy dependence of PLR and photopotentiation in rd/rd mice. (○) Irradiance–response curve for initial PLR to white light (halogen). (●) Irradiance response curve for photopotentiation of PLR subsequent to a range of bright white light intensities (halogen). (Zhu et al. 2007)

in bistable crayfish rhodopsin. High intensity $R \rightarrow M$ stimulus was shown to "damage" both the dark-dependent and light-dependent (with $M \rightarrow R$) photoregeneration pathway, suggesting the existence of a second photosensitive "regenerating" system in addition to the bistable $R \rightleftharpoons M$ system, in which the photosensitive unit is likely to be protein-bound replacement chromophore. Such photosensitive unit is suggestive of retinochrome of cephalopod mollusks (Hara and Hara 1972), as present also in the eyes of bees (Pepe and Cugnoli 1980; Schwemer et al. 1984).

Additionally, the origin of the photopotentiation was tested testing both ipsilateral and contralateral pupillary responses (Section 3.2), with the photopotentiation occurring only in the eye receiving saturating stimulus, demonstrating the photopotentiation do occur either before bilateral integration in the olivary pretectal nucleus (OPN) or within the eye on the efferent limb. Finally, the PLR protocol was extended to a comparable *in vitro* multielectrode array (MEA) recording from an adult *rd/rd* mouse (5 weeks old) where in contrast to the PLR protocol, no photopotentiation was found for the ipRGC firing (Zhu et al. 2007). The wavelength-dependence in ipRGC firing was found (sensitivity higher for 430 nm than fro 530 nm) comparable to the established wavelength sensitivity. The authors concluded that the observed photopotentiation occurs downstream of the photopigment and immediate phototransduction event itself, more exactly at the synapse between ipRGC and OPN. The photopotentiation was suggested to counteract the adaptation of melanopsin-ipRGCs (Wong et al. 2007 and see 2.4.8) ensuring minimum pupil size even under

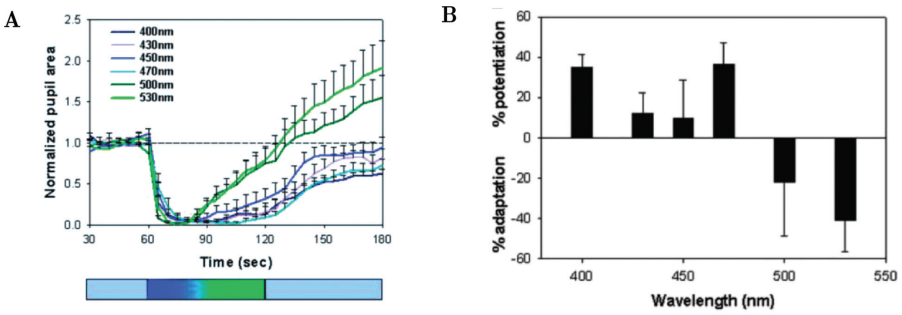

Figure 49: **(A)** Time-course of PLR to different wavelengths of saturating monochromatic light exposure (10^{15} photons/cm^2/s). The same animals were tested at all wavelengths. **(B)** Wavelength dependence of photopotentiation in *rd/rd* mice. Single irradiance relative response spectrum for photopotentiation in rd/rd mice. Photopotentiation of pupillary responses subsequent to stimulation with intense monochromatic lights of equal irradiance (10^{15} photons/cm^2/s for all colors) was examined. One-minute 470-nm light pulses (IR_{50}) were used to compare PLR sensitivity before and after intense light exposure. (Zhu et al. 2007)

high irradiances. Similarly the explanation would be compatible with the shown persistence of rat SCN cell firing *in vivo* in response to light stimuli up to 30 minutes (Meijer et al. 1998).

5 RESEARCH PROJECTS

5.1 BACKGROUND

The first presented research subproject (Section 5.2) is a continuation of the previous study by Mure et al. 2009 with Ludovic S. Mure. The study is focused on studying the dark regeneration time of the melanopsin and whether a "photic memory" (Hochstein et al. 1973) is exhibited in the melanopsin system, in other words if the melanopsin system is able to "remember" its state when left in the dark for 8 hours.

The second subproject (Section 5.3) was related to a melatonin suppression study done by Raymond P. Najjar in the same team. The goal was to quantify the effect of lens density for melatonin suppression between young and aged subjects for what a easily implementable and low-cost psychophysical method was realized for crude estimation of the lens density.

The third subproject (5.4) is a result from a collaboration with Véronique Daneault and Gilles Vandewalle in Montreal, in which the age-dependent pupillary light reflex (PLR) changes are studied. The last fourth subproject (Section 5.5) provides a quantitative framework for predicting the responses of bistable photopigment systems including the putative bistable melanopsin pigment system. The initially planned projects on studying differential photoreceptor contributions on NIF responses (2.4.5), and the use of PLR and especially its melanopsin-dependence on glaucoma diagnosis were never realized (Section 3.9).

5.1.1 *PLR Setup*

The PLR setup used in the study (Section 5.2) is almost the same as previously used by Mure et al. 2009, thus it is essential in the interpretation of the results presented in this work and previously obtained in the same team. The schematic of the consensual PLR measurement system is given in Figure 50, and the physical setup in our laboratory in Figure 51.

The homogeneity of the light distribution in the visual field was quantified using Photolux software (Dumortier et al. 2005), as shown in Figure 52. The system consists of Nikon 5000 digital camera with a fisheye lens and Photolux software developed in ENTPE, Lyon, France. The system is typically used for quantifying the luminance distribution in architectural lighting settings helping the lighting de-

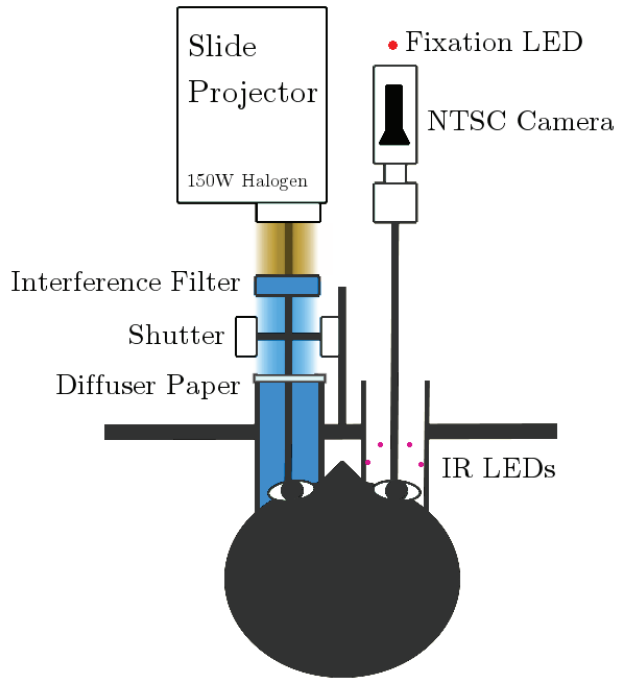

Figure 50: **Schematics of the used PLR setup.** The light is delivered consensually (left eye dilated with tropicamide) by photographic slide projector (24V/150W halogen light), the interference filter (hbw = 10 nm) is placed on the slide slot. The light output is controlled mechanically using a computer-controlled shutter (Uniblitz®). The filtered light is projected via mirror to a sheet of tracing paper glued on the end of a PVC tube (∅ = 6 cm). The inside of the PVC tube is painted with a white spray paint. The distance between the diffuser paper and the eye is ~10 cm. The right eye is illuminated by an array of concentrically placed IR LEDs (λ_{max}~ 950 nm), and monitored with an analogue NTSC camera (ViewPoint, Arrington®) digitized with a sampling rate of 60 Hz and a resolution of 640 x 480. The subject is asked to fixate to red LED (λ_{max}~ 950 nm) with a cross-shaped mask placed on top of the camera at the distance of ~17 cm.

signers verifying their designs (Rea 2003). There is also a simplified version of the software for iPhone (iPhotoLux, © 2011, Dominique Dumortier, LASH, ENTPE).

In the previous study by Mure et al. 2009, the IR LED illumination consisted of only one infrared LED placed on top of the camera objective. This was in many cases insufficient for the the used Arrington ViewPoint eyetracking system to detect pupil properly. The illumination was improved with an off-axis illumination from a total of eight infrared LEDs ($\lambda_{max} \sim 950$ nm) placed concentrically around the eye (Morimoto et al. 2000; Teikari 2007a). Additionally, the fluctuations in the pupil size were not around the mean "correct" pupil size in Gaussian manner, but rather fluctuated either between the "correct" pupil contour and some contour detected by the program inside or outside the "correct" pupil contour.

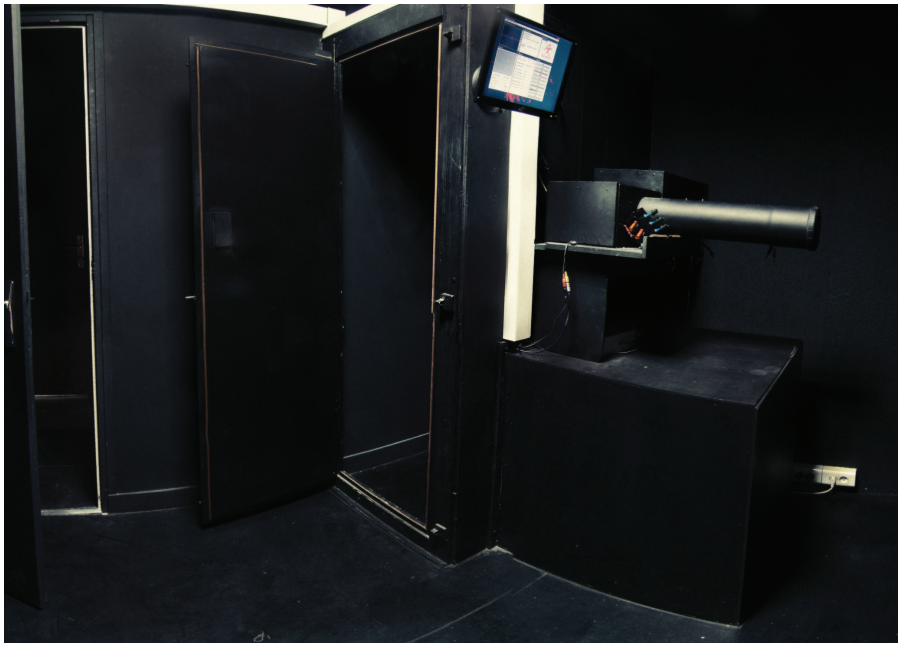

Figure 51: **Physical PLR setup.** The subject enters the light-proof-cabin in which there is a seat with a chinrest. External to the cabin there is a LCD monitor for helping to set the individual focus distance and camera positioning. The long tube is for housing of the fixation LED if its distance from the eye need to be increased.

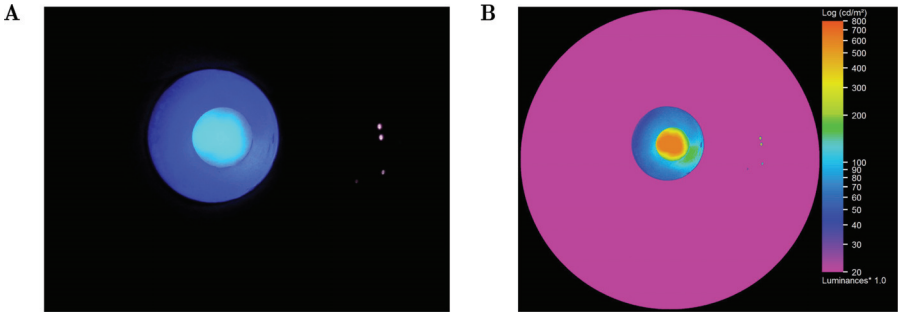

Figure 52: **Luminance homogeneity of PLR setup. (A)** Photo of the tube used for the light delivery. The bright spots on the right are the infrared LEDs ($\lambda_{max} \sim 950$ nm) which are seen in the photo due to different spectral sensitivity of the used camera compared to human visual system. **(B)** The corresponding luminance map with Photolux system (Dumortier et al. 2005), demonstrates a bright central region (~400-800 cd/m²) corresponding to a visual angle ~34° [diameter of the diffuser disk is 6 cm and the distance between the eye and the disk is ~ 10 cm, these values allowing more quantitative retinal irradiance calculations (Weber et al. 2004; Sliney 2008)] with surrounding area of ~1 log unit lower luminance (40-80 cd/m²).

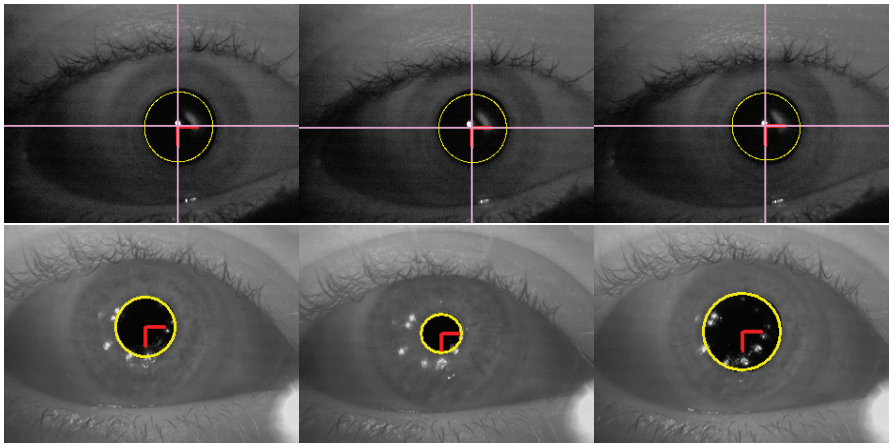

Figure 53: **Pupil image quality. (Top row)** Pupil image recorded with only one IR LED placed on top of the camera objective as used in the study by Mure et al. 2009. **(Bottom row)** The image quality was improved by changing the one IR LED setup for eight IR LEDs placed concentrically around the eye. The change in illumination setup can be seen in corneal reflections (Purkinje images, e.g. Said and Weale 1959; Cornsweet and Crane 1973; Tabernero et al. 2006), there being only one in the old setup (very near the detected centroid of the pupil perimeter) and multiple corneal reflections seen in the bottom row corresponding to individual LEDs. The dynamic fitting behavior of the system cannot be illustrated well with static images, thus the difference in pupil size recording quality between the image quality of top and bottom row is illustrated in Figure 106. The subject for the both rows is the same.

The improvement in image quality is illustrated in Figure 53 with clearly improved iris-pupil contrast with the new lighting condition accompanied with lower variation in pupil recordings in general as shown in Figure 106. Brown irises were found to give the best image quality as the reflectance of iris for near-infrared light is higher (Medina et al. 2011), thus producing the best iris-pupil contrast. The geometric distortions of the imaging system were defined using Imatest (Boulder, Colorado, USA) as defined in Teikari and Rautkylä 2008, and were found to be non-significant.

5.1.2 *Individual PLR variability*

As a part of the collaboration with Véronique Daneault, a pilot study was conducted on the diurnal variability of the PLR. The experimental methods were the same as in the previous study by Mure et al. 2009 and in the "photic memory" study (Section 5.2). The four subjects (one of them did only 6 experimental conditions) were exposed to monochromatic 480 nm light (hbw = 10 nm, irradiance ~10^{12} photons/cm^2/sec) at 8 different time points (02h, 05h, 08h, 11h, 14h, 17h, 20h, 23h) split to two consecutive days so that each subject did 4

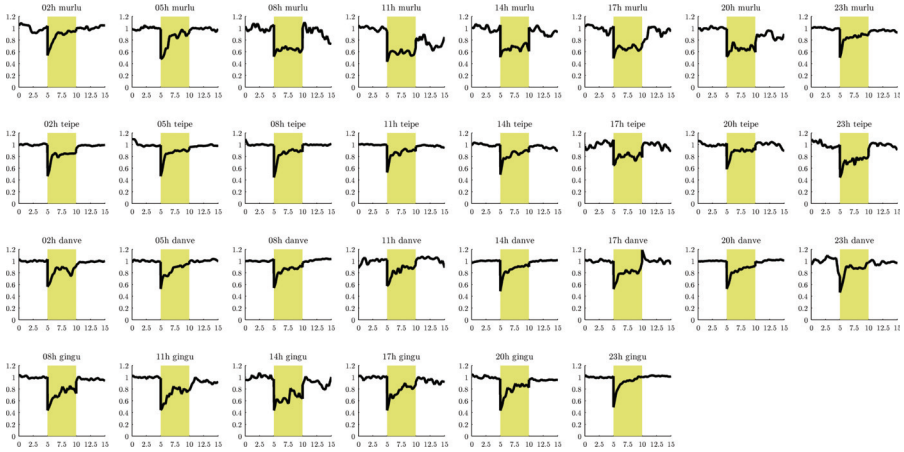

Figure 54: **Individual variability of PLR waveform.** Each row corresponds to subject and the columns the different time points tested. Circadian rhythmicity cannot be derived from these graphs as the sleeping, food intake and environmental light exposure were not controlled.

sessions per day. Pupil was recorded first 5 minutes in darkness (pre-light baseline) and then exposed to 5 minutes of light, and the again for 5 minutes in darkness (post-light baseline). The focus was on diurnal and general variability on the PLR responses on the same subject for the same light stimulus, thus no constant routine protocol (Wirz-Justice 2007) was used to assess circadian rhythmicity as done in the study by Zele et al. 2011. The subjects were free to sleep between the sessions as they felt like, and the food intake and the environmental light exposure were not controlled.

The results of the PLR waveform (see 3.2.2) variation are shown in Figure 54. Intriguingly, the subject MURLU demonstrates a "switch-like" behavior between pupillary escape (02h, 05h, 23h) and pupillary capture (08h, 11h, 14h, 17h, 20h). Other subjects show less drastic variable PLR when examining only the shape of the PLR waveform.

The results of the PLR component variation are shown in Figure 54. The pre-light baseline (0-300 sec, 1st column) functioned as the baseline for the pupil size thus all the time points have a value of 1.0, and each component time point was always compared to the baseline of that given time point. A significant variation in response components can be seen, in addition to the inter-individual responses in the relative response amplitude. The subject MURLU again differs from other subject showing more pronounced sustained response, whereas in other subject the sustained response have decayed close to the baseline value. In regard to the "bistable photopotentiaton", the subjects with weak sustained response are not the most optimal objects (as discussed with IRCs in 2.4.3). As the "pupil resolution" between the test and reference pulse can be insufficient for proper characterization of potentiation and depression of the following response.

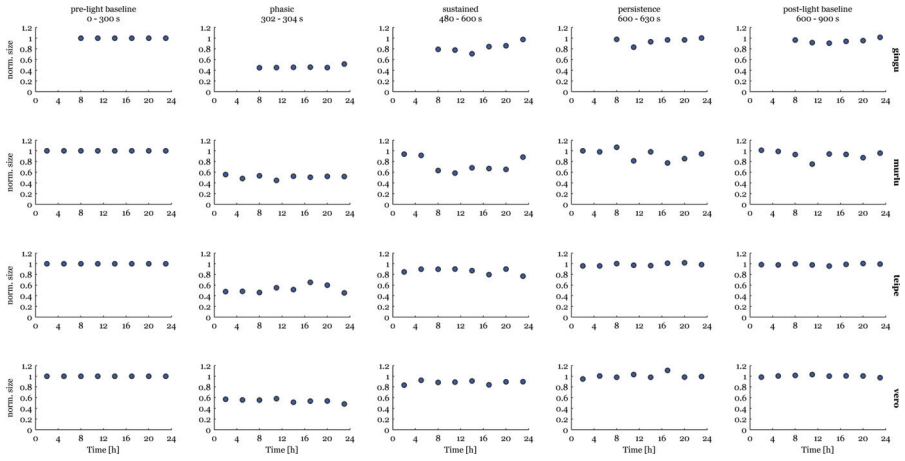

Figure 55: **Individual variability of PLR components**. Each row corresponds to subject and the columns the different time points tested. Circadian rhythmicity cannot be derived from these graphs as the sleeping, food intake and environmental light exposure were not controlled.

5.2 DARK REGENERATION OF MELANOPSIN

DARK AND PHOTIC REGENERATION IN MELANOPSIN-DRIVEN PLR-RESPONSES

Petteri Teikari[#1,2], *Ludovic S. Mure*[#1,2], *Howard M. Cooper*[1,2]

[1] Stem Cell and Brain Research Institute, INSERM U846, 18 avenue Doyen Lépine 69500, Bron – France, [2] Université Claude Bernard, Lyon I, Lyon, France.

# *These authors contributed equally to this work*

5.2.1 *Introduction*

To avoid overlap in this thesis, introduction to melanopsin bistability is found in Section 5.5.1, and for bistability in general in 4. In this study we examined the dark regeneration of melanopsin photopigment using PLR as tool as done in the previous study in our team (Mure et al. 2009). In the previous study (Mure et al. 2009), dark regeneration was not seen when keeping the dark period between the test and the reference pulse in 45 minutes. For this study, an overnight condition was introduced with a dark period of 8 hours between the reference/adapting and the test stimulus with three different adapting conditions (460 nm, darkness and 590 nm). The hypothesis was that there would be "photic memory" phenomenon observed in the in melanopsin regeneration behavior, term introduced by Hochstein et al. 1973 for bistable barnacle. In practive this means that the relative concentrations of the R and the M state would be unaltered after a long 8 hour dark period compared to the shorter 45 min dark condition of previous study (Mure et al. 2009).

5.2.2 *Material and Methods*

5.2.2.1 *Subjects*

Seven subjects with normal color vision participated in this study [2 males and 5 females, 22.3 ± 2.3 years (mean ± SD)]. The selection for the final seven subjects was based on the pilot recordings of the short session with 590 nm adapting light (Figure 56), particularly in regard to the subjects' ability to fixate well, and whether the subjects exhibited the potentiation in PLR seen in previous study of Mure et al. 2009. The latter criterion introduced a slight selection bias for the experiment as later seen in Figure 57B. All experiments were performed in accordance with Institutional guidelines and the research protocol received the necessary ethical approvals. Written informed consent was obtained from each subject prior to inclusion in the experiment. Subjects were examined for normal color vision, visual field and verified that there was no detectable ophthalmic problems. Subjects were

emmetropic and none were under medication during the testing period.

5.2.2.2 *Pupil Measures*

Monochromatic light stimulations were used to record consensual pupillary constriction responses. The pupil size was recorded from the unilluminated eye using an infrared video pupil tracking system (ViewPoint, Arrington®). A video camera was set in a plane parallel to the cornea, with infrared LEDs ($\lambda_{max} \approx$ 950 nm) set obliquely to the cornea ensuring high reflection from the iris while keeping the pupil as dark as possible. By placing the infrared LEDs closer to the eye obliquely, higher corneal irradiance and iris-pupil contrast was achieved compared to the condition of previous study from our group (Mure et al. 2009) with only one infrared LED used placed on top of the camera. Behind the recording system, a small red LED ($\lambda_{max} \approx$ 650 nm) was located to allow the subject to keep a stable gaze on the same point during the entire experiment. Pupil aperture size measures are based on online thresholding algorithm provided at a sampling rate of 60 images/sec by the software (ViewPoint, Arrington®). The circularity is calculated for each fitted ellipsoid as a ratio between aperture height and aperture width.

5.2.2.3 *Light stimulation*

Monochromatic stimulation was produced using a tungsten halogen light source (24 V–150 W Eke bulb) with heat absorbing, collimating lenses and Schott® interference filters (hbw=10 nm). Light was projected through an opal diffuser providing a uniform, pattern-less stimulus that encompassed the entire visual field of one eye. Stimulus irradiance and duration was controlled with an electronic shutter (Uniblitz®) under a computer program. Irradiance levels and spectral distribution were monitored with a photometer (International Light® IL700) and spectrophotometer (Ocean Optics® S4000). The pupil of the stimulated eye was dilated by topical application of tropicamide on the cornea.

5.2.2.4 *Protocol and Data analysis*

General

The data were analyzed using custom-written program on Matlab® (Mathworks). Artifacts in pupil measures, for example due to eye movements or eye blinks were eliminated using the circularity coefficient of the pupil outline. Sample sequences containing more than 15% deviation from unity circularity were excluded from the analysis. To correct for individual variations in pupil size, data were normalized for each subject to mean pupil area measured during the last 5

minutes of dark adaptation prior to light exposures. Pupil data were smoothed using a non-parametric locally weighted linear regression (Lowess, span 0.40, Cleveland 1979).

Kinetics and of the PLR

Different temporal sequences of the pupillary response were analyzed during several time windows of the initial pupillary constriction between 0–30 seconds after lights-on (phasic and tonic responses (Clarke et al. 2003a; Gamlin et al. 2007; McDougal and Gamlin 2010). The steady-state of the pupil constriction was measured during the prolonged constant light exposure (3–5 minutes). Finally, post-stimulus persistence of pupillary constriction was analyzed during the first minute after lights-off.

Effects of prior light exposure on the PLR

To assay the effects of prior light exposure we used procedures previously applied to studies of invertebrate photoreception (Lisman and Sheline 1976; Stavenga 1975; 1976; Hillman et al. 1983), in the mouse (Mure et al. 2007), and in humans (Mure et al. 2009). In this study we used 480 nm light as the test and reference stimuli since this has been reported as the peak wavelength of sensitivity for melanopsin expressed in vitro (Panda et al. 2005; Koyanagi et al. 2005; Torii et al. 2007; Terakita et al. 2008), and for retinal mRGCs recordings (Berson et al. 2002; Tu et al. 2005; Dacey et al. 2005). Test wavelength of 480 nm had a photon density of 10^{12} photons/cm^2/sec, while the adapting light stimuli (460 nm and 590 nm) had a photon density of 10^{14} photons/cm^2/sec. The protocol is illustrated in Figure 56. The experiment always took place at ~22h (corresponding to 0 minute in Figure 56) in contrast to our previous study done in midday (Mure et al. 2009).

5.2.3 *Results*

The results from the study are seen in Figure 57 for three different time bins corresponding to the same time bins previously used by Mure et al. 2009: A) Phasic component (2-4 sec after light onset), B) Sustained / steady-state component (3-5 min after light onset), and C) Persistent component (0-1 min after light offset). In the phasic component (Figure 57A), no statistically significant modulation of the PLR in response to test light by the adapting light stimulus was seen.

In the sustained component, adapting light stimulus is seen to modulate the PLR with some of the results reaching statistical significance as assessed with Kruskal-Wallis test (Kruskal and Wallis 1952) . In the short condition, there is a difference between the 590 nm and darkness condition (p=0.048), but not between 590 nm and 460 nm (p=0.123) nor between darkness and 460 nm (p=0.935). In the long

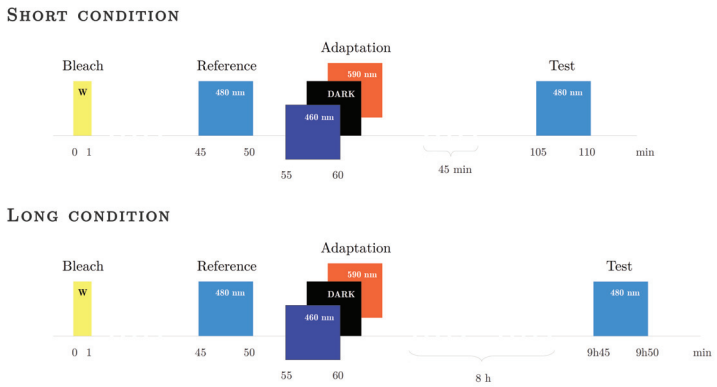

Figure 56: **Experiment protocol.** Protocol design corresponds to the experimental design of Mure et al. 2009 with an initial bleaching white light stimulus for rods and cones ($f_{Me} \sim 0.19$, followed by 45 minutes of dark adaptation, 5 min reference light pulse (480 nm, $f_{Me} \sim 0.71$), 5 minutes of dark, 5 minute adapting light [460 nm, $f_{Me} \sim 0.74$; darkness, $f_{Me} \sim 0.71$ after 480 nm; or 590 nm, $f_{Me} \sim 0.01$ (simulated threshold wavelength for total $R \rightarrow M$ conversion was 602 nm]. In the "short condition" (above), the second 480 nm (Test) light pulse is followed after a dark adaptation of 45 min, whereas in the "long condition" (below), the dark adaptation time is 8 hours during which the subjects can sleep. The f_{Me} values were calculated using Eq. (18) with the peak values of 482 nm for R and 587 nm for M state. The nomograms were created using the definition by Govardovskii et al. 2000 using the β-band with no self-screening correction (2.3.3).

condition, there is a difference between 590 nm and 460 nm (p=0.042), and darkness and 460 nm (p=0.028), but not between 590 nm and darkness (p=0.749). Between the short and long conditions, there is only a difference between short 590 nm and long 460 nm condition (p=0.004), other interactions between the two conditions not reaching statistical significance. In the persistent response, differences can be seen but none of them are statistically significant due to high variability.

Alternatively the results could be plotted as the individual changes between the short and long sessions for each given condition (590 nm, dark and 460 nm) as shown in Figure 58. It can be seen that the phasic component exhibits very little variability which is to be expected from low melanopsin drive during the initial PLR (McDougal and Gamlin 2010). The sustained and especially persistence responses exhibit high variability, some subjects showing more potentiation (second data point higher than the first data point per time bin) after long conditions whereas some other show the depression (second data point lower than the first data point per time bin). The individual values for each condition are shown in Figure 58.

5.2.3.1 *Robustness of bistability-mediated potentiation in PLR*

In the process of recruiting subjects, more subjects were tested with the short 590 nm protocol than the final seven subjects, and the results for these non-selected subjects along with the subjects (total n = 24 subjects) from the previous study by Mure et al. 2009 are shown in Figure 59 (individual values in Table 9 and the individual PLR traces and "difference signals" shown in Section C.5). The choice of subjects for the full protocol was based on whether they exhibited potentiation in the 590 nm condition and whether they were behaviorally suitable for the protocol, i.e. being able to fixate well. The results demonstrate a significant inter-individual variability in the responses, the potentiation value of the sustained response being closer to zero compared to the results of Mure et al. 2009. The persistence response exhibits depression of the response after prior 590 nm adapting light exposure.

5.2.3.2 *Effect of data conditioning on the results*

The sensitivity of the obtained results for the LOWESS *span* [Matlab command YY = SMOOTH(X,Y,SPAN,'RLOWESS')], higher *span* values resulting in smoother plots. The data were smoothed piecewise in three 5 minute bins (pre-light baseline, light exposure, and post-light baseline) so that the phasic component would not be smoothed too much. The robust version of the LOWESS was chosen to minimize the effects of outliers to the smoothing results. It can be seen in Figure 60 with the data set analyzed that the *span* parameter did not have a dramatic effect on the sustained nor the phasic component.

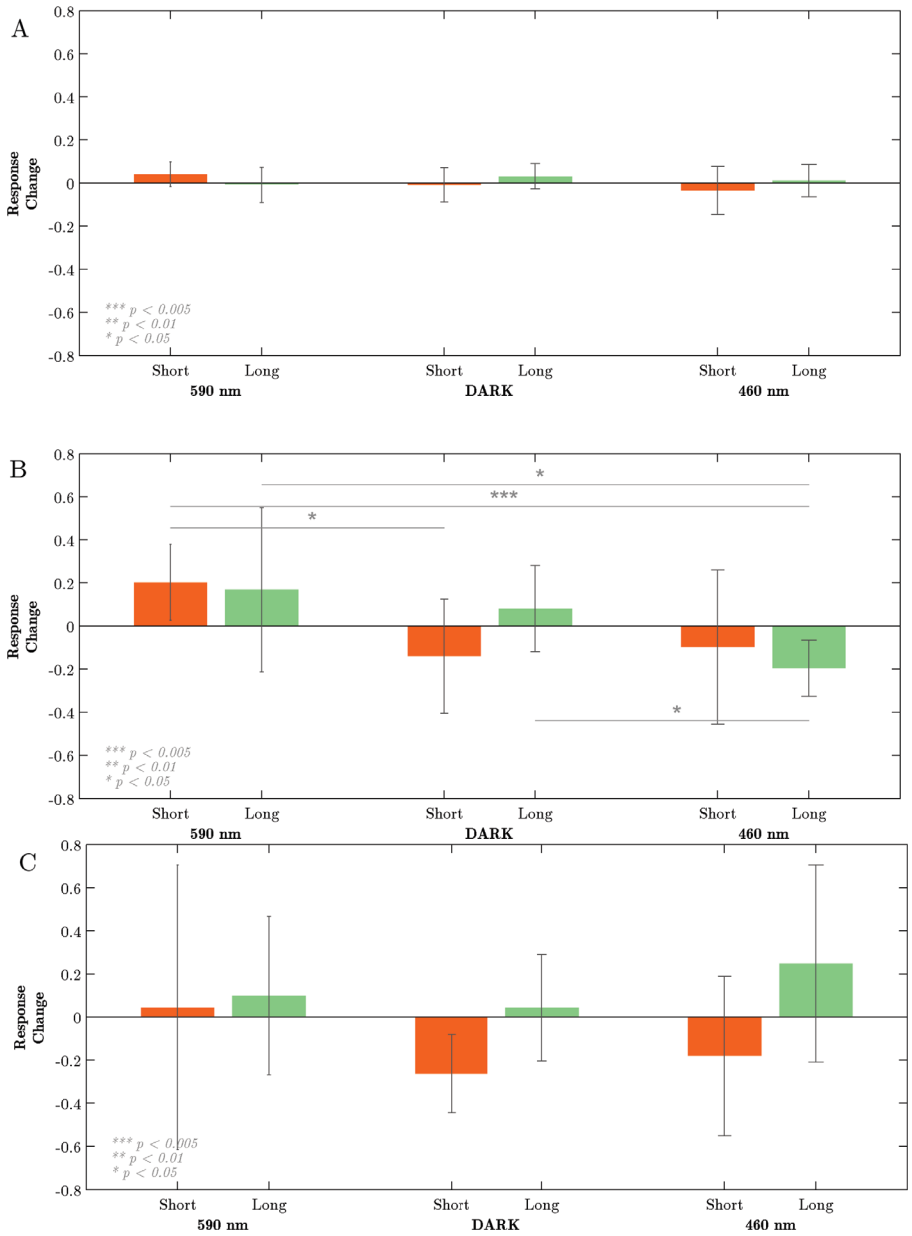

Figure 57: **Alteration of PLR response following pre-exposure of adapting light in short and long condition. (A)** Phasic response (2-4 sec after light onset), **(B)** Sustained response (180-300 sec after light onset), and **(C)** Persistent response (0-60 sec after light offset)

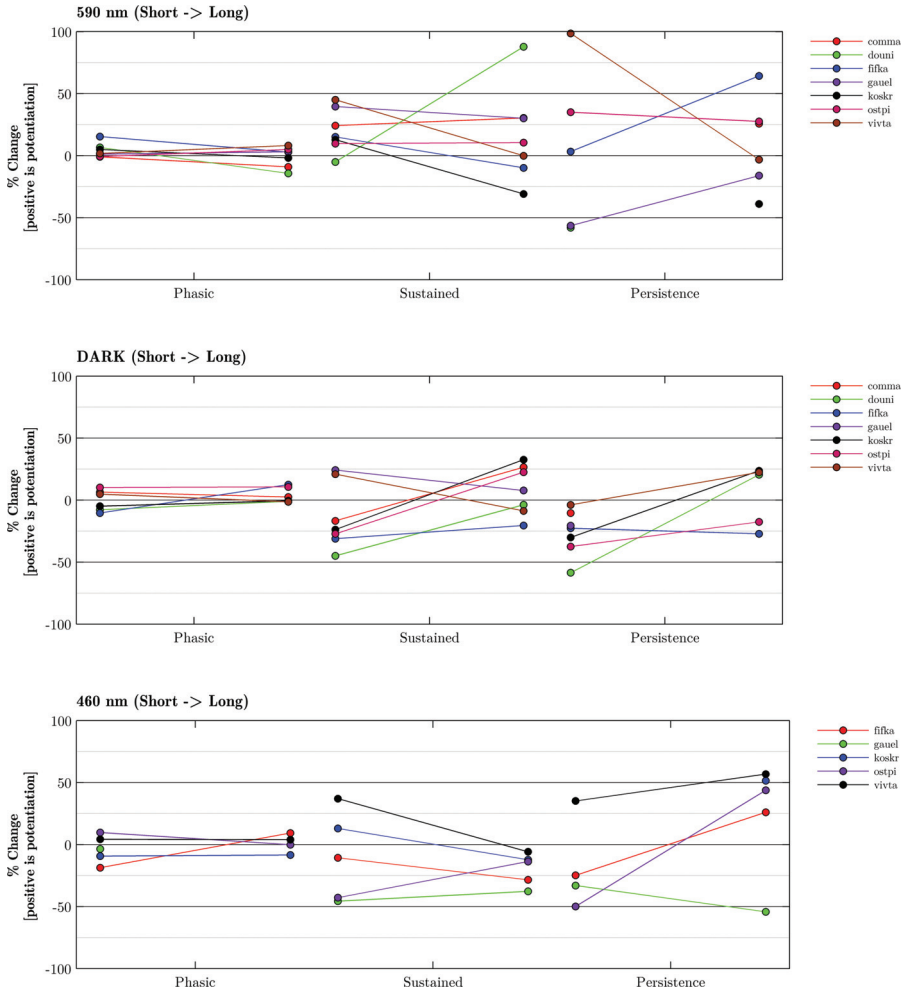

Figure 58: **Individual Changes** The plot can shows how if the "photic memory" phenomenon would have been very robust, all the subjects would responded roughly in the same way between the short and long conditions. This is not the case for majority of the conditions, some subjects exhibiting potentiation and some others attenuation (comparing "short and "long" conditions) for the same adapting light condition (460 nm, dark, 590 nm). The "NaN-threshold" to reject outliers were set to 100%, thus the single points missing a connection line to either short or long conditions were due to the other marked as an outlier.

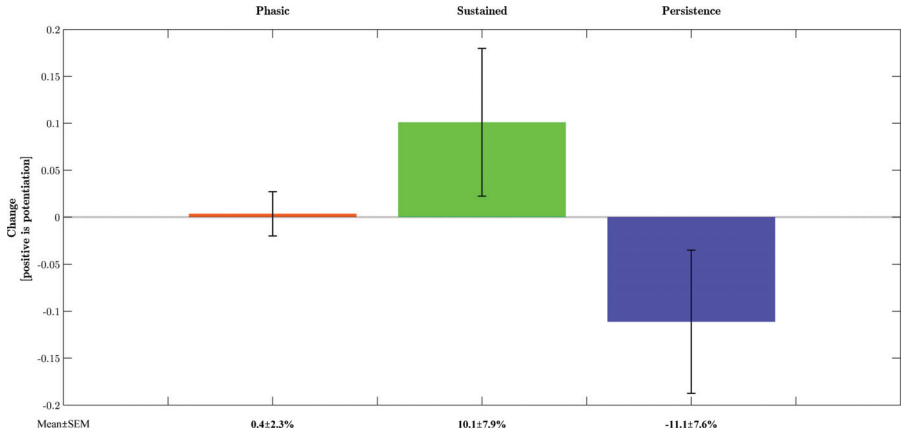

Figure 59: **PLR component analysis of the short 590 nm condition**. The averaged responses ± SEM of all subjects (n=24, see values in Table 9) tested for the short 590 nm condition for three time bins. LOWESS span used was 0.20. The "NaN-threshold" to reject outliers was set to 100%.

With the persistence component the conclusion weather the adapting light stimulus caused potentiation or depression depended on the *span* parameter (potentation at *span*=0.20 and depression at *span*=0.3 and 0.4). These results highlight the need for high quality recordings in order to make correct conclusion from the measured data as discussed in 3.5.1 and in 5.1.1.

5.2.4 *Discussion*

In contrast to the previous study by Mure et al. 2009, a less robust bistable photopotentiation effect was found in both short and especially in the long study condition. The mean response for the sustained PLR component with the 590 nm adaptation light was roughly similar to the results obtained by Mure et al. 2009, whereas with the dark control the response suppression was found to be stronger than with the adapting 460 nm light. However, none of these differences results reached statistical significance due to highly variable responses. The obtained results for the difference between the short and long condition did not seem to support either a pure "photic memory" hypothesis nor a combination of "photic memory" and "dark regeneration". Similarly, possible contribution of upregulation of the melanopsin pigment after prolonged darkness with or without circadian drive for pigment concentration (2.4.9) and/or pupillary light reflex (Section 3.6) could not be derived from the results.

There were mainly three differences in the experimental design compared to the previous one (Mure et al. 2009). The first one was the use of 590 nm adapting light as the "maximal potentiator" light instead of the 620 nm used previously. The 590 nm was chosen as the experimental wavelength as it corresponded to the putative peak

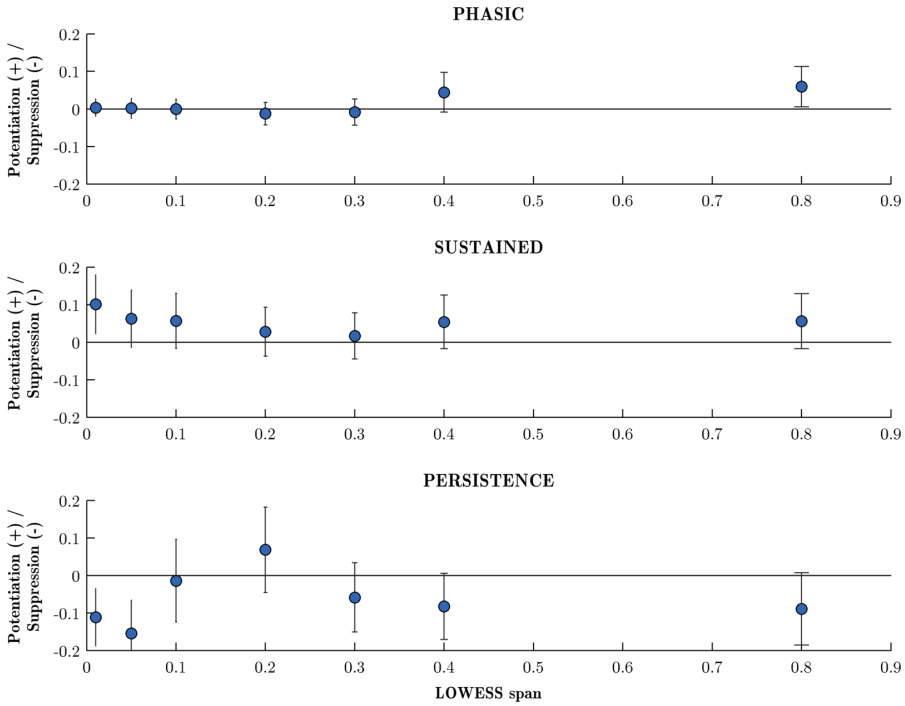

Figure 60: The effect of LOWESS span (mean ± SEM) is illustrated for the same 24 subjects in Figure 59 for various LOWESS span values (x-axis) for the three analyzed time bins: phasic, sustained and persistence. The phasic and sustained are more or less insensitive for LOWESS span while still yielding different means. The persistence response can be either potentiated by prior 590 nm light exposure or suppressed depending on the LOWESS smooth parameter. . For comparison, the highest 0.8 was used in the study presented in Section 5.4. The 0.01 and 0.05 values are insufficient for our PLR recordings at least when visually inspecting the smoothed individual PLR recordings.

of the "meta-melanopsin". The 590 nm wavelength in equilibrium results a f_{Me} of 0.01 while the 620 nm is able to shift all the pigment to the R state in theory (see equilibrium spectrum in Figure 37 with zero values at that wavelength). Thus, the change in adapting wavelength to 590 nm from 620 nm would in theory lower also the maximum possible potentiation. The second difference is in the experimental time, as the previous study was done during midday whereas this study was undertaken late in the evening starting at 22h. Strict control of prior light history and subject behavior was not possible due to resource limitation, while extreme chronotypes were excluded and subjects were asked to have regular sleep-wake cycles before the experimental sessions.

Third difference was the improvement of infrared (IR) illumination discussed in detail previously in 5.1.1. Qualitatively examining the traces in Figure 106 and Figure 107 from this current study and from the previous study (subjects with code starting with ORI are from Mure et al. 2009), one could suggest that the results obtained previously could be partly explained by the previous noisy recording of the pupil diameter. The recorded pupil size is seen to oscillate significantly more than in the majority of recordings for the current study (BYRSO and GAUEL being notable exceptions). As shown above in Figure 60, the choice of smoothness parameter (*span* in our case when using LOWESS) can significantly affect the obtained final results. Furthermore higher *span* values result less variable estimates of the time bins (lower standard deviation as data points from which the time bin mean is calculated become less variable), if the original variability in the raw data is taken into account as was the case with Mure et al. 2009. Surprisingly, the fit of difference spectrum with 5th degree polynomial was found to have R^2 value close to unity (Figure 61A), and being visually comparable to nomogram fitting for photometric data in *Rh2* of *Drosophila* (Figure 61A) obtained by Salcedo et al. 1999.

Additionally, statistically non-significant trend was found for the subjects from the Mediterranean region (subjects DOUNI, FIFKA, GILAL, SPAMA, BOUNE, BYRSO) in regard to the sustained component behavior. The sustained component decayed qualitatively closer to the baseline at the end of light stimulus, suggesting a possible long-term adaptation for environmental light exposure experienced during childhood. Similar claims were made for the differences found in light sensitivity between indoor and outdoor workers in the studies by Rufiange et al. 2007 and Beaulieu et al. 2009, being mediated via "photostasis"-like phenomenon shown in rats (Penn and Williams 1986). In rats reduced environmental light have shown to cause elongation of the rod outer segments to compensate for the reduced retinal irradiance.

In conclusion one cannot reject the hypothesis of melanopsin bistability based on the results presented here, but one could hypothesize that the PLR would not be optimal tool to demonstrate it in humans

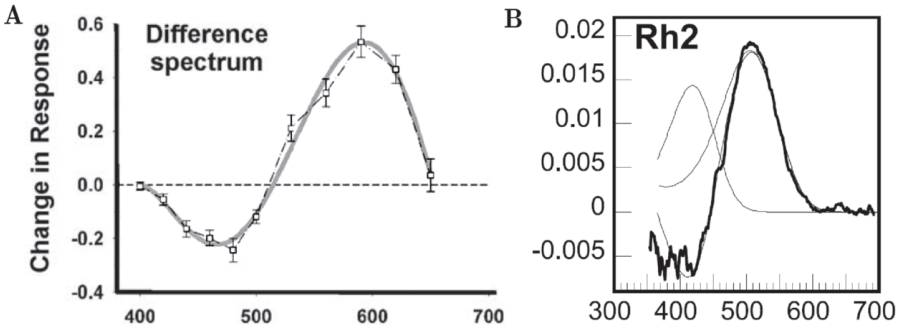

Figure 61: **Experimental difference spectra**. **(A)** The difference spectrum was obtained by measuring the change in pupil constriction between the two identical reference and test stimulations (480 nm, 10^{12} photons/cm^2/sec, 5 min duration) subsequent to a 5 min pre-exposure period for 11 different wavelengths (n = 4 subjects; iso-irradiance of 14.1± 0.2 log photons/cm^2/s). Consistent with typical difference spectra of invertebrates, the response function (5-degree polynomial, R^2 = 0.91) shows two domains: a decrease in the response between 400–515 nm (min = 466 nm) and an increase in constriction for longer wavelengths (515–650 nm, max = 592 nm). The response function also shows an isosbestic point that corresponds to the wavelength at which the pre-exposure stimulation has a neutral effect (514.3±1.2 nm). (Graph from Mure et al. 2009) **(B)** In each case the difference spectra were calculated from spectra measured after illumination with adapting lights (using a single-adapting light and subtracting from the dark-adapted state or with λ_1 and λ_2) which were 418 and 524 nm for Rh2. Difference spectrum (bold trace) was fit with calculated rhodopsin and metarhodopsin absorption profiles (*Stavenga et al. 1993*). Curve fits of the difference spectrum and the R- and M-forms are shown as fine traces in each panel. (Graph from Salcedo et al. 1999)

especially using the current paradigm. One could want a method that more directly assesses the pigment-level changes in melanopsin phototransduction rather than being too-many-synapses away with PLR recording (Section 3.2). The discussion is continued in 6 with alternative paradigms and alternative explanations for the observed phenomena offered.

5.3 OCULAR MEDIA DENSITY MEASUREMENT

HETEROCHROMATIC FLICKER PHOTOMETRY FOR ESTIMATING HUMAN OCULAR MEDIA DENSITY

Petteri Teikari[#1,2], *Raymond P. Najjar*[#1,2], *Pierre-Loïc Cornut*[1,2,3], *Philippe Denis*[1,2,4], *Kenneth Knoblauch*[1,2], *Howard M. Cooper*[1,2], *Claude Gronfier*[1,2]

[1] Stem Cell and Brain Research Institute, INSERM U846, 18 avenue Doyen Lépine 69500, Bron – France, [2] Université Claude Bernard, Lyon I, Lyon, France; [3] Department of Ophthalmology, CHU de Lyon Hopital Edouard Herriot, Lyon, France. [4] Department of Ophthalmology, CHU de Lyon Hopital Edouard Herriot, Lyon, France.

# *These authors contributed equally to this work*

5.3.1 *Introduction*

Aging is associated to many anatomical and physiological alterations at the eye level. Although distinct from age related eye diseases, these alterations produce similar yet smaller photoreception changes. Lens yellowing is one of these alterations and gradually leads to the most documented cause of blindness in developed countries: cataract.

With aging many changes occur at the eye level. Most of these anatomic and physiologic processes, that follow a gradual decline, can solely be attributed to the aging process. Although these processes are distinct from the aging eye diseases, the vision changes they produce may be similar, albeit smaller. Lens yellowing is one of these phenomenon and gradually leads, at some point, to the most documented cause of blindness is developed countries: cataract (Michael and Bron 2011). Lens yellowing most commonly occur as a result of aging and exposure to environmental factors as ultraviolet light (Taylor et al. 1988; Hodge et al. 1995; Vrensen 2009). However cataract may occur secondary to hereditary factors (Sacca et al. 2009), trauma (Shah et al. 2011), metabolic or nutritional disorders (Lutze and Bresnick 1991; Wegner and Khoramnia 2011), smoking (Hammond et al. 1999), non-ionizing (Söderberg et al. 2009) and ionizing radiation (Fillmore 1952; Lipman et al. 1988; Ainsbury et al. 2009). The effect of cataract for visual perception have been simulated for example in regard to painter Claude Monet's paintings (Marmor 2006), and glare in night-time driving (Ikaunieks et al. 2009; Pamplona et al. 2011).

The relationship between healthy aging and ocular lens density have been studied by many (van Norren and Vos 1974; Werner 1982; Pokorny et al. 1987; De Natale et al. 1988; Sample et al. 1988; 1991; Johnson et al. 1993; Hammond et al. 1997b; Wooten et al. 2007). These studies show a decreased transmission (increased density) of the intraocular lens, especially for short wavelength lights with age. This increase is even more pronounced in individuals with cataract (Sample et al. 1988). Recently Dillon et al. 2004 and Broendsted et al.

2011 demonstrated a good correlation between *ex vivo* techniques for donor lenses, and non-invasive *in vivo* technique.

Lens yellowing and cataract have been quantified using various method *in vivo* including Purkinje images (Said and Weale 1959; Johnson et al. 1993; Savage et al. 2001), visual evoked potentials (Werner 1982), psychophysical techniques (van Norren and Vos 1974; Wooten et al. 2007; Barbur et al. 2010), slit lamp photographs with manual (Chew et al. 2010) or automated analysis (Li et al. 2010), photoacoustic imaging (Lerman et al. 1978; Silverman et al. 2010), Shack-Hartmann wavefront sensing (Donnelly et al. 2004), imaging spectrograph for fundus reflection (van de Kraats and van Norren 2008; Gimenez et al. 2010), femtosecond optical coherence tomography (OCT, Palanker et al. 2010), retro-illuminated image processing techniques (Camparini et al. 2000), dynamic light scattering technique (Datiles et al. 2002; Datiles et al. 2008), Raman spectroscopy (Hogg et al. 2007), autofluorescence imaging (Broendsted et al. 2011), parallax barrier-based method using a smart mobile phone (Pamplona et al. 2011), and Scheimpflug photography (Bosem et al. 1994; Nishimoto and Sasaki 1995).

Scheimpflug photography is the most commonly used technique for lens density clinically (Wegener and Laser-Junga 2009), implemented commercially in Pentacam® (Oculus, Germany) has been shown to correlate well (Pei et al. 2008; Grewal et al. 2009; Magalhães et al. 2011) with the subjective Lens Opacities Classification System III (LOCS-III, from 1, clear lens, to 5, cataract; (Chylack et al. 1993) employed by ophthalmologists.

Psychophysical methods are easy and low cost to implement both in clinical and experimental settings. Early scotopic psychophysical studies used long dark adaptation times (van Norren and Vos 1974; Pokorny et al. 1987), up to 45 minutes, making these cumbersome in real-life settings. Several attempts have been made to shorten the measurement time. In photopic color matching (Davies and Morland 2002), no long dark-adaptation is required, however the obtained results are influenced by combined rod and cone responses, that is not in accord with the univariance principle of additivity (Naka and Rushton 1966). Additionally, the results may be subject to individual variability in the L/M cones ratio (Carroll et al. 2002). Whether photopic methods are equivalent to scotopic methods have been addressed previously by Wooten et al. 2007, authors demonstrating strong relation (R^2 = 0.80) between scotopic and photopic heterochromatic flicker match, suggesting that reliable photopic psychophysical estimates would be possible. Wooten et al. 2007 also suggested that relative thresholds might even be superior to absolute thresholds in relation to maintaining steady state absolute adaptation as no fixed adaptive state is required. Similar results were obtained by Barbur et al. 2010 elaborating the idea of Moreland et al. 2001 using a normal

computer monitor for flicker photometry with notch filters, allowing reliable photopic estimation of macular pigment and lens density.

To be clinically significant cataract should cause a significant reduction in visual acuity or other visual impairments. The eye does not only serve for visual purposes as a non-visual melanopsin (ipRGCs) based photoreceptive system has recently been discovered (Berson et al. 2002) . Together with the conventional visual photoreceptors (rods, cones), this system conveys photic information for non-visual functions such as pupillary light reflex (PLR) and circadian photoentrainment (Güler et al. 2008). Knowing that the visual system usually compensates for visual impairments, the question remains how pre-cataract lens opacification affects entrainment of the circadian system. Therefore lens opacification should be measured objectively and compared to non visual sensitivity to light, even before visual impairments.

Moreover assessing the amount and spectral composition of light reaching retinas' photopigments is crucial for studying photoreceptor contribution in non visual photoreception (Brainard et al. 1997; Brainard et al. 2001; Thapan et al. 2001; Mure et al. 2009; Gooley et al. 2010). Amongst the factors that could alter light penetrating through the ocular media, pupil size, corneal filtration, eye chambers filtration and lens opacification. Compared to other ocular medias the lens alters spectral composition of light reaching the retina. Therefore having a system that could give objective ocular media spectral transmittance is a necessity in the circadian photoreception and vision field. Moreover a debated has been going on about the the potential risks and benefits of blue light blocking intraocular lenses (IOLs) after cataract surgery. These artificial lenses that filter a considerable amount of blue light were suggested to provide photoprotection against the risks of development or progression of age related macular degeneration (AMD) and enhance visual performance by reducing glare (Davison et al. 2011) . For other authors these IOLs filter short wavelengths that are crucial for circadian photoentrainment and might have potential risks on scotopic and mesopic vision (Mainster 2006).

In our study we evaluated an improved scotopic flicker photometry technique to assess the age-related changes in lens density. Psychophysical technique of absolute threshold detection in the same subjects. In addition we also diminished the DA period from 45 min to 5 min and to 0 min, and compared the results. Another aim of this paper is to compare three methods of lens opacification assessment, using psychophysical testing, Scheimpflug imaging (Oculus Pentacam) and a grading system commonly used with slit lamps by ophthalmologists [LOCS III (Chylack et al. 1993), Oxford Clinical Cataract Classification and Grading System (Sparrow et al. 1986) or The WHO simplified cataract grading system (Thylefors et al. 2002)]

5.3.2 *Material and Methods*

Subject's lens density was assessed using an improved light emitting diode driven (LED) heterochromatic flicker photometry system developed at our institute (INSERM U846, Bron, France)

5.3.2.1 *Principle of lens transmission measurement*

Except for the lens and the macular pigment, the ocular media have been shown to be wavelength neutral or to show very little change in transmittance with age (van de Kraats and van Norren 2007a). Since the macular pigment has an effect mainly on the cones in the fovea, testing peripheral vision using the psychophysical procedure to be described provides a nearly pure measure of changes in lens density as a function of age (Sample et al. 1988). The action spectrum of rhodopsin is genetically determined (Nathans et al. 1986), stable with age, and very well known. When measuring individual aphakics (Wright 1951; Griswold and Stark 1992), it is clear that their scotopic spectral sensitivity curve is highly similar to the relative absorption curve based on the extinction spectrum of rhodopsin (Wald 1949). Therefore, based on a nomogram (Govardovskii et al. 2000) for rhodopsin sensitivity [λ_{max}= 495 nm (points from Kraft et al. 1993 refitted with Govardovskii et al. 2000), β-band included, and axial density d_{Rh} of 0.40 OD (Lamb 1995)] pairs of wavelengths with equal absolute threshold are chosen ($L1$ and $L2$). Without any filtering by the ocular lens in vivo, the scotopic threshold for $L1$ and $L2$ is obtained at the same irradiance ($I1 = I2$). A different threshold is obtained ($I1 \neq I2$) when a non-homogeneous filtering of the light spectrum occurs due to lens filtering (Figure 2).

5.3.2.2 *Subjects*

Thirty nine subjects participated in this study (21 males and 18 females). Subjects were sorted by age groups, 17 young (26.7 ± 3.4 years old), 9 middle aged (45.3 ± 5.7 years old) and 13 old (62.4 ± 2.9 years old) and were tested using a scotopic heterochromatic flicker photometry technique. All experiments were performed in accordance with Institutional guidelines and the research protocol received the necessary ethical approvals (RBM Co6-17 and Co8-13). Written informed consent was obtained from each subject prior to inclusion in the experiment. Subjects were examined for normal color vision, visual field and verified that there was no detectable ophthalmic problems. All experiments were performed between 9:00 and 19:00 hrs and were conducted between Jan 2011 to July 2011. Subjects also filled in 3 questionnaires: Horne and Ostberg questionnaire (Horne and Östberg 1976), Munich chronotype questionnaire (Roenneberg

et al. 2003), and sleep quality [Pittsburg Sleep Quality Index (PSQI], Buysse et al. 1989).

5.3.2.3 *Apparatus*

Apparatus consisted of a full field covering black box with a chin rest and a two way joystick with a confirm button. System was placed in a convenient dark painted room. A 3° wide annulus was projected using LEDs on a diffusing paper placed in front of the subject at a 15° to 18° visual periphery. The two LEDs used to produce light stimulus had wavelength peaks at 405nm (LedEngin, Inc., UV LED, LZ1-10UA00, 700mA) and 530nm (Philips Lumileds® Luxeon III LED, LXHL-LM3C, 1000mA). The LEDs were attached to heat sinks (Aavid Thermalloy, part no. 601403b06000) with a thermal adhesive (Aavid Thermalloy, Ther-O-Bond 1500) to ensure sufficient heat dissipation from the LEDs (Tao and Hui 2012). Light emitted by these LEDs was collimated (Ledil® LE1-RS Lens, ±4° angle for 405 nm LED, and L2® 3° Spot for the 530 nm LED) and filtered respectively by 410nm monochromatic filter (BFI Optilas® IF 410 +/- 0.4nm, FWHM = 3 +/- 0.4nm) and 560nm monochromatic filter (BFI Optilas® IF 560 +/- 0.4nm, FWHM 3 +/- 0.4nm). The resulting chromaticity (CIE xy) for 410 nm light was x=0.18, y=0.03, and for the 560 nm light x=0.41, y= 0.58.

Light intensity was attenuated to scotopic levels (10^{-2} to 10^{-6} cd/m^2) by different neutral density filters (ND) ranging from ND2.5 to ND5.0 (Omega Optical®). Light attenuation and ND's used were dependent to subjects' scotopic threshold. LEDs were controlled by constant current LED drivers (XP Power® LDU0830S350, 350 mA) and intensity was modulated using pulse width modulation signal (PWM) controlled by a data acquisition card (DAQ, National Instruments® USB-6210). The software front-end was developed by the author using LabView® development environment (Figure 62). The output current (350 mA) of the LED drivers was chosen to be lower than the nominal current of the LEDs to avoid reduction in light output and shift in the peak emission with heating of the LEDs even with the heatsinks (Watanabe et al. 1992; Pousset et al. 2010). Initially, in place of the DAQ card a low-cost sound card was used as described by Puts et al. 2005, but the quality of our sound card with the accompanying amplifier was not sufficient for a good-quality square-wave required by the LED drivers.

Light intensity was directly controlled by the subject, using the joystick , depending on the task he was instructed to perform. Therefore in order to increase or decrease light intensity subject pushed up or down the joystick lever. Joystick also had a confirm button to acquire subject's responses on the PC. Irradiance levels were monitored using a radiometer (International Light ® IL 1700) and a luminancemeter (Minolta® LS-110). The spectral emission characteristics of the system

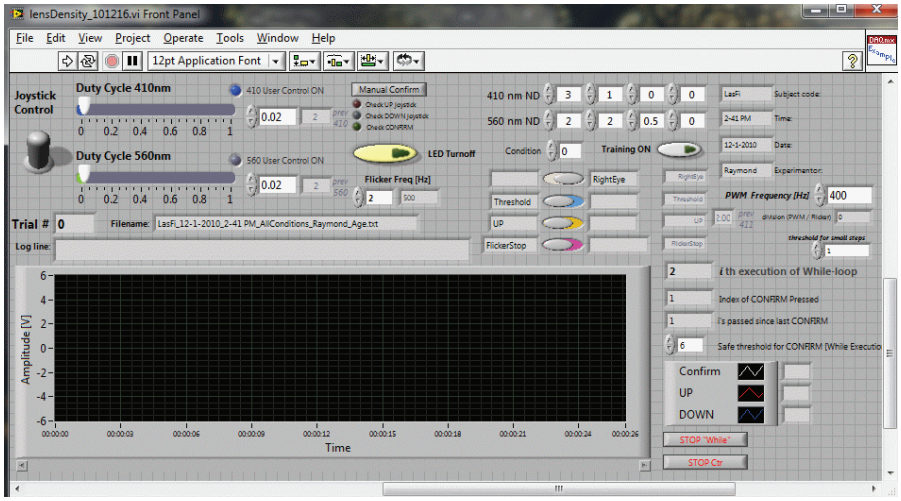

Figure 62: **LabView interface for lens density program.** The subject controls the duty cycle of 410 nm in the flicker photometry condition with the joystick.

were measured using a spectrophotometer (Ocean Optics USB4000®). Data were analyzed using a custom-written Matlab program (Mathworks©).

5.3.2.4 *Method*

In this study we used scotopic heterochromatic flicker photometry technique to measure lens yellowing. After receiving proper explanations about the experiment and safety procedures, subject dark adapted for 45 minutes to ensure full dark adaptation. After this dark adaptation (DA) period 99.9% of the rhodopsin photopigment contained in rod photoreceptors of the retina would have been regenerated and be responsive to light (Lamb and Pugh 2004; Reuter 2011). DA period was followed by a training phase in which the subject increased light intensity until he reached his scotopic threshold and detected, with his non-preferred eye, a flickering 3° wide annulus in free-view (Newtonian view) at a 15° to 18° visual periphery (63, right). Free-view had been shown previously to correspond well to the results obtained with Maxwellian view (Wooten et al. 1999; Wooten et al. 2007), allowing simplification of the optical setup as summarized by Howells et al. 2011 for macular pigment measurement. Subjects' preferred eye was occluded using an eye patch.

In order to adjust the annulus light intensity, the subject used an one-axis (up, down) joystick confirming the detection intensity when the scotopic annulus is detected by pressing on a button (63, left). Once the subject has understood the indications and localized the flickering annulus in his peripheral vision, the testing starts. On average, total measurement time, including DA and instructions, is about 90 min. Subjects fixation was aided by a small centered ~10' red fixa-



Figure 63: **Physical lens density setup.** The implementation of the lens density setup in Montreal, Canada. **(left)** Overall view of the setup with the joystick and the confirm button shown on the left of the setup. **(right)** The view of the annulus as seen by the subject. The subject positions himself to the chinr est and sees the annulus flickering in scotopic conditions. The wightness of the annulus is due to the white tracing paper to diffuse the light.

tion light (λ_{peak}= 650 nm, luminance of 7 to 10 cd/m^2). Zagers and van Norren 2004 had suggested that the variability in their intra-session macular pigment density results was the result of fixation errors, with the less experienced subjects showing greater variability. Some subjects reported difficulties in fixating, and they were instructed upon problems to close eyes for couple of seconds. Additional reason for the requested blinking and small pauses was to minimize Troxler's effect (Troxler 1804), a fading of the peripherally viewed stimulus that sometimes makes the extrafoveal flicker match difficult.

The homogeneity of the light distribution in the visual field was quantified using Photolux software (Dumortier et al. 2005). The system consists of Nikon 5000 digital camera with a fisheye lens and Photolux software developed in ENTPE, Lyon, France. The system is typically used for quantifying the luminance distribution in architectural lighting settings helping the lighting designers verifying their designs (Cai and Chung 2010; Hua et al. 2011). There is also a simplified version of the software for iPhone (iPhotoLux, © 2011, Dominique Dumortier, LASH, ENTPE). The observed homogeneity of the annulus was very good due to the use of multiple diffusing sheets (Figure 64), and especially when compared to the less homogenous luminance map of the PLR setup (Figure 52).

Absolute scotopic threshold detection

Based on the principle described earlier, this technique allows to estimate lens density by directly comparing absolute scotopic thresholds to rhodopsin absorption curve (van Norren and Vos 1974). Such comparisons yield *in vivo* spectral density curves that generally agree with

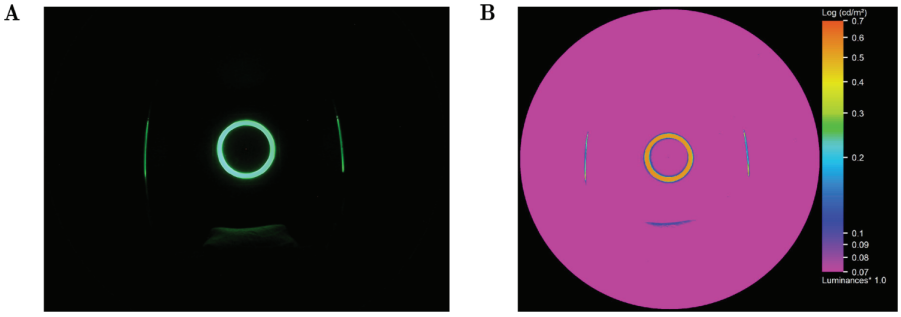

Figure 64: **(A)** Photo of the annulus with a long exposure time resulting the color being a mixture of the 410 nm and 560 nm. The vertical reflections on the sides come from the chin rest metal frame, and one in the below of the annulus from the chin rest. **(B)** The corresponding luminance map (as presented also for Figure 52) with Photolux system (Dumortier et al. 2005).

ex vivo curves suggesting that this technique is valid. The method is also widely regarded as valid because, as it is clearly rod-driven, the underlying template being univariant (Naka and Rushton 1966). While fixating a centred red dot with his preferred eye, subject controlled the annulus light intensity until he could detect it flickering in his peripheral vision field. The flicker frequency was chosen to be 2 Hz (500 ms of light, 500 ms of dark) based on earlier pilot study and the temporal summation characteristics of Hecht et al. 1942. . Once the annulus is detected, subject confirmed by pressing on the button. Intensity at which annulus is detected represents absolute scotopic threshold of the subject for the wavelength used. This procedure was repeated 5 times with 410 nm light and 5 times with 560 nm light. Under scotopic conditions both lights are detected as gray. Each trial yielded an estimate of the difference of quantal light intensities expressed as:$\Delta I = I_{ph,410nm} - I_{ph,560nm}$ (both $I_{ph,410nm}$ and $I_{ph,560nm}$ being in log units) which was used for calculation of the lens density index (see 5.3.2.4). The possible diurnal variation of absolute threshold (Bassi and Powers 1986; O'Keefe and Baker 1987; Tassi et al. 2000a) has no influence on our results, as it has a symmetric effect for both test lights, the underlying spectral sensitivity being univariant.

Critical Fusion Frequency detection (CFF)

The aim of this step was to detect subjects' flicker sensitivity, the critical fusion frequency [CFF (Conner 1982; Hammond and Wooten 2005)] in scotopic conditions. The CFF thresholds were obtained with the same optical setup as the above described absolute threshold method. Only the 560 nm reference light was used in this condition with a square-wave modulation at the maximal modulation depth (half of the cycle period light on, and the other half of the cycle the light was completely off). The intensity of the 560 nm light was set at 1 Log unit above individual threshold, and the flicker frequency

(range of 0.2 - 60 Hz) was controlled by the subject using a joystick (method of adjustment).

Subjects were instructed to: 1) Start the flickering of the annulus by decreasing its flicker frequency (descending condition), 2) stop the flickering of the annulus by increasing its flicker frequency (ascending condition). Both ascending and descending condition were repeated 5 times. CFF threshold was considered to be the point at which the subject detected (mean of all trials) the annulus flickering while decreasing its frequency. The latter option of decreasing the frequency was shown to be more robust against flicker adaptation lowering the CFF of the subject with increased exposure to flickering light (Nygaard and Frumkes 1985). It has been shown previously that CFF have high test-retest reliability (Gortlemeyer and Wieman 1982), thus the obtained CFF can be considered a reliable estimate for our purposes. Hammond and Wooten 2005 had refined the approximate CFF threshold from method of limits approach (six ascending and six descending steps) using a constant stimuli approach with 40 trials.

Heterochromatic flicker photometry

Lens density was finally assessed using the heterochromatic flicker photometry (HFP, Wagner and Boynton 1972; Bone and Landrum 2004), in which the subjects were instructed to minimize or eliminate the perception of flicker by adjusting light intensity of the test light (410 nm light) while the reference (560 nm) was kept constant. The HFP technique has been validated for example by Werner et al. 1987 for macular pigment (MP) measuring the entire spectral absorption curve, which closely matched the *ex vivo* measurement of the MP absorption spectrum.

The 560 nm and the 410 nm lights were square wave-modulated in counterphase with a frequency of 2 Hz (500 ms of test, 500 ms of reference) as used by Wooten et al. 2007), and this frequency was found to give reliable results with little complaints from all subjects. The measured CFF of the subject was left unexploited (Hammond and Wooten 2005).

It was seen in a study by Barbur et al. 2010 that a subject with low CFF will have a wide flicker nulling range, while a subject with high CFF may not be able to null the perception of flicker completely, particularly when fixation instability is large. The nulling range is defined as the difference between flicker null intensity while approaching the flicker null zone with increasing intensity and with decreasing intensity.

The 560 nm light was set one log unit above the measured absolute threshold, and the subject had to adjust the light intensity of the 410 nm in order to stop the annulus from flickering. Since both lights are still seen as gray under these conditions (scotopic vision) total fusion can only be achieved once both lights are detected at the

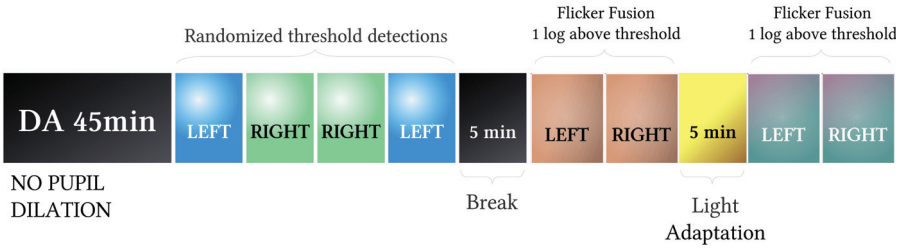

Figure 65: **Lens density measurement protocol.** After 45 minutes of DA, subject performed a threshold detection training phase with his non preferred eye in which he had to increase light intensity of 560 until he detects the annuls flickering. Training was followed by threshold detection procedure for 560nm and 410nm with preferred eye. In a second step subject had to detect their CFF by increasing (UP) or decreasing (DOWN) annulus flickering frequency. In the last step of the protocol (Flicker Fusion) subject had to minimize the perception of flicker by adjusting light intensity of the measuring wavelength (410nm) either by increasing it (UP) or decreasing it (DOWN). Flicker fusion was made using both eyes, once at a time.

same intensity. At this point the difference between the intensities of two wavelengths is an indicator of the lens density. The subject was instructed to perform the adjustment by first increasing then 410 nm light intensity, and then decreasing the light intensity. Fusion point was chosen as the mean of these two measures (end points of nulling range) as done previously by Barbur et al. 2010. Both eyes were tested individually using this technique and five trials were obtained for each condition and each eye. The lens density was calculated as with absolute scotopic threshold detection (see 5.3.2.4).

Lens density index calculation

The lens density index was calculated from the obtained detection difference of scotopic threshold condition (5.3.2.4) or the flicker null of the HFP condition (5.3.2.4) $\Delta I = I_{ph,410nm} - I_{ph,560nm}$ based on the formulation of van Norren and Vos 1974 customized for our measurement technique. The average lens density difference $D_{stdDiff}$ between the used spectral power distributions (SPD) of the experimental lights (photon densities $L_1(\lambda)$ for 410 and $L_2(\lambda)$ for 560 nm in linear scale) was calculated from the standard observer lens density $D_{stdObs}(\lambda)$ from the human ocular media model (Eq. (62)) of van de Kraats and van Norren 2007a by setting the *age* to 25 years:

$$D_{stdDiff} = log_{10}\left(\frac{\int_{380}^{780} L_1(\lambda) \times 10^{D_{stdObs}(\lambda)} d\lambda}{\int_{380}^{780} L_2(\lambda) \times 10^{D_{stdObs}(\lambda)} d\lambda}\right) \tag{54}$$

Now the obtained $D_{stdDiff}$ is the same as the "scaling factor" used in van Norren and Vos 1974, and for our choice of experimental lights, the $D_{stdDiff}$ was ~0.775 log units. This approach of integrating the "ef-

fective lens density" over the full light spectrum (from 380 nm to 780 nm) avoids the cumbersome use of tabulated values of van Norren and Vos 1974 that are only valid for very monochromatic lights (like ours), but start to deviate from "ground truth" as the half-bandwidth (HBW) of the light starts to increase as it is the case for unfiltered LEDs pointed out by Wooten et al. 2007.

Lens density index D_{lens} for each subject is calculated by subtracting the ΔI from the obtained $D_{stdDiff}$:

$$D_{lens} = D_{stdDiff} - \Delta I \tag{55}$$

The lens density index D_{lens} now represents the difference in lens density between the imaginary "standard observer" and the subject tested, and thus can be negative if the subject has a very low lens density or due to calibration offsets in the system. The D_{lens} is the ideal lens density assuming that our test lights ($L_1(\lambda)$ and $L_2(\lambda)$) stimulated equally rhodopsin and the spectral transmittance of the measurement system was spectrally neutral. However, this was not the case and the following corrections had to be made for the D_{lens}.

First, our method is sensitive for the correct parameters chosen for rhodopsin peak wavelength λ_{max}, peak density d_{Rh} and the nomogram model for rhodopsin $S(\lambda)$, as pointed out by van de Kraats and van Norren 2007a in regard to the previously published method from the same authors (van Norren and Vos 1974). In practice the experimental lights do not have to stimulate equally rhodopsin if the stimulation difference $\triangle R$ is exactly known expressed as following:

$$\triangle R = log_{10}\left(\frac{\int_{380}^{780} L_1(\lambda) \times S(\lambda) d\lambda}{\int_{380}^{780} L_2(\lambda) \times S(\lambda) d\lambda}\right) \tag{56}$$

In the paper by van Norren and Vos 1974, peak wavelength λ_{max} was chosen to be 493 nm (Wald and Brown 1958), and the peak density d_{Rh} of 0.20 (Rushton 1972) while using the Dartnall template (Dartnall 1953). We chose slightly different values based on recent literature with a peak wavelength λ_{max} estimate of 495 nm by re-fitting the points given by Kraft et al. 1993 with the nomogram provided by Govardovskii et al. 2000. The self-screening correction was done with an estimate of 0.40 for peak density d_{Rh} for rhodopsin in dark-adapted human rods (Lamb 1995) as following:

$$S(\lambda)_{ss} = log_{10}\left\{\frac{1 - \left[S(\lambda) \cdot \left(1 - 10^{-d_{Rh}}\right)\right]}{-d_{Rh}}\right\} \tag{57}$$

where $S(\lambda)_{ss}$ is the spectral sensitivity for rhodopsin, corrected for the self-screening effect. The human rod is only 25 µm long (Baylor et al. 1984), thus the correction for spectral absorbance change as a function of outer segment length was found to be non-significant for our purposes (Warrant and Nilsson 1998). With our parameter values

the 410 nm light stimulated 0.08 log units more the rhodopsin than the used 560 nm lights, whereas with the parameter values of van Norren and Vos 1974 our 410 nm light would have stimulated 0.19 log units more than the 560 nm light.

The self-screening effect of rhodopsin peak density d_{rh} had negligible effect on rhodopsin stimulation, d_{rh} decreasing from 0.40 to 0.20 caused a simulated increase of 0.004 log units in rhodopsin stimulation at λ_{max}~495 nm. The results of these calculations are shown in Section C.1. This invariant behavior on pigment density is beneficial considering that there is evidence for photopigment density decrease in cones with age differentially for fovea and perifovea (Swanson and Fish 1996). Renner et al. 2004 noticed a paradoxical increase of L and M cone photopigment in the parafovea with age improving the photon catch, and likely counteracts the typically seen loss of visual sensitivity with age.

Additionally, the apparatus with its diffusing sheets (Chen et al. 2008) differentially filtered blue light especially via Rayleigh scattering causing blue light to scatter more and to be attenuated significantly in the optical system of the apparatus. The optical system of the apparatus was measured to attenuate our 410 nm test light 0.60 log units more than the 560 nm test light.

Estimation of spectral attenuation from lens density index

The lens density index was calculated by fitting the ocular media model of van de Kraats and van Norren 2007a to the measured two data points (410 nm and 560 nm), with only the *age* as free parameter (Matlab function FMINCON, from Optimization Toolbox) in the model (Eq. (62)) resulting a "virtual age" estimate for each subject. This virtual age is conceptually similar to the virtual age used by van Norren and van de Kraats 2007 to estimate the spectral behavior of intraocular lenses (IOL) in regard to their photoreception and photoprotection characteristics. The virtual age of the lens allowed the approximation of the full spectral attenuation profile of the ocular lens. The human ocular media model $D_{media}(\lambda)$ is defined in general form as a sum of five spectral components and a spectrally neutral offset:

$$\begin{aligned} D_{media}(\lambda) \quad = \quad & d_{RL}(age) \times M_{RL}(\lambda) \\ & + M_{TP}(\lambda) \\ & + d_{LY}(age) \times M_{LY}(\lambda) \\ & + d_{LOUV}(age) \times M_{LOUV}(\lambda) \\ & + d_{LO}(age) \times M_{LO}(\lambda) \\ & + d_{neutral} \end{aligned} \tag{58}$$

where M_i are the templates (M for media) describing the spectral shape of each component and d_i are age-dependent scalar weights, i.e. the density coefficients. The subscripts RL, TP, LY, LOUV, and LO are Rayleigh loss, tryptophan, lens young, lens old UV, and lens old, respectively.

The templates M_{TP} and M_{RL} represent the light losses in the ocular media as a whole, the former is based on tryptophan absorption occurring heavily below 310 nm (Gakamsky et al. 2011), and the latter for Rayleigh scatter arising from light interaction with submicroscopic density fluctuations in the ocular media including the aqueous and vitreous humors (Ambach et al. 1994), and cornea (Boettner and Wolter 1962; Kolozsvári et al. 2002). Without the Rayleigh scatter, the humors and the cornea can be considered to consist mainly of water, and to be transparent for the visible light. The water in the eye start to absorb beyond 700 nm and can the transmittance be modeled then using the tabulated water absorption up to 2500 nm (van den Berg and Spekreijse 1997).

The three lens templates (LY, LOUV and LO) are based on the absorbance characteristics of kynurenine derivatives (Gaillard et al. 2000) in the human eye, dominating absorber being the the 3-hydroxy-kynurenine glucoside (3HKG) with contributions from kynurenine and 3-hydroxy-kynurenine (3HK). With aging, the lens proteins undergo changes in structure or in binding of kynurenine products (Bloemendal et al. 2004; Lynnerup et al. 2008; Su et al. 2011), for example the total amount of 3HKG is reduced to about 30% at the age of 50 compared to the young lens (Gaillard et al. 2000). The three lens templates and the tryptophan template can be described with a single Gaussian:

$$M_{i,gaussian} = norm \times exp\left(-\left\{\left[w \times \left(\lambda - \lambda_{peak}\right)\right]^2\right\}\right) \tag{59}$$

where the *norm* is the the normalization factor for the template to normalize the template to unity at 300 nm, w is the width factor (in nm^{-1}) describing the "narrowness" of the spectral template analogous to the definition of half-bandwidth in Gaussian light sources, and the $\lambda$is the wavelength vector and the λ_{peak} is a scalar wavelength describing the maximum absorption of the spectral template. The Rayleigh scatter component M_{RL} is described as monotonically decreasing function with wavelength, typical for Rayleigh scatter (Bohren and Huffman 1998):

$$M_{RL}(\lambda) = (400/\lambda)^4 \tag{60}$$

The age relationship for d_i was found by the authors best described by a quadratic age relationship rather than by a linear one:

$$d_i = d_{i,0} + \alpha_i \times age^2 \tag{61}$$

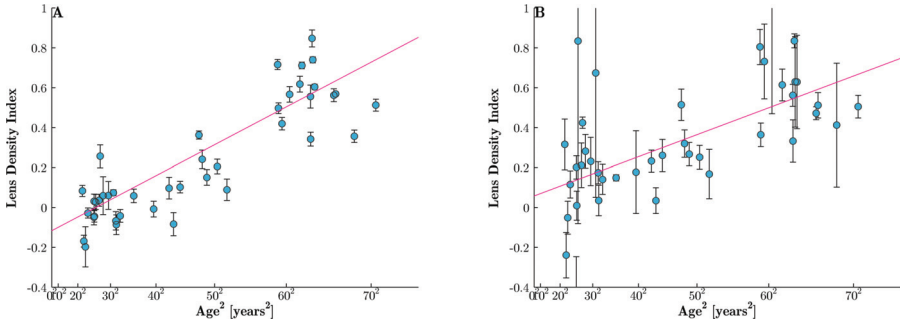

Figure 66: **Lens density index as a function of age. (A)** Lens density index as a function of age in the heterochromatic flicker photometry (HFP) condition (age coefficient a_i= 0.000168 (Eq. (61)), R^2~0.79). **(B)** Lens density index as a function of age in the absolute scotopic threshold condition(age coefficient a_i= 0.000144 (Eq. (61)), R^2~0.59).

with $d_{i,0}$ the density at age 0 (the intercept), α_i the aging in years^{-2} (quadratic slope), and *age* in years.

The human ocular media model $D_{media}(\lambda)$ can be expressed in its final form with all the numerical values derived by van de Kraats and van Norren 2007a, combining the Gaussian expression (Eq. (59); for TP, LY, LOUV and LO) and Rayleigh scatter (Eq. (60)) with the aging trend (Eq. (61); excluding M_{TP} which was not found to depend on age) resulting the following:

$$\begin{aligned} D_{media}(\lambda) \quad = \quad & (0.446 + 0.000031 \times age^2) \times (400/\lambda)^4 \\ & +14.19 \times 10.68 \times exp\left(-\left\{[0.057 \times (\lambda - 273)]^2\right\}\right) \\ & + (0.998 - 0.000063 \times age^2) \\ & \times 2.13 \times exp\left(-\left\{[0.029 \times (\lambda - 370)]^2\right\}\right) \\ & + (0.059 - 0.000186 \times age^2) \\ & \times 11.95 \times exp\left(-\left\{[0.021 \times (\lambda - 325)]^2\right\}\right) \\ & + (0.016 - 0.000132 \times age^2) \\ & \times 1.43 \times exp\left(-\left\{[0.008 \times (\lambda - 325)]^2\right\}\right) \\ & +0.111 \end{aligned} \tag{62}$$

5.3.3 *Results*

Lens density index when plotted as a function of squared age (age^2 as done in van de Kraats and van Norren 2007a) shows a clear increasing trend with age in both heterochromatic flicker photometry (HFP) condition (Figure 66A), as well as in the absolute scotopic threshold condition (Figure 66B). However, the HFP condition exhibits significantly less variability as a function of age as it can be seen from R^2 values (R^2~0.79 for the HFP, R^2~0.59 for the scotopic threshold.

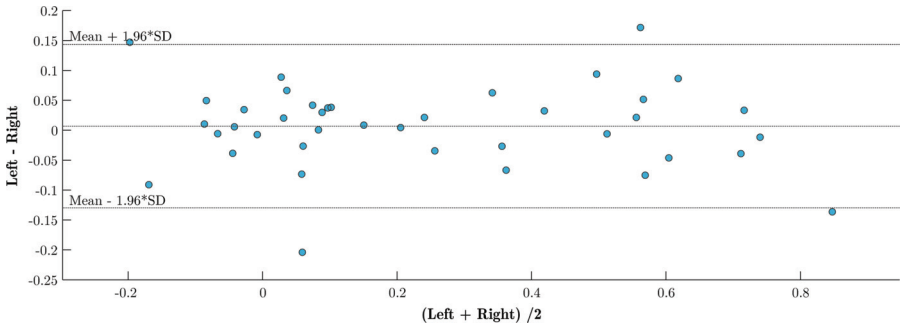

Figure 67: Left vs. right eye as done with heterochromatic flicker photometry (HFP) technique. Bland-Altman plot (Bland and Altman 1986).

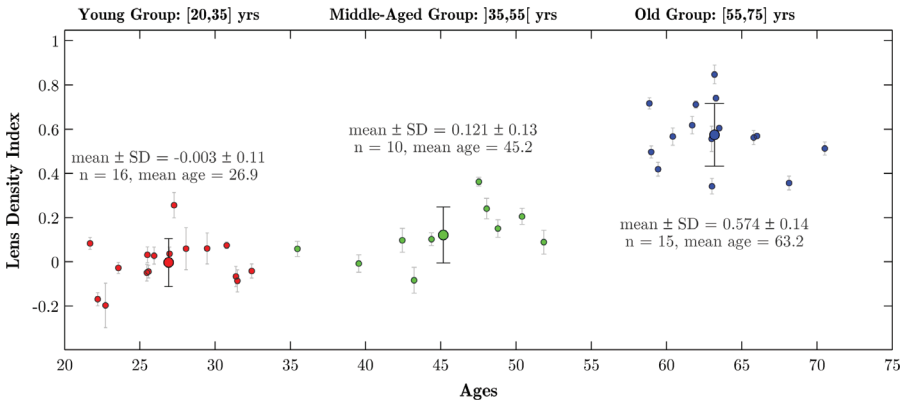

Figure 68: Lens density results for three age groups: young group, [20,35] year olds; middle age group]35,55[year olds; and the old group [55,70] year olds.

Left vs. right

Left and right eye did not correlate with the original version of Bland-Altman (Bland and Altman 1986) as shown in Figure 67.

Age-grouped

Our results are normalized to lens density of standard observer (25 yo). Data is presented as mean ± SD. Our preliminary results in 39 subjects (17 young, 9 middle aged and 13 old) show a significant increase in lens density index between young group, middle aged group compared to old group in blue (t-test p<0.05). Increase in lens density index was not significant between young group and middle aged group (Figure 68).

Used in van de Kraats and van Norren 2007a ocular media model this increase in lens density index leads to a diminished transmittance over the entire visible spectrum in the elderly compared to young and middle aged group. Moreover, filtering is particularly pronounced in the short wavelength range (<500 nm) a result that is similar to the one recently reported by Gimenez et al. 2010 using a different tech-

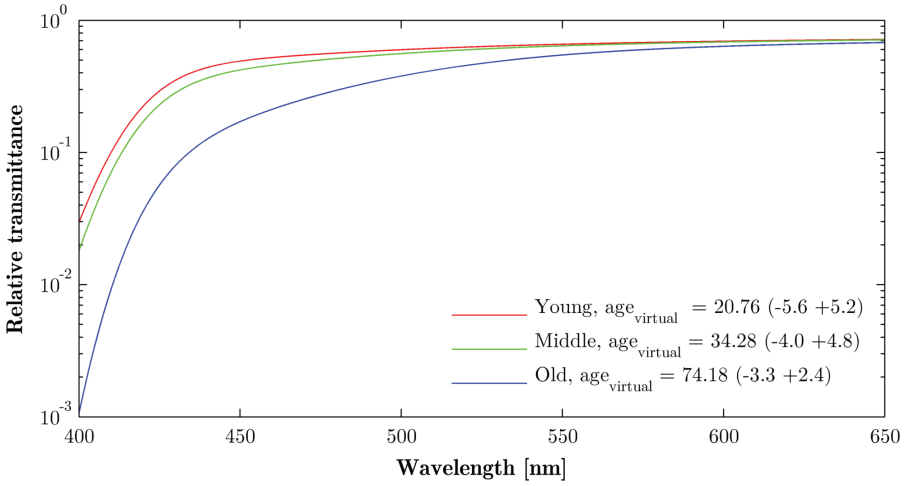

Figure 69: Spectral attenuation of the three age groups as expressed in virtual age: young group, [20,35] year olds; middle age group]35,55[year olds; and the old group [55,70] year olds.

nique. Our data using fusion technique are in agreement with Sample et al. 1988 and showing a strong correlation (R^2 = 0.96) between left and right (non-cataractous) eyes using the fusion technique.

Our results using our flicker photometry system show a significant increase of lens density and therefore lens filtration with age (Figure 68). These results are in total agreement with previous literature data. The system developed in our laboratory is therefore fully efficient for measuring lens yellowing in vivo. Moreover, the Fusion technique we developed seems to be less variable and repetitive than traditional threshold detection technique (results are still under analysis).

Spectral attenuation estimates based on the model of van de Kraats and van Norren 2007a are shown in Figure 69 based on the calculations outlined in 5.3.2.4.

CFF

Shown in Figure 70A, no age-dependent effects were found for CFF threshold, in contrast to the results found in the study of Hammond and Wooten 2005 which had shown a decreasing CFF threshold with age, while however demonstrating high variability. The results are roughly in accordance with the three-phase age dependence of temporal contrast sensitivity (TCS, i.e. flicker sensitivity), TCS increasing up to an age of ~16 years, then remaining relatively constant until 60 years followed by a decline after 60 years (Kim and Mayer 1994; Tyler 1989). The individual CFF did not correlate well with the individual flicker nulling range as shown in Figure 70B.

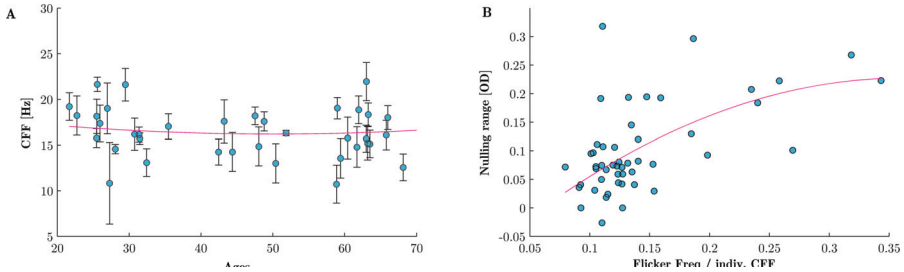

Figure 70: **Behavior of CFF in the descending frequency condition (A)** CFF as a function of age. The fit (red line) is a 2nd order polynomial with a R^2~0.02. **B)** Nulling range defined in optical densities [OD] as a function of flicker frequency used normalized to the individual CFF threshold. In other words if 2 Hz was used and individual's CFF threshold was 20 Hz, the normalized value for x-axis was 0.1. Note that there are more data points than subjects as some subjects were tested with various flicker frequencies. The fit (red line) is a 2nd order polynomial with a R^2~0.22.

5.3.4 *Discussion*

The estimates of short-wavelength light absorption by the ocular media correlated well with the age of the subject (Pokorny et al. 1987; Weale 1988; van de Kraats and van Norren 2007a). A large variation in ocular media optical density between individuals (Sample et al. 1988), and in many cases the use of average values is not indicative of a individual lens OD. Mathematical models have been produced to predict the expected changes in the absorption characteristics of the aging lens (van de Kraats and van Norren 2007a) they cannot present individual changes for real observers. This is in contrast with the typical corrections applied in NIF photoreception studies, typically using the standard observer lens density template provided by Stockman et al. 1999.

For the lens media correction to be meaningful, the transmittance of the lens media should be measured before the actual experimental session. The ocular media transmittance can be then used to correct the experimental corneal irradiance to a level giving equal retinal irradiance for all the tested subjects. The change of the spectral sensitivity occurring in the ocular media from the corneal irradiance to the retinal irradiance can be done *post hoc*. The correction the NIF responses for wavelength-dependent light attenuation can be complicated by the nonlinear irradiance response curves (sigmoidal relationship) for majority of NIF responses such as for melatonin suppression (McIntyre et al. 1989; Brainard et al. 2001; West et al. 2011), light-induced alertness (Cajochen et al. 2000) and PLR (Reeves 1920; 3.3.2). In other words, a reduction of irradiance in the ocular media by 0.40 log units for example would not necessarily lead to a reduction of the measured response by 0.40 log units, the reduction depending on the

individual irradiance response curve that might be subject to light/-dark adaptation effects and individual variations.

The example of a lens media correction with confusing results can be seen in the melatonin suppression study by Thapan et al. 2001 using the lens media template of Stockman et al. 1999 *post hoc* of the study. The results showed a maximal retinal sensitivity for melatonin suppression at ~420 nm, thus significantly blue-shifted compared to the current knowledge of melanopsin λ_{max}~ 480 nm (see 2.4.2). Additionally, the authors were fitting a "Dartnall template" (Dartnall et al. 1983) derived from donor retinas for the corneal sensitivity data (showing a λ_{max}~ 468 nm, R^2~ 0.85), which in theory could never fit if there is a filtering ocular media between the light stimulus and the retina. Furthermore, the attempt to fit the same template (Dartnall et al. 1983) to ocular media corrected sensitivity gave a λ_{max}~ 459 nm with a worse fit (R^2~ 0.74). The exact reasons for the deviation from the other published melatonin suppression action spectra (Brainard et al. 2001; 2008b) is hard to estimate afterwards.

In contrast, in the studies by Brainard et al. 2001; 2008b, the corneal irradiance was increased to compensate the losses in ocular media based on the mean estimates from their previous study (Brainard et al. 1997). This approach in theory provides more conceptually correct correction of ocular media, whilst suffering from the lack of individual measurements of ocular media (e.g. Gimenez et al. 2010). van de Kraats and van Norren 2007b re-analyzed the ocular media corrections used in the melatonin suppression studies, and they surprisingly proposed the best fit for melatonin suppression action spectrum, to be the same as for photodependent oxygen uptake in retinal pigment epithelial (RPE) cells [approximated by an exponential function, (Rózanowska et al. 1995)] for both melatonin suppression datasets. This highlights the difficulty and importance of ocular media correction as also addressed by Takahashi et al. 2011. Additionally, there is evidence that the spectral sensitivity of the human visual system may change with age (Kraft and Werner 1994) to compensate the reduced retinal short-wavelength irradiance. See 6.4.1 for more discussion on practical implications of ocular media on lighting and NIF photoreception.

Strictly speaking, the used psychophysical heterochromatic flicker photometry (HFP) cannot distinguish the lens density component from other ocular absorbers, and the result is an estimate of the whole eye absorption difference between 410 nm and 560 nm. By choosing a peripheral retinal location (3° wide annulus between 15° to 18°) the contribution of macular pigment was avoided (Delori et al. 2001), even considering the noted variability in the peak density and the rate of decrease amongst individuals (Hammond et al. 1997a), and the possible spread of macular pigment towards the periphery of retina with age (Chen et al. 2001b). The cornea, the aqueous and the vitreous

humors, and lens capsule (Murata 1987) were implicitly incorporated to the human ocular model (van de Kraats and van Norren 2007a), and their significance to the obtained lens density results cannot be separated. In previous reports, however the optical density contribution of the cornea (Boettner and Wolter 1962; van den Berg and Tan 1994) and the humors (Boettner and Wolter 1962), were found not be effected by aging making their contribution to final results less complex.

In a study of Van Loo and Enoch 1975, a wavelength-dependent directionality was found for the human rods in a Maxwellian view setup. The extreme directionality difference at 3.5 mm displacement from the center of the pupil, was found to be 0.17 log units between the used monochromatic 433 nm light and the broadband light with wavelengths below 433 nm filtered out. The directionally difference was found to be negligible up to 1.5 mm displacement from the center, and combined this with our approach to use the free-view optical setup the directionality for the used wavelengths can be assumed to be non-existent.

Crystalline lens has been shown to fluorescence in response to light mainly at two spectral bands, the blue fluorescence and green fluorescence (Van Best and Kuppens 1996). Excitation of the lens at 413 nm causes a fluorescence emission with a peak at ~480 nm (Zuclich et al. 1992). Fluorescence may be assumed to add a uniform component to the retinal point spread function (PSF) degrading the visual performance by adding a "veiling glare" on top of the retinal image (van den Berg et al. 2009b). Weale 1985 has estimated that the reciprocal ratio between the luminance of a patch of sky and the fluorescence it induces is ~0.002 for the normal lens of a 30-year-old human, increasing to 0.017 for a 60 year old and to 0.121 for an 80 year old, the two latter ones starting to be visually noticeable. With aging, fluorescent intensity increases roughly linear with age (Van Best and Kuppens 1996) and fluorophores emerging with age that emit at even longer wavelengths (Cooper and Robson 1969; Yu et al. 1985), the upper limit for excitation being roughly 650 nm for older lenses (Yu et al. 1985). The absorbance of fluorescence by the ocular media itself has been also used to quantify the lens absorption (Weale 1996; Broendsted et al. 2011)

As the fluorescence induced outlasts the duration of the exciting stimulus, in our psychophysical paradigm it can be assumed that in theory there is an added "visual component" both during the 410 nm light and decaying fluorescence during 560 nm light, the exact "artifact luminance" depending on the photon densities at a given time. The prolonged impairment is qualitatively similar of the "flash blindness" phenomenon (Brown 1965b) referred in Zuclich et al. 1992 with lens fluorescence causing a prolonged glare/visual impairment for example from the blue-enriched headlights of by-passing cars in

night-time driving conditions (Gray et al. 2011). van den Berg 1993 estimated quantal sensitivity of the blue fluorescence (induced for example by our 410 nm light) to be between 0.004 and 0.025 fluorescent quanta per exciting quantum.

In theory, the transmural transmittance of the ocular wall and iris transmittance could have contributed to our results by attenuating the test light at 410 nm more, but the attenuation values found in the literature were in order of 2 log units even for the light-eyed subjects (van den Berg et al. 1991). These estimated iris transmittance values combined with the dark-adapted pupil, and thus smaller iris area, the effect of iris transmittance in our ocular media density values can be assumed to be non-significant.

There has been some evidence of other sources of yellowing of the ocular media existing in the human eye. Geeraets et al. 1960 found short-wavelength absorption in human neurosensory retina (outside the anatomic fovea that contains the macular pigment), while at the time it was considered a postmortem artifact. The report of Snodderly et al. 1984 suggest the existence of two additional yellow pigments with absorbance maxima at 410 and 435 nm, located in the outer nuclear layer or the inner segment layer of retinal tissue both inside and outside the anatomic fovea. Furthermore, Bowmaker et al. 1991 reported another yellow ocular pigment, located in the inner segments of both rods and cones of old world monkeys with a peak absorbance at 420 nm. Any or all of these yellow pigments could contribute to the filtering of the light before reaching the rods in our scotopic measurement conditions.

Hubbard and Kropf 1958 had originally shown that normal photobleaching could be prevented if additional light was absorbed by the bleaching intermediates, referred as the "photoreversal" of bleaching (Williams 1964). Similar phenomenon was observed in early receptor potential (ERP) recordings of a rat, with complete bleaching of rhodopsin abolishing early receptor potential, but being recordable again after a blue light flash regenerating rhodopsin (Cone 1967). The most likely intermediate photoproduct being photoreversed was suggested to be metarhodopsin II, that has a peak absorbance at ~380 nm with a 1.2 times higher excinction coefficient than rhodopsin (Weale 1967; Bartl and Vogel 2007). Further rat study *in vivo* by Grimm et al. 2000 estimated the quantum efficiency of photoisomerization to be roughly ~0.3, while demonstrating that light at 550 nm was able to fully bleach the rhodopsin, in contrast to the "rhodopsin-equal" exposure at 403 nm that left significant portion of rhodopsin to the unbleached state. This blue-enhanced photoreversal was linked to the increased susceptibility for blue-light damage (Grimm et al. 2001).

Additionally, some residual photoregeneration could occur via the putative retinal G protein-coupled receptor (RGR) photoisomerase pathway (Chen et al. 2001a), with Wenzel et al. 2005 showing dim

light an 4-fold effect in accelerating rhodopsin regeneration, although independent of RGR. Authors suggested a plausible candidate for accelerated recovery to be the light-dependent palmitoylation of sRPE65 to mRPE65, as palmitoylation of retinal pigment epithelial protein 65 (RPE65) has shown to accelerate the delivery of retinyl esters to the isomerohydrolase (Xue et al. 2004). The authors (Wenzel et al. 2005), however did not extend their protocol to include the wavelength-dependent effect of such acceleration making quantification of their findings problematic for our purposes. An equilibrium photoreversal at 1% of the rate of photobleaching (metarhodopsin II and rhodopsin stimulation ratio in response to the used white fluorescent light) was estimate in their study being practically insignificant.

In conclusion, the proposed method is able to provide a relatively low-cost estimate of the ocular media density that is a clear improvement compared to the approach of using standardized ocular media templates. For more exact estimation of ocular media on melanopsin photoreception, a third light source could be added for the wavelength region of 480 nm. In that case two distinct heterochromatic flicker pairs (410 nm vs. 560 nm, and 480 nm vs. 560 nm) would be need to done for each subject resulting three points for the curve fitting algorithm (B.3), thus improving the accuracy of the full spectral attenuation estimate.

5.4 PUPILLARY LIGHT REFLEX WITH AGING

DOES PUPIL CONSTRICTION UNDER BLUE AND GREEN MONOCHROMATIC LIGHT EXPOSURE CHANGE WITH AGE?

Véronique Daneault[#1,2,6], Gilles Vandewalle[#1,2,6], Marc Hébert[3], Petteri Teikari[4,5], Ludovic S. Mure[4,5], Julien Doyon[1,6], Claude Gronfier[4,5], Howard M. Cooper[4,5], Marie Dumont[2], Julie Carrier[1,2,6]*

[1] Functional Neuroimaging Unit, University of Montreal Geriatric Institute, 4565, chemin Queen-Mary, Montréal, Québec, Canada, H3W 1W5; [2] Center for Advanced Research in Sleep Medicine (CARSM), Hôpital du Sacré-Cœur de Montréal, 5400 boulevard Gouin Ouest, Montréal, Québec, Qc., Canada, H4J 1C5; [3] Centre de recherche Université Laval Robert-Giffard, 2601 Chemin de la Canardière, Québec, QC, Canada, G1J 2G3; [4] Stem Cell and Brain Research Institute, INSERM U846, 18 avenue Doyen Lépine 69500, Bron – France, [5] Université Claude Bernard, Lyon I, Lyon, France; [6] Department of Psychology, Université de Montréal, CP 6128, succursale Centre-Ville, Montréal, Québec, Canada, H3C 3J7.

 # These authors contributed equally to this work

5.4.1 *Introduction*

Light is perceived by the visual system to allow conscious vision but also by a photoreceptive system based on light sensitive melanopsin-expressing intrinsically photosensitive ganglion cells (ipRGCs, mRGCs, pRGCs) optimized to detect changes in light irradiance rather than to participate in image formation (Brown et al. 2010; Hatori and Panda 2010; Schmidt et al. 2011). This non-image-forming (NIF) photoreceptive system is responsible for circadian entrainment but also acutely regulates many other non-visual functions such as melatonin secretion, sleep, alertness, performance, cognitive brain functions and pupillary constriction (Brainard and Hanifin 2005; Chellappa et al. 2011; Hatori and Panda 2010; Schmidt et al. 2011). The NIF system shows a peak sensitivity at around 460-480 nm (blue light) (Brainard and Hanifin 2005) so that the impact of light on non-visual functions is greater under short-wavelength blue light compared to lights of longer-wavelength such as green light (Cajochen et al. 2005; Lockley et al. 2003; Lockley et al. 2006; Mure et al. 2009; 2007; Vandewalle et al. 2011; 2009). This maximal sensitivity to short wavelength light is primarily due to the recruitment of mRGCs, which receives additional modulatory inputs from rods and cones (Berson 2003; Hatori and Panda 2010; Provencio et al. 2000; Schmidt et al. 2011). mRGCs project directly to numerous brain regions including the suprachiasmatic nuclei (SCN), site of the master circadian clock, the ventrolateral preoptic nucleus (VLPO) which contains sleep active neurons, and the olivary pretectal nucleus (OPN), crucial for pupillary constriction (Berson et al. 2010; Hatori and Panda 2010; Schmidt et al. 2011).

Aging is associated with changes in functions affected by the non-visual photoreception system including sleep and circadian entrainment (Turner et al. 2010). For instance, studies have demonstrated that healthy aging is associated with advanced sleep timing, more wakefulness during the sleep episode, and increased rate of napping (Buysse et al. 1992; Carrier et al. 1996; 2001; Landolt and Borbély 2001, Landolt et al. 1996). Aging also induces significant changes in the circadian timing system (phase advance and reduced amplitude of circadian rhythms) and problems to adapt to circadian challenges (e.g., shift work, jet lag) (Carrier et al. 1996; Duffy et al. 1998; Kawinska et al. 2005; Moline et al. 1992; Monk et al. 1995; Van Cauter et al. 1996). These age-related modifications may be triggered in part by a decreased sensibility to light or by the ability for light to drive non-visual functions. Indeed, the impact of light on the circadian phase, and therefore on the circadian entrainment, seems to diminish with aging [significant impact found in Duffy et al. 2007 but not in Sletten et al. 2009]. Recent evidence also suggests that acute effects of light such as melatonin suppression, subjective alertness enhancement and PERIOD2 expression decrease with age for blue but not for green light (Herljevic et al. 2005; Jud et al. 2009; Sletten et al. 2009). However, age-related alterations on pupillary light reflex (PLR), which regulates the amount of light reaching the retina (see Section 3.1), remain poorly understood.

Major modifications occur with aging at the level of the eye such as a decrease in scotopic and photopic sensitivity, as well as in the number of retinal photoreceptors (Sturr et al. 1997; Hébert et al. 2004; Freund et al. 2011). Due to progressive opacification and yellowing of the lens (see Section 5.3), light transmission decreases with age, especially for shorter wavelength (blue) light (Kessel et al. 2010). In addition, aging is associated with a substantial decrease in pupil size (senile miosis) in darkness and under various light irradiance levels (Bitsios et al. 1996a; Winn et al. 1994). Yet, how aging affects the wavelength sensitivity of pupil constriction and its response dynamics as a function of irradiance change is unknown.

In the present study, we first assessed how the amount of light reaching the retina changes with age by measuring pupil size under green (550nm) and blue (480nm) light exposures at different irradiance levels in healthy young and older individuals. We then assessed PLR, i.e. the relative change in pupil size under these light conditions, to investigate whether the ability of light to trigger this non-visual response changes with aging. We anticipated that, in older compared to young subjects, a smaller pupil size would be observed under all light conditions, accompanied with a reduction in PLR, particularly for blue light.

5.4.2 *Materials and methods*

Subjects

Healthy subjects, 16 young (22.8 ± 4y; 10 females) and 14 older (61 ± 4.4; 10 females), participated in the present study. Recruitment interviews established the absence of medical, traumatic, psychiatric, or sleep disorders. Questionnaires were used to exclude candidates with extreme chronotype (Horne and Östberg 1976), poor sleep quality (Buysse et al. 1989), high anxiety (Beck et al. 1988) or depression (Steer et al. 1997) scores (see Supplementary Table 8 for detailed subject characteristics). Candidates with a body mass index > 27 were excluded. None had worked on night shifts during the preceding year or traveled across more than one time zone during the last two months. All participants were nonsmokers, moderate caffeine and alcohol consumers and were not using medication, except for hormonal contraceptive in 9 out of 10 young women. Prior to participation, subjects went through an extensive professional ocular examination to confirm normal color vision and absence of ocular problems. The absence of cataract was assessed subjectively using the Lens Opacities Classification System III (LOCS-III, from 1, clear lens, to 5, cataract; (Chylack et al. 1993). All young subjects had clear lenses (level 1) and all older subjects' lenses were classified below level 4. This experiment was performed in accordance with institutional guidelines and received the necessary ethical approvals. Written informed consent was obtained from each subject.

Protocol

Upon arrival, subjects were dark-adapted for 15 minutes (0 lux) and baseline pupil size was assessed at the end of this adaptation period (Figure 71). Pupil size was then measured under blue (480nm, full width at half maximum - FWHM: 10nm) and green (550nm, FWHM: 10nm) monochromatic light exposures presented at low (7×10^{12}ph/ cm^2/s), medium (3×10^{13}ph/ cm^2/s), and high (10^{14}ph/ cm^2/s) irradiance levels. Light exposures lasted 45s, during which subjects were asked to maintain a fixed gaze, and were separated by 2 min of darkness (0 lux, free gaze or eyes closed). Three light exposures of each wavelength were administered for the three irradiance levels (pseudo-random order; high irradiance was never administered first). The order of blue and green monochromatic lights was counter balanced between subjects and groups (Supplementary Table 8). Pre-exposure pupil size was assessed at the end of each 2 min period in darkness. Note that we verified that pseudo-randomization prevented an exposure to significantly affect the subsequent exposure (supplementary material). Data was collected during the day between 10:00h and 20:00h. Average clock time of testing did not differ between the

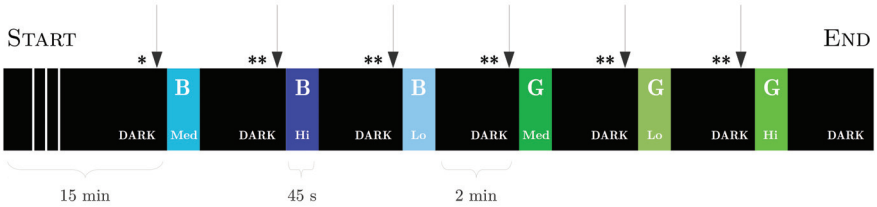

Figure 71: **Experimental Protocol**. Legend: *↓ = baseline pupil value; **↓ = pre-exposure pupil value; B_{Lo}; B_{Med}, B_{Hi} = Blue light; lower, medium and higher irradiances, respectively; G_{Lo}; G_{Med}, G_{Hi} = Green light; lower, medium, higher irradiance, respectively. Example for one subject, wavelength and irradiance conter balanced between subjects and groups.

two groups and all experiments were carried in the Fall season (Supplementary Table 8).

Light settings and data acquisition

Narrow interference band-pass filters (Edmund Optic, NJ, USA) were used to produce blue and green monochromatic lights using a white light source (PL950, Dolan-Jenner Industries, MA, USA). Switch between filters was achieved using a filter wheel (AB301-T, Spectral Products, NM, USA) inserted between the light source and an optic fiber (Dolan-Jenner Industries). The latter brought light to a diffusing glass placed 2cm in front of the subject's left eye. The light source and the filter wheel were computer-controlled and synchronized with pupil data acquisition using COGENT2000 under Matlab 7.0.4 (R14SP2, 2005, Mathwork Inc., MA, USA). Light spectra was assessed at the level of the diffuser (Lightspex, GretagMacbeth, NY, USA) and confirmed to peak at 480nm and 550nm. Irradiance levels were verified using a calibrated radiometer (PM100D, Thorlabs, NJ, USA).

Pupil size was recorded using an eye tracking device (EyeFrame Scene systems, Arrington Research Inc., AZ, USA) consisting of an infrared camera mounted on the frames of eyeglasses in front of the subject's right eye. As PLR is a consensual mechanism (i.e. light in one eye constricts the pupil in the other eye), light was administered to the subjects' left eye while pupil size was captured from the right eye. Pupils were not pharmacologically dilated. Pupil width and height (arbitrary units) were acquired at a sampling rate of 60Hz and the frame image size used was constant for all acquisitions to assure equivalence of the unit size.

Data analysis

Data was analyzed using Matlab 7.10 (R14SP3, 2005). Artifacts in pupil measures, including eye movements and blinks, were excluded using a circularity coefficient exclusion criteria (ratio between width

and height <0.70 or >1.30). According to literature on pupil analysis (Canver et al. 2010; Wyatt 2010), pupil data was smoothed using a non-parametric locally weighted linear regression (function: *smooth*, type: *'rlowess'*; span: *0.8*), for the effect of smoothing parameter on the analysis results see Figure 60. PLR is characterized by an initial transient robust constriction at light onset (phasic response) followed by a tonic or sustained steady-state response at a lower constriction level (McDougal and Gamlin 2010; Mure et al. 2009). In our experimental setting, the transition between light-on and light-off was not sharply regulated (~ 500ms for full illumination or extinction) therefore not allowing a reliable analysis of the phasic response. In consequence, we excluded the first 6s of each illumination to make sure that we only included stable response and averaged pupil size during the remaining 39s of each light exposure. Baseline pupil size and pre-exposure pupil size were estimated by averaging the last second (60 data points) of the 15 or 2 min. of darkness prior to illumination, respectively. Pupil size referring to pupil area was inferred by computing the ellipsoidal surface obtained with width and height arbitrary units PLR was estimated by normalizing mean pupil size during the illumination according to baseline pupil size or pre-exposure pupil size. Statistical analysis was computed in SPSS 17.0 (IBM SPSS Statistics) using two-tailed Student t test to assess difference in baseline pupil size, and a 3-way repeated-measure analysis of variance (ANOVA) with wavelength (blue, green) and irradiance (lower, medium, higher) as within subject factors and age (young, older) as between subject factor. Due to technical issues, three older subjects had missing values (two men with data of 1 light condition missing and one woman with data of 2 light conditions missing). We estimated these missing values with Yates replacement technique (Kirk 2012).

5.4.3 *Results*

Analysis of baseline pupil size (i.e. following 15min. in darkness) showed that older subjects (arbitrary units *a.u.*, mean ± SEM: 0.08 ± 0.009) had smaller pupil size than young subjects (0.11±0.008) [$T(28)$ = 2.73, P =0.01]. This represents an average reduction in surface area of about 27% in older subjects.

Repeated-measure 3-way ANOVA on absolute pupil size during illumination (no normalization) with light wavelength (blue, green) and light irradiance (lower, medium, higher) as within subject factors, and age group (young, older) as between subject factor, revealed a significant interaction between age groups and irradiance [$F(2,56)$ = 7.29, P=0.006] (see 72 for the interaction). Older subjects showed smaller absolute pupil size at each irradiance level but the age-related difference was higher at lower irradiance (low: young = 0.049 ± 0.004, older = 0.030 ± 0.004 [$F(1,28)$ = 11.47, P=0.002] - medium: young =

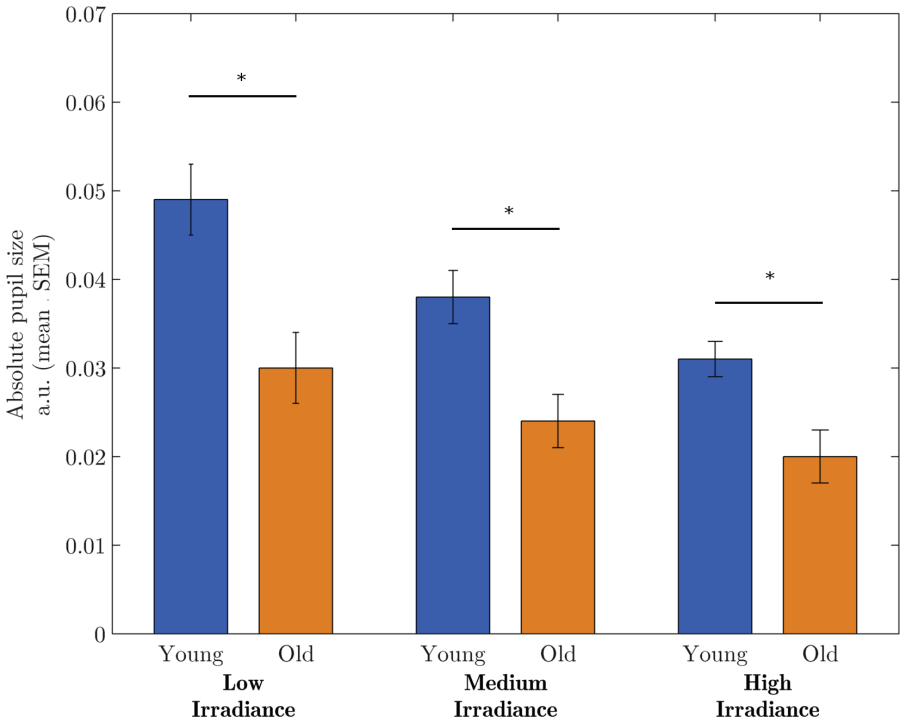

Figure 72: **Significant interaction between age group and light intensity on absolute pupil size.** Mean sustained pupil values ($a.u.\pm$SEM) during light exposure in young (blue bars) and in old (orange bars) group at lower, medium, and higher irradiances. Blue and green wavelengths are combined to show the significant interaction between between age-group and light irradiance. Young and older subjects show stronger differences on absolute pupil size at lower irradiance level. Significant differences : $p < 0.003$ * Significant differences : $p \leq 0.005$ **.

0.038 $\pm$ 0.003, older = 0.024 $\pm$ 0.003 [$F(1,28)$ = 10.05, P =0.004] - high: young = 0.031 $\pm$ 0.002, older = 0.020 $\pm$ 0.003 [$F(1,28)$ = 9.35, P =0.005]). This analysis also revealed a significant effect of light wavelength [$F(1,28)$ = 4.69, P =0.039], with smaller pupil size under blue light (0.031 $\pm$ 0.002), as compared to green light (0.033 $\pm$ 0.002). No other interactions were significant (light wavelength by age group: [$F(1,28)$ = 2.73, P =0.110] - light wavelength by light irradiance: [$F(2,56)$= 2.87, P =0.683] - light wavelength by light irradiance by age group: [$F(2,56)$= 0.055, P =0.898]).

We then normalized sustained pupil size during light exposure according to baseline pupil size to analyze PLR (Figure 73). Repeated-measure 3-way ANOVA of normalized pupil values revealed that blue light induced significantly more constriction (66.67% $\pm$ 2.10), than green light (64.47% $\pm$ 2.25) [$F(1,28)$ = 6.43, P =0.017]. Moreover, constriction was greater with increasing irradiances (low: 57.83% $\pm$ 2.71 - medium: 66.67%$\pm$2.04 - high: 72.21% $\pm$ 1.81) [$F(2,56)$ = 89.18, $P < 0.001$]. The main effect of age was not significant [$F(1,28)$ = 0.514, P = 0.479] and none of the interactions, including the age group by ir-

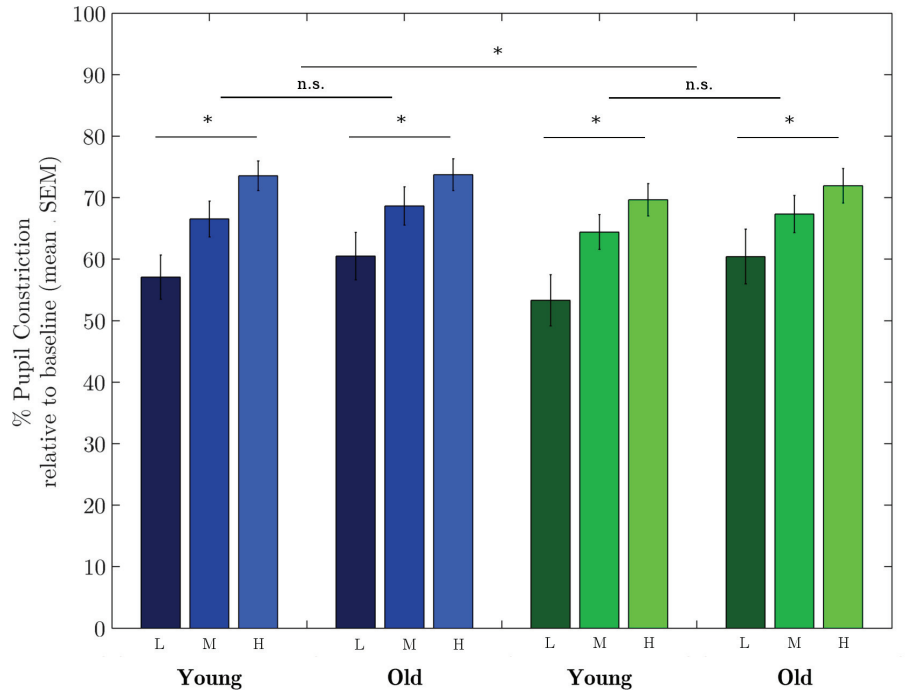

Figure 73: **Pupil light reflex in young and older individuals.** Color bars: Mean pupillary constriction relative to baseline±SEM in each age group. Blue bars: blue light at lower (*L*), medium (*M*), and higher (*H*) irradiances; Green bars: green light at lower (*L*), medium (*M*) and higher irradiances (*H*). Effects of wavelength and irradiances levels were significant (*; $p < 0.05$) but there was no difference between age group and no interaction with age (*n.s.* : non significant).

radiance were significant (irradiance by age group: $[F(2,56) = 1.78, P = 0.19]$, light wavelength by age group: $[F(2,56) = 1.75, P = 0.20]$, light wavelength by light irradiance: $[F(2,56) = 0.24, P = 0.75]$, light wavelength by light irradiance by age group: $[F(2,56) = 0.33, P = 0.68]$). Finally, statistical analysis performed on normalized pupil size data according to pre-exposure pupil size gave similar results (C.3).

5.4.4 *Discussion*

This study investigated the effects of age on pupil size and PLR using shorter (blue, 480 nm) and longer (green, 550 nm) wavelength monochromatic light exposures at three different irradiance levels. Our results confirm that older subjects have smaller pupil size than young subjects (Bitsios et al. 1996a; Winn et al. 1994). This difference was observed both after prolonged dark adaptation and during blue and green light exposures at the three irradiance levels. The observed interaction between irradiance level and age groups is in agreement with previous results that report larger age-related decreases in pupil size under lower, compared to higher irradiance level (Winn et al.

1994). Our results also support previous reports showing that PLR is greater under blue than green light exposure and for higher irradiances (Mure et al. 2009; West et al. 2011). However, despite the fact that irradiance levels exerted a stronger impact on the absolute pupil size of younger compared to older individuals, PLR did not differ between the two age groups for either blue or green light exposures at the 3 irradiance levels.

A previous study by Bitsios et al. 1996a showed no age-related differences under white light for the latency of the phasic PLR, while other parameters of the phasic response were affected by age (amplitude, maximum constriction velocity, maximum constriction acceleration). However, in this previous study, sustained pupil constriction was not investigated.

At the eye level, senile miosis is one of the primary functional mechanisms reducing the amount of light reaching the retina (Winn et al. 1994). In our sample, the observed age-related reduction in pupil size (~30%) is comparable with previous reports in young and older populations (Bitsios et al. 1996a). Senile miosis may constitute a contributing factor to the reduced impact of light on non-visual functions in older subjects (Herljevic et al. 2005; Jud et al. 2009; Sletten et al. 2009). Indeed, in young subjects, studies have reported a correlation between pupil size and light-induced melatonin suppression (Gaddy et al. 1993; Higuchi et al. 2008). In our study, despite the 30% reduction in pupil size (0.15 log attenuation of retinal irradiance) and the increase in lens opacification (professional assessment, LOCS-III [Steer et al. 1997, see Section 5.3] score on Table 8), older subjects showed a steady-state PLR similar to that of younger subjects.

One explanation for the lack of difference could be that compensatory mechanisms may allow a normal PLR despite the age-related decrease in the amount of light reaching the retina. For instance, an increased sensitivity to light may develop with age to compensate for chronic exposure to lower levels of light due to lens opacification. Several studies in young individuals have shown that, following prolonged exposure to low light level, exposure to light induces stronger suppression and phase shift of melatonin secretion (Hébert and Stacia 2002; Jasser et al. 2006; Chang et al. 2011). An alternative explanation for the smaller pupil size in the aged, despite the lack of a difference in relative pupil constriction, is a loss of tonic control of pupil dilation, suggested by the study of Clarke et al. 2003a in the non-human primate. These authors reported that pharmacological blockade of the sympathetic pupillodilator pathway reduces pupil size but does not affect PLR dynamics to different broadband white light intensities. The idea of a loss of autonomic control in the aged is consistent with the the results in our study that show smaller absolute pupil areas in the older subjects, but no difference in PLR under blue or green wavelength light exposures.

Statistical power analysis on our normalized data (i.e. PLR) indicated a small effect size for the main effect of age (0.13) supporting the notion that age did not affect PLR response in the present study. However, the interactions between group and irradiance and between group and wavelength showed medium effect size (0.24 and 0.30, respectively). Future studies with a larger sample size will contribute to a better understanding of age-related interaction according to wavelength and irradiance light levels.

In general agreement with previous hypotheses (Revell and Skene 2010), our data suggests that, although aging alters several non-visual functions regulated by light, the degree to which the impact of light on these functions is reduced may vary considerably. It is worth noting that our sample was slightly younger than previous studies showing age-related differences in non-visual effects of light [4 years (Jud et al. 2009; Sletten et al. 2009) or 7 years (Duffy et al. 2007) on average]. However, such limited age differences appear unlikely to fully explain the very limited effect of aging on PLR in our data compared to these other studies. Interestingly, another recent investigation did not find a significant impact of age on the ability of light to phase shift circadian rhythmicity (Sletten et al. 2009), contrary to a previous investigation (Duffy et al. 2007) suggesting that aging may not impact all non-visual functions similarly.

The lack of age-related differences in PLR response compared to other non-visual responses reported by previous studies may be related to the involvement of different melanopsin ganglion cell types and their target brain structures, or the output pathways involved. For example, recent studies in rodents have found that light sensitivity is not equivalent for all non-visual functions regulated by light. The sensitivity of the circadian system for entrainment and phase shift was greater than that of PLR or masking (Hut et al. 2008; Butler and Silver 2010). There is evidence that different populations of mRGCs may mediate these light sensitivity differences. Five types of these mRGCs (M1 to M5) have been identified to date, their projections overlapping only partially (Berson et al. 2010; Ecker et al. 2010; Schmidt et al. 2011; see also 2.4.1). In addition, two subtypes of M1 cells have been identified, with one subtype innervating the SCN while the other projects to all other known brain targets of mRGCs including the OPN (Chen et al. 2011). In this respect, it appears plausible that the impact of aging varies for different non-visual functions regulated by light, such as circadian entrainment, melatonin secretion, and PLR, which present different light sensitivities and are mediated, at least in part, by different populations of mRGCs.

5.5 MODEL OF BISTABLE MELANOPSIN

MODELING THE PIGMENT KINETICS AND PHOTORESPONSE OF THE BISTABLE MELANOPSIN SYSTEM

Petteri Teikari[1,2], *Ludovic S. Mure*[1,2], *Howard M. Cooper*[1,2]

[1] Stem Cell and Brain Research Institute, INSERM U846, 18 avenue Doyen Lépine 69500, Bron – France, [2] Université Claude Bernard, Lyon I, Lyon, France.

5.5.1 *Introduction*

In this chapter, a simplified model for pigment kinetics coupled to the membrane potential mediated via "transmitter gating" model (Carpenter et al. 1987) is presented. The model for the visual pigment kinetics is derived from the model described by Stavenga and Hardie 2010 for bistable invertebrate photoreception. The transmitter model for bistable invertebrate phototransduction was described by Öğmen and Gagné 1987, and it was used as a basis for the bistable melanopsin model presented here. The model allows quantitative predictions of pigment-level changes, and how these pigment modulation are coupled to the photoreceptor responses. Given the scarce information on the quantitative aspects of melanopsin phototransduction, the proposed framework should be interpreted as a "order-of-magnitude" estimate of the function with tunable model parameters that can be improved as more research is done on melanopsin.

5.5.2 *Analytical Methods*

Response types in bistable pigment systems

In 4.4, the typical photoreceptor response types used to quantify the bistability photopigment systems were reviewed. In order to avoid overlap and needless repetition, only the very key points are reviewed here briefly.

Stimulus types

A. Neutral stimulus. Neutral stimulus is defined as not inducing a net pigment shift from the R state to the M state, or vice versa. In other words, the relative stimulation of two states is the same when the illuminant is changed. For example in increase of light intensity with no changes in the spectral content of the light, will typically result an increased photoresponse without net pigment shift.

B. $R \rightarrow M$ stimulus. The change from the R state (rhodopsin in flies) to the M state (metarhodopsin in flies) is maximal when

the stimulus wavelength is at the peak of the equilibrium spectrum (see 4.3.3) , in the study of Mure et al. 2009, the peak wavelength of equilibrium spectum was found to be around ~460 nm.

c. $M \rightarrow R$ stimulus. The most effective light stimulus for shifting pigment from the M state to the R state occurs slightly red-shifted from the peak of the M state spectral sensitivity (see e.g. Figure 56) as there is an overlap of the R and the M state spectral sensitivities at the peak spectral sensitivity of the M state.

PLR as a tool for melanopsin bistability

The shape of the human pupil response (i.e. the waveform) to light can be roughly generalized having three distinct components, phasic, sustained and post-illumination persistence. Phasic component is the rapid initial constriction, that is followed by a slight dilation to a steady-state (tonic) pupil diameter (also referred as a pupillary escape (Lowenstein and Loewenfeld 1959; Hung and Stark 1979; Sun et al. 1983). With higher light intensities the steady-state pupil size is more or less equal to the initial phasic size (see for example Fig. 2A in Mure et al. 2009) and this is referred as pupillary capture (Usui and Stark 1978; Sun and Stark 1983). The two components have rough correspondences at the level of olivary pretectal nucleus (OPN) where two types of neurons were found in macaques based on their firing patterns, burst-sustained ("phasic-sustained") neurons and transient neurons that responded both to lights-ON and lights-OFF (Pong and Fuchs 2000a).

After light offset, the pupil does not immediately return to its dark-adapted diameter, and this behavior is referred as the post-illumination persistence. At light offset there might be an initial dilation followed by reconstriction as shown first by Alpern and Campbell 1963. It was further shown (Newsome 1971) that after extremely bright light (3.5 x 10^6 Td) the pupil remained constricted in darkness as long as ~5-6 minutes reaching full pupil size after 15-18 minutes of light offset as seen in Figure 20A. The recontraction and initial dilation was shown to depend on the light intensity (Figure 20B). The pupil reconstriction was shown to disappear with light stimuli shorter than 1 sec (Figure 20C) presumably corresponding to sluggish response of the yet undiscovered ipRGCs. Similar results were obtained in a study by Alpern and Ohba 1972 with recordings of post-stimulation pupil size extending up to 30-40 minutes in the darkness.

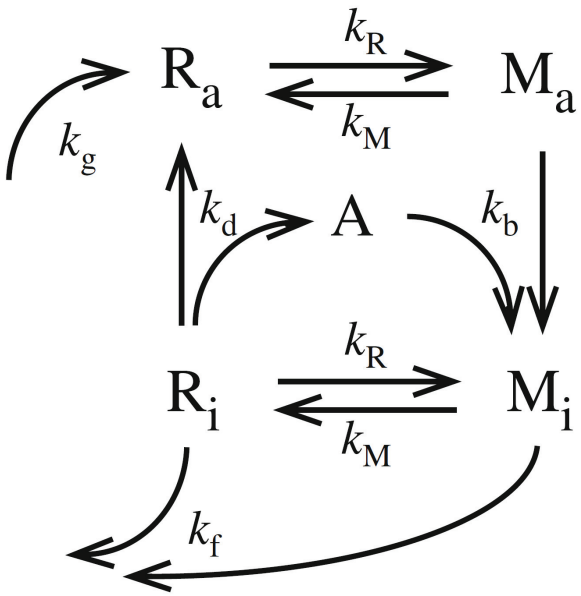

Figure 74: **Visual pigment-arrestin cycle.** Photoconversion of active rhodopsin, R_a, creates active metarhodopsin, M_a, which upon binding arrestin, A, becomes inactive metarhodopsin, M_i. Photoconversion of M_i creates inactive rhodopsin, R_i, which upon arrestin release converts into the native rhodopsin, R_a. The light-induced conversion processes have rate constants k_R and k_M, the rate constants of arrestin binding and dissociation are k_b and k_d. R_i and M_i are degraded with rate constant k_f, and R_a is regenerated with rate constant k_g. (Stavenga and Hardie 2010).

5.5.3 *Pigment kinetics*

The simplified model for describing visual pigment-arrestin kinetics (74) in flies by Stavenga and Hardie 2010 was reviewed in Section 4.6. Photoconversion of the native, active rhodopsin (R_a) creates the active metarhodopsin state (M_a, at a rate of k_R) , this M_a state triggers the phototransduction. Upon binding arrestin (A) the photoresponse is quenched and M_a converts into inactive metarhodopsin (M_i, at a rate of k_b). Photoconversion of M_i creates inactive rhodopsin (R_i, at a rate of k_M), which upon arrestin release return to the active rhodopsin state R_a (at a rate of k_d). Inactive metarhodopsin (M_i) is phosphorylated when photoconverted from M_a, dephosphorylation occurring upon photoconversion from R_i to R_a (Kiselev and Subramaniam 1994).

In comparison to *Drosophila* bistable rhodopsin, some parameter values need to be estimated for the bistable melanopsin system. The rate constants k_R and k_M (s^{-1}, Eq. (16)) depend on the light intensity, increasing intensity driving the pigment-arrestin system more quickly to photoequilibrium (smaller rate constants), following an exponential time course with time constant $\tau_c = 1/(k_R + k_M)$ (Eq. (20)). The behavior of the system (i.e. rate constants for the $R \rightleftharpoons M$ transi-

tions) depends furthermore on the values of quantum efficiencies (γ_i), the molecular absorbance coefficient (α_{max}), and on the absorbance coefficient of the rhabdomere / outer segment medium (κ_{max}). Typical values for these value from the literature are listed in Table 6 in B).

The parameters for melanopsin system were estimated to be (see also Section B.4) 1.0 for relative quantum efficiency ($\varphi = \gamma_M/\gamma_R$) as done in Mure et al. 2009, without any quantitative estimates published on the forward ($R \rightarrow M$) and backward ($M \rightarrow R$) conversion quantum efficiencies. The molecular absorbance coefficient $\alpha_{max} \sim 5.5 \times 10^{-5} \cdot \mu m^2$ was obtained by fitting an exponential recovery function for the pupil recordings obtained in our group, and estimating the time constant τ_c for the pupil to reach steady-state. The obtained estimate for the time constant τ_c was roughly 37 sec using the following equation:

$$\alpha_{max} = \frac{1/\tau_c}{k_R + k_M} \tag{63}$$

with the light-dependent rate constant $k_R$and k_M calculated using 480 nm light stimulus (*hbw*= 10 nm) with a photon density of 10^{12} ph·cm^{-2}·s^{-1}. Absorbance coefficient κ_{max} of the photoreceptive medium (see Section 4.6 for details) was set to unity due to the very low pigment density of melanopsin (Do et al. 2009; see also B.3.3) making the calculations simpler.

Strictly speaking, the time constant τ_c estimated from pupil response might not reflect the conformational changes of the melanopsin photopigment (discussed later also in Section 6.1), this PLR-based assumption was based on Mure et al. 2009 where the equilibrium in pupil response was interpreted as an equilibirum in melanopsin pigment kinetics. Another limitation of the pigment kinetic model here is the assumption of first-order pigment kinetics, whereas Mahroo and Lamb 2004 (see also 2.3.6) recently proposed cone and rod bleaching and regeneration to follow rate-limited kinetics deviating from previously reported first order kinetics (e.g. Boynton and Whitten 1970; Paupoo et al. 2000). The rate limit was suggested to arise from a limitation in the delivery of 11-*cis*-retinoid to the photoreceptor outer segments, which might not be the case with "non-bleaching" bistable melanopsin (see Wang and Kefalov 2011 for a review on classical photoreceptor regeneration mechanisms).

Bistable melanopsin photopigment behavior

The pigment model described by the set of linear differential equations can be then simulated using Matlab and its ODE45 solver on ordinary differential equations based on the Runge-Kutta method (Shampine and Reichelt 1997). In an ideal bistable photopigment system (see 4.2.1), the system being infinitely stable on the M state, the stimulus wavelength only having an effect on the relative R and M

state pigment concentration on equilibrium state. This relative R and M state concentration is described with f_M and f_{Me} from now on, the former describing the fraction of pigment in M state at a given moment, and the latter fraction of pigment in M state in equilibrium e denoting equilibrium. In our case with melanopsin, the quantitative effects of arrestin in the visual pigment are not examined in detail as melanopsin "visual cycle" (e.g. Sexton et al. 2012) and the role of arrestin in melanopsin deactivation (Hatori and Panda 2009; Frederick et al. 2009) are not well known.

The intensity-dependence of pigment kinetics is simulated in Figure 75. Condition similar to the one used in a study of Mure et al. 2009 is used as the simulation condition. First (Figure 75A), the pigment shift kinetics from the fully dark-adapted state (f_{Me}= 0) to an equilibrium state of f_{Me}~0.70 is induced by a 480 nm (hbw = 10 nm) light stimulus ($R \rightarrow M$) at various photon densities is shown. intensities high enough. Note that in Mure et al. 2009 the initial f_{Me} was around 0.19 due to the 1 minute bleaching white light 45 minutes before the reference stimulus. The two lowest intensities (-2.0 and -3.0 LOG) were shown to be too weak to drive the system to the equilibrium during the 5 minute simulation time period.

The pigment shift back from the M state (f_{Me}~ 0.70) to the R state was driven with a a 620 nm (hbw = 10 nm) light stimulus ($M \rightarrow R$) at same light intensities as in Figure 75A. The effect of pigment turnover was modeled in Figure 75C,D using otherwise the same values as in Figure 75A,B, but the thermal stability of the M state was weakened significantly by setting the rate constants $k_f \sim 0.28$ s^{-1} for pigment degradation and $k_g \sim 0.08$ s^{-1} for pigment regeneration. These values present very rapid pigment turnover maybe only found in hypsochromic invertebrates, but are shown to demonstrate the possible "ciliary behavior" of bistable photopigment system. The equilibrium is now reached faster with the inclusion of pigment turnover, with an overall decrease of f_{Me} in practice keeping more photopigment in responsive state at moderate light intensities, whereas there is no difference in f_{Me} between the Figure 75A,C with the simulated values for the highest intensity. The faster pigment turnover favors low f_{Me}, thus in Figure 75D only a faster return back to baseline is seen, without any additional phenomena observed.

The wavelength dependence of the pigment kinetics is simulated in Figure 76. The effect of various wavelengths on pigment kinetics, from a dark-adapted initial state (f_{Me} = 0) is shown in Figure 76A. The same simulation wavelengths as in in Figure 76A is used to simulate the wavelength-dependent drive of the pigment back to the R state (Figure 76B) from an initial state of f_{Me} = 0.53 being higher. The 700 nm stimulates the M state so weakly that eventually all pigment would be regenerated but the 300 seconds is not enough for that. Photon density for both simulations was fixed to 12.5 log photons·cm^{-2}·s^{-1}. The

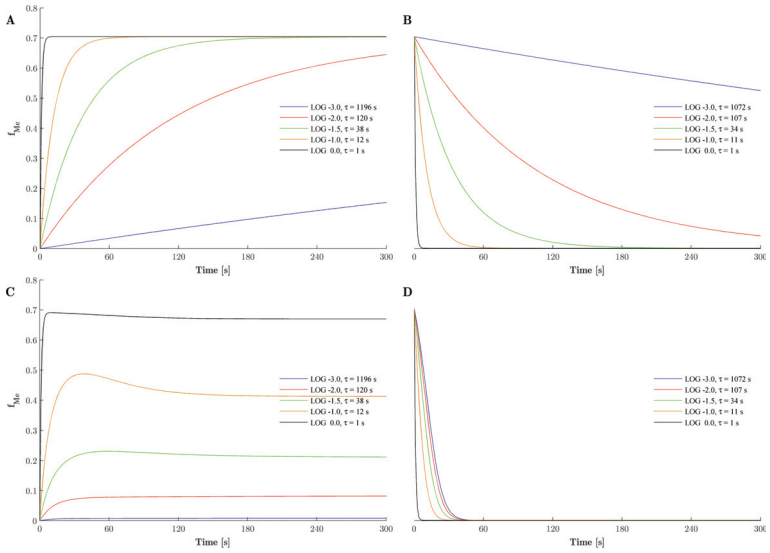

Figure 75: **Intensity dependence of pigment kinetics.** (A) The pigment shift from f_{Me}= 0 induced by a 480 nm (*hbw* = 10 nm) light stimulus ($R \rightarrow M$) at various photon densities to the equilibrium state of f_{Me}~0.70 with intensities high enough. The highest intensity (LOG 0.0) now set to 13.5 log photon density based on the parameter estimates given in Section 5.5.3. **(B)** The pigment shift back from the M state to R state, initial state being the f_{Me}~ 0.70 as the system left from **(A)** with a 620 nm (*hbw* = 10 nm) light stimulus ($M \rightarrow R$) at same light intensities as in **(A)**. The **(C,D)** are the same as **(A,B)** but the thermal stability of the M state is weakened significantly by setting the rate constants $k_f \sim 0.28$ s^{-1} for pigment degradation and $k_g \sim 0.08$ s^{-1} for pigment regeneration. Note that these values present very rapid pigment turnover maybe only found in monochromatic invertebrates, but are shown to demonstrate the possible "ciliary behavior" of bistable photopigment system. Note also that the time constant τ_c is not changed as defined using the k_R and k_M while the system itself reaches an equilibrium faster.

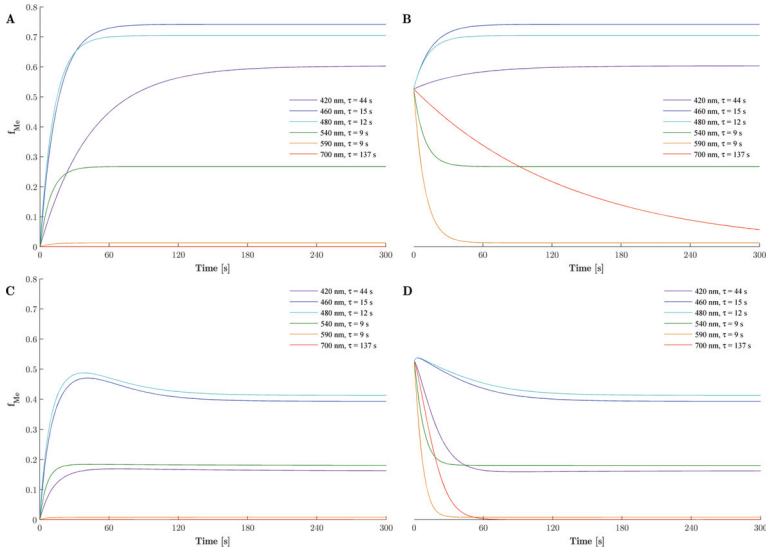

Figure 76: **Wavelength dependence of pigment kinetics. (A)** The effect of various wavelengths on pigment kinetics, from the initial state all the pigment is in the M state (f_{Me} = 0). **(B)** The same simulation wavelengths as in (A), but the initial state f_{Me} = 0.53 being higher. The 700 nm stimulates the M state so weakly that eventually all pigment would be regenerated but the 300 seconds is not enough for that. Photon density for both simulations was fixed to 12.5 log photons·cm^{-2}·s^{-1}. In **(C,D)** the pigment turnover was simulated to be very rapid (same values as in Figure 75), demonstrating the same overall decrease in f_{Me} values as in Figure 75.

rapid pigment turnover (Figure 76C,D) is shown to have the same overall decrease in f_{Me} values and faster time for equilibrium, as in the intensity simulations (Figure 75C,D).

The model for pigment kinetics was implemented also for an easy to use Matlab program with a graphical user interface (GUI) as shown in Figure 77, allowing quick simulation of the pigment behavior.

5.5.4 *Transmitter gating model*

The model of Öğmen and Gagné 1987 describes the invertebrate bistable photopigment with the system using the transmitter gating model proposed by Carpenter et al. 1987. The model was intended to improve the phototransduction model of Baylor et al. 1974a for vertebrate photoreception. The model comprises of three blocks (Figure 78), the first "Pigment Kinetics" block corresponding to the visual-arrestin cycle described above (Section 5.5.3) which is coupled to the last photoreceptor membrane potential both directly to the membrane block (upper arrow in Figure 78), and via "Transmitter gating" block (lower arrow in Figure 78).

The principle of transmitter dynamics model is shown in Figure 79 as modified from Carpenter et al. 1987. The modulation signal S in

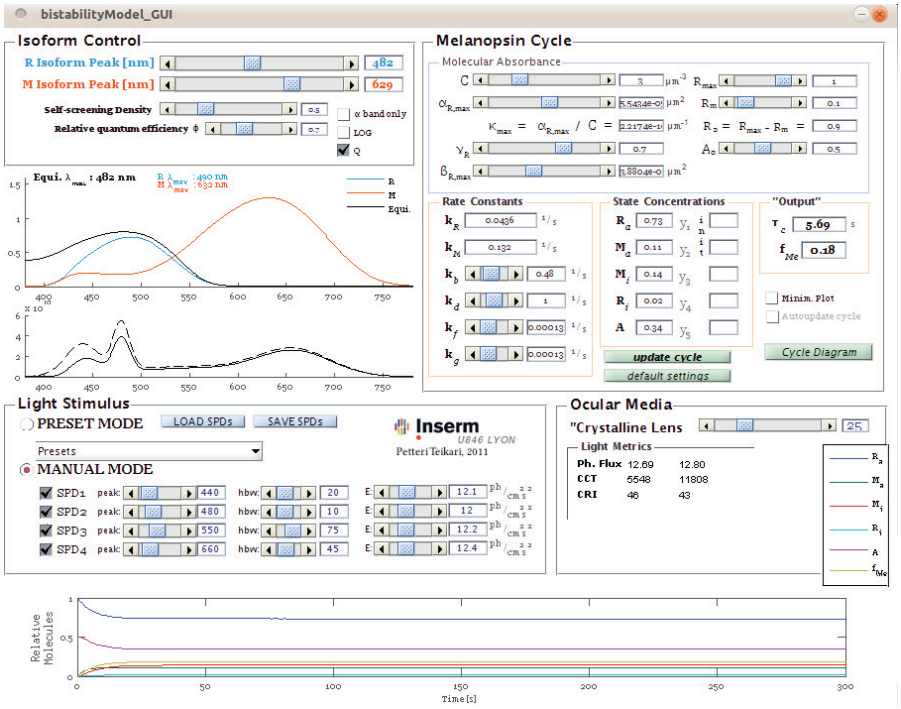

Figure 77: Matlab GUI for pigment kinetic model.

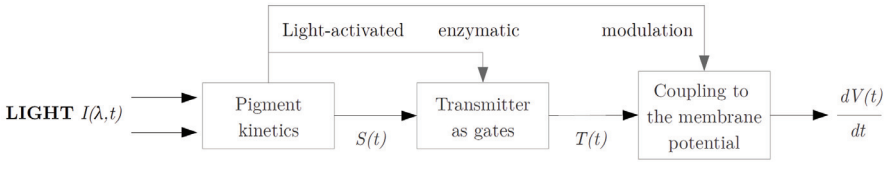

Figure 78: Block diagram of the transmitter model phototransduction, redrawn from Öğmen and Gagné 1987.

the transmitter model causing the transmitter z to be released at a rate of of $T = Sz$, where further the S can be thought to depend on the visual pigment kinetics (dR_a/dt for example). Whenever two processes, such as S and z are multiplied, they interact by mass action. Thus, the z gates S to release a net signal T, and the cell tries to replenish z to maintain the system's sensitivity to S (Carpenter et al. 1987). Transmitter turnover studies in neural preparations have been done for example by Esplin and Zablocka-Esplin 1971, and a gating concept appears in the model of Hemilä 1977; 1978 for rod adaptation in frog retina. The terms $(L - w)$ and w are added to distinguish the transmitter between bound or storage form and transmitter that is available, or mobilized. The transmitter dynamics between the mobilized transmitter $z(t)$ and storage transmitter $w(t)$ can be expressed as following:

$$dw/dt = K\,(L - w) - (Mw - Nz) \tag{64}$$

$$dz/dt = (Mw - Nz) - Sz \tag{65}$$

The term in Eq. (64) states that $w(t)$ tries to maintain a level L via transmitter accumulation (or production and feedback inhibition). The term $-(Mw - Nz)$ in Eq. (64) says that storage transmitter w is mobilized at a rate M whereas mobilized transmitter z is demobilized and restored at a rate N until the two processes equilibrate. Term $(Mw - Nz)$ in Eq. (65) states that w's loss is z's gain, and the term Sz in Eq. (65) says that the mobilized transmitter is released at rate $-Sz$ as it couple to the signal S by mass action. More details of the model can be read from Carpenter et al. 1987.

Depolarization amount ($x = V - V_0$) is defined as the difference between the resting membrane potential V_0 and the absolute depolarization V. The resting membrane potential V_0 is found when putting $dV(t)/dt$. The dynamic equation for the depolarization is then defined as following (Öğmen and Gagné 1987):

$$\frac{dx}{dt} = -\left(g^+ + g^-\right) x + \left(V^+ - V_0\right) g^+ + \left(V^- - V_0\right) g^- \tag{66}$$

where g^+ and g^- are respectively positive and negative ion conductances; $V^+$and V^- are respectively the positive and negative depolarization saturation points. The signal $T(t)$ from the transmitter block is coupled to the standard membrane equation (Eq. (67)) via the positive conductance g^+ which can be interpreted as the opening of ion channels. The standard membrane equation translates the conductance change into membrane potential as following (Cole 1968):

$$C\frac{dU(t)}{dt} = \left(U^+ - U\right) g^+ + \left(U^- - U\right) g^- + \left(U^p - U\right) g^p \tag{67}$$

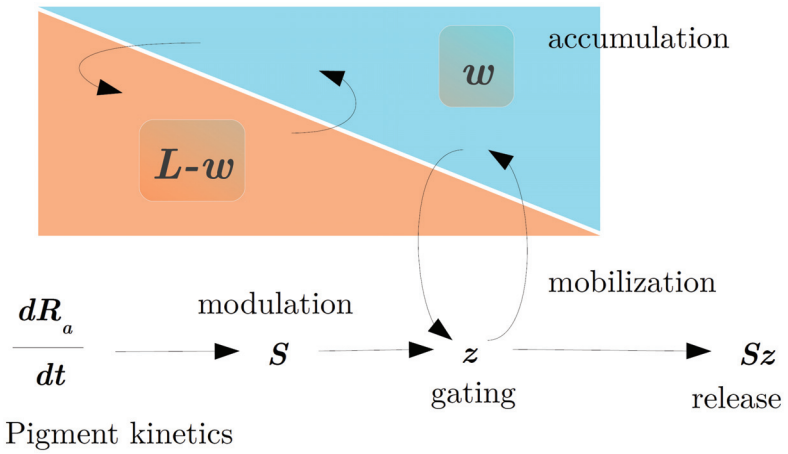

Figure 79: **Transmitter dynamics.** Transmitter w accumulates until a target level is reached. Accumulated transmitter is mobilized until an equilibrium between mobilized and unmobilized transmitter fractions is attained. The signal S is gated by mobilized transmitter which is released by mass action. The signal also modulates the accumulation and/or mobilization process. Redrawn from Öğmen and Gagné 1987 and Carpenter et al. 1987.

Where U^+, U^+ and U^+ are respectively the positive, negative and passive saturation points; U is the voltage difference across the membrane; C is the membrane capacity [typically 1 $\mu F \cdot cm^{-2}$ (Cole 1968)]. To formulate the coupling of pigment kinetics to the membrane equation, Öğmen and Gagné 1987 used a mass action law with g_m being maximum number of pores, g_0 the number of open pores at the resting potential and $g^+$the number of open pores at a given moment. The signal T will open the closed pores, which amount to $(g_m - g^+)$, at a rate proportional to its strength and to a given constant J. This is formulated as following:

$$\frac{dg^+}{dt} = JT\left(g_m - g^+\right) \tag{68}$$

To keep g^+at its resting level against the fluctuations and stimulus offset, an antagonistic component is needed for condition $g^+ \leqq g_m$ that increase the number of open pores by mass action. This is presented as (Öğmen and Gagné 1987):

$$\frac{dg^+}{dt} = H\left(g_0 - g^+\right) \tag{69}$$

Combining Eq. (68) and Eq. (69), first equation for the coupling system is obtained

$$\frac{dg^+}{dt} = H\left(g_0 - g^+\right) + JT\left(g_m - g^+\right) \tag{70}$$

If $g^+ < g_0$, the two terms (Eq. (68), Eq. (69)) both increases the conductance g^+, but as once g^+ exceeds g_0 the equilibrium level (Eq. (68))

starts to oppose the effect of Eq. (69), its tendency being to keep g^+at this level.

The signal $T(t)$ originates from the pigment transformations ands its amplitude depends partly on their kinetics. On the other hand the antagonistic component (Eq. (69)) has H as opposition rate (Öğmen and Gagné 1987). If H were constant, the behavior of g^+ would be limited as in practice small increments in light stimuli are amplified to a larger variations in $T(t)$, and a large T would saturate the cell by opening all available pores. Öğmen and Gagné 1987 proposed an "enzymatic gain modulation strategy" to couple the pigment kinetics directly to the membrane making the H to depend on pigment kinetics $f(\cdot)$ as following:

$$\frac{dH(t)}{dt} = -u\,(H - H_0) + \epsilon f(\cdot)H \tag{71}$$

where H_0 is the resting level of H, u a constant and $f(\cdot)$ a function of the closed pigment system defined in Eq. (37), Eq. (38), Eq. (39) and Eq. (40). The $f(\cdot)$ is chosen to correspond the $R_a \rightarrow M_a$ conversion (dR_a/dt, Eq. (37)), as this conversion activity reflects the activation of photoresponse. The ϵ is a gain depending on the magnitude of $f(\cdot)$ which in our case is a constant simply scaling the $f(\cdot)$ for physiologically meaningful outputs.

In our case the signal T from the transmitter block transmitter block can be estimated using a sigmoid function typically used for the irradiance response curve (IRC) with the following 4-parameter model (see also Matlab implementation in B.8):

$$Y(x) = \frac{min + (max - min)}{[1 + (x/X_{50})]^{coeff}} \tag{72}$$

Approximate irradiance behavior of mRGC subtypes M1 and M2 can be obtained from the study of Schmidt and Kofuji 2009, and an approximation for the photoresponse latency was obtained from the study by Tu et al. 2005 in 10-day postnatal mice (P10). These values can be taken as an order-of-magnitude estimates for the mRGC behavior.

In the case of a PDA-inductive (4.4.4) stimulus we have a case where the the R pigment population is decreasing ($f(\cdot) < 0$). The PDA induction rises from the inequality between the antagonistic drive at light offset and resting state [$H(t_{offset}) < H_o$], and in the differential positive gains for LRP and PDA ($\Gamma_{g^+PDA} < \Gamma_{g^+LRP}$). The positive gain is defined as following derived from Eq. (70):

$$\Gamma_{g^+} = H + JT \tag{73}$$

In a post-stimulus conditions, the light-dependent $T = 0$ and the positive gain $\Gamma_{g^+} = H$. Thus the observed prolongation of the depolarization and action potential firing after light offset (see e.g. Section

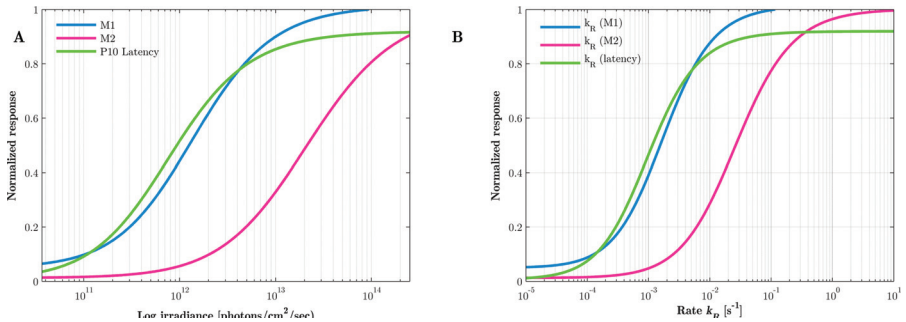

Figure 80: **Light drive (T) defined with an irradiance-response curve (IRC). (A)** Irradiance response curve (IRC) obtained for mRGC (subtypes M1 and M2, see 2.4.1) using 5 second 480 nm light pulses (Schmidt and Kofuji 2009, Fig. 2F), same figure as Figure 12B redrawn using a sigmoid fit (Eq. (72)). The irradiance-response for normalized latency is obtained from Tu et al. 2005 (Fig. 6D) **(B)** The abscissa of IRC transformed from photon density to rate factor k_R $[s^{-1}]$ using a synthetic 480 nm light with a half-bandwidth of 10 nm and the corresponding photon densities of **(A)**. Irradiance and rate constants were defined in logarithmic units for the sigmoid fit.
Sigmoid parameters: **(A) M1:** min=0, max=1, $X_{50} = 12.2$, $coeff$=-29.6, **M2:** min=0, max=1, $X_{50} = 13.3$, $coeff$=-29.1, **Latency:** min=0, max=0.92, $X_{50} = 11.9$, $coeff$=-28.9. **(B) M1:** min=0, max=1, $X_{50} = 12.2$, $coeff$=6.00, **M2:** min=0, max=1, $X_{50} = 12.2$, $coeff$=4.77, **Latency:** min=0, max=0.92, $X_{50} = -3.06$, $coeff$=6.02.

2.4 and 3.2.2) depends on the behavior of the H (see later Figure 81; Figure 82; Figure 83).

In the case of a PDA depression (4.4.4), PDA-antagonist stimulus ($M \rightarrow R$) follows the PDA-inductive one ($R \rightarrow M$), the M pigment population need be thus decreasing in the model formulation ($f(\cdot) > 0$). The return of the amount of depolarization x now depends on the strength of gain $f(\cdot) - u$.

The anti-PDA phenomenon requires (4.4.4) a PDA antagonist stimulus to precede a PDA-inductive one. The behavior of the PDA induced by the second PDA-inducing stimulus after the initial one depends on the decay of H back to its baseline, and namely on the variable u (Figure 82). The smaller the gain u is, the longer the decay back to baseline, and longer the interval needed between the PDA-inducing stimuli for the anti-PDA phenomenon to decay.

Finally, in the case of PDA facilitation effect (4.4.4) the second PDA induced have been shown to be facilitated (in contrast to anti-PDA) given that the first PDA was not "too strong" (too high f_{Me}). The duration difference in induced PDA in the model comes from the difference in the gains of x and H. Even if x would have decayed to the baseline, this would not necessarily mean that H has returned to its resting values.

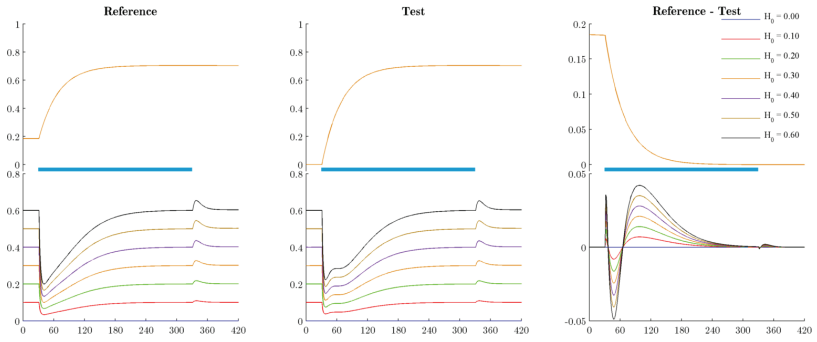

Figure 81: **Behavior of H as a function of H_0.** The parameter H_0 is the baseline antagonistic drive affecting the behavior of H (Eq. (71)). We can see that larger the baseline H_0 is the larger are the responses of H in response to light pulses, the kinetics of H remaining unchanged. See text for further details. *add labels, increase resolution*

Transmitter gating model behavior

Simplistic behavior of the transmitter gating model is simulated using the experimental paradigm used for *Limulus* (Lisman and Sheline 1976) and for human PLR (Mure et al. 2009). The responses to the two different 480 nm light stimuli (*hbw* = 10 nm, 12 log photons·cm^{-2}·s^{-1}) used in the study of Mure et al. 2009, are analyzed (reference being the first 480 nm light pulse, and the test being the second light pulse being modulated by adapting light), and the "reference - test" is the difference between these two conditions. Note the test stimulus correspond to the 480 nm delivered after adapting light of 620 nm (f_{Me}= 0), and the reference stimulus is administered to an initial state of f_{Me}~ 0.19 to which the system is left after the bleaching white light before the reference pulse (see Figure 56) if one assumes that during 45 minutes there is no dark regeneration. Alternatively the initial state of f_{Me}~ 0.19 can be taken as an initial state that can be "potentiated" in contrast to the initial state of f_{Me} = 0 when all the pigment is already in the R state and cannot be further potentiated more with an adapting light. The light pulse is administered at 30 seconds for 5 minutes with an 1 minute post-stimulus behavior included in the simulation.

The behavior of the antagonistic drive H is simulated in regard to baseline antagonistic drive H_0 (Figure 81), "antagonistic difference" gain u (Figure 82), and the scaling factor ϵ added to the original formulation of Öğmen and Gagné 1987 to function as a gain parameter for the strength of the pigment kinetic drive $f(\cdot)$ for H (Figure 83). The behavior of the depolarization amount x is not shown for this report, it requiring further work and it will be published in the future as fully functional implementation.

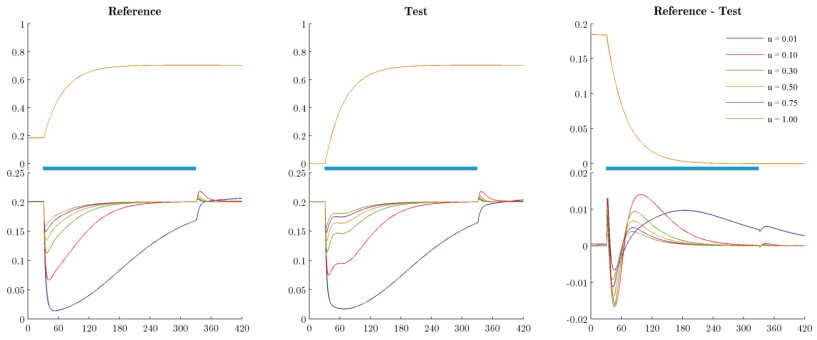

Figure 82: **Behavior of H as a function of u.** The parameter u is a constant gain affecting the difference between baseline antagonistic drive and the antagonistic drive at a given moment $(H - H_0)$, defined in Eq. (71). We can see that the smaller the gain u is the longer the return to baseline accompanied with a different amplitude. See text for further details. *add labels, increase resolution*

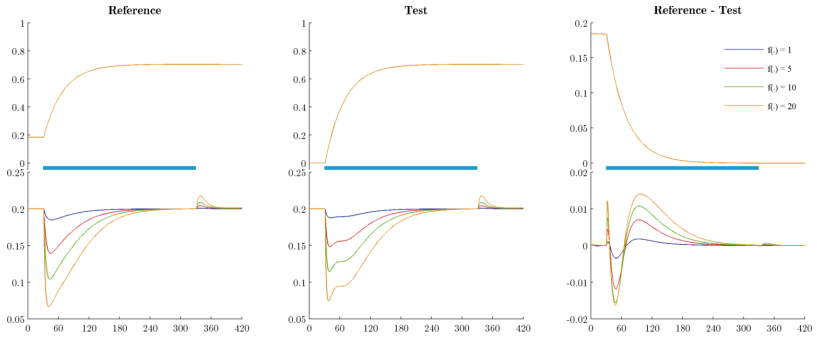

Figure 83: **Behavior of H as a function of ϵ scaling $f(\cdot)$.** The parameter ϵ is gain scaling $(\epsilon f(\cdot))$ the "pigment drive" $f(\cdot)$, that is a dynamic variable depending on the rate of change from active R state $R_a$to active M state M_a (dR_a/dt), affecting the minimal equation Eq. (71). The choice of ϵ only affects amplitude and the kinetics of H. See text for further details. *add labels, increase resolution, change $f(\cdot)$ to ϵ*

5.5.5 *Discussion*

The presented model describes a mathematical framework for simulating the behavior of a putatively bistable melanopsin in regard to the pigment kinetics and their coupling to the membrane potential. The intrinsic limitation of the model is that most of the simulation parameter were estimated from scarce information available on the quantitative behavior of melanopin phototransduction. Additionally, many of the bistable phenomenon such as anti-PDA and PDA facilitation have not been explicitly tested in melanopsin (see later Section 6.2), and the whole phenomenon of *in vivo* bistability in human PLR remaining still uncertain (see later Section 6.1). In order for the experiment designed to test bistability, the measured response should reflect the pigment level changes as well as possible which might not be the case with the sustained pupil component (see detailed discussion later in 6).

Previously in Section 5.2, the study designed to test the hypothesis of a "photic memory" (Hochstein et al. 1973) was presented. In other words, whether a lack of dark regeneration could be observed in the melanopsin as shown by lack of change in response after 45 minutes in darkness compared to 8 hours of darkness. The study was not able to provide statistically nor qualitatively compelling evidence for either lack or the existence of dark regeneration. The study however highlighted the high inter- and intra-individual variability in human PLR response (combined with the results from a short pilot study on human PLR variability presented in 5.1.2).

Additionally as illustrated in Figure 75 for intensity dependence and in Figure 76 for wavelength dependence, the photopigment system exhibits quantitatively rather distinct responses depending whether it is treated as time-independent (no pigment turnover) or as time-dependent system not exhibiting the "photic memory".

As discussed previously with intermediate photoproducts (4.5.1) and to be discussed in more detail in 6.1.4, the intermediates in melanopsin "photo cycle" are not well known including the effects of arrestin (Hatori and Panda 2009; Frederick et al. 2009), phosphorylation (Reingruber and Holcman 2008; Robinson et al. 2009) and signaling intermediates (6.1.5). On a system level, the melanopsin response deactivation is modeled above with an arrestin binding and release without any specific variable addressed for phosphorylation which was assumed not to be play a role to simplify the model scheme. Additionally, a signaling intermediate was not included for the current implementation in lack of proper evidence for the existence of such, but more intermediates could be rather easily added to the scheme if their mutual relations are known with decent accuracy. Other such intermediates would be possible short-lived intermediate melanopsin analogies for bathorhodopsin and lumirhodopsin (6.1.4).

Finally, the proposed framework does not contain any long-term adaptation mechanisms shown for example by Wong et al. 2007; 2011; 2005 (see also review by Do and Yau 2010 on melanopsin properties), which in practice on the model level could have an effect on both the pigment level behavior and the transmitter gating block. One could predict based on the literature in flies (French 1979; Jusola and Hardie 2001a;b) and in classical vertebrate photoreceptors (Burns and Baylor 2001; Kefalov et al. 2003; Arshavsky and Burns 2012) that most likely the adaptation changes occur downstream from the photopigment itself, the target for modification in the model being the transmitter gating model. Given that majority of the studies for melanopsin are done for rather short light pulses, the simulation of whole days would not be possible with the available information if one further considers the possible modulation of melanopsin photoresponses by the circadian (Hannibal et al. 2002; Sakamoto et al. 2005; Mathes et al. 2007) and ambient light intensity modulation (Hannibal et al. 2005) reviewed in 2.4.9. In conclusion, the predictive and explaining power of the framework currently is limited, but the parameters can be updated to match the future studies.

6 DISCUSSION

The phenomenon of melanopsin bistability is still rather poorly understood in the non-image forming photoreception community that can be illustrated with a quote from McDougal and Gamlin 2010:

> "Mure et al. 2009 propose that the dynamic nature of the spectral sensitivity of the human PLR is due to the bistable nature of melanopsin, and that as stimulus duration is increased the absorbance spectrum is shifted by the light induced transformation of M-state melanopsin into the R-state, with each state having a different peak absorbance. Furthermore, the authors contend that in the steady-state condition, in which a complete transition from M to R states is achieved, the action spectrum of melanopsin would shift to ~460 nm, as opposed to the more commonly reported peak of ~480 nm (e.g. Berson et al. 2002; Dacey et al. 2005; Gamlin et al. 2007; Hankins and Lucas 2002 and Hattar et al. 2003)."

Where the authors with an extensive publishing record on PLR (Gamlin and Clarke 1995; Gamlin 2000; Gamlin et al. 2007; McDougal and Gamlin 2008) first got the R and M states mixed up, and then understood the equilibrium being defined as a complete transition to to the other state, instead of interpreting equilibrium as a state where the net change is zero between the states.

6.1 MELANOPSIN BISTABILITY INTERPRETATION

6.1.1 *Melanopsin properties*

Despite the discovery of melanopsin over 10 years ago (Provencio et al. 1998) and its role in non-image forming (NIF) photoreception (Berson et al. 2002), a lot is still unknown. Probably the most characteristic difference between mRGCs and classical photoreceptors, rods and cones, is the depolarization of mRGCs with production of action potential in response to light compared to graded hyperpolarization of rods and cones. The exact mechanism of the molecular machinery is not well understood at the moment, and it has been suggested that the phototransduction steps resemble those found in *Drosophila* photoreceptors (Sekaran et al. 2007; Graham et al. 2008; see Section 4.1).

There is evidence (Sexton et al. 2012; Provencio and Warthen 2012) pointing that melanopsin seem to have a second messenger cascade

using $G\alpha_{q/11}$-type G protein signaling (Graham et al. 2008) and phospholipase C (PLC) signaling (Isoldi et al. 2005; Koyanagi et al. 2005; Gomez et al. 2009; Angueyra et al. 2012; Pulido et al. 2012). The disruption of G protein signaling in heterologously expressed melanopsin interferes with melanopsin-driven light responses (Qiu et al. 2005; Melyan et al. 2005). Additionally, $G_q$inhibitors and antibodies with PLC inhibitors (Yau and Hardie 2009) reduce light responses (Qiu et al. 2005; Panda et al. 2005), but $G_{i/o}$ do not (Melyan et al. 2005).

The channel(s) needed to produce the observed are yet to be determined, and canonical TRP channels as the effector channels have been suggested (Sexton et al. 2012), as they are the mammalian homologs of the invertebrate TRP channels activated by rhabdomeric opsins (Hardie and Postma 2008; Hardie 2011). Especially the types TRPC6 and TRPC7 (subfamily C, and member 6 and 7) have been of an interest as they are localized to mRGCs (Warren et al. 2006; Hartwick et al. 2007). However, in mice lacking TRPC3, TRPC6, or TRPC7 light-dependent mRGC responses were demonstrated, suggesting the presence of an additional effector channel (Perez-Leighton et al. 2011). Recent report found TRP-channel TRPM1 (subfamily M, member 1; Oancea and Wicks 2011) to be involved in non-image forming responses to light shown using pupillary light reflex (PLR), in addition to their better known role in the depolarizing light responses of ON bipolar cells (Morgans et al. 2009). Additionally mutations of the *Trpm1* gene have been identified as a primary cause of stationary night blindness (van Genderen et al. 2009).

Another hallmark of melanopsin-mediated photoreception is the sluggish response both for lights ON and for lights OFF as seen both at photoreception level (see Section 2.4) and in the downstream NIF responses such as in PLR (see 3.2.2). The molecular mechanism for this observed persistence is not known. The persistence was modeled on a system level (Section 5.5) using the "arrestin deactivation" scheme from *Drosophila* (Stavenga and Hardie 2010) combined with the transmitter model (Carpenter et al. 1987) employed to describe prolonged depolarization afterpotential (PDA, see 4.4.4) in *Drosophila* (Öğmen and Gagné 1987). With increasing irradiance the response latency to lights ON is reduced (Tu et al. 2005), and the persistence of the photoresponse is prolonged and enhanced (Berson et al. 2002).

Additionally, mRGCs are rather insensitive for light and require high light intensity for maximal response. The melanopsin molecule itself exhibits larger single-photon responses than rodent rods or cones (Do et al. 2009). The density of melanopsin protein is 10,000-fold lower compared to rods and cones (see B.3.3), and together with lack of light-absorbing organelles similar to the outer segments (Do et al. 2009) of the classical visual photoreceptors, the probability of photon capture for M1 subtype is roughly million-fold lower than for rodent rods and cones for a given irradiance falling upon a unit area of retina

(Do et al. 2009; Sexton et al. 2012). Furthermore, the subtypes M2-M5 (see 2.4.1) have suggested to contain even less melanopsin (Schmidt et al. 2011) and functioning maybe *in vivo* primarily as conduits for signals from classical photoreceptors as shown in general for mRGC signaling (Güler et al. 2008).

The mRGCs can also be distinguished from conventional RGCs by their expression of pituitary adenylyl cyclaseactivating protein (PACAP), a peptide neuromodulator that may play an important role in nonimage vision (Hannibal et al. 2004). Many brain targets of the ipRGCs express PACAP receptors, and animals with impaired PACAP signaling are defective in circadian photoentrainment, among other functions (Colwell et al. 2004).

In all mammalian species that have been studied, melanopsin exists only as long and short splice variants of a single gene (Torii et al. 2007; Pires et al. 2009; Davies et al. 2010). By contrast, non-mammalian vertebrates possess two evolutionary lineages of the melanopsin gene family, *opn4m* and *opn4x* (Davies et al. 2010; Bellingham et al. 2006). Recent results from Davies et al. 2011 in zebrafish indicate that there are both vertebrate monostable and invertebrate bistable photopigments in the same species. Photopigments encoded by *opn4m-2*, *opn4x-1* and *opn4x-2* functioned as classical monostable vertebrate photoreceptors, whereas the photopigments encoded by *opn4m-1* and *opn4m-3* functioned as typical invertebrate bistable photopigments.

6.1.2 *Novel non-melanopsin photopigments*

In addition to melanopsin (Opn4), the mammalian retina may express other functional photopigments and photoisomerases including encephalopsin/panopsin (Opn3, Blackshaw and Snyder 1999), neuropsin (Opn5, Tarttelin et al. 2003), peropsin (Koyanagi et al. 2002), retinal G protein coupled receptor (RGR, Jiang et al. 1993; Chen et al. 2001a; Wenzel et al. 2005; see 6.1.4 below), vertebrate ancient (VA) opsin (Soni and Foster 1997) and cone opsins expressed in inner retina (Semo et al. 2007). Around the discovery of melanopsin and mRGCs, cryptochromes were also proposed to mediate the NIF photoreception in humans but no evidence to date for their photoreceptor function in mammals have been provided (Somers et al. 1998; Van Gelder et al. 2003; Fogle et al. 2011; for cryptochrome spectral sensitivity see Hsu et al. 1996).

Neuropsin (OpnPN5) has been recently identified as a deep brain photoreceptor in birds (Nakane et al. 2010, $\lambda_{max} \sim 420$ nm), and found localized within some types of amacrine cells and some cells in the ganglion cell layer of the retinas of chicken (Yamashita et al. 2010). In chicken, the Opn5 was found to be exhibit properties like suggested for melanopsin (4), the authors suggesting that the UV-sensitive Opn5

and blue-sensitive melanopsin, may concertedly control the activity of dopaminergic amacrine neurons (Van Hook et al. 2012), resulting in retinal adaptation. Furthermore, it was hypothesized that despite UV light-absorbing compounds in human ocular media (see 2.2.3 and Section 5.3), the human eye and brain might a potential ability to receive UV radiation through Opn5.

The *in vitro* results were recently extended by Nieto et al. 2011 showing intrinsic light responses in the rat retina using the mammalian retinal ganglion cell line RGC-5 (Wood et al. 2010). The authors hypothesized that Opn5 expression in the retina of mammals might be responsible for the detection of some remaining light such as observed in non-rod, non-cone, non-melanopsin animals (Gnat1$^{-/-}$ Cnga3$^{-/-}$ Opn4$^{-/-}$- mice) in which certain non-image forming tasks (a residual pupillary light reflex) are still observed (Hattar et al. 2003; Allen et al. 2010). As in pinealocytes neonatal rats, expression of both rod-specific and cone-specific phototransduction were previously demonstrated in the study of Blackshaw and Snyder 1997. It was suggested that the mammalian pineal gland could be physiologically photosensitive during early life, Opn5 being one of the elements involved in non-visual light detection (Blackshaw and Snyder 1997; Tosini et al. 2000)

Recently, Kojima et al. 2011 provided the first evidence that Opn5 is expressed also in humans, using the cell line of HEK293S stably expressing human Opn5. The human Opn5 was shown to exhibit similar properties as the also studied mouse Opn5 such as sensitivity to UV irradiation (λ_{max}~ 380 nm) and bistable photoreversal with a λ_{max} ~471 nm ("M-state" sensitivity). In mice, the OPN5 protein is present in a subset of non-rod/non-cone retinal neurons, as well as in the muscle and epidermal cells of the outer ears. Authors suggested that even if human OPN5 would be present in the retina, it would be unlikely to be activated effectively by light in the UV region. Instead, non-retinal tissues such as the testis and its related tissue (epididymus) showed detectable levels of human Opn5 mRNA expression. Thus, further research is needed to elucidate the role of Opn5 in humans.

Encephalopsin/panopsin (both names used in the literature, still referring to the same Opn3) have been recently found in the human brain using *post mortem* donor brains (Nissilä et al. 2011) part of the research initiatives related to a commercial product Valkee (Oulu, Finland) designed to deliver light treatment via earbuds directly to the ear canal for example to treat seasonal depression (Timonen et al. 2011). The first evidence for a photoresponsive mammalian cerebral cortex was presented by Wade et al. 1988 who showed that high intensity light was able to penetrate fur, scalp, skull, and dura mater of a rat. The results suggest that ambient light may be sufficient to alter the release of transmitters from mammalian cerebral cortex i*n vivo*.

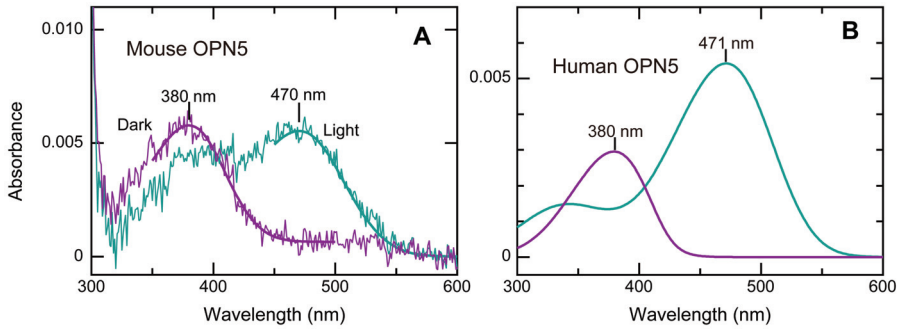

Figure 84: **Bistability of mouse and human *Opn5*. (A)** Absorption spectra of mouse Opn5 (Dark) and its photoproduct (Light). The Opn5 (λ_{max}~ 380 nm) was irradiated with UV light (357 nm; *hbw* = 10 nm; 28 µW/cm2) for 32 min, resulting in formation of a blue-absorbing photoproduct (λ_{max} ~470 nm). **(B)** Estimation of the absorption spectrum for human Opn5. The spectra for human OPN5 and its photoproduct were estimated from difference spectra (shown in Kojima et al. 2011) by using spectral template by Govardovskii et al. 2000 for opsin-type photopigments (Kojima et al. 2011).

Alternatively, one could hypothesize that the light signal in the brain could be mediated via biophoton communication, the light stimulus being able to generate biophotons conducted along nerve fibers (Sun et al. 2010), conceptually similar to the hypothesis of humoral transport of light (Grass and Kasper 2008). However, one should interpret the results of human brain photosensitivity with caution, as the field lacks research.

Finally, there is evidence that melanopsin is expressed also outside the retinal ganglion cells in mammalian retina including the retinal pigment epithelium (RPE) of *Xenopus* (Provencio et al. 1998), mouse (Peirson et al. 2004), and with contradictory results in humans for being partly explained by retinal contamination during dissection of tissues (Provencio et al. 2000) and with a recent report of allegedly non-contamined finding of melanopsin in human RPE (Carr et al. 2011). Müller glial cells (Jadhav et al. 2009) have closer contacts with mRGCs than with other RGCs (Viney et al. 2007), and the finding of melanopsin in Müller cells (Hollborn et al. 2011) could be related to the "melanopsin visual cycle" yet uncharacterized (Sexton et al. 2012), as Müller glial cells are involved in visual cycle of human cone photopigments (Wang and Kefalov 2011). melanopsin expression have been also reported in specific subset of human cone pigments (Dkhissi-Benyahya et al. 2006) with the possible functional significance of this being unknown.

Recently melanopsin was found directly on the iris of many vertebrate species (excluding primates) driving the pupillary light reflex (Xue et al. 2011) together with retina, as found previously with chick (Tu et al. 2004) and frog iris (Barr and Alpern 1963). Furthermore,

horizontal cells have been shown to express melanopsin in teleost fish (Cheng et al. 2009) and in chick (Verra et al. 2011).

6.1.3 *Photoreceptor contributions*

As reviewed previously above for classical photoreception (2.3.5), for non-image forming (NIF) responses in general (2.4.5), and more specifically for pupillary light reflex (PLR; 3.3.3 and 3.3.4) there is evidence that most of the NIF responses are driven jointly by multiple photoreceptor classes. In the study by Mure et al. 2009, it was assumed that the sustained component of the PLR was purely melanopsin-mediated mainly based on the results obtained by Gamlin et al. 2007. This view of melanopsin-only sustained response has been challenged for pupillary light reflex, complicating the evaluation of melanopsin bistability using the sustained component of PLR (see below Section 6.2 also).

McDougal and Gamlin 2010 found significant rod contribution (see 3.3.4 for details) for the sustained component (100 seconds the longest recording duration) using criterion response paradigm (e.g. Webster et al. 1968) opposed to action spectrum derivation from response amplitude used in Mure et al. 2009 (with partial irradiance-response correction). For a review on the differences between approaches in general one is recommended the review by Brainard and Hanifin 2005. In regard to melatonin suppression, one can compare the criterion response paradigm of Brainard et al. 2001; 2008b (action spectrum derived from half-maximal irradiance) to the "response amplitude" of Thapan et al. 2001. The rod contribution was assessed mathematically using the Quick pooling model (Quick 1974) described in 3.3.4 from the shape of the action spectrum, and the Quick pooling model can be seen as an indirect estimate of photoreceptor contribution while possible reflecting the underlying physiology.

The studies with rodent models have suggested also contribution of other photoreceptor classes to the PLR. Thompson et al. 2011 compared wild-type mice with *Nob4* (mice lacking ON-bipolar cell function) and *rd* (rodless mice). The results indicated alternative rod-cone input to the PLR not being entirely dependent on the ON bipolar cells possibly mediated according to the authors via M2 mRGC subtype (see 2.4.1). Lall et al. 2010 found a cone contribution at moderate light intensities with an evidence for "winner takes it all" situation (described by McDougal and Gamlin 2010), melanopsin solely driving the PLR at high light intensities.

In a recent study, Allen et al. 2011 demonstrated a distinct contribution of S-cones to sustained responses (30 sec recording) recorded directly in the mouse olivary pretectal nucleus (OPN, see Section 3.2) with minimal rod contribution. Authors used mice with the M cone opsin replaced genetically modified by human red cone opsin (Small-

wood et al. 2003) allowing the delivery of "melanopsin-silent" long-wavelength stimuli (Lall et al. 2010; Brown et al. 2011b; 2010). Furthermore, the S-cone input was shown to drive a strong OFF-inhibition at high irradiances, observed also in *Opn4*$^{-/-}$ mice. In other words, photic drive from S-cones was able to cut off the persistent OPN firing back to baseline even in the presence of melanopsin, immediately after light offset in contrast to the sluggish decay of mRGCs described above (6.1.1).

In addition to typical characterization of spectral and irradiance dependences, the temporal characteristics of the mice were studied varying the frequency of sinusoidal light stimuli. The results were in accordance with the view that M/L-cones encode the rapid changes in light intensity, S-cone pathway tracking significantly lower changes in light intensity. The multiple cone pathways with different temporal frequency was hypothesized to extend the sensory capabilities of the mouse olivary pretectal nucleus (OPN) extending the results of Dacey et al. 2005 and Schmidt and Kofuji 2010 for S-cone pathway in NIF responses. Recent report (Estevez et al. 2011), suggested that the M4 mRGC subtype was synaptically driven by the S-cone input covering a wide dynamic range (10^{10}-10^{15} photons·cm^{-2}·s^{-1}) supporting the involvement of S-cones in the NIF system.

In general, several approaches not relying on genetic models, have been used recently to distinguish the distinct photoreceptor contribution from different photoreceptor classes. These approaches include differential dichroic absorption ratio measurement *in vitro* conditions studying intermediate photoproducts (Kolesnikov et al. 2003; see also 4.5.1); using the "silent substitution" method (Estévez and Spekreijse 1982; Klee et al. 2011) allowing in theory differential stimulation of photoreceptor classes as used with PLR (Tsujimura et al. 2010; Viénot et al. 2012) and electroretinography (ERG; Fukuda et al. 2010); mathematically fitting spectral absorption profiles for measured action spectra (McDougal and Gamlin 2010); filtering selectively (notch filter) certain portions of light to mimic the loss of excitation on that wavelength region as done with circadian rhythms (Rahman et al. 2008) and PLR (Ishikawa et al. 2012); and isolating the photoreceptor responses based on the assumed differences in temporal response properties (e.g. De Lange DZN 1954; Shinomori and Werner 2008), M/L-cone being able to respond to highest frequencies while rods, S-cones and melanopsin not being able to track as fast-changing stimulus [defined for example with critical flicker frequency (CFF), see 5.3.2.4] as used with PLR (Tsujimura and Tokuda 2011; Allen et al. 2011; Doerning et al. 2011).

Furthermore, the observed OFF-response from S-cones (Dacey et al. 2005; Allen et al. 2011) combined with the poor understanding of the S-cone OFF pathway (Shinomori and Werner 2008; Lee et al. 2009; Li and Chen 2011), the S-cone OFF could be hypothesized to be in-

volved in the possible adaptation of human NIF system to reduced illuminance (senile miosis, increased lens density) and spectral filtering of short wavelengths cue to increased lens density with age (see 2.2.3 and Section 5.3). The increase in lens filtering at the short wavelength region in humans has the largest impact on S-cones (λ_{max}~ 420 nm, see Figure 7), the corneal spectral sensitivity peak shifting to 448 nm (Stockman and Sharpe 2007) with S-cone stimulation reducing roughly ~0.45 log units between 25 year and 65 year old standard observes simulated with the ocular media model of van de Kraats and van Norren 2007a. The loss of S-cone response (Shinomori and Werner 2006) could prolong the neuronal firing for example in OPN and in suprachiasmatic nucleus (SCN) compensating the decreased retinal irradiance with age (Owsley 2011). Similar loss of inhibition have been demonstrated in inhibitory cortical connections in aged monkeys (Leventhal et al. 2003)

In conclusion, the assumption of "melanopsin-pure" drive of sustained PLR response in Mure et al. 2009 (test/reference light of 480 nm, *hbw* = 10 nm, 10^{15} photons·cm^{-2}·s^{-1}, on average producing half-maximal pupil constriction) might have been unsubstantiated, and the observed chromatically modulated pupil responses might have arisen from a combined drive of multiple photoreceptors. It should be noted also that majority of the studies on PLR and melanopsin phototranducstion have been using relatively short light stimuli, and the relative contribution of different photopigments in more natural conditions of hour would be of an interest. Recent report recorded mRGC responses with a multielectrode array during 1-hour light exposure (Wong et al. 2011). Significant adaptation of mRGC was found (~1 log unit decrease in sensitivity) extending the previous findings on mRGC adaptation (Wong et al. 2005), highlighting the dynamic nature of even melanopsin-mediated photoreception. Further research is needed to quantify the photoreceptors involved in the sustained response and possible mediation via bistable melanopsin (see Section 6.2 for possible paradigms).

6.1.4 *Regeneration, melanopsin visual cycle*

The existence of dark regeneration in melanopsin as studied with PLR in humans was presented above in Section 5.2. The results were seen to be highly variable making quantification of the dark regeneration impossible, and only highlighting the suitability for PLR sustained response as a tool to study melanopsin bistability. The "melanopsin visual cycle", in other words how melanopsin photoreception system restores its visual sensitivity is still not well understood (Sexton et al. 2012), Figure 85 demonstrates the three possible simplified models for melanopsin regeneration. The photoreversal model refers to the "bistable" scheme reviewed in 4, the dark regeneration scheme refer-

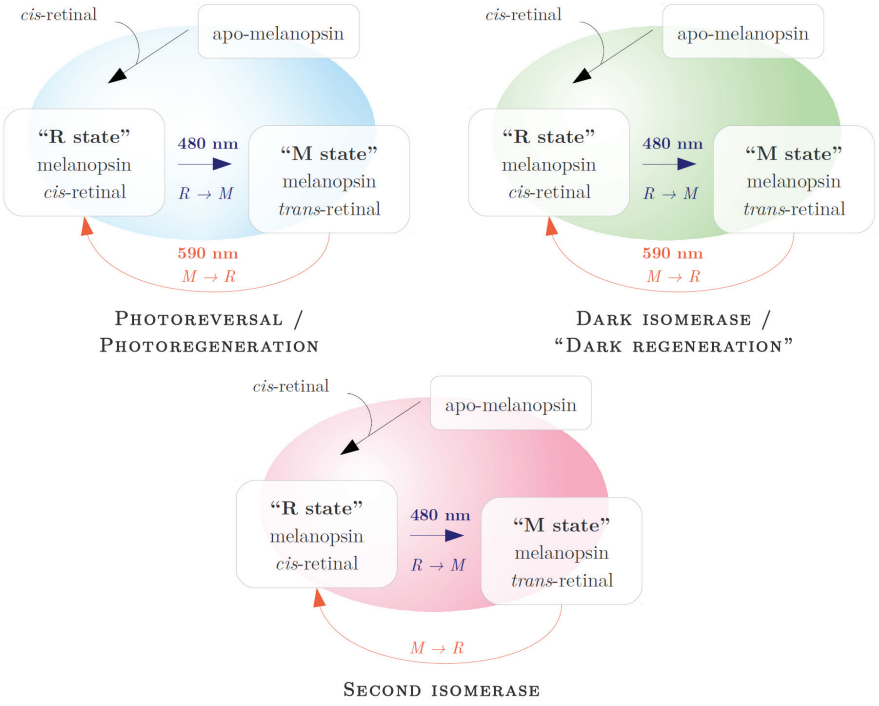

Figure 85: Potential models for cell-autonomous and non-autonomous melanopsin chromophore recycling. Three possibly non-mutually exclusive models for chromophore recycling, including photoreversal/photoregeneration (i.e. "bistability", see 4), dark isomerase/-dark regeneration (Section 5.2), and second (photo)isomerase activity (4.5.1). Schematic models redrawn from Sexton et al. 2012.

ring to light-independent pathway found in classical photoreception with rods and cones, and the third possibility would employ second photoisomerase demonstrated in some invertebrates (Pepe and Cugnoli 1992). It should be noted that the three proposed models do not need to be necessarily mutually exclusive.

The first "bistable" regeneration pathway has been thoroughly reviewed in 4, and it still remains unclear whether melanopsin in humans functions like a bistable photopigment and what are the practical implications of bistability behaviorally if the pigment itself is bistable (Hochstein 1979; Rollag 2008). The light-driven photoregeneration from the M state to R state in flies seems to be very fast and exhibiting irradiance dependency (Stavenga and Hardie 2010 and Section 4.6), with some evidence for a non-transducing inactive R state (Levine et al. 1987, in the model of Section 4.6 referred as R_i). To date, no reports exist on the quantitative behavior of phototransduction cascade of human melanopsin with detailed analysis of intermediate photoproducts, only mouse melanopsin intermediated being studied by Walker 2008, Walker et al. 2008, the results summarized in Figure 86.

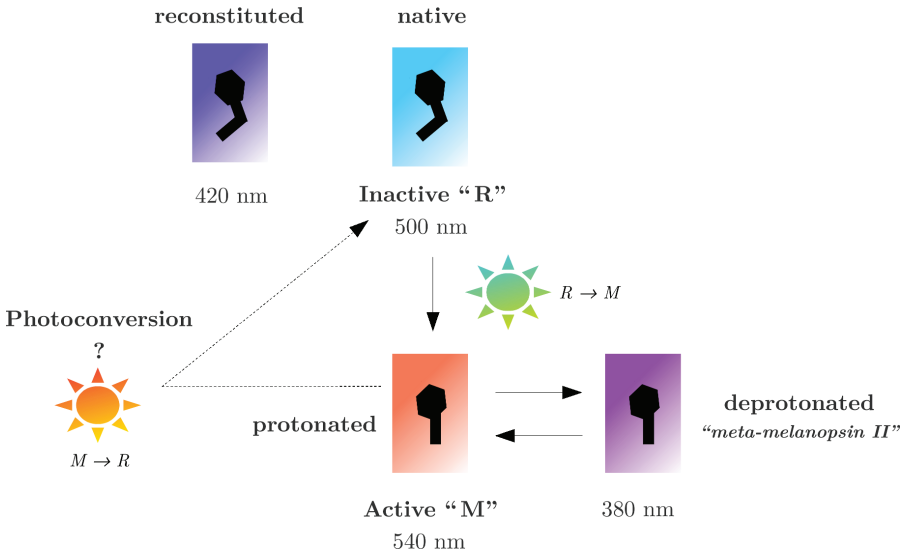

Figure 86: **Melanopsin intermediates.** Summary of endogenous mouse melanopsin properties. Inactive ("dark adapted") melanopsin has an absorbance maximum λ_{max}~500 nm which is upon absorption converted to two distinct "meta-melanopsin" isoforms with absorbance maxima at $\lambda_{max,"Meta-I"}$~540 nm and $\lambda_{max,"Meta-II"}$~380 nm. Reconstituted melanopsin with λ_{max}~420 nm refers to the reconstituted expressed melanopsin with exogenously added 9-*cis*-retinal. The results (Walker et al. 2008) indicated that the native melanopsin must also use some other light-independent retinoid regeneration mechanism in addition to bistability to return to the dark state, The schematic redrawn from Walker 2008.

The dark regeneration (enzymatic visual pigment turnover) kinetics differ significantly between different invertebrate species (Stavenga and Hardie 2010 and Section 4.1), two rough categories of time course existing depending whether the species is bathochromic (R peak blue-shifted compared to M) or hypsochromic (R peak red-shifted compared to M). The hypsochromic species are able to regenerate their pigments very rapidly (in minutes in butterflies, Bernard 1983), whereas the dark regeneration in bathochromic species such as in fly, the dark regeneration may take several hours (Pak and Lidington 1974; Stavenga 1975; Bruno et al. 1977; Schwemer 1989), and in the moth *Galleria* several days (Goldman et al. 1975).

For melanopsin dark regeneration, there are contradictory information available. Walker et al. 2008 found only 11-*cis*-retinal using melanopsin chromophore extractions from dark-adapted retinas, suggesting that even if melanopsin functions as a bistable photopigment, there must also exist some other light-independent regeneration mechanism to return the "meta-melanopsin" to the R state (Walker 2008). In contrast, the studies done with heterologously expressed melanopsin after illumination and conversion from 11-*cis* to all-*trans*-state, no recovery of responsiveness was found after 20 (Melyan et al. 2005) and 60 minutes (Giesbers et al. 2008) in darkness. Bistability in melanopsin could be indirectly to be supported by the noticed resistance of ipRGC function to systemic vitamin A depletion (Thompson et al. 2001; Sexton et al. 2012).

The third possible pathway would employ a second photoisomerase, in addition or without the putative photoisomerase ability of melanopsin to regenerate the pigment to the responsive state. In a fly, there seems to be evidence for the existence of all three photoregeneration pathways in addition to the "bistable photoregeneration" and with a recent "re-discovery" (Arshavsky 2010; Wang et al. 2010; von Lintig et al. 2010; Wang et al. 2012) of the previously found light-independent dark regeneration in flies over 30 years ago (Mayer and Santer 1980; Schwemer 1984). The photoisomerization of all-*trans* to 11-*cis*-retinal is mediated with a λ_{max} = 420 nm (Isono et al. 1988).

Additional phenomenon in the second photoisomerase pathway have been demonstrated in crayfish (Cronin and Goldsmith 1984), that has a hypsochromically shifted rhodopsin ($\lambda_{R,max}$~530 nm, and $\lambda_{M,max}$~510 nm). Crayfish are known to regenerate in darkness (Cronin and Goldsmith 1982a) with an evidence of membrane cycling in their photoreceptors (Eguchi and Waterman 1979), newly synthesized protein continuously being added to the rhabdom (Hafner and Bok 1977). Cronin and Goldsmith 1984 demonstrated that the sensitivity recovery was significantly prolonged after orange exposure (note, now the orange light is the $R \rightarrow M$ stimulus as the R peak is red-shifted in regard to the M state) but not after blue light. Several hypotheses were proposed for the observed phenomenon, the most intuitive

explanation of a direct photodamage to photoregenerating mechanism rejected. The authors (Cronin and Goldsmith 1984), found the most plausible explanation to be that the wavelength of the adapting exposure (orange in this case) might not only affect the bistable rhodopsin, but also a photosensitive regenerating system, such that short-wavelength exposure ($M \rightarrow R$ stimulus for rhodopsin) leaves more replacement capacity in the photoreceptor than does long-wavelength exposure ($M \rightarrow R$ stimulus for rhodopsin). After an exposure to long-wavelength light, for example, regeneration of rhodopsin might be limited by the rate at which new chromophore (presumably 11-*cis* retinal) is made available. Thus, the actual store of chromophore would be photosensitive, and being modulated by chromatic exposure independently of the visual pigments.

Qualitatively this would fit the results obtained in the "photic memory" experimented presented in Section 5.2 (see Figure 57B) where the response is suppressed even after eight hours of darkness following an intense 460 nm light. However, the similar mechanism might not exist for putatively bathochromic melanopsin ($\lambda_{R,max}$~ 480 nm, $\lambda_{M,max}$~ 590 nm) as exist in hypsochromic crayfish. Additionally, the large intra and inter-individual variations complicate the interpretation of the results while one should note that the response after eight hours of darkness followed by 460 nm light shows the least variability.

In mammalian retina, there is contradictory reports on a putative RGR-photoisomerase pathway with Chen et al. 2001a finding a light-dependent rhodopsin regeneration in mice, whereas Wenzel et al. 2005 found dim illumination accelerating rhodopsin regeneration 4-fold in mice, however being independent of RGR. Wenzel et al. 2005 suggested the light-dependent palmitoylation of of sRPE65 to mRPE65 (Redmond. et al. 1998) being a possible mechanism for the observed phenomenon, palmitoylation of RPE65 accelerating the delivery of retinyl esters to the isomerohydrolase (Xue et al. 2004). In humans, the mutation in the RGR encoding gene have been associated with retinitis pigmentosa (Morimura et al. 1999) and age-related macular degeneration (AMD; Fong et al. 2006). Recent report of Radu et al. 2008 suggest that retinal pigment epithelium (RPE; Travis et al. 2010) in humans would be intrinsically photosensitive due to the RGR, and the RGR being involved in the visual cycle.

6.1.5 *Intermediate photoproducts*

The intermediate photoproduct cycle and their putative role in signaling light information in invertebrate and vertebrate phototransduction was reviewed earlier in 4.5.1, with the simplified quantitative model presented in Section 5.5.3 and Section 5.5. Considering that vertebrate rhodopsin intermediate photoproduct cycle is not completely

understood in respect to the biochemical steps (Bartl and Vogel 2007) and behavioral implications (Lamb and Pugh 2004; Reuter 2011), it is not surprising that even less is known about melanopsin intermediates. Similarly to melanopsin, the role of cone intermediates in vertebrate phototransduction is not well understood (Vissers et al. 1998; Kuwayama et al. 2005; Golobokova and Govardovskii 2006).

One of the first evidence of intermediate photoproduct involvement in human rhodopsin was obtained by Hubbard and Kropf 1958 whose results suggested that normal photobleaching could be prevented if additional light was absorbed by bleaching intermediates (reviewed in more detail in Section 4.5, and see Figure 45). This finding was later replicated (Williams 1970; 1974; 1966; 1964; Williams and Webbers 1995), and termed as photoreversal of bleaching most likely mediated via photoreversible metarhodopsin-II [Grimm et al. 2000; λ_{max}~380 nm (Kolesnikov et al. 2003)]. Additionally, it was shown that photosensitivity for early receptor potential (ERP) can be restored after a bleaching stimulus with a short-wavelength light pulse in albino rats (Cone 1967, see Figure 45B). The photoreversal was further suggested to aggravate blue light hazard (van Norren and Gorgels 2011, see 1.2.5), as higher number of photons per unit of time would be absorbed by rhodopsin (Grimm et al. 2001). Thus, conceptually human rhodopsin function as previously described bistable photopigments, however with a crucial difference in regard to its relative strength compared to dark regeneration not allowing full light-driven regeneration (see for example Wenzel et al. 2005).

In humans, further support for the intermediate photoproduct signaling have been obtained from dark adaptation studies (reviewed in Lamb and Pugh 2004; Reuter 2011) where an "equivalent background" phenomenon have been noticed (Stiles and Crawford 1932). The recovery of visual sensitivity after moderately bleaching light stimulus have been noticed to be slower than the regeneration of the visual pigment, suggesting that there could be a buildup of intermediate photoproducts still activating transducin (e.g. Govardovskii and Firsov 2011), the intermediate photoproducts functioning as "virtual light sources". Over the years, suggestions for the threshold-elevating species have been one (or more) of the following (Lamb and Pugh 2004): a metarhodopsin photoproduct , "free opsin" (apoopsin), or all-*trans* retinal, the latter two of which are formed when metarhodopsin is hydrolyzed. For example, one "free opsin" molecule has been estimated to be able to produce ~ 10^{-5} Rh·s^{-1}(Melia et al. 1997) to 10^{-6} Rh·s^{-1}(Cornwall and Fain 1994) equivalent to a steady-state illumination, in other being able to activate transducin and phototransduction 10^{-6}- 10^{-5} less effectively than light (for photoisomerization calculations see Lyubarsky et al. 2004).

With melanopsin, there is scarce evidence for the intermediate photoproduct signaling. The findings of Zhu et al. 2007 (reviewed in 4.7.1)

who demonstrated an increased pupil constriction after intense light with a λ_{max} blue-shifted from 480 nm while still being dependent on melanopsin as the phenomenon was abolished in mice without melanopsin. The "paradoxical potentiation", being spectrally shifted towards shorter wavelengths compared to longer wavelength shift expected from "bistable photopotentiation" (Mure et al. 2009), could be interpreted as arising from yet unknown intermediate photoproduct that builds up at high light intensities. "Paradoxical potentiation" was also found in the study by Hansen et al. 2011, where both red (660 nm) and blue (470 nm) light were shown to potentiate the PLR in humans (Hansen et al. 2011), with no mechanism for the observed phenomena suggested by the authors.

In *Drosophila*, a buildup of M′ photoproduct was seen at high light intensities (Franceschini et al. 1981) which was shown to give a larger fluorescence signal than the M state (Stark et al. 1977; Stavenga 1983). Additionally, Razmjoo and Hamdorf 1980 had included a "buildup product" for their "photopigment model" to provide a quantitative explanation for the prolonged depolarization afterpotential (PDA, see 4.4.4) phenomenon in *Drosophila*. Putative intermediate photoproduct scheme for melanopsin is shown in Figure 87 modified from fly intermediate schemes (Kruizinga et al. 1983; Vought et al. 2000), the buildup of photosensitive M′ state explaining the potentiation seen in Zhu et al. 2007.

Additionally, the deactivation of melanopsin photoresponse is not well understood, namely whether there is a functional arrestin deactivating melanopsin. There is preliminary evidence for arrestin in melanopsin phototransduction (Hatori and Panda 2009), neither rod nor cone arrestin found in mRGC with an evidence for both arrestin-2 and arrestin-3 at both mRNA and protein levels in mice mRGCs (Frederick et al. 2009). Recently, the role of β-arrestin (Lohse et al. 1990) in non-bleaching parapinopsin of lamprey pineal was elucidated by Kawano-Yamashita et al. 2011. The authors demonstrated that β-arrestin is responsible for eliminating the stable photoproduct and restoring cell conditions to the original dark state. The β-arrestin mediated internalization was shown to be necessary for the selective and complete removal of the stable photoproduct from the outer segments (the signal transduction locus) resulting in a decrease of parapinopsin function. This downregulation was hypothesized to partially contribute to the light adaptation and desensitization of photoreceptor cells (Terakita et al. 2012), similar to the downregulation of ligand-binding GPCRs through internalization (Krupnick and Benovic 1998).

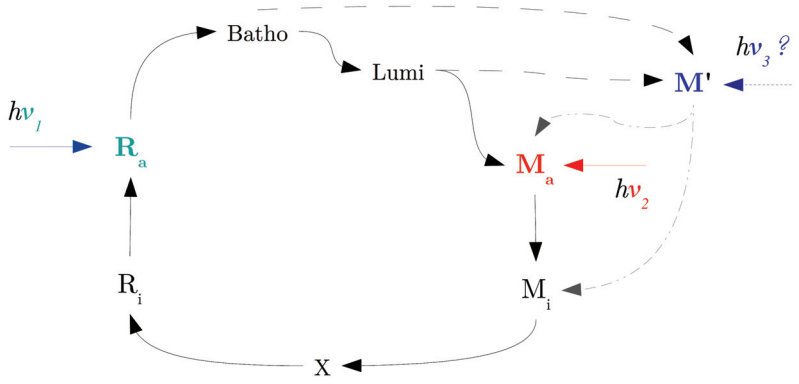

Figure 87: **Putative intermediate cycle of** melanopsin**.** The pigment states R_a, M_a, M_i, R_i are the same as modeled in Section 5.5, and the very short-lived intermediates bathorhodopsin and lumirhodopsin are those shown with fly intermediate scheme previously in Figure 43. The component M′ is now added based on findings of Franceschini et al. 1981 demonstrating another form of metarhodopsin, building up especially with high light intensities (reviewed in 4.5.1). The M′ could be photosensitive maximally for light v_3 blue-shifted from melanopsin peak sensitivity v_1, explaining the paradoxal spectral sensitivity found by Zhu et al. 2007 for pupil constriction in mice. The state X is added between M_i, R_i based on the observations of a possible short-lived intermediate in flies (Kruizinga et al. 1983). Scheme modified from Kruizinga et al. 1983 and Vought et al. 2000.

6.1.6 *Absolute versus relative pigment concentration*

In melanopsin phototransduction, the relation between responsive (R state) melanopsin pigment concentration and sensitivity has not been addressed well. In "bistable photopotentiation", the short-term potentiation and depression effects of photoresponses can be seen to arise from changes in relative concentration ratio between the R and M state (f_M), whereas in natural conditions the adaptive state of the retina might contribute more to the elicited light response.

In *Drosophila*, Razmjoo and Hamdorf 1976 the increased pigment concentration was found to produce a small desensitization of photoreceptor response due to the light excited M state, yet estimated to have very little significance in natural conditions. Similarly in a study by Smakman and Stavenga 1986, the photoreceptor response was found to be independent of pigment concentration with only differences seen in the broadening of the spectral absorption profile with high pigment concentration (due to self-screening, see 2.3.3) and increased contribution from sensitizing pigment at low concentrations (4.1.4).

In albino Wistar rats, a significant modulation for the melanopsin expression was found (Hannibal et al. 2005, see also 2.4.9), constant light (LL) decreasing melanopsin protein concentration in the eye 7.5-

fold, and constant darkness (DD) increasing the protein concentration 10-fold, however without addressing the effect of this modulation on NIF response. The changes in protein amount were accompanied with morphological changes, melanopsin immunosensitivity spreading from soma and proximal dendrites more extensively in DD condition compared to the LL condition. In previous studies there had been evidence for additional circadian (Hannibal et al. 2002) and synaptic modulation from rods and cones to melanopsin protein expression (Sakamoto et al. 2004; Mathes et al. 2007). These highlight the adaptivity of melanopsin system to the environmental lighting conditions, and thus partly contributing to the age-related plasticity as seen in classical photoreceptors (Freund et al. 2011; Owsley 2011). The age-related plasticity in the visual system have been for example demonstrated with increased bipolar sprouting in aged mice (Liets et al. 2006) and in aged humans (Eliasieh et al. 2007).

In contrast to the initial idea of mRGCs not adapting their sensitivity to light stimulus (Berson 2003) has been suggested not to be true, mRGCs clearly showing light adaptation for prolonged light exposure (Wong et al. 2007; 2011; 2005, see also 2.4.8). The suggested adaptation of mRGC photoresponses could be either reflected in downstream NIF responses with a linear or nonlinear dependency on photoresponse, or it could be compensated via post-receptoral processing as suggested for PLR (Zhu et al. 2007) and SCN firing (Meijer et al. 1998). This unknown dependency between the changes between photopigments and photoreceptors, and the resulting downstream response further adds to uncertainty to the already mentioned aspects in using the sustained component of PLR for quantifying bistability in melanopsin.

In *Drosophila*, the light adaptation process is even more sensitive, initialized significantly already from the absorption of a single photon (French 1979; French et al. 1993; Juusola and Hardie 2001a). In contrast to the duplex retina (rod and cones) of humans, the same photoreceptors are used in flies for the whole dynamic range of ambient light intensity (see Section 4.1). To avoid the dealing with highly nonlinear responses, the bistability studies in *Drosophila* have been done using ERG responses with fairly linear dependence on pigment concentrations focusing on pigment level changes [e.g. early receptor potential (ERP) and late receptor potential (LRP) see 4.4]. Alternatively, the pigment dynamics are quantified using photometric method measuring either the transmittance (lower transmittance with higher f_M; *Stark and Thomas 2004*) or the fluorescence (higher fluorescence with higher f_M; Franceschini et al. 1981; Stavenga 1983). The correspondence between the sensitivity measurements with ERG and the photometric measurements have been noticed to be fairly linear (Tsukahara and Horridge 1977). Furthermore, the visual sensitivity is affected significantly less in *Limulus* compared for example to rat

retina. In *Limulus* increasing f_M to 0.5 lowers the maximum sensitivity no more than 0.7 log units (Tsukahara and Horridge 1977), whereas the same rhodopsin bleaching in rat lowers the maximum sensitivity by 3 log units (Weinstein et al. 1967).

For melanopsin, Do et al. 2009 found the single-photon response of mRGCs to be larger than those of rods and cones, while the macroscopic response was found to be smaller due to sparsity of mRGCs and low melanopsin pigment concentration. Additionally, the subtype M1 is shown to express roughly at least one order of magnitude more melanopsin compared to the other mRGC subtypes (M2, M3, M4, M5, see review by Schmidt et al. 2011). M1 subtypes have higher sensitivity for light, the non-M1 subtypes most likely function more as "relay cells" for rod and cone signals. The quantification of melanopsin bistability from downstream response such as PLR is further complicated by the noticed similarity between photoresponses of L-cone and rod photopigment (Kefalov et al. 2003), and S-cone and rod pigment (Shi et al. 2007). The differences in gain and kinetic mainly being modulated by the downstream phototransduction proteins (Makino et al. 2003; Krispel et al. 2006), and furthermore the post-receptoral retinal cells (e.g. Fain et al. 2001; Burns and Arshavsky 2005).

In conclusion, optimally one would have a method of directly measuring the changes at each step of the NIF phototransduction cascade from photopigment concentration changes via photoreceptor output to the downstream nuclei (olivary pretectal nuclei, in the case of PLR) and the resulting pupillary light response (for future methodology predictions, see Section 6.5). Based on the information reviewed, the results obtained in the study Mure et al. 2009 and in Section 5.2 could in theory be interpreted in multiple ways, and the approach of using sustained pupil response very likely do not reflect the pigment-level changes being unsuitable for quantifying melanopsin bistability.

6.2 PARADIGMS TO TEST THE MELANOPSIN BISTABILITY

General frameworks are presented in the following subsections in regard to practical experimental design are briefly outlined.

6.2.1 *Bistable response modulation*

Probably the simplest scheme to test the bistability of a given pigment system is to employ the design used for example in Lisman and Sheline 1976, and then further adapted for human PLR by Mure et al. 2009. The effect of an "Adaptation" light (Figure 88) to "Test" light is studied using the "Reference" as the control for the observed response. In the example case (Figure 88) the "Test" and "Reference" are chosen to be 460 nm corresponding to the maximum pigment shift

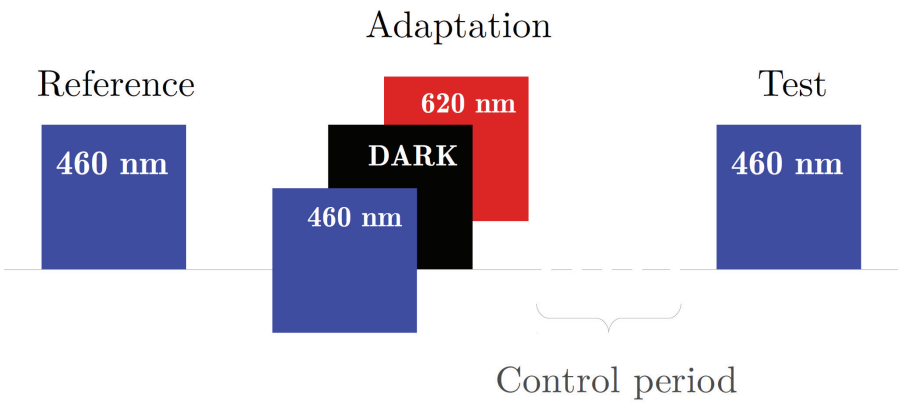

Figure 88: **Response modulation test paradigm.** The effect of the Adaptation stimulus is determined by comparing the difference between the Reference and Test stimulus as done for example by Lisman and Sheline 1976 and Mure et al. 2009. The optimal response to be studied depend then on the available resources and the model organism.

in a melanopsin system assuming the R state peak of ~480 nm and M state peak of ~590. The "Adaptation" light wavelength can span from maximum $R \rightarrow M$ activation (highest f_{Me}, i.e. 460 nm) to minimal $R \rightarrow M$ activation occurring when the equilibrium spectrum has the lowest values (i.e. with melanopsin system $\gtrsim$ 620 nm). The two extremes combined with a "neutral" dark allow the possible extreme values to be measured, the addition of intermediate wavelengths (between 460 nm and 620 nm) increasing the spectral resolution. Note that the maximum and minimum responses of the bistable pigment system do not match the peaks of the R and M states as shown in 4.3.3 and in Section 5.5.

Lisman and Sheline 1976 studied the early receptor potential (ERP, 4.4.1) of *Limulus*, the ERP known to have a linear dependence on pigment shifts, whereas Mure et al. 2009 used the sustained response of PLR (3.2.2) assuming that it reflects melanopsin-only response to the measured PLR. In the former case, the obtained equilibrium spectrum (4.3.3) expresses the amount of relative pigment concentrations (R and M states), whereas in the latter case the measured equilibrium spectrum is more indirect measure of the photopigment dynamics in response to the "Adaptation" light complicating the interpretation of the results (see 5.2.4 and Section 6.1).

6.2.2 *PDA Suppression*

For mammalian melanopsin studies, an improved method in studying the bistability would be to quantify the PDA suppression as a function of wavelength and intensity as done in an unpublished study

by Qiu and Berson 2007 (and see discussion in Do and Yau 2010). The basic idea of the paradigm is to induce a strong PDA (4.4.4) characterized by a persistent pupil constriction long after the light offset (see Figure 20, Newsome 1971), and study the light-dependent "shut-off" of the persistence with many different wavelengths for spectral sensitivity derivation (Figure 89). In invertebrate bistable systems it is possible to suppress the induced PDA in a wavelength-dependent manner (see 4.4.4). The spectral sensitivity of the PDA induction have shown to correspond the R state sensitivity, and the PDA suppression spectral sensitivity of the M state sensitivity.

In vertebrate photoreception, no significant "PDA suppression"-like phenomenon have been shown, thus the demonstration of light-dependent fast return of depolarization to baseline level would offer strong evidence for the melanopsin bistability. It is possible that human PLR is "too many" synapses away from the pigment-dependent PDA suppression complicating the quantification of melanopsin bistability for example due to chromatic interactions for PLR (3.3.3). Measurement directly on a mRGC level (*in vitro* multielectrode array for example in Zhu et al. 2007) or the measurement in the olivary pretectal nucleus (OPN, see Allen et al. 2011 in mice and Clarke et al. 2003b in monkeys) wouldoffer a more direct estimate of the "bistable modulation" of the melanopsin photopigment.

Furthermore, it could be hypothesized that the bistability or the lack of it in melanopsin phototransduction could be shown with significantly shorter experiments compared to the long dark periods and long light pulses needed in the study of Mure et al. 2009. In the study of Newsome 1971, "PDA-like" pupil constriction persistence was found in light pulse durations longer than 1 second as long as the light intensity was high. Additionally if one assumes that melanopsin could be regenerated with long wavelength light, there would be no need for the long dark adaptation [45 minutes used in Mure et al. 2009 ensuring maximum dark adaptation of the rod photoreceptors (Reuter 2011)]. Intense long wavelength light ($\gtrsim$ 620 nm) would in theory shift all the melanopsin pigment to the R state, the exact kinetics of the process requiring further research. One could further assume that the contribution of the rod and cone photoreceptors at high light intensities would be non-significant (McDougal and Gamlin 2010) independent of the initial pigment concentrations (Mahroo and Lamb 2004).

The length of "Control period" in Figure 89 would require some experimental optimization as there is evidence for initial pupil dilation at light offset followed by recontraction ("pupil persistence") as shown in Figure 20. The "Suppression period" with $M \rightarrow R$ could be timed to occur after the pupil recontraction when a rough equilibrium in pupil persistence is reached. The short period of experimental condition would also allow the averaging of PLR waveforms improv-

ing the quality of pupil recordings given the possible intra-individual variability in human PLR (Tryon 1975; Semmlow et al. 1975; see 5.1.2).

6.2.3 *Anti-PDA*

There is an "invisible phenomenon" in bistable pigment system termed as anti-PDA (see 4.4.4). The anti-PDA is characterized by a refractory period between two PDA-inductive stimulus (460 nm Reference and Test in Figure 90) during which the PDA has a lower amplitude in response to the second $R \rightarrow M$ stimulus (Test in Figure 90). The dependence of anti-PDA on stimulus amount and decay period was shown previously in Figure 41, with currently no information available of anti-PDA behavior for the melanopsin system to the author's knowledge. The exact mechanism of the anti-PDA is not known either in invertebrates, and it was suggested to be caused by photoreceptors loaded with arrestin (Stavenga and Hardie 2010), and the arrestin translocation in microvilli () which is not the case with melanopsin-containing RGCs that does not have similar structure.

In practice, anti-PDA would have implications for rapidly pulsed light stimuli such as in the protocol used by Fontaine and Hébert 2011 (the effect of 3 ms of blue light, 11 ms of red light for heart rate) in which one could hypothesize that the decay of mRGC responses (see Figure 13) is shortened if the anti-PDA behavior is significant in melanopsin photoreception. However, one could assume that the cone drive for transient stimuli would increase (Lall et al. 2010; Zeitzer et al. 2011) complicating the analysis of melanopsin contribution of the given NIF response. Furthermore, if the transition from inactive R state (R_i) to active R state (R_a) represents the anti-PDA in the modeling framework illustrated in Figure 47, one could assume that the light would have no effect on the anti-PDA decay time (Figure 90B), it being rate-limited by $R_i \rightarrow R_a$. In other words, the long wavelength stimulation ($M \rightarrow R$) could not potentiate this step while short wavelength stimulus ($R \rightarrow M$) would amplify the anti-PDA.

6.2.4 *PDA Facilitation*

The last PDA-related phenomenon is the least understood phenomenon termed the "PDA facilitation" (discussed in 4.4.4). PDA facilitation is characterized by the opposite behavior to the anti-PDA so that the subsequent stimulus ("Test" in Figure 91) identical to the first stimulus ("Reference" in Figure 91) induces a larger PDA than the first one (Hillman et al. 1976). The facilitatory effect is however only seen with experimental lights that do not shift the pigment "too much" [$R \rightarrow M$ stimulus transferring 14% ($f_{Me} = 0.14$) of the pigment to the M state used in Hillman et al. 1976]. The "Refractory period" in Figure 91 refers to the protocol used in Hillman et al. 1976 (see also

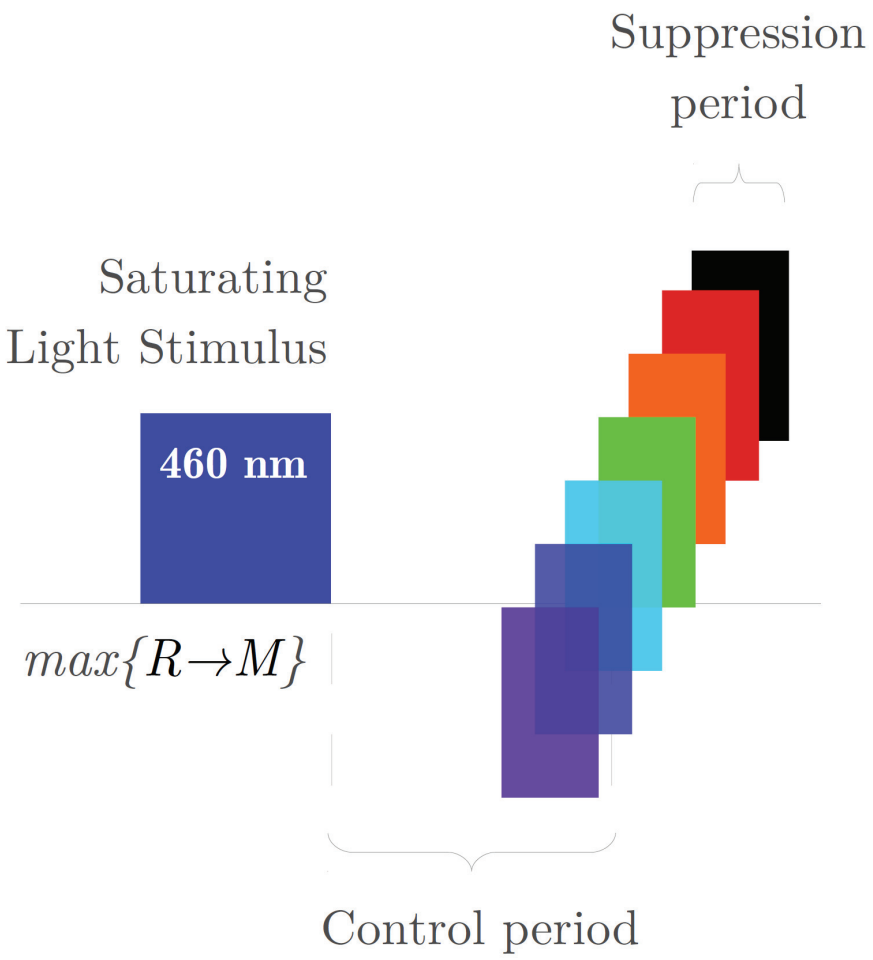

Figure 89: **PDA suppression test paradigm.** Maximum PDA is induced by the peak wavelength of the equilibrium spectrum (max{$R \rightarrow M$}, with melanopsin λ_{max}~ 460 nm derived by Mure et al. 2009), followed by the PDA suppressing light. The PDA suppression in invertebrate system is modulated by the $M \rightarrow R$ pigment shift, thus the observed spectral sensitivity should be slightly long wavelength-shifted from the M state spectral sensitivity as there is some "canceling" of the $M \rightarrow R$ pigment shift by the overlap of R and M sensitivities at peak spectral sensitivity of the M state.

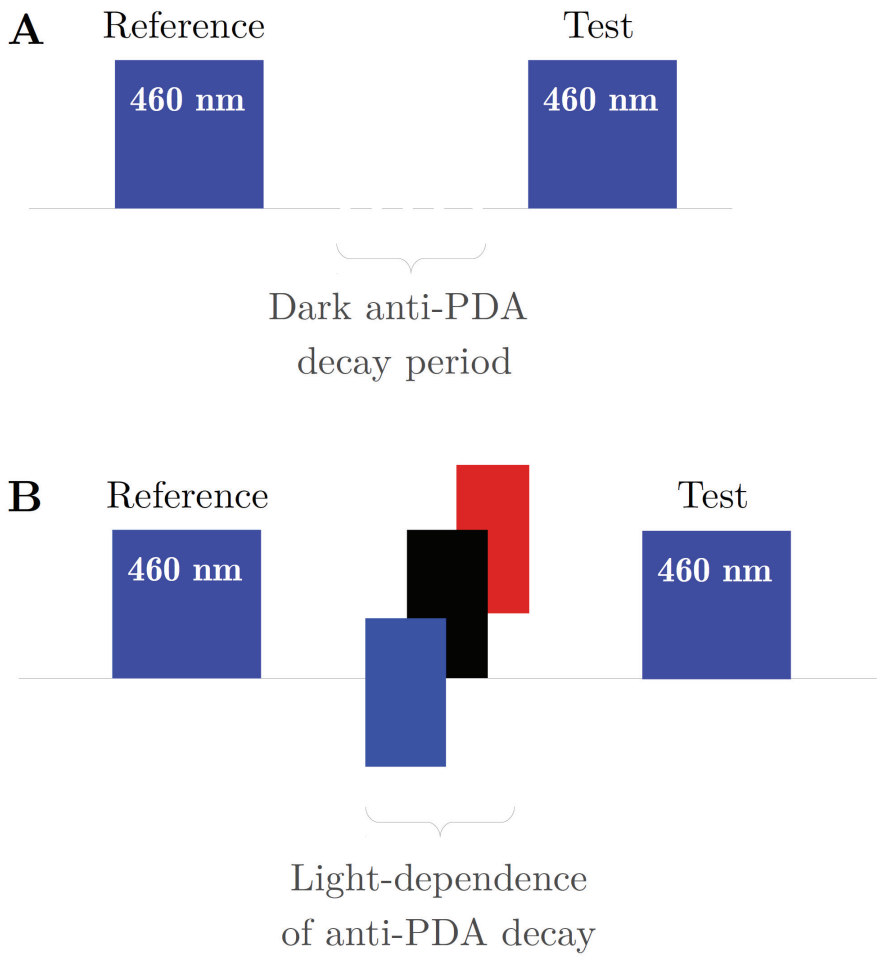

Figure 90: **Anti-PDA test paradigm. (A)** Dark protocol for quantifying the anti-PDA decay time. **(B)** Protocol for testing the light-dependence of anti-PDA decay. With melanopsin there is no evidence for anti-PDA, thus one should derive the time course of the anti-PDA as a function of light intensity, light duration and "light amount" ($I \times d$).

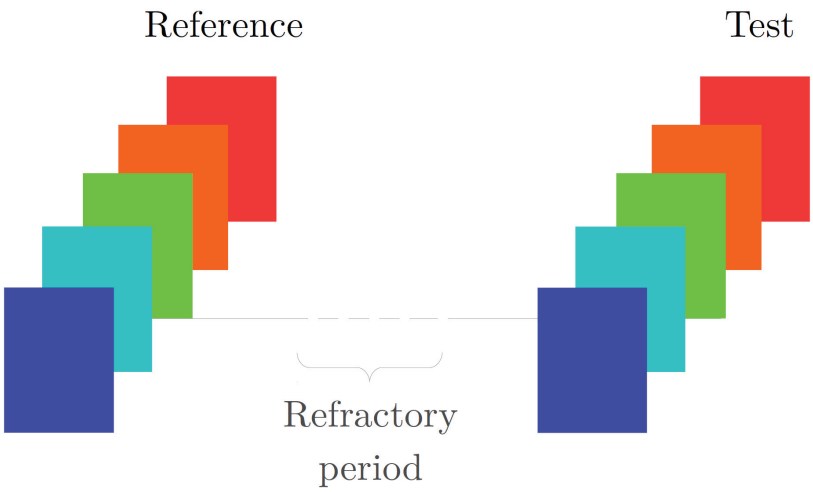

Figure 91: **PDA facilitation test paradigm.** Identical light pairs are chosen, inducing varying f_{Me} values. Based on invertebrate model (Hillman et al. 1976), "PDA facilitation" should be seen with "not-too-high" f_{Me} values [f_{Me}~0.14 in Hillman et al. 1976]. The refractory period should be long enough to ensure that the first PDA has completely decay.

Figure 42) so that the PDA was let decay completely before delivering the second light stimulus. As the mechanism of PDA facilitation is unknown even in invertebrates, it is hard to predict the behavior with melanopsin, and the f_{Me} threshold could be very different or the phenomenon could be simply non-existent with melanopsin. PDA Facilitation was modeled in Öğmen and Gagné 1987 to arise from the antagonistic component to the "light drive" that decays at a different rate than the actual pigment states explaining this underlying latent nonlocal process.

6.3 ECOLOGY AND ATMOSPHERIC MODELING

One could hypothesize that the two-peak bistable melanopsin pigment system could be exploited in tracking environmental spectral changes occurring during the day, and even during the year (for reviews on visual ecology and evolution of opsins, see e.g. Lythgoe 1984; Arendt 2003; Peirson et al. 2009; Davies et al. 2010). Conceptually similar two-opsin (both opsins co-expressed in the same photoreceptor with λ_{max} ~ 495 and 430 nm) system is employed in the parietal eyes of lizards (Solessio and Engbretson 1993; Solessio and Engbretson 1999; Su et al. 2006) which unlike the post-receptoral color opponent system of humans (2.3.4) have the opponency directly at the photoreceptor level. Although the exact behavioral function of this opponent mechanism in lizards is not known, it has been proposed to work as a "twilight detector", detecting the spectral changes of environmental light upon dawn and dusk (Solessio and Engbretson 1993).

The spectral power distribution (SPD) of the environmental light can be roughly composed into direct sunlight, blue skylight and the diffused light from clouds. The surface temperature of the sun is roughly a constant ~6'500 K throughout the day and year, and changes its spectral appearance are due to the atmospheric filtration (Okuno 2008; Pavlov and Pavlova 2010). The sun light scatters in the atmosphere due the presence of aerosols, small particles or droplets [e.g smog (Jacovides et al. 2000)] suspended in the air. The scattering from air-suspended molecules is stronger for blue light than for red light (Rayleigh scatter, see for example 5.3.2.4 ocular media), thus making the sky look blue and the sunset red (Petty 2006; Kerola 2006). The cloud cover reduces the overall light intensity reaching the earth and increases correlated color temperature (CCT) attenuating the long wavelength light more (Hernández-Andrés et al. 1999; Rozanov and Kokhanovsky 2004).

The spectral power distribution during the day is more or less constant being influenced by moving cloud cover and fluctuating particle concentrations in the atmosphere, while the largest changes in environmental light spectrum occurs during dawn and dusk (Figure 92). As the solar elevation decreases from +20° to –20° (sunset), the downwelling irradiance is first relatively spectrally neutral, then long-wavelength dominated, followed with short-wavelength domination, and then either spectrally neutral or long wavelength dominated depending on the presence or absence of the moon (i.e. white to red to blue and then back to white or red, as perceived by humans). The intense blue of skylight during nautical twilight is not due to the wavelength-dependent Rayleigh light scattering, but to the absorption by ozone (Hulburt 1953; Rozenberg 1966). In addition to its strong absorption at ultraviolet wavelengths, ozone also has a

broad absorption band in the visible, known as the Chappuis Band (see discussion in relation to visual ecology in Lythgoe 1984).

The same pattern in opposite order occurs at sunrise (Johnsen et al. 2006; Pavlov and Pavlova 2010), and upon moonrise and moonset, given that the moonlight is reflected sunlight (Johnsen et al. 2006; Sweeney et al. 2011). At temperate and tropical latitudes, the rate of solar and lunar elevation change near the horizon is approximately 1° every 4–6·min (determined using US Naval Observatory tables Office). Thus, these intensity and spectral changes occur over a period of 2.5–4·h, with the central 20° range that exhibits the largest changes occurring in 80–120 min.

Recently, Johnsen et al. 2006 extended the previous studies (McFarland et al. 1999; Rickel and Genin 2005) for twilight and nocturnal light perception in animals with environmental twilight spectral measurements. Previously, in terrestrial invertebrate and vertebrate species twilight shifts in irradiance spectrum have been shown to be physiologically relevant to visual activities such as foraging (Kelber et al. 2002; Roth and Kelber 2004). In the study, star and moon-free night spectra was found to be composed primarily of airglow (emission spectra of the various molecular components of the upper atmosphere) and zodiacal light (sunlight scattered from the dust in the plane of the solar system; Leinert et al. 2004; Benn and Ellison 1998). The stars were found to contribute approximately 23-33% of the total irradiance, the average star emission spectrum taken from Mattila 1980.

This study was followed by the study by Sweeney et al. 2011 on the twilight spectral dynamics on coral reef invertebrate spawning response. The twilight light spectrum was measured and used for modeling the optimal dichromatic visual system discriminating twilight spectrum, the resulting optimal photosensitivity peaks being found to be at 434 nm and 546 nm (compare the peak spectral sensitivities of bistable pigment systems reviewed in Hillman et al. 1983).

Furthermore, the late twilight color was found to be relatively unaltered by intermittent cloud cover, the twilight mainly originating from sub-horizon sunlight scattering at the altitude of ~40km (Bohren and Clothiaux 2006), the cloud cover being significantly lower. The measured underwater (on a coral reef) twilight spectrum was found to be similar to terrestrial spectrum, demonstrating similar twilight blue-shift in the absence of long-wavelength-shifted moonlight (in comparison to direct sunlight).

Somewhat counterintuitive finding was that the best design proposed by the authors (Sweeney et al. 2011) for optimal light detector design was an "a broad, unobstructed sheet of photoreceptive tissue" like that present in corals, sea urchins (Millott 1976), and in mammalian eyes with melanopsin forming a photoreceptive nondirectionally sensitive net (Provencio et al. 2002). The angular reso-

lution (acuity) impeding the organism to distinguish colors as there is a trade-off between packing the photoreceptive organ with only one photoreceptor class (high angular resolution) and photoreceptors with varying spectral classes for color perception (Land and Nilsson 2002). Furthermore it was pointed out by Sweeney et al. 2011 that any organisms that may be using these phenomena as cues must perceive the color of ambient light rather than the colors of objects in a scene, in other words the organism must lack a color constancy mechanism such as the one found in humans (Foster 2011a; Ratnasingam et al. 2011). That is, the visual system used for this task must lack an "auto white-balance" (Rastislav 2008) function to account for changes in background illumination when perceiving colors. A visual system like this has already been postulated for organisms that maintain position in an isolume in the pelagic ocean, and would require many of the same characteristics were hypothesized for observing twilight color (Nilsson 2009).

In addition to the "natural" spectral changes in environmental light, the artificial lighting red-shifts the airglow (e.g. 589.0 and 589.6 nm narrow spectral lines from low-pressure lamps), the exact magnitude shift depending on the light sources used, see for example Elvidge et al. 2010. This opposite spectral shift is possibly affecting twilight-sensitive species, along with possible changes in light polarization "invisible" to humans (Horváth et al. 2009; Kyba et al. 2011b). Most of the light pollution studies have concentrated on cloudless skies as it is the most relevant in astronomic contents (Smith 2009), but there is recent evidence for the amplification effect of cloud coverage to ecological disturbances caused by artificial light pollution (Kyba et al. 2011a).

6.3.1 *SMARTS2 Simulation*

The effects of diurnal changes in environmental light spectrum on bistable melanopsin responses was modeled here using the SMARTS2 model (Gueymard 2001). SMARTS2 is intended for a variety of applications requiring higher resolution and more flexible estimates of spectral irradiance than the standard ASTM/ISO terrestrial spectra (ASTM 1987), these application include for example in daylighting (Henderson and Hodgkiss 1963; Chain et al. 2001; Pechacek et al. 2008; Andersen et al. 2008; Stokes et al. 2008; Iversen et al. 2012), and in solar energy applications (Gueymard 2004). The algorithms used by SMARTS were developed to match the output from the MODTRAN (Berk et al. 1987) complex band models within 2%. The algorithms were implemented in compiled FORTRAN code (source available from: NREL's website) with a graphical user interface provided for Microsoft Excel. The model comes with ten different reference atmospheres, consisting of different vertical profiles of temperature,

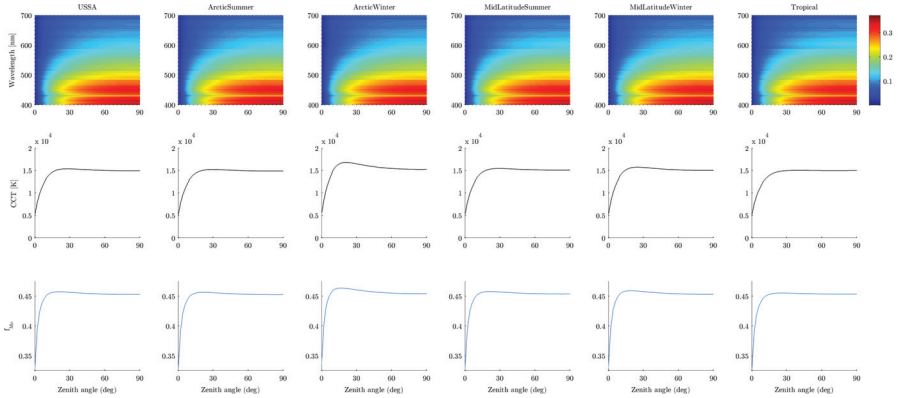

Figure 92: SMARTS2 (Gueymard 2001) simulation with six different reference atmospheres used (Anderson et al. 1986). The first row shows the light spectrum as a function of zenith angle (sunset 0 to midday 90, the 90 to 180 being the same with an inverse pattern), thus normalizing the differences in daylength. The used irradiance type was DIFFUSE HORIZONTAL IRRADIANCE ($W \cdot m^{-2}$) with CIRCUMSOLAR set ON to simulate a radiometer (see full input file in B.5.1). The second row shows the color temperature (CCT) variation. The third row shows the "meta-melanopsin" f_{Me} fraction (see 4.2.1). The irradiance was converted for photon flux for f_{Me} calculation. It can be seen that the light spectrum on average is constant during the day with very rapid changes upon dawn (similar in dusk but not shown).

pressure, and of the concentrations of the main atmospheric gases (Anderson et al. 1986).

The results of a simple simulation are shown in Figure 92 (see B.5.1 for parameters used) with six different reference atmospheres. It can be seen that the time windows for spectral changes upon dawn and dusk, the largest changes occurring with the "Arctic Winter" atmosphere. The higher the correlated color temperature (CCT), the higher the R state activation thus higher the amount of melanopsin in M state (f_{Me}, see 4.2.1). The blue-shifted twilight (higher CCT, see 6.3 above) should therefore prime the melanopsin system to have a lower responsiveness (higher f_{Me}) for subsequent light stimulus, and red-shifted twilight to potentiate (or ensure maximum responsiveness if all the melanopsin is already regenerated to R state during the night) the melanopsin system for subsequent light stimulus.

6.3.2 *Personal NIF dosimetry*

Instead of measuring the physical environmental light changes, it is often more valuable to obtain naturalistic estimates on light exposure received by people which is referred in this subsection as "personal NIF dosimetry" in the absence of a standardized term (Teikari 2006b; Rea 2011a). Typically the naturalistic light exposure has been measured using a wrist-worn actimeter (Savides et al. 1986; Campbell

et al. 1986; Koller et al. 1993; Tamura and Iwata 2001; Heil and Mathis 2002) which have been argued not to correlate that well with the actual light exposure received by the eyes of the individual (Cole et al. 1990). For a comparison of commercial actimeter-based light dosimetry devices see the review by Price et al. 2012. For comparison, similar approach has been taken to quantify naturalistic light exposure experienced by flies (van Hateren 1997, see insect visual system in Section 4.1).

The new generation of personal light dosimeter have increased the number of spectral bands instead of the photopic $V(\lambda)$-based single channel light intensity (defined in lux) sensors including RGB sensor actimeters (Thorne et al. 2009; Santhi et al. 2011), a RGB dosimeter (with additional ultraviolet and near-infrared channels) placed on spectacles (EUCLOCK, LightWatcher, Kolodyazhniy et al. 2011); and two-channel approaches including one photopic and another "circadian" channel as implemented in LichtBlick/LuxBlick system (Hubalek et al. 2006; 2010), and in Daysimeter (van Derlofske et al. 2002; Bierman et al. 2005; Rea et al. 2008; Rea 2011a).

Additionally, the inclusion of multiple spectral bands allows in theory the reconstruction of full light spectrum from sensor data (López-Álvarez et al. 2007; Ratnasingam and Hernández-Andrés 2011). In future, full spectrum estimates could be obtained using smart phones containing cameras simply by placing a light-dispersing grating on top of the lens as done by Chu et al. 2011. The use of smart phones in scientific contexts is emerging trend (Want 2009; Evanko 2010; Pavlou and Diamandis 2011) as employed also in ophthalmic applications quantifying refraction errors (Pamplona et al. 2010), cataract severity (Pamplona et al. 2011).

6.4 PRACTICAL LIGHTING IMPLICATIONS

With the recent emergence of solid state lighting use in general lighting such as light emitting diodes (LEDs; Rea 2010; Tsao et al. 2010 Haitz and Tsao 2011) and organic LEDs (OLEDs; So et al. 2008; Reineke et al. 2009; Leo 2011), the flexibility and controllability of general lighting have improved significantly. The control of spectral power distribution (SPD), spatial distribution, color temperature, temporal modulation, and polarization properties is a lot easier than with conventional light sources (Schubert and Kim 2005). It is possible to dynamically control the color temperature of the LED (Su and Lu 2009; Lo et al. 2011; Oh et al. 2011;) allowing dynamic stimulation of the R and M states (thus a dynamic f_{Me}) in a similar fashion as employed in "non-NIF" lighting (Izsó 2009; Izso et al. 2009; Moeller et al. 2011) and in horticultural lighting (Pinho et al. 2011).

The recent advances in LED technologies have improved the LED color rendering capabilities (Ohno 2005; Smet et al. 2011) suiting bet-

ter for general lighting purposes with little adverse health effect in practice (Behar-Cohen et al. 2011; Wilkins et al. 2010). Given the small size of the LEDs, it is also possible to provide the light stimulus in a novel way (Kim et al. 2010), for example placing a LED directly on a contact lens (Lingley et al. 2011). For more energy-efficient lighting, more advanced lighting control schemes have been proposed (Claudio 2009; Bhardwaj et al. 2010; Hutchison et al. 2010; Lohr 2012), including an internet address for every light bulb (Butgereit et al. 2011), that could be integrated into one "smart lighting" scheme including the spectral and intensity modulation for the "NIF system".

6.4.1 *Implications of aging ocular media*

The implications of ocular media filtration in general (2.2.3) and for the non-image forming system were already discussed previously (Section 5.3). Some practical conclusion can be further derived for architectural lighting practice in relation to recent trend in using high color temperature lighting to improve "human health" (Rea et al. 2002; Boyce 2006; van Bommel 2006; Veitch 2008; Rea et al. 2010; Bellia et al. 2011a; Andersen et al. 2012). The special consideration for aged individuals has been a part of "standard" lighting design practice (Schierz 2011) with a general tendency to be increase lighting levels for elderly to ensure optimal visual performance (Boyce 1973; Boyce 2003; Cheng et al. 2012).

Figure 93 shows an simulation of the effect of ocular media filtration on typical fluorescent light spectrum. The fluorescent lamp with correlated color temperature (CCT) of ~4 000 K [color rendering index (CRI) ~80 thus model number of 840) was chosen to represent the generic office lighting, to be compared to high color temperature "blue-enriched circadian lights" from Osram (Skywhite CCT = 8 000 K) and Philips (ActiViva, CCT = 17 000K). The ocular media was simulated using the model defined by van de Kraats and van Norren 2007a using ages 25 and 65 in Eq. (62). The color temperatures for the measured *in situ* light spectrum and simulated ocular media filtrated light spectra were calculated using the analytical definition by Hernández-Andrés et al. 1999 instead of the older geometrical model of McCamy 1992.

The "meta-melanopsin" fraction f_{Me} was calculated first transforming the irradiance defined in energy to photon density so that all the fluorescent spectra had the total photon density. Then the relative rate constants k_R and k_M were calculated from the light spectrum (Eq. (16)) which were used to derive the f_{Me} using the Eq. (19). The NIF-response was calculated by weighing the nomogram of Govardovskii et al. 2000 with a λ_{max}= 482 nm (β-band included) as the action spectrum. The definition of Enezi et al. 2011 was not used as all the light spectra were in normalized units, and the highest "nomo-

gram response" (unfiltered *in situ* 17 000 K light) was then normalized to unity and then all the other relative NIF responses were in relation to this. It should be noted that the obtained NIF-responses in linear units might be hard to link to specific responses, and they should be interpreted more as rough estimates of "melanopsin stimulation".

The simulation shown in Figure 93 demonstrates a significant attenuation of the short wavelength peaks of the fluorescent spectra especially with the high color temperature fluorescent lamps. This reduction of short wavelength peak has a clear effect on the "retinal color temperature" normalizing the differences between difference light spectra especially for the 65 yr. old observer. Similarly melanopsin responses were reduced, more melanopsin pigment remaining in the photoresponsive R state (lower f_{Me}) in the equilibrium state accompanied with lower NIF values.

The effects of "blue-enriched light" have been addressed in numerous recent studies in an attempt to provide the companies selling arguments for their lamps [e.g. Philips ActiViva, 17,000 K (Mills et al. 2007; Viola et al. 2008; Francis et al. 2008; Revell et al. 2010; Rautkylä et al. 2010; Mottram et al. 2011; Gordijn et al. 2012); and Osram Skywhite 8000 K (Gall and Bieske 2004; Figueiro et al. 2006; Vetter et al. 2011)]. The studies have yielded mixed with yet no established supremacy for the blue-enriched lighting for the NIF system. With similar hopes, the blue-enriched lighting have been used in aged population (e.g. van Hoof et al. 2009; Lederle 2010 ; Morgan 2011).

Confusingly, the national German standardization organization DIN (Deutsches Institut für Normung) adopted a "circadian sensitivity function" $C(\lambda)$ (Lang 2011) with a λ_{max} based on the retinal action spectra for melatonin suppression derived by Brainard et al. 2001; 2008b. The $C(\lambda)$ was designed to be used similarly as $V(\lambda)$ (Stockman et al. 2008; Sharpe et al. 2010) to quantify the visual efficacy of light sources. The inclusion of ocular media especially the observed retinal sensitivity of the 460 nm would shift considerably towards longer wavelengths, accompanied with the mathematical "trick" of fitting the nomogram for logarithmic suppression values (Foster 2011b) and obtaining roughly a ~20 nm shift towards longer wavelengths around the proposed 480 nm peak sensitivity of melanopsin (2.4.2). Furthermore, the measured action spectrum of melatonin suppression seems to be fitted poorly by a nomogram implying an involvement of multiple photoreceptors for the melatonin suppression (e.g. Gooley et al. 2010) violating the principle of univariance (Naka and Rushton 1966; Stockman et al. 2008).

van Hoof et al. 2009 compared the effects of 2,700 K and 17,000 K fluorescent luminaires in institutionalized older people with dementia. They measured the variation of color temperate at the eye level in real-life settings as a combination of the luminaires and daylight during the day. For the 2,700 K condition, the color temperature varied

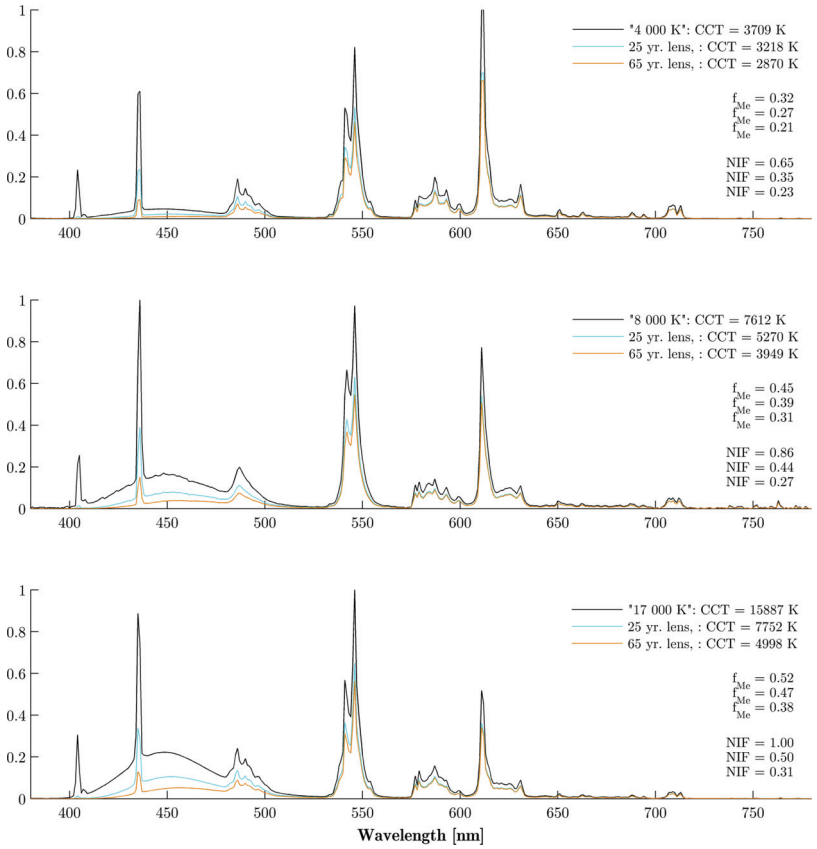

Figure 93: **Light source simulation with aging ocular media.** The properties of three different fluorescent lamp spectra [4,000K at top (generic 840), 8,000K in middle (Osram Skywhite 880) and 17,000 K at the bottom (Philips Activiva)] were compared with three different levels of ocular media filtration [*in situ* light spectrum, 25 yr old lens media filtered, 65 yr. old lens media] using the ocular media model of van de Kraats and van Norren 2007a for 25 yr. and 65 yr. standard observers. Observing the simulations, it is clear that the phosphor used around ~435 nm to increase the color temperature (CCT) of the lamp is significantly attenuated in the ocular media. This attenuation has a significant effect on the "retinal color temperature". Similarly, the increased filtration with age reduces the melanopsin response defined both as "meta-melanopsin" f_{Me} and arbitrary "NIF-response" using the Govardovskii et al. 2000 with a λ_{max}= 482 nm and β-band included as the action spectrum. The spectra were normalized for display to have a peak at unity while the calculations were done for normalized photon density.

between 2,800 and 3,460 K with peaks up to well over 8,000 K. The 17,000 K condition had a mean range from 7,400 to 8,400 K with maximum values of 11,500 and 12,500 K. Furthermore changes in ambient temperature was estimated to be able to cause deviation of 0.005 in CIE XY coordinates corresponding to color temperature shifts up to 2,000 K (see for example for fluorescent technology Thorington 1950; Franz et al. 1989; and Kang 2006 for CIE colorimetry).

The higher color temperature was actually found to worsen the observed behavioral problems in the institutionalized elderly. This was not in contrast with previous finding of "reseting" of high color temperature preference in the demented elderly, compared to normal elderly who preferred high color temperature lighting over lower color temperature (Ishi and Kakitsuba 2003).

There are additional problems using the CCT to predict the NIF responses of light. Correlated color temperature is defined using the corresponding color perception on a Planckian locus (Kelly 1963) based on the electromagnetic blackbody radiation spectrum (Boyer 1969), thus the equivalent correlated color temperature is obtained with various CIE XY coordinates (metamery, e.g. Díaz et al. 1998). The phenomenon is illustrated in 94 using the Philips ActiViva fluorescent lamp with a CCT of 17,000 K and a synthetic light source with a smooth quasi-Gaussian spectral power distribution (SPD). The smooth synthetic light source behaves is less affected by the ocular media filtering in regard to CCT and the melanopsin responses due to the pronounced filtering of the short-wavelength peak of ActiViva. This highlights the importance of ocular media filtering even in the practical lighting design. The observed ambiguity in using a scalar CCT is similar to the problem of using photometric lux to predict human (Anderson et al. 2009) and animal NIF responses (Bullough et al. 2006), complicating the interpretation of studies comparing different color temperature lighting and physiological responses (e.g. Deguchi and Sato 1992; Morita and Tokura 1996; Noguchi and Sakaguchi 1999 Yasukouchi et al. 2000; Kozaki et al. 2005; Yasukouchi and Ishibashi 2005)

Combining the findings on daylight, the environmental reflectance variation (color of walls, furniture, etc), the ambient temperature in the study of van Hoof et al. 2009, and the ocular media simulations one could argue that the differences in theoretical NIF-simulations would be canceled out in real-life settings. Furthermore, the large "real-life" variations even of engineered lighting systems and aging ocular media filtering (see Figure 95 for simulation of R and M state sensitivities and the bistable action spectra applying the same lens media corrections as above for Figure 93, for calculation see 4.2.1) could also be argued to have also an impact on lighting design optimizing putative "bistable responses" by manipulating the spectral content of the light sources. The theoretical optimization of R and M

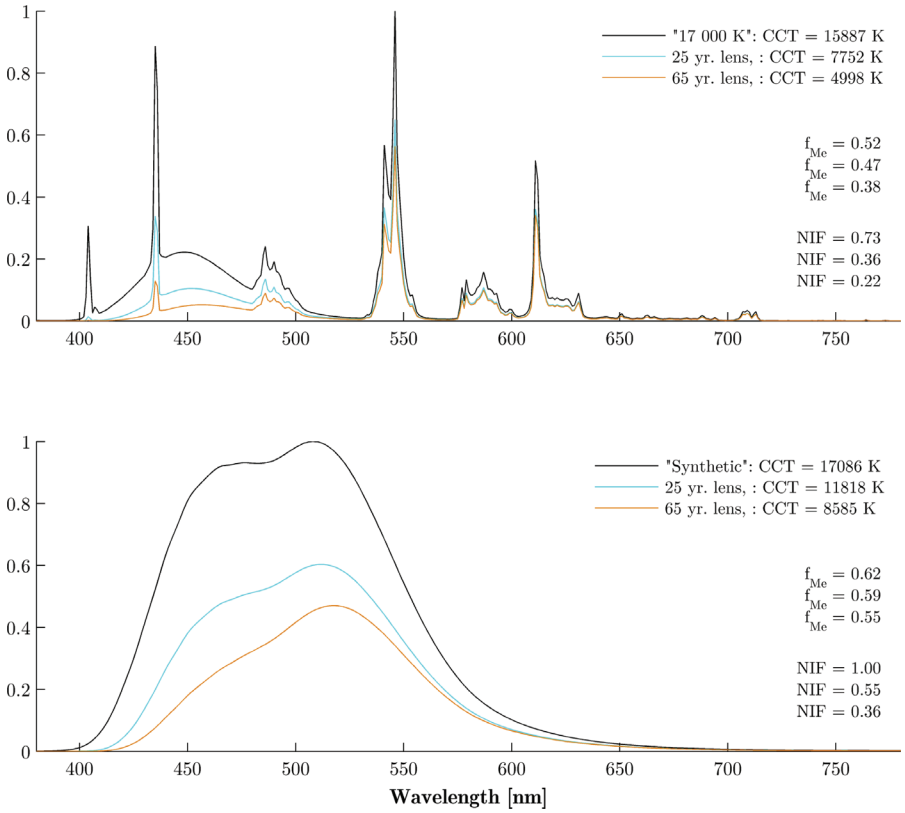

Figure 94: The effect of ocular media filtering on two different light spectra with roughly the same correlated color temperature (CCT) despite the large differences in spectral shape. The synthetic light source (below) is affected by less the ocular media in regard to CCT and the melanopsin metrics. Derivation of the graph identical to Figure 93.

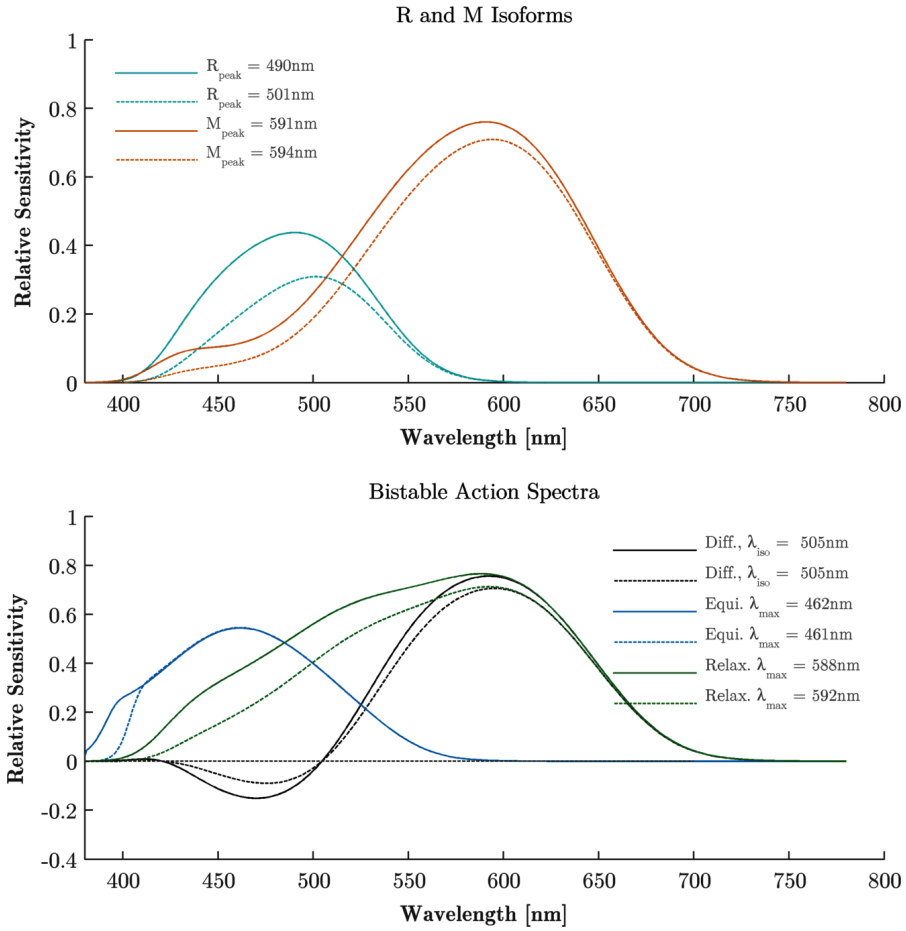

Figure 95: Effect of ocular media for bistable action spectra. (Above) Spectral sensitivities of the R and M state (retinal $\lambda_{max,R}$ = 482 nm and $\lambda_{max,M}$ = 587 nm) filtered with the model lens media of 25 yr old (solid line) and 65 yr old (dashed line) "standard observer" (van de Kraats and van Norren 2007a). (Below) The corresponding bistable action spectra with ocular media filtration. See Section 4.3 for explanation of the bistable spectra, and Figure 37 for the plot of retinal sensitivities of the same spectra.

state stimulation would most likely be eliminated in practice, excluding settings such as NASA space programs (Mallis and DeRoshia 2005), where strict control of lighting geometry and gaze control is possible.

6.4.2 *Implications on architectural lighting design*

In the field studies of the "non-visual lighting" and its effect on well-being (e.g. Bellia et al. 2011b), very rarely are the psychological (Heerwagen and Heerwagen 1986; Veitch 2001) and aesthetic (McVay et al. 1995; Schell et al. 2011) aspects addressed that might be counteracting the physiological effects of the hypothesized "non-visual" effects. An example of psychological "rule-of-thumb" theory in lighting de-

sign is the Kruithof's rule (Kruithof 1941) stating that people tend to prefer psychologically warmer color temperatures with lower illuminances, the preference being reversed for higher color temperatures as illuminance is increased. Additionally, there is some evidence of seasonal (Ishi and Kakitsuba 2003), gender (Knez 1995; Knez and Kers 2000; Knez 2001) and age variation (Ishi and Kakitsuba 2003) in Kruithof's rule. Recently Kruithof's rule was revisited with LED lighting in regard to mRGCs as well and their contribution to luminance perception (Viénot et al. 2009; see also 2.4.10). The psychological preference for certain color temperatures might artifact the results from field studies when in moderate light intensities the ambient light is switched from warm to cool, possibly being experienced unpleasant by the subjects (for such changes, see for example the studies of Viola et al. 2008; Rautkylä et al. 2010; Mottram et al. 2011; Gordijn et al. 2012).

In respect to color psychology, some evidence suggest that red light can be more stimulating than blue light (Stone 2003; Hill and Barton 2005), opposed to what one would expect from more "physiological" studies such as Lockley et al. 2006; Vandewalle et al. 2007a; Figueiro et al. 2009. Additionally, the perception of red color prior a cognitive task have shown to impair the performance (Elliot et al. 2007; Mehta and Zhu 2009) roughly in accordance of the blue-preference of NIF literature (Vandewalle et al. 2009).

There is evidence also for color preference in laboratory animals, one report demonstrating the preference for white cage in mice with the least preference for red cage (Sherwin and Glen 2003). Another study done in gorillas and chimpanzees (Wells et al. 2008), demonstrated that the apes showed significant color preferences, paying significantly less attention to the red, than to the blue or green colored stimuli. With animal studies, there is an added complexity of interpreting the results due to differences between humans and animals in emotional processing (Nagel 1974; Paul et al. 2005; Burn 2008), but results from the animal studies suggest that there might be some hard-wired color preference.

Finally, in regard to daylight and daylit offices (Galasiu and Veitch 2006; Reinhart and Wienold 2011), there is evidence for daylight preference even with visual discomfort from glare (Heerwagen and Zagreus 2005) highlighting the psychophysical experience of our environments rather than the experience being deducible to an easily measured terms (Hawkes 2011). According to the "biophilia hypothesis" introduced by Wilson 1984, humans have an intrinsic tendency to affiliate with life and life-like processes, partly explaining the strong emotional responses to aesthetic environments as a whole (Zajonc 1995; Hildebrand 1999; Botton 2008; Kellert et al. 2011), rather than to one optimized parameters such as "circadian efficacy" of lighting for example (Rea et al. 2010; Lang 2011).

6.5 FUTURE METHODOLOGY

6.5.1 *Adaptive Optics*

In recent years, the use of adaptive optics (AO) based systems in vision science and clinical opthalmologic have increased rapidly (Carroll et al. 2011; in biological imaging Pastrana 2011), AO driving a *paradigm shift* in how to do ophthalmoscopy and vision science (Roorda 2011). The basic idea of adaptive optics is to correct dynamically the aberrations of dynamic media to improve the image quality for example for the correcting the refractive index fluctuations caused by atmospheric turbulence in ground-based astronomy (Babcock 1953; Hardy et al. 1977).

The first implementation of adaptive optics system for the human eye was realized in 1997 by the group of David R. Williams at the University of Rochester (Liang and Williams 1997). In practice the use of adaptive optics approach allows sharper images to be captured of the retina (Rossi and Roorda 2010; Yang et al. 2010; Doble et al. 2011), and spatially precise light stimulus to be delivered even on a accuracy of a single photoreceptor (Hofer et al. 2005; Vohnsen and Rativa 2011b). Additionally adaptive optics have been used for example with *in vivo* imaging of the retinal pigment epithelium (Morgan et al. 2009), the outer segment renewal (Jonnal et al. 2010), and three-dimensional volumetric cone imaging (Kocaoglu et al. 2011).

The principle of adaptive optics use in vision research is shown in 96. The wavefront sensor [typically a Shack-Hartman sensor (Liang et al. 1994), or a novel methods of pyramid sensing (Chamot et al. 2006) and curvature sensing (Gruppetta et al. 2005)] measures the ocular wave aberrations (i.e. the optical distortion caused by the eye). The waveform corrector (deformable mirrors or liquid crystal spatial light modulator, see Hampson 2008) corrects the wavefront according to the algorithm defined by the AO controller (review of control methods, see for example Hofer et al. 2001 and Diaz-Santana et al. 2003). Alternatively, the optomechanical setup could be simplified by replacing the spatial light modulator and lenslet array with numerical processing based on the principles of digital holography (Liu and Kim 2011). The correction sampling rate depends on the technology used, typical values being in the order of typical video sampling rates (25-60 Hz) with AO scanning laser ophthalmoscope (AOSLO) reaching cone-level eye tracking at frequencies over 1 kHz (Yang et al. 2010; Lu et al. 2012). For methodological reviews of retinal adaptive optics systems, one is referred to the reviews by Porter et al. 2006; Hampson 2008; Miller and Roorda 2009; and Vera-Díaz and Doble 2012.

Figure 97 shows a more detailed setup schematic used in the *in vivo* study of cone photoreceptor mosaic (Jonnal et al. 2007). The different light sources allow differential stimulation of different photoreceptor

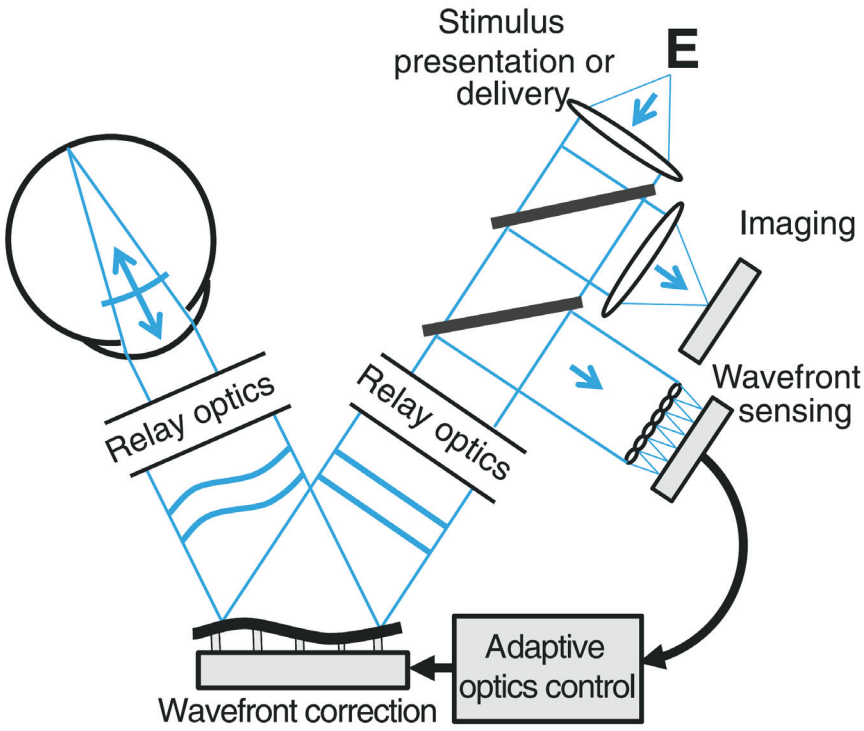

Figure 96: Basic layout of an adaptive optics (AO) system for imaging and vision testing. (Roorda 2011)

classes while the photoreceptor mosaic is recorded with the science CCD. The pupil camera is included for fixation monitoring purposes, but in practice could be used also for characterizing pupillary light reflex (PLR, see 3) allowing more information to be extracted from the same experimental session. As in previous studies, the reflectance of cone pigments (or oscillation of the cone reflectance) to near-infrared (NIR) was seen to correlate with the amount of bleached cone pigment (Rha et al. 2006; Jonnal et al. 2007; Hunter et al. 2011). One could suggest that it could be possible at some point to quantify the conformational states of melanopsin photopigment in the R and in the M state (see 4). These AO-based findings can be seen as upgrades of the classical light-evoked IR studying *in vitro* phototransduction process (see for example Harary et al. 1978; Hofmann et al. 1976; Pepperberg et al. 1988; see also 4.5.3), the measurement now being able *in vivo* conditions.

The cone signal scintillation (reflectance originating from the inner and outer segment refractive index transition, see Gao et al. 2008) in the study by Jonnal et al. 2007 was shown to occur quickly after the stimulus onset (5 to 10 ms) with high stimuli strength, the scintillation lasting roughly 300 to 400 ms. This observed time course was in accordance with human cone ERG data (Hood and Birch 1995), supporting the claim that the observed scintillation was linked to the cone phototransduction. The noticed duration of 300 to 400 ms was

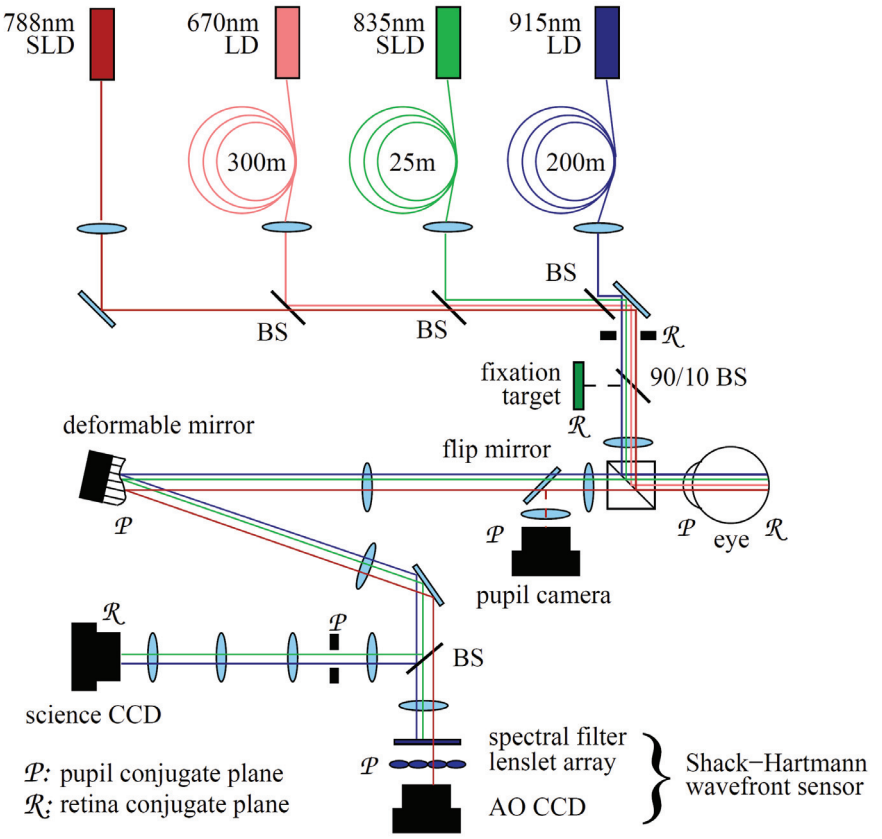

Figure 97: **Layout of the AO retina camera**. The camera consists of four subsystems, **described in the text**. Custom dielectric beamsplitters were designed to reflect and transmit the various light sources, allowing simultaneous retinal imaging, wavefront correction, and stimulation without loss or mixing of light. LD = laser diode, SLD = superluminescent diode, BS = beamsplitter. (Jonnal et al. 2007)

similar with the previous reported interval (Srinivasan et al. 2006), while significantly shorter than the previous reports of a duration of 1 - 3 s obtained with optical coherence tomography (Yao et al. 2005; Bizheva et al. 2006), but the different imaging modality could have made the comparison not possible.

Furthermore, the change in scintillation was shown to be nonlinear suggesting that the scintillation is not directly due to changes in concentration of activated opsin, activated G-protein, or phosphodiesterase, since these are known to change linearly in response to stimulation (Pugh and Lamb 1993), regardless of whether the scintillation effect is mediated by scattering or refractive index. Most likely candidate for the scintillation source was suggested to be situated within the cone photoreceptor itself following changes in the the properties of the outer segment (OS) membrane, or changes in the physical size of OS due to cell swelling. Photopigment activation was rejected as an explanation due to the long observed 300-400 ms scintillation period, as the photoactivation of rhodopsin molecule is completed in well under one millisecond (Menon et al. 2001).

In case with studying melanopsin-dependent photoresponses *in vivo* in humans, the problem is the low number of mRGCs in human retina (~1% of all retinal ganglion cells, ~1000 cells, see Section 2.4) and the very low photopigment density being ~4 log units lower than for rod and cone photopigments (B.3.3). The imaging of ganglion cell layer is further complicated by the fact that their reflectance is roughly 60 times less than that of cones and have a similar refractive index as the Müller and the amacrine cells (Gray et al. 2006). Gray et al. 2006 were able to image ganglion cells using retrograde labeling in monkeys with observed *in vivo* labeling up to five months. This long labeling duration is useful in quantifying retinal disease progression (for example in glaucoma). Additionally functional ganglion cells could be distinguished from pathological ones by selective dye injections into different regions of the lateral geniculate nucleus (LGN). In the future, adaptive optics could be married with an emerging "genetic tag" (Siegert et al. 2009; Gollisch and Meister 2010) approach, in theory allowing different retinal cell types to be studied and their responses isolated with cell-specific markers reviewed in next section.

6.5.2 *Genetic fluorescent tagging*

As reviewed briefly in Gollisch and Meister 2010, it has become possible recently to genetically tag specific neuronal cell types, including retinal cell types during development allowing them to be labeled fluorescently (Siegert et al. 2009). This approach brings various advantages (Gollisch and Meister 2010), first the specific cell types are easily found for electrode placement due to fluorescence allowing

even rare cell types to be studied in dedicated fashion (Huberman et al. 2008), being especially needed for mRGC subtype experiments (Schmidt and Kofuji 2011a; see 2.4.1). Second, the marking can reveal both the shape of the cell, synaptic outputs (Lo and Anderson 2011), and its connectivity with other surrounding cells and brain projections as done by Fox and Guido 2011 for mRGCs. Third, the genetic tag can be also engineered to be activated and deactivated with light when wanted (Lagali et al. 2008). Gollisch and Meister 2010 predicted a future where every retinal cell type would come with a genetic handle but which it could be easily marked and its function to be manipulated, dissolving also ambiguities in morphological definitions between different laboratories as the cell types would be easily labeled.

Recently, in a study by Lin et al. 2008 visual sensitivity was restored as quantified using PLR among other techniques by expressing melanopsin ectopically in the eye, as done earlier also with channelrhodopsin-2 (Tomita et al. 2010). Channelrhodopsin (Thyagarajan et al. 2010; Schoenenberger et al. 2011) have been used with halorhodopsin (Li et al. 2011) in optogenetic studies (Deisseroth 2011) for creating light-sensitive neuronal population that would not otherwise show any light sensitivity, allowing specific switching of neuronal population as done studying sleep for example (Adamantidis et al. 2010). Ye et al. 2011 utilized melanopsin to create an optogenetic system capable of secreting glucagon-like peptide 1 in response to light in synthetic implants for the treatment of diabetes, highlighting the suitability of melanopsin for optogenetic systems also.

In conclusion for the future, one could want a method able to measure the melanopsin pigment concentration *in vivo* in human eye analogously to existing methods of reflection densitometry with (Roorda and Williams 1999) and without adaptive optics (Kremers et al. 2000), ERP (Sieving 1981) and adaptive optics near-infrared scatter (Jonnal et al. 2007) for classical humans photoreceptors, and *in vivo* fluorescence measurement of visual pigment concentrations in fly eye (Franceschini et al. 1981; Stavenga 1983). The photopigment level could then be combined with electrophysiological techniques in animals *in vivo* electrodes placed for example to suprachiasmatic nucleus (SCN) for circadian studies (Meijer et al. 1996; Mure et al. 2007; Brown and Piggins 2007; Brown et al. 2011b), and for olivary pretectal nucleus (OPN) for pupillary light reflex studies (Pong and Fuchs 2000a; Clarke et al. 2003b; Allen et al. 2011). Methodological advances both in "ophthalmic optics" and genetic fluorescent tagging hold a great promise for the future also for melanopsin-related studies.

A

SCIENTIFIC PRODUCTION

A.1 PUBLICATIONS

- **Teikari P**, Mure LS, Cooper HM. "Modelling the kinetics of the bistable melanopsin system", *in preparation.*
- **Teikari P***, Mure LS*, Cooper HM. "Dark regeneration in melanopsin-driven PLR-responses", *in preparation.*
- Najjar RP, **Teikari P**, Cornut PL, Claustrat B, Denis P, Cooper HM, Gronfier C . "Altered non-visual sensitivity to light in the elderly: effect of lens opacification?", *in preparation.*
- **Teikari P***, Najjar RP*, Knoblauch K, Cooper HM, Gronfier C. "An Improved Flicker Photometry Technique to Measure the Ocular Lens Density", *in preparation.*
- Najjar RP*, **Teikari P***, Knoblauch K, Cooper HM, Gronfier C. "Ocular media density assessment and its implication on circadian photoreception and cataract diagnostics", *in preparation.*
- **Teikari P***, Najjar RP*, Cooper HM, Gronfier C. "A low-cost Arduino-based open source system for multi-channel LED visual stimulation", *in preparation.*
- Daneault V, Vandewalle G, Hébert M, **Teikari P**, Mure LS, Gronfier C, Cooper HM, Dumont M, Carrier J. "Does pupil constriction under blue and green monochromatic light changes with age?", *accepted for publication, J Biol Rhythms*

* *equal contribution*

A.2 CONFERENCE PROCEEDINGS

- Rautkylä R, **Teikari P**, Puolakka M, Halonen L. "Evaluation of Today's Research Methods for Assessing Light-induced Alertness", In: EXPERIENCING LIGHT 2009 International Conference on the Effects of Light on Wellbeing (Eds. Y.A.W. de Kort, W.A. IJsselsteijn, I.M. Vogels, M. Aarts, A. Tenner, and K.C.H.J. Smolders), 2009, pp. 162-173.
- Gligor V, **Teikari P**, Eloholma M, Halonen L. "The effect of melatonin on visual performance - study case for equal melatonin

suppression under different light spectra." Conference proceeding at Symposium Light, Performance and Quality of life (SOLG), Eindhoven, the Netherlands, 8 November 2007.

A.3 ORAL & POSTER PRESENTATIONS

- **Teikari P**, Mure LS, Najjar RP, Cornut P-L, Denis P, Gronfier C, Cooper HM. *"Modelling the kinetics of the bistable melanopsin system"* Poster presentation at XII. Congress of the European Biological Rhythms Society, Oxford, UK, August 20-26 2011.
- Najjar RP, **Teikari P**, Cornut P-L, Claustrat B, Denis P, Cooper HM, Gronfier C. *"Aging of non-visual sensitivity to light: compensatory mechanisms"* Oral presentation at XII European Biological Rhythms Society (EBRS), Oxford, UK, August 20-26 2011.
- **Teikari P,** Mure LS, Najjar RP, Cornut P-L, Denis P, Gronfier C, Cooper HM. *"The kinetics of the bistable melanopsin system - Implications for architectural lighting"* Poster presentation at 23rd Annual Meeting of the SLTBR, Montreal, Canada, July 10-13 2011.
- Daneault V, Vandewalle G, **Teikari P**, Mure LS, Hébert M, Doyon J, Gronfier C, Cooper HM, Dumont M, Carrier J. *"Effect of blue monochromatic light on non-visual functions in aging"* Oral presentation at 23rd Annual Meeting of the SLTBR, Montreal, Canada, July 10-13 2011.
- Najjar RP, **Teikari P**, Cornut P-L, Claustrat B, Denis P, Cooper HM, Gronfier C *"Aging of non-visual sensitivity to light: compensatory mechanisms?"* Poster presentation at Gordon Research Conference: Chronobiology. Integration: From Molecule to Organism, Lucca, Italy, June 12-17 2011.
- Daneault V, Vandewalle G, **Teikari P**, Mure LS, Hébert M, Doyon J, Gronfier C, Cooper HM, Dumont M, Carrier J *"Pupil light reflex in response to monochromatic light stimuli in younger and older subjects"* Poster presentation at SLEEP 2011 25th Anniversary Meeting of the Associated Professional Sleep Societies, LLC (APSS), Minneapolis, USA, June 11– 15 2011.
- Daneault V, Vandewalle G, **Teikari P**, Mure LS, Hébert M, Doyon J, Gronfier C, Cooper HM, Dumont M, Carrier J "Aging and effect of blue monochromatic light on non-visual functions" Poster presentation at CERNEC, *"Le cerveau à travers les âges"* , Manoir Saint-Sauveur, Canada, March 25-26 2011.
- **Teikari P**, Mure LS, Point C, Dumortier D, Cooper HM. *"Modelling the effects of bistability on melanopsin responses to light"* Poster presentation at SFC, Antibes, France, x to x September 2010.

- Najjar R, **Teikari P**, Claustrat B, Cornut PL, Denis P, Cooper HM, Gronfier C. *"Circadian photoreception and Aging"*, Journée Scientifique de l'Ecole Doctorale Neurosciences et cognition, Lyon, France, November 3 2010.

- **Teikari P**, Mure LS, Gronfier C, Dumortier D, Cooper HM. *"Consequences of Different Lighting Conditions on Melanopsin Bistable properties"* Poster presentation at SRBR 12th Biennial Meeting, Florida, USA, 22nd to 26th May 2010.

- **Teikari P**, Mure LS, Point C, Dumortier D, Cooper HM. *"Modelling the effects of prior light exposure on melanopsin responses to light"* Poster presentation at XI. Congress of the European Biological Rhythms Society, Strasbourg, France, 22nd to 28th August 2009.

- **Teikari P**, Mure LS, Cooper HM. *"Exploring the role of melanopsin in pupillary responses to light"* Poster presentation at SLTBR Annual Meeting 2009, Berlin, Germany, 23rd to 27th June 2009.

- **Teikari P**. *"Melanopsin bistability: The effect of preceding long-wavelength light exposure to light-induced alertness and melatonin suppression in humans"* Poster presentation at EUCLOCK: Summer School 2008, Laulasmaa, Estonia, 7th to 14th June 2008.

B

TABLES AND CALCULATIONS

B.1 LIGHT

B.1.1 *Gaussian spectral power distribution*

As briefly reviewed in Section 2.1, spectral power distributions (SPD) from LEDs, lasers and interference filters among others can be approximated with good accuracy with the knowledge of peak wavelength and half-bandwidth [HBW, same as full-width half maximum (FWHM)], see Eq. (2). The Matlab implementation is given in B.1.

Algorithm B.1 Light SPD as Gaussian-

```
% sigma / deviation of the gaussian is defined as a function of FWHM
sigma = (FWHM*2) / 2.355; % e.g., http://cp.literature.agilent.com/litweb/pdf/5980-0746E.pdf

% create a wavelength vector
lambda = (xLimits(1) : xRes : xLimits(2))';

%% create a GAUSSIAN Spectral Power Distribution (SPD) with the above
%% parameters and lambda
f = gauss_distribution(lambda, peak, sigma);
SPD = f / max(f); % normalize

  %% subfunction for Gaussian distribution
  function f = gauss_distribution(x, mu, s)

    % x         x vector (i.e. wavelength)
    % mu        mean / peak nm
    % sigma     standard deviation
    p1 = -.5 * ((x - mu)/s) .^ 2;
    p2 = (s * sqrt(2*pi));
    f = exp(p1) ./ p2;
```

B.2 OCULAR MEDIA CORRECTIONS

B.2.1 *Ocular media (crystalline lens)*

The state-of-the-art age-dependent ocular media model has been defined by van de Kraats and van Norren 2007a and reviewed in detail in 5.3.2.4. The model defines the spectral filtration of the environmental light in the ocular media due to absorption of crystalline lens and the Rayleigh scattering occurring on all components of the ocular media. The Matlab implementation is given in B.2.

The lens density index was calculated by fitting the ocular media model of van de Kraats and van Norren 2007a to the measured two data points (410 nm and 560 nm), with only the *age* as free parameter (Matlab function FMINCON, from Optimization Toolbox) in the model (Eq. (62)) resulting a "virtual age" estimate of each subject. See main

Algorithm B.2 Ocular media model of van de Kraats and van Norren 2007a

```
A = 25; % age
lambda = (380 : 1 : 780)'; % wavelength vector [nm]
offset = 0.111; % spectrally neutral offset ('ND filter')

% TRYPTOPHAN
ones273 = 273 * ones(length(lambda),1);
lensMedia.TP = 14.19 * 10.68 ...
                    * exp(-1 .* ((0.057 * (lambda - ones273))) .^ 2);

% YOUNG LENS
ones370 = 370 * ones(length(lambda),1);
lensMedia.LY = (0.998 - (0.000063 * (A .^ 2))) * 2.13 ...
                    * exp(-1 .* ((0.029 * (lambda - ones370))) .^ 2);

% OLD LENS UV
ones325 = 325 * ones(length(lambda),1);
lensMedia.LOUV = (0.059 + (0.000186 * (A .^ 2))) * 11.95 ...
                    * exp(-1 .* ((0.021 * (lambda - ones325))) .^ 2);

% OLD LENS
lensMedia.LO = (0.016 + (0.000132 * (A .^ 2))) * 1.43 ...
                    * exp(-1 .* ((0.008 * (lambda - ones325))) .^ 2);

% SCATTER (for large fields)
offs = 0.225;
lensMedia.rayleighScatter = (offs + (0.000031 * (A .^ 2))) * ((400 ./ lambda) .^ 4);

%  TOTAL MEDIA
lensMedia.totalMedia = lensMedia.rayleighScatter...
                       + lensMedia.TP...
                       + lensMedia.LY...
                       + lensMedia.LOUV...
                       + lensMedia.LO...
                       + offset;
```

text of lens density measurement in 5.3.2.4 for details and Matlab implementation in B.3.

B.2.2 *Macular Pigment*

The macular pigment (2.2.3) is situated mainly between the outer and the inner segment of the classical photoreceptors, thus having little significance for melanopsin-dependent photoreception as the light does not pass the macular pigment before being absorbed by the melanopsin. Spectral profile of nacular pigment absorption is defined analytically by Walraven (2003) (cited by Zagers 2004 and Van de Kraats 2008) as following (for Matlab implementation see B.4):

$$\begin{aligned} MP(\lambda) \quad = \quad & 0.32exp\left[-0.0012 \times (436-\lambda)^2\right] \\ & 0.32exp\left[-0.0012 \times (480-\lambda)^2\right] \\ & 0.123exp\left[-0.0012 \times (458-\lambda)^2\right] \\ & 0.12042exp\left[-0.006 \times (457-\lambda)^2\right] \end{aligned} \tag{74}$$

Algorithm B.3 Main parts of the Matlab implementation of fitting the van de Kraats and van Norren 2007a to the lens measurements.

```
% PSEUDOCODE OF THE MAIN COMPONENTS
function [templates, virtualAges] = lensTemplate_fromDescriptor(ages, descr, descrStr, model,
      lambda, offset, field, SPD1, SPD2, handles)

  % average(i) now is the mean of the "Lens Density Index (NEW)" and the stdev(i) the SD of
       that estimate, scaleFactor is the difference of attenuation between used lights (SPD1
        and SPD2) for standard observer, this being the rationale of replacing old
       definitions of "lens index" which depend on the experimental situations

  % Call the subfunction for the fit (i refers to the number of subjects)
  templates(:,i), virtualAgesMean(i,1), virtualAgesSD(i,:)] = fit_vanDeKraats_forDescriptor(
       average(i), stdev(i), lambda, offset, SPD1, SPD2, compPath, ages(i), scaleFactor);

% SUBFUNCTION FOR THE FIT
function [template, virtualAge, virtualAge_SD] = fit_vanDeKraats_forDescriptor(average, stdev
     , lambda, neutrOffset, SPD1, SPD2, compPath, age, scaleFactorStd)

    % correct the input average with the scale factor
  average = average + scaleFactorStd;

  % define the function for the fitting procedure
  fitFunc = @(ageOptim) minimScaleFactor(ageOptim, average, stdev, lambda, SPD1, SPD2,
       neutrOffset, currDir, compPath);

  % define the input age as the initial guess
  A0 = age;

  % define optimization parameters
  optimOpt = optimset('fmincon');
  optimOpt = optimset(optimOpt, 'Algorithm', 'interior-point', 'Display', 'notify');

  % constrain the age
  lb = 0; % lowest possible age
  ub = 80; % highest possible age

  % empty variables for fmincon
  A = []; b = []; Aeq = []; beq = []; nonlcon = [];

  % use the function "fmincon" from "Optimization Toolbox"
  ageOptim_mean  = fmincon(fitFunc, A0, A, b, Aeq, beq, lb, ub, nonlcon, optimOpt);
```

Algorithm B.4 Macular pigment absorption

```
% create the scalar vector needed for vectorized version of the
ones436 = 436 * ones(length(lambda(:,1)), 1);
ones480 = 480 * ones(length(lambda(:,1)), 1);
ones458 = 458 * ones(length(lambda(:,1)), 1);
ones457 = 457 * ones(length(lambda(:,1)), 1);

% create the template
opticalDensity =  (0.32 .* exp(-0.0012 .* ((ones436 - lambda) .^ 2))) ...
                + (0.32 .* exp(-0.0012 .* ((ones480 - lambda) .^ 2))) ...
                - (0.123 .* exp(-0.0012 .* ((ones458 - lambda) .^ 2))) ...
                + (0.12042 .* exp(-0.006 .* ((ones457 - lambda) .^ 2)));

% normalize to unity at 460 nm
mp_density_norm = opticalDensity / max(opticalDensity);
```

B.2.3 *Humors*

used for the humor absorbance the equivalent absorbance of 24 mm of water as the defined with the tabulated water absorption (Smith and Baker 1981):

$$\alpha_{water} = l_{pathLength} \times K_w^{sw} \tag{75}$$

where K_w^{sw} is diffuse attenuation coefficient for irradiance [m^{-1}] for clear sea water and $l_{pathLength}$ is the distance [m] that the light travels.

B.3 PHOTOTRANSDUCTION

B.3.1 *Nomogram*

The nomogram defines the shape of the spectral absorption of a photopigment as a function of wavelength λ (see 2.3.2). The state-of-the art nomogram template is defined analytically by Govardovskii et al. 2000 modifying the previosu template Lamb 1995. The α-band is defined as following for vitamin A1 pigments (mammalian photoreception):

$$S(x) = \frac{1}{exp\left[A\left(a-x\right)\right] + exp\left[B\left(b-x\right)\right] + exp\left[C\left(c-x\right)\right] + D} \tag{76}$$

where $x = \lambda_{max}/\lambda$, and b, c, A, B, C and$D$ are constants; $A = 69.7$, $B = 28.0$, $C = -14.9$, $b = 0.922$, $c = 1.104$, $d = 0.674$. The parameter a is modified from constant in Lamb 1995 to depend on the peak spectral sensitivity λ_{max} improving the fit of the template at long-wave end of the spectrum ($x \to 0$), as following:

$$a = 0.8795 + 0.0459exp\left[-\left(\lambda_{max} - 300\right)^2/11940\right] \tag{77}$$

The β-band is defined as following:

$$S_\beta(\lambda) = A_\beta exp\left\{-\left[\left(\lambda - \lambda_{m\beta}\right)/b\right]^2\right\} \tag{78}$$

where $\lambda_{m\beta} = 189 + 0.315 \cdot \lambda_{max}$ and $b = -40.5 + 0.195 \cdot \lambda_{max}$. Both bands are implemented in Matlab in B.5.

The obtained nomogram $S(\lambda)$ (quantal sensitivity in linear domain) can be corrected for self-screening effect (2.3.3) as in Matlab (B.6).

where the *pigmentDensity* is the photopigment density (OD) in logarithmic units, and the *pigmentTransmittance* defines how much the photopigment filters the incoming light. The quantal sensitivity $S_{corr}(\lambda)$ can be transformed to energy sensitivity $S_E(\lambda)$ as following: (Matlab in B.7)

$$S_E(\lambda) = \frac{S_{quantal}(\lambda)}{hc/\lambda} \tag{79}$$

Algorithm B.5 Govardovskii's nomogram (2000)

```
peak_nm = 482; % desired peak wavelength
lambda = (380 : 1 : 780)'; % wavelength vector

% Parameters (alpha-band)
  a = 0.8795 + (0.0459 * exp(-1 * (((peak_nm - 300)^2) / 11940)));
  b = 0.922; c = 1.104;
  A = 69.7; B = 28.0; C = -14.9; D = 0.674;

% Vectorize the variables to avoid using a for-loop
  onesVector = ones(1, length(lambda));
  A = A * onesVector; B = B * onesVector; C = C * onesVector; D = D * onesVector;
  a = a * onesVector; b = b * onesVector; c = c * onesVector;

%% Calculating spectral sensitivities
  % ALPHA
    % Defining denominator terms as their own variables
    denom_term1 = exp(A .* (a - (peak_nm ./ lambda) ) );
    denom_term2 = exp(B .* (b - (peak_nm ./ lambda) ) );
    denom_term3 = exp(C .* (c - (peak_nm ./ lambda) ) );
    denom_term4 = D;
    S_alpha = (1 ./ (denom_term1 + denom_term2 + denom_term3 + denom_term4))';

  % BETA
    peakBeta = 189 + (0.315 * peak_nm); % nm
    b = -40.5 + (0.195 * peak_nm); % nm
    A_beta  = 0.26;
    x = lambda - peakBeta;

    S_beta = (A_beta * exp(-1* ((x/b) .^2)))';

  % SUM
    S = S_alpha + S_beta;
```

Algorithm B.6 Self-screening correction

```
% corrected, in LINEAR units
pigmentTransmittance = (10 .^ (-1 * (pigmentDensity * (10 .^ S))));
S_corr = onesVector - transmittance;
```

where h is Planck's constant, c is the speed of light and λ is the wavelength.

Algorithm B.7 Quantal→Energy sensitivity conversion

```
h = 6.62606896 * 10^-34; % Planck's constant [J*s]
c = 299792458; % Speed of light [m/s]
photonEnergy_vector = (h * c) ./ (lambda * 10^-9); % [J]
E = S_corr ./ photonEnergy_vector;
```

B.3.2 *Irradiance response curve (IRC)*

In order to fit an 4-parameter irradiance response curve (IRC, defined analytically in Eq. (72)) in Matlab, the code in B.8 can be used.

B.3.3 *Photopigment density*

The photopigment densities for human photoreceptors are shown in Table 5, these values can be used then for the self-screening effect correction discussed in 2.3.3.

Algorithm B.8 Irradiance response curve (IRC) fit

```
% INPUT
x = irradiance; % in logarithmic units
y = response; % in linear units

% DEFINE Hill Equation Sigmoid
sigmoid = @(beta,x)beta(1)+(beta(2)-beta(1))./(1+(x/beta(3)).^beta(4));

% Initial parameter guesses
mino = min(y);
maxo = max(y);
X50_o = mean([mino maxo]);
coeffo = 1;

% Use the 'nlinfit' routine
[coeffs,r,J] = nlinfit(x,y,sigmoid,[mino maxo X50_o coeffo]);
```

Table 5: Estimates of optical densities for human dark-adapted pigments

Pigment	Peak Optical Density	Reference
Rods	0.40	Lamb 1995
S-cones	0.30	Stockman et al. 1999
L/M-cones	0.38	Stockman et al. 1999
	0.27	Lamb 1995
M-cones	0.4 - 0.5 ^{prot}	Miller 1972
	0.3 ^{prot}	Smith and Pokorny 1973
	0.27^{prot}	Burns and Elsner 1993
	0.39 ^{dichr}	Berendschot et al. 1996
	0.66	Renner et al. 2004
L-cones	0.5 - 0.6 ^{deut}	Miller 1972
	0.4 ^{deut}	Smith and Pokorny 1973
	0.48^{deut}	Burns and Elsner 1993
	0.42 ^{dichr}	Berendschot et al. 1996
	0.65	Renner et al. 2004
Melanopsin	0.50	Tsujimura et al. 2010
	0.1	Viénot et al. 2009
	$\sim 0.4 \times 10^{-4}$ *	Do et al. 2009

^{prot} *protanope dichromat*
^{deut} *deuteranope dichromat*
^{dichr} *dichromat (unspecified)*
* *"10^4 less than for cones/rods"*

B.4 MELANOPSIN PHOTOTRANSDUCTION CALCULATIONS

B.4.1 *Visual pigment-arrestin cycle - parameter estimates*

B.5 DAYLIGHT SIMULATION

B.5.1 *SMARTS2 Parameters*

Put the parameters used here so that it could be reproduced if wanted.

Algorithm B.9 Input text file for SMARTS2 simulation (see) to be used for "Arctic Summer' atmosphere model (5th line, '*AS*'). See full explanation for the used parameters in the *SMARTS2 User Manual v. 2.9.5*.

```
USSA_AOD=0.084_ASTM_G173'
1
1013.25 0 0
1
'AS'
1
1
1
370
0
'SRA_URBAN'
0
0.084
38
1
38 37. 180.
380 780 1.0 1366.1
2
380 780 1
3
8 9 10
1
0 2.9 0
0
0
0
1
0 0
2 0
4 0
6 0
8 0
10 0
12 0
14 0
16 0
18 0
20 0
22 0
24 0
26 0
28 0
30 0
32 0
34 0
36 0
38 0
40 0
42 0
44 0
46 0
48 0
50 0
52 0
54 0
56 0
58 0
60 0
62 0
64 0
66 0
68 0
70 0
72 0
74 0
76 0
78 0
80 0
82 0
84 0
86 0
88 0
90 0
90 0
```

Table 6: **Parameter estimates for the visual pigment-arrestin cycle 1/2.** Relative quantum efficiency (φ); the molecular absorbance coefficient (α_{max}); concentration C of the photopigment; ρ_m pigment density; r_m radius of the photoreceptor, γ_R and γ_M the quantum efficiencies of forward (R→M) and backward (M→R) isomerizations, respectively; and ϵ_R and ϵ_M the molar extinction coefficient of forward (R→M) and backward (M→R) isomerizations, respectively. Rh. is rhodopsin, and OPN4 melanopsin.

Parameter	Value	Species	Reference
$\epsilon_R : \epsilon_M$	~35,000 : 56,000 $M^{-1}cm^{-1}$	*Drosophila* Rh.	Ostroy 1978
	~40,000 : 60,000 $M^{-1}cm^{-1}$	squid Rh.	Hubbard and St. George 1958
γ_R: γ_M	0.69 : 0.49	crayfish Rh.	Cronin and Goldsmith 1982b
	0.67 : ?	bovine Rh.	Dartnall 1972
φ	0.94	*Calliphora* Rh.	Schwemer 1979
	0.7	*Drosophila* Rh.	Stark and Johnson 1980
	0.69	crayfish Rh.	Cronin and Goldsmith 1982b
	1.0	human OPN4 (estimate)	Mure et al. 2009
α_{max}	2.0×10^{-8} μm^2	*Drosophila* Rh.	Stavenga and Hardie 2010
	1.56×10^{-8} μm^2	bovine Rh.	Dartnall 1972
	5.5×10^{-5} μm^2 §	human OPN4	estimated from PLR ofMure et al. 2009
κ_{max}	5.0×10^{-3} μm^{-1}	*Drosophila* Rh.	**?**
	2.8×10^{-2} μm^{-1}	Human Rh.	Alpern and Pugh 1974
	3.5×10^{-2} μm^{-1}	Macaque Cone	Bowmaker et al. 1978
	4×10^{-2} μm^{-1}	Macaque Rh	Bowmaker et al. 1978
	3×10^{-6} μm^{-1}	OPN4	Do et al. 2009

§ *estimating τ_c from mean PLR of Mure et al. 2009 fitting a exponential curve, yielding $\tau_c \approx 37$ sec. This estimate was then used as followed: $\alpha_{max} = [(1/\tau_c) / (k_R + k_M)]$ with the $k_R$and k_M calculated from 480 nm light (hbw = 10 nm) with a photon density of 10^{12} ph/cm²/s⁻¹. Note that now the estimate of α_{max} is physically not valid and represents the measured equilibrium behavior of the PLR. Most likely the absorbance coefficient of melanopsin is close to other opsins. For a review of κ_{max} values, see Warrant and Nilsson 1998*

Table 7: **Parameter estimates for the visual pigment-arrestin cycle 2/2.** Relative quantum efficiency (φ); the molecular absorbance coefficient (α_{max}); concentration C of the photopigment; ρ_m pigment density; r_m radius of the photoreceptor, γ_R and γ_M the quantum efficiencies of forward (R→M) and backward (M→R) isomerizations, respectively; and ϵ_R and ϵ_M the molar extinction coefficient of forward (R→M) and backward (M→R) isomerizations, respectively. Rh. is rhodopsin, and OPN4 melanopsin.

Parameter	Value	Species	Reference
C	$2.5 \times 10^5 \mu m^{-3}$	*Drosophila* Rh.	Hardie and Postma 2008; Stavenga and Hardie 2010
	~3.5 mM	vertebrate	Hárosi 1975
	$1{,}560\ \mu m^{-3}$¥	*in situ* mice OPN4	Do et al. 2009
ρ	$3\ \mu m^{-2}$	mice OPN4	Do et al. 2009
	$25{,}000\ \mu m^{-2}$	mouse rod	Liebman et al. 1987
	$4{,}000\ \mu m^{-2}$	*Drosophila* Rh.	Hardie and Postma 2008
	$4{,}214\ \mu m^{-2}$	*Drosophila* Rh.	Harris et al. 1977
	$8{,}000\ \mu m^{-2}$	*Drosophila* Rh.	Lisman and Bering 1977
	$10{,}000$ - $20{,}000\ \mu m^{-2}$	crayfish Rh.	Goldsmith and Wehner 1977
r_{mRGC}	$5\ \mu m$	mice OPN4	Do et al. 2009
l_{mRGC}	?		
A_{dendr}	$9{,}600 \pm 700\ \mu m^2$	mice OPN4	Do et al. 2009
A_{soma}	$1{,}000 \pm 500\ \mu m^2$	mice OPN4	Do et al. 2009
A_{s+d}	$100{,}600 \pm 860\ \mu m^2$	mice OPN4	Do et al. 2009
$CA_{\mu F}$	$1\ \mu F/cm^2$	*Drosophila* Rh.	Cole 1968; Lisman and Bering 1977

¥ *10^4 fold lower in mice than for rods/cones, ($C_{drosophila,Rh.} \times (25{,}000/4{,}000) \times 10^{-4}$), assuming that the relation between density and concentration is linear (vertebrate rhodopsin higher than invertebrate, thus scaling needed). For a review of κ_{max} values, see Warrant and Nilsson 1998*

C

SUPPLEMENTARY GRAPHS AND TABLES

C.1 LENS DENSITY MEASUREMENT

Sensitivity for the described lens density method for the self-screening effect (photopigment density, see 2.3.3) and peak spectral sensitivity λ_{max} of human rhodopsin are illustrated in Figure 98 and Figure 99. For discussion of the parameters see the main text in 5.3.2.4.

C.2 BISTABLE PHOTORECEPTION SIMULATIONS

C.2.1 *Equilibrium spectrum*

C.2.2 *Relaxation spectrum*

C.2.3 *Effect of quantum efficiency on bistable spectra*

C.2.4 *Effect of pigment density*

C.3 PUPIL AND AGING

Supplementary info related to the study presented in Section 5.4.

Impact of an exposure on the next exposure

Our protocol included only 2 min. of darkness between light exposures. Retinal photoreceptors could not fully recover and return to baseline level between two exposures and a given exposure to light could affect the subsequent one. However, pseudo-randomization prevented this bias to significantly affect our results. A repeated measure ANOVA across all participants (irrespective of age group) with the 6 pre-exposure pupil size as within subject factor did not reveal any significant difference between pre-exposure pupil measures [$F(5, 145) = 0.60$, $P = 0.67$], indicating that, on average, pre-exposure pupil size remained stable across light conditions.

Normalization of pupil size according to pre-exposure to measure PLR

Repeated measure ANOVA of normalized pupil values according to pre-exposure baseline pupil size with light condition (blue, green) and light intensity (low, medium, high) as within subject factors and age groups (young, older) as between subject factor revealed that PLR

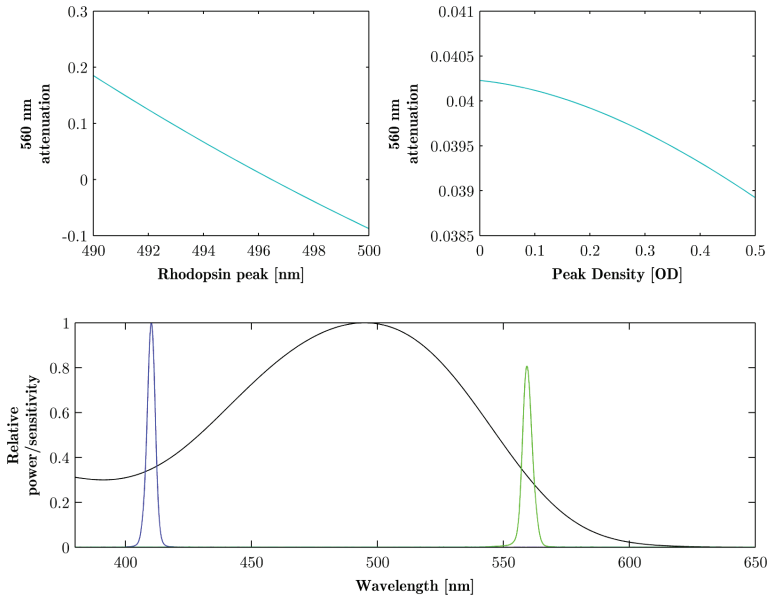

Figure 98: **Sensitivity of the method for rhodopsin parameters.** Separate analysis for rhodopsin peak sensitivity λ_{max} (left, above) and rhodopsin axial pigment density d_{rh} (right, above). Values used by us are λ_{max} = 495 nm and d_{rh} = 0.40. The nomogram (Govardovskii et al. 2000) includes the β-band, thus the short-wavelength lobe is elevated. The lights are normalized to have the same total photon density, thus the green 560 nm has a lower peak value.

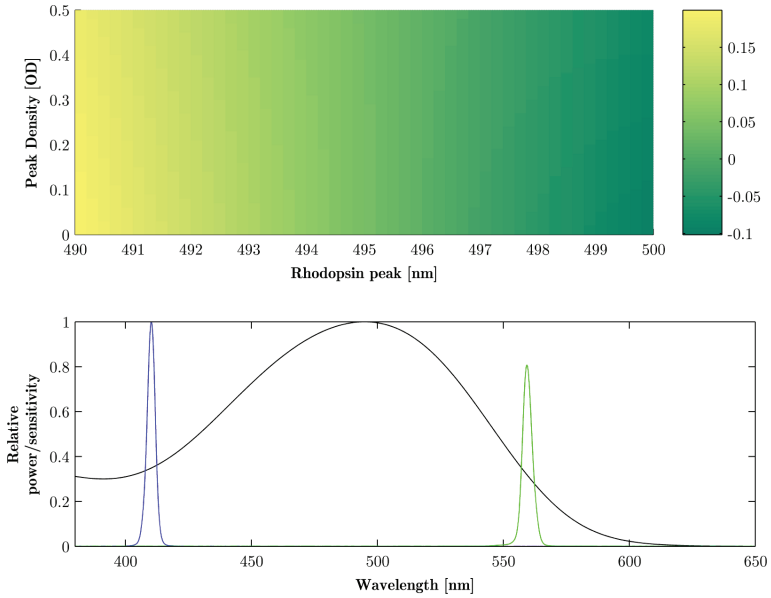

Figure 99: **Sensitivity of the method for rhodopsin parameters (three-dimensional color-coded plot).** Combined analysis for rhodopsin peak sensitivity λ_{max} and rhodopsin axial pigment density d_{rh} (above). Values used by us are λ_{max} = 495 nm and d_{rh} = 0.40. The nomogram (Govardovskii et al. 2000) includes the β-band, thus the short-wavelength lobe is elevated. The lights are normalized to have the same total photon density, thus the green 560 nm has a lower peak value.

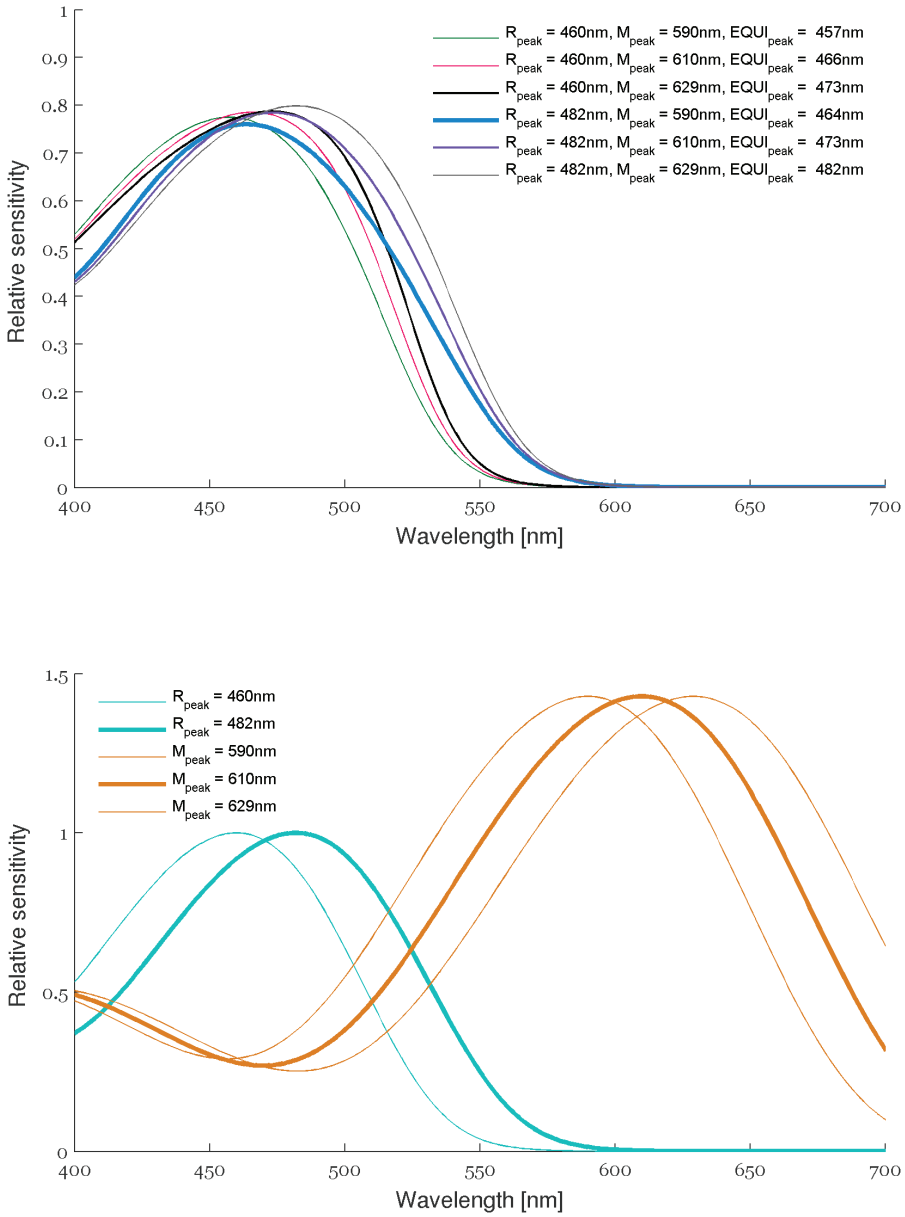

Figure 100: **Equilibrium spectrum shape** Effect of different R and M spectral sensitivities to the shape of the equilibrium spectrum.

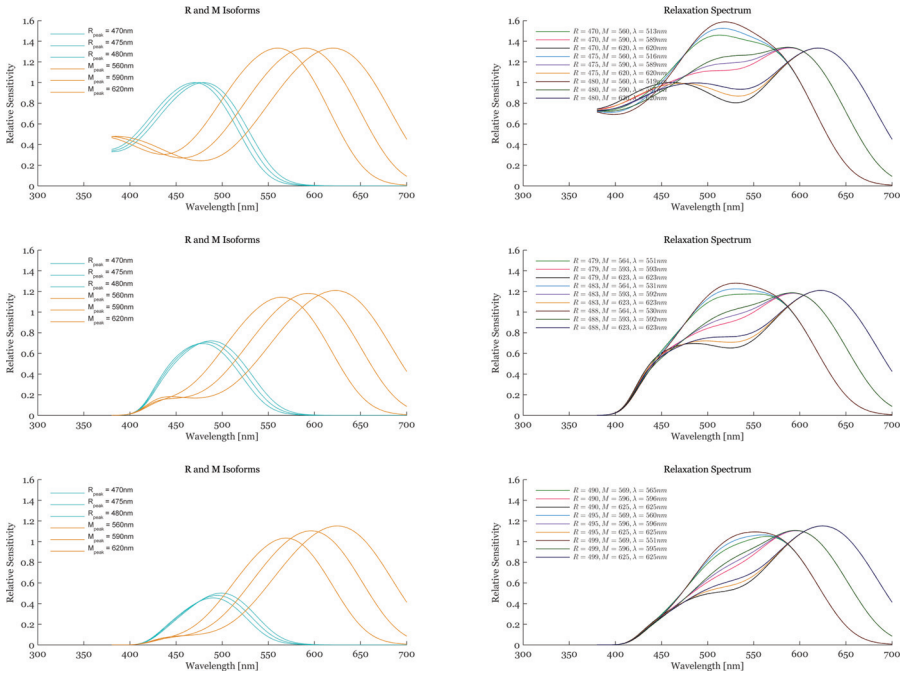

Figure 101: **Relaxation spectrum shape** Effect of different R and M spectral sensitivities to the shape of the relaxation spectrum. Relaxation spectrum will tell you the spectral sensitivity of the system before it reaces equilibrium.

was significantly greater under blue (64.44% ± 2.05) than green light exposure (61.73% ± 2.17) [$F(1,28) = 6.72$, P =0.015], and that PLR was greater with increasing irradiances (low: 54.43% ± 2.74 - medium: 64.68% ± 1.95 - high: 70.14% ± 1.76) [$F(2,56) = 69.55$, $P < 0.001$]. No age effect was obtained [$F(1,28)$= 0.09, P =0.77] and none of the interactions, including the group by intensity interaction, were significant (light intensity by age group: [$F(2,56) = 0.29$, $P = 0.68$], light condition by age group: [$F(2,56) = 0.11$, $P = 0.74$], light condition by light intensity: [$F(2,56) = 0.39$, P =0.63], light condition by light intensity by age group: [$F(2,56) = 1.79$, P =0.18]). These statistical results, obtained when normalizing according to pre-exposure pupil size, are therefore similar to those obtained when normalizing according to baseline pupil size.

C.4 PHOTIC MEMORY

See 5.2 on page 141 for full details of the study.

C.4.1 *Individual PLR recordings*

The individual traces of the "photic memory" PLR recordings are shown in Figure 104. The "normalized difference" between the reference (first 480 nm light pulse) and the test pulse (second 480 nm light

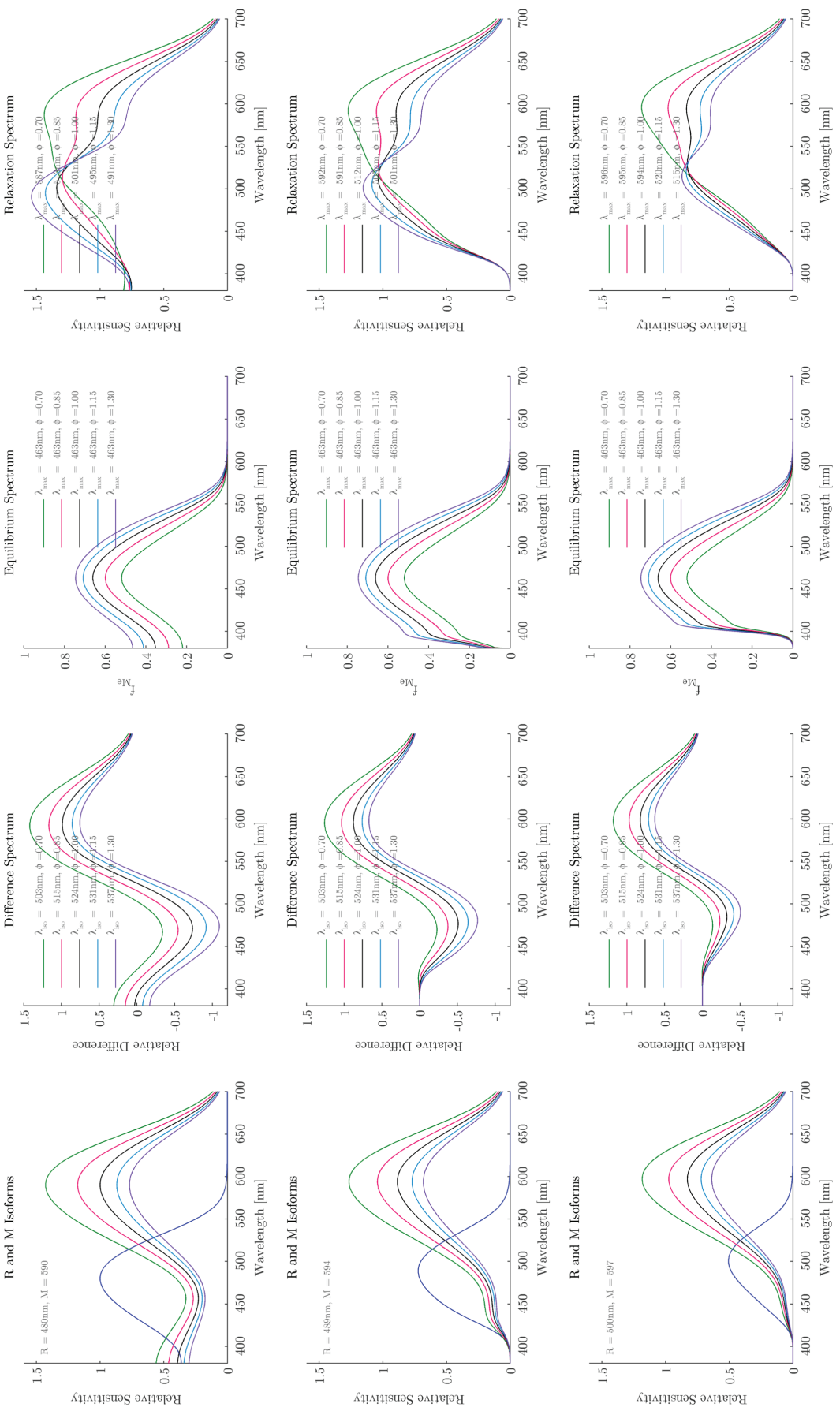

Figure 102: Effect of relative quantum efficiency (ϕ, B.4.1) on bistable action spectra.

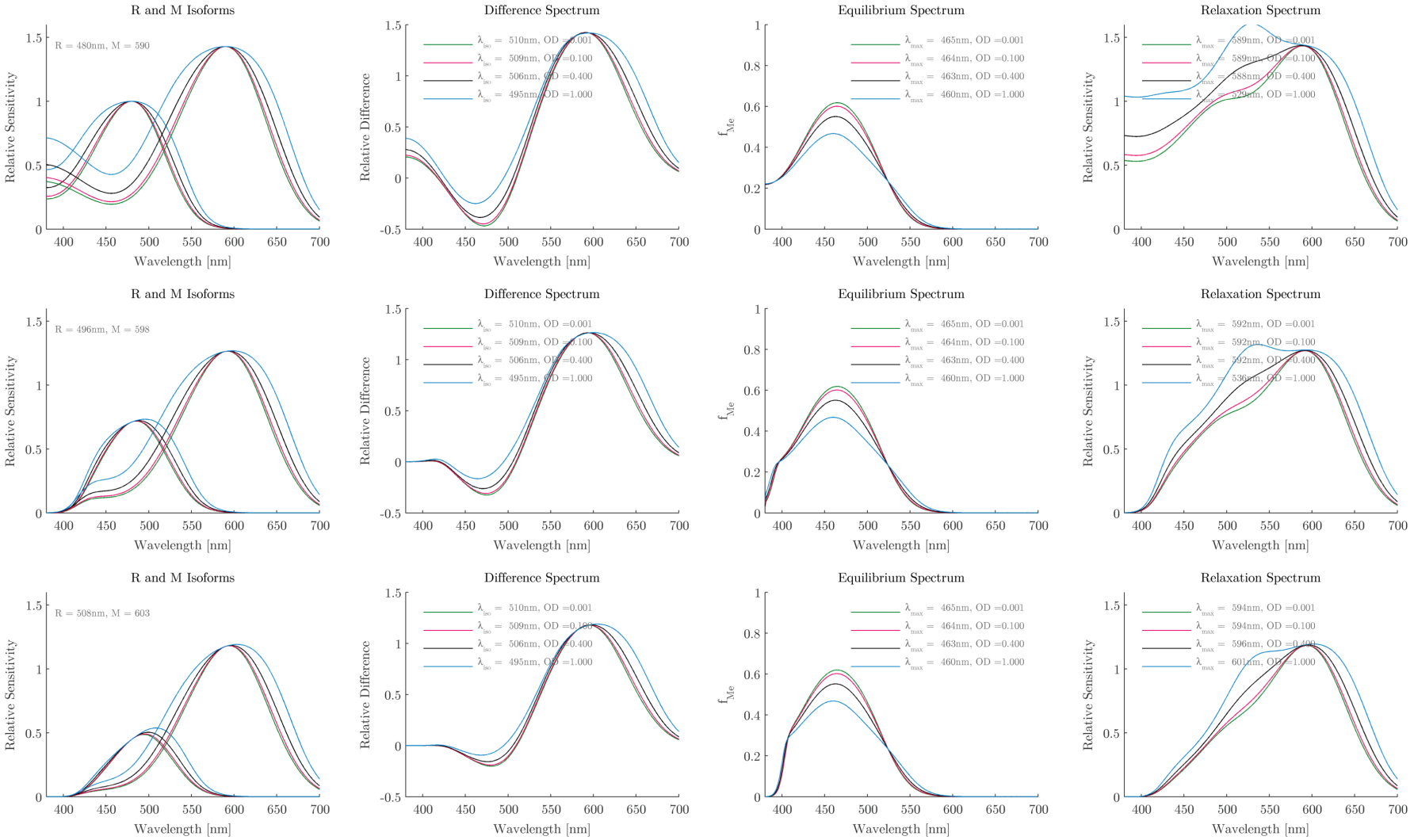

Figure 103: Effect of photopigment density (B.3.3) on bistable action spectra .

Table 8: **Detailed subjects characteristics** [mean +/- SD]

GROUP	Older	Younger	P-value
n	14	16	
Age [Older ≥55 ; Younger ≤18, ≥30 y.o]	61 ± 4.4	22.8 ± 4	<0.001
Sex [M/F]	10/4	10/6	0.605
Depression level (Steer et al. 1997)	3± 4.3	3 ± 2	1.000
Anxiety level (Beck et al. 1988)	1.9 ± 3	3.9 ± 3.7	0.132
Sleep disturbance, as assessed by the PSQI (Buysse et al. 1989)	3.2 ± 1.4	2.9 ± 1.3	0.485
Chronotype (Horne and Östberg 1976)	55.9 ± 8.3	40558	0.606
Ethnicity [Afro-American/Caucasian]	0/14	1/15	0.92
Date of the experiment [dd/mm/yy]	27/10/09 ± 30d	26/10/09 ± 34d	0.978
Hour of the experiment	14:04 ± 2:57	13:58 ± 2:44	0.924
LOCS-III (Chylack et al. 1993)	2.4 ± 0.7	1.00 ± 0	0.000
ORDER: Blue before green (BG) / Green before blue (GB)	9 BG/5 GB	8BG/8 GB	0.431

Table 9: **The individual responses for the three time bins** (Figure 59). The "NaN-threshold" to reject outliers was set to 100%. For individual PLR and "difference signal" waveforms see Section C.5. The subjects with code starting with ORI are from previous study by Mure et al. 2009.

PHASIC		SUSTAINED		PERSISTENCE	
subject	**value**	**subject**	**value**	**subject**	**value**
agahu	6.13	agahu	-2.93	agahu	NaN
orica	-22.44	orica	-55.78	orica	NaN
comma	-3.42	comma	18.72	comma	NaN
cordi	-2.77	cordi	-39.90	cordi	-29.59
douni	10.86	douni	21.23	douni	1.59
oriel	0.24	oriel	83.21	oriel	26.31
jidfa	26.63	jidfa	-14.25	jidfa	NaN
fifka	14.62	fifka	6.23	fifka	-9.51
garma	-14.72	garma	-13.20	garma	32.90
gauel	-1.46	gauel	35.11	gauel	-48.59
gilal	-9.20	gilal	0.19	gilal	16.48
masju	-8.87	masju	-30.20	masju	-58.73
orij	10.68	orij	72.20	orij	7.23
koskr	6.23	koskr	31.14	koskr	NaN
spama	-12.13	spama	-31.76	spama	-31.71
orimg	3.65	orimg	19.91	orimg	NaN
orimr	8.58	orimr	NaN	orimr	NaN
boune	NaN	boune	-28.64	boune	-36.55
ostpi	-4.46	ostpi	9.98	ostpi	22.92
mispi	-12.27	mispi	-3.66	mispi	34.94
oripi	2.77	oripi	-3.80	oripi	-2.62
orirb	17.57	orirb	18.46	orirb	NaN
byrso	-6.82	byrso	96.47	byrso	-91.86
vivta	-1.01	vivta	43.48	vivta	NaN

pulse) is shown in Figure 105, the difference calculated as $difference = (reference - test) \,/\, reference$.

C.5 BISTABILITY POTENTIATION IN HUMAN PLR

See 5.2.3.1 on page 145 for discussion of the plots.

C.5.1 *Individual PLR recordings*

The individual traces PLR recordings of the "short 590 nm condition" of the above "photic memory" experiment, with all tested subjects and subjects from previous study, are shown in Figure 106. The "normalized difference" between the reference (first 480 nm light pulse) and the test pulse (second 480 nm light pulse) is shown in Figure 107, the difference calculated as $difference = (reference - test) \,/\, reference$. The plots are identical by definition to the ones in C.4.1. The individual mean values for the three bins are shown in Table 9.

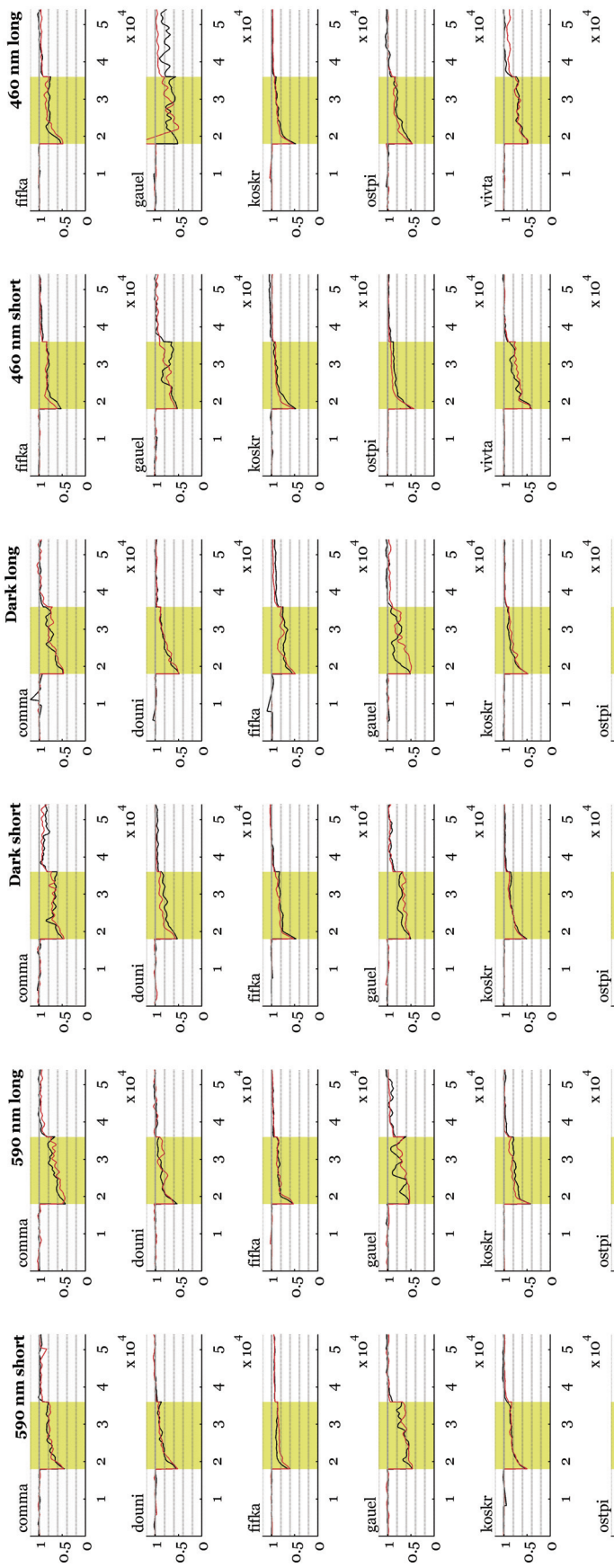

Figure 104: **Individual PLRs** Individual plots of all recordings done. The black line corresponds to the *reference* light stimulus (480 nm), and the red line is for the *test* light applied after the *adapting* light (460 nm, dark control and 590 nm). Full protocol was not completed for 2 subjects for the 460 nm condition, thus the empty subplot boxes at the bottom-right corner. The responses are normalized so that the mean of the first 5 minutes is unity (0 -18'000 data samples), the light was administered at 5 minutes (18'001th data sample) for 5 minutes (until 36'000 data sample), followed by a 5 minute post-light dark period (until 54'000 data points).

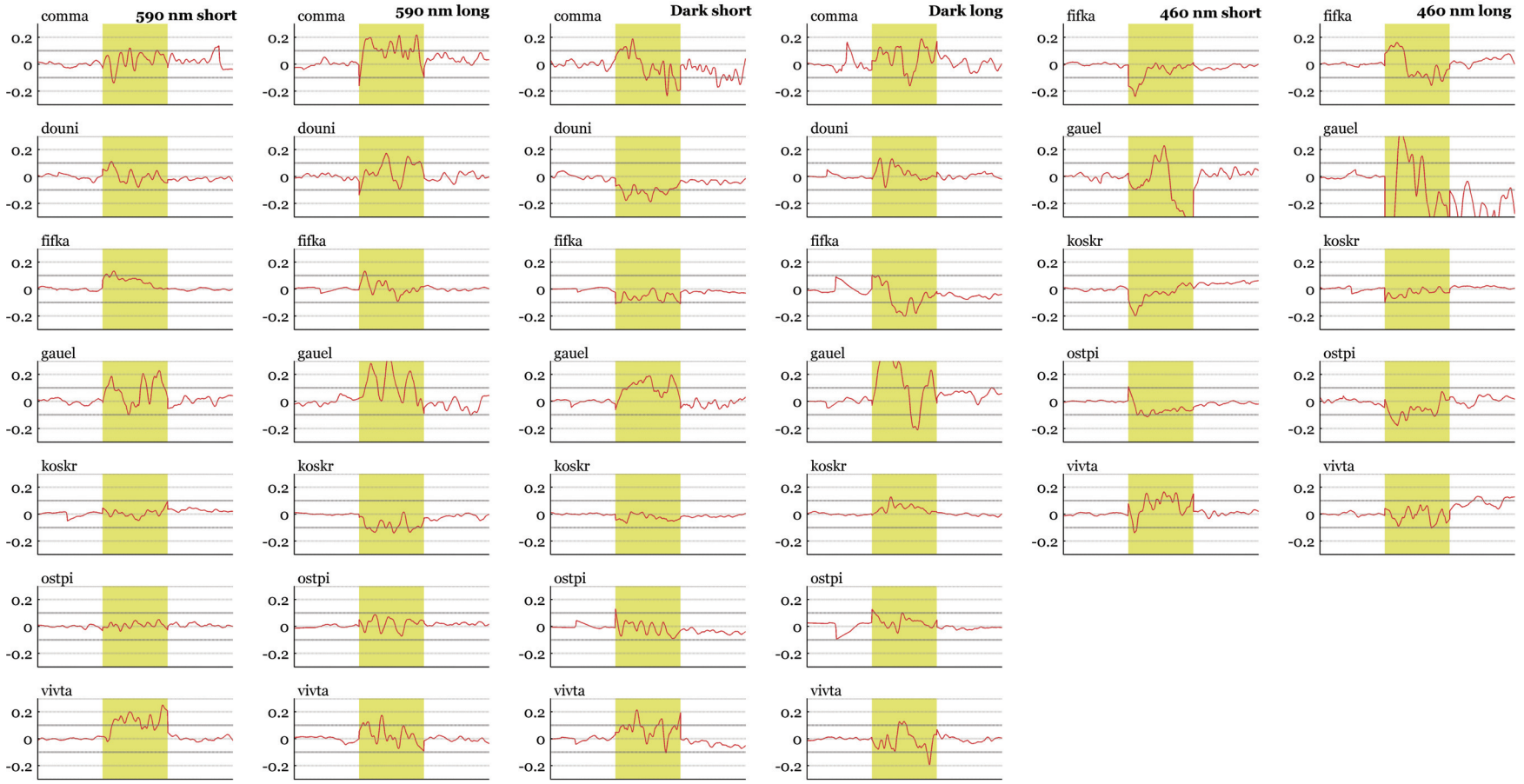

Figure 105: **Individual Difference** Individual differences of the traces shown in . The difference (i.e. the potentiation or suppression) was calculated as before in Mure et al. 2009 as $difference = (reference - test)/reference$. These results are used for all subsequent analysis and this plot serves as a visual tool for inspecting the "goodness" of the PLR responses. The plot demonstrates at which time the potentiation or suppression has occurred, as only potentiation could be expected in more steady-state opposed to the phasic portion. Additionally we can see that the subject "GAUEL" exhibit very oscillatory pupil behavior both here and in individual PLR recordings (Figure 104) indicating that he/she was not that suitable as a subject. Full protocol was not completed for 2 subjects for the 460 nm condition, thus the empty subplot boxes at the bottom-right corner.

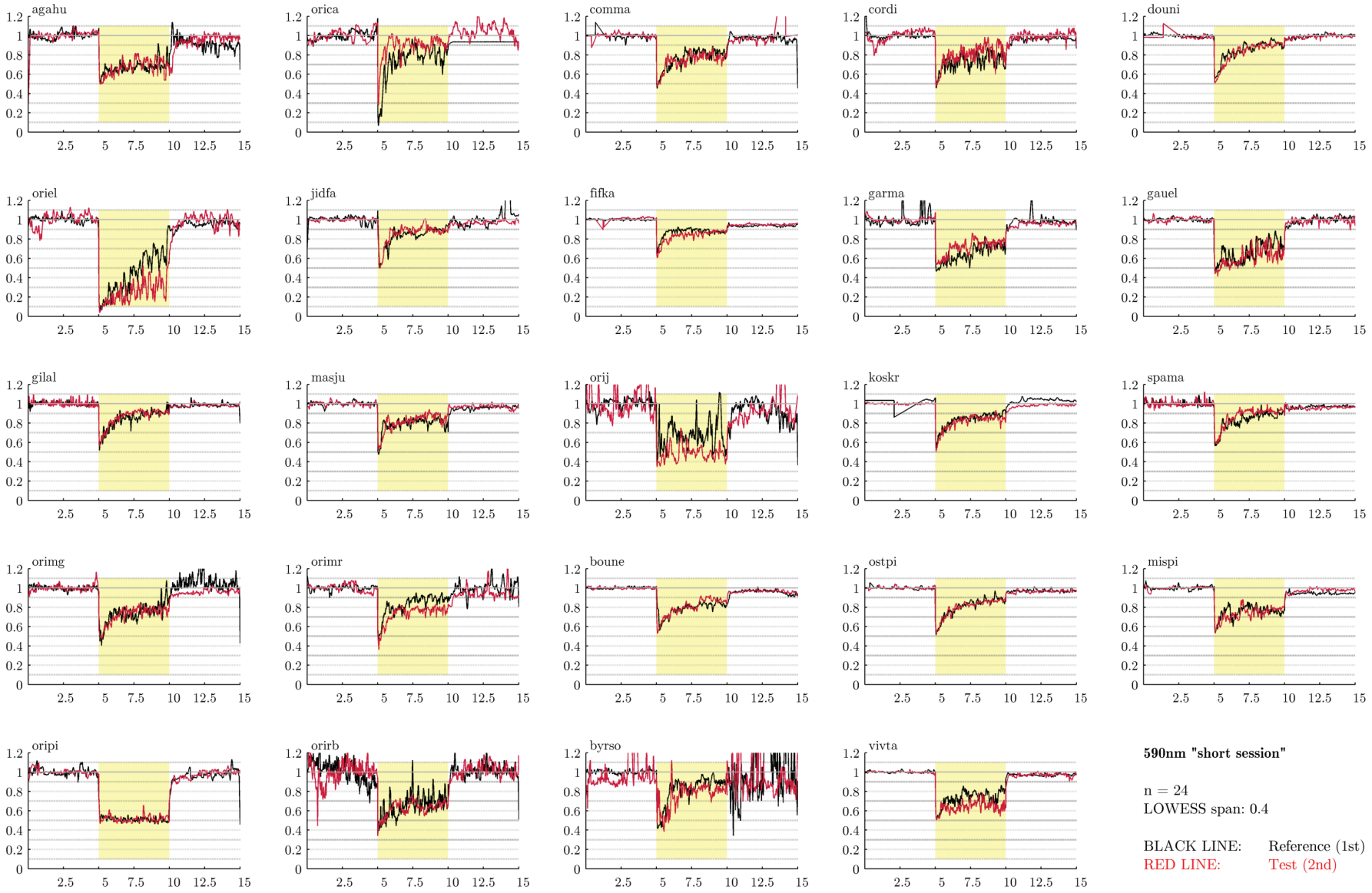

Figure 106: **Individual PLRs** Individual plots of all recordings done. The black line corresponds to the *reference* light stimulus (480 nm), and the red line is for the *test* light applied after the *adapting* light (590 nm). The responses are normalized so that the mean of the first 5 minutes is unity, the light was administered at 5 minutes for 5 minutes, followed by a 5 minute post-light dark period. The subjects with code starting with ORI are from previous study by Mure et al. 2009, and they clearly have more noisy PLR waveforms for the reasons discussed in 5.1.1 on page 135.

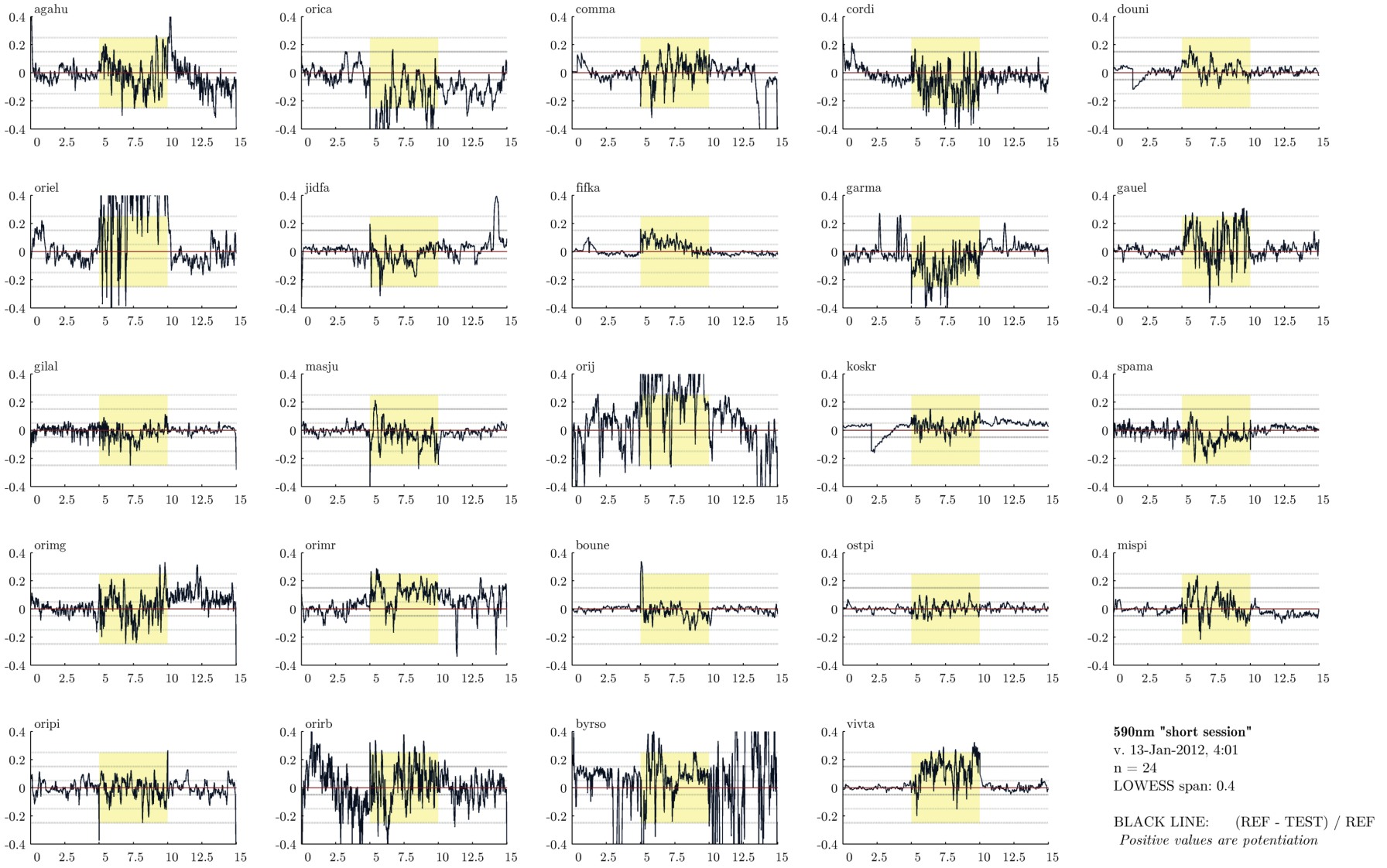

Figure 107: **Individual Difference** Individual differences of the traces shown in . The difference (i.e. the potentiation or suppression) was calculated as before in Mure et al. 2009 as $difference = (reference - test)/reference$. These results are used for all subsequent analysis and this plot serves as a visual tool for inspecting the "goodness" of the PLR responses. The plot demonstrates at which time the potentiation or suppression has occurred, as only potentiation could be expected in more steady-state opposed to the phasic portion. The subjects with code starting with ORI are from previous study by Mure et al. 2009, and they clearly have more noisy PLR waveforms for the reasons discussed in 5.1.1 on page 135.

BIBLIOGRAPHY

W. d. W. Abney. *Researches in Colour Vision*. Longmans, Green, London, 1913.

W. d. W. Abney and E. R. Festing. Colour photometry. *Philosophical Transactions of the Royal Society*, 177:423–456, 1886.

A. Adamantidis, M. C. Carter, and L. d. Lecea. Optogenetic deconstruction of sleep–wake circuitry in the brain. *Frontiers in Molecular Neuroscience*, 2:31, 2010. http://dx.doi.org/10.3389/neuro.02.031.2009.

P. Addison, J. Walker, and R. Guido. Time–frequency analysis of biosignals. *Engineering in Medicine and Biology Magazine, IEEE*, 28(5):14–29, 2009. http://dx.doi.org/10.1109/MEMB.2009.934244.

E. H. Adelson. Saturation and adaptation in the rod system. *Vision Research*, 22(10):1299–1312, 1982. http://dx.doi.org/10.1016/0042-6989(82)90143-2.

J. S. Adler, D. F. Kripke, R. T. Loving, and S. L. Berga. Peripheral vision suppression of melatonin. *Journal of Pineal Research*, 12 (1):49–52, Jan. 1992. http://dx.doi.org/10.1111/j.1600-079X.1992.tb00025.x.

N. C. Aggelopoulos and H. Meissl. Responses of neurones of the rat suprachiasmatic nucleus to retinal illumination under photopic and scotopic conditions. *J Physiol*, 523(1):211–222, Feb. 2000. http://dx.doi.org/10.1111/j.1469-7793.2000.t01-1-00211.x.

J. P. Aggleton. *The Amygdala: Neurobiological Aspects of Emotion, Memory, and Mental Dysfunction*. Wiley-Liss, Feb. 1992.

P. K. Ahnelt, H. Kolb, and R. Pflug. Identification of a subtype of cone photoreceptor, likely to be blue sensitive, in the human retina. *The Journal of Comparative Neurology*, 255(1):18–34, Jan. 1987. http://dx.doi.org/10.1002/cne.902550103.

E. A. Ainsbury, S. D. Bouffler, W. Dörr, J. Graw, C. R. Muirhead, A. A. Edwards, and J. Cooper. Radiation cataractogenesis: A review of recent studies. *Radiation Research*, 172(1):1–9, 2009. http://dx.doi.org/10.1667/RR1688.1.

H. Akaike. A new look at the statistical model identification. *IEEE Transactions on Automatic Control*, 19(6):716– 723, Dec. 1974.

P. Ala-Laurila, A. V. Kolesnikov, R. K. Crouch, E. Tsina, S. A. Shukolyukov, V. I. Govardovskii, Y. Koutalos, B. Wiggert, M. E. Estevez, and M. C. Cornwall. Visual cycle: Dependence of retinol production and removal on photoproduct decay and cell morphology. *The Journal of General Physiology*, 128(2):153–169, Aug. 2006. http://dx.doi.org/10.1085/jgp.200609557.

C. Albani, G. N. Nöll, and S. Yoshikami. Rhodopsin regeneration, calcium, and the control of the dark current in vertebrate rods. *Photochemistry and Photobiology*, 32(4):515–520, Oct. 1980. http://dx.doi.org/10.1111/j.1751-1097.1980.tb03797.x.

T. S. Aleman, S. G. Jacobson, J. D. Chico, M. L. Scott, A. Y. Cheung, E. A. M. Windsor, M. Furushima, T. M. Redmond, J. Bennett, K. Palczewski, and A. V. Cideciyan. Impairment of the transient pupillary light reflex in rpe65-/- mice and humans with leber congenital amaurosis. *Investigative Ophthalmology & Visual Science*, 45(4):1259 –1271, Apr. 2004. http://dx.doi.org/10.1167/iovs.03-1230.

K. R. Alexander and S. A. Kelly. The influence of cones on rod saturation with flashed backgrounds. *Vision Research*, 24 (5):507–511, 1984. http://dx.doi.org/10.1016/0042-6989(84)90048-8.

E. Alexandridis and E. Dodt. Pupillenlichtreflexe und pupillenweite einer stäbchenmonochromatin. *Albrecht von Graefes Archiv für Klinische und Experimentelle Ophthalmologie*, 173:153–161, 1967. http://dx.doi.org/10.1007/BF00405718.

E. Alexandridis and E. R. Koeppe. Die spektrale empfindlichkeit der für den pupillenlichtreflex verantwortlichen photoreceptoren beim menschen. *Albrecht von Graefes Archiv für Klinische und Experimentelle Ophthalmologie*, 177:136–151, 1969. http://dx.doi.org/10.1007/BF00431624.

M. Ali. Pattern of EEG recovery under photic stimulation by light of different colors. *Electroencephalography and Clinical Neurophysiology*, 33(3):332–335, Sept. 1972. http://dx.doi.org/10.1016/0013-4694(72)90162-9.

A. E. Allen, M. A. Cameron, T. M. Brown, A. A. Vugler, and R. J. Lucas. Visual responses in mice lacking critical components of all known retinal phototransduction cascades. *PloS One*, 5(11):e15063, 2010. http://dx.doi.org/10.1371/journal.pone.0015063.

A. E. Allen, T. M. Brown, and R. J. Lucas. A distinct contribution of Short-Wavelength-Sensitive cones to Light-Evoked activity in the mouse pretectal olivary nucleus. *The Journal of Neuroscience: The Official Journal of the Society for Neuroscience*, 31(46):16833–16843, Nov. 2011. http://dx.doi.org/10.1523/JNEUROSCI.2505-11.2011.

E. Almagor, P. Hillman, and B. Minke. Upper limit on translational diffusion of visual pigment in intact unfixed barnacle photoreceptors. *Biophysics of Structure and Mechanism*, 5:243–248, 1979. http://dx.doi.org/10.1007/BF00535453.

M. Alpern and D. J. Benson. Directional sensitivity of the pupillomotor photoreceptors. *American Journal of Optometry and Archives of American Academy of Optometry*, 30(11):

569–580, Nov. 1953. http://www.ncbi.nlm.nih.gov/pubmed/13104602.

M. Alpern and F. W. Campbell. The spectral sensitivity of the consensual light reflex. *The Journal of physiology*, 164:478–507, Dec. 1962. http://www.ncbi.nlm.nih.gov/pubmed/14012269.

M. Alpern and F. W. Campbell. The behaviour of the pupil during dark-adaptation. *J. Physiol.*, 165:5–7, 1963.

M. Alpern and N. Ohba. The effect of bleaching and backgrounds on pupil size. *Vision Research*, 12(5):943–951, May 1972. http://dx.doi.org/10.1016/0042-6989(72)90016-8.

M. Alpern and E. N. Pugh. The density and photosensitivity of human rhodopsin in the living retina. *The Journal of Physiology*, 237(2):341–370, Mar. 1974. http://www.ncbi.nlm.nih.gov/pubmed/4825455.

M. Alpern and F. Zwas. The wavelength variation of the directional sensitivity of the stiles [pi]1([mu]). *Vision Research*, 19(10):1077–1087, 1979. http://dx.doi.org/10.1016/0042-6989(79)90002-6.

M. Alpern, S. Kitai, and J. D. Isaacson. The dark-adaptation process of the pupillomotor photoreceptors. *American Journal of Ophthalmology*, 48(5)Pt 2:583–593, Nov. 1959. http://www.ncbi.nlm.nih.gov/pubmed/13792913.

M. Alpern, C. C. Ching, and K. Kitahara. The directional sensitivity of retinal rods. *The Journal of Physiology*, 343:577–592, Oct. 1983. http://www.ncbi.nlm.nih.gov/pubmed/6644624.

M. Alpern, H. Kitahara, and G. Fielder. The change in color matches with retinal angle of incidence of the colorimeter beams. *Vision Research*, 27(10):1763–1778, 1987. http://dx.doi.org/10.1016/0042-6989(87)90105-2.

C. M. Altimus, A. D. Güler, K. L. Villa, D. S. McNeill, T. A. LeGates, and S. Hattar. Rods-cones and melanopsin detect light and dark to modulate sleep independent of image formation. *Proceedings of the National Academy of Sciences*, 105(50):19998–20003, 2008. http://dx.doi.org/10.1073/pnas.0808312105.

C. M. Altimus, A. D. Guler, N. M. Alam, A. C. Arman, G. T. Prusky, A. P. Sampath, and S. Hattar. Rod photoreceptors drive circadian photoentrainment across a wide range of light intensities. *Nat Neurosci*, 13(9):1107–1112, 2010. http://dx.doi.org/10.1038/nn.2617.

W. Ambach, M. Blumthaler, T. Schöpf, E. Ambach, F. Katzgraber, F. Daxecker, and A. Daxer. Spectral transmission of the optical media of the human eye with respect to keratitis and cataract formation. *Documenta Ophthalmologica*, 88(2):165–173, June 1994. http://dx.doi.org/10.1007/BF01204614.

M. Andersen, S. Kleindienst, L. Yi, J. Lee, M. Bodart, and B. Cutler. An intuitive daylighting performance analysis and optimization approach. *Building Research & Information*, 36(6):593–607, 2008. http://dx.doi.org/10.1080/09613210802243159.

M. Andersen, J. Mardaljevic, and S. W. Lockley. A framework for predicting the non-visual effects of daylight – part i: photobiology- based model. *Lighting Research and Technology*, 44(1):37–53, Mar. 2012. http://dx.doi.org/10.1177/1477153511435961.

G. Anderson, S. Clough, F. Kneizys, J. Chetwynd, and E. Shettle. AFGL atmospheric constituent profiles (0–120 km). Technical Report Technical report AFGL-TR-86-0110,, Air Force Geophysics Laboratory, Hanscom AFB, MA, 1986.

J. L. Anderson, C. A. Glod, J. Dai, Y. Cao, and S. W. Lockley. Lux vs. wavelength in light treatment of seasonal affective disorder. *Acta Psychiatrica Scandinavica*, 9999(9999), 2009. http://dx.doi.org/10.1111/j.1600-0447.2009.01345.x.

M. L. Anderson and R. L. Purple. Circadian rhythms and variability of the clinical electro-oculogram. *Investigative Ophthalmology & Visual Science*, 19(3):278–288, Mar. 1980. http://www.ncbi.nlm.nih.gov/pubmed/7358478.

K. Ando and D. F. Kripke. Light attenuation by the human eyelid. *Biological Psychiatry*, 39(1):22–25, Jan. 1996. http://dx.doi.org/10.1016/0006-3223(95)00109-3.

J. M. Angueyra, C. Pulido, G. Malagón, E. Nasi, and M. D. P. Gomez. Melanopsin-Expressing amphioxus photoreceptors transduce light via a phospholipase c signaling cascade. *PloS One*, 7(1):e29813, 2012. http://dx.doi.org/10.1371/journal.pone.0029813.

D. Arendt. Evolution of eyes and photoreceptor cell types. *The International Journal of Developmental Biology*, 47(7-8):563–71, 2003. http://www.ncbi.nlm.nih.gov/pubmed/14756332.

V. Y. Arshavsky. Like night and day: Rods and cones have different pigment regeneration pathways. *Neuron*, 36(1):1–3, Sept. 2002. http://dx.doi.org/10.1016/S0896-6273(02)00937-6.

V. Y. Arshavsky. The retinoid cycle in drosophila. *Current Biology*, 20(3):R96–R98, Feb. 2010. http://dx.doi.org/10.1016/j.cub.2009.12.039.

V. Y. Arshavsky and M. E. Burns. Photoreceptor signaling: Supporting vision across a wide range of light intensities. *Journal of Biological Chemistry*, 287(3):1620 –1626, Jan. 2012. http://dx.doi.org/10.1074/jbc.R111.305243.

K. Asakawa, N. Shoji, H. Ishikawa, and K. Shimizu. New approach for the glaucoma detection with pupil perimetry. *Clinical Ophthalmology (Auckland, N.Z.)*, 4:617–623, 2010. http://dx.doi.org/10.2147/OPTH.S9936.

J. Aschoff. Exogenous and endogenous components in circadian rhythms. *Cold Spring Harbor Symposia on Quantitative Biology*, 25: 11–28, 1960. http://www.ncbi.nlm.nih.gov/pubmed/13684695.

J. Aschoff and C. Goetz. Masking of circadian activity rhythms in hamsters by darkness. *Journal of Comparative Physiology A*, 162(4):559–562, 1988. http://dx.doi.org/10.1007/BF00612521.

J. Aschoff, M. Fatranska, H. Giedke, P. Doerr, D. Stamm, and H. Wisser. Human circadian rhythms in continuous darkness: Entrainment by social cues. *Science*, 171(3967): 213 –215, Jan. 1971. http://dx.doi.org/10.1126/science.171.3967.213.

ASTM. Standard tables for terrestrial direct normal solar spectral irradiance for air mass 1.5 standard no. e891-87. Technical report, American Society for Testing and Materials, Philadelphia, Pennsylvania, 1987.

G. Aston-Jones and J. D. Cohen. An integrative theory of locus coeruleus-norepinephrine function: adaptive gain and optimal performance. *Annual Review of Neuroscience*, 28:403–450, 2005. http://dx.doi.org/10.1146/annurev.neuro.28.061604.135709.

Z. Atzmon, P. Hillman, and S. Hochstein. Visual response in barnacle photoreceptors is not initiated by transitions to and from metarhodopsin. *Nature*, 274(5666):74–76, July 1978. http://dx.doi.org/10.1038/274074a0.

Z. Atzmon, S. Hochstein, and P. Hillman. Transduction in photoreceptors: Determination of the pigment transition or state coupled to excitation. *Biophysics of Structure and Mechanism*, 5:249–253, 1979. http://dx.doi.org/10.1007/BF00535454.

E. J. Augenstein and J. Pugh, E N. The dynamics of the pi 1 colour mechanism: further evidence for two sites of adaptation. *The Journal of Physiology*, 272(2):247–281, Nov. 1977. http://www.ncbi.nlm.nih.gov/pubmed/592192.

R. Azeredo da Silveira and B. Roska. Cell types, circuits, computation. *Current Opinion in Neurobiology*, 21(5):664–671, Oct. 2011. http://dx.doi.org/10.1016/j.conb.2011.05.007.

H. Babcock. The possibility of compensating astronomical seeing. *Publications of the Astronomical Society of the Pacific*, 65(386):229, 1953.

P. Badia, B. Myers, M. Boecker, J. Culpepper, and J. R. Harsh. Bright light effects on body temperature, alertness, EEG and behavior. *Physiology & behavior*, 50(3):583–8, Sept. 1991. http://dx.doi.org/10.1016/0031-9384(91)90549-4.

J. E. Baggs, T. S. Price, L. DiTacchio, S. Panda, G. A. FitzGerald, and J. B. Hogenesch. Network features of the mammalian circadian clock. *PLoS Biology*, 7(3): e52, 2009. http://dx.doi.org/10.1371%2Fjournal.pbio.1000052.

K. Bär, W. Greiner, T. Jochum, M. Friedrich, G. Wagner, and H. Sauer. The influence of major depression and its treatment on heart rate variability and pupillary light reflex parameters. *Journal of Affective Disorders*, 82(2):245–252, Oct. 2004. http://dx.doi.org/10.1016/j.jad.2003.12.016.

K. Bär, M. K. Boettger, S. Till, J. Dolicek, and H. Sauer. Lateralization of pupillary light reflex parameters. *Clinical Neurophysiology: Official Journal of the International Federation of Clinical Neurophysiology*, 116(4):790–8, Apr. 2005. http://dx.doi.org/10.1016/j.clinph.2004.11.007.

J. L. Barbur, A. J. Harlow, and A. Sahraie. Pupillary responses to stimulus structure, colour and movement. *Ophthalmic and Physiological Optics*, 12(2):137–141, 1992. http://dx.doi.org/10.1111/j.1475-1313.1992.tb00276.x.

J. L. Barbur, J. Wolf, and P. Lennie. Visual processing levels revealed by response latencies to changes in different visual attributes. *Proceedings. Biological Sciences / The Royal Society*, 265(1412):2321–2325, Dec. 1998. http://dx.doi.org/10.1098/rspb.1998.0578.

J. L. Barbur, S. Moro, J. A. Harlow, B. L. Lam, and M. Liu. Comparison of pupil responses to luminance and colour in severe optic neuritis. *Clinical Neurophysiology*, 115 (11):2650–2658, Nov. 2004. http://dx.doi.org/10.1016/j.clinph.2004.05.022.

J. L. Barbur, E. Konstantakopoulou, M. Rodriguez-Carmona, J. A. Harlow, A. G. Robson, and J. D. Moreland. The macular assessment profile test – a new VDU-based technique for measuring the spatial distribution of the macular pigment, lens density and rapid flicker sensitivity. *Ophthalmic and Physiological Optics*, 30(5):470–483, 2010. http://dx.doi.org/10.1111/j.1475-1313.2010.00748.x.

H. B. Barlow and W. R. Levick. Changes in the maintained discharge with adaptation level in the cat retina. *The Journal of Physiology*, 202(3):699–718, June 1969. http://www.ncbi.nlm.nih.gov/pubmed/5789945.

J. Barlow, R B, E. Kaplan, G. H. Renninger, and T. Saito. Efferent control of circadian rhythms in the limulus lateral eye. *Neuroscience Research. Supplement: The Official Journal of the Japan Neuroscience Society*, 2: S65–78, 1985. http://www.ncbi.nlm.nih.

gov/pubmed/2867510.

R. Barlow and H. R. Helga Kolb. Circadian and efferent modulation of visual sensitivity. In *Concepts and Challenges in Retinal Biology (Progress in Brain Research)*, volume Volume 131, pages 487–503. Elsevier, 2001. http://dx.doi.org/10.1016/S0079-6123(01)31039-7.

R. B. Barlow. Dark and light adaptation: Psychophysics. In D. Jameson and L. Hurvich, editors, *Handbook of Sensory Physiology*, page 1–28. Springer-Verlag, Berlin, 1972.

S. N. Barnes and T. H. Goldsmith. Dark adaptation, sensitivity, and rhodopsin level in the eye of the lobster,Homarus. *Journal of Comparative Physiology A*, 120:143–159, 1977. http://dx.doi.org/10.1007/BF00619311.

L. Barr and M. Alpern. Photosensitivity of the frog iris. *The Journal of General Physiology*, 46(6):1249 –1265, July 1963. http://dx.doi.org/10.1085/jgp.46.6.1249.

F. J. Bartl and R. Vogel. Structural and functional properties of metarhodopsin III: recent spectroscopic studies on deactivation pathways of rhodopsin. *Physical Chemistry Chemical Physics*, 9:1648, 2007. http://dx.doi.org/10.1039/b616365c.

C. J. Bassi and M. K. Powers. Daily fluctuations in the detectability of dim lights by humans. *Physiology & Behavior*, 38(6):871–877, 1986. http://dx.doi.org/10.1016/0031-9384(86)90056-9.

R. Batra and R. B. Barlow. Efferent control of temporal response properties of the limulus lateral eye. *The Journal of General Physiology*, 95(2):229 –244, Feb. 1990. http://dx.doi.org/10.1085/jgp.95.2.229.

B. Battelle. Circadian efferent input to limulus eyes: anatomy, circuitry, and impact. *Microscopy Research and Technique*, 58(4):345–355, Aug. 2002. http://dx.doi.org/10.1002/jemt.10142.

F. Baumann and B. Hadjilazaro. A depolarizing aftereffect of intense light in the drone visual receptor. *Vision Research*, 12(1):17–31, Jan. 1972. http://dx.doi.org/10.1016/0042-6989(72)90134-4.

S. B. Baver, G. E. Pickard, P. J. Sollars, and G. E. Pickard. Two types of melanopsin retinal ganglion cell differentially innervate the hypothalamic suprachiasmatic nucleus and the olivary pretectal nucleus. *European Journal of Neuroscience*, 27(7):1763–1770, 2008. http://dx.doi.org/10.1111/j.1460-9568.2008.06149.x.

B. E. Bayer. Color imaging array, July 1976.

D. Baylor. Photoreceptor signals and vision. proctor lecture. *Invest. Ophthalmol. Vis. Sci.*, 28(1):34–49, Jan. 1987. http://www.ncbi.nlm.nih.gov/pubmed/3026986.

D. A. Baylor and A. L. Hodgkin. Changes in time scale and sensitivity in turtle photoreceptors. *The Journal of Physiology*, 242 (3):729–758, Nov. 1974. http://www.ncbi.nlm.nih.gov/pubmed/4449053.

D. A. Baylor, A. L. Hodgkin, and T. D. Lamb. Reconstruction of the electrical responses of turtle cones to flashes and steps of light. *The Journal of Physiology*, 242(3):759–791, Nov. 1974a. http://www.ncbi.nlm.nih.gov/pubmed/4449054.

D. A. Baylor, A. L. Hodgkin, and T. D. Lamb. The electrical response of turtle cones to flashes and steps of light. *The Journal of Physiology*, 242(3):685–727, Nov. 1974b. http://www.ncbi.nlm.nih.gov/pubmed/4449052.

D. A. Baylor, T. D. Lamb, and K. W. Yau. Responses of retinal rods to single photons. *The Journal of Physiology*, 288:613–634, Mar. 1979. http://www.ncbi.nlm.nih.gov/pubmed/112243.

D. A. Baylor, B. J. Nunn, and J. L. Schnapf. The photocurrent, noise and spectral sensitivity of rods of the monkey macaca fascicularis. *The Journal of Physiology*, 357:575–607, Dec. 1984. http://www.ncbi.nlm.nih.gov/pubmed/6512705.

D. A. Baylor, B. J. Nunn, and J. L. Schnapf. Spectral sensitivity of cones of the monkey macaca fascicularis. *The Journal of Physiology*, 390(1):145–160, 1987. http://www.ncbi.nlm.nih.gov/pubmed/3443931.

J. Beatty. Phasic not tonic pupillary responses vary with auditory vigilance performance. *Psychophysiology*, 19(2):167–172, Mar. 1982. http://dx.doi.org/10.1111/j.1469-8986.1982.tb02540.x.

J. Beatty and B. Lucero-Wagoner. The pupillary system. In J. Cacioppo and L. G. Tassimary, editors, *Handbook of Psychophysiology*, pages 142–162. Cambridge University Press, 2 edition, 2000.

J. Beatty and B. Wagoner. Pupillometric signs of brain activation vary with level of cognitive processing. *Science*, 199(4334):1216 –1218, Mar. 1978. http://dx.doi.org/10.1126/science.628837.

C. Beaulieu, M. Rufiange, M. Dumont, and P. Lachapelle. Modulation of ERG retinal sensitivity parameters with light environment and photoperiod. *Documenta Ophthalmologica*, 118(2):89–99, Apr. 2009. http://dx.doi.org/10.1007/s10633-008-9137-6.

A. T. Beck, N. Epstein, G. Brown, and R. A. Steer. An inventory for measuring clinical anxiety: Psychometric properties. *Journal of Consulting and Clinical Psychology*, 56(6):893–897, Dec. 1988. http://dx.doi.org/10.1037/0022-006X.56.6.893.

D. G. M. Beersma, B. J. Hoenders, A. M. J. Huiser, and P. Van Toorn. Refractive index of the fly rhabdomere. *Journal of the Optical Society of America*, 72(5):583–588, May 1982. http://dx.doi.org/10.1364/JOSA.

72.000583.

F. Behar-Cohen, C. Martinsons, F. Viénot, G. Zissis, A. Barlier-Salsi, J. Cesarini, O. Enouf, M. Garcia, S. Picaud, and D. Attia. Light-emitting diodes (LED) for domestic lighting: Any risks for the eye? *Progress in Retinal and Eye Research*, 30(4):239–257, July 2011. http://dx.doi.org/10.1016/j.preteyeres.2011.04.002.

D. Behn, A. Doke, J. Racine, C. Casanova, S. Chemtob, and P. Lachapelle. Dark adaptation is faster in pigmented than albino rats. *Documenta Ophthalmologica. Advances in Ophthalmology*, 106(2):153–159, Mar. 2003. http://dx.doi.org/10.1023/A:1022511918823.

K. G. Belani, D. I. Sessler, M. D. Larson, M. A. Lopez, D. E. Washington, M. Ozaki, J. McGuire, B. Merrifield, and M. Schroeder. The pupillary light reflex. effects of anesthetics and hyperthermia. *Anesthesiology*, 79(1):23–27, July 1993. http://www.ncbi.nlm.nih.gov/pubmed/8342824.

M. A. Belenky, C. A. Smeraski, I. Provencio, P. J. Sollars, and G. E. Pickard. Melanopsin retinal ganglion cells receive bipolar and amacrine cell synapses. *The Journal of Comparative Neurology*, 460(3):380–393, June 2003. http://dx.doi.org/10.1002/cne.10652.

A. Bell, A. C. James, M. Kolic, R. W. Essex, and T. Maddess. Dichoptic multifocal pupillography reveals afferent visual field defects in early type 2 diabetes. *Investigative Ophthalmology & Visual Science*, 51(1):602 –608, Jan. 2010. http://dx.doi.org/10.1167/iovs.09-3659.

L. Bellia, F. Bisegna, and G. Spada. Lighting in indoor environments: Visual and non-visual effects of light sources with different spectral power distributions. *Building and Environment*, 46(10):1984–1992, Oct. 2011a. http://dx.doi.org/10.1016/j.buildenv.2011.04.007.

L. Bellia, F. Bisegna, and G. Spada. Lighting in indoor environments: Visual and non-visual effects of light sources with different spectral power distributions. *Building and Environment*, 46(10):1984–1992, Oct. 2011b. http://dx.doi.org/10.1016/j.buildenv.2011.04.007.

J. Bellingham, S. S. Chaurasia, Z. Melyan, C. Liu, M. A. Cameron, E. E. Tarttelin, P. M. Iuvone, M. W. Hankins, G. Tosini, and R. J. Lucas. Evolution of melanopsin photoreceptors: Discovery and characterization of a new melanopsin in nonmammalian vertebrates. *PLoS Biology*, 4(8), Aug. 2006. http://dx.doi.org/10.1371/journal.pbio.0040254.

G. Belušič. ERG in drosophila. In *Electroretinograms*, page 238. InTech, Aug. 2011.

G. Belušič, P. Pirih, and D. G. Stavenga. Photoreceptor responses of fruitflies with normal and reduced arrestin content studied by simultaneous measurements of visual pigment fluorescence and ERG. *Journal of Comparative Physiology A*, 196(1):23–35, 2010. http://dx.doi.org/10.1007/s00359-009-0489-5.

E. E. Benarroch. The melanopsin system: Phototransduction, projections, functions, and clinical implications. *Neurology*, 76(16):1422–1427, Apr. 2011. http://dx.doi.org/10.1212/WNL.0b013e31821671a5.

W. Bender. The effect of pain and emotional stimuli and alcohol upon pupillary reflex activity. *Psychological Monographs*, 1933.

J. J. Benedetto and G. E. Pfander. Periodic wavelet transforms and periodicity detection. *SIAM Journal on Applied Mathematics*, 62(4):1329–1368, Apr. 2002.

S. Benloucif, M. J. Guico, K. J. Reid, L. F. Wolfe, M. L'Hermite-Baleriaux, and P. C. Zee. Stability of melatonin and temperature as circadian phase markers and their relation to sleep times in humans. *J Biol Rhythms*, 20(2):178–188, Apr. 2005. http://dx.doi.org/10.1177/0748730404273983.

S. Benloucif, K. Green, M. L'Hermite-Baleriaux, S. Weintraub, L. Wolfe, and P. Zee. Responsiveness of the aging circadian clock to light. *Neurobiology of Aging*, 27(12):1870–1879, Dec. 2006. http://dx.doi.org/10.1016/j.neurobiolaging.2005.10.011.

S. Benloucif, H. J. Burgess, E. B. Klerman, A. J. Lewy, B. Middleton, P. J. Murphy, B. L. Parry, and V. L. Revell. Measuring melatonin in humans. *Journal of Clinical Sleep Medicine: JCSM: Official Publication of the American Academy of Sleep Medicine*, 4(1):66–9, Feb. 2008. http://www.ncbi.nlm.nih.gov/pubmed/18350967.

C. Benn and S. Ellison. Brightness of the night sky over la palma. *New Astronomy Reviews*, 42(6-8):503–507, Nov. 1998. http://dx.doi.org/10.1016/S1387-6473(98)00062-1.

J. L. Benovic, F. Mayor, R. L. Somers, M. G. Caron, and R. J. Lefkowitz. Light-dependent phosphorylation of rhodopsin by [beta]-adrenergic receptor kinase. *Nature*, 321(6073):869–872, June 1986. http://dx.doi.org/10.1038/321869a0.

T. T. Berendschot and D. van Norren. On the age dependency of the macular pigment optical density. *Experimental Eye Research*, 81(5):602–609, Nov. 2005. http://dx.doi.org/10.1016/j.exer.2005.03.019.

T. T. Berendschot, J. van de Kraats, and D. van Norren. Foveal cone mosaic and visual pigment density in dichromats. *The Journal of Physiology*, 492(Pt 1):307–314, Apr. 1996. http://www.ncbi.nlm.nih.gov/pubmed/8730604/.

O. Bergamin and R. H. Kardon. Greater pupillary escape differentiates central from peripheral visual field loss. *Ophthalmology*, 109(4):771–780, Apr. 2002. http://dx.doi.org/10.1016/S0161-6420(01)01026-0.

O. Bergamin and R. H. Kardon. Latency of the pupil light reflex: Sample rate, stimulus intensity, and variation in normal subjects. *Invest. Ophthalmol. Vis. Sci.*, 44(4): 1546–1554, Apr. 2003. http://dx.doi.org/10.1167/iovs.02-0468.

O. Bergamin, A. Schoetzau, K. Sugimoto, and M. Zulauf. The influence of iris color on the pupillary light reflex. *Graefe's Archive for Clinical and Experimental Ophthalmology*, 236(8):567–570, July 1998. http://dx.doi.org/10.1007/s004170050122.

O. Bergamin, M. B. Zimmerman, and R. H. Kardon. Pupil light reflex in normal and diseased eyes: Diagnosis of visual dysfunction using waveform partitioning. *Ophthalmology*, 110(1):106–114, Jan. 2003. http://dx.doi.org/10.1016/S0161-6420(02)01445-8.

A. Berk, L. S. Bernstein, and D. C. Robertson. MODTRAN: a moderate resolution model for LOWTRAN. Technical report, July 1987. http://adsabs.harvard.edu/abs/1987ssi..reptR....B.

S. Berman, D. Jewett, G. Fein, G. Saika, and F. Ashford. Photopic luminance does not always predict perceived room brightness. *Lighting Research and Technology*, 22(1):37 – 41, Mar. 1990. http://dx.doi.org/10.1177/096032719002200103.

S. M. Berman. A new retinal photoreceptor should affect lighting practice. *Lighting Research and Technology*, 40(4):373–376, Dec. 2008. http://dx.doi.org/10.1177/1477153508097975.

S. M. Berman and R. D. Clear. Past vision studies can support a novel human photroreceptor. *Light & Engineering*, 16(2):88–94, 2008.

G. D. Bernard. Dark-processes following photoconversion of butterfly rhodopsins. *Biophysics of Structure and Mechanism*, 9:277–286, 1983. http://dx.doi.org/10.1007/BF00535663.

G. D. Bernard and W. Miller. What does antenna engineering have to do with insect eyes? *IEEE Student J.*, 1970.

D. Berson. Phototransduction in ganglion-cell photoreceptors. *Pflügers Archiv European Journal of Physiology*, 454(5):849–855, 2007. http://dx.doi.org/10.1007/s00424-007-0242-2.

D. M. Berson. Strange vision: ganglion cells as circadian photoreceptors. *Trends in Neurosciences*, 26(6):314–320, June 2003. http://dx.doi.org/10.1016/S0166-2236(03)00130-9.

D. M. Berson. Retinal ganglion cell types and their central projections. In *The Senses: A Comprehensive Reference*. Elsevier/Academic, New York, NY, USA, 2008.

D. M. Berson, F. A. Dunn, and M. Takao. Phototransduction by retinal ganglion cells that set the circadian clock. *Science*, 295 (5557):1070–1073, 2002. http://dx.doi.org/10.1126/science.1067262.

D. M. Berson, A. M. Castrucci, and I. Provencio. Morphology and mosaics of melanopsin-expressing retinal ganglion cell types in mice. *The Journal of Comparative Neurology*, 518(13):2405–2422, 2010. http://dx.doi.org/10.1002/cne.22381.

M. Bertalmio, G. Sapiro, V. Caselles, and C. Ballester. Image inpainting. In *Proceedings of the 27th annual conference on Computer graphics and interactive techniques*, SIGGRAPH '00, page 417–424, New York, NY, USA, 2000. ACM Press/Addison-Wesley Publishing Co. http://dx.doi.org/10.1145/344779.344972.

Bhalla and U. S. Ravi Iyengar. Emergent properties of networks of biological signaling pathways. *Science*, 283(5400):381 –387, Jan. 1999. http://dx.doi.org/10.1126/science.283.5400.381.

S. Bhardwaj, T. Ozcelebi, J. Lukkien, and R. Verhoeven. Semantic interoperability in a heterogeneous smart lighting system. In *2010 IEEE Symposium on Computers and Communications (ISCC)*, pages 1035–1040. IEEE, June 2010. http://dx.doi.org/10.1109/ISCC.2010.5546628.

W. Bi, S. Tsujimura, G. T. Plant, and J. L. Barbur. The contribution of the Rod/Melanopsin driven ganglion cells to the dynamic pupil light reflex response. *ARVO Meeting Abstracts*, 52(6):5287, Apr. 2011.

A. Bierman. Will switching to LED outdoor lighting increase sky glow? *Lighting Research and Technology*, Feb. 2012. http://dx.doi.org/10.1177/1477153512437147.

A. Bierman, T. R. Klein, and M. S. Rea. The daysimeter: a device for measuring optical radiation as a stimulus for the human circadian system. *Measurement Science and Technology*, 16(11):2292–2299, 2005. http://dx.doi.org/10.1088/0957-0233/16/11/023.

D. L. Bimler and G. V. Paramei. Bezold-Brücke effect in normal trichromats and protanopes. *Journal of the Optical Society of America A*, 22(10):2120–2136, Oct. 2005. http://dx.doi.org/10.1364/JOSAA.22.002120.

P. Bitsios, R. Prettyman, and E. Szabadi. Changes in autonomic function with age: A study of pupillary kinetics in healthy young and old people. *Age Ageing*, 25(6): 432–438, Nov. 1996a. http://dx.doi.org/10.1093/ageing/25.6.432.

P. Bitsios, E. Szabadi, and C. Bradshaw. The inhibition of the pupillary light reflex by the threat of an electric shock: a potential laboratory model of human anxiety. *J Psychopharmacol*, 10(4):279–287, Jan. 1996b. http://dx.doi.org/10.1177/026988119601000404.

K. Bizheva, R. Pflug, B. Hermann, B. Povazay, H. Sattmann, P. Qiu, E. Anger, H. Reitsamer, S. Popov, J. R. Taylor, A. Unterhuber, P. Ahnelt, and W. Drexler. Optophysiology: depth-resolved probing of retinal physiology with functional ultrahigh-resolution optical coherence tomography. *Proceedings of the National Academy of Sciences of the United States of America*, 103(13): 5066–5071, Mar. 2006. http://dx.doi.org/10.1073/pnas.0506997103.

S. Blackshaw and S. H. Snyder. Developmental expression pattern of phototransduction components in mammalian pineal implies a light-sensing function. *The Journal of Neuroscience: The Official Journal of the Society for Neuroscience*, 17(21):8074–8082, Nov. 1997. http://www.ncbi.nlm.nih.gov/pubmed/9334383.

S. Blackshaw and S. H. Snyder. Encephalopsin: A novel mammalian extraretinal opsin discretely localized in the brain. *The Journal of Neuroscience*, 19(10):3681 –3690, May 1999. http://www.ncbi.nlm.nih.gov/pubmed/10234000.

T. J. Blanche and N. V. Swindale. Nyquist interpolation improves neuron yield in multiunit recordings. *Journal of Neuroscience Methods*, 155(1):81–91, July 2006. http://dx.doi.org/10.1016/j.jneumeth.2005.12.031.

M. J. Bland and D. G. Altman. Statistical methods for assessing agreement between two methods of clinical measurement. *The Lancet*, 327(8476):307–310, Feb. 1986. http://dx.doi.org/10.1016/S0140-6736(86)90837-8.

J. R. Blasic, R. Lane Brown, and P. R. Robinson. Light-dependent phosphorylation of the carboxy tail of mouse melanopsin. *Cellular and Molecular Life Sciences*, Dec. 2011. http://dx.doi.org/10.1007/s00018-011-0891-3.

A. Bloch. Experiences sur la vision. *CR Seances Society of Biology Paris*, Ser 8(5):493, 1885.

H. Bloemendal, W. de Jong, R. Jaenicke, N. H. Lubsen, C. Slingsby, and A. Tardieu. Ageing and vision: structure, stability and function of lens crystallins. *Progress in Biophysics and Molecular Biology*, 86(3):407–485, Nov. 2004. http://dx.doi.org/10.1016/j.pbiomolbio.2003.11.012.

S. C. Blumen, V. Feiler-Ofry, and A. D. Korczyn. The pupil cycle time in horner's syndrome. *Journal of Clinical Neuro-Ophthalmology*, 6(4):232–235, Dec. 1986. http://www.ncbi.nlm.nih.gov/pubmed/2947928.

E. A. Boettner and J. R. Wolter. Transmission of the ocular media. *Invest. Ophthalmol. Vis. Sci.*, 1(6):776–783, Dec. 1962.

M. Böhme, M. Dorr, M. Graw, T. Martinetz, and E. Barth. A software framework for simulating eye trackers. pages 251–258, Savannah, Georgia, 2008. ACM. http://dx.doi.org/10.1145/1344471.1344529.

C. F. Bohren and E. E. Clothiaux. *Fundamentals of atmospheric radiation: an introduction with 400 problems*. Physics textbook. Wiley-VCH, 2006.

C. F. Bohren and D. R. Huffman. *Absorption and Scattering of Light by Small Particles*. Wiley-VCH, 1998.

R. A. Bone and J. T. Landrum. Heterochromatic flicker photometry. *Archives of Biochemistry and Biophysics*, 430(2):137–142, Oct. 2004. http://dx.doi.org/10.1016/j.abb.2004.04.003.

R. A. Bone, B. Brener, and J. C. Gibert. Macular pigment, photopigments, and melanin: Distributions in young subjects determined by four-wavelength reflectometry. *Vision Research*, 47(26):3259–3268, Dec. 2007. http://dx.doi.org/10.1016/j.visres.2007.09.002.

A. A. Borbély. A two process model of sleep regulation. *Human Neurobiology*, 1(3):195–204, 1982. http://www.ncbi.nlm.nih.gov/pubmed/7185792.

H. Borgmann. Die pupillenfunktion im 24-Std-Rhythmus. *Ber Zusammenkunft Dtsch Ophthalmol Ges*, 67:123–127, 1966.

M. H. Bornstein. Color vision and color naming: A psychophysiological hypothesis of cultural difference. *Psychological Bulletin*, 80(4):257–285, Oct. 1973. http://dx.doi.org/10.1037/h0034837.

J. E. Bos. Detection of the pupil constriction latency. *Medical & Biological Engineering & Computing*, 29:529–534, Sept. 1991. http://dx.doi.org/10.1007/BF02442326.

M. E. Bosem, P. A. Sample, G. A. Martinez, M. Lusky, and R. N. Weinreb. Age-related changes in the human lens: a comparison of scheimpflug photography and lens density index. *Journal of Cataract and Refractive Surgery*, 20(1):70–73, Jan. 1994. http://www.ncbi.nlm.nih.gov/pubmed/8133484.

A. D. Botton. *The Architecture of Happiness*. Vintage, Apr. 2008.

H. Bouma. Size of the static pupil as a function of wave-length and luminosity of the light incident on the human eye. *Nature*, 193(4816):690–691, Feb. 1962. http://dx.doi.org/10.1038/193690a0.

H. Bouma and L. Baghuis. Hippus of the pupil: Periods of slow oscillations of unknown origin. *Vision Research*, 11(11):1345–1351, Nov. 1971. http://dx.doi.org/10.1016/0042-6989(71)90016-2.

K. E. Bowles and T. W. Kraft. ERG critical flicker frequency assessment in humans. *Advances in Experimental Medicine and Biology*, 723:503–509, 2012. http://dx.doi.org/10.1007/978-1-4614-0631-0_63.

J. Bowmaker, S. Astell, D. Hunt, and J. Mollon. Photosensitive and photostable pigments in the retinae of old world monkeys. *J Exp Biol*, 156(1):1–19, Mar. 1991. http://www.ncbi.nlm.nih.gov/pubmed/2051127.

J. K. Bowmaker, H. J. Dartnall, J. N. Lythgoe, and J. D. Mollon. The visual pigments of rods and cones in the rhesus monkey, macaca mulatta. *The Journal of Physiology*, 274:329–348, Jan. 1978. http://www.ncbi.nlm.nih.gov/pubmed/415133.

P. Boyce. Age, illuminance, visual performance and preference. *Lighting Research and Technology*, 5(3):125 –144, 1973. http://dx.doi.org/10.1177/096032717300500301.

P. R. Boyce. *Human Factors in Lighting, Second Edition*. CRC, 2 edition, Apr. 2003.

P. R. Boyce. Lemmings, light and health. *LEUKOS - The Journal of the Illuminating Engineering Society of North America*, 2(3), Jan. 2006.

T. H. Boyer. Derivation of the blackbody radiation spectrum without quantum assumptions. *Physical Review*, 182(5):1374–1383, June 1969. http://dx.doi.org/10.1103/PhysRev.182.1374.

R. M. Boynton. Some temporal factors in vision. In *Sensory Communication*. MIT Press, Cambridge, MA, 1961.

R. M. Boynton and D. N. Whitten. Visual adaptation in monkey cones: Recordings of late receptor potentials. *Science*, 170(3965):1423 –1426, Dec. 1970. http://www.sciencemag.org/content/170/3965/1423.abstract.

J. C. Bradley, K. C. Bentley, A. I. Mughal, H. Bodhireddy, R. S. Young, and S. M. Brown. The effect of gender and iris color on the Dark-Adapted pupil diameter. *Journal of Ocular Pharmacology and Therapeutics*, 26(4):335–340, Aug. 2010. http://dx.doi.org/10.1089/jop.2010.0061.

D. H. Brainard, D. R. Williams, and H. Hofer. Trichromatic reconstruction from the interleaved cone mosaic: Bayesian model and the color appearance of small spots. *Journal of Vision*, 8(5), May 2008a. http://www.journalofvision.org/content/8/5/15.abstract.

G. C. Brainard and J. P. Hanifin. Photons, clocks, and consciousness. *J Biol Rhythms*, 20(4):314–325, Aug. 2005. http://dx.doi.org/10.1177/0748730405278951.

G. C. Brainard, M. D. Rollag, and J. P. Hanifin. Photic regulation of melatonin in humans: Ocular and neural signal transduction. *J Biol Rhythms*, 12(6):537–546, Dec. 1997. http://dx.doi.org/10.1177/074873049701200608.

G. C. Brainard, J. P. Hanifin, J. M. Greeson, B. Byrne, G. Glickman, E. Gerner, and M. D. Rollag. Action spectrum for melatonin regulation in humans: Evidence for a novel circadian photoreceptor. *J. Neurosci.*, 21(16):6405–6412, Aug. 2001. http://www.ncbi.nlm.nih.gov/pubmed/11487664.

G. C. Brainard, D. Sliney, J. P. Hanifin, G. Glickman, B. Byrne, J. M. Greeson, S. Jasser, E. Gerner, and M. D. Rollag. Sensitivity of the human circadian system to Short-Wavelength (420-nm) light. *J Biol Rhythms*, 23(5):379–386, Oct. 2008b. http://dx.doi.org/10.1177/0748730408323089.

G. Brecher. Discussion of "The dark-adaptation process of the pupillomotor photoreceptors. *Am J Ophthalmol*, 48:592, 1959.

F. D. Bremner. Pupil assessment in optic nerve disorders. *Eye*, 18(11):1175–1181, 2004. http://dx.doi.org/10.1038/sj.eye.6701560.

P. C. Bressloff and C. V. Wood. Spontaneous oscillations in a nonlinear delayed-feedback shunting model of the pupil light reflex. *Physical Review E*, 58(3):3597–3605, 1998. http://dx.doi.org/10.1103/PhysRevE.58.3597.

P. C. Bressloff, C. V. Wood, and P. A. Howarth. Nonlinear shunting model of the pupil light reflex. *Proceedings. Biological Sciences / The Royal Society*, 263(1373):953–60, Aug. 1996. http://dx.doi.org/10.1098/rspb.1996.0141.

M. E. Breton, A. W. Schueller, T. D. Lamb, and E. N. Pugh. Analysis of ERG a-wave amplification and kinetics in terms of the g-protein cascade of phototransduction. *Investigative Ophthalmology & Visual Science*, 35(1):295 –309, Jan. 1994. http://www.ncbi.nlm.nih.gov/pubmed/8113014.

G. S. Brindley. The Bunsen-Roscoe law for the human eye at very short durations. *The Journal of Physiology*, 118(1):135–139, Sept. 1952. http://www.ncbi.nlm.nih.gov/pubmed/13000697.

P. J. Brockwell and R. A. Davis. *Introduction to Time Series and Forecasting*. Springer, 2nd edition, Mar. 2002.

A. E. Broendsted, M. Stormly Hansen, H. Lund-Andersen, B. Sander, and L. Kessel. Human lens transmission of blue light: A comparison of Autofluorescence-Based and direct spectral transmission determination. *Ophthalmic Research*, 46(3):118–124, 2011. http://dx.doi.org/10.1159/000323576.

A. J. Bron, R. C. Tripathi, and B. J. Tripathi. *Wolff's Anatomy of the Eye and Orbit*. Oxford University Press, USA, 8 edition, Jan. 1997.

H. M. Brown and M. C. Cornwall. Spectral correlates of a quasi-stable depolarization in barnacle photoreceptor following red light. *The Journal of Physiology*, 248(3):555–578, July 1975. http://www.ncbi.nlm.nih.gov/pubmed/1151837.

J. Brown. Flicker an intermittent stimulation. In C. H. Graham, editor, *Vision and Visual Perception*. John Wiley & Sons Inc, New York, 1965a.

J. L. Brown. Flash blindness. *American Journal of Ophthalmology*, 60(3):505–520, Sept. 1965b. http://www.ncbi.nlm.nih.gov/pubmed/5825155.

K. T. Brown and M. Murakami. A new receptor potential of the monkey retina with no detectable latency. *Nature*, 201(4919):626–628, Feb. 1964. http://dx.doi.org/10.1038/201626a0.

S. A. Brown, K. Schmitt, and A. Eckert. Aging and circadian disruption: Causes and effects. *Aging*, 3(8), Aug. 2011a.

T. M. Brown and H. D. Piggins. Electrophysiology of the suprachiasmatic circadian clock. *Progress in Neurobiology*, 82(5):229–255, Aug. 2007. http://dx.doi.org/10.1016/j.pneurobio.2007.05.002.

T. M. Brown, C. Gias, M. Hatori, S. R. Keding, M. Semo, P. J. Coffey, J. Gigg, H. D. Piggins, S. Panda, and R. J. Lucas. Melanopsin contributions to irradiance coding in the Thalamo-Cortical visual system. *PLoS Biol*, 8(12):e1000558, Dec. 2010. http://dx.doi.org/10.1371/journal.pbio.1000558.

T. M. Brown, J. Wynne, H. D. Piggins, and R. J. Lucas. Multiple hypothalamic cell populations encoding distinct visual information. *The Journal of Physiology*, Jan. 2011b. http://dx.doi.org/10.1113/jphysiol.2010.199877.

M. S. Bruno, S. N. Barnes, and T. H. Goldsmith. The visual pigment and visual cycle of the lobster, homarus. *Journal of Comparative Physiology ? A*, 120(2):123–142, 1977. http://dx.doi.org/10.1007/BF00619310.

J. Bullough, M. Rea, and M. Figueiro. Of mice and women: Light as a circadian stimulus in breast cancer research. *Cancer Causes and Control*, 17:375–383, May 2006. http://dx.doi.org/10.1007/s10552-005-0574-1.

J. Burge and W. S. Geisler. Optimal defocus estimation in individual natural images. *Proceedings of the National Academy of Sciences*, 2011. http://dx.doi.org/10.1073/pnas.1108491108.

H. J. Burgess, V. L. Revell, and C. I. Eastman. A three pulse phase response curve to three milligrams of melatonin in humans. *J Physiol*, 586(2):639–647, Jan. 2008. http://dx.doi.org/10.1113/jphysiol.2007.143180.

D. W. Burke and K. N. Ogle. Comparison of visual and pupillary light thresholds in periphery. *Arch Ophthalmol*, 71(3):400–408, Mar. 1964. http://www.ncbi.nlm.nih.gov/pubmed/14100766.

D. A. Burkhardt. Light adaptation and photopigment bleaching in cone photoreceptors in situ in the retina of the turtle. *The Journal of Neuroscience: The Official Journal of the Society for Neuroscience*, 14(3 Pt 1):1091–1105, Mar. 1994. http://www.ncbi.nlm.nih.gov/pubmed/8120614.

C. C. Burn. What is it like to be a rat? rat sensory perception and its implications for experimental design and rat welfare. *Applied Animal Behaviour Science*, 112(1-2):1–32, July 2008. http://dx.doi.org/10.1016/j.applanim.2008.02.007.

M. E. Burns and V. Y. Arshavsky. Beyond counting photons: Trials and trends in vertebrate visual transduction. *Neuron*, 48(3):387–401, Nov. 2005. http://dx.doi.org/10.1016/j.neuron.2005.10.014.

M. E. Burns and D. A. Baylor. Activation, deactivation, and adaptation in vertebrate photoreceptor cells. *Annual Review of Neuroscience*, 24:779–805, 2001. http://dx.doi.org/10.1146/annurev.neuro.24.1.779.

S. A. Burns and A. E. Elsner. Color matching at high illuminances: the color-match-area effect and photopigment bleaching. *Journal of the Optical Society of America A*, 2(5):698–704, May 1985. http://dx.doi.org/10.1364/JOSAA.2.000698.

S. A. Burns and A. E. Elsner. Color matching at high illuminances: photopigment optical density and pupil entry. *Journal of the Optical Society of America A*, 10(2):221–230, Feb. 1993. http://dx.doi.org/10.1364/JOSAA.10.000221.

V. Busskamp and B. Roska. Optogenetic approaches to restoring visual function in retinitis pigmentosa. *Current Opinion in Neurobiology*, (0), 2011. http://dx.doi.org/10.1016/j.conb.2011.06.001.

L. Butgereit, L. Coetzee, and A. C. Smith. Turn me on! using the "Internet of things" to turn things on and off. In *2011 6th International Conference on Pervasive Computing and Applications (ICPCA)*, pages 4–10. IEEE, Oct. 2011. http://dx.doi.org/10.1109/ICPCA.2011.6106469.

M. P. Butler and R. Silver. Divergent photic thresholds in the non-image-forming visual system: entrainment, masking and pupillary light reflex. *Proceedings. Biological Sciences / The Royal Society*, Sept. 2010. http://dx.doi.org/10.1098/rspb.2010.1509.

D. J. Buysse, C. F. Reynolds III, T. H. Monk, S. R. Berman, and D. J. Kupfer. The pittsburgh sleep quality index: A new instrument for psychiatric practice and research. *Psychiatry Research*, 28(2):193–213, May 1989. http://dx.doi.org/10.1016/0165-1781(89)90047-4.

D. J. Buysse, K. E. Browman, T. H. Monk, r. Reynolds, C F, A. L. Fasiczka, and D. J. Kupfer. Napping and 24-hour sleep/wake patterns in healthy elderly and young adults. *Journal of the American Geriatrics Society*, 40(8):779–786, Aug. 1992. http://www.ncbi.nlm.nih.gov/pubmed/1634721.

T. Byk, M. Bar-Yaacov, Y. N. Doza, B. Minke, and Z. Selinger. Regulatory arrestin cycle secures the fidelity and maintenance of the fly photoreceptor cell. *Proceedings of the National Academy of Sciences*, 90(5):1907–1911, Mar. 1993. http://www.ncbi.nlm.nih.gov/pubmed/8446607.

R. Cabestrero, A. Crespo, and P. QuiróS. Pupillary dilation as an index of task demands. *Perceptual and Motor Skills*, 109(3):664–678, Dec. 2009. http://dx.doi.org/10.2466/pms.109.3.664-678.

A. Cagnacci, J. A. Elliott, and S. S. Yen. Melatonin: a major regulator of the circadian rhythm of core temperature in humans. *The Journal of Clinical Endocrinology and Metabolism*, 75(2):447–452, Aug. 1992. http://dx.doi.org/10.1210/jc.75.2.447.

H. Cahill and J. Nathans. The optokinetic reflex as a tool for quantitative analyses of nervous system function in mice: Application to genetic and Drug-Induced variation. *PLoS ONE*, 3(4), 2008. http://dx.doi.org/10.1371/journal.pone.0002055.

H. Cai and T. M. Chung. Improving the quality of high dynamic range images. *Lighting Research and Technology*, Aug. 2010. http://dx.doi.org/10.1177/1477153510371356.

C. Cajochen. Alerting effects of light. *Sleep Medicine Reviews*, 11(6):453–464, 2007. http://dx.doi.org/10.1016/j.smrv.2007.07.009.

C. Cajochen, J. M. Zeitzer, C. A. Czeisler, and D. J. Dijk. Dose-response relationship for light intensity and ocular and electroencephalographic correlates of human alertness. *Behavioural Brain Research*, 115(1):75–83, Oct. 2000. http://dx.doi.org/10.1016/S0166-4328(00)00236-9.

C. Cajochen, M. Munch, S. Kobialka, K. Kräuchi, R. Steiner, P. Oelhafen, S. Orgul, and A. Wirz-Justice. High sensitivity of human melatonin, alertness, thermoregulation, and heart rate to short wavelength light. *J Clin Endocrinol Metab*, 90(3):1311–1316, Mar. 2005. http://dx.doi.org/10.1210/jc.2004-0957.

G. Calcagnini, F. Censi, S. Lino, and S. Cerutti. Spontaneous fluctuations of human pupil reflect central autonomic rhythms. *Methods of Information in Medicine*, 39(2):142–145, June 2000. http://www.ncbi.nlm.nih.gov/pubmed/10892249.

D. J. Calkins. Seeing with s cones. *Progress in Retinal and Eye Research*, 20(3):255–287, May 2001. http://dx.doi.org/10.1016/S1350-9462(00)00026-4.

D. J. Calkins. Linking retinal circuits to color opponency. In L. M. Chalupa and J. S. Werner, editors, *The Visual Neurosciences*, pages 989–1002. The MIT Press, Cambridge, MA, 2-vol. set edition, Nov. 2003.

P. D. Calvert and C. L. Makino. The time course of light adaptation in vertebrate retinal rods. *Advances in Experimental Medicine and Biology*, 514:37–60, 2002. http://www.ncbi.nlm.nih.gov/pubmed/12596914.

P. D. Calvert, K. J. Strissel, W. E. Schiesser, E. N. Pugh Jr, and V. Y. Arshavsky. Light-driven translocation of signaling proteins in vertebrate photoreceptors. *Trends in Cell Biology*, 16(11):560–568, Nov. 2006. http://dx.doi.org/10.1016/j.tcb.2006.09.001.

M. Cameron, A. Barnard, and R. Lucas. The electroretinogram as a method for studying circadian rhythms in the mammalian retina. *Journal of Genetics*, 87(5):459–466, Dec. 2008. http://dx.doi.org/10.1007/s12041-008-0068-5.

M. Camparini, C. Macaluso, L. Reggiani, and G. Maraini. Retroillumination versus Reflected-Light images in the photographic assessment of posterior capsule opacification. *Investigative Ophthalmology & Visual Science*, 41(10):3074 –3079, 2000. http://www.ncbi.nlm.nih.gov/pubmed/10967066.

F. W. Campbell and M. Alpern. Pupillomotor spectral sensitivity curve and color of the fundus. *Osaka City Medical Journal*, 52:1084, Sept. 1962. http://www.ncbi.nlm.nih.gov/pubmed/13876028.

F. W. Campbell and D. G. Green. Optical and retinal factors affecting visual resolution. *The Journal of Physiology*, 181(3):576–593, Dec. 1965.

F. W. Campbell and R. W. Gubisch. Optical quality of the human eye. *The Journal of Physiology*, 186(3):558–578, Oct. 1966. http://www.ncbi.nlm.nih.gov/pubmed/5972153.

S. S. Campbell, J. C. Gillin, and D. F. Kripke. Ambulatory recording of rest/activity, body temperature and light exposure in normal elderly and alzheimer's disease. *Sleep Res*, 5:264, 1986.

M. C. Canver, A. C. Canver, K. E. Revere, D. Amado, J. Bennett, and D. C. Chung. Algorithm for pupillometric data analysis. In *Bioengineering Conference, Proceedings of the 2010 IEEE 36th Annual Northeast*, pages 1–2. IEEE, Mar. 2010. http://dx.doi.org/10.1109/NEBC.2010.5458283.

S. M. Carcieri, A. L. Jacobs, and S. Nirenberg. Classification of retinal ganglion cells: a statistical approach. *Journal of Neurophysiology*, 90(3):1704–1713, Sept. 2003. http://dx.doi.org/10.1152/jn.00127.2003.

C. F. Carle, A. C. James, M. Kolic, R. W. Essex, and T. L. Maddess. Targeting melanopsin with mfPOP: blue multifocal pupillographic objective perimetry in glaucoma. *ARVO Meeting Abstracts*, 52(6):5491, Apr. 2011a.

C. F. Carle, A. C. James, M. Kolic, Y. Loh, and T. Maddess. High-Resolution multifocal pupillographic objective perimetry in glaucoma. *Investigative Ophthalmology & Visual Science*, 52(1):604 –610, Jan. 2011b. http://dx.doi.org/10.1167/iovs.10-5737.

C. F. Carle, T. Maddess, and A. C. James. Contraction anisocoria: Segregation, summation, and saturation in the pupillary pathway. *Investigative Ophthalmology & Visual Science*, 52(5):2365 –2371, Apr. 2011c. dx.doi.org/10.1167/iovs.10-6335.

G. A. Carpenter, S. Grossberg, and S. Grossberg. Adaptation and transmitter gating in vertebrate photoreceptors. In *The Adaptive Brain II Vision, Speech, Language, and Motor Control*, volume Volume 43, pages 273–310. North-Holland, 1987. http://dx.doi.org/10.1016/S0166-4115(08)61764-1.

M. B. Carpenter and R. J. Pierson. Pretectal region and the pupillary light reflex. an anatomical analysis in the monkey. *The Journal of Comparative Neurology*, 149(3): 271–299, June 1973. http://dx.doi.org/10.1002/cne.901490302.

A. Carr, A. A. Vugler, L. Yu, M. Semo, P. Coffey, S. E. Moss, and J. Greenwood. The expression of retinal cell markers in human retinal pigment epithelial cells and their augmentation by the synthetic retinoid fenretinide. *Molecular Vision*, 17:1701–1715, June 2011.

R. E. Carr and I. M. Siegel. Action spectrum of the human early receptor potential. *Nature*, 225(5227):88–89, Jan. 1970. http://dx.doi.org/10.1038/225088a0.

J. Carrier, T. H. Monk, D. J. Buysse, and D. J. Kupfer. Amplitude reduction of the circadian temperature and sleep rhythms in the elderly. *Chronobiology International*, 13 (5):373–386, Nov. 1996. http://www.ncbi.nlm.nih.gov/pubmed/8957588.

J. Carrier, S. Land, D. J. Buysse, D. J. Kupfer, and T. H. Monk. The effects of age and gender on sleep EEG power spectral density in the middle years of life (ages 20–60 years old). *Psychophysiology*, 38(2):232–242, Mar. 2001. http://dx.doi.org/10.1111/1469-8986.3820232.

J. Carroll, J. Neitz, and M. Neitz. Estimates of L:M cone ratio from ERG flicker photometry and genetics. *Journal of Vision*, 2(8), Nov. 2002. http://dx.doi.org/10.1167/2.8.1.

J. Carroll, M. Pircher, and R. J. Zawadzki. Introduction: Feature issue on cellular imaging of the retina. *Biomedical Optics Express*, 2(6):1778–1780, June 2011. http://dx.doi.org/10.1364/BOE.2.001778.

S. Cerutti, G. Baselli, A. M. Bianchi, E. Caiani, D. Contini, R. Cubeddu, F. Dercole, L. D. Rienzo, D. Liberati, L. Mainardi, P. Ravazzani, S. Rinaldi, M. G. Signorini, and A. Torricelli. Biomedical signal and image processing. *IEEE Pulse*, 2(3):41–54, June 2011.

L. Cervetto, V. Torre, G. Rispoli, and P. Marroni. Mechanisms of light adaptation in toad rods. *Experimental Biology*, 44(3):147–157, 1985. http://www.ncbi.nlm.nih.gov/pubmed/3934000.

C. Chain, D. Dumortier, and M. Fontoynont. Consideration of daylight's colour. *Energy and Buildings*, 33(3):193–198, Feb. 2001. http://dx.doi.org/10.1016/S0378-7788(00)00081-5.

T. K. Chakraborty, A. L. Ogilvie, R. C. Heading, and D. J. Ewing. Abnormal cardiovascular reflexes in patients with gastro-oesophageal reflux. *Gut*, 30(1):46 –49, Jan. 1989. http://dx.doi.org/10.1136/gut.30.1.46.

S. Chamberlain and R. Barlow. Control of structural rhythms in the lateral eye of limulus: interactions of natural lighting and circadian efferent activity. *J. Neurosci.*, 7(7):2135–2144, July 1987. http://www.ncbi.nlm.nih.gov/pubmed/3612232.

S. R. Chamot, C. Dainty, and S. Esposito. Adaptive optics for ophthalmic applications using a pyramid wavefront sensor. *Optics Express*, 14(2):518–526, Jan. 2006. http://dx.doi.org/10.1364/OPEX.14.000518.

A. Chang, F. A. J. L. Scheer, and C. A. Czeisler. The human circadian system adapts to prior photic history. *The Journal of Physiology*, 589(5):1095 –1102, Mar. 2011. http://dx.doi.org/10.1113/jphysiol.2010.201194.

W. N. Charman. Optics of the eye. In M. Bass, editor, *Handbook of Optics*. McGraw-Hill Inc.,US, 1995.

W. N. Charman. Age, lens transmittance, and the possible effects of light on melatonin suppression. *Ophthalmic and Physiological Optics*, 23(2):181–187, 2003. http://dx.doi.org/10.1046/j.1475-1313.2003.00105.x.

S. Chatterjee and E. M. Callaway. Parallel colour-opponent pathways to primary visual cortex. *Nature*, 426(6967):668–671, Dec. 2003. http://dx.doi.org/10.1038/nature02167.

S. L. Chellappa, R. Steiner, P. Blattner, P. Oelhafen, T. Götz, and C. Cajochen. Non-Visual effects of light on melatonin, alertness and cognitive performance: Can Blue-Enriched light keep us alert? *PLoS ONE*, 6 (1):e16429, Jan. 2011. http://dx.doi.org/10.1371/journal.pone.0016429.

J. Chen, C. Makino, N. Peachey, D. Baylor, and M. Simon. Mechanisms of rhodopsin inactivation in vivo as revealed by a COOH-

terminal truncation mutant. *Science*, 267 (5196):374 –377, Jan. 1995. http://dx.doi.org/10.1126/science.7824934.

P. Chen, W. Hao, L. Rife, X. P. Wang, D. Shen, J. Chen, T. Ogden, G. B. Van Boemel, L. Wu, M. Yang, and H. K. Fong. A photic visual cycle of rhodopsin regeneration is dependent on rgr. *Nat Genet*, 28(3):256–260, July 2001a. http://dx.doi.org/10.1038/90089.

S. Chen, T. C. Badea, and S. Hattar. Photoentrainment and pupillary light reflex are mediated by distinct populations of ipRGCs. *Nature*, 476(7358):92–95, 2011. http://dx.doi.org/10.1038/nature10206.

S. F. Chen, Y. Chang, and J. C. Wu. The spatial distribution of macular pigment in humans. *Current Eye Research*, 23(6):422–434, Dec. 2001b. http://www.ncbi.nlm.nih.gov/pubmed/12045892.

T. F. Chen, G. V. G. Baranoski, and K. F. Lin. Bulk scattering approximations for HeNe laser transmitted through paper. *Optics Express*, 16(26):21762–21771, Dec. 2008. http://dx.doi.org/10.1364/OE.16.021762.

Y. Chen, H. J. Wyatt, and W. H. Swanson. Pupillary evaluation of retinal asymmetry: Development and initial testing of a technique. *Vision Research*, 45(19):2549–2563, Sept. 2005. http://dx.doi.org/10.1016/j.visres.2005.04.003.

N. Cheng, T. Tsunenari, and K. Yau. Intrinsic light response of retinal horizontal cells of teleosts. *Nature*, 460(7257):899–903, 2009. http://dx.doi.org/10.1038/nature08175.

W. Cheng, J. Ju, Y. Sun, and Y. Lin. The effect of LED lighting on color discrimination and preference of elderly people. *Human Factors and Ergonomics in Manufacturing & Service Industries*, Early View, 2012. http://dx.doi.org/10.1002/hfm.20333.

E. Y. Chew, J. Kim, R. D. Sperduto, M. B. Datiles, H. R. Coleman, D. J. S. Thompson, R. C. Milton, J. A. Clayton, L. D. Hubbard, R. P. Danis, and F. L. Ferris. Evaluation of the Age-Related eye disease study clinical lens grading system AREDS report no. 31. *Ophthalmology*, 117(11):2112–2119.e3, Nov. 2010. http://dx.doi.org/10.1016/j.ophtha.2010.02.033.

T. C. Chou, T. E. Scammell, J. J. Gooley, S. E. Gaus, C. B. Saper, and J. Lu. Critical role of dorsomedial hypothalamic nucleus in a wide range of behavioral circadian rhythms. *The Journal of Neuroscience*, 23(33):10691 –10702, Nov. 2003. http://www.ncbi.nlm.nih.gov/pubmed/14627654.

K. Chu, Z. J. Smith, A. R. Espenson, S. Lane, and S. Wachsmann-Hogiu. Microscopy and spectroscopy on a cell phone. San Jose, California, USA, Oct. 2011.

J. Chylack, L T, J. K. Wolfe, D. M. Singer, M. C. Leske, M. A. Bullimore, I. L. Bailey, J. Friend, D. McCarthy, and S. Y. Wu. The lens opacities classification system III. the longitudinal study of cataract study group. *Archives of Ophthalmology*, 111(6):831–836, June 1993. http://www.ncbi.nlm.nih.gov/pubmed/8512486.

C. V. Clark. Ocular autonomic nerve function in proliferative diabetic retinopathy. *Eye (London, England)*, 2 (Pt 1):96–101, 1988. http://www.ncbi.nlm.nih.gov/pubmed/3044851.

C. V. Clark and D. J. Ewing. Ocular autonomic function in progressive autonomic failure. *Documenta Ophthalmologica*, 70:309–321, Dec. 1988. http://dx.doi.org/10.1007/BF00157061.

C. V. Clark and R. Mapstone. Pupil cycle time in primary closed-angle glaucoma. *Canadian Journal of Ophthalmology. Journal Canadien D'ophtalmologie*, 21(3):88–91, Apr. 1986. http://www.ncbi.nlm.nih.gov/pubmed/3708430.

C. V. Clark and R. Mapstone. Anterior segment autonomic dysfunction in ocular hypertension. *Documenta Ophthalmologica*, 64:201–207, 1987. http://10.1007/BF00159994.

A. H. Clarke. Image processing techniques for the measurement of eye movement. In *Eye Movements in Reading*, pages 21–38. Elsevier, Oxford, NY, 1994.

R. Clarke and H. Ikeda. Luminance and darkness detectors in the olivary and posterior pretectal nuclei and their relationship to the pupillary light reflex in the rat. *Experimental Brain Research*, 57(2):224–232, Jan. 1985. http://dx.doi.org/10.1007/BF00236527.

R. J. Clarke, H. Zhang, and P. D. R. Gamlin. Characteristics of the pupillary light reflex in the alert rhesus monkey. *J Neurophysiol*, 89(6):3179–3189, June 2003a. http://dx.doi.org/10.1152/jn.01131.2002.

R. J. Clarke, H. Zhang, and P. D. R. Gamlin. Primate pupillary light reflex: Receptive field characteristics of pretectal luminance neurons. *J Neurophysiol*, 89(6):3168–3178, June 2003b. http://dx.doi.org/10.1152/jn.01130.2002.

L. Claudio. Switch on the night: policies for smarter lighting. *Environmental Health Perspectives*, 117(1):A28–31, Jan. 2009. http://www.ncbi.nlm.nih.gov/pubmed/19165375.

W. S. Cleveland. Robust locally weighted regression and smoothing scatterplots. *Journal of the American Statistical Association*, 74 (368):829–836, Dec. 1979. http://dx.doi.org/10.2307/2286407.

M. Clynes. Unidirectional rate sensitivity: a biocybernetic law of reflex and humoral systems as physiologic channels of con-

trol and communication. *Annals of the New York Academy of Sciences*, 92:946–969, July 1961. http://dx.doi.org/10.1111/j.1749-6632.1961.tb40968.x.

L. Cohen. Time-frequency distributions-a review. *Proceedings of the IEEE*, 77(7):941–981, July 1989. http://dx.doi.org/10.1109/5.30749.

K. S. Cole. *Membranes, ions, and impulses*. University of California Press, 1968.

R. Cole, D. F. Kripke, W. Gruen, and J. Nava. Ambulatory monitoring of light exposure: Comparison of measurements at forehead and wrist. *Sleep Res*, 19:364, 1990.

C. S. Colwell. Linking neural activity and molecular oscillations in the SCN. *Nat Rev Neurosci*, 12(10):553–569, Oct. 2011. http://dx.doi.org/10.1038/nrn3086.

C. S. Colwell, S. Michel, J. Itri, W. Rodriguez, J. Tam, V. Lelièvre, Z. Hu, and J. A. Waschek. Selective deficits in the circadian light response in mice lacking PACAP. *American Journal of Physiology - Regulatory, Integrative and Comparative Physiology*, 287(5):R1194 –R1201, Nov. 2004. http://dx.doi.org/10.?1152/?ajpregu.?00268.?2004.

R. A. Cone. Early receptor potential of the vertebrate retina. *Nature*, 204(4960):736–739, Nov. 1964. http://dx.doi.org/10.1038/204736a0.

R. A. Cone. Early receptor potential: Photoreversible charge displacement in rhodopsin. *Science*, 155(3766):1128 –1131, Mar. 1967. http://dx.doi.org/10.1126/science.155.3766.1128.

J. D. Conner. The temporal properties of rod vision. *The Journal of Physiology*, 332:139–155, Nov. 1982. http://www.ncbi.nlm.nih.gov/pubmed/7153925.

M. N. Cook, R. W. Williams, and L. Flaherty. Anxiety-related behaviors in the elevated zero-maze are affected by genetic factors and retinal degeneration. *Behavioral Neuroscience*, 115(2):468–476, Apr. 2001. http://dx.doi.org/10.1037/0735-7044.115.2.468.

J. L. Coombs and L. M. Chalupa. The plasticity of retinal ganglion cells. In L. M. Chalupa, N. Berardi, M. Caleo, L. Galli-Resta, and T. Pizzorusso, editors, *Cerebral Plasticity: New Perspectives*. The MIT Press, Cambridge, MA, 1 edition, May 2011.

G. F. Cooper and J. G. Robson. The yellow colour of the lens of man and other primates. *The Journal of Physiology*, 203(2):411–417, Aug. 1969. http://www.ncbi.nlm.nih.gov/pubmed/4978734.

H. M. Cooper and L. S. Mure. Expected and unexpected properties of melanopsin signaling. *Journal of Biological Rhythms*, 23(5):392–3, Oct. 2008. http://dx.doi.org/10.1177/0748730408323064.

J. E. Coppens, L. Franssen, and T. J. van den Berg. Wavelength dependence of intraocular straylight. *Experimental Eye Research*, 82(4):688–692, Apr. 2006. http://dx.doi.org/10.1016/j.exer.2005.09.007.

R. Coppola, R. Tabor, and M. S. Buchsbaum. Signal to noise ratio and response variability measurements in single trial evoked potentials. *Electroencephalography and Clinical Neurophysiology*, 44(2):214–222, Feb. 1978. http://dx.doi.org/10.1016/0013-4694(78)90267-5.

J. E. Corbett and M. Carrasco. Visual performance fields: Frames of reference. *PLoS ONE*, 6(9):e24470, 2011. http://dx.doi.org/10.1371/journal.pone.0024470.

R. M. Corless, G. H. Gonnet, D. E. G. Hare, D. J. Jeffrey, and D. E. Knuth. On the LambertW function. *Advances in Computational Mathematics*, 5:329–359, Dec. 1996. http://dx.doi.org/10.1007/BF02124750.

A. Cornish-Bowden. *Fundamentals of Enzyme Kinetics*. Portland Press Limited, London, rev sub edition, July 1995.

T. N. Cornsweet and H. D. Crane. Accurate two-dimensional eye tracker using first and fourth purkinje images. *Journal of the Optical Society of America*, 63(8):921–928, 1973. http://dx.doi.org/10.1364/JOSA.63.000921.

M. C. Cornwall and G. L. Fain. Bleached pigment activates transduction in isolated rods of the salamander retina. *The Journal of Physiology*, 480 (Pt 2):261–279, Oct. 1994. http://www.ncbi.nlm.nih.gov/pubmed/7532713.

D. Cosens and D. Briscoe. A switch phenomenon in the compound eye of the white-eyed mutant of drosophila melanogaster. *Journal of Insect Physiology*, 18(4):627–632, Apr. 1972. http://dx.doi.org/10.1016/0022-1910(72)90190-4.

B. H. Crawford. The integration of the glare effects from a number of glare sources. *Proceedings of the Physical Society*, 48:35–37, Jan. 1936. http://dx.doi.org/10.1088/0959-5309/48/1/305.

B. H. Crawford. The scotopic visibility function. *Proceedings of the Physical Society. Section B*, 62(5):321–334, May 1949. http://dx.doi.org/10.1088/0370-1301/62/5/305.

T. Cronin, R. Caldwell, and M. Erdmann. Tuning of photoreceptor function in three mantis shrimp species that inhabit a range of depths. i. visual pigments. *Journal of Comparative Physiology A: Sensory, Neural, and Behavioral Physiology*, 188(3):179–186, Apr. 2002. http://dx.doi.org/10.1007/s00359-002-0291-0.

T. W. Cronin and T. H. Goldsmith. Photosensitivity spectrum of crayfish rhodopsin measured using fluorescence of metarhodopsin. *The Journal of General Phys-*

iology, 79(2):313–332, Feb. 1982a. http://www.ncbi.nlm.nih.gov/pubmed/7057163.

T. W. Cronin and T. H. Goldsmith. Quantum efficiency and photosensitivity of the rhodopsin equilibrium metarhodopsin conversion in crayfish photoreceptors. *Photochemistry and Photobiology*, 36(4):447–454, Oct. 1982b. http://dx.doi.org/10.1111/j.1751-1097.1982.tb04401.x.

T. W. Cronin and T. H. Goldsmith. Dark regeneration of rhodopsin in crayfish photoreceptors. *The Journal of General Physiology*, 84 (1):63 –81, July 1984. http://dx.doi.org/10.1085/jgp.84.1.63.

C. A. Curcio, K. R. Sloan, R. E. Kalina, and A. E. Hendrickson. Human photoreceptor topography. *The Journal of Comparative Neurology*, 292(4):497–523, Feb. 1990. http://dx.doi.org/10.1002/cne.902920402.

C. A. Czeisler, T. L. Shanahan, E. B. Klerman, H. Martens, D. J. Brotman, J. S. Emens, T. Klein, and J. F. Rizzo. Suppression of melatonin secretion in some blind patients by exposure to bright light [see comments]. *N Engl J Med*, 332:6 – 11, 1995.

C. A. Czeisler, J. F. Duffy, T. L. Shanahan, E. N. Brown, J. F. Mitchell, D. W. Rimmer, J. M. Ronda, E. J. Silva, J. S. Allan, J. S. Emens, D. Dijk, and R. E. Kronauer. Stability, precision, and Near-24-Hour period of the human circadian pacemaker. *Science*, 284(5423):2177 –2181, June 1999. http://dx.doi.org/10.1126/science.284.5423.2177.

S. Daan, D. G. Beersma, and A. A. Borbely. Timing of human sleep: recovery process gated by a circadian pacemaker. *Am J Physiol Regul Integr Comp Physiol*, 246(2):R161–183, Feb. 1984. http://www.ncbi.nlm.nih.gov/pubmed/6696142.

D. M. Dacey. Primate retina: cell types, circuits and color opponency. *Progress in Retinal and Eye Research*, 18(6):737–763, Nov. 1999. http://dx.doi.org/10.1016/S1350-9462(98)00013-5.

D. M. Dacey, B. B. Peterson, F. R. Robinson, and P. D. Gamlin. Fireworks in the primate retina: In vitro photodynamics reveals diverse LGN-Projecting ganglion cell types. *Neuron*, 37(1):15–27, Jan. 2003. http://dx.doi.org/10.1016/S0896-6273(02)01143-1.

D. M. Dacey, H. Liao, B. B. Peterson, F. R. Robinson, V. C. Smith, J. Pokorny, K. Yau, and P. D. Gamlin. Melanopsin-expressing ganglion cells in primate retina signal colour and irradiance and project to the LGN. *Nature*, 433(7027):749–54, Feb. 2005. http://dx.doi.org/10.1038/nature03387.

K. V. Danilenko, I. L. Plisov, A. Wirz-Justice, and M. Hébert. Human retinal light sensitivity and melatonin rhythms following four days in near darkness. *Chronobiology International*, 26(1):93, 2009. http://dx.doi.org/10.1080/07420520802689814.

K. V. Danilenko, I. L. Plisov, H. M. Cooper, A. Wirz-Justice, and M. Hébert. Human cone light sensitivity and melatonin rhythms following 24-hour continuous illumination. *Chronobiology International*, 28: 407–414, May 2011. http://dx.doi.org/10.3109/07420528.2011.567425.

H. J. Dartnall and J. N. Lythgoe. The spectral clustering of visual pigments. *Vision Research*, 5(3):81–100, Apr. 1965. http://dx.doi.org/10.1016/0042-6989(65)90057-X.

H. J. A. Dartnall. The interpretation of spectral sensitivity curves. *British Medical Bulletin*, 9(1):24–30, 1953. http://dx.doi.org/10.1016/0042-6989(73)90098-9.

H. J. A. Dartnall. Photosensitivity. In H. J. A. Dartnall, editor, *Handbook of Sensory physiology. Photochemistry of Vision*, pages 122–145. Springer, 1972.

H. J. A. Dartnall, C. F. Goodeve, and R. J. Lythgoe. The quantitative analysis of the photochemical bleaching of visual purple solutions in monochromatic light. *Proceedings of the Royal Society of London. Series A, Mathematical and Physical Sciences*, 156(887):158–170, 1936. http://www.jstor.org/stable/96721.

H. J. A. Dartnall, J. K. Bowmaker, and J. D. Mollon. Human visual pigments: microspectrophotometric results from the eyes of seven persons. *Proceedings of the Royal Society of London. Series B, Containing Papers of a Biological Character. Royal Society (Great Britain)*, 220(1218):115–130, Nov. 1983. http://www.ncbi.nlm.nih.gov/pubmed/6140680.

M. B. Datiles, R. R. Ansari, K. I. Suh, S. Vitale, G. F. Reed, J. S. Zigler, and F. L. Ferris. Clinical detection of precataractous lens protein changes using dynamic light scattering. *Arch Ophthalmol*, 126(12):1687–1693, Dec. 2008. http://dx.doi.org/10.1001/archophthalmol.2008.507.

M. B. I. Datiles, R. R. Ansari, and G. F. Reed. A clinical study of the human lens with a dynamic light scattering device. *Experimental Eye Research*, 74(1):93–102, Jan. 2002. http://dx.doi.org/10.1006/exer.2001.1106.

A. Daurat, J. Foret, Y. Touitou, and O. Benoit. Detrimental influence of bright light exposure on alertness, performance, and mood in the early morning. *Neurophysiologie Clinique/Clinical Neurophysiology*, 26(1): 8–14, 1996. http://dx.doi.org/10.1016/0987-7053(96)81529-2.

N. P. Davies and A. B. Morland. Color matching in diabetes: Optical density of the crystalline lens and macular pigments. *Investigative Ophthalmology & Visual Science*, 43 (1):281 –289, Jan. 2002. http://www.ncbi.nlm.nih.gov/pubmed/11773043.

W. I. L. Davies, L. Zheng, S. Hughes, T. K. Tamai, M. Turton, S. Halford, R. G. Foster, D. Whitmore, and M. W. Hankins. Functional diversity of melanopsins and their global expression in the teleost retina. *Cellular and Molecular Life Sciences: CMLS*, Aug. 2011. http://dx.doi.org/10.1007/s00018-011-0785-4.

W. L. Davies, M. W. Hankins, and R. G. Foster. Vertebrate ancient opsin and melanopsin: divergent irradiance detectors. *Photochem. Photobiol. Sci.*, 9(11):1444–1457, Oct. 2010. http://dx.doi.org/10.1039/C0PP00203H.

J. A. Davison, A. S. Patel, J. P. Cunha, J. Schwiegerling, and O. Muftuoglu. Recent studies provide an updated clinical perspective on blue light-filtering IOLs. *Graefe's Archive for Clinical and Experimental Ophthalmology*, 249(7):957–968, May 2011. http://dx.doi.org/10.1007/s00417-011-1697-6.

J. Daymude and R. Refinetti. Phase-Shifting effects of single and multiple light pulses in the golden hamster. *Biological Rhythm Research*, 30(2):202–215, 1999. http://dx.doi.org/10.1076/brhm.30.2.202.1421.

A. de Candolle. *Phisiologie végétale*. 1832.

S. G. De Groot and J. W. Gebhard. Pupil size as determined by adapting luminance. *Journal of the Optical Society of America*, 42 (7):492–495, July 1952. http://dx.doi.org/10.1364/JOSA.42.000492.

H. De Lange DZN. Relationship between critical Flicker-Frequency and a set of Low-Frequency characteristics of the eye. *Journal of the Optical Society of America*, 44(5): 380–388, May 1954. http://dx.doi.org/10.1364/JOSA.44.000380.

J. De Launay. A note on the Photo-Pupil reflex. *Journal of the Optical Society of America*, 39(5):364–367, May 1949. http://dx.doi.org/10.1364/JOSA.39.000364.

R. De Natale, J. Flammer, M. Zulauf, and T. Bebie. Influence of age on the transparency of the lens in normals: A population study with help of the lens opacity meter 701. *Ophthalmologica*, 197:14–18, 1988. http://dx.doi.org/10.1159/000309911.

A. De Santis and D. Iacoviello. Optimal segmentation of pupillometric images for estimating pupil shape parameters. *Computer Methods and Programs in Biomedicine*, 84(2-3):174–187, Dec. 2006. http://dx.doi.org/10.1016/j.cmpb.2006.07.005.

D. A. Dean, D. B. Forger, and E. B. Klerman. Taking the lag out of jet lag through Model-Based schedule design. *PLoS Comput Biol*, 5(6):e1000418, June 2009. http://dx.doi.org/10.1371/journal.pcbi.1000418.

D. Deaver, J. Davies, and D. Sliney. Vertical visual fields-of-view in outdoor daylight. *Lasers Light Ophthalmology*, 7:121–125, 1996.

J. Debecker and A. Zanen. Intensity functions of the early receptor potential and of the melanin fast photovoltage in the human eye. *Vision Research*, 15(1):101–106, Jan. 1975. http://dx.doi.org/10.1016/0042-6989(75)90066-8.

S. S. Deeb. Genetics of variation in human color vision and the retinal cone mosaic. *Current Opinion in Genetics & Development*, 16(3):301–307, June 2006. http://dx.doi.org/10.1016/j.gde.2006.04.002.

T. Deguchi and M. Sato. The effect of color temperature of lighting sources on mental activity level. *The Annals of Physiological Anthropology = Seiri Jinruigaku Kenkyūkai Kaishi*, 11(1):37–43, Jan. 1992. http://www.ncbi.nlm.nih.gov/pubmed/1567518.

J. Deijen, M. Heemstra, and J. Orlebeke. Pupillometric assessment of compensatory effort in a memory search task under physical and pharmacologically induced suboptimal states. *Canadian Journal of Experimental Psychology*, 49(3):387–396, 1995. http://dx.doi.org/10.1037/1196-1961.49.3.387.

K. Deisseroth. Optogenetics. *Nat Meth*, 8(1): 26–29, Jan. 2011. http://dx.doi.org/10.1038/nmeth.f.324.

F. Delori and K. P. Pflibsen. Spectral reflectance of the human ocular fundus. *Applied Optics*, 28(6):1061–1077, Mar. 1989. http://dx.doi.org/10.1364/AO.28.001061.

F. Delori, D. G. Goger, B. R. Hammond, D. M. Snodderly, and S. A. Burns. Macular pigment density measured by autofluorescence spectrometry: comparison with reflectometry and heterochromatic flicker photometry. *Journal of the Optical Society of America A*, 18(6):1212–1230, June 2001. http://dx.doi.org/10.1364/JOSAA.18.001212.

K. Demos, W. Kelley, S. Ryan, F. Davis, and P. Whalen. Human amygdala sensitivity to the pupil size of others. *Cerebral Cortex*, 18(12):2729 –2734, Dec. 2008. http://dx.doi.org/10.1093/cercor/bhn034.

J. J. A. Denissen, L. Butalid, L. Penke, and M. A. G. van Aken. The effects of weather on daily mood: a multilevel approach. *Emotion (Washington, D.C.)*, 8(5): 662–667, Oct. 2008. http://dx.doi.org/10.1037/a0013497.

J. A. Díaz, A. Chiron, and F. Viénot. Tracing a metameric match to individual variations of color vision. *Color Research & Application*, 23(6):379–389, Dec. 1998. http://dx.doi.org/10.1002/(SICI)1520-6378(199812)23:6<379::AID-COL6>3.0.CO;2-E.

L. Diaz-Santana, C. Torti, I. Munro, P. Gasson, and C. Dainty. Benefit of higher closed–loop bandwidths in ocular adaptive optics. *Optics Express*, 11(20):2597–2605,

Oct. 2003. http://dx.doi.org/10.1364/OE.11.002597.

K. B. Digre. *Principles and Techniques of Examination of the Pupil, Accommodation, and the Lacrimal SYstem*. Lippincott Williams & Wilkins, 2005.

D. Dijk and S. N. Archer. Light, sleep, and circadian rhythms: Together again. *PLoS Biol*, 7(6):e1000145, June 2009. http://dx.doi.org/10.1371/journal.pbio.1000145.

J. Dillon, L. Zheng, J. C. Merriam, and E. R. Gaillard. Transmission spectra of light to the mammalian retina. *Photochemistry and Photobiology*, 71(2):225–229, 2000. http://dx.doi.org/10.1562/0031-8655(2000)0710225TSOLTT2.0.CO2.

J. Dillon, L. Zheng, J. C. Merriam, and E. R. Gaillard. Transmission of light to the aging human retina: possible implications for age related macular degeneration. *Experimental Eye Research*, 79(6):753–759, Dec. 2004. http://dx.doi.org/10.1016/j.exer.2004.06.025.

DJ-Skene. Optimization of light and melatonin to Phase-Shift human circadian rhythms. *Journal of Neuroendocrinology*, 15 (4):438–441, 2003. http://dx.doi.org/10.1046/j.1365-2826.2003.01006.x.

O. Dkhissi-Benyahya, C. Rieux, R. A. Hut, and H. M. Cooper. Immunohistochemical evidence of a melanopsin cone in human retina. *Investigative Ophthalmology & Visual Science*, 47(4):1636 –1641, Apr. 2006. http://dx.doi.org/10.1167/iovs.05-1459.

O. Dkhissi-Benyahya, C. Gronfier, W. D. Vanssay, F. Flamant, and H. M. Cooper. Modeling the role of Mid-Wavelength cones in circadian responses to light. *Neuron*, 53(5):677–687, Mar. 2007. http://dx.doi.org/10.1016/j.neuron.2007.02.005.

M. T. H. Do and K. Yau. Intrinsically photosensitive retinal ganglion cells. *Physiological Reviews*, 90(4):1547 –1581, Oct. 2010. http://dx.doi.org/10.1152/physrev.00013.2010.

M. T. H. Do, S. H. Kang, T. Xue, H. Zhong, H. Liao, D. E. Bergles, and K. Yau. Photon capture and signalling by melanopsin retinal ganglion cells. *Nature*, 457:281–287, 2009. http://dx.doi.org/10.1038/nature07682.

N. Doble, S. S. Choi, J. L. Codona, J. Christou, J. M. Enoch, and D. R. Williams. In vivo imaging of the human rod photoreceptor mosaic. *Optics Letters*, 36(1):31–33, Jan. 2011. http://dx.doi.org/10.1364/OL.36.000031.

F. A. Dodge, B. W. Knight, and J. Toyoda. Voltage noise in limulus visual cells. *Science*, 160(3823):88 –90, Apr. 1968. http://dx.doi.org/10.1126/science.160.3823.88.

C. M. Doerning, C. R. Quinones, and A. T. Hartwick. Isolating the contribution of ipRGCs to the rat pupillary light reflex based on temporal properties of Melanopsin-Based photoreception. *ARVO Meeting Abstracts*, 52(6):3461, Apr. 2011.

N. Dokuchaev. On sub-ideal causal smoothing filters. *Signal Processing*, 92(1):219–223, Jan. 2012. http://dx.doi.org/10.1016/j.sigpro.2011.07.009.

R. P. Dolan and P. H. Schiller. Effects of ON channel blockade with 2-Amino-4-Phosphonobutyrate (APB) on brightness and contrast perception in monkeys. *Visual Neuroscience*, 11(01):23–32, 1994. http://dx.doi.org/10.1017/S095252380001107X.

P. Dolph, R. Ranganathan, N. Colley, R. Hardy, M. Socolich, and C. Zuker. Arrestin function in inactivation of g protein-coupled receptor rhodopsin in vivo. *Science*, 260 (5116):1910 –1916, June 1993. http://dx.doi.org/10.1126/science.8316831.

P. Dolph, A. Nair, and P. Raghu. Electroretinogram recordings of drosophila. *Cold Spring Harbor Protocols*, 2011(1):pdb.prot5549, Jan. 2011a. http://dx.doi.org/10.1101/pdb.prot5549.

P. Dolph, A. Nair, and P. Raghu. Whole-Cell Patch-Clamp analysis of adult drosophila photoreceptors. *Cold Spring Harbor Protocols*, 2011(1): pdb.prot5551, Jan. 2011b. http://dx.doi.org/10.1101/pdb.prot5551.

r. Donnelly, William J, K. Pesudovs, J. D. Marsack, E. J. Sarver, and R. A. Applegate. Quantifying scatter in Shack-Hartmann images to evaluate nuclear cataract. *Journal of Refractive Surgery (Thorofare, N.J.: 1995)*, 20 (5):S515–522, Oct. 2004. http://www.ncbi.nlm.nih.gov/pubmed/15523968.

K. Donner and T. Reuter. The photoproducts of rhodopsin in the isolated retina of the frog. *Vision Research*, 9(7):815–847, July 1969. http://dx.doi.org/10.1016/0042-6989(69)90017-0.

K. O. Donner and W. A. H. Rushton. Retinal stimulation by light substitution. *The Journal of Physiology*, 149(2):288–302, 1959a. http://www.ncbi.nlm.nih.gov/pubmed/13817555.

K. O. Donner and W. A. H. Rushton. Rod-cone interaction in the frog's retina analysed by the Stiles-Crawford effect and by dark adaptation. *The Journal of Physiology*, 149:303–317, Dec. 1959b. http://www.ncbi.nlm.nih.gov/pubmed/13817556.

G. Donnert, C. Eggeling, and S. W. Hell. Major signal increase in fluorescence microscopy through dark-state relaxation. *Nat Meth*, 4 (1):81–86, Jan. 2007. http://dx.doi.org/10.1038/nmeth986.

R. C. Dorf and R. H. Bishop. *Modern Control Systems*. Prentice Hall, 12 edition, July 2010.

G. K. Doring and E. Schaffers. Über die tagesrhytmik der pupillenweite beim menschen. *Pflugers Arch*, 252:537–541, 1950. http://dx.doi.org/10.1007/BF00463530.

S. Douglas and R. Losada. Adaptive filters in matlab: from novice to expert. pages 168–173, 2002. http://dx.doi.org/10.1109/DSPWS.2002.1231097.

J. E. Dowling. Chemistry of visual adaptation in the rat. *Nature*, 188(4745):114–118, Oct. 1960. http://dx.doi.org/10.1038/188114a0.

J. E. Dowling. Neural and photochemical mechanisms of visual adaptation in the rat. *The Journal of General Physiology*, 46:1287–1301, July 1963. http://www.ncbi.nlm.nih.gov/pubmed/14043003.

J. E. Dowling. *The Retina: An Approachable Part of the Brain*. Belknap Press of Harvard University Press, 1 edition, Jan. 1987.

S. E. Doyle, A. M. Castrucci, M. McCall, I. Provencio, and M. Menaker. Nonvisual light responses in the rpe65 knockout mouse: rod loss restores sensitivity to the melanopsin system. *Proceedings of the National Academy of Sciences of the United States of America*, 103(27):10432–7, July 2006. http://dx.doi.org/10.1073/pnas.0600934103.

S. E. Doyle, M. S. Grace, W. McIvor, and M. Menaker. Circadian rhythms of dopamine in mouse retina: the role of melatonin. *Visual Neuroscience*, 19(5):593–601, Mar. 2009. http://dx.doi.org/10.1017/S0952523802195058.

P. Drew, R. Sayres, K. Watanabe, and S. Shimojo. Pupillary response to chromatic flicker. *Experimental Brain Research. Experimentelle Hirnforschung. Expérimentation Cérébrale*, 136(2):256–262, Jan. 2001. http://dx.doi.org/10.1007/s002210000605.

E. Drouyer, C. Rieux, R. A. Hut, and H. M. Cooper. Responses of suprachiasmatic nucleus neurons to light and dark adaptation: relative contributions of melanopsin and rod-cone inputs. *The Journal of Neuroscience: The Official Journal of the Society for Neuroscience*, 27(36):9623–31, Sept. 2007. http://dx.doi.org/10.1523/JNEUROSCI.1391-07.2007.

J. F. Duffy, R. E. Kronauer, and C. A. Czeisler. Phase-shifting human circadian rhythms: influence of sleep timing, social contact and light exposure. *The Journal of physiology*, 495 (Pt 1):289–97, Aug. 1996. http://www.ncbi.nlm.nih.gov/sites/entrez?cmd=Retrieve&db=PubMed&list_uids=8866371&dopt=Citation.

J. F. Duffy, D. J. Dijk, E. B. Klerman, and C. A. Czeisler. Later endogenous circadian temperature nadir relative to an earlier wake time in older people. *Am J Physiol*, 275: R1478 – R1487, 1998.

J. F. Duffy, J. M. Zeitzer, and C. A. Czeisler. Decreased sensitivity to phase-delaying effects of moderate intensity light in older subjects. *Neurobiology of Aging*, 28(5):799–807, May 2007. http://dx.doi.org/10.1016/j.neurobiolaging.2006.03.005.

D. Dulić, S. J. van der Molen, T. Kudernac, H. T. Jonkman, J. J. D. de Jong, T. N. Bowden, J. van Esch, B. L. Feringa, and B. J. van Wees. One-Way optoelectronic switching of photochromic molecules on gold. *Physical Review Letters*, 91(20):207402, Nov. 2003. http://dx.doi.org/10.1103/PhysRevLett.91.207402.

O. N. Dumitrescu, F. G. Pucci, K. Y. Wong, and D. M. Berson. Ectopic retinal ON bipolar cell synapses in the OFF inner plexiform layer: Contacts with dopaminergic amacrine cells and melanopsin ganglion cells. *The Journal of Comparative Neurology*, 517(2):226–244, 2009. http://dx.doi.org/10.1002/cne.22158.

D. Dumortier, B. Coutelier, T. Faulcon, and F. Roy. PHOTOLUX: a new luminance mapping system based on nikon coolpix digital cameras. Berlin, Germany, 2005.

F. A. Dunn, M. J. Lankheet, and F. Rieke. Light adaptation in cone vision involves switching between receptor and post-receptor sites. *Nature*, 449(7162):603–606, Oct. 2007. http://dx.doi.org/10.1038/nature06150.

J. L. Ecker, O. N. Dumitrescu, K. Y. Wong, N. M. Alam, S. Chen, T. LeGates, J. M. Renna, G. T. Prusky, D. M. Berson, and S. Hattar. Melanopsin-Expressing retinal Ganglion-Cell photoreceptors: Cellular diversity and role in pattern vision. *Neuron*, 67(1):49–60, July 2010. http://dx.doi.org/10.1016/j.neuron.2010.05.023.

L. Edinger. Über den verlauf der centralen hirnnervenbahnen mit demonstrationen von präparaten. *Arch. Psychiat. Nervenkr.*, 16:858–859, 1885.

E. Eguchi and T. H. Waterman. Longterm dark induced fine structural changes in crayfish photoreceptor membrane. *Journal of Comparative Physiology ? A*, 131:191–203, 1979. http://dx.doi.org/10.1007/BF00610428.

C. M. Einterz, J. W. Lewis, and D. S. Kliger. Spectral and kinetic evidence for the existence of two forms of bathorhodopsin. *Proceedings of the National Academy of Sciences*, 84(11):3699 –3703, June 1987. http://www.pnas.org/content/84/11/3699.abstract.

K. Eliasieh, L. C. Liets, and L. M. Chalupa. Cellular reorganization in the human retina during normal aging. *Investigative Ophthalmology & Visual Science*, 48(6):2824 –2830, June 2007. http://dx.doi.org/10.1167/iovs.06-1228.

O. Elibol, T. Alçe, N. Yüksel, and Y. Çağlar. The influence of drop size of cyclopentolate, phenylephrine and tropicamide

on pupil dilatation and systemic side effects in infants. *Acta Ophthalmologica Scandinavica*, 75(2):178–180, Apr. 1997. http://dx.doi.org/10.1111/j.1600-0420.1997.tb00119.x.

A. J. Elliot, M. A. Maier, A. C. Moller, R. Friedman, and J. Meinhardt. Color and psychological functioning: the effect of red on performance attainment. *Journal of Experimental Psychology. General*, 136(1):154–168, Feb. 2007. http://dx.doi.org/10.1037/0096-3445.136.1.154.

D. Elliott, D. Whitaker, and D. MacVeigh. Neural contribution to spatiotemporal contrast sensitivity decline in healthy ageing eyes. *Vision Research*, 30(4):541–547, 1990. http://dx.doi.org/10.1016/0042-6989(90)90066-T.

C. J. Ellis. The pupillary light reflex in normal subjects. *The British journal of ophthalmology*, 65(11):754–9, Nov. 1981. http://www.ncbi.nlm.nih.gov/pubmed/7326222.

C. D. Elvidge, D. M. Keith, B. T. Tuttle, and K. E. Baugh. Spectral identification of lighting type and character. *Sensors*, 10:3961–3988, Apr. 2010. http://dx.doi.org/10.3390/s100403961.

J. A. Enezi, V. Revell, T. Brown, J. Wynne, L. Schlangen, and R. Lucas. A "melanopic" spectral efficiency function predicts the sensitivity of melanopsin photoreceptors to polychromatic lights. *Journal of Biological Rhythms*, 26(4):314–323, Aug. 2011. http://dx.doi.org/10.1177/0748730411409719.

J. M. Enoch. Optical properties of the retinal receptors. *Journal of the Optical Society of America*, 53(1):71–85, Jan. 1963. http://dx.doi.org/10.1364/JOSA.53.000071.

J. M. Enoch and V. Lakshminarayanan. 75th anniversary of the Stiles–Crawford effect(s): a celebratory special symposium: October 23 2008, rochester, new york. *Journal of Modern Optics*, 56(20):2164–2175, 2009. http://dx.doi.org/10.1080/09500340903023766.

I. R. Epstein. Can droplets and bubbles think? *Science*, 315(5813):775 –776, Feb. 2007. http://dx.doi.org/10.1126/science.1138325.

C. J. Erkelens. A dual visual–local feedback model of the vergence eye movement system. *Journal of Vision*, 11(10), 2011. http://dx.doi.org/10.1167/11.10.21.

T. Erneux. *Applied Delay Differential Equations*. Springer, 1 edition, Mar. 2009.

D. W. Esplin and B. Zablocka-Esplin. Rates of transmitter turnover in spinal monosynaptic pathway investigated by electrophysiological techniques. *Journal of Neurophysiology*, 34(5):842–859, Sept. 1971. http://www.ncbi.nlm.nih.gov/pubmed/4398563.

G. Esquiva, I. Gonzalez-Menedez, L. Fernandez-Sanchez, E. Garcia-Martin, I. Pinilla, J. Garcia-Fernandez, and N. Cuenca. Degeneration of melanopsin photosensitive ganglion cells in human retinas with aging and in animal models of retinitis pigmentosa. *ARVO Meeting Abstracts*, 51(5):680, Apr. 2010.

M. E. Estevez, S. Weng, E. C. Chan, and D. M. Berson. Form and function of m4 and m5 intrinsically photosensitive retinal ganglion cells. *ARVO Meeting Abstracts*, 52(6):5285, Apr. 2011.

O. Estévez and H. Spekreijse. The "silent substitution" method in visual research. *Vision Research*, 22(6):681–691, 1982. http://dx.doi.org/10.1016/0042-6989(82)90104-3.

D. Evanko. The scientist and the smartphone. *Nature Methods*, 7(2):87, Feb. 2010. http://dx.doi.org/10.1038/nmeth0210-87.

J. A. Evans, J. A. Elliott, and M. R. Gorman. Dim nighttime illumination accelerates adjustment to timezone travel in an animal model. *Current Biology*, 19(4):R156–R157, Feb. 2009. http://dx.doi.org/10.1016/j.cub.2009.01.023.

J. A. Evans, J. A. Elliott, and M. R. Gorman. Dim nighttime illumination interacts with parametric effects of bright light to increase the stability of circadian rhythm bifurcation in hamsters. *Chronobiology International*, 28:488–496, July 2011. http://dx.doi.org/10.3109/07420528.2011.591952.

G. L. Fain, H. R. Matthews, M. C. Cornwall, and Y. Koutalos. Adaptation in vertebrate photoreceptors. *Physiological Reviews*, 81(1):117–151, Jan. 2001. http://www.ncbi.nlm.nih.gov/pubmed/11152756.

X. Fan, J. H. Miles, N. Takahashi, and G. Yao. Abnormal transient pupillary light reflex in individuals with autism spectrum disorders. *Journal of Autism and Developmental Disorders*, 39:1499–1508, June 2009a. http://dx.doi.org/10.1007/s10803-009-0767-7.

X. Fan, J. H. Miles, N. Takahashi, and G. Yao. Sex-Specific lateralization of contraction anisocoria in transient pupillary light reflex. *Invest. Ophthalmol. Vis. Sci.*, 50(3):1137–1144, Mar. 2009b. http://dx.doi.org/10.1167/iovs.08-2329.

N. Fang, H. Lee, C. Sun, and X. Zhang. Sub-Diffraction-Limited optical imaging with a silver superlens. *Science*, 308(5721):534 –537, Apr. 2005. http://dx.doi.org/10.1126/science.1108759.

A. A. Fawzi, N. Lee, J. H. Acton, A. F. Laine, and R. T. Smith. Recovery of macular pigment spectrum in vivo using hyperspectral image analysis. *Journal of Biomedical Optics*, 16:106008, 2011. http://dx.doi.org/10.1117/1.3640813.

A. M. Fay, S. L. Trokel, and J. A. Myers. Pupil diameter and the principal ray. *Journal of Cataract and Refractive Surgery*, 18(4):348–351, July 1992. http://www.ncbi.nlm.nih.

gov/pubmed/1501085.

B. Feigl, A. J. Zele, S. M. Fader, A. N. Howes, C. E. Hughes, K. A. Jones, and R. Jones. The post-illumination pupil response of melanopsin-expressing intrinsically photosensitive retinal ganglion cells in diabetes. *Acta Ophthalmologica*, Aug. 2011. http://dx.doi.org/10.1111/j.1755-3768.2011.02226.x.

R. Feinberg and E. Podolak. Latency of pupillary reflex to light stimulation and its relationship to aging. In A. Welford and J. Birren, editors, *Aging and the Nervous System*, pages 326–329. CC Thomas, Springfield, IL, USA, 1965.

J. E. J. Ferrell. Self-perpetuating states in signal transduction: positive feedback, double-negative feedback and bistability. *Current Opinion in Cell Biology*, 14(2):140–148, Apr. 2002. http://dx.doi.org/10.1016/S0955-0674(02)00314-9.

M. Fetter. Vestibulo-Ocular reflex. In A. Straube and U. Büttner, editors, *Developments in Ophthalmology*, volume 40, pages 35–51. KARGER, Basel, 2007. http://dx.doi.org/10.1159/000100348.

G. Field and E. Chichilnisky. Information processing in the primate retina: Circuitry and coding. *Annual Review of Neuroscience*, 30 (1):1–30, July 2007. http://dx.doi.org/10.1146/annurev.neuro.30.051606.094252.

M. Figueiro, A. Bierman, B. Plitnick, and M. Rea. Preliminary evidence that both blue and red light can induce alertness at night. *BMC Neuroscience*, 10(1): 105, 2009. http://dx.doi.org/10.1186/1471-2202-10-105.

M. G. Figueiro, J. D. Bullough, R. H. Parsons, and M. S. Rea. Preliminary evidence for spectral opponency in the suppression of melatonin by light in humans. *Neuroreport*, 15(2):313–6, Feb. 2004. http://www.ncbi.nlm.nih.gov/pubmed/15076759.

M. G. Figueiro, J. D. Bullough, A. Bierman, and M. S. Rea. Demonstration of additivity failure in human circadian phototransduction. *Neuro Endocrinology Letters*, 26(5): 493–8, Oct. 2005. http://www.ncbi.nlm.nih.gov/pubmed/16264413.

M. G. Figueiro, M. S. Rea, and J. D. Bullough. Circadian effectiveness of two polychromatic lights in suppressing human nocturnal melatonin. *Neuroscience Letters*, 406(3): 293–297, Oct. 2006. http://dx.doi.org/10.1016/j.neulet.2006.07.069.

M. G. Figueiro, A. Bierman, and M. S. Rea. Retinal mechanisms determine the subadditive response to polychromatic light by the human circadian system. *Neuroscience Letters*, 438(2):242–245, June 2008. http://dx.doi.org/10.1016/j.neulet.2008.04.055.

P. G. Fillmore. The medical examination of hiroshima patients with radiation cataracts. *Science*, 116(3013):322 –323, 1952. http://dx.doi.org/10.1126/science.116.3013.322.

J. M. Findlay and R. Walker. A model of saccade generation based on parallel processing and competitive inhibition. *The Behavioral and Brain Sciences*, 22(4):661–674; discussion 674–721, Aug. 1999. http://www.ncbi.nlm.nih.gov/pubmed/11301526.

M. Fioretto, G. Piero Fava, R. Lotti, and W. G. Sannita. Early receptor potentials recorded in humans via dermal electrodes. *Documenta Ophthalmologica*, 79(2):109–116, 1992. http://dx.doi.org/10.1007/BF00156570.

M. Firsov, A. Kolesnikov, E. Golobokova, and V. Govardovskii. Two realms of dark adaptation. *Vision Research*, 45(2):147–151, Jan. 2005. http://dx.doi.org/10.1016/j.visres.2004.08.005.

M. L. Firsov, K. Donner, and V. I. Govardovskii. pH and rate of 'dark' events in toad retinal rods: test of a hypothesis on the molecular origin of photoreceptor noise. *The Journal of Physiology*, 539(3):837 –846, Mar. 2002. http://dx.doi.org/10.1113/jphysiol.2001.013207.

M. A. Fischler and R. C. Bolles. Random sample consensus: a paradigm for model fitting with applications to image analysis and automated cartography. *Communications of the ACM*, 24:381–395, June 1981. http://dx.doi.org/10.1145/358669.358692.

N. Fishkin, Y. Jang, Y. Itagaki, J. R. Sparrow, and K. Nakanishi. A2-rhodopsin: a new fluorophore isolated from photoreceptor outer segments. *Organic & Biomolecular Chemistry*, 1(7):1101–1105, Apr. 2003. http://www.ncbi.nlm.nih.gov/pubmed/12926382.

K. J. Fogle, K. G. Parson, N. A. Dahm, and T. C. Holmes. CRYPTOCHROME is a Blue-Light sensor that regulates neuronal firing rate. *Science*, 331(6023):1409 –1413, Mar. 2011. http://dx.doi.org/10.1126/science.1199702.

H. K. Fong, M. Lin, and S. Pandey. Exon-skipping variant of RGR opsin in human retina and pigment epithelium. *Experimental Eye Research*, 83(1):133–140, July 2006. http://dx.doi.org/10.1016/j.exer.2005.11.013.

C. I. Fontaine and M. Hébert. Possible implication of melanopsin bistability for the increase of human heart rate influenced by bichromatic blue and red light. In *Poster*, Montreal, Canada, 2011.

M. Forejt, J. Hollan, K. Skocovský, and R. Skotnica. Sleep disturbances by light at night:two queries made in 2003 in czechia. Graz, Austria, Oct. 2004.

J. S. Fosnaugh, E. B. Bunker, and W. B. Pickworth. Daily variation and effects of ambient light and circadian factors on the human light reflex. *Methods and Findings in Experimental and Clinical Pharmacology*, 14(7): 545–553, Sept. 1992. http://www.ncbi.nlm.nih.gov/pubmed/1287379.

D. H. Foster. Color constancy. *Vision Research*, 51(7):674–700, Apr. 2011a. http://dx.doi.org/10.1016/j.visres.2010.09.006.

R. G. Foster. Body clocks, light, sleep and health. In *Oral presentation at Velux 2011*, Lausanne, Switzerland, 2011b.

R. G. Foster and M. W. Hankins. Circadian vision. *Current Biology*, 17(17):R746–R751, Sept. 2007. http://dx.doi.org/10.1016/j.cub.2007.07.007.

D. F. Fotiou, C. G. Brozou, A. Haidich, D. Tsiptsios, M. Nakou, A. Kabitsi, C. Giantselidis, and F. Fotiou. Pupil reaction to light in alzheimer's disease: evaluation of pupil size changes and mobility. *Aging Clinical and Experimental Research*, 19(5): 364–71, Oct. 2007. http://www.ncbi.nlm.nih.gov/pubmed/18007114.

M. A. Fox and W. Guido. Shedding light on Class-Specific wiring: Development of intrinsically photosensitive retinal ganglion cell circuitry. *Molecular Neurobiology*, 44(3): 321–329, Aug. 2011. http://dx.doi.org/10.1007/s12035-011-8199-8.

N. Franceschini and K. Kirschfeld. Le contrôle automatique du flux lumineux dans l'oeil composé des diptères. *Biological Cybernetics*, 21:181–203, 1976. http://dx.doi.org/10.1007/BF00344164.

N. Franceschini, K. Kirschfeld, and B. Minke. Fluorescence of photoreceptor cells observed in vivo. *Science*, 213(4513):1264 –1267, 1981. http://dx.doi.org/10.1126/science.7268434.

G. Francis, L. Bishop, C. Luke, B. Middleton, P. Williams, and J. Arendt. Sleep during the antarctic winter: preliminary observations on changing the spectral composition of artificial light. *Journal of Sleep Research*, 17(3):354–360, Sept. 2008. http://dx.doi.org/10.1111/j.1365-2869.2008.00664.x.

D. W. Frank, J. A. Evans, and M. R. Gorman. Time-Dependent effects of dim light at night on Re-Entrainment and masking of hamster activity rhythms. *Journal of Biological Rhythms*, 25(2):103 –112, Apr. 2010. http://dx.doi.org/10.1177/0748730409360890.

K. A. Franz, W. G. Kehr, A. Siggel, J. Wieczoreck, and W. Adam. Luminescent materials. *Book Title Ullmann's Encyclopedia of Industrial Chemistry Ullmann's Encyclopedia of Industrial Chemistry*, 1989. http://dx.doi.org/10.1002/14356007.a15_519.

P. L. Franzen, D. J. Buysse, R. E. Dahl, W. Thompson, and G. J. Siegle. Sleep deprivation alters pupillary reactivity to emotional stimuli in healthy young adults. *Biological Psychology*, 80(3):300–305, Mar. 2009. http://dx.doi.org/10.1016/j.biopsycho.2008.10.010.

C. E. Frederick, S. Weng, and D. M. Berson. Arrestin and response termination in ganglion-cell photoreceptors. *ARVO Meeting Abstracts*, 50(5):5032, Apr. 2009.

M. S. Freedman, R. J. Lucas, B. Soni, M. von Schantz, M. Muñoz, Z. David-Gray, and R. Foster. Regulation of mammalian circadian behavior by non-rod, non-cone, ocular photoreceptors. *Science*, 284(5413):502 –504, Apr. 1999. http://dx.doi.org/10.1126/science.284.5413.502.

M. Freeman. *Optics*. Butterworth-Heinemann, Oxford, 10 edition, 1990.

A. French, M. Korenberg, M. Järvilehto, E. Kouvalainen, M. Juusola, and M. Weckström. The dynamic nonlinear behavior of fly photoreceptors evoked by a wide range of light intensities. *Biophysical Journal*, 65(2): 832–839, Aug. 1993. http://dx.doi.org/10.1016/S0006-3495(93)81116-0.

A. S. French. The effect of light adaptation on the dynamic properties of phototransduction in the fly, phormia regina. *Biological Cybernetics*, 32:115–123, 1979. http://www.springerlink.com/content/u6jq318671n72121/.

P. R. Freund, J. Watson, G. S. Gilmour, F. Gaillard, and Y. Sauvé. Differential changes in retina function with normal aging in humans. *Documenta Ophthalmologica*, 122(3): 177–190, May 2011. http://dx.doi.org/10.1007/s10633-011-9273-2.

E. Fromm, C. Horlebein, A. Meergans, M. Niesner, and C. Randler. Evaluation of a dawn simulator in children and adolescents. *Biological Rhythm Research*, 42(5):417–425, 2011. http://dx.doi.org/10.1080/09291016.2010.525851.

Y. Fu, H. Zhong, M. H. Wang, D. Luo, H. Liao, H. Maeda, S. Hattar, L. J. Frishman, and K. Yau. Intrinsically photosensitive retinal ganglion cells detect light with a vitamin a-based photopigment, melanopsin. *Proceedings of the National Academy of Sciences of the United States of America*, 102(29):10339–10344, July 2005. http://dx.doi.org/10.1073/pnas.0501866102.

Y. Fukuda, S. Tsujimura, S. Higuchi, A. Yasukouchi, and T. Morita. The ERG responses to light stimuli of melanopsin-expressing retinal ganglion cells that are independent of rods and cones. *Neuroscience Letters*, 479(3): 282–286, Aug. 2010. http://dx.doi.org/10.1016/j.neulet.2010.05.080.

K. Fuld, B. R. Wooten, and L. Katz. The Stiles-Crawford hue shift following photopigment depletion. *Nature*, 279(5709): 152–154, May 1979. http://dx.doi.org/10.1038/279152a0.

P. M. Fuller, J. Lu, and C. B. Saper. Differential rescue of light- and Food-Entrainable circadian rhythms. *Science*, 320(5879):1074–1077, May 2008. http://dx.doi.org/10.1126/science.1153277.

M. G. Fuortes and S. Yeandle. Probability of occurrence of discrete potential waves in the eye of limulus. *The Journal of General Physiology*, 47:443–463, Jan. 1964. http://www.ncbi.nlm.nih.gov/pubmed/14100964.

M. G. F. Fuortes and A. L. Hodgkin. Changes in time scale and sensitivity in the ommatidia of limulus. *The Journal of Physiology*, 172(2):239–263, July 1964. http://www.ncbi.nlm.nih.gov/pubmed/14205019.

J. R. Gaddy, M. Edelson, K. Stewart, and G. C. Brainard. Possible retinal spatial summation in melatonin suppression. Walter De Gruyter Inc, 1992.

J. R. Gaddy, M. D. Rollag, and G. C. Brainard. Pupil size regulation of threshold of light-induced melatonin suppression. *The Journal of Clinical Endocrinology and Metabolism*, 77(5):1398–1401, Nov. 1993. http://dx.doi.org/10.1210/jc.77.5.1398.

N. Gadoth, N. Schlaen, D. Maschkowski, and M. Bechar. The pupil cycle time in familial dysautonomia. further evidence for denervation hypersensitivity. *Metabolic, Pediatric, and Systemic Ophthalmology*, 7(3):131–134, 1983. http://www.ncbi.nlm.nih.gov/pubmed/6656621.

E. R. Gaillard, L. Zheng, J. C. Merriam, and J. Dillon. Age-related changes in the absorption characteristics of the primate lens. *Investigative Ophthalmology & Visual Science*, 41(6):1454–1459, May 2000. http://www.ncbi.nlm.nih.gov/pubmed/10798662.

D. M. Gakamsky, B. Dhillon, J. Babraj, M. Shelton, and S. D. Smith. Exploring the possibility of early cataract diagnostics based on tryptophan fluorescence. *Journal of The Royal Society Interface*, 8(64):1616 –1621, Nov. 2011. http://dx.doi.org/10.1098/rsif.2010.0608.

A. D. Galasiu and J. A. Veitch. Occupant preferences and satisfaction with the luminous environment and control systems in daylit offices: a literature review. *Energy and Buildings*, 38(7):728–742, July 2006. http://dx.doi.org/10.1016/j.enbuild.2006.03.001.

D. Gall. Die messung circadianer strahlungsgrößen, 2004.

D. Gall and K. Bieske. Definition and measurement of circadian radiometric quantities. CIE x027:2004, pages 129–132, Vienna, Austria, 2004.

T. Gallaway, R. N. Olsen, and D. M. Mitchell. The economics of global light pollution. *Ecological Economics*, 69(3):658–665, Jan. 2010. http://dx.doi.org/10.1016/j.ecolecon.2009.10.003.

H. D. Gambill, K. N. Ogle, and T. P. Kearns. Mydriatic effect of four drugs determined with pupillograph. *Archives of Ophthalmology*, 77(6):740–746, June 1967. http://www.ncbi.nlm.nih.gov/pubmed/6026181.

P. D. Gamlin and R. J. Clarke. The pupillary light reflex pathway of the primate. *Journal of the American Optometric Association*, 66(7):415–8, July 1995. http://www.ncbi.nlm.nih.gov/pubmed/7560728.

P. D. Gamlin, D. H. McDougal, J. Pokorny, V. C. Smith, K. Yau, and D. M. Dacey. Human and macaque pupil responses driven by melanopsin-containing retinal ganglion cells. *Vision Research*, 47(7):946–954, Mar. 2007. http://dx.doi.org/10.1016/j.visres.2006.12.015.

P. D. R. Gamlin. Functions of the Edinger-Westphal nucleus. In G. Burnstock, editor, *Nervous Control of the Eye*, pages 117–154. Harwood Academic, 2000.

P. D. R. Gamlin. Neural mechanisms for the control of vergence eye movements. *Annals of the New York Academy of Sciences*, 956(1):264–272, Apr. 2002. http://dx.doi.org/10.1111/j.1749-6632.2002.tb02825.x.

P. D. R. Gamlin, H. Zhang, and R. J. Clarke. Luminance neurons in the pretectal olivary nucleus mediate the pupillary light reflex in the rhesus monkey. *Experimental Brain Research*, 106(1):177–180, 1995. http://dx.doi.org/10.1007/BF00241367.

P. D. R. Gamlin, B. B. Peterson, and D. M. Dacey. Physiology and morphology of retinal ganglion cells projecting to the pretectal olivary nucleus of the rhesus monkey. *Investigative Ophthalmology & Visual Science*, 42((Suppl)):676, 2001.

W. Gao, B. Cense, Y. Zhang, R. S. Jonnal, and D. T. Miller. Measuring retinal contributions to the optical Stiles-Crawford effect with optical coherence tomography. *Optics Express*, 16(9):6486–6501, Apr. 2008. http://dx.doi.org/10.1364/OE.16.006486.

J. Garcia-Ojalvo. Physical approaches to the dynamics of genetic circuits: A tutorial. *arXiv:1105.4335*, May 2011. http://dx.doi.org/10.1080/00107514.2011.588432.

P. Garrigan, C. P. Ratliff, J. M. Klein, P. Sterling, D. H. Brainard, and V. Balasubramanian. Design of a trichromatic cone array. *PLoS Comput Biol*, 6(2):e1000677, Feb. 2010. http://dx.doi.org/10.1371/journal.pcbi.1000677.

P. Gaudiano. Simulations of x and y retinal ganglion cell behavior with a nonlinear push-pull model of spatiotemporal retinal processing. *Vision Research*, 34(13):1767–1784, July 1994. http://dx.doi.org/10.1016/0042-6989(94)90131-7.

W. J. Geeraets, R. C. Williams, G. Chan, W. T. Ham, D. Guerry, and F. H. Schmidt. The loss of light energy in retina and choroid.

Archives of Ophthalmology, 64:606–615, Oct. 1960. http://www.ncbi.nlm.nih.gov/pubmed/13704161.

W. Gern and C. Ralph. Melatonin synthesis by the retina. *Science*, 204(4389):183 –184, Apr. 1979. http://dx.doi.org/10.1126/science.432640.

H. M. Gibbs. *Optical bistability: controlling light with light*. Academic Press Inc, Orlando, FL, USA, 1985.

M. E. Giesbers, N. Shirzad-Wasei, G. J. C. G. M. Bosman, and W. J. De Grip. Functional expression, targeting and ca2+ signaling of a mouse Melanopsin-eYFP fusion protein in a retinal pigment epithelium cell line†. *Photochemistry and Photobiology*, 84(4):990–995, 2008. http://dx.doi.org/10.1111/j.1751-1097.2008.00347.x.

M. C. Giménez, M. Hessels, M. van de Werken, B. de Vries, D. G. M. Beersma, and M. C. M. Gordijn. Effects of artificial dawn on subjective ratings of sleep inertia and dim light melatonin onset. *Chronobiol Int*, 27(6):1219–1241, 2010. http://dx.doi.org/10.3109/07420528.2010.496912.

M. C. Gimenez, M. J. Kanis, D. G. M. Beersma, B. A. E. van der Pol, D. van Norren, and M. C. M. Gordijn. In vivo quantification of the retinal reflectance spectral composition in elderly subjects before and after cataract surgery: Implications for the Non-Visual effects of light. *J Biol Rhythms*, 25(2):123–131, Apr. 2010. http://dx.doi.org/10.1177/0748730409360888.

G. Glickman, J. P. Hanifin, M. D. Rollag, J. Wang, H. M. Cooper, and G. C. Brainard. Inferior retinal light exposure is more effective than superior retinal exposure in suppressing melatonin in humans. *Journal of Biological Rhythms*, 18(1):71–9, Feb. 2003. http://dx.doi.org/10.1177/0748730402239678.

S. Goldberg, T. Frumkes, and R. Nygaard. Inhibitory influence of unstimulated rods in the human retina: evidence provided by examining cone flicker. *Science*, 221(4606):180 –182, July 1983. http://dx.doi.org/10.1126/science.6857279.

L. J. Goldman, S. N. Barnes, and T. H. Goldsmith. Microspectrophotometry of rhodopsin and metarhodopsin in the moth galleria. *The Journal of General Physiology*, 66(3):383 –404, 1975. http://dx.doi.org/10.1085/jgp.66.3.383.

T. H. Goldsmith. The natural history of invertebrate visual pigments. In H. J. A. Dartnall, editor, *Handbook of Sensory physiology. Photochemistry of Vision*, pages 685–719. Springer, 1972.

T. H. Goldsmith and R. Wehner. Restrictions on rotational and translational diffusion of pigment in the membranes of a rhabdomeric photoreceptor. *The Journal of General Physiology*, 70(4):453–490, Oct. 1977. http://dx.doi.org/10.1007/BF02442326.

B. E. Goldstein and E. L. Berson. Cone dominance of the human early receptor potential. *Nature*, 222(5200):1272–1273, June 1969. http://dx.doi.org/10.1038/2221272a0.

E. B. Goldstein and E. L. Berson. Rod and cone contributions to the human early receptor potential. *Vision Research*, 10(3):207–218, Mar. 1970. http://dx.doi.org/10.1016/0042-6989(70)90126-4.

T. Gollisch and M. Meister. Eye smarter than scientists believed: Neural computations in circuits of the retina. *Neuron*, 65(2):150–164, Jan. 2010. http://dx.doi.org/10.1016/j.neuron.2009.12.009.

E. Golobokova and V. Govardovskii. Late stages of visual pigment photolysis in situ: Cones vs. rods. *Vision Research*, 46(14):2287–2297, July 2006. http://dx.doi.org/10.1016/j.visres.2005.12.017.

M. d. P. Gomez, J. M. Angueyra, and E. Nasi. Light-transduction in melanopsin-expressing photoreceptors of amphioxus. *Proceedings of the National Academy of Sciences*, 106(22):9081 –9086, June 2009. http://dx.doi.org/10.1073/pnas.0900708106.

R. C. Gonzalez and R. E. Woods. *Digital Image Processing*. Prentice Hall, 2nd edition, Jan. 2002.

C. F. Goodeve, R. J. Lythgoe, and E. E. Schneider. The photosensitivity of visual purple solutions and the scotopic sensitivity of the eye in the Ultra-Violet. *Proceedings of the Royal Society of London. Series B - Biological Sciences*, 130(861):380 –395, May 1942. http://dx.doi.org/10.1098/rspb.1942.0007.

J. J. Gooley, J. Lu, T. C. Chou, T. E. Scammell, and C. B. Saper. Melanopsin in cells of origin of the retinohypothalamic tract. *Nat Neurosci*, 4(12):1165, Dec. 2001. http://dx.doi.org/10.1038/nn768.

J. J. Gooley, S. M. W. Rajaratnam, G. C. Brainard, R. E. Kronauer, C. A. Czeisler, and S. W. Lockley. Spectral responses of the human circadian system depend on the irradiance and duration of exposure to light. *Science Translational Medicine*, 2(31):31ra33, May 2010. http://dx.doi.org/10.1126/scitranslmed.3000741.

M. Gordijn, D. 't Mannetje, and Y. Meesters. The effects of blue-enriched light treatment compared to standard light treatment in seasonal affective disorder. *Journal of Affective Disorders*, 136(1–2):72–80, Jan. 2012. http://dx.doi.org/10.1016/j.jad.2011.08.016.

T. G. Gorgels and D. V. Norren. Spectral transmittance of the rat lens. *Vision Research*, 32(8):1509–1512, Aug. 1992. http://dx.doi.org/10.1016/0042-6989(92)90206-X.

R. Gortlemeyer and H. Wieman. Retest reliability and construct validity of critical flicker fusion frequency. *Pharmacopsychia-*

try, 15(Suppl. 1):24–28, 1982.

P. G. Gottschalk and J. R. Dunn. Determining the error of dose estimates and minimum and maximum acceptable concentrations from assays with nonlinear dose-response curves. *Computer Methods and Programs in Biomedicine*, 80(3):204–215, Dec. 2005. http://dx.doi.org/10.1016/j.cmpb.2005.08.003.

V. I. Govardovskii and M. L. Firsov. Unknown mechanisms regulating the GPCR signal cascade in vertebrate photoreceptors. *Neuroscience and Behavioral Physiology*, 42(2):180–192, Dec. 2011. http://dx.doi.org/10.1007/s11055-011-9551-1.

V. I. Govardovskii, N. Fyhrquist, T. Reuter, D. G. Kuzmin, and K. Donner. In search of the visual pigment template. *Visual Neuroscience*, 17(04):509–528, 2000. http://dx.doi.org/10.1017/S0952523800174036.

D. Göz, K. Studholme, D. A. Lappi, M. D. Rollag, I. Provencio, and L. P. Morin. Targeted destruction of photosensitive retinal ganglion cells with a saporin conjugate alters the effects of light on mouse circadian rhythms. *PLoS ONE*, 3(9): e3153, 2008. http://dx.doi.org/10.1371/journal.pone.0003153.

D. Graham. Melanopsin ganglion cells: A bit of fly in the mammalian eye. In H. Kolb, E. Fernandez, and R. Nelson, editors, *Webvision: The Organization of the Retina and Visual System*. Salt Lake City (UT): University of Utah Health Sciences Center, Aug. 2008.

D. M. Graham, K. Y. Wong, P. Shapiro, C. Frederick, K. Pattabiraman, and D. M. Berson. Melanopsin ganglion cells use a membrane-associated rhabdomeric phototransduction cascade. *Journal of Neurophysiology*, 99(5):2522–2532, May 2008. http://dx.doi.org/10.1152/jn.01066.2007.

N. V. S. Graham. *Visual Pattern Analyzers*. Oxford University Press, USA, 1 edition, Aug. 2001.

E. Granholm, S. Morris, D. Galasko, C. Shults, E. Rogers, and B. Vukov. Tropicamide effects on pupil size and pupillary light reflexes in alzheimer's and parkinson's disease. *International Journal of Psychophysiology*, 47(2):95–115, Feb. 2003. http://dx.doi.org/10.1016/S0167-8760(02)00122-8.

F. Grass and S. Kasper. Humoral phototransduction: Light transportation in the blood, and possible biological effects. *Medical Hypotheses*, 71(2):314–317, Aug. 2008. http://dx.doi.org/10.1016/j.mehy.2008.01.034.

D. C. Gray, W. Merigan, J. I. Wolfing, B. P. Gee, J. Porter, A. Dubra, T. H. Twietmeyer, K. Ahamd, R. Tumbar, F. Reinholz, and D. R. Williams. In vivo fluorescence imaging of primate retinal ganglion cells and retinal pigment epithelial cells. *Optics Express*, 14(16):7144–7158, 2006. http://dx.doi.org/10.1364/OE.14.007144.

R. Gray, S. A. Perkins, R. Suryakumar, B. Neuman, and W. A. Maxwell. Reduced effect of glare disability on driving performance in patients with blue light–filtering intraocular lenses. *Journal of Cataract & Refractive Surgery*, 37(1):38–44, Jan. 2011. http://dx.doi.org/10.1016/j.jcrs.2010.07.034.

A. Greenwood. Sarcoma of the choroid not demonstrable by the ordinary transilluminator. *Transactions of the American Ophthalmological Society*, 13(Pt 2):503–508, 1913. http://www.ncbi.nlm.nih.gov/pubmed/16692297.

D. S. Grewal, G. S. Brar, and S. P. S. Grewal. Correlation of nuclear cataract lens density using scheimpflug images with lens opacities classification system III and visual function. *Ophthalmology*, 116(8):1436–1443, Aug. 2009. http://dx.doi.org/10.1016/j.ophtha.2009.03.002.

F. G. Gribakin and K. Y. Ukhanov. Is the white eye of insect eye-color mutants really white? *Journal of Comparative Physiology A*, 167(5), Nov. 1990. http://dx.doi.org/10.1007/BF00192666.

K. Grieve and A. Roorda. Intrinsic signals from human cone photoreceptors. *Invest. Ophthalmol. Vis. Sci.*, 49(2):713–719, Feb. 2008. http://dx.doi.org/10.1167/iovs.07-0837.

C. Grimm, C. E. Remé, P. O. Rol, and T. P. Williams. Blue light's effects on rhodopsin: Photoreversal of bleaching in living rat eyes. *Investigative Ophthalmology & Visual Science*, 41(12):3984 –3990, Nov. 2000. http://www.ncbi.nlm.nih.gov/pubmed/11053303.

C. Grimm, A. Wenzel, T. P. Williams, P. O. Rol, F. Hafezi, and C. E. Remé. Rhodopsin-Mediated Blue-Light damage to the rat retina: Effect of photoreversal of bleaching. *Investigative Ophthalmology & Visual Science*, 42(2):497 –505, Feb. 2001. http://www.ncbi.nlm.nih.gov/pubmed/11157889.

M. S. Griswold and W. S. Stark. Scotopic spectral sensitivity of phakic and aphakic observers extending into the near ultraviolet. *Vision Research*, 32(9):1739–1743, Sept. 1992. http://dx.doi.org/10.1016/0042-6989(92)90166-G.

J. Grünberger, L. Linzmayer, E. Majda, A. Reitner, and H. Walter. Pupillary dilatation test and fourier analysis of pupillary oscillations in patients with multiple sclerosis. *European Archives of Psychiatry and Clinical Neuroscience*, 246(4):209–212, June 1996. http://dx.doi.org/10.1007/BF02188955.

U. Grünert, P. R. Jusuf, S. C. S. Lee, and D. T. Nguyen. Bipolar input to melanopsin containing ganglion cells in primate retina. *Visual Neuroscience*, FirstView:1–12, 2010. http://dx.doi.org/

10.1017/S095252381000026X.

S. Gruppetta, L. Koechlin, F. Lacombe, and P. Puget. Curvature sensor for the measurement of the static corneal topography and the dynamic tear film topography in the human eye. *Optics Letters*, 30(20):2757–2759, Oct. 2005. http://dx.doi.org/10.1364/OL.30.002757.

C. A. Gueymard. Parameterized transmittance model for direct beam and circumsolar spectral irradiance. *Solar Energy*, 71(5):325–346, Nov. 2001. http://dx.doi.org/10.1016/S0038-092X(01)00054-8.

C. A. Gueymard. The sun's total and spectral irradiance for solar energy applications and solar radiation models. *Solar Energy*, 76(4):423–453, Apr. 2004. http://dx.doi.org/10.1016/j.solener.2003.08.039.

R. Guido, P. Addison, and J. Walker. Introducing wavelets and time–frequency analysis. *Engineering in Medicine and Biology Magazine, IEEE*, 28(5):13, 2009. http://dx.doi.org/10.1109/MEMB.2009.934243.

A. D. Güler, J. L. Ecker, G. S. Lall, S. Haq, C. M. Altimus, H. Liao, A. R. Barnard, H. Cahill, T. C. Badea, H. Zhao, M. W. Hankins, D. M. Berson, R. J. Lucas, K. Yau, and S. Hattar. Melanopsin cells are the principal conduits for rod-cone input to non-image-forming vision. *Nature*, 453(7191):102–105, May 2008. http://dx.doi.org/10.1038/nature06829.

A. Hachol, W. Szczepanowska-Nowak, H. Kasprzak, I. Zawojska, A. Dudzinski, R. Kinasz, and D. Wygledowska-Promienska. Measurement of pupil reactivity using fast pupillometry. *Physiological Measurement*, 28:61–72, Jan. 2007. http://dx.doi.org/10.1088/0967-3334/28/1/006.

G. S. Hafner and D. Bok. The distribution of 3H-leucine labeled protein in the retinula cells of the crayfish retina. *The Journal of Comparative Neurology*, 174(3):397–416, Aug. 1977. http://www.ncbi.nlm.nih.gov/pubmed/903413.

W. A. Hagins and R. E. McGaughy. Molecular and thermal origins of fast photoelectric effects in the squid retina. *Science*, 157 (3790):813 –816, 1967. http://dx.doi.org/10.1126/science.157.3790.813.

R. Haitz and J. Y. Tsao. Solid-state lighting: 'The case' 10 years after and future prospects. *Physica Status Solidi (a)*, 208(1):17–29, Jan. 2011. http://dx.doi.org/10.1002/pssa.201026349.

K. Hamdorf. The physiology of invertebrate visual pigments. In H. Autrum, editor, *Handbook of Sensory physiology. Comparative Physiology and Evolution of Vision in Invertebrates. A. Invertebrate Photoreceptors*, volume 7, pt. 6A, pages 145–224. Springer-Verlag, Berlin, 1979.

K. Hamdorf and S. Razmjoo. The prolonged depolarizing afterpotential and its contribution to the understanding of photoreceptor function. *Biophysics of Structure and Mechanism*, 3:163–170, 1977. http://dx.doi.org/10.1007/BF00535813.

K. Hamdorf and S. Razmjoo. Photoconvertible pigment states and excitation in calliphora; the induction and properties of the prolonged depolarising afterpotential. *Biophysics of Structure and Mechanism*, 5:137–161, 1979. http://dx.doi.org/10.1007/BF00535444.

K. Hamdorf and J. Schwemer. Photoregeneration and the adaptation process in insect photoreceptors. In A. W. Snyder and R. Menzel, editors, *Photoreceptor optics*, pages 263–289. Springer, Berlin, Heidelberg, New York, 1975.

K. Hamdorf, G. Höglund, and H. Langer. Photoregeneration of visual pigments in a moth. a microphotometric study. *Journal of Comparative Physiology*, 86:247–263, 1973a.

K. Hamdorf, R. Paulsen, and J. Schwemer. Photoregeneration and sensitivity control of photoreceptors of invertebrates. In H. Langer, editor, *Biochemistry and physiology of visual pigments*, pages 155–166. Springer, Berlin, Heidelberg, New York, 1973b.

B. R. Hammond, B. R. Wooten, J. E. Náñez, and A. J. Wenzel. Smoking and lens optical density. *Ophthalmic and Physiological Optics*, 19(4):300–305, July 1999. http://dx.doi.org/10.1046/j.1475-1313.1999.00444.x.

B. R. J. Hammond and B. R. Wooten. CFF thresholds: relation to macular pigment optical density. *Ophthalmic and Physiological Optics*, 25(4):315–319, July 2005. http://dx.doi.org/10.1111/j.1475-1313.2005.00271.x.

C. J. Hammond, H. Snieder, T. D. Spector, and C. E. Gilbert. Factors affecting pupil size after dilatation: the twin eye study. *British Journal of Ophthalmology*, 84(10):1173 –1176, Oct. 2000. http://dx.doi.org/10.1136/bjo.84.10.1173.

J. Hammond, B. R. Wooten, and D. M. Snodderly. Individual variations in the spatial profile of human macular pigment. *Journal of the Optical Society of America A*, 14 (6):1187–1196, June 1997a. http://dx.doi.org/10.1364/JOSAA.14.001187.

J. Hammond, B R, B. R. Wooten, and D. M. Snodderly. Density of the human crystalline lens is related to the macular pigment carotenoids, lutein and zeaxanthin. *Optometry and Vision Science: Official Publication of the American Academy of Optometry*, 74(7):499–504, July 1997b. http://www.ncbi.nlm.nih.gov/pubmed/9293517.

K. M. Hampson. Adaptive optics and vision. *Journal of Modern Optics*, 55(21):3425–3467, 2008. http://dx.doi.org/10.1080/

09500340802541777.

M. Hanani and P. Hillman. Absorption of light by metarhodopsin modifies the effect of a conditioning light on the barnacle photoreceptor. *Biophysics of Structure and Mechanism*, 5:231–235, 1979. http://dx.doi.org/10.1007/BF00535451.

M. W. Hankins and R. J. Lucas. The primary visual pathway in humans is regulated according to long-term light exposure through the action of a nonclassical photopigment. *Current Biology: CB*, 12(3): 191–8, Feb. 2002. http://dx.doi.org/10.1016/S0960-9822(02)00659-0.

J. Hannibal and J. Fahrenkrug. Target areas innervated by PACAP-immunoreactive retinal ganglion cells. *Cell and Tissue Research*, 316:99–113, Apr. 2004. http://dx.doi.org/10.1007/s00441-004-0858-x.

J. Hannibal, P. Hindersson, S. M. Knudsen, B. Georg, and J. Fahrenkrug. The photopigment melanopsin is exclusively present in pituitary adenylate cyclase-activating polypeptide-containing retinal ganglion cells of the retinohypothalamic tract. *J Neurosci*, 22:RC191, 2002.

J. Hannibal, P. Hindersson, J. Ostergaard, B. Georg, S. Heegaard, P. J. Larsen, and J. Fahrenkrug. Melanopsin is expressed in PACAP-Containing retinal ganglion cells of the human retinohypothalamic tract. *Invest. Ophthalmol. Vis. Sci.*, 45(11):4202–4209, Nov. 2004. http://dx.doi.org/10.1167/iovs.04-0313.

J. Hannibal, B. Georg, P. Hindersson, and J. Fahrenkrug. Light and darkness regulate melanopsin in the retinal ganglion cells of the albino wistar rat. *Journal of Molecular Neuroscience*, 27(2):147–155, Oct. 2005. http://dx.doi.org/10.1385/JMN:27:2:147.

D. W. Hansen and Q. Ji. In the eye of the beholder: A survey of models for eyes and gaze. *Pattern Analysis and Machine Intelligence, IEEE Transactions on*, 32(3):478–500, 2010. http://dx.doi.org/10.1109/TPAMI.2009.30.

J. Hansen and R. G. Stevens. Night shiftwork and breast cancer risk: overall evidence. *Occupational and Environmental Medicine*, 68(3): 236, Mar. 2011. http://dx.doi.org/10.1136/oem.2010.061630.

M. S. Hansen, B. Sander, A. Kawasaki, A. E. Brondsted, C. Nissen, and H. Lund-Andersen. Prior light exposure enhances the pupil response to subsequent short wavelength (Blue) light. *J Clinic Experiment Ophthalmol*, 2:152, 2011. http://dx.doi.org/10.4172/2155-9570.1000152.

L. Hao, C. Sihai, D. Shan, and Y. Xinjian. Bionic ommatidia based on microlens array. *Optical Engineering*, 48(6):063401–5, June 2009. http://dx.doi.org/10.1117/1.3156019.

T. Hara and R. Hara. Cephalopod retinochrome. In H. J. A. Dartnall, editor, *Handbook of Sensory Physiology . Vol. VII/1 : Photochemistry of Vision*, pages 720–746. Springer-Verlag, Berlin, 1972.

H. Harary, J. Brown, and L. Pinto. Rapid light-induced changes in near infrared transmission of rods in bufo marinus. *Science*, 202 (4372):1083–1085, Dec. 1978. http://dx.doi.org/10.1126/science.102035.

R. Hardeland. Melatonin: Signaling mechanisms of a pleiotropic agent. *BioFactors*, 35(2):183–192, Mar. 2009. http://dx.doi.org/10.1002/biof.23.

R. Hardie, K. Vogt, and A. Rudolph. The compound eye of the tsetse fly (Glossina morsitans morsitans and glossina palpalis palpalis). *Journal of Insect Physiology*, 35(5):423–431, 1989. http://dx.doi.org/10.1016/0022-1910(89)90117-0.

R. C. Hardie. The photoreceptor array of the dipteran retina. *Trends in Neurosciences*, 9 (0):419–423, 1986. http://dx.doi.org/10.1016/0166-2236(86)90136-0.

R. C. Hardie. Phototransduction in drosophila melanogaster. *Journal of Experimental Biology*, 204(20):3403 –3409, Oct. 2001. http://www.ncbi.nlm.nih.gov/pubmed/11707492.

R. C. Hardie. A brief history of trp: commentary and personal perspective. *Pflügers Archiv - European Journal of Physiology*, 461 (5):493–498, Feb. 2011. http://dx.doi.org/10.1007/s00424-011-0922-9.

R. C. Hardie. Polarization vision: Drosophila enters the arena. *Current Biology*, 22(1):R12–R14, Jan. 2012. http://dx.doi.org/10.1016/j.cub.2011.11.016.

R. C. Hardie and M. Postma. Phototransduction in microvillar photoreceptors of drosophila and other invertebrates. In A. Basbaum, editor, *The senses: a comprehensive reference*, volume Vol. 1, pages 77–130. Academic Press, San Diego, California, vision i edition, 2008.

R. C. Hardie and P. Raghu. Visual transduction in drosophila. *Nature*, 413(6852):186–193, 2001. http://dx.doi.org/10.1038/35093002.

R. C. Hardie, N. Franceschini, and P. D. McIntyre. Electrophysiological analysis of fly retina II: spectral and polarisation sensitivity in r7 and r8. *Journal of Comparative Physiology ? A*, 133:23–39, 1979. http://dx.doi.org/10.1007/BF00663107.

J. W. Hardy, J. E. Lefebvre, and C. L. Koliopoulos. Real-time atmospheric compensation. *Journal of the Optical Society of America*, 67 (3):360–369, Mar. 1977. http://dx.doi.org/10.1364/JOSA.67.000360.

F. I. Hárosi. Absorption spectra and linear dichroism of some amphibian photoreceptors. *The Journal of General Physiology*, 66 (3):357 –382, 1975. http://dx.doi.org/10.

1085/jgp.66.3.357.

F. I. Hárosi and F. E. Malerba. Plane-polarized light in microspectrophotometry. *Vision Research*, 15(3):379–388, Mar. 1975. http://dx.doi.org/10.1016/0042-6989(75)90086-3.

R. E. Harrington. Effect of color temperature on apparent brightness. *Journal of the Optical Society of America*, 44(2):113–116, Feb. 1954. http://dx.doi.org/10.1364/JOSA.44.000113.

W. A. Harris, W. S. Stark, and J. A. Walker. Genetic dissection of the photoreceptor system in the compound eye of drosophila melanogaster. *The Journal of Physiology*, 256 (2):415–439, Apr. 1976. http://www.ncbi.nlm.nih.gov/pubmed/16992509.

W. A. Harris, D. F. Ready, E. D. Lipson, A. J. Hudspeth, and W. S. Stark. Vitamin a deprivation and drosophila photopigments. *Nature*, 266(5603):648–650, Apr. 1977. http://dx.doi.org/10.1038/266648a0.

N. S. Hart. The visual ecology of avian photoreceptors. *Progress in Retinal and Eye Research*, 20(5):675–703, Sept. 2001. http://dx.doi.org/10.1016/S1350-9462(01)00009-X.

A. T. E. Hartwick, J. R. Bramley, J. Yu, K. T. Stevens, C. N. Allen, W. H. Baldridge, P. J. Sollars, and G. E. Pickard. Light-Evoked calcium responses of isolated Melanopsin-Expressing retinal ganglion cells. *The Journal of Neuroscience*, 27(49):13468 –13480, Dec. 2007. http://dx.doi.org/10.1523/?JNEUROSCI.3626-07.2007.

M. H. Hastings and E. Maywood. Two decades of circadian time. *Journal of Neuroendocrinology*, 20(6):812–819, 2008. http://dx.doi.org/10.1111/j.1365-2826.2008.01715.x.

M. H. Hastings, A. B. Reddy, and E. S. Maywood. A clockwork web: circadian timing in brain and periphery, in health and disease. *Nat Rev Neurosci*, 4(8):649–661, 2003. http://dx.doi.org/10.1038/nrn1177.

T. Hätönen, A. Alila-Johansson, S. Mustanoja, and M. Laakso. Suppression of melatonin by 2000-lux light in humans with closed eyelids. *Biological Psychiatry*, 46(6):827–831, Sept. 1999. http://dx.doi.org/10.1016/S0006-3223(98)00357-6.

M. Hatori and S. Panda. The role of arrestin in melanopsin function. *Journal of Vision*, 9 (14):41, Dec. 2009. http://dx.doi.org/10.1167/9.14.41.

M. Hatori and S. Panda. The emerging roles of melanopsin in behavioral adaptation to light. *Trends in Molecular Medicine*, Aug. 2010. http://dx.doi.org/10.1016/j.molmed.2010.07.005.

M. Hatori, H. Le, C. Vollmers, S. R. Keding, N. Tanaka, C. Schmedt, T. Jegla, and S. Panda. Inducible ablation of Melanopsin-Expressing retinal ganglion cells reveals their central role in Non-Image forming visual responses. *PLoS ONE*, 3(6):e2451, 2008. http://dx.doi.org/10.1371/journal.pone.0002451.

S. Hattar, H. W. Liao, M. Takao, D. M. Berson, and K. W. Yau. Melanopsin-containing retinal ganglion cells: architecture, projections, and intrinsic photosensitivity. *Science*, 295: 1065 – 1070, 2002. http://dx.doi.org/10.1126/science.1069609.

S. Hattar, R. J. Lucas, N. Mrosovsky, S. Thompson, R. H. Douglas, M. W. Hankins, J. Lem, M. Biel, F. Hofmann, R. G. Foster, and K. Yau. Melanopsin and rod-cone photoreceptive systems account for all major accessory visual functions in mice. *Nature*, 424(6944):75–81, July 2003. http://dx.doi.org/10.1038/nature01761.

S. Hattar, M. Kumar, A. Park, P. Tong, J. Tung, K. Yau, and D. M. Berson. Central projections of melanopsin-expressing retinal ganglion cells in the mouse. *The Journal of Comparative Neurology*, 497(3):326–349, 2006. http://dx.doi.org/10.1002/cne.20970.

D. Hawkes. The measurable and the unmeasurable, 2011.

P. He, G. Wilson, C. Russell, and M. Gerschutz. Removal of ocular artifacts from the EEG: a comparison between time-domain regression method and adaptive filtering method using simulated data. *Medical & Biological Engineering & Computing*, 45:495–503, Mar. 2007. http://dx.doi.org/10.1007/s11517-007-0179-9.

M. Hébert and K. M. Stacia. The effects of prior light history on the suppression of melatonin by light in humans. *Journal of Pineal Research*, 33(4):198–203, 2002. http://dx.doi.org/10.1034/j.1600-079X.2002.01885.x.

M. Hébert, C. W. Beattie, E. M. Tam, L. N. Yatham, and R. W. Lam. Electroretinography in patients with winter seasonal affective disorder. *Psychiatry Research*, 127(1-2): 27–34, June 2004. http://dx.doi.org/10.1016/j.psychres.2004.03.006.

J. Hecht. *Understanding Lasers*. Longman Higher Education, 1st edition, Nov. 1988.

S. Hecht. Rods, cones, and the chemical basis of vision. *Physiological Reviews*, 17(2):239 – 290, Apr. 1937.

S. Hecht, S. Schlaer, and E. L. Smith. Intermittent stimulation by light and the duplicity theory of vision. *Cold Spring Harbor Symposia on Quantitative Biology*, 3:237 –244, Jan. 1935. http://dx.doi.org/10.1101/SQB.1935.003.01.027.

S. Hecht, S. Shlaer, and M. H. Pirenne. Energy, quanta and vision. *J. Gen. Physiol.*, 25(6): 819–840, July 1942. http://dx.doi.org/10.1085/jgp.25.6.819.

M. Heck, S. A. Schädel, D. Maretzki, F. J. Bartl, E. Ritter, K. Palczewski, and K. P. Hofmann. Signaling states of rhodopsin. *Journal of Biological Chemistry*, 278(5):3162 –3169, Jan. 2003. http://dx.doi.org/10.1074/jbc.M209675200.

J. Heerwagen and D. Heerwagen. Lighting and psychological comfort. *Lighting Design and Application*, 16(4):47–51, 1986.

J. H. Heerwagen and L. Zagreus. The human factors of sustainable building design: Post-Occupancy evaluation of the philip merrill environmental center, annapolis, MD. U.S. department of energy report, University of California, Berkeley, CA, USA, 2005.

H. Heikkinen, F. Vinberg, S. Nymark, and A. Koskelainen. Mesopic background lights enhance dark-adapted cone ERG flash responses in the intact mouse retina: a possible role for gap junctional decoupling. *Journal of Neurophysiology*, Mar. 2011. http://dx.doi.org/10.1152/jn.00536.2010.

D. P. Heil and S. R. Mathis. Characterizing free-living light exposure using a wrist-worn light monitor. *Applied Ergonomics*, 33(4):357–363, July 2002. http://dx.doi.org/10.1016/S0003-6870(02)00007-8.

S. Hemilä. Background adaptation in the rods of the frog's retina. *The Journal of Physiology*, 265(3):721–741, Mar. 1977. http://www.ncbi.nlm.nih.gov/pubmed/300800.

S. Hemilä. An analysis of rod outer segment adaptation based on a simple equivalent circuit. *Biophysics of Structure and Mechanism*, 4(2):115–128, 1978. http://dx.doi.org/10.1007/BF00539226.

S. R. Henderson, H. Reuss, and R. C. Hardie. Single photon responses in drosophila photoreceptors and their regulation by ca2+. *The Journal of Physiology*, 524(1):179 –194, Apr. 2000. http://dx.doi.org/10.1111/j.1469-7793.2000.00179.x.

S. T. Henderson and D. Hodgkiss. The spectral energy distribution of daylight. *British Journal of Applied Physics*, 14:125–131, Mar. 1963. http://dx.doi.org/10.1088/0508-3443/14/3/307.

R. Hengstenberg. Multisensory control in insect oculomotor systems. *Reviews of Oculomotor Research*, 5:285–298, 1993. http://www.ncbi.nlm.nih.gov/pubmed/8420553.

K. Herbst, B. Sander, D. Milea, H. Lund-Andersen, and A. Kawasaki. Test–Retest repeatability of the pupil light response to blue and red light stimuli in normal human eyes using a novel pupillometer. *Frontiers in Neurology*, 2, 2011. http://dx.doi.org/10.3389/fneur.2011.00010.

M. Herljevic, B. Middleton, K. Thapan, and D. J. Skene. Light-induced melatonin suppression: age-related reduction in response to short wavelength light. *Experimental Gerontology*, 40(3):237–242, Mar. 2005. http://dx.doi.org/10.1016/j.exger.2004.12.001.

J. Hernández-Andrés, R. L. Lee, and J. Romero. Calculating correlated color temperatures across the entire gamut of daylight and skylight chromaticities. *Applied Optics*, 38 (27):5703–5709, Sept. 1999. http://dx.doi.org/10.1364/AO.38.005703.

E. D. Herzog. Neurons and networks in daily rhythms. *Nature Reviews. Neuroscience*, 8 (10):790–802, Oct. 2007. http://dx.doi.org/10.1038/nrn2215.

C. Hess. Untersuchungen zur physiologie und pathologie des pupillenspieles. *Arch. Augenheilk*, 60:327–389, 1908.

E. H. Hess. Attitude and pupil size. *Scientific American*, 212(4):46–54, 1965.

E. H. Hess and J. M. Polt. Pupil size as related to interest value of visual stimuli. *Science*, 132(3423):349 –350, 1960. http://dx.doi.org/10.1126/science.132.3423.349.

E. H. Hess and J. M. Polt. Pupil size in relation to mental activity during simple Problem-Solving. *Science*, 143(3611):1190–1192, Mar. 1964. http://dx.doi.org/10.1126/science.143.3611.1190.

E. H. Hess, A. L. Seltzer, and J. M. Shlien. Pupil response of hetero- and homosexual males to pictures of men and women: A pilot study. *Journal of Abnormal Psychology;Journal of Abnormal Psychology*, 70 (3):165–168, 1965. http://dx.doi.org/10.1037/h0021978.

H. Hibino. Red-green and yellow-blue opponent-color responses as a function of retinal eccentricity. *Vision Research*, 32(10): 1955–1964, Oct. 1992. http://dx.doi.org/10.1016/0042-6989(92)90055-N.

S. Higuchi, Y. Motohashi, K. Ishibashi, and T. Maeda. Less exposure to daily ambient light in winter increases sensitivity of melatonin to light suppression. *Chronobiology International*, 24(1):31–43, 2007. http://dx.doi.org/10.1080/07420520601139805.

S. Higuchi, K. Ishibashi, S. Aritake, M. Enomoto, A. Hida, M. Tamura, T. Kozaki, Y. Motohashi, and K. Mishima. Inter-individual difference in pupil size correlates to suppression of melatonin by exposure to light. *Neuroscience Letters*, 440 (1):23–26, July 2008. http://dx.doi.org/10.1016/j.neulet.2008.05.037.

G. Hildebrand. *Origins of Architectural Pleasure*. University of California Press, 1 edition, June 1999.

A. V. Hill. The heat of shortening and the dynamic constants of muscle. *Proceedings of the Royal Society of London. Series B, Biological Sciences*, 126(843):136–195, Oct. 1938.

R. A. Hill and R. A. Barton. Psychology: Red enhances human performance in contests. *Nature*, 435(7040):293, May 2005. http:

//dx.doi.org/10.1038/435293a.

P. Hillman, S. Hochstein, and B. Minke. A visual pigment with two physiologically active stable states. *Science (New York, N.Y.)*, 175(29):1486–8, Mar. 1972. http://dx.doi.org/10.1126/science.175.4029.1486.

P. Hillman, S. Hochstein, and B. Minke. Nonlocal interactions in the photoreceptor transduction process. *The Journal of General Physiology*, 68(2):227–245, Aug. 1976. http://www.ncbi.nlm.nih.gov/pubmed/182904.

P. Hillman, S. Hochstein, and B. Minke. Transduction in invertebrate photoreceptors: role of pigment bistability. *Physiological Reviews*, 63(2):668–772, Apr. 1983. http://www.ncbi.nlm.nih.gov/pubmed/6340134.

Y. Hirata, K. Yamaji, H. Sakai, and S. Usui. Function of the pupil in vision and information capacity of retinal image. *Systems and Computers in Japan*, 34(9):48–57, Aug. 2003. http://dx.doi.org/10.1002/scj.10344.

S. Hochstein. *Electrophysiologal Study of Wavelength-Dependent Photoreceptor Responses*. PhD thesis, Hebrew University, Jerusalem, Israel, 1972.

S. Hochstein. On the implications of bistability of visual pigment systems. *Biophysics of Structure and Mechanism*, 5(2-3):129–136, 1979. http://dx.doi.org/10.1007/BF00535443.

S. Hochstein, B. Minke, and P. Hillman. Antagonistic components of the late receptor potential in the barnacle photoreceptor arising from different stages of the pigment process. *J. Gen. Physiol.*, 62(1):105–128, July 1973. http://www.ncbi.nlm.nih.gov/pubmed/4767023.

S. Hochstein, B. Minke, P. Hillman, and B. W. Knight. The kinetics of visual pigment systems i: Mathematical analysis. *Biological Cybernetics*, 30(1):23–32, 1978. http://dx.doi.org/10.1007/BF00365480.

W. Hodge, J. Whitcher, and W. Satariano. Risk factors for age-related cataracts. *Epidemiologic reviews*, 17(2):336, 1995. http://www.ncbi.nlm.nih.gov/pubmed/8654515.

H. Hofer, L. Chen, G. Yoon, B. Singer, Y. Yamauchi, and D. R. Williams. Improvement in retinal image quality with dynamic correction of the eye's aberrations. *Optics Express*, 8(11):631–643, May 2001. http://dx.doi.org/10.1364/OE.8.000631.

H. Hofer, B. Singer, and D. R. Williams. Different sensations from cones with the same photopigment. *Journal of Vision*, 5(5), May 2005. http://dx.doi.org/10.1167/5.5.5.

M. Höfle, R. Kenntner-Mabiala, P. Pauli, and G. W. Alpers. You can see pain in the eye: Pupillometry as an index of pain intensity under different luminance conditions. *International Journal of Psychophysiology*, 70 (3):171–175, 2008. http://dx.doi.org/10.1016/j.ijpsycho.2008.06.008.

K. P. Hofmann, R. Uhl, W. Hoffmann, and W. Kreutz. Measurements of fast light-induced light-scattering and -absorption changes in outer segments of vertebrate light sensitive rod cells. *European Biophysics Journal*, 2(1):61–77, Mar. 1976. http://dx.doi.org/10.1007/BF00535653.

K. P. Hofmann, P. Scheerer, P. W. Hildebrand, H. Choe, J. H. Park, M. Heck, and O. P. Ernst. A g protein-coupled receptor at work: the rhodopsin model. *Trends in Biochemical Sciences*, 34(11):540–552, Nov. 2009. http://dx.doi.org/10.1016/j.tibs.2009.07.005.

W. A. Hofstra and A. W. de Weerd. How to assess circadian rhythm in humans: A review of literature. *Epilepsy & Behavior*, 13(3):438–444, Oct. 2008. http://dx.doi.org/10.1016/j.yebeh.2008.06.002.

R. E. Hogg, M. B. Zlatkova, U. Chakravarthy, and R. S. Anderson. Investigation of the effect of simulated lens yellowing, transparency loss and refractive error on in vivo resonance raman spectroscopy. *Ophthalmic and Physiological Optics*, 27(3):225–231, May 2007. http://dx.doi.org/10.1111/j.1475-1313.2007.00478.x.

F. Hölker, C. Wolter, E. K. Perkin, and K. Tockner. Light pollution as a biodiversity threat. *Trends in Ecology & Evolution*, 25(12):681–682, Dec. 2010. http://dx.doi.org/10.1016/j.tree.2010.09.007.

M. Hollborn, E. Ulbricht, K. Rillich, S. Dukic-Stefanovic, A. Wurm, L. Wagner, A. Reichenbach, P. Wiedemann, G. A. Limb, A. Bringmann, and L. Kohen. The human müller cell line MIO-M1 expresses opsins. *Molecular Vision*, 17:2738–2750, 2011.

K.-i. Honma, S. Hashimoto, M. Nakao, and S. Honma. Period and phase adjustments of human circadian rhythms in the real world. *J Biol Rhythms*, 18(3):261–270, June 2003. http://dx.doi.org/10.1177/0748730403018003008.

D. C. Hood and D. G. Birch. Phototransduction in human cones measured using the a-wave of the ERG. *Vision Research*, 35(20):2801–2810, Oct. 1995. http://dx.doi.org/10.1016/0042-6989(95)00034-W.

J. A. Horne and O. Östberg. A self-assessment questionnaire to determine morningness-eveningness in human circadian rhythms. *International Journal of Chronobiology*, 4(2):97–110, 1976. http://www.ncbi.nlm.nih.gov/pubmed/1027738.

G. Horváth, G. Kriska, P. Malik, and B. Robertson. Polarized light pollution: a new kind of ecological photopollution. *Frontiers in Ecology and the Environment*, 7(6):317–325, 2009. http://dx.doi.org/10.1890/080129.

H. Hoshi, W. Liu, S. C. Massey, and S. L. Mills. ON inputs to the OFF layer: bipolar cells that break the stratification rules of the retina. *The Journal of Neuroscience: The Official Journal of the Society for Neuroscience*, 29 (28):8875–8883, July 2009. http://dx.doi.org/10.1523/JNEUROSCI.0912-09.2009.

R. Hou, R. Langley, E. Szabadi, and C. Bradshaw. Comparison of diphenhydramine and modafinil on arousal and autonomic functions in healthy volunteers. *Journal of Psychopharmacology*, 21(6):567 –578, 2007. http://dx.doi.org/10.1177/0269881106071022.

J. Howard, B. Blakeslee, and S. B. Laughlin. The intracellular pupil mechanism and photoreceptor signal: noise ratios in the fly lucilia cuprina. *Proceedings of the Royal Society of London. Series B, Containing Papers of a Biological Character. Royal Society (Great Britain)*, 231(1265):415–435, Sept. 1987. http://www.ncbi.nlm.nih.gov/pubmed/2892201.

P. A. Howarth, G. Heron, and L. Whittaker. The measurement of pupil cycling time. *Graefe's Archive for Clinical and Experimental Ophthalmology*, 238(10):826–32, Oct. 2000. http://dx.doi.org/10.1007/s004170000175.

O. Howells, F. Eperjesi, and H. Bartlett. Measuring macular pigment optical density in vivo: a review of techniques. *Graefe's Archive for Clinical and Experimental Ophthalmology*, 249(3):315–347, Jan. 2011. http://dx.doi.org/10.1007/s00417-010-1577-5.

D. S. Hsu, X. Zhao, S. Zhao, A. Kazantsev, R. Wang, T. Todo, Y. Wei, and A. Sancar. Putative human Blue-Light photoreceptors hCRY1 and hCRY2 are flavoproteins†. *Biochemistry*, 35(44):13871–13877, 1996. http://dx.doi.org/10.1021/bi962209o.

K. Hu, E. J. W. Van Someren, S. A. Shea, and F. A. J. L. Scheer. Reduction of scale invariance of activity fluctuations with aging and alzheimer's disease: Involvement of the circadian pacemaker. *Proceedings of the National Academy of Sciences*, 106(8):2490–2494, Feb. 2009. http://dx.doi.org/10.1073/pnas.0806087106.

Y. Hua, A. Oswald, and X. Yang. Effectiveness of daylighting design and occupant visual satisfaction in a LEED gold laboratory building. *Building and Environment*, 46 (1):54–64, Jan. 2011. http://dx.doi.org/10.1016/j.buildenv.2010.06.016.

N. E. Huang and S. Shen. *The Hilbert-Huang Transform and Its Applications*. World Scientific Publishing Company, Sept. 2005.

N. E. Huang, Z. Shen, S. R. Long, M. C. Wu, H. H. Shih, Q. Zheng, N. Yen, C. C. Tung, and H. H. Liu. The empirical mode decomposition and the hilbert spectrum for nonlinear and non-stationary time series analysis. *Proceedings of the Royal Society of London. Series A: Mathematical, Physical and Engineering Sciences*, 454(1971):903 –995, Mar. 1998. http://dx.doi.org/10.1098/rspa.1998.0193.

S. Hubalek, D. Zoschg, and C. Schierz. Ambulant recording of light for vision and non-visual biological effects. *Lighting Research and Technology*, 38(4):314–321, Dec. 2006. http://dx.doi.org/10.1177/1477153506070687.

S. Hubalek, M. Brink, and C. Schierz. Office workers' daily exposure to light and its influence on sleep quality and mood. *Lighting Research and Technology*, page 1477153509355632, Jan. 2010. http://dx.doi.org/10.1177/1477153509355632.

R. Hubbard and A. Kropf. The action of light on rhodopsin. *Proceedings of the National Academy of Sciences of the United States of America*, 44(2):130–139, Feb. 1958. http://www.ncbi.nlm.nih.gov/pubmed/16590155.

R. Hubbard and R. C. C. St. George. The rhodopsin system of the squid. *The Journal of General Physiology*, 41(3):501–528, Jan. 1958. http://www.ncbi.nlm.nih.gov/pubmed/13491819.

A. D. Huberman, M. Manu, S. M. Koch, M. W. Susman, A. B. Lutz, E. M. Ullian, S. A. Baccus, and B. A. Barres. Architecture and Activity-Mediated refinement of axonal projections from a mosaic of genetically identified retinal ganglion cells. *Neuron*, 59(3):425–438, Aug. 2008. http://dx.doi.org/10.1016/j.neuron.2008.07.018.

G. Huet. Pupil size and light reactivity in hypothermic infants and adults. *Intensive Care Medicine*, 15:216–217, 1989. http://dx.doi.org/10.1007/BF01058578.

A. Hughes. A schematic eye for the rabbit. *Vision Research*, 12(1):123–IN6, Jan. 1972. http://dx.doi.org/10.1016/0042-6989(72)90143-5.

A. Hughes. A schematic eye for the rat. *Vision Research*, 19(5):569–588, 1979. http://dx.doi.org/10.1016/0042-6989(79)90143-3.

E. O. Hulburt. Explanation of the brightness and color of the sky, particularly the twilight sky. *Journal of the Optical Society of America*, 43(2):113–118, Feb. 1953. http://dx.doi.org/10.1364/JOSA.43.000113.

G. Hung and L. Stark. Interpretation of kernels. III. positive off-diagonal kernels as correlates of the dynamic process of pupillary escape. *Mathematical Biosciences*, 46(3-4):189–203, Oct. 1979. http://dx.doi.org/10.1016/0025-5564(79)90066-X.

J. J. Hunter, B. Masella, A. Dubra, R. Sharma, L. Yin, W. H. Merigan, G. Palczewska, K. Palczewski, and D. R. Williams. Images of photoreceptors in living primate eyes using adaptive optics two-photon ophthalmoscopy. *Biomedical Optics Express*, 2(1): 139–148, Jan. 2011. http://dx.doi.org/10.

1364/BOE.2.000139.

J. J. Hunter, J. I. Morgan, W. H. Merigan, D. H. Sliney, J. R. Sparrow, and D. R. Williams. The susceptibility of the retina to photochemical damage from visible light. *Progress in Retinal and Eye Research*, 31(1): 28–42, Jan. 2012. http://dx.doi.org/10.1016/j.preteyeres.2011.11.001.

J. Hupé, C. Lamirel, and J. Lorenceau. Pupil dynamics during bistable motion perception. *Journal of Vision*, 9(7):1–19, July 2009. http://dx.doi.org/10.1167/9.7.10.

C. M. Hurvich, J. S. Simonoff, and C. Tsai. Smoothing parameter selection in nonparametric regression using an improved akaike information criterion. *Journal of the Royal Statistical Society: Series B (Statistical Methodology)*, 60(2):271–293, Jan. 1998. http://dx.doi.org/10.1111/1467-9868.00125.

R. Z. Hussain, S. C. Hopkins, E. M. Frohman, T. N. Eagar, P. C. Cravens, B. M. Greenberg, S. Vernino, and O. Stüve. Direct and consensual murine pupillary reflex metrics: Establishing normative values. *Autonomic Neuroscience*, 151(2):164–167, Dec. 2009. http://http://dx.doi.org/10.1016/j.autneu.2009.07.021.

R. A. Hut, M. Oklejewicz, C. Rieux, and H. M. Cooper. Photic sensitivity ranges of hamster pupillary and circadian phase responses do not overlap. *Journal of Biological Rhythms*, 23(1):37–48, Feb. 2008. http://dx.doi.org/10.1177/0748730407311851.

D. Hutchison, T. Kanade, J. Kittler, J. M. Kleinberg, F. Mattern, J. C. Mitchell, M. Naor, O. Nierstrasz, C. Pandu Rangan, B. Steffen, M. Sudan, D. Terzopoulos, D. Tygar, M. Y. Vardi, G. Weikum, C. Tomishima, M. Miki, M. Ashibe, T. Hiroyasu, and M. Yoshimi. Distributed control of illuminance and color temperature in intelligent lighting system. In L. Rutkowski, R. Scherer, R. Tadeusiewicz, L. A. Zadeh, and J. M. Zurada, editors, *Artifical Intelligence and Soft Computing*, volume 6114, pages 411–419. Springer Berlin Heidelberg, Berlin, Heidelberg, 2010. http://dx.doi.org/10.1007/978-3-642-13232-2_50.

H. E. Huxley. Fifty years of muscle and the sliding filament hypothesis. *European Journal of Biochemistry*, 271(8):1403–1415, Apr. 2004. http://dx.doi.org/10.1111/j.1432-1033.2004.04044.x.

A. Hyvärinen, J. Karhunen, and E. Oja. *Independent Component Analysis*. Wiley-Interscience, 1 edition, May 2001.

D. Iacoviello and M. Lucchetti. Parametric characterization of the form of the human pupil from blurred noisy images. *Computer Methods and Programs in Biomedicine*, 77(1): 39–48, Jan. 2005. http://dx.doi.org/10.1016/j.cmpb.2004.09.001.

I. Ihrke, G. Wetzstein, and W. Heidrich. A theory of plenoptic multiplexing. In *Computer Vision and Pattern Recognition (CVPR), 2010 IEEE Conference on*, pages 483–490, 2010. dx.doi.org/10.1109/CVPR.2010.5540174.

H. Ijima, A. Ohsumi, and R. Okui. A method of detection of signals corrupted by nonstationary random noise via stationarization of the data. *Electronics and Communications in Japan (Part III: Fundamental Electronic Science)*, 90(8):29–38, Aug. 2007. http://dx.doi.org/10.1002/ecjc.20302.

J. Ijspeert, P. de Waard, T. van den Berg, and P. de Jong. The intraocular straylight function in 129 healthy volunteers; dependence on angle, age and pigmentation. *Vision Research*, 30(5):699–707, 1990. http://dx.doi.org/10.1016/0042-6989(90)90096-4.

G. Ikaunieks, M. Colomb, and M. Ozolinsh. Light scattering in artificial fog and simulated with light scattering filter. *Ophthalmic and Physiological Optics*, 29(3):351–356, May 2009. http://dx.doi.org/10.1111/j.1475-1313.2009.00664.x.

M. Ishi and N. Kakitsuba. Preferred color temperatures at 200 lx during exposure to cool or warm environments for Middle-Aged female subjects. *Journal of the Human-Environment System*, 6(2):93–100, 2003. http://dx.doi.org/10.1618/jhes.6.93.

M. Ishihara. Versuch einer deutung der photoelektrischen schwankungen am froschauge. *Pflüger, Archiv für die Gesammte Physiologie des Menschen und der Thiere*, 114:569–618, Oct. 1906. http://dx.doi.org/10.1007/BF01677147.

H. Ishikawa, K. Asakawa, and T. Yoshitomi. Pupillary near reflex. *Neuro-Ophthalmology Japan*, 21(3):280–285, 2004.

H. Ishikawa, A. Onodera, K. Asakawa, S. Nakadomari, and K. Shimizu. Effects of selective-wavelength block filters on pupillary light reflex under red and blue light stimuli. *Japanese Journal of Ophthalmology*, Jan. 2012. http://dx.doi.org/10.1007/s10384-011-0116-1.

M. C. Isoldi, M. D. Rollag, A. M. de Lauro Castrucci, and I. Provencio. Rhabdomeric phototransduction initiated by the vertebrate photopigment melanopsin. *Proceedings of the National Academy of Sciences of the United States of America*, 102(4):1217 –1221, Jan. 2005. http://dx.doi.org/10.1073/pnas.0409252102.

K. Isono, T. Tanimura, Y. Oda, and Y. Tsukahara. Dependency on light and vitamin a derivatives of the biogenesis of 3-hydroxyretinal and visual pigment in the compound eyes of drosophila melanogaster. *The Journal of General Physiology*, 92(5):587 –600, Nov. 1988. http://dx.doi.org/10.1085/jgp.92.5.587.

M. E. Itkis, X. Chi, A. W. Cordes, and R. C. Haddon. Magneto-Opto-Electronic bistability in a Phenalenyl-Based neutral radical. *Science*, 296(5572):1443 –1445, May 2002. http://dx.doi.org/10.1126/science.1071372.

P. C. Ivanov, K. Hu, M. F. Hilton, S. A. Shea, and H. E. Stanley. Endogenous circadian rhythm in human motor activity uncoupled from circadian influences on cardiac dynamics. *Proceedings of the National Academy of Sciences*, 104(52):20702–20707, Dec. 2007. http://dx.doi.org/10.1073/pnas.0709957104.

A. Iversen, S. Svendsen, and T. R. Nielsen. The effect of different weather data sets and their resolution in Climate-Based daylight modelling. *Lighting Research and Technology*, Mar. 2012. http://dx.doi.org/10.1177/1477153512440545.

H. E. Ives. Critical frequency relations in scotopic vision. *Journal of the Optical Society of America*, 6(3):254–267, May 1922. http://dx.doi.org/10.1364/JOSA.6.000254.

L. Izsó. Appropriate dynamic lighting as a possible basis for a smart ambient lighting. In C. Stephanidis, editor, *Universal Access in Human-Computer Interaction. Intelligent and Ubiquitous Interaction Environments*, volume 5615, pages 67–74. Springer Berlin Heidelberg, Berlin, Heidelberg, 2009. http://dx.doi.org/10.1007/978-3-642-02710-9_8.

L. Izso, L. Laufer, and S. Suplicz. Effects of dynamic lighting on the visual performance of older adults. *Lighting Research and Technology*, page 1477153509336802, Aug. 2009. http://dx.doi.org/10.1177/1477153509336802.

G. H. Jacobs. The distribution and nature of colour vision among the mammals. *Biological Reviews*, 68(3):413–471, Aug. 1993. http://dx.doi.org/10.1111/j.1469-185X.1993.tb00738.x.

G. H. Jacobs and G. A. Williams. L and m cone proportions in polymorphic new world monkeys. *Visual Neuroscience*, 23(3-4):365–370, Aug. 2006. http://dx.doi.org/10.1017/S0952523806233066.

G. H. Jacobs and G. A. Williams. Contributions of the mouse UV photopigment to the ERG and to vision. *Documenta Ophthalmologica*, 115:137–144, May 2007. http://dx.doi.org/10.1007/s10633-007-9055-z.

C. P. Jacovides, M. D. Steven, and D. N. Asimakopoulos. Spectral solar irradiance and some optical properties for various polluted atmospheres. *Solar Energy*, 69(3):215–227, 2000. http://dx.doi.org/10.1016/S0038-092X(00)00062-1.

A. P. Jadhav, K. Roesch, and C. L. Cepko. Development and neurogenic potential of müller glial cells in the vertebrate retina. *Progress in Retinal and Eye Research*, 28(4):249–262, July 2009. http://dx.doi.org/10.1016/j.preteyeres.2009.05.002.

S. Jain, G. J. Siegle, C. Gu, C. G. Moore, L. S. Ivanco, S. Studenski, J. T. Greenamyre, and S. R. Steinhauer. Pupillary unrest correlates with arousal symptoms and motor signs in parkinson disease. *Movement Disorders*, 26(7):1344–1347, June 2011. http://dx.doi.org/10.1002/mds.23628.

A. C. James, M. Kolic, S. M. Bedford, and T. Maddess. Stimulus parameters for multifocal pupillographic objective perimetry. *Journal of Glaucoma*, page 1, May 2011. http://dx.doi.org/10.1097/IJG.0b013e31821e8413.

J. M. L. Janssen. Discontinuous low-frequency delay line with continuously variable delay. *Nature*, 169(4291):148–149, Jan. 1952. http://dx.doi.org/10.1038/169148a0.

M. Järvilehto. The physiology of invertebrate visual pigments. In H. Autrum, editor, *Handbook of Sensory physiology. Comparative Physiology and Evolution of Vision in Invertebrates. A. Invertebrate Photoreceptors*, volume 7, pt. 6A, pages 145–224. Springer-Verlag, Berlin, 1979.

S. A. Jasser, J. P. Hanifin, M. D. Rollag, and G. C. Brainard. Dim light adaptation attenuates acute melatonin suppression in humans. *J Biol Rhythms*, 21(5):394–404, Oct. 2006. http://dx.doi.org/10.1177/0748730406292391.

K. Jeong, J. Kim, and L. P. Lee. Biologically inspired artificial compound eyes. *Science*, 312(5773):557 –561, Apr. 2006. http://dx.doi.org/10.1126/science.1123053.

M. Jiang, S. Pandey, and H. K. Fong. An opsin homologue in the retina and pigment epithelium. *Investigative Ophthalmology & Visual Science*, 34(13):3669–3678, Dec. 1993. http://www.ncbi.nlm.nih.gov/pubmed/8258527.

M. Joesch, B. Schnell, S. V. Raghu, D. F. Reiff, and A. Borst. ON and OFF pathways in drosophila motion vision. *Nature*, 468(7321):300–304, Nov. 2010. http://dx.doi.org/10.1038/nature09545.

S. Johnsen, A. Kelber, E. Warrant, A. M. Sweeney, E. A. Widder, R. L. Lee, and J. Hernández-Andrés. Crepuscular and nocturnal illumination and its effects on color perception by the nocturnal hawkmoth deilephila elpenor. *Journal of Experimental Biology*, 209(5):789 –800, Mar. 2006. http://dx.doi.org/10.1242/jeb.02053.

C. A. Johnson, D. L. Howard, D. Marshall, and H. Shu. A noninvasive video-based method for measuring lens transmission properties of the human eye. *Optometry and Vision Science: Official Publication of the American Academy of Optometry*, 70(11):944–55, Nov. 1993. http://www.ncbi.nlm.nih.gov/pubmed/8302531.

M. S. Johnson. Activity and distribution of certain wild mice in relation to biotic communities. *Journal of Mammalogy*, 7(4):245–277, Nov. 1926. http://dx.doi.org/10.2307/1373575.

W. Johnson and J. Shah. How green is your lighting? In *Cement Industry Technical Conference, 2011 IEEE-IAS/PCA 53rd*, pages 1–15. IEEE, May 2011. http://dx.doi.org/10.1109/CITCON.2011.5934567.

I. Jolliffe. Principal component analysis. In *Encyclopedia of Statistics in Behavioral Science*. Wiley, 2005. http://dx.doi.org/10.1002/0470013192.bsa501.

P. D. Jones, M. Loeb, and A. Cohen. Effects of intense continuous- and impact-type noise on pupil size and visual acuity. *Journal of the American Audiology Society*, 2(6):202–207, June 1977. http://www.ncbi.nlm.nih.gov/pubmed/893189.

R. S. Jonnal, J. Rha, Y. Zhang, B. Cense, W. Gao, and D. T. Miller. In vivo functional imaging of human cone photoreceptors. *Optics Express*, 15(24):16141–16160, Nov. 2007. http://dx.doi.org/10.1364/OE.15.016141.

R. S. Jonnal, J. R. Besecker, J. C. Derby, O. P. Kocaoglu, B. Cense, W. Gao, Q. Wang, and D. T. Miller. Imaging outer segment renewal in living human cone photoreceptors. *Optics Express*, 18(5):5257–5270, Mar. 2010. http://dx.doi.org/10.1364/OE.18.005257.

C. Jud, S. Chappuis, V. L. Revell, T. L. Sletten, D. Saaltink, C. Cajochen, D. J. Skene, and U. Albrecht. Age-dependent alterations in human PER2 levels after early morning blue light exposure. *Chronobiology International*, 26(7):1462–1469, Oct. 2009. http://dx.doi.org/10.3109/07420520903385564.

H. T. Juslén. *Lighting, Productivity and Preferred Illuminances – Field Studies in the Industrial Environment*. PhD thesis, Helsinki University of Technology, Espoo, Finland, 2007.

P. R. Jusuf, S. C. S. Lee, J. Hannibal, and U. Grunert. Characterization and synaptic connectivity of melanopsin-containing ganglion cells in the primate retina. *European Journal of Neuroscience*, 26(10):2906–2921, 2007. http://dx.doi.org/10.1111/j.1460-9568.2007.05924.x.

M. Juusola and R. C. Hardie. Light adaptation in drosophila photoreceptors: II. rising temperature increases the bandwidth of reliable signaling. *The Journal of General Physiology*, 117(1):27–42, Jan. 2001a. http://dx.doi.org/10.1085/jgp.117.1.27.

M. Juusola and R. C. Hardie. Light adaptation in drosophila photoreceptors. *The Journal of General Physiology*, 117(1):3 –25, Jan. 2001b. http://jgp.rupress.org/content/117/1/3.abstract.

M. Kalloniatis and R. S. Harwerth. Spectral sensitivity and adaptation characteristics of cone mechanisms under white-light adaptation. *Journal of the Optical Society of America. A, Optics and Image Science*, 7(10):1912–1928, Oct. 1990. http://dx.doi.org/10.1364/JOSAA.7.001912.

S. Kanaya, K. Hashimoto, and E. Kichize. Subjective balance between general color rendering index color temperature and illuminance of interior lighting. In *Proceedings of the CIE 19th Session*, Kyoto, 1979.

H. R. Kang. *Computational color technology*. SPIE Press, 2006.

P. P. Kanjilal, J. Bhattacharya, and G. Saha. Robust method for periodicity detection and characterization of irregular cyclical series in terms of embedded periodic components. *Physical Review E*, 59(4):4013, Apr. 1999. http://dx.doi.org/10.1103/PhysRevE.59.4013.

L. Kankipati, C. A. Girkin, and P. D. Gamlin. Post-illumination pupil response in subjects without ocular disease. *Invest. Ophthalmol. Vis. Sci.*, 51(5):2764–2769, May 2010. http://dx.doi.org/10.1167/iovs.09-4717.

L. Kankipati, C. A. Girkin, and P. D. Gamlin. The Post-Illumination pupil response is reduced in glaucoma patients. *Investigative Ophthalmology & Visual Science*, Jan. 2011. http://dx.doi.org/10.1167/iovs.10-6023.

T. Kantermann and T. Roenneberg. Is Light-at-Night a health risk factor or a health risk predictor? *Chronobiology International: The Journal of Biological and Medical Rhythm Research*, 26(6):1069, 2009. http://dx.doi.org/10.1080/07420520903223984.

E. Kaplan and R. B. Barlow. Circadian clock in limulus brain increases response and decreases noise of retinal photoreceptors. *Nature*, 286(5771):393–395, July 1980. http://dx.doi.org/10.1038/286393a0.

E. Kaplan, R. B. Barlow, G. Renninger, and K. Purpura. Circadian rhythms in limulus photoreceptors. II. quantum bumps. *The Journal of General Physiology*, 96(3):665 –685, 1990. http://dx.doi.org/10.1085/jgp.96.3.665.

M. A. Karaçorlu, Z. Sürel, T. Cakiner, E. Hanyaloğlu, T. Saylan, and C. Mat. Pupil cycle time and early autonomic involvement in ocular leprosy. *The British Journal of Ophthalmology*, 75(1):45–48, Jan. 1991. http://dx.doi.org/10.1136/bjo.75.1.45.

R. Kardon. Pupillary light reflex. *Current Opinion in Ophthalmology*, 6(6):20–6, Dec. 1995. http://www.ncbi.nlm.nih.gov/pubmed/10160414.

R. Kardon, S. C. Anderson, T. G. Damarjian, E. M. Grace, E. Stone, and A. Kawasaki. Chromatic pupillometry in patients with

retinitis pigmentosa. *Ophthalmology*, 118(2): 376–381, Feb. 2011. http://dx.doi.org/10.1016/j.ophtha.2010.06.033.

R. H. Kardon. Anatomy and physiology of the autonomic nervous system. In N. R. Miller, editor, *Walsh and Hoyt's Clinical Neuro-Ophthalmology*, pages 649–714. Lippincott Williams & Wilkins, 2005.

L. Kass and G. H. Renninger. Circadian change in function of limulus ventral photoreceptors. *Visual Neuroscience*, 1(01):3–11, 1988. http://dx.doi.org/10.1017/S0952523800000985.

S. Kasthurirangan and A. Glasser. Characteristics of pupil responses during far-to-near and near-to-far accommodation. *Ophthalmic and Physiological Optics*, 25(4):328–339, 2005. http://dx.doi.org/10.1111/j.1475-1313.2005.00293.x.

S. Kasthurirangan and A. Glasser. Age related changes in the characteristics of the near pupil response. *Vision Research*, 46(8-9):1393–1403, Apr. 2006. http://dx.doi.org/10.1016/j.visres.2005.07.004.

C. Katti, K. Kempler, M. L. Porter, A. Legg, R. Gonzalez, E. Garcia-Rivera, D. Dugger, and B. Battelle. Opsin co-expression in limulus photoreceptors: differential regulation by light and a circadian clock. *Journal of Experimental Biology*, 213(15):2589 –2601, 2010. http://dx.doi.org/10.1242/jeb.043869.

E. Kawano-Yamashita, M. Koyanagi, Y. Shichida, T. Oishi, S. Tamotsu, and A. Terakita. Beta-Arrestin functionally regulates the Non-Bleaching pigment parapinopsin in lamprey pineal. *PLoS ONE*, 6(1):e16402, Jan. 2011. http://dx.doi.org/10.1371/journal.pone.0016402.

A. Kawasaki. Disorders of pupillary function, accommodation, and lacrimation. In N. R. Miller, editor, *Walsh and Hoyt's Clinical Neuro-Ophthalmology*, pages 649–714. Lippincott Williams & Wilkins, 2005.

A. Kawasaki, K. Herbst, B. Sander, and D. Milea. Selective wavelength pupillometry in leber hereditary optic neuropathy. *Clinical & Experimental Ophthalmology*, Feb. 2010. http://dx.doi.org/10.1111/j.1442-9071.2010.02212.x.

A. Kawinska, M. Dumont, B. Selmaoui, J. Paquet, and J. Carrier. Are modifications of melatonin circadian rhythm in the middle years of life related to habitual patterns of light exposure? *Journal of Biological Rhythms*, 20(5):451 –460, Oct. 2005. http://dx.doi.org/10.1177/0748730405280248.

Y. Kayama, R. R. Riso, J. R. Bartlett, and R. W. Doty. Luxotonic responses of units in macaque striate cortex. *Journal of Neurophysiology*, 42(6):1495–1517, Nov. 1979. http://www.ncbi.nlm.nih.gov/pubmed/115968.

L. Kayumov, A. Lowe, S. Rahman, R. Casper, and C. Shapiro. Prevention of melatonin suppression by nocturnal lighting: relevance to cancer. *European Journal of Cancer Prevention*, 16(4):357–362, 2007. http://dx.doi.org/10.1097/01.cej.0000215622.59122.d4.

C. E. Keeler. Iris movements in blind mice. *American Journal of Physiology*, 81(1):107 –112, June 1927.

V. Kefalov, Y. Fu, N. Marsh-Armstrong, and K. Yau. Role of visual pigment properties in rod and cone phototransduction. *Nature*, 425(6957):526–531, Oct. 2003. http://www.ncbi.nlm.nih.gov/pubmed/14523449.

A. Kelber, A. Balkenius, and E. J. Warrant. Scotopic colour vision in nocturnal hawkmoths. *Nature*, 419(6910):922–925, Oct. 2002. http://dx.doi.org/10.1038/nature01065.

M. C. Keller, B. L. Fredrickson, O. Ybarra, S. Côté, K. Johnson, J. Mikels, A. Conway, and T. Wager. A warm heart and a clear head. *Psychological Science*, 16(9):724 –731, 2005. http://dx.doi.org/10.1111/j.1467-9280.2005.01602.x.

S. R. Kellert, J. Heerwagen, and M. Mador. *Biophilic Design: The Theory, Science and Practice of Bringing Buildings to Life*. John Wiley and Sons, Sept. 2011.

K. L. Kelly. Lines of constant correlated color temperature based on MacAdam's (u,u) uniform chromaticity transformation of the CIE diagram. *Journal of the Optical Society of America*, 53(8):999–1002, 1963. http://dx.doi.org/10.1364/JOSA.53.000999.

J. S. Kenkre, N. A. Moran, T. D. Lamb, and O. A. R. Mahroo. Extremely rapid recovery of human cone circulating current at the extinction of bleaching exposures. *The Journal of Physiology*, 567(1):95–112, 2005. http://dx.doi.org/10.1113/jphysiol.2005.088468.

D. Kennedy. Neural photoreception in a lamellibranch mollusc. *The Journal of General Physiology*, 44:277–299, Nov. 1960. http://www.ncbi.nlm.nih.gov/pubmed/13752503.

D. X. Kerola. Modelling artificial night-sky brightness with a polarized multiple scattering radiative transfer computer code. *Monthly Notices of the Royal Astronomical Society*, 365(4):1295–1299, Feb. 2006. http://dx.doi.org/10.1111/j.1365-2966.2005.09821.x.

L. Kessel, J. H. Lundeman, K. Herbst, T. V. Andersen, and M. Larsen. Age-related changes in the transmission properties of the human lens and their relevance to circadian entrainment. *Journal of Cataract and Refractive Surgery*, 36(2):308–312, Feb. 2010. http://dx.doi.org/10.1016/j.jcrs.2009.08.035.

C. K. Kier and S. C. Chamberlain. Dual controls for screening pigment movement in photoreceptors of the limulus lateral eye: circadian efferent input and light. *Visual Neuroscience*, 4(3):237–255, Mar. 1990. http://dx.doi.org/10.1017/S0952523800003382.

C. B. Y. Kim and M. J. Mayer. Foveal flicker sensitivity in healthy aging eyes. II. cross-sectional aging trends from 18 through 77 years of age. *Journal of the Optical Society of America A*, 11(7):1958–1969, July 1994. http://dx.doi.org/10.1364/JOSAA.11.001958.

J. Kim, R. Horstmeyer, I. Kim, and R. Raskar. Highlighted depth-of-field photography: Shining light on focus. *ACM Transactions on Graphics (TOG)*, 30:24:1–24:9, May 2011. http://dx.doi.org/10.1145/1966394.1966403.

R. Kim, D. Kim, J. Xiao, B. H. Kim, S. Park, B. Panilaitis, R. Ghaffari, J. Yao, M. Li, Z. Liu, V. Malyarchuk, D. G. Kim, A. Le, R. G. Nuzzo, D. L. Kaplan, F. G. Omenetto, Y. Huang, Z. Kang, and J. A. Rogers. Waterproof AlInGaP optoelectronics on stretchable substrates with applications in biomedicine and robotics. *Nat Mater*, 9(11):929–937, Nov. 2010. http://dx.doi.org/10.1038/nmat2879.

E. Kimura and R. S. Young. Nature of the pupillary responses evoked by chromatic flashes on a white background. *Vision Research*, 35(7):897–906, Apr. 1995. http://dx.doi.org/10.1016/0042-6989(94)00188-R.

E. Kimura and R. S. Young. A chromatic-cancellation property of human pupillary responses. *Vision Research*, 36(11):1543–1550, June 1996. http://dx.doi.org/10.1016/0042-6989(95)00229-4.

E. Kimura and R. S. L. Young. S-cone contribution to pupillary responses evoked by chromatic flash offset. *Vision Research*, 39(6):1189–1197, Mar. 1999. http://dx.doi.org/10.1016/S0042-6989(98)00154-0.

E. Kimura and R. S. L. Young. Sustained pupillary constrictions mediated by an l- and m- cone opponent process. *Vision Research*, 50(5):489–496, Mar. 2010. http://dx.doi.org/10.1016/j.visres.2010.01.001.

R. E. Kirk. *Experimental Design: Procedures for Behavioral Sciences*. Sage Publications (CA), 4 edition, Jan. 2012.

K. Kirschfeld. The absolute sensitivity of lens and compound eyes. *Zeitschrift Für Naturforschung. Section C: Biosciences*, 29C(9-10):592–596, Oct. 1974. http://www.ncbi.nlm.nih.gov/pubmed/4278301.

K. Kirschfeld, R. Feiler, and N. Franceschini. A photostable pigment within the rhabdomere of fly photoreceptors no. 7. *Journal of Comparative Physiology ? A*, 125:275–284, 1978a. http://dx.doi.org/10.1007/BF00656606.

K. Kirschfeld, R. Feiler, and B. Minke. The kinetics of formation of metarhodopsin in intact photoreceptors of the fly. *Zeitschrift Für Naturforschung. Section C: Biosciences*, 33(11-12):1009–1010, Dec. 1978b. http://www.ncbi.nlm.nih.gov/pubmed/154219.

K. Kirschfeld, R. Feiler, and K. Vogt. Evidence for a sensitizing pigment in the ocellar photoreceptors of the fly (Musca, calliphora). *Journal of Comparative Physiology A*, 163:421–423, 1988. http://dx.doi.org/10.1007/BF00604896.

A. Kiselev and S. Subramaniam. Activation and regeneration of rhodopsin in the insect visual cycle. *Science*, 266(5189):1369 –1373, Nov. 1994. http://dx.doi.org/10.1126/science.7973725.

T. Kitakawa, S. Nakadomari, I. Kuriki, and K. Kitahara. Evaluation of early state of cyanopsia with subjective color settings immediately after cataract removal surgery. *Journal of the Optical Society of America A*, 26(6):1375–1381, June 2009. http://dx.doi.org/10.1364/JOSAA.26.001375.

S. Klee, D. Link, P. Bessler, and J. Haueisen. Optoelectrophysiological stimulation of the human eye using fundus-controlled silent substitution technique. *Journal of Biomedical Optics*, 16(1):015002, Feb. 2011. http://dx.doi.org/10.1117/1.3528616.

I. Kloog, A. Haim, R. G. Stevens, and B. A. Portnov. Global Co-Distribution of light at night (LAN) and cancers of prostate, colon, and lung in men. *Chronobiology International*, 26(1):108, 2009. http://dx.doi.org/10.1080/07420520802694020.

I. Kloog, B. A. Portnov, H. S. Rennert, and A. Haim. Does the modern urbanized sleeping habitat pose a breast cancer risk? *Chronobiology International*, 28(1):76–80, Feb. 2011. http://dx.doi.org/10.3109/07420528.2010.531490.

R. D. Knaggs, I. M. Crighton, T. F. Cobby, A. J. P. Fletcher, and G. J. Hobbs. The pupillary effects of intravenous morphine, codeine, and tramadol in volunteers. *Anesthesia & Analgesia*, 99(1):108 –112, July 2004. http://dx.doi.org/10.1213/01.ANE.0000116924.16535.BA.

A. G. Knapp. *The visual role of the rabbit's ON channel*. PhD thesis, Massachusetts Institute of Technology, Department of Neuroscience, Cambridge, MA, 1986.

L. Knels, M. Valtink, C. Roehlecke, A. Lupp, J. de la Vega, M. Mehner, and R. H. W. Funk. Blue light stress in retinal neuronal (R28) cells is dependent on wavelength range and irradiance. *European Journal of Neuroscience*, 34(4):548–558, Aug. 2011. http://dx.doi.org/10.1111/j.1460-9568.2011.07790.x.

I. Knez. Effects of indoor lighting on mood and cognition. *Journal of Environmental Psychology*, 15(1):39–51, Mar. 1995. http://dx.

doi.org/10.1016/0272-4944(95)90013-6.

I. Knez. Effects of colour of light on nonvisual psychological processes. *Journal of Environmental Psychology*, 21(2):201–208, June 2001. http://dx.doi.org/10.1006/jevp.2000.0198.

I. Knez and C. Kers. Effects of indoor lighting, gender, and age on mood and cognitive performance. *Environment and Behavior*, 32(6):817–831, Nov. 2000. http://dx.doi.org/10.1177/0013916500326005.

A. Knowles, H. J. A. Dartnall, and H. Davson. The photobiology of vision. In *The Eye*, volume 2B. Academic Press, New York, 1977.

O. P. Kocaoglu, S. Lee, R. S. Jonnal, Q. Wang, A. E. Herde, J. C. Derby, W. Gao, and D. T. Miller. Imaging cone photoreceptors in three dimensions and in time using ultrahigh resolution optical coherence tomography with adaptive optics. *Biomedical Optics Express*, 2(4):748–763, Apr. 2011. http://dx.doi.org/10.1364/BOE.2.000748.

M. Kocifaj. A numerical experiment on light pollution from distant sources. *Monthly Notices of the Royal Astronomical Society*, 415(4):3609–3615, Aug. 2011. http://dx.doi.org/10.1111/j.1365-2966.2011.18977.x.

M. Kocifaj, M. Aubé, and I. Kohút. The effect of spatial and spectral heterogeneity of ground-based light sources on night-sky radiances. *Monthly Notices of the Royal Astronomical Society*, 409(3):1203–1212, Dec. 2010. http://dx.doi.org/10.1111/j.1365-2966.2010.17385.x.

L. Kocsis, P. Herman, and A. Eke. The modified Beer–Lambert law revisited. *Physics in Medicine and Biology*, 51(5):N91–N98, Mar. 2006. http://dx.doi.org/10.1088/0031-9155/51/5/N02.

M. Kohn and M. Clynes. Color dynamics of the pupil. *Annals of the New York Academy of Sciences*, 156(Rein Control or Unidirectional Rate Sensitivity a Fundamental Dynamic and Organizing Function in Biology):931–950, 1969. http://dx.doi.org/10.1111/j.1749-6632.1969.tb14024.x.

D. Kojima, S. Mori, M. Torii, A. Wada, R. Morishita, and Y. Fukada. UV-Sensitive photoreceptor protein OPN5 in humans and mice. *PLoS ONE*, 6(10):e26388, Oct. 2011. http://dx.doi.org/10.1371/journal.pone.0026388.

A. V. Kolesnikov, E. Y. Golobokova, and V. I. Govardovskii. The identity of metarhodopsin III. *Visual Neuroscience*, 20(03):249–265, 2003. http://dx.doi.org/10.1017/S0952523803203047.

M. Koller, M. Kundi, H. G. Stidl, T. Zidek, and M. Haider. Personal light dosimetry in permanent night and day workers. *Chronobiology international*, 10(2):143–55, Apr. 1993. http://www.ncbi.nlm.nih.gov/pubmed/8500191.

V. Kolodyazhniy, J. Späti, S. Frey, T. Götz, A. Wirz-Justice, K. Kräuchi, C. Cajochen, and F. H. Wilhelm. Estimation of human circadian phase via a Multi-Channel ambulatory monitoring system and a multiple regression model. *Journal of Biological Rhythms*, 26(1):55 –67, Feb. 2011. http://dx.doi.org/10.1177/0748730410391619.

L. Kolozsvári, A. Nógrádi, B. Hopp, and Z. Bor. UV absorbance of the human cornea in the 240- to 400-nm range. *Investigative Ophthalmology & Visual Science*, 43(7):2165–2168, July 2002. http://www.ncbi.nlm.nih.gov/pubmed/12091412.

H. Komatsu. The neural mechanisms of perceptual filling-in. *Nat Rev Neurosci*, 7(3):220–231, Mar. 2006. http://dx.doi.org/10.1038/nrn1869.

S. M. Korogod and I. B. Kulagina. Electrical bistability in a neuron model with monostable dendritic and axosomatic membranes. *Neurophysiology*, 32:73–76, Mar. 2000. http://dx.doi.org/10.1007/BF02515172.

A. Koskelainen, P. Ala-Laurila, N. Fyhrquist, and K. Donner. Measurement of thermal contribution to photoreceptor sensitivity. *Nature*, 403(6766):220–223, Jan. 2000. http://dx.doi.org/10.1038/35003242.

V. Koudas, A. Nikolaou, E. Hourdaki, S. G. Giakoumaki, P. Roussos, and P. Bitsios. Comparison of ketanserin, buspirone and propranolol on arousal, pupil size and autonomic function in healthy volunteers. *Psychopharmacology*, 205:1–9, Mar. 2009. http://dx.doi.org/10.1007/s00213-009-1508-5.

M. Koyanagi, A. Terakita, K. Kubokawa, and Y. Shichida. Amphioxus homologs of go-coupled rhodopsin and peropsin having 11-cis- and all-trans-retinals as their chromophores. *FEBS Letters*, 531(3):525–528, Nov. 2002. http://dx.doi.org/10.1016/S0014-5793(02)03616-5.

M. Koyanagi, K. Kubokawa, H. Tsukamoto, Y. Shichida, and A. Terakita. Cephalochordate melanopsin: Evolutionary linkage between invertebrate visual cells and vertebrate photosensitive retinal ganglion cells. *Current Biology*, 15(11):1065–1069, June 2005. http://dx.doi.org/10.1016/j.cub.2005.04.063.

T. Kozaki, S. Kitamura, Y. Higashihara, K. Ishibashi, H. Noguchi, and A. Yasukouchi. Effect of color temperature of light sources on slow-wave sleep. *Journal of PHYSIOLOGICAL ANTHROPOLOGY and Applied Human Science*, 24(2):183–186, 2005. http://dx.doi.org/10.2114/jpa.24.183.

R. Kozakov and H. Schoepp. Proposal for the standard evaluation procedure for Non-Visual action of light. *Journal of Light & Visual Environment*, 35(3):274–277, 2011.

J. M. Kraft and J. S. Werner. Spectral efficiency across the life span: flicker photometry and

brightness matching. *Journal of the Optical Society of America A*, 11(4):1213–1221, Apr. 1994. http://dx.doi.org/10.1364/JOSAA.11.001213.

T. W. Kraft. Photocurrents of cone photoreceptors of the golden-mantled ground squirrel. *The Journal of Physiology*, 404:199–213, Oct. 1988. http://www.ncbi.nlm.nih.gov/pubmed/3253431.

T. W. Kraft, D. M. Schneeweis, and J. L. Schnapf. Visual transduction in human rod photoreceptors. *The Journal of Physiology*, 464:747–765, May 1993. http://www.ncbi.nlm.nih.gov/pubmed/8229828.

H. G. Krapp and M. Wicklein. Central processing of visual information in insects. In A. Basbaum, editor, *The senses: a comprehensive reference*, volume Vol. 1, pages 132–203. Academic Press, San Diego, California, vision i edition, 2008.

H. Krastel, E. Alexandridis, and J. Gertz. Pupil increment thresholds are influenced by color opponent mechanisms. *Ophthalmologica*, 191:35–38, 1985. http://content.karger.com/ProdukteDB/produkte.asp?Doi=309536.

J. Krauskopf and G. Karl. Color discrimination and adaptation. *Vision Research*, 32(11): 2165–2175, Nov. 1992. http://dx.doi.org/10.1016/0042-6989(92)90077-V.

R. J. Krauzlis. The control of voluntary eye movements: new perspectives. *The Neuroscientist: A Review Journal Bringing Neurobiology, Neurology and Psychiatry*, 11(2):124–137, Apr. 2005. http://www.ncbi.nlm.nih.gov/pubmed/15746381.

L. Kreitzman. *The 24 Hour Society*. Profile Books Ltd, London, new edition edition, Oct. 1999.

J. Kremers, H. P. N. Scholl, H. Knau, T. T. J. M. Berendschot, T. Usui, and L. T. Sharpe. L/M cone ratios in human trichromats assessed by psychophysics, electroretinography, and retinal densitometry. *Journal of the Optical Society of America A*, 17(3):517–526, Mar. 2000. http://dx.doi.org/10.1364/JOSAA.17.000517.

W. Krenz and L. Stark. Neuronal population model for the pupil-size effect. *Mathematical Biosciences*, 68(2):247–265, Apr. 1984. http://dx.doi.org/10.1016/0025-5564(84)90034-8.

W. Krenz, M. Robin, S. Barez, and L. Stark. Neurophysiological model of the normal and abnormal human pupil. *Biomedical Engineering, IEEE Transactions on*, BME-32 (10):817–825, 1985. http://dx.doi.org/10.1109/TBME.1985.325497.

C. M. Krispel, D. Chen, N. Melling, Y. Chen, K. A. Martemyanov, N. Quillinan, V. Y. Arshavsky, T. G. Wensel, C. Chen, and M. E. Burns. RGS expression Rate-Limits recovery of rod photoresponses. *Neuron*, 51(4): 409–416, Aug. 2006. http://dx.doi.org/10.1016/j.neuron.2006.07.010.

A. Kristek. The physiological pupillogram of the human eye. pages 42–51, Jan. 1965.

L. E. Krueger. Reconciling fechner and stevens: Toward a unified psychophysical law. *Behavioral and Brain Sciences*, 12(02): 251–267, 1989. http://dx.doi.org/10.1017/S0140525X0004855X.

A. A. Kruithof. Tubular luminescence lamps for general illumination. *Philips Tech. Rev.*, 6(3):65–73, 1941.

B. Kruizinga, R. L. Kamman, and D. G. Stavenga. Laser induced visual pigment conversions in fly photoreceptors measured in vivo. *Biophysics of Structure and Mechanism*, 9:299–307, 1983. http://dx.doi.org/10.1007/BF00535665.

J. G. Krupnick and J. L. Benovic. The role of receptor kinases and arrestins in g protein-coupled receptor regulation. *Annual Review of Pharmacology and Toxicology*, 38(1): 289–319, Apr. 1998. http://dx.doi.org/10.1146/annurev.pharmtox.38.1.289.

W. H. Kruskal and W. A. Wallis. Use of ranks in One-Criterion variance analysis. *Journal of the American Statistical Association*, 47 (260):583–621, Dec. 1952. http://dx.doi.org/10.2307/2280779.

L. S. Kumnick. Aging and the latency and duration of pupil constriction in response to light and sound stimuli. *Journal of Gerontology*, 11(4):391 –396, Oct. 1956. www.ncbi.nlm.nih.gov/pubmed/13367380.

Y. Kuo, W. Lin, S. Shieh, and W. Wang. Exploring bistability in rotating Bose–Einstein condensates by a quotient transformation invariant continuation method. *Physica D: Nonlinear Phenomena*, 240(1):78–88, Jan. 2011. http://dx.doi.org/10.1016/j.physd.2010.08.008.

A. Kurtenbach, S. Meierkord, and J. Kremers. Spectral sensitivities in dichromats and trichromats at mesopic retinal illuminances. *Journal of the Optical Society of America A*, 16(7):1541–1548, July 1999. http://dx.doi.org/10.1364/JOSAA.16.001541.

T. G. Kusakabe, N. Takimoto, M. Jin, and M. Tsuda. Evolution and the origin of the visual retinoid cycle in vertebrates. *Philosophical Transactions of the Royal Society B: Biological Sciences*, 364(1531):2897–2910, Oct. 2009. http://dx.doi.org/10.1098/rstb.2009.0043.

S. Kuwayama, H. Imai, T. Morizumi, and Y. Shichida. Amino acid residues responsible for the meta-III decay rates in rod and cone visual pigments. *Biochemistry*, 44(6): 2208–2215, Feb. 2005. http://dx.doi.org/10.1021/bi047994g.

D. Kwiatkowski, P. C. Phillips, P. Schmidt, and Y. Shin. Testing the null hypothesis of stationarity against the alternative of a unit

root: How sure are we that economic time series have a unit root? *Journal of Econometrics*, 54(1-3):159–178, Dec. 1992. http://dx.doi.org/10.1016/0304-4076(92)90104-Y.

C. C. M. Kyba, T. Ruhtz, J. Fischer, and F. Hölker. Cloud coverage acts as an amplifier for ecological light pollution in urban ecosystems. *PLoS ONE*, 6(3):e17307, Mar. 2011a. http://dx.doi.org/10.1371/journal.pone.0017307.

C. C. M. Kyba, T. Ruhtz, J. Fischer, and F. Hölker. Lunar skylight polarization signal polluted by urban lighting. *Journal of Geophysical Research*, Paper in Press, 2011b. http://dx.doi.org/10.1029/2011JD016698.

C. P. Kyriacou and M. H. Hastings. Circadian clocks: genes, sleep, and cognition. *Trends in Cognitive Sciences*, Apr. 2010. http://dx.doi.org/10.1016/j.tics.2010.03.007.

E. La Hey, J. K. IJspeert, T. J. van den Berg, and A. Kijlstra. Quantitative analysis of iris translucency in fuchs' heterochromic cyclitis. *Investigative Ophthalmology & Visual Science*, 34(10):2931 –2942, 1993. http://www.ncbi.nlm.nih.gov/pubmed/8360026.

T. Labhart and D. Nilsson. The dorsal eye of the dragonfly sympetrum: specializations for prey detection against the blue sky. *Journal of Comparative Physiology A*, 176, Apr. 1995. http://dx.doi.org/10.1007/BF00196410.

B. Laeng, S. Sirois, and G. Gredebäck. Pupillometry. *Perspectives on Psychological Science*, 7(1):18 –27, Jan. 2012. http://dx.doi.org/10.1177/1745691611427305.

P. S. Lagali, D. Balya, G. B. Awatramani, T. A. Munch, D. S. Kim, V. Busskamp, C. L. Cepko, and B. Roska. Light-activated channels targeted to ON bipolar cells restore visual function in retinal degeneration. *Nat Neurosci*, 11(6):667–675, June 2008. http://dx.doi.org/10.1038/nn.2117.

G. S. Lall, V. L. Revell, H. Momiji, J. Al Enezi, C. M. Altimus, A. D. Güler, C. Aguilar, M. A. Cameron, S. Allender, M. W. Hankins, and R. J. Lucas. Distinct contributions of rod, cone, and melanopsin photoreceptors to encoding irradiance. *Neuron*, 66(3):417–428, May 2010. http://dx.doi.org/10.1016/j.neuron.2010.04.037.

T. D. Lamb. Photoreceptor spectral sensitivities: Common shape in the long-wavelength region. *Vision Research*, 35(22):3083–3091, Nov. 1995. http://dx.doi.org/10.1016/0042-6989(95)00114-F.

T. D. Lamb. Evolution of vertebrate retinal photoreception. *Philosophical Transactions of the Royal Society B: Biological Sciences*, 364 (1531):2911–2924, Oct. 2009. http://dx.doi.org/10.1098/rstb.2009.0102.

T. D. Lamb and E. N. Pugh. Dark adaptation and the retinoid cycle of vision. *Progress in Retinal and Eye Research*, 23(3):307–380, May 2004. http://dx.doi.org/10.1016/j.preteyeres.2004.03.001.

T. D. Lamb and E. N. Pugh. Phototransduction, dark adaptation, and rhodopsin regeneration: The proctor lecture. *Invest. Ophthalmol. Vis. Sci.*, 47(12):5138–5152, Dec. 2006. http://dx.doi.org/10.1167/iovs.06-0849.

M. F. Land. The physiology of invertebrate visual pigments. In H. Autrum, editor, *Handbook of Sensory physiology. Comparative Physiology and Evolution of Vision in Invertebrates. A. Invertebrate Photoreceptors*, volume 7, pt. 6B, pages 471–592. Springer-Verlag, Berlin, 1981.

M. F. Land and D. Nilsson. *Animal Eyes*. Oxford University Press, USA, Feb. 2002.

H. Landolt and A. A. Borbély. Age-dependent changes in sleep EEG topography. *Clinical Neurophysiology*, 112(2):369–377, Feb. 2001. http://dx.doi.org/10.1016/S1388-2457(00)00542-3.

H. Landolt, D. Dijk, P. Achermann, and A. A. Borbély. Effect of age on the sleep EEG: slow-wave activity and spindle frequency activity in young and middle-aged men. *Brain Research*, 738(2):205–212, Nov. 1996. http://dx.doi.org/10.1016/S0006-8993(96)00770-6.

D. Lang. Energy efficient lighting for the biological clock. *SPIE Newsroom*, Feb. 2011. http://dx.doi.org/10.1117/2.1201101.003442.

P. Lapuerta and S. J. Schein. A four-surface schematic eye of macaque monkey obtained by an optical method. *Vision Research*, 35(16):2245–2254, Aug. 1995. http://dx.doi.org/10.1016/0042-6989(94)00320-L.

M. D. Larson, D. I. Sessler, J. McGuire, and J. M. Hynson. Isoflurane, but not mild hypothermia, depresses the human pupillary light reflex. *Anesthesiology*, 75(1):62–67, July 1991. http://www.ncbi.nlm.nih.gov/pubmed/2064062.

T. A. Lasko, D. F. Kripke, and J. A. Elliot. Melatonin suppression by illumination of upper and lower visual fields. *Journal of Biological Rhythms*, 14(2):122 –125, Apr. 1999. http://dx.doi.org/10.1177/074873099129000506.

H. Laurens. Studies on the relative physiological value of spectral lights: III. the pupillomotor effects of Wave-Lengths of equal energy content. *American Journal of Physiology*, 64(1):97 –119, Mar. 1923.

P. Lavie. Ultradian rhythms in alertness – a pupillometric study. *Biological Psychology*, 9(1):49–62, July 1979. http://dx.doi.org/10.1016/0301-0511(79)90022-X.

A. Le Floch, G. Ropars, J. Enoch, and V. Lakshminarayanan. The polarization sense in

human vision. *Vision Research*, 50(20):2048–2054, Sept. 2010. http://dx.doi.org/10.1016/j.visres.2010.07.007.

G. Leal, C. Neves, and P. Vieira. Wavelet analysis of the autonomic outflowof the pupil's variation in normal subjects, given stimuli. In *Bioengineering (ENBENG), 2011. ENBENG 2011. 1st Portuguese Meeting in*, pages 1–4. IEEE, Mar. 2011. http://dx.doi.org/10.1109/ENBENG.2011.6026066.

K. A. Lederle. *Light effects on sleep, activity and mood in older people*. PhD thesis, Faculty of Health and Medical Sciences, University of Surrey, Guildford, UK, 2010.

B. B. Lee, V. C. Smith, J. Pokorny, and J. Kremers. Rod inputs to macaque ganglion cells. *Vision Research*, 37(20):2813–2828, Oct. 1997. http://dx.doi.org/10.1016/S0042-6989(97)00108-9.

D. D. Lee and H. S. Seung. Learning the parts of objects by non-negative matrix factorization. *Nature*, 401(6755):788–791, Oct. 1999. http://dx.doi.org/10.1038/44565.

H. Lee, Y. Kim, and J. Park. Pupil cycle time and contrast sensitivity in type II diabetes mellitus patients: a pilot study. *Indian Journal of Ophthalmology*, 59(3):201–205, June 2011. http://www.ncbi.nlm.nih.gov/pubmed/21586840.

J. Lee and C. F. Stromeyer. Contribution of human short-wave cones to luminance and motion detection. *The Journal of Physiology*, 413(1):563 –593, June 1989. http://www.ncbi.nlm.nih.gov/pubmed/2600863.

R. D. Lee, C. F. Thomas, R. G. Marietta, and W. S. Stark. Vitamin a, visual pigments, and visual receptors in drosophila. *Microscopy Research and Technique*, 35(6):418–430, Dec. 1996. http://dx.doi.org/10.1002/(SICI)1097-0029(19961215)35:6<418::AID-JEMT2>3.0.CO;2-E.

R. E. Lee, G. H. Cohen, and R. M. Boynton. Latency variation in human pupil contraction due to stimulus luminance and/or adaptation level. *Journal of the Optical Society of America*, 59(1):97–100, Jan. 1969. http://dx.doi.org/10.1364/JOSA.59.000097.

R. J. Lee, J. D. Mollon, Q. Zaidi, and H. E. Smithson. Latency characteristics of the short-wavelength-sensitive cones and their associated pathways. *Journal of Vision*, 9(12), Nov. 2009. http://dx.doi.org/10.1167/9.12.5.

C. Leinert, S. Bowyer, L. K. Haikala, M. S. Hanner, M. G. Hauser, A. C. Levasseur-Regourd, I. Mann, K. Mattila, W. T. Reach, W. Schlosser, J. J. Staude, G. N. Toller, J. L. Weiland, J. L. Weinberg, and A. N. Witt. The 1997 reference of diffuse night sky brightness. Technical report, 2004.

P. Lennie. The physiological basis of variations in visual latency. *Vision Research*, 21(6):815–824, 1981. http://dx.doi.org/10.1016/0042-6989(81)90180-2.

K. Leo. Organic light-emitting diodes: Efficient and flexible solution. *Nat Photon*, 5(12):716–718, Dec. 2011. http://dx.doi.org/10.1038/nphoton.2011.288.

L. Léon, S. V. Crippa, F. Borruat, and A. Kawasaki. Differential effect of long versus short wavelength light exposure on pupillary re-dilation in patients with outer retinal disease. *Clinical & Experimental Ophthalmology*, Accepted article, 2011. http://dx.doi.org/10.1111/j.1442-9071.2011.02665.x.

F. E. Lepore, G. E. Sanborn, and J. T. Slevin. Pupillary dysfunction in myasthenia gravis. *Annals of Neurology*, 6(1):29–33, July 1979. http://dx.doi.org/10.1002/ana.410060107.

S. Leppämäki, Y. Meesters, J. Haukka, J. Lönnqvist, and T. Partonen. Effect of simulated dawn on quality of sleep – a community-based trial. *BMC Psychiatry*, 3(1):14, Oct. 2003. http://dx.doi.org/10.1186/1471-244X-3-14.

S. Lerman, B. Yamanashi, R. Palmer, J. Roark, and R. Borkman. Photoacoustic, fluorescence and light transmission spectra of normal, aging and cataractous lenses. *Ophthalmic Research*, 10(3):168–176, 1978. http://dx.doi.org/10.1159/000264951.

A. B. Lerner, J. D. Case, Y. Takahashi, T. H. Lee, and W. Mori. Isolation of melatonin: a pineal factorthat tightens melanocytes. *J. Am. Chem. Soc.*, 80(10):2587, 1958. http://dx.doi.org/10.1021/ja01543a060.

P. Levatin. Pupillary escape in disease of the retina or optic nerve. *Arch Ophthalmol*, 62:768–779, 1959.

A. G. Leventhal, Y. Wang, M. Pu, Y. Zhou, and Y. Ma. GABA and its agonists improved visual cortical function in senescent monkeys. *Science*, 300(5620):812 –815, May 2003. http://dx.doi.org/10.1126/science.1082874.

E. Levine, E. Crain, P. Robinson, and J. Lisman. Nontransducing rhodopsin. *The Journal of General Physiology*, 90(4):575 –586, Oct. 1987. http://dx.doi.org/10.1085/jgp.90.4.575.

J. Levine and E. J. MacNichol. Microspectrophotometry of primate photoreceptors: art, artifact, and analysis. In A. Fein and J. Levine, editors, *The Visual System*, pages 73–87. Alain R. Liss, New York, 1985.

J. Levine, P. Funes, H. Dowse, and J. Hall. Signal analysis of behavioral and molecular cycles. *BMC Neuroscience*, 3(1):1, 2002. http://dx.doi.org/10.1186/1471-2202-3-1.

A. Lewy, T. Wehr, F. Goodwin, D. Newsome, and S. Markey. Light suppresses melatonin secretion in humans. *Science*, 210(4475):1267–1269, Dec. 1980. http://dx.doi.org/

10.1126/science.7434030.

D. Li, D. Winfield, and D. Parkhurst. Starburst: A hybrid algorithm for video-based eye tracking combining feature-based and model-based approaches. volume 3, page 79, 2005. http://dx.doi.org/10.1109/CVPR.2005.531.

H. Li, J. H. Lim, J. Liu, P. Mitchell, A. G. Tan, J. J. Wang, and T. Y. Wong. A computer-aided diagnosis system of nuclear cataract. *IEEE Transactions on Bio-Medical Engineering*, 57(7):1690–1698, July 2010. http://dx.doi.org/10.1109/TBME.2010.2041454.

N. Li, G. Pelled, A. A. Gilad, P. Walczak, and N. V. Thakor. An in vivo optical system: Control and monitor cortical activity with improved laser speckle contrast imaging and optogenetics. In *2011 5th International IEEE/EMBS Conference on Neural Engineering (NER)*, pages 76–79. IEEE, May 2011. http://dx.doi.org/10.1109/NER.2011.5910492.

W. Li and S. Chen. The origin of the "S-Off" signal in a mammalian retina. In *E-Abstract*, Fort Lauderdale, Florida, USA, 2011.

J. Liang and D. R. Williams. Aberrations and retinal image quality of the normal human eye. *Journal of the Optical Society of America A*, 14(11):2873–2883, Nov. 1997. http://dx.doi.org/10.1364/JOSAA.14.002873.

J. Liang, B. Grimm, S. Goelz, and J. F. Bille. Objective measurement of wave aberrations of the human eye with use of a Hartmann-Shack wave-front sensor. *J. Opt. Soc. Am. A*, 11(7):1949, 1994. http://dx.doi.org/10.1364/JOSAA.11.001949.

T. C. Lie and E. F. Domino. Effects of tobacco smoking on the human pupil. *International Journal of Clinical Pharmacology and Therapeutics*, 37(4):184–188, Apr. 1999. http://www.ncbi.nlm.nih.gov/pubmed/10235421.

P. A. Liebman, K. R. Parker, and E. A. Dratz. The molecular mechanism of visual excitation and its relation to the structure and composition of the rod outer segment. *Annual Review of Physiology*, 49:765–791, 1987. http://dx.doi.org/10.1146/annurev.ph.49.030187.004001.

L. C. Liets, K. Eliasieh, D. A. van der List, and L. M. Chalupa. Dendrites of rod bipolar cells sprout in normal aging retina. *Proceedings of the National Academy of Sciences*, 103(32):12156 –12160, 2006. http://dx.doi.org/10.1073/pnas.0605211103.

B. Lin, A. Koizumi, N. Tanaka, S. Panda, and R. H. Masland. Restoration of visual function in retinal degeneration mice by ectopic expression of melanopsin. *Proceedings of the National Academy of Sciences*, 105(41):16009–16014, Oct. 2008. http://dx.doi.org/10.1073/pnas.0806114105.

D. L. Lindsley and E. H. Grell. Genetic variations of drosophila melanogaster. Technical Report Publication no. 627., Carnegie Institution of Washington, 1967.

A. R. Lingley, M. Ali, Y. Liao, R. Mirjalili, M. Klonner, M. Sopanen, S. Suihkonen, T. Shen, B. P. Otis, H. Lipsanen, and B. A. Parviz. A single-pixel wireless contact lens display. *Journal of Micromechanics and Microengineering*, 21(12):125014, Dec. 2011. http://dx.doi.org/10.1088/0960-1317/21/12/125014.

N. Link and L. Stark. Latency of the pupillary response. *IEEE Transactions on Biomedical Engineering*, 35(3):214–218, Mar. 1988. http://dx.doi.org/10.1109/10.1365.

R. M. Lipman, B. J. Tripathi, and R. C. Tripathi. Cataracts induced by microwave and ionizing radiation. *Survey of Ophthalmology*, 33(3):200–210, Dec. 1988. http://dx.doi.org/10.1016/0039-6257(88)90088-4.

S. G. Lisberger. Visual guidance of Smooth-Pursuit eye movements: Sensation, action, and what happens in between. *Neuron*, 66(4):477–491, May 2010. http://dx.doi.org/10.1016/j.neuron.2010.03.027.

J. E. Lisman and H. Bering. Electrophysiological measurement of the number of rhodopsin molecules in single limulus photoreceptors. *The Journal of General Physiology*, 70(5):621–633, Nov. 1977. http://www.ncbi.nlm.nih.gov/pubmed/591915.

J. E. Lisman and Y. Sheline. Analysis of the rhodopsin cycle in limulus ventral photoreceptors using the early receptor potential. *The Journal of General Physiology*, 68(5):487–501, Nov. 1976. http://www.ncbi.nlm.nih.gov/pubmed/11271.

C. Liu and M. K. Kim. Digital holographic adaptive optics for ocular imaging: proof of principle. *Optics Letters*, 36(14):2710–2712, July 2011. http://dx.doi.org/10.1364/OL.36.002710.

C. Liu, A. K. Satoh, M. Postma, J. Huang, D. F. Ready, and R. C. Hardie. Ca2+-Dependent metarhodopsin inactivation mediated by calmodulin and NINAC myosin III. *Neuron*, 59(5):778–789, Sept. 2008. http://dx.doi.org/10.1016/j.neuron.2008.07.007.

L. Lo and D. J. Anderson. A Cre-Dependent, anterograde transsynaptic viral tracer for mapping output pathways of genetically marked neurons. *Neuron*, 72(6):938–950, Dec. 2011. http://dx.doi.org/10.1016/j.neuron.2011.12.002.

M. Lo, T. Yang, and C. Lee. Fabrication of a tunable daylight simulator. *Applied Optics*, 50(9):C95–C99, Mar. 2011. http://dx.doi.org/10.1364/AO.50.000C95.

E. S. Lobanova, R. Herrmann, S. Finkelstein, B. Reidel, N. P. Skiba, W. Deng, R. Jo, E. R. Weiss, W. W. Hauswirth, and V. Y. Arshavsky. Mechanistic basis for the failure of cone transducin to translocate: Why cones are never blinded by light. *The*

Journal of Neuroscience, 30(20):6815 –6824, May 2010. http://dx.doi.org/10.1523/JNEUROSCI.0613-10.2010.

S. W. Lockley and J. J. Gooley. Circadian photoreception: Spotlight on the brain. *Current Biology*, 16(18):R795–R797, Sept. 2006. http://dx.doi.org/10.1016/j.cub.2006.08.039.

S. W. Lockley, G. C. Brainard, and C. A. Czeisler. High sensitivity of the human circadian melatonin rhythm to resetting by short wavelength light. *The Journal of Clinical Endocrinology and Metabolism*, 88(9): 4502–5, Sept. 2003. http://www.ncbi.nlm.nih.gov/pubmed/12970330.

S. W. Lockley, E. E. Evans, F. A. J. L. Scheer, G. C. Brainard, C. A. Czeisler, and D. Aeschbach. Short-wavelength sensitivity for the direct effects of light on alertness, vigilance, and the waking electroencephalogram in humans. *Sleep*, 29(2):161–8, Feb. 2006. http://www.ncbi.nlm.nih.gov/pubmed/16494083.

I. E. Loewenfeld. Pupillary changes related to age. In H. Thompson, R. Daroff, and L. Frisen, editors, *Topics in Neurophthalmology*, pages 124–150. Williams and Wilkins, Baltimore, 1979.

I. E. Loewenfeld. *The Pupil: Anatomy, Physiology, and Clinical Applications*. Butterworth-Heinemann, 2 edition, Sept. 1999.

I. E. Loewenfeld and O. Lowenstein. *The Pupil: Anatomy, Physiology and Clinical Applications*, volume 1. Iowa State University Press, Ames, 1993.

Y. Loewenstein, S. Mahon, P. Chadderton, K. Kitamura, H. Sompolinsky, Y. Yarom, and M. Häusser. Bistability of cerebellar purkinje cells modulated by sensory stimulation. *Nature Neuroscience*, 8(2):202–211, Feb. 2005. http://www.ncbi.nlm.nih.gov/pubmed/15665875.

C. Lohr. *Semantic light: building blocks*. Master's thesis, University of Maryland, Baltimore, USA, Apr. 2012.

M. Lohse, J. Benovic, J. Codina, M. Caron, and R. Lefkowitz. beta-Arrestin: a protein that regulates beta-adrenergic receptor function. *Science*, 248(4962):1547 –1550, June 1990. http://dx.doi.org/10.1126/science.2163110.

X. Long, O. Tonguz, and A. Kidernan. Real time pupil size monitoring as a screening method for diabetic retinopathy. pages 215–218, 2007. http://dx.doi.org/10.1109/BIOCAS.2007.4463347.

R. S. Longhurst. *Geometrical and Physical Optics*. Longman Group, UK, 3 edition, June 1974.

A. Longtin and J. Milton. Modelling autonomous oscillations in the human pupil light reflex using non-linear delay-differential equations. *Bulletin of Mathematical Biology*, 51(5):605–624, 1989. http://dx.doi.org/10.1007/BF02459969.

A. Longtin, J. G. Milton, J. E. Bos, and M. C. Mackey. Noise and critical behavior of the pupil light reflex at oscillation onset. *Physical Review A*, 41(12):6992, June 1990. http://dx.doi.org/10.1103/PhysRevA.41.6992.

M. A. López-Álvarez, J. Hernández-Andrés, E. M. Valero, and J. Romero. Selecting algorithms, sensors, and linear bases for optimum spectral recovery of skylight. *Journal of the Optical Society of America A*, 24(4): 942–956, Apr. 2007. http://dx.doi.org/10.1364/JOSAA.24.000942.

R. T. Loving, D. F. Kripke, and L. K. Glazner. Circadian rhythms in the human pupil and eyelid. *The American Journal of Physiology*, 271(2 Pt 2):R320–324, Aug. 1996. http://www.ncbi.nlm.nih.gov/pubmed/8770129.

O. Lowenstein. Clinical pupillary symptoms in lesions of the optic nerve, optic chiasm, and optic tract. *A.M.A. Archives of Ophthalmology*, 52(3):385–403, Sept. 1954. http://www.ncbi.nlm.nih.gov/pubmed/13188481.

O. Lowenstein. The argyll robertson pupillary syndrome; mechanism and localization. *American Journal of Ophthalmology*, 42 (4 Part 2):105–121, Oct. 1956. http://www.ncbi.nlm.nih.gov/pubmed/13372660.

O. Lowenstein and E. D. Friedman. Pupillographic studies: I present state of pupillography; its method and diagnostic significance. *Arch Ophthal*, 27(5):969–993, May 1942. http://dx.doi.org/10.1001/archopht.27.5.969.

O. Lowenstein and I. E. Loewenfeld. Scotopic and photopic thresholds of the pupillary light reflex in normal man. *American Journal of Ophthalmology*, 48(1, Part 2):87–98, July 1959. http://www.ncbi.nlm.nih.gov/pubmed/13670267.

O. Lowenstein and I. E. Loewenfeld. Effect of various light stimuli. page 274. Academic Press, New York, NY, USA, 1969.

O. Lowenstein, R. Feinberg, and I. E. Loewenfeld. Pupillary movements during acute and chronic fatigue: A new test for the objective evaluation of tiredness. *Invest. Ophthalmol. Vis. Sci.*, 2(2):138–157, Apr. 1963.

J. Lu, Y. H. Zhang, T. C. Chou, S. E. Gaus, J. K. Elmquist, P. Shiromani, and C. B. Saper. Contrasting effects of ibotenate lesions of the paraventricular nucleus and subparaventricular zone on sleep-wake cycle and temperature regulation. *The Journal of Neuroscience: The Official Journal of the Society for Neuroscience*, 21(13):4864–4874, July 2001. http://www.ncbi.nlm.nih.gov/pubmed/11425913.

J. Lu, G. Shi, and Y. Zhang. Adaptive optics confocal scanning laser ophthalmoscope. In R. K. Tyson, editor, *Topics in Adaptive Op-*

tics. InTech, Jan. 2012.

R. J. Lucas and R. G. Foster. Neither functional rod photoreceptors nor rod or cone outer segments are required for the photic inhibition of pineal melatonin. *Endocrinology*, 140(4):1520–1524, Apr. 1999. http://www.ncbi.nlm.nih.gov/pubmed/10098483.

R. J. Lucas, M. S. Freedman, M. Muñoz, J. Garcia-Fernández, and R. G. Foster. Regulation of the mammalian pineal by non-rod, non-cone, ocular photoreceptors. *Science*, 284(5413):505 –507, Apr. 1999. http://dx.doi.org/10.1126/science.284.5413.505.

R. J. Lucas, R. H. Douglas, and R. G. Foster. Characterization of an ocular photopigment capable of driving pupillary constriction in mice. *Nat Neurosci*, 4:621 – 626, 2001.

R. J. Lucas, S. Hattar, M. Takao, D. M. Berson, R. G. Foster, and K. Yau. Diminished pupillary light reflex at high irradiances in Melanopsin-Knockout mice. *Science*, 299 (5604):245–247, Jan. 2003. http://dx.doi.org/10.1126/science.1077293.

H. Lüdtke, B. Wilhelm, M. Adler, F. Schaeffel, and H. Wilhelm. Mathematical procedures in data recording and processing of pupillary fatigue waves. *Vision Research*, 38(19): 2889–2896, Oct. 1998. http://dx.doi.org/10.1016/S0042-6989(98)00081-9.

D. Luo, V. J. Kefalov, and K. Yau. Phototransduction in retinal rods and cones. In A. Basbaum, editor, *The Senses: A Comprehensive Reference*. Elsevier/Academic, New York, 2008.

D. Lupi, H. Oster, S. Thompson, and R. G. Foster. The acute light-induction of sleep is mediated by OPN4-based photoreception. *Nat Neurosci*, 11(9):1068–1073, 2008. http://dx.doi.org/10.1038/nn.2179.

M. Lutze and G. H. Bresnick. Lenses of diabetic patients "yellow" at an accelerated rate similar to older normals. *Investigative Ophthalmology & Visual Science*, 32(1):194 – 199, Jan. 1991. http://www.ncbi.nlm.nih.gov/pubmed/1987100.

N. Lynnerup, H. Kjeldsen, S. Heegaard, C. Jacobsen, and J. Heinemeier. Radiocarbon dating of the human eye lens crystallines reveal proteins without carbon turnover throughout life. *PLoS ONE*, 3(1):e1529, Jan. 2008. http://dx.plos.org/10.1371/journal.pone.0001529.

J. Lythgoe. Visual pigments and environmental light. *Vision Research*, 24(11):1539–1550, 1984. http://dx.doi.org/10.1016/S0042-6989(84)80003-6.

A. L. Lyubarsky, L. L. Daniele, and J. Pugh, Edward N. From candelas to photoisomerizations in the mouse eye by rhodopsin bleaching in situ and the light-rearing dependence of the major components of the mouse ERG. *Vision Research*, 44(28):3235–3251, Dec. 2004. http://dx.doi.org/10.1016/j.visres.2004.09.019.

J. Lyytimäki. *Unohdetut ympäristöongelmat*. Gaudeamus, Helsinki, 2006.

R. Ma, G. Jiang, H. Duan, L. Bracchini, and S. Loiselle. Effective upwelling irradiance depths in turbid waters: a spectral analysis of origins and fate. *Optics Express*, 19(8): 7127–7138, Apr. 2011. http://dx.doi.org/10.1364/OE.19.007127.

H. Maclean and B. Dhillon. Pupil cycle time and human immunodeficiency virus (HIV) infection. *Eye (London, England)*, 7 (Pt 6): 785–786, 1993. http://www.ncbi.nlm.nih.gov/pubmed/8119434.

E. J. MacNichol. A unifying presentation of photopigment spectra. *Vision Research*, 26 (9):1543–1556, 1986. http://dx.doi.org/10.1016/0042-6989(86)90174-4.

T. Maddess, S. M. Bedford, X. Goh, and A. C. James. Multifocal pupillographic visual field testing in glaucoma. *Clinical & Experimental Ophthalmology*, 37(7):678–686, Sept. 2009. http://dx.doi.org/10.1111/j.1442-9071.2009.02107.x.

F. P. Magalhães, E. F. Costa, A. J. Cariello, E. B. Rodrigues, and A. L. Hofling-Lima. Comparative analysis of the nuclear lens opalescence by the lens opacities classification system III with nuclear density values provided by oculus pentacam: a cross-section study using pentacam nucleus staging software. *Arquivos Brasileiros de Oftalmologia*, 74(2), 2011. http://dx.doi.org/10.1590/S0004-27492011000200008.

O. A. R. Mahroo and T. D. Lamb. Recovery of the human photopic electroretinogram after bleaching exposures: estimation of pigment regeneration kinetics. *The Journal of Physiology*, 554(Pt 2):417–37, Jan. 2004. http://dx.doi.org/10.1113/jphysiol.2003.051250.

M. A. Mainster. Violet and blue light blocking intraocular lenses: photoprotection versus photoreception. *Br J Ophthalmol*, 90(6): 784–792, June 2006. http://dx.doi.org/10.1136/bjo.2005.086553.

C. L. Makino, X. Wen, and J. Lem. Piecing together the timetable for visual transduction with transgenic animals. *Current Opinion in Neurobiology*, 13(4):404–412, Aug. 2003. http://dx.doi.org/10.1016/S0959-4388(03)00091-6.

W. Makous. Scotopic vision. In L. Chalupa and J. S. Werner, editors, *The Visual Neurosciences*, volume 1, pages 838–850. MIT Press, Cambridge, MA, 2004.

M. M. Mallis and C. W. DeRoshia. Circadian rhythms, sleep, and performance in space. *Aviation, space, and environmental medicine*, 76(6 Suppl):B94–107, June 2005. http://www.ncbi.nlm.nih.gov/sites/entrez?Db=pubmed&Cmd=

ShowDetailView&TermToSearch=15943202&ordinalpos=1&itool=EntrezSystem2.PEntrez.Pubmed.Pubmed_ResultsPanel.Pubmed_RVDocSum.

T. Malmström and R. H. H. Kröger. Pupil shapes and lens optics in the eyes of terrestrial vertebrates. *The Journal of Experimental Biology*, 209(Pt 1):18–25, Jan. 2006. http://dx.doi.org/10.1242/jeb.01959.

R. S. Manor, Y. Yassur, and I. Ben Sira. Pupil cycle time in space occupying lesions of anterior optic pathways. *Annals of Ophthalmology*, 14(11):1030–1031, Nov. 1982. http://www.ncbi.nlm.nih.gov/pubmed/7181334.

P. Marchand and L. Marmet. Binomial smoothing filter: A way to avoid some pitfalls of least-squares polynomial smoothing. *Review of Scientific Instruments*, 54(8):1034–1041, Aug. 1983. http://dx.doi.org/10.1063/1.1137498.

S. Marcos, E. Moreno, and R. Navarro. The depth-of-field of the human eye from objective and subjective measurements. *Vision Research*, 39(12):2039–2049, June 1999. http://dx.doi.org/10.1016/S0042-6989(98)00317-4.

E. Marg and J. Morgan, M W. The pupillary near reflex; the relation of pupillary diameter to accommodation and the various components of convergence. *American Journal of Optometry and Archives of American Academy of Optometry*, 26(5):183–198, May 1949. http://www.ncbi.nlm.nih.gov/pubmed/18153968.

E. L. Markwell. *Intrinsically photosensitive melanopsin retinal ganglion cell contributions to the post-illumination pupil response and circadian rhythm*. Master's thesis, Queensland University of Technology, Brisbane, Australia, 2011.

E. L. Markwell, B. Feigl, and A. J. Zele. Intrinsically photosensitive melanopsin retinal ganglion cell contributions to the pupillary light reflex and circadian rhythm. *Clinical and Experimental Optometry*, 93(3):137–149, 2010. http://dx.doi.org/10.1111/j.1444-0938.2010.00479.x.

M. F. Marmor. Ophthalmology and art: Simulation of monet's cataracts and degas' retinal disease. *Arch Ophthalmol*, 124(12):1764–1769, Dec. 2006. http://dx.doi.org/10.1001/archopht.124.12.1764.

D. Marr and E. Hildreth. Theory of edge detection. *Proceedings of the Royal Society of London. Series B. Biological Sciences*, 207(1167):187 –217, Feb. 1980. http://dx.doi.org/10.1098/rspb.1980.0020.

R. T. Marrocco. Possible neural basis of brightness magnitude estimations. *Brain Research*, 86(1):128–133, Mar. 1975. http://www.ncbi.nlm.nih.gov/pubmed/1115988.

J. Marshall and T. W. Cronin. Polarisation vision. *Current Biology*, 21(3):R101–R105, Feb. 2011. http://dx.doi.org/10.1016/j.cub.2010.12.012.

J. Marshall, J. Mellerio, and D. Palmer. A schematic eye for the pigeon. *Vision Research*, 13(12):2449–IN9, Dec. 1973. http://dx.doi.org/10.1016/0042-6989(73)90242-3.

G. R. Martin. Schematic eye models in vertebrates. In D. Ottoson, editor, *Progress in sensory physiology*, volume 4, pages 43–81. Springer, Berlin, 1983.

S. Martinez-Conde, S. L. Macknik, and D. H. Hubel. The role of fixational eye movements in visual perception. *Nature Reviews. Neuroscience*, 5(3):229–240, Mar. 2004. http://dx.doi.org/10.1038/nrn1348.

S. Martinez-Conde, S. L. Macknik, X. G. Troncoso, and D. H. Hubel. Microsaccades: a neurophysiological analysis. *Trends in Neurosciences*, 32(9):463–475, Sept. 2009. http://dx.doi.org/10.1016/j.tins.2009.05.006.

R. H. Masland. The fundamental plan of the retina. *Nat Neurosci*, 4(9):877–886, 2001. http://dx.doi.org/10.1038/nn0901-877.

R. H. Masland. Cell populations of the retina: The proctor lecture. *Investigative Ophthalmology & Visual Science*, 52(7):4581 –4591, June 2011. http://dx.doi.org/10.1167/iovs.10-7083.

N. L. Mata, R. A. Radu, R. C. Clemmons, and G. H. Travis. Isomerization and oxidation of vitamin a in cone-dominant retinas: a novel pathway for visual-pigment regeneration in daylight. *Neuron*, 36(1):69–80, Sept. 2002. http://dx.doi.org/10.1016/S0896-6273(02)00912-1.

A. Mathes, L. Engel, H. Holthues, T. Wolloscheck, and R. Spessert. Daily profile in melanopsin transcripts depends on seasonal lighting conditions in the rat retina. *Journal of Neuroendocrinology*, 19(12):952–957, 2007. http://dx.doi.org/10.1111/j.1365-2826.2007.01608.x.

H. Matsumoto and T. Yamada. Phosrestins i and II: arrestin homologs which undergo differential light-induced phosphorylation in the drosophila photoreceptor in vivo. *Biochemical and Biophysical Research Communications*, 177(3):1306–1312, June 1991. http://dx.doi.org/10.1016/0006-291X(91)90683-X.

R. L. Matsuoka, K. T. Nguyen-Ba-Charvet, A. Parray, T. C. Badea, A. Chedotal, and A. L. Kolodkin. Transmembrane semaphorin signalling controls laminar stratification in the mammalian retina. *Nature*, 470(7333):259–263, Feb. 2011. http://dx.doi.org/10.1038/nature09675.

D. Matthews, D. Lang, M. Burnett, and R. Turner. Control of pulsatile insulin secretion in man. *Diabetologia*, 24, Apr. 1983. http://dx.doi.org/10.1007/BF00282705.

H. R. Matthews, R. L. W. Murphy, G. L. Fain, and T. D. Lamb. Photoreceptor light adaptation is mediated by cytoplasmic calcium concentration. *Nature*, 334(6177):67–69, July 1988. http://dx.doi.org/10.1038/334067a0.

R. G. Matthews, R. Hubbard, P. K. Brown, and G. Wald. Tautomeric forms of metarhodopsin. *The Journal of General Physiology*, 47(2):215–240, Nov. 1963. http://www.ncbi.nlm.nih.gov/pubmed/14080814.

K. Mattila. Synthetic spectrum of the integrated starlight between 3,000 and 10,000 Å. i - method of calculation and results. *Astronomy and Astrophysics Supplement Series*, 39:53–65, Jan. 1980.

K. Mawad and R. N. Van Gelder. Absence of long-wavelength photic potentiation of murine intrinsically photosensitive retinal ganglion cell firing in vitro. *Journal of Biological Rhythms*, 23(5):387–91, Oct. 2008. http://dx.doi.org/10.1177/0748730408323063.

P. J. May and S. Warren. Ultrastructure of the macaque ciliary ganglion. *Journal of Neurocytology*, 22(12):1073–1095, Dec. 1993. http://dx.doi.org/10.1007/BF01235750.

H. Mayer and J. Santer. Synthese von optisch aktiven, naturlichen carotinoiden undstrukturell verwandten naturprodukten. VII. synthese von (3R)-3-Hydroxyretinol, (3R)-3-Hydroxyretinal und (3R)-3-Hydroxyretinsaure. *Helv. chim. Acta*, 63:1467–1472, 1980.

C. S. McCamy. Correlated color temperature as an explicit function of chromaticity coordinates. *Color Research & Application*, 17 (2):142–144, 1992. http://dx.doi.org/10.1002/col.5080170211.

D. H. McDougal and P. D. Gamlin. The influence of intrinsically photosensitive retinal ganglion cells on the spectral sensitivity and response dynamics of the human pupillary light reflex. *Vision Research*, 50(1): 72–87, 2010. http://dx.doi.org/10.1016/j.visres.2009.10.012.

D. H. McDougal and P. D. R. Gamlin. Pupillary control pathways. In *The Senses: A Comprehensive Reference*. Elsevier/Academic, New York, 2008.

W. N. McFarland, C. Wahl, T. Suchanek, and F. McAlary. The behavior of animals around twilight with emphasis on coral reef communities. In S. Archer, M. Djamgoz, E. Loew, J. Partridge, and S. Vallerga, editors, *Adaptive Mechanisms in the Ecology of Vision*. Springer, Boston, MA, USA, 1 edition, 1999.

I. M. McIntyre, T. R. Norman, G. D. Burrows, and S. M. Armstrong. Human melatonin suppression by light is intensity dependent. *Journal of Pineal Research*, 6(2):149–56, 1989. http://www.ncbi.nlm.nih.gov/pubmed/2915324.

J. W. McLaren, P. J. Hauri, S. Lin, and C. D. Harris. Pupillometry in clinically sleepy patients. *Sleep Medicine*, 3(4):347–352, July 2002. http://dx.doi.org/10.1016/S1389-9457(02)00017-5.

S. McVay, A. Katcher, C. McCarthy, G. Wilkins, R. Ulrich, P. Shepard, S. S. Antoine, J. Diamond, G. Orians, R. Nelson, M. Gadgil, L. Margulis, E. Lawrence, J. Heerwagen, and G. Orians. Humans, habitats and aesthetics. In S. R. Kellert and E. O. Wilson, editors, *The Biophilia Hypothesis*. Island Press, 1 edition, Mar. 1995.

J. B. Meddings, R. B. Scott, and G. H. Fick. Analysis and comparison of sigmoidal curves: application to dose-response data. *The American Journal of Physiology*, 257(6 Pt 1):G982–989, Dec. 1989. http://www.ncbi.nlm.nih.gov/pubmed/2610264.

J. M. Medina, L. M. Pereira, H. T. Correia, and S. M. C. Nascimento. Hyperspectral optical imaging of human iris in vivo: characteristics of reflectance spectra. *Journal of Biomedical Optics*, 16:076001, 2011. http://dx.doi.org/10.1117/1.3595710.

R. Mehta and R. J. Zhu. Blue or red? exploring the effect of color on cognitive task performances. *Science*, 323(5918):1226 –1229, Feb. 2009. http://dx.doi.org/10.1126/science.1169144.

J. Meijer, K. Watanabe, L. Détári, and J. Schaap. Circadian rhythm in light response in suprachiasmatic nucleus neurons of freely moving rats. *Brain Research*, 741(1-2):352–355, Nov. 1996. http://dx.doi.org/10.1016/S0006-8993(96)01091-8.

J. H. Meijer, K. Watanabe, J. Schaap, H. Albus, and L. Détári. Light responsiveness of the suprachiasmatic nucleus: long-term multiunit and single-unit recordings in freely moving rats. *The Journal of Neuroscience: The Official Journal of the Society for Neuroscience*, 18(21):9078–9087, Nov. 1998. http://www.ncbi.nlm.nih.gov/pubmed/9787011.

T. J. Melia, C. Cowan, J. Angleson, and T. Wensel. A comparison of the efficiency of g protein activation by ligand-free and light-activated forms of rhodopsin. *Biophysical Journal*, 73(6):3182–3191, Dec. 1997. http://dx.doi.org/10.1016/S0006-3495(97)78344-9.

Z. Melyan, E. E. Tarttelin, J. Bellingham, R. J. Lucas, and M. W. Hankins. Addition of human melanopsin renders mammalian cells photoresponsive. *Nature*, 433(7027):741–745, Feb. 2005. http://dx.doi.org/10.1038/nature03344.

S. T. Menon, M. Han, and T. P. Sakmar. Rhodopsin: structural basis of molecular physiology. *Physiological Reviews*, 81(4): 1659–1688, Oct. 2001. http://www.ncbi.nlm.nih.gov/pubmed/11581499.

S. L. Merbs and J. Nathans. Absorption spectra of human cone pigments. *Nature*, 356

(6368):433–435, Apr. 1992. http://dx.doi.org/10.1038/356433a0.

S. L. Merritt, A. P. Keegan, and P. W. Mercer. Artifact management in pupillometry. *Nursing research*, 43(1):56–9, 1994. http://dx.doi.org/10.1097/00006199-199401000-00012.

N. Michael, M. Johns, C. Owen, and J. Patterson. Effects of caffeine on alertness as measured by infrared reflectance oculography. *Psychopharmacology*, 200:255–260, June 2008. http://dx.doi.org/10.1007/s00213-008-1202-z.

R. Michael and A. J. Bron. The ageing lens and cataract: a model of normal and pathological ageing. *Philosophical Transactions of the Royal Society B: Biological Sciences*, 366 (1568):1278 –1292, Apr. 2011. http://dx.doi.org/10.1098/rstb.2010.0300.

R. Michael, L. J. Van Rijn, T. J. T. P. Van Den Berg, R. I. Barraquer, G. Grabner, H. Wilhelm, T. Coeckelbergh, M. Emesz, P. Marvan, and C. Nischler. Association of lens opacities, intraocular straylight, contrast sensitivity and visual acuity in european drivers. *Acta Ophthalmologica*, 87(6): 666–671, Sept. 2009. http://dx.doi.org/10.1111/j.1755-3768.2008.01326.x.

D. T. Miller and A. Roorda. Adaptive optics in retinal microscopy and vision. In M. Bass, editor, *Handbook of Optics, Vol. III*. Optical Society of America, Rochester, USA, 2009.

S. D. Miller and H. S. Thompson. Edge-light pupil cycle time. *The British Journal of Ophthalmology*, 62(7):495–500, July 1978a. http://www.ncbi.nlm.nih.gov/pubmed/678506.

S. D. Miller and H. S. Thompson. Pupil cycle time in optic neuritis. *American Journal of Ophthalmology*, 85(5 Pt 1):635–642, May 1978b. http://www.ncbi.nlm.nih.gov/pubmed/655242.

S. S. Miller. Psychophysical estimates of visual pigment densities in red-green dichromats. *The Journal of Physiology*, 223(1):89–107, May 1972. http://www.ncbi.nlm.nih.gov/pubmed/4537944.

N. Millott. The photosensitivity of echinoids. *Advances in Marine Biology*, 13, 1976.

P. Mills, S. Tomkins, and L. Schlangen. The effect of high correlated colour temperature office lighting on employee wellbeing and work performance. *Journal of Circadian Rhythms*, 5(1):2, 2007. http://dx.doi.org/10.1186/1740-3391-5-2.

J. G. Milton and A. Longtin. Evaluation of pupil constriction and dilation from cycling measurements. *Vision Research*, 30 (4):515–25, 1990. http://dx.doi.org/10.1016/0042-6989(90)90063-Q.

J. G. Milton, A. Longtin, T. H. Kirkham, and G. S. Francis. Irregular pupil cycling as a characteristic abnormality in patients with demyelinative optic neuropathy. *American Journal of Ophthalmology*, 105(4):402–407, Apr. 1988. http://www.ncbi.nlm.nih.gov/pubmed/3358432.

B. Minke. Transduction in photoreceptors with bistable pigments: Intermediate processes. *Biophysics of Structure and Mechanism*, 5(2-3):163–174, 1979. http://dx.doi.org/10.1007/BF00535445.

B. Minke and K. Kirschfeld. Microspectrophotometric evidence for two photointerconvertible states of visual pigment in the barnacle lateral eye. *The Journal of General Physiology*, 71(1):37–45, Jan. 1978. http://www.ncbi.nlm.nih.gov/pubmed/621493.

B. Minke and K. Kirschfeld. The contribution of a sensitizing pigment to the photosensitivity spectra of fly rhodopsin and metarhodopsin. *The Journal of General Physiology*, 73(5):517–540, May 1979. http://www.ncbi.nlm.nih.gov/pubmed/458418.

B. Minke and K. Kirschfeld. Fast electrical potentials arising from activation of metarhodopsin in the fly. *The Journal of General Physiology*, 75(4):381–402, Apr. 1980. http://www.ncbi.nlm.nih.gov/pubmed/7381425.

B. Minke, S. Hochstein, and P. Hillman. Early receptor potential evidence for the existence of two thermally stable states in the barnacle visual pigment. *The Journal of General Physiology*, 62(1):87–104, July 1973. http://www.ncbi.nlm.nih.gov/pubmed/4767025/.

B. Minke, S. Hochstein, and P. Hillman. Derivation of a quantitative kinetic model for a visual pigment from observations of early receptor potential. *Biophysical Journal*, 14(6):490–512, June 1974. http://dx.doi.org/10.1016/S0006-3495(74)85929-1.

B. Minke, C. F. Wu, and W. L. Pak. Isolation of light-induced response of the central retinula cells from the electroretinogram of drosophila. *Journal of Comparative Physiology A*, 98:345–355, 1975. http://dx.doi.org/10.1007/BF00709805.

B. Minke, S. Hochstein, and P. Hillman. The kinetics of visual pigment systems II: application to measurements on a bistable pigment system. *Biological Cybernetics*, 30(1): 33–43, 1978. http://dx.doi.org/10.1007/BF00365481.

M. J. Minzenberg and C. S. Carter. Modafinil: A review of neurochemical actions and effects on cognition. *Neuropsychopharmacology*, 33(7):1477–1502, 2007. http://dx.doi.org/10.1038/sj.npp.1301534.

Y. Minzhong, M. Russo, D. Johnson, and G. Kamimori. Oculomotor measures over 30-hours of continuous wake with and without caffeine. *Sleep*, 27(Supplement): A138, 2004.

P. Mirtaheri. A novel low-cost design of a digital infrared pupillometer using a web cam-

era. In *Unitech2010*, Oslo, Norway, 2010.

R. E. Mistlberger and D. J. Skene. Nonphotic entrainment in humans? *J Biol Rhythms*, 20(4):339–352, Aug. 2005. http://dx.doi.org/10.1177/0748730405277982.

D. Mitchell and W. Rushton. The red/green pigments of normal vision. *Vision Research*, 11(10):1045–1056, Oct. 1971. http://dx.doi.org/10.1016/0042-6989(71)90111-8.

E. Miyahara, J. Pokorny, and V. C. Smith. Increment threshold and purity discrimination spectral sensitivities of x-chromosome-linked color-defective observers. *Vision Research*, 36(11):1597–1613, June 1996. http://dx.doi.org/10.1016/0042-6989(95)00215-4.

Y. Miyasako, Y. Umezaki, and K. Tomioka. Separate sets of cerebral clock neurons are responsible for light and temperature entrainment of drosophila circadian locomotor rhythms. *Journal of Biological Rhythms*, 22(2):115 –126, Apr. 2007. http://dx.doi.org/10.1177/0748730407299344.

K. Moeller, V. Grote, K. Keller, D. Lorenz, M. Moser, and T. Q. Khanh. LED office lighting to promote performance and Well-Being. In M. M. Robertson, editor, *Ergonomics and Health Aspects of Work with Computers*, volume 6779, pages 68–77. Springer Berlin Heidelberg, Berlin, Heidelberg, 2011. http://dx.doi.org/10.1007/978-3-642-21716-6_8.

M. L. Moline, C. P. Pollak, T. H. Monk, L. S. Lester, D. R. Wagner, S. M. Zendell, R. C. Graeber, C. A. Salter, and E. Hirsch. Age-related differences in recovery from simulated jet lag. *Sleep*, 15(1):28–40, Feb. 1992. http://www.ncbi.nlm.nih.gov/pubmed/1557592.

T. H. Monk, D. J. Buysse, C. F. Reynolds III, and D. J. Kupfer. Inducing jet lag in an older person: Directional asymmetry. *Experimental Gerontology*, 30(2):137–145, Apr. 1995. http://dx.doi.org/10.1016/0531-5565(94)00059-X.

P. Moon and D. E. Spencer. On the Stiles-Crawford effect. *Journal of the Optical Society of America*, 34(6):319–329, June 1944. http://dx.doi.org/10.1364/JOSA.34.000319.

R. Y. Moore and V. B. Eichler. Loss of a circadian adrenal corticosterone rhythm following suprachiasmatic lesions in the rat. *Brain Research*, 42(1):201–206, July 1972. http://dx.doi.org/10.1016/0006-8993(72)90054-6.

R. Y. Moore and D. C. Klein. Visual pathways and the central neural control of a circadian rhythm in pineal serotonin n-acetyltransferase activity. *Brain Research*, 71 (1):17–33, May 1974. http://dx.doi.org/10.1016/0006-8993(74)90188-7.

Y. Morad, H. Lemberg, N. Yofe, and Y. Dagan. Pupillography as an objective indicator of fatigue. *Current eye research*, 21(1):535–42, July 2000.

J. D. Moreland, A. G. Robson, and J. J. Kulikowski. Macular pigment assessment using a colour monitor. *Color Research & Application*, 26(S1):S261–S263, Jan. 2001. http://dx.doi.org/10.1002/1520-6378(2001)26:1+<::AID-COL56>3.0.CO;2-6.

J. I. W. Morgan, A. Dubra, R. Wolfe, W. H. Merigan, and D. R. Williams. In vivo autofluorescence imaging of the human and macaque retinal pigment epithelial cell mosaic. *Investigative Ophthalmology & Visual Science*, 50(3):1350 –1359, Mar. 2009. http://dx.doi.org/10.1167/iovs.08-2618.

P. L. Morgan. *The light environment in care homes: resident light exposure and the effects on rest-activity rhythms*. PhD thesis, Faculty of Health and Medical Sciences, University of Surrey, Guildford, UK, 2011.

C. W. Morgans, J. Zhang, B. G. Jeffrey, S. M. Nelson, N. S. Burke, R. M. Duvoisin, and R. L. Brown. TRPM1 is required for the depolarizing light response in retinal ON-bipolar cells. *Proceedings of the National Academy of Sciences*, 106(45):19174 –19178, Nov. 2009. http://dx.doi.org/10.1073/pnas.0908711106.

C. H. Morimoto and M. R. Mimica. Eye gaze tracking techniques for interactive applications. *Computer Vision and Image Understanding*, 98(1):4–24, Apr. 2005. http://dx.doi.org/10.1016/j.cviu.2004.07.010.

C. H. Morimoto, D. Koons, A. Amir, and M. Flickner. Pupil detection and tracking using multiple light sources. *Image and Vision Computing*, 18(4):331–335, Mar. 2000. http://dx.doi.org/10.1016/S0262-8856(99)00053-0.

H. Morimura, F. Saindelle-Ribeaudeau, E. L. Berson, and T. P. Dryja. Mutations in RGR, encoding a light-sensitive opsin homologue, in patients with retinitis pigmentosa. *Nat Genet*, 23(4):393–394, Dec. 1999. http://dx.doi.org/10.1038/70496.

L. Morin and C. Allen. The circadian visual system, 2005. *Brain Research Reviews*, 51(1): 1–60, June 2006. http://dx.doi.org/10.1016/j.brainresrev.2005.08.003.

L. Morin and K. Studholme. Millisecond light pulses make mice stop running, then display prolonged Sleep-Like behavior in the absence of light. *J Biol Rhythms*, 24(6):497–508, Dec. 2009. http://dx.doi.org/10.1177/0748730409349059.

L. P. Morin, J. H. Blanchard, and I. Provencio. Retinal ganglion cell projections to the hamster suprachiasmatic nucleus, intergeniculate leaflet, and visual midbrain: Bifurcation and melanopsin immunoreactivity. *The Journal of Comparative Neurology*, 465(3):401–416, Oct. 2003. http://dx.doi.

org/10.1002/cne.10881.

T. Morita and H. Tokura. Effects of lights of different color temperature on the nocturnal changes in core temperature and melatonin in humans. *Applied Human Science*, 15 (5):243–246, 1996. http://dx.doi.org/10.2114/jpa.15.243.

S. I. Moro, M. L. Rodriguez-Carmona, E. C. Frost, G. T. Plant, and J. L. Barbur. Recovery of vision and pupil responses in optic neuritis and multiple sclerosis. *Ophthalmic and Physiological Optics*, 27(5):451–460, 2007. http://dx.doi.org/10.1111/j.1475-1313.2007.00501.x.

A. Morte, L. Benito, E. Grasa, S. Clos, J. Riba, and M. Barbanoj. Effects of tobacco smoking on the kinetics of the pupillary light reflex: A comparison between smokers and Non-Smokers. *Neuropsychobiology*, 52:169–175, 2005. http://dx.doi.org/10.1159/000088859.

M. J. Moseley, S. C. Bayliss, and A. R. Fielder. Light transmission through the human eyelid: in vivo measurement. *Ophthalmic & Physiological Optics: The Journal of the British College of Ophthalmic Opticians (Optometrists)*, 8(2):229–30, 1988. http://dx.doi.org/10.1111/j.1475-1313.1988.tb01043.x.

V. Mottram, B. Middleton, P. Williams, and J. Arendt. The impact of bright artificial white and 'blue-enriched' light on sleep and circadian phase during the polar winter. *Journal of Sleep Research*, 20(1pt2):154–161, Mar. 2011. http://dx.doi.org/10.1111/j.1365-2869.2010.00875.x.

M. S. Mould, D. H. Foster, K. Amano, and J. P. Oakley. A simple nonparametric method for classifying eye fixations. *Vision Research*, 57(0):18–25, Mar. 2012. http://dx.doi.org/10.1016/j.visres.2011.12.006.

N. Mrosovsky. In praise of masking: Behavioural responses of retinally degenerate mice to dim light, chronobiology international, informa healthcare. *Chronobiology International*, 11(6):343–348, 1994. http://dx.doi.org/10.3109/07420529409057251.

N. Mrosovsky. Masking: history, definitions, and measurement. *Chronobiology International*, 16(4):415–429, July 1999. http://dx.doi.org/10.3109/07420529908998717.

N. Mrosovsky and P. A. Salmon. Learned arbitrary responses to light in mice without rods or cones. *Naturwissenschaften*, 89:525–527, Nov. 2002. http://dx.doi.org/10.1007/s00114-002-0369-0.

H. Muijser, J. T. Leutscher-Hazelhoff, D. G. Stavenga, and J. W. Kuiper. Photopigment conversions expressed in receptor potential and membrane resistance of blowfly visual sense cells. *Nature*, 254(5500):520–522, Apr. 1975. http://dx.doi.org/10.1038/254520a0.

S. Mukherjee and S. Vernino. Dysfunction of the pupillary light reflex in experimental autoimmune autonomic ganglionopathy. *Autonomic Neuroscience*, 137(1-2):19–26, Dec. 2007. http://dx.doi.org/10.1016/j.autneu.2007.05.005.

W. Müller, H. Töpke, J. Gauß, and S. Pietscher. The inter- and intraindividual variations of the early receptor potentials (ERP). *Graefe's Archive for Clinical and Experimental Ophthalmology*, 219(5):222–224, Nov. 1982. http://dx.doi.org/10.1007/BF00231239.

A. Müller-Jensen and R. Hagenah. Untersuchungen zur variabilität des phasischen pupillenlichtreflexes. *Journal of Neurology*, 212:123–132, Apr. 1976. http://dx.doi.org/10.1007/BF00329155.

A. Müller-Jensen and R. Hagenah. Simultaneous recording of pupillary hippus and EEG. pages 213–218, 1978. http://dx.doi.org/10.1007/BF00312964.

M. Münch, S. Kobialka, R. Steiner, P. Oelhafen, A. Wirz-Justice, and C. Cajochen. Wavelength-dependent effects of evening light exposure on sleep architecture and sleep EEG power density in men. *Am J Physiol Regul Integr Comp Physiol*, 290(5): R1421–1428, May 2006. http://dx.doi.org/10.1152/ajpregu.00478.2005.

M. Murakami and W. L. Pak. Intracellularly recorded early receptor potential of the vertebrate photoreceptors. *Vision Research*, 10 (10):965–XV, Oct. 1970. http://dx.doi.org/10.1016/0042-6989(70)90074-X.

Y. Murata. Light absorption characteristics of the lens capsule. *Ophthalmic Research*, 19 (2):107–112, 1987. http://dx.doi.org/10.1159/000265481.

L. S. Mure. *Caracterisation des proprietes spectrales de la melanopsine*. PhD, Universite Claude Bernard - Lyon 1, Lyon, Nov. 2009.

L. S. Mure, C. Rieux, S. Hattar, and H. M. Cooper. Melanopsin-Dependent nonvisual responses: Evidence for photopigment bistability in vivo. *J Biol Rhythms*, 22(5): 411–424, Oct. 2007. http://dx.doi.org/10.1177/0748730407306043.

L. S. Mure, P. Cornut, C. Rieux, E. Drouyer, P. Denis, C. Gronfier, and H. M. Cooper. Melanopsin bistability: A fly's eye technology in the human retina. *PLoS ONE*, 4(6): e5991, June 2009. http://dx.doi.org/10.1371/journal.pone.0005991.

L. Muscat and L. Morin. Intergeniculate leaflet: Contributions to photic and nonphotic responsiveness of the hamster circadian system. *Neuroscience*, 140(1):305–320, 2006. http://dx.doi.org/10.1016/j.neuroscience.2006.01.050.

G. Myers and L. Stark. Level dependent signal flow in the light pupil reflex i latency of time domain responses to transient stimuli. *Biological Cybernetics*, 68(3):229–234,

Jan. 1993. http://dx.doi.org/10.1007/BF00224856.

G. A. Myers and L. Stark. Topology of the near response triad. *Ophthalmic and Physiological Optics*, 10(2):175–181, Apr. 1990. http://dx.doi.org/10.1111/j.1475-1313.1990.tb00972.x.

G. A. Myers, J. A. Gannon, and L. W. Stark. Level dependent signal flow in the light pupil reflex II phase velocity of responses to sinusoidal light stimuli. *Biological Cybernetics*, 68:235–240, Jan. 1993. http://dx.doi.org/10.1007/BF00224857.

F. Naarendorp, K. S. Rice, and P. A. Sieving. Summation of rod and s cone signals at threshold in human observers. *Vision Research*, 36(17):2681–2688, Sept. 1996. http://dx.doi.org/10.1016/0042-6989(96)00023-5.

T. Nagel. What is it like to be a bat? *The Philosophical Review*, 83(4):435–450, Oct. 1974. http://dx.doi.org/10.2307/2183914.

K. S. Nair, S. M. Hanson, A. Mendez, E. V. Gurevich, M. J. Kennedy, V. I. Shestopalov, S. A. Vishnivetskiy, J. Chen, J. B. Hurley, V. V. Gurevich, and V. Z. Slepak. Light-Dependent redistribution of arrestin in vertebrate rods is an Energy-Independent process governed by Protein-Protein interactions. *Neuron*, 46(4):555–567, May 2005. http://dx.doi.org/10.1016/j.neuron.2005.03.023.

K. I. Naka and W. A. H. Rushton. An attempt to analyse colour reception by electrophysiology. *The Journal of Physiology*, 185(3):556–586, Aug. 1966. http://www.ncbi.nlm.nih.gov/pubmed/5918059/.

Y. Nakane, K. Ikegami, H. Ono, N. Yamamoto, S. Yoshida, K. Hirunagi, S. Ebihara, Y. Kubo, and T. Yoshimura. A mammalian neural tissue opsin (Opsin 5) is a deep brain photoreceptor in birds. *Proceedings of the National Academy of Sciences*, 107 (34):15264 –15268, 2010. http://dx.doi.org/10.1073/pnas.1006393107.

D. R. Nässel and M. Hagberg. Ocellar interneurones in the blowfly calliphora erythrocephala morphology and central projections. *Cell and Tissue Research*, 242(2): 417–426, Nov. 1985. http://dx.doi.org/10.1007/BF00214556.

J. Nathans, D. Thomas, and D. Hogness. Molecular genetics of human color vision: the genes encoding blue, green, and red pigments. *Science*, 232(4747):193–202, Apr. 1986. http://dx.doi.org/10.1126/science.2937147.

K. J. Navara and R. J. Nelson. The dark side of light at night: physiological, epidemiological, and ecological consequences. *Journal of Pineal Research*, 43(3):215–224, 2007. http://dx.doi.org/10.1111/j.1600-079X.2007.00473.x.

R. Navarro, P. Artal, and D. R. Williams. Modulation transfer of the human eye as a function of retinal eccentricity. *Journal of the Optical Society of America A*, 10(2):201–212, Feb. 1993. http://dx.doi.org/10.1364/JOSAA.10.000201.

J. Neitz and G. H. Jacobs. Polymorphism of the long-wavelength cone in normal human colour vision. *Nature*, 323(6089):623–625, Oct. 1986. http://dx.doi.org/10.1038/323623a0.

J. Neitz and M. Neitz. Colour vision: The wonder of hue. *Current Biology*, 18(16):R700–R702, Aug. 2008. http://dx.doi.org/10.1016/j.cub.2008.06.062.

J. Neitz and M. Neitz. The genetics of normal and defective color vision. *Vision Research*, 51(7):633–651, Apr. 2011. http://dx.doi.org/10.1016/j.visres.2010.12.002.

L. A. Newman, M. T. Walker, R. L. Brown, T. W. Cronin, and P. R. Robinson. Melanopsin forms a functional short-wavelength photopigment. *Biochemistry*, 42: 12734 – 12738, 2003. http://dx.doi.org/10.1021/bi035418z.

R. H. Newman, M. D. Fosbrink, and J. Zhang. Genetically encodable fluorescent biosensors for tracking signaling dynamics in living cells. *Chem. Rev.*, 111(5):3614–3666, 2011. http://dx.doi.org/10.1021/cr100002u.

D. A. Newsome. Afterimage and pupillary activity following strong light exposure. *Vision Research*, 11(3):275–288, Mar. 1971. http://dx.doi.org/10.1016/0042-6989(71)90191-X.

R. Ng, M. Levoy, M. Brédif, G. Duval, M. Horowitz, and P. Hanrahan. Light field photography with a hand-held plenoptic camera. Tech. Rep. Computer Science CSTR 2005-02, Stanford University, 2005. http://graphics.stanford.edu/papers/lfcamera/.

P. M. Niedenthal and N. Cantor. Affective responses as guides to category-based inferences. *Motivation and Emotion*, 10(3):217–232, Sept. 1986. http://dx.doi.org/10.1007/BF00992317.

L. Niehaus, B. Guldin, and B. Meyer. Influence of transcranial magnetic stimulation on pupil size. *Journal of the Neurological Sciences*, 182(2):123–128, Jan. 2001. http://dx.doi.org/10.1016/S0022-510X(00)00462-7.

P. S. Nieto, D. J. Valdez, V. A. Acosta-Rodríguez, and M. E. Guido. Expression of novel opsins and intrinsic light responses in the mammalian retinal ganglion cell line RGC-5. presence of OPN5 in the rat retina. *PLoS ONE*, 6(10):e26417, Oct. 2011. http://dx.doi.org/10.1371/journal.pone.0026417.

A. Nikolaou, S. Schiza, S. Giakoumaki, P. Roussos, N. Siafakas, and P. Bitsios. The 5-min pupillary alertness test is sensitive to modafinil: a placebo controlled study in patients with sleep apnea. *Psychopharmacology*, 196(2):167–175, Feb. 2008. http://dx.doi.org/10.1007/s00213-007-0949-y.

C. Niles and M. Bartiss. Increased pupillary cycle time in primary open angle glaucoma. *Investigative Ophthalmology & Visual Science*, 32:1110, 1991.

D. Nilsson. The evolution of eyes and visually guided behaviour. *Philosophical Transactions of the Royal Society B: Biological Sciences*, 364(1531):2833 –2847, Oct. 2009. http://dx.doi.org/10.1098/rstb.2009.0083.

K. Nishimoto and K. Sasaki. In vivo light scattering intensity in the lens versus in vitro spectral transmission in the nuclear region. *Ophthalmic Research*, 27:1–11, 1995. http://dx.doi.org/10.1159/000267560.

J. Nishiyama, K. Tanida, M. Kusumi, and Y. Hirata. The pupil as a possible premonitor of drowsiness. pages 1586–1589, 2007.

I. Nisida, H. Okada, and O. Nakano. The activity of the ciliospinal centers and their inhibition in pupillary light reflex. *The Japanese Journal of Physiology*, 10:73–84, Feb. 1960. http://www.ncbi.nlm.nih.gov/pubmed/14427324.

J. Nissilä, S. Mänttäri, H. Tuominen, T. Särkioja, M. Timonen, and S. Saarela. The abundance and distribution of the encephalopsin (OPN3) in the human brain, Aug. 2011.

H. Noguchi and T. Sakaguchi. Effect of illuminance and color temperature on lowering of physiological activity. *Applied Human Science*, 18(4):117–123, 1999. http://dx.doi.org/10.2114/jpa.18.117.

J. Nolte and J. E. Brown. Electrophysiological properties of cells in the median ocellus of limulus. *The Journal of General Physiology*, 59(2):167–185, Feb. 1972. http://www.ncbi.nlm.nih.gov/pubmed/5058473.

R. A. Normann and I. Perlman. The effects of background illumination on the photoresponses of red and green cones. *The Journal of Physiology*, 286:491–507, Jan. 1979.

W. Nowak, A. Hachol, and H. Kasprzak. Time-frequency analysis of spontaneous fluctuation of the pupil size of the human eye. *Optica Applicata*, XXXVIII(2), 2008.

R. Nygaard and T. Frumkes. Frequency dependence in scotopic flicker sensitivity. *Vision Research*, 25(1):115–127, 1985. http://dx.doi.org/10.1016/0042-6989(85)90085-9.

E. Oancea and N. L. Wicks. TRPM1: new trends for an old TRP. *Advances in Experimental Medicine and Biology*, 704:135–145, 2011. http://dx.doi.org/10.1007/978-94-007-0265-3_7.

N. A. Office. *The Astronomical Almanac*. Nautical Almanac Office, Washington, D.C.

K. Ogawa, Y. Ito, and K. Nakano. Efficient canny edge detection using a GPU. In *International Conference on Natural Computation*, volume 0, pages 279–280, Los Alamitos, CA, USA, 2010. IEEE Computer Society. http://dx.doi.org/10.1109/IC-NC.2010.13.

J. H. Oh, J. R. Oh, H. K. Park, Y. Sung, and Y. R. Do. New paradigm of multi-chip white LEDs: combination of an InGaN blue LED and full down-converted phosphor-converted LEDs. *Optics Express*, 19(S3): A270–A279, May 2011. http://dx.doi.org/10.1364/OE.19.00A270.

N. Ohba and M. Alpern. Adaptation of the pupil light reflex. *Vision Research*, 12(5): 953–967, May 1972. http://dx.doi.org/10.1016/0042-6989(72)90017-X.

Y. Ohno. Spectral design considerations for white LED color rendering. *Optical Engineering*, 44(11):111302–111302–9, Nov. 2005. http://dx.doi.org/10.1117/1.2130694.

K. Ohtsuka, K. Asakura, H. Kawasaki, and M. Sawa. Respiratory fluctuations of the human pupil. *Experimental Brain Research*, 71, June 1988. http://dx.doi.org/10.1007/BF00247537.

L. P. O'Keefe and H. D. Baker. Diurnal changes in human psychophysical luminance sensitivity. *Physiology & Behavior*, 41 (3):193–200, 1987. http://dx.doi.org/10.1016/0031-9384(87)90353-2.

T. Okuno. Hazards of solar blue light. *Applied Optics*, 47(16):2988–2992, June 2008. http://dx.doi.org/10.1364/AO.47.002988.

W. O'Neill and K. Trick. The narcoleptic cognitive pupillary response. *Biomedical Engineering, IEEE Transactions on*, 48(9):963–968, 2001.

W. D. O'Neill and S. Zimmerman. Neurological interpretations and the information in the cognitive pupillary response. *Methods of Information in Medicine*, 39(2):122–4, June 2000. http://www.ncbi.nlm.nih.gov/pubmed/10892244.

J. Ostergaard, J. Hannibal, and J. Fahrenkrug. Synaptic contact between Melanopsin-Containing retinal ganglion cells and rod bipolar cells. *Invest Ophthalmol Vis Sci*, 48: 3812 – 3820, 2007. http://dx.doi.org/10.1167/iovs.06-1322.

S. E. Ostroy. Characteristics of drosophila rhodopsin in wild-type and norpA vision transduction mutants. *The Journal of General Physiology*, 72(5):717–732, Nov. 1978. http://www.ncbi.nlm.nih.gov/pubmed/105082.

T. Ou-Yang, M. Tsai, C. Yen, and T. Lin. An infrared range camera-based approach for three-dimensional locomotion tracking and pose reconstruction in a rodent. *Jour-*

nal of Neuroscience Methods, 201(1):116–123, Sept. 2011. http://dx.doi.org/10.1016/j.jneumeth.2011.07.019.

H. Öğmen and S. Gagné. Phototransduction in invertebrates: The prolonged depolarizing afterpotential. *Biological Cybernetics*, 56: 27–35, Apr. 1987. http://dx.doi.org/10.1007/BF00333065.

M. Overgaard. Visual experience and blindsight: a methodological review. *Experimental Brain Research*, 209:473–479, Feb. 2011. http://dx.doi.org/10.1007/s00221-011-2578-2.

C. Owsley. Aging and vision. *Vision Research*, 51(13):1610–1622, July 2011. http://dx.doi.org/10.1016/j.visres.2010.10.020.

O. Packer and D. R. Williams. Light, the retinal image, and photoreceptors. In S. K. Shevell, editor, *The Science of Color, Second Edition*, pages 64–66. Elsevier Science, Amsterdam, Boston, 2 edition, July 2003.

W. L. Pak and K. J. Lidington. Fast electrical potential from a Long-Lived, Long-Wavelength photoproduct of fly visual pigment. *The Journal of General Physiology*, 63 (6):740–756, June 1974. http://dx.doi.org/10.1085/jgp.63.6.740.

N. R. Pal and S. K. Pal. A review on image segmentation techniques. *Pattern Recognition*, 26(9):1277–1294, Sept. 1993. http://dx.doi.org/10.1016/0031-3203(93)90135-J.

D. V. Palanker, M. S. Blumenkranz, D. Andersen, M. Wiltberger, G. Marcellino, P. Gooding, D. Angeley, G. Schuele, B. Woodley, M. Simoneau, N. J. Friedman, B. Seibel, J. Batlle, R. Feliz, J. Talamo, and W. Culbertson. Femtosecond laser-assisted cataract surgery with integrated optical coherence tomography. *Science Translational Medicine*, 2(58):58ra85, Nov. 2010. http://dx.doi.org/10.1126/scitranslmed.3001305.

K. Palczewski, T. Kumasaka, T. Hori, C. A. Behnke, H. Motoshima, B. A. Fox, I. L. Trong, D. C. Teller, T. Okada, R. E. Stenkamp, M. Yamamoto, and M. Miyano. Crystal structure of rhodopsin: A g Protein-Coupled receptor. *Science*, 289(5480):739 – 745, 2000. http://dx.doi.org/10.1126/science.289.5480.739.

V. F. Pamplona, M. M. Oliveira, and G. V. G. Baranoski. Photorealistic models for pupil light reflex and iridal pattern deformation. *ACM Transactions on Graphics (TOG)*, 28: 106:1–106:12, Sept. 2009. http://dx.doi.org/10.1145/1559755.1559763.

V. F. Pamplona, A. Mohan, M. M. Oliveira, and R. Raskar. NETRA: interactive display for estimating refractive errors and focal range. *ACM Trans. Graph.*, 29(4):1–8, 2010. http://dx.doi.org/10.1145/1833349.1778814.

V. F. Pamplona, E. B. Passos, J. Zizka, M. M. Oliveira, E. Lawson, E. Clua, and R. Raskar. CATRA: interactive measuring and modeling of cataracts. In *ACM SIGGRAPH 2011 papers*, SIGGRAPH '11, page 47:1–47:8, Vancouver, British Columbia, Canada, 2011. ACM. http://dx.doi.org/10.1145/1964921.1964942.

S. Panda, S. K. Nayak, B. Campo, J. R. Walker, J. B. Hogenesch, and T. Jegla. Illumination of the melanopsin signaling pathway. *Science*, 307:600 – 604, 2005. http://dx.doi.org/10.1126/science.1105121.

S. R. Pandi-Perumal, M. Smits, W. Spence, V. Srinivasan, D. P. Cardinali, A. D. Lowe, and L. Kayumov. Dim light melatonin onset (DLMO): a tool for the analysis of circadian phase in human sleep and chronobiological disorders. *Progress in Neuro-Psychopharmacology & Biological Psychiatry*, 31(1):1–11, Jan. 2007. http://dx.doi.org/10.1016/j.pnpbp.2006.06.020.

H. Park. *Remembering the starry night (SkyAct): Using smartphones and social networking to raise community awareness to light pollution*. M.Des., York University, Toronto, Canada, Dec. 2011.

J. C. Park, A. L. Moura, A. S. Raza, D. W. Rhee, R. H. Kardon, and D. C. Hood. Toward a clinical protocol for assessing rod, cone and melanopsin contributions to the human pupil response. *Investigative Ophthalmology & Visual Science*, July 2011. http://dx.doi.org/10.1167/iovs.11-7586.

T. Partonen and A. Magnusson. *Seasonal Affective Disorder: Practice and Research*. Oxford University Press, USA, 1 edition, Dec. 2001.

M. Passatore and V. E. Pettorossi. Efferent fibers in the cervical sympathetic nerve influenced by light. *Experimental Neurology*, 52(1):66–82, July 1976. http://dx.doi.org/10.1016/0014-4886(76)90201-6.

E. Pastrana. Adaptive optics for biological imaging. *Nat Meth*, 8(1):45, Jan. 2011. http://dx.doi.org/10.1038/nmeth.f.333.

E. S. Paul, E. J. Harding, and M. Mendl. Measuring emotional processes in animals: the utility of a cognitive approach. *Neuroscience & Biobehavioral Reviews*, 29(3):469–491, May 2005. http://dx.doi.org/10.1016/j.neubiorev.2005.01.002.

S. M. Pauley. Lighting for the human circadian clock: recent research indicates that lighting has become a public health issue. *Medical Hypotheses*, 63(4):588–596, 2004. http://dx.doi.org/10.1016/j.mehy.2004.03.020.

A. A. V. Paupoo, O. A. R. Mahroo, C. Friedburg, and T. D. Lamb. Human cone photoreceptor responses measured by the electroretinogram a-wave during and after exposure to intense illumination. *The Journal of Physiology*, 529(2):469–482, Dec. 2000. http://dx.doi.org/10.1111/j.1469-7793.2000.00469.x.

M. Pavlou and E. P. Diamandis. I detected my cancer with my smart phone. *Clinical Chemistry*, 57(9):1221 –1223, 2011. http://dx.doi.org/10.1373/clinchem.2011.165761.

A. Pavlov and N. Pavlova. Effect of solar radiation refraction on the zenith angle and times of the sunrise and sunset in the atmosphere. *Geomagnetism and Aeronomy*, 50(2): 219–224, Apr. 2010. http://dx.doi.org/10.1134/S001679321002009X.

C. S. Pechacek, M. Andersen, and S. W. Lockley. Preliminary method for prospective analysis of the circadian efficacy of (Day)Light with applications to healthcare architecture. *LEUKOS*, 5(1):1–26, 2008.

X. Pei, Y. Bao, Y. Chen, and X. Li. Correlation of lens density measured using the pentacam scheimpflug system with the lens opacities classification system III grading score and visual acuity in age-related nuclear cataract. *British Journal of Ophthalmology*, 92(11):1471 –1475, Nov. 2008. http://dx.doi.org/10.1136/bjo.2007.136978.

S. N. Peirson, P. H. Bovee-Geurts, D. Lupi, G. Jeffery, W. J. DeGrip, and R. G. Foster. Expression of the candidate circadian photopigment melanopsin (Opn4) in the mouse retinal pigment epithelium. *Molecular Brain Research*, 123(1–2):132–135, Apr. 2004. http://dx.doi.org/10.1016/j.molbrainres.2004.01.007.

S. N. Peirson, S. Halford, and R. G. Foster. The evolution of irradiance detection: melanopsin and the non-visual opsins. *Philosophical Transactions of the Royal Society B: Biological Sciences*, 364(1531):2849–2865, Oct. 2009. http://dx.doi.org/10.1098/rstb.2009.0050.

J. S. Penn and T. P. Williams. Photostasis: regulation of daily photon-catch by rat retinas in response to various cyclic illuminances. *Experimental Eye Research*, 43(6): 915–28, Dec. 1986. http://dx.doi.org/10.1016/0014-4835(86)90070-9.

I. Pepe and C. Cugnoli. Isolation and characterization of a water-soluble photopigment from honeybee compound eye. *Vision Research*, 20(2):97–102, 1980. http://dx.doi.org/10.1016/0042-6989(80)90150-9.

I. M. Pepe and C. Cugnoli. New trends in photobiology: Retinal photoisomerase: Role in invertebrate visual cells. *Journal of Photochemistry and Photobiology B: Biology*, 13(1): 5–17, Apr. 1992. http://dx.doi.org/10.1016/1011-1344(92)80035-T.

D. R. Pepperberg, M. Kahlert, A. Krause, and K. P. Hofmann. Photic modulation of a highly sensitive, near-infrared light-scattering signal recorded from intact retinal photoreceptors. *Proceedings of the National Academy of Sciences of the United States of America*, 85(15):5531–5535, 1988. http://www.ncbi.nlm.nih.gov/pubmed/3399504.

C. E. Perez-Leighton, T. M. Schmidt, J. Abramowitz, L. Birnbaumer, and P. Kofuji. Intrinsic phototransduction persists in melanopsin-expressing ganglion cells lacking diacylglycerol-sensitive TRPC subunits. *The European Journal of Neuroscience*, Jan. 2011. http://dx.doi.org/10.1111/j.1460-9568.2010.07583.x.

I. Perlman. Dark-adaptation in abnormal (RCS) rats studied electroretinographically. *The Journal of Physiology*, 278:161–175, May 1978. http://www.ncbi.nlm.nih.gov/pubmed/671282.

F. Perrin, P. Peigneux, S. Fuchs, S. Verhaeghe, S. Laureys, B. Middleton, C. Degueldre, G. Del Fiore, G. Vandewalle, E. Balteau, R. Poirrier, V. Moreau, A. Luxen, P. Maquet, and D. Dijk. Nonvisual responses to light exposure in the human brain during the circadian night. *Current Biology*, 14:1842–1846, Oct. 2004. http://dx.doi.org/10.1016/j.cub.2004.09.082.

D. Petersen and R. Cone. The electric dipole moment of rhodopsin solubilized in triton x-100. *Biophysical Journal*, 15(12):1181–1200, Dec. 1975. http://dx.doi.org/10.1016/S0006-3495(75)85894-2.

G. W. Petty. *A First Course in Atmospheric Radiation*. Sundog Publishing, 2 edition, Apr. 2006.

N. Phillips, B. Winn, and B. Gilmartin. Absence of pupil response to blur-driven accommodation. *Vision Research*, 32(9):1775–1779, Sept. 1992. http://dx.doi.org/10.1016/0042-6989(92)90170-N.

G. E. Pickard. The afferent connections of the suprachiasmatic nucleus of the golden hamster with emphasis on the retinohypothalamic projection. *The Journal of Comparative Neurology*, 211(1):65–83, Oct. 1982. http://dx.doi.org/10.1002/cne.902110107.

G. E. Pickard, S. B. Baver, M. D. Ogilvie, and P. J. Sollars. Light-Induced fos expression in intrinsically photosensitive retinal ganglion cells in melanopsin knockout (Opn4-/-) mice. *PLoS ONE*, 4(3), 2009. http://dx.doi.org/10.1371/journal.pone.0004984.

A. R. Pieprzyk, W. W. Weiner, and S. C. Chamberlain. Mechanisms controlling the sensitivity of the limulus lateral eye in natural lighting. *Journal of Comparative Physiology A: Neuroethology, Sensory, Neural, and Behavioral Physiology*, 189(8):643–653, 2003. http://dx.doi.org/10.1007/s00359-003-0437-8.

J. R. Pierce. *An Introduction to Information Theory: Symbols, Signals and Noise*. Dover Publications, 2nd revised ed. edition, Nov. 1980.

J. W. Pillow, L. Paninski, V. J. Uzzell, E. P. Simoncelli, and E. J. Chichilnisky. Prediction and decoding of retinal ganglion cell responses with a probabilistic spiking model. *J. Neurosci.*, 25(47):11003–11013,

Nov. 2005. http://dx.doi.org/10.1523/JNEUROSCI.3305-05.2005.

P. Pinho, K. Jokinen, and L. Halonen. Horticultural lighting - present and future challenges. *Lighting Research and Technology*, Nov. 2011. http://dx.doi.org/10.1177/1477153511424986.

S. S. Pires, S. Hughes, M. Turton, Z. Melyan, S. N. Peirson, L. Zheng, M. Kosmaoglou, J. Bellingham, M. E. Cheetham, R. J. Lucas, R. G. Foster, M. W. Hankins, and S. Halford. Differential expression of two distinct functional isoforms of melanopsin (Opn4) in the mammalian retina. *The Journal of Neuroscience: The Official Journal of the Society for Neuroscience*, 29(39):12332–12342, Sept. 2009. http://dx.doi.org/10.1523/JNEUROSCI.2036-09.2009.

V. F. Pires and J. F. A. Silva. Teaching nonlinear modeling, simulation, and control of electronic power converters using MATLAB/SIMULINK. *IEEE Transactions on Education*, 45:253–261, Aug. 2002. http://dx.doi.org/10.1109/TE.2002.1024618.

J. R. Platt. Carotene-Donor-Acceptor complexes in photosynthesis. *Science*, 129 (3346):372 –374, Feb. 1959. http://dx.doi.org/10.1126/science.129.3346.372.

J. Poirrier, L. Poirrier, P. Leprince, and P. Maquet. Gemvid, an open source, modular, automated activity recording system for rats using digital video. *Journal of circadian rhythms*, 4:10, 2006. http://dx.doi.org/10.1186/1740-3391-4-10.

J. Pokorny, V. C. Smith, and M. Lutze. Aging of the human lens. *Applied Optics*, 26(8): 1437, 1987. http://dx.doi.org/10.1364/AO.26.001437.

J. Pokorny, Q. Jin, and V. C. Smith. Spectral-luminosity functions, scalar linearity, and chromatic adaptation. *Journal of the Optical Society of America A*, 10(6):1304–1313, June 1993. http://dx.doi.org/10.1364/JOSAA.10.001304.

J. Pokorny, H. E. Smithson, and J. Quinlan. Photostimulator allowing independent control of rods and the three cone types. *Visual Neuroscience*, 21(03):263–267, 2004. http://dx.doi.org/10.1017/S0952523804213207.

D. D. Pollak, M. T. Rogan, T. Egner, D. L. Perez, T. K. Yanagihara, and J. Hirsch. A translational bridge between mouse and human models of learned safety. *Annals of Medicine*, 42(2):115–122, Mar. 2010. http://dx.doi.org/10.3109/07853890903583666.

M. Pong and A. F. Fuchs. Characteristics of the pupillary light reflex in the macaque monkey: discharge patterns of pretectal neurons. *Journal of Neurophysiology*, 84(2): 964–74, Aug. 2000a. http://www.ncbi.nlm.nih.gov/pubmed/10938320.

M. Pong and A. F. Fuchs. Characteristics of the pupillary light reflex in the macaque monkey: metrics. *Journal of Neurophysiology*, 84(2):953–63, Aug. 2000b. http://www.ncbi.nlm.nih.gov/pubmed/10938319.

J. Porter, H. Queener, J. Lin, K. Thorn, and A. A. S. Awwal. *Adaptive Optics for Vision Science: Principles, Practices, Design and Applications*. Wiley-Interscience, 1 edition, July 2006.

M. Potmesil and I. Chakravarty. A lens and aperture camera model for synthetic image generation. pages 297–305. ACM Press, 1981. http://dx.doi.org/10.1145/800224.806818.

N. Pousset, B. Rougié, and A. Razet. Impact of current supply on LED colour. *Lighting Research and Technology*, 42(4):371 –383, Dec. 2010. http://dx.doi.org/10.1177/1477153510373315.

N. Pozdeyev, G. Tosini, L. Li, F. Ali, S. Rozov, R. H. Lee, and P. M. Iuvone. Dopamine modulates diurnal and circadian rhythms of protein phosphorylation in photoreceptor cells of mouse retina. *European Journal of Neuroscience*, 27(10):2691–2700, 2008. http://dx.doi.org/10.1111/j.1460-9568.2008.06224.x.

B. Prasad, Y. K. Choi, T. E. Weaver, and D. W. Carley. Pupillometric assessment of sleepiness in narcolepsy. 2(35):1–7, 2011. http://dx.doi.org/10.3389/fpsyt.2011.00035.

F. H. Previc. Functional specialization in the lower and upper visual fields in humans: Its ecological origins and neurophysiological implications. Technical report, 1990.

L. L. Price, M. Khazova, and J. B. O'Hagan. Performance assessment of commercial circadian personal exposure devices. *Lighting Research and Technology*, Jan. 2012. http://dx.doi.org/10.1177/1477153511433171.

C. Privitera and L. Stark. A binocular pupil model for simulation of relative afferent pupil defects and the swinging flashlight test. *Biological Cybernetics*, 94(3):215–224, Mar. 2006. http://dx.doi.org/10.1007/s00422-005-0042-8.

H. Proenca and L. Alexandre. A method for the identification of inaccuracies in pupil segmentation. page 5 pp., 2006. http://dx.doi.org/10.1109/ARES.2006.9.

I. Provencio and D. M. Warthen. Melanopsin, the photopigment of intrinsically photosensitive retinal ganglion cells. *Wiley Interdisciplinary Reviews: Membrane Transport and Signaling*, Early View, 2012. http://dx.doi.org/10.1002/wmts.29.

I. Provencio, G. Jiang, W. J. De Grip, W. P. A. Hayes, and M. D. Rollag. Melanopsin: An opsin in melanophores, brain, and eye. *Proceedings of the National Academy of Sciences of the United States of America*, 95(1):340–345, Jan. 1998. http://www.ncbi.nlm.nih.gov/

pubmed/9419377.

I. Provencio, I. R. Rodriguez, G. Jiang, W. P. Hayes, E. F. Moreira, and M. D. Rollag. A novel human opsin in the inner retina. *J Neurosci*, 20:600 – 605, 2000. http://www.ncbi.nlm.nih.gov/pubmed/10632589.

I. Provencio, M. D. Rollag, and A. M. Castrucci. Anatomy: Photoreceptive net in the mammalian retina. *Nature*, 415(6871):493, Jan. 2002. http://dx.doi.org/10.1038/415493a.

E. J. Pugh, S. Nikonov, and T. Lamb. Molecular mechanisms of vertebrate photoreceptor light adaptation. *Current Opinion in Neurobiology*, 9(4):410–418, Aug. 1999. http://dx.doi.org/10.1016/S0959-4388(99)80062-2.

J. Pugh, E N and T. D. Lamb. Amplification and kinetics of the activation steps in phototransduction. *Biochimica Et Biophysica Acta*, 1141(2-3):111–149, Mar. 1993. http://www.ncbi.nlm.nih.gov/pubmed/8382952.

J. Pugh, E N and T. D. Lamb. Phototransduction in vertebrate rods and cones: molecular mechanisms of amplification, recovery and light adaptation. In D. G. Stavenga, W. J. De Grip, and J. Pugh, E N, editors, *Handbook of biological physics. Molecular mechanisms of visual transduction*, volume 3, pages 183–255. Elsevier, 2000.

E. Pukkala, A. Auvinen, and G. Wahlberg. Incidence of cancer among finnish airline cabin attendants, 1967-92. *BMJ*, 311(7006):649–652, Sept. 1995. http://dx.doi.org/10.1136/bmj.311.7006.649.

C. Pulido, G. Malagón, C. Ferrer, J. K. Chen, J. M. Angueyra, E. Nasi, and M. D. P. Gomez. The light-sensitive conductance of melanopsin-expressing joseph and hesse cells in amphioxus. *The Journal of General Physiology*, 139(1):19–30, Jan. 2012. http://dx.doi.org/10.1085/jgp.201110717.

A. Pumir, J. Graves, R. Ranganathan, and B. I. Shraiman. Systems analysis of the single photon response in invertebrate photoreceptors. *Proceedings of the National Academy of Sciences*, 105(30):10354 –10359, July 2008. http://dx.doi.org/10.1073/pnas.0711884105.

D. Purves. *Neuroscience*. Sinauer Associates, Inc., 4th edition, July 2008.

M. J. Puts, J. Pokorny, J. Quinlan, and L. Glennie. Audiophile hardware in vision science; the soundcard as a digital to analog converter. *Journal of Neuroscience Methods*, 142(1):77–81, Mar. 2005. http://dx.doi.org/10.1016/j.jneumeth.2004.07.013.

X. Qiu and D. M. Berson. Melanopsin bistability in ganglion cell photoreceptors. *Investigative Ophthalmology & Visual Science*, 48:E–Abstract 612, 2007.

X. Qiu, T. Kumbalasiri, S. M. Carlson, K. Y. Wong, V. Krishna, I. Provencio, and D. M. Berson. Induction of photosensitivity by heterologous expression of melanopsin. *Nature*, 433(7027):745–749, Feb. 2005. http://dx.doi.org/10.1038/nature03345.

R. F. Quick. A vector-magnitude model of contrast detection. *Biological Cybernetics*, 16(2):65–67, June 1974. http://dx.doi.org/10.1007/BF00271628.

R. A. Radu, J. Hu, J. Peng, D. Bok, N. L. Mata, and G. H. Travis. Retinal pigment Epithelium-Retinal g protein Receptor-Opsin mediates light-dependent translocation of all-trans-retinyl esters for synthesis of visual chromophore in retinal pigment epithelial cells. *Journal of Biological Chemistry*, 283(28):19730 –19738, July 2008. http://dx.doi.org/10.1074/jbc.M801288200.

S. A. Rahman, A. Kollara, T. J. Brown, and R. F. Casper. Selectively filtering short wavelengths attenuates the disruptive effects of nocturnal light on endocrine and molecular circadian phase markers in rats. *Endocrinology*, pages en.2007–1742, Aug. 2008. http://dx.doi.org/10.1210/en.2007-1742.

S. M. Rajaratnam and J. Arendt. Health in a 24-h society. *The Lancet*, 358(9286):999–1005, Sept. 2001. http://dx.doi.org/10.1016/S0140-6736(01)06108-6.

T. Åkerstedt and S. Folkard. The three-process model of alertness and its extension to performance, sleep latency, and sleep length. *Chronobiology international*, 14(2):115–23, Mar. 1997. http://dx.doi.org/10.3109/07420529709001149.

T. Åkerstedt, S. Folkard, and C. Portin. Predictions from the three-process model of alertness. *Aviation, space, and environmental medicine*, 75(3 Suppl):A75–83, Mar. 2004.

M. Ralph, R. Foster, F. Davis, and M. Menaker. Transplanted suprachiasmatic nucleus determines circadian period. *Science*, 247(4945):975 –978, Feb. 1990. http://dx.doi.org/10.1126/science.2305266.

R. Ranganathan and C. F. Stevens. Arrestin binding determines the rate of inactivation of the g protein-coupled receptor rhodopsin in vivo. *Cell*, 81(6):841–848, June 1995. http://dx.doi.org/10.1016/0092-8674(95)90004-7.

S. W. Ranson and H. W. Magoun. The central path of the pupilloconstrictor reflex in response to light. *Arch Neurol Psychiatry*, 30(6):1193–1204, Dec. 1933.

S. Raphael and D. I. A. MacLeod. Mesopic luminance assessed with minimum motion photometry. *Journal of Vision*, 11(9), 2011. http://dx.doi.org/10.1167/11.9.14.

L. Rastislav. New framework for automatic white balancing of digital camera images. *Signal Processing*, 88(3):582–593, Mar. 2008. http://dx.doi.org/10.1016/j.sigpro.2007.09.007.

S. Ratnasingam and J. Hernández-Andrés. Illuminant spectrum estimation at a pixel. *Journal of the Optical Society of America A*, 28(4):696–703, Apr. 2011. http://dx.doi.org/10.1364/JOSAA.28.000696.

S. Ratnasingam, S. Collins, and J. Hernández-Andrés. Extending "color constancy" outside the visible region. *Journal of the Optical Society of America A*, 28(4):541–547, Apr. 2011. http://dx.doi.org/10.1364/JOSAA.28.000541.

E. Rautkyä, M. Puolakka, and L. Halonen. Alerting effects of daytime light exposure - a proposed link between light exposure and brain mechanisms. *Lighting Research and Technology*, 2011. http://dx.doi.org/10.1177/1477153511409294.

E. Rautkylä. *Research Methods and Neurophysiological Mechanisms Behind the Alerting Effects of Daytime Light Exposure*. PhD thesis, Aalto University, Espoo, Finland, 2011.

E. Rautkylä, M. Puolakka, E. Tetri, and L. Halonen. Effects of correlated colour temperature and timing of light exposure on daytime alertness in lecture environments. *Journal of Light & Visual Environment*, 34(2):59–68, 2010. http://dx.doi.org/10.2150/jlve.34.59.

K. Rayner. Eye movements in reading and information processing: 20 years of research. *Psychological Bulletin*, 124(3):372–422, Nov. 1998. http://dx.doi.org/10.1037/0033-2909.124.3.372.

S. Razmjoo and K. Hamdorf. Visual sensitivity and the variation of total photopigment content in the blowfly photoreceptor membrane. *Journal of Comparative Physiology A*, 105:279–286, Oct. 1976. http://dx.doi.org/10.1007/BF01379288.

S. Razmjoo and K. Hamdorf. In support of the "photopigment model" of vision in invertebrates. *Journal of Comparative Physiology A*, 135:209–215, 1980. http://dx.doi.org/10.1007/BF00657248.

M. Rea, M. Figueiro, and J. Bullough. Circadian photobiology: an emerging framework for lighting practice and research. *Lighting Research and Technology*, 34(3):177–187, Sept. 2002. http://dx.doi.org/10.1191/1365782802lt057oa.

M. Rea, A. Bierman, M. Figueiro, and J. Bullough. A new approach to understanding the impact of circadian disruption on human health. *Journal of Circadian Rhythms*, 6 (1):7, 2008. http://dx.doi.org/10.1186/1740-3391-6-7.

M. S. Rea. *The Iesna Lighting Handbook: Reference & Application*. Illuminating Engineering Society of North America, 9th edition edition, May 2003.

M. S. Rea. Opinion: The future of LED lighting: Greater benefit or just lower cost. *Lighting Research and Technology*, 42(4):370, Dec. 2010. http://dx.doi.org/10.1177/1477153510390978.

M. S. Rea. Biophotonics: Circadian photonics. *Nat Photon*, 5(5):271–272, May 2011a. http://dx.doi.org/10.1038/nphoton.2011.71.

M. S. Rea. Toward a definition of circadian light. *Journal of Light & Visual Environment*, 35(3):250–254, 2011b.

M. S. Rea, M. G. Figueiro, J. D. Bullough, and A. Bierman. A model of phototransduction by the human circadian system. *Brain Research Reviews*, 50(2):213–228, Dec. 2005. http://dx.doi.org/10.1016/j.brainresrev.2005.07.002.

M. S. Rea, M. G. Figueiro, A. Bierman, and J. D. Bullough. Circadian light. *Journal of Circadian Rhythms*, 8(1):2, 2010. http://dx.doi.org/10.1186/1740-3391-8-2.

U. Redlin and N. Mrosovsky. Masking by light in hamsters with SCN lesions. *Journal of Comparative Physiology A: Sensory, Neural, and Behavioral Physiology*, 184:439–448, May 1999. http://dx.doi.org/10.1007/s003590050343.

T. M. Redmond., S. Yu, E. Lee, D. Bok, D. Hamasaki, N. Chen, P. Goletz, J. Ma, R. K. Crouch, and K. Pfeifer. Rpe65 is necessary for production of 11-cis-vitamin a in the retinal visual cycle. *Nat Genet*, 20(4): 344–351, Dec. 1998. http://dx.doi.org/10.1038/3813.

A. Reeves. Transient tritanopia: Its abolition at high intensities. *Vision Research*, 21(5):665–672, 1981. http://dx.doi.org/10.1016/0042-6989(81)90074-2.

A. Reeves, S. Wu, and J. Schirillo. The effect of photon noise on the detection of white flashes. *Vision Research*, 38(5):691–703, Mar. 1998. http://dx.doi.org/10.1016/S0042-6989(97)00201-0.

P. Reeves. Rate of pupillary dilation and contraction. *Psychological Review*, 25(4):330–340, July 1918. http://dx.doi.org/10.1037/h0075293.

P. Reeves. The response of the average pupil to various intensities of light. *Journal of the Optical Society of America*, 4(2):35–43, Mar. 1920. http://dx.doi.org/10.1364/JOSA.4.000035.

R. Refinetti. Dark adaptation in the circadian system of the mouse. *Physiology & Behavior*, 74(1-2):101–107, 2001. http://dx.doi.org/10.1016/S0031-9384(01)00546-7.

R. Refinetti. Effects of prolonged exposure to darkness on circadian photic responsiveness in the mouse. *Chronobiology International*, 20(3):417–440, 2003. http://dx.doi.org/10.1081/CBI-120021443.

R. Refinetti. Enhanced circadian photoresponsiveness after prolonged dark adaptation in seven species of diurnal and nocturnal rodents. *Physiology & Behavior*, 90(2-3):431–7, Feb. 2007. http://dx.doi.org/10.1016/

j.physbeh.2006.10.004.

R. Refinetti, G. Cornélissen, and F. Halberg. Procedures for numerical analysis of circadian rhythms. *Biological Rhythm Research*, 38(4):275, 2007. http://dx.doi.org/10.1080/09291010600903692.

S. Reineke, F. Lindner, G. Schwartz, N. Seidler, K. Walzer, B. Lussem, and K. Leo. White organic light-emitting diodes with fluorescent tube efficiency. *Nature*, 459(7244):234–238, May 2009. http://dx.doi.org/10.1038/nature08003.

J. Reingruber and D. Holcman. The dynamics of phosphodiesterase activation in rods and cones. *Biophysical Journal*, 94(6):1954–70, Mar. 2008. http://dx.doi.org/10.1529/biophysj.107.116202.

G. Reinhard and H. Lachnit. Differential conditioning of anticipatory pupillary dilation responses in humans. *Biological Psychology*, 60(1):51–68, July 2002. http://dx.doi.org/10.1016/S0301-0511(02)00011-X.

C. F. Reinhart and J. Wienold. The daylighting dashboard – a simulation-based design analysis for daylit spaces. *Building and Environment*, 46(2):386–396, Feb. 2011. http://dx.doi.org/10.1016/j.buildenv.2010.08.001.

R. J. Reiter, C. M. Craft, J. Johnson, J E, T. S. King, B. A. Richardson, G. M. Vaughan, and M. K. Vaughan. Age-associated reduction in nocturnal pineal melatonin levels in female rats. *Endocrinology*, 109(4):1295–1297, Oct. 1981. http://dx.doi.org/10.1210/endo-109-4-1295.

R. J. Reiter, D. Tan, L. Fuentes-Broto, and L. Martini. Melatonin: A multitasking molecule. In *Neuroendocrinology: The Normal Neuroendocrine System*, volume Volume 181, pages 127–151. Elsevier, 2010. http://dx.doi.org/10.1016/S0079-6123(08)81008-4.

S. Remtulla and P. Hallett. A schematic eye for the mouse, and comparisons with the rat. *Vision Research*, 25(1):21–31, 1985. http://dx.doi.org/10.1016/0042-6989(85)90076-8.

A. B. Renner, H. Knau, M. Neitz, J. Neitz, and J. S. Werner. Photopigment optical density of the human foveola and a paradoxical senescent increase outside the fovea. *Visual Neuroscience*, 21(06):827–834, 2004. http://dx.doi.org/10.1017/S0952523804216030.

T. Reuter. Fifty years of dark adaptation 1961–2011. *Vision Research*, 51(21-22):2243–2262, Nov. 2011. http://dx.doi.org/10.1016/j.visres.2011.08.021.

V. L. Revell and D. J. Skene. Impact of age on human non-visual responses to light. *Sleep and Biological Rhythms*, 8(2):84–94, 2010. http://dx.doi.org/10.1111/j.1479-8425.2009.00418.x.

V. L. Revell, D. C. G. Barrett, L. J. M. Schlangen, and D. J. Skene. Predicting human nocturnal nonvisual responses to monochromatic and polychromatic light with a melanopsin photosensitivity function. *Chronobiology International*, 27(9-10):1762–1777, Oct. 2010. http://dx.doi.org/10.3109/07420528.2010.516048.

J. Rha, R. S. Jonnal, K. E. Thorn, J. Qu, Y. Zhang, and D. T. Miller. Adaptive optics flood-illumination camera for high speed retinal imaging. *Optics Express*, 14(10):4552–4569, May 2006. http://dx.doi.org/10.1364/OE.14.004552.

C. Ribelayga, Y. Cao, and S. C. Mangel. The circadian clock in the retina controls Rod-Cone coupling. *Neuron*, 59(5):790–801, Sept. 2008. http://dx.doi.org/10.1016/j.neuron.2008.07.017.

C. Rich and T. Longcore. *Ecological Consequences of Artificial Night Lighting*. Island Press, Washington, D.C., USA, Nov. 2005.

F. Richer and J. Beatty. Pupillary dilations in movement preparation and execution. *Psychophysiology*, 22(2):204–207, 1985. http://dx.doi.org/10.1111/j.1469-8986.1985.tb01587.x.

S. Rickel and A. Genin. Twilight transitions in coral reef fish: the input of light-induced changes in foraging behaviour. *Animal Behaviour*, 70:133–144, July 2005. http://dx.doi.org/10.1016/j.anbehav.2004.10.014.

F. Rieke and D. A. Baylor. Single-photon detection by rod cells of the retina. *Reviews of Modern Physics*, 70(3):1027, July 1998. http://dx.doi.org/10.1103/RevModPhys.70.1027.

M. Rietkerk, S. C. Dekker, P. C. de Ruiter, and J. van de Koppel. Self-Organized patchiness and catastrophic shifts in ecosystems. *Science*, 305(5692):1926 –1929, 2004. http://dx.doi.org/10.1126/science.1101867.

J. Robinson, S. C. Bayliss, and A. R. Fielder. Transmission of light across the adult and neonatal eyelid in vivo. *Vision Research*, 31(10):1837–1840, 1991. http://dx.doi.org/10.1016/0042-6989(91)90031-Y.

P. R. Robinson, J. R. Blasic, S. Hattar, and R. L. Brown. Light-Dependent phosphorylation of melanopsin in vitro. *ARVO Meeting Abstracts*, 50(5):5034, Apr. 2009.

J. Robson and N. Graham. Probability summation and regional variation in contrast sensitivity across the visual field. *Vision Research*, 21(3):409–418, 1981. http://dx.doi.org/10.1016/0042-6989(81)90169-3.

J. Roebroek and D. Stavenga. Insect pupil mechanisms IV: spectral characteristics and light intensity dependence in the blowfly, calliphora erythrocephala. *Journal of Comparative Physiology A*, 166, Feb. 1990a. http://dx.doi.org/10.1007/BF00192024.

J. G. Roebroek and D. G. Stavenga. On the effective optical density of the pupil mechanism in fly photoreceptors. *Vision Research*, 30(8):1235–1242, 1990b. http://dx.doi.org/10.1016/0042-6989(90)90178-N.

T. Roenneberg, M. Lotze, and N. von Steinbüchel. Diurnal variation in human visual sensitivity determined by incremental thresholds. *Clinical vision sciences*, 7(2):83–91, 1992.

T. Roenneberg, A. Wirz-Justice, and M. Merrow. Life between clocks: Daily temporal patterns of human chronotypes. *J Biol Rhythms*, 18(1):80–90, Feb. 2003. http://dx.doi.org/10.1177/0748730402239679.

K. J. Rohan, K. A. Roecklein, and D. A. Haaga. Biological and psychological mechanisms of seasonal affective disorder: A review and integration. *Current Psychiatry Reviews*, 5(1):37–47, 2009. http://dx.doi.org/10.2174/157340009787315299.

M. D. Rollag. Does melanopsin bistability have physiological consequences? *Journal of Biological Rhythms*, 23(5):396–9, Oct. 2008. http://dx.doi.org/10.1177/0748730408323067.

A. Roorda. Adaptive optics for studying visual function: A comprehensive review. *Journal of Vision*, 11(5), June 2011. http://dx.doi.org/10.1167/11.5.6.

A. Roorda and D. R. Williams. The arrangement of the three cone classes in the living human eye. *Nature*, 397(6719):520–522, Feb. 1999. http://dx.doi.org/10.1038/17383.

M. L. Rosenberg and M. H. Kroll. Pupillary hippus: an unrecognized example of biologic chaos. *Journal of Biological Systems (JBS)*, 7(1):85–94, 1999. http://dx.doi.org/10.1142/S0218339099000085.

N. E. Rosenthal, D. A. Sack, J. C. Gillin, A. J. Lewy, F. K. Goodwin, Y. Davenport, P. S. Mueller, D. A. Newsome, and T. A. Wehr. Seasonal affective disorder: A description of the syndrome and preliminary findings with light therapy. *Arch Gen Psychiatry*, 41 (1):72–80, Jan. 1984. http://dx.doi.org/10.1001/archpsyc.1984.01790120076010.

G. Rosner. Adaptation und photoregeneration im fliegenauge. *Journal of Comparative Physiology ? A*, 102:269–295, Dec. 1975. http://dx.doi.org/10.1007/BF01464341.

E. A. Rossi and A. Roorda. The relationship between visual resolution and cone spacing in the human fovea. *Nat Neurosci*, 13(2): 156–157, Feb. 2010. http://dx.doi.org/10.1038/nn.2465.

L. S. V. Roth and A. Kelber. Nocturnal colour vision in geckos. *Proceedings of the Royal Society B: Biological Sciences*, 271:S485–S487, Dec. 2004. http://dx.doi.org/10.1098/rsbl.2004.0227.

K. Roy, P. Bhattacharya, and C. Y. Suen. Iris segmentation using variational level set method. *Optics and Lasers in Engineering*, 49(4):578–588, Apr. 2011. http://dx.doi.org/10.1016/j.optlaseng.2010.09.011.

V. V. Rozanov and A. A. Kokhanovsky. Semianalytical cloud retrieval algorithm as applied to the cloud top altitude and the cloud geometrical thickness determination-from top-of-atmosphere reflectance measurements in the oxygen a band. *Journal of Geophysical Research*, 109:21, Mar. 2004. http://dx.doi.org/10.1029/2003JD004104.

M. Różanowska and T. Sarna. Light-induced damage to the retina: Role of rhodopsin chromophore revisited. *Photochemistry and Photobiology*, 81(6):1305–1330, Nov. 2005. http://dx.doi.org/10.1562/2004-11-13-IR-371.

M. Rózanowska, J. Jarvis-Evans, W. Korytowski, M. E. Boulton, J. M. Burke, and T. Sarna. Blue light-induced reactivity of retinal age pigment. in vitro generation of oxygen-reactive species. *The Journal of Biological Chemistry*, 270(32):18825–18830, Aug. 1995. http://dx.doi.org/10.1074/jbc.270.32.18825.

G. V. Rozenberg. *Twilight;: A study in atmospheric optics*. Plenum Press, first english edition edition, 1966.

K. H. Ruddock. Evidence for macular pigmentation from colour matching data. *Vision Research*, 3(9-10):417–429, 1963. http://dx.doi.org/10.1016/0042-6989(63)90093-2.

M. Rufiange, C. Beaulieu, P. Lachapelle, and M. Dumont. Circadian light sensitivity and rate of retinal dark adaptation in indoor and outdoor workers. *Journal of Biological Rhythms*, 22(5):454–7, Oct. 2007. http://dx.doi.org/10.1177/0748730407305375.

M. Rüger, M. C. M. Gordijn, D. G. M. Beersma, B. de Vries, and S. Daan. Nasal versus temporal illumination of the human retina: Effects on core body temperature, melatonin, and circadian phase. *J Biol Rhythms*, 20(1): 60–70, Feb. 2005. http://dx.doi.org/10.1177/0748730404270539.

A. C. Rupp, C. M. Altimus, and S. Hattar. Melanopsin drives acute Light-Dependent changes in body temperature against Cone-Mediated inhibition. *ARVO Meeting Abstracts*, 52(6):3463, Apr. 2011.

W. Rushton. The difference spectrum and the photosensitivity of rhodopsin in the living human eye. *The Journal of Physiology*, 134 (1):11–29, Oct. 1956. http://www.ncbi.nlm.nih.gov/pubmed/13377309.

W. Rushton. Visual pigments in man. In H. J. A. Dartnall, editor, *Handbook of Sensory physiology. Photochemistry of Vision*, pages 481–528. Springer, 1972.

W. Rushton and D. S. Powell. The rhodopsin content and the visual threshold of human rods. *Vision Research*, 12(6):1073–1081, June

1972. http://dx.doi.org.gate1.inist.fr/10.1016/0042-6989(72)90098-3.

W. Rushton, F. W. Campbell, W. A. Hagins, and G. S. Brindley. The bleaching and regeneration of rhodopsin in the living eye of the albino rabbit and of man. *Optica Acta*, 1:183–190, 1955. http://dx.doi.org/10.1016/0042-6989(68)90040-0.

W. A. H. Rushton. Excitation pools in the frog's retina. *The Journal of Physiology*, 149: 327–345, Dec. 1959. http://www.ncbi.nlm.nih.gov/pubmed/14440252.

S. Sacca, C. Bolognesi, A. Battistella, A. Bagnis, and A. Izzotti. Gene–environment interactions in ocular diseases. *Mutation Research/Fundamental and Molecular Mechanisms of Mutagenesis*, 667(1-2):98–117, July 2009. http://dx.doi.org/10.1016/j.mrfmmm.2008.11.002.

R. L. Sack, A. J. Lewy, D. L. Erb, W. M. Vollmer, and C. M. Singer. Human melatonin production decreases with age. *Journal of Pineal Research*, 3(4):379–388, Oct. 1986. http://dx.doi.org/10.1111/j.1600-079X.1986.tb00760.x.

A. Sadeh. The role and validity of actigraphy in sleep medicine: An update. *Sleep Medicine Reviews*, Jan. 2011. http://dx.doi.org/10.1016/j.smrv.2010.10.001.

A. B. Safran, A. Walser, A. Roth, and G. Gauthier. Influence of central depressant drugs on pupil function: an evaluation with the pupil cycle induction test. *Ophthalmologica. Journal International D'ophtalmologie. International Journal of Ophthalmology. Zeitschrift Für Augenheilkunde*, 183(4):214–219, 1981. http://www.ncbi.nlm.nih.gov/pubmed/6121313.

K. Sagawa and Y. Takahashi. Spectral luminous efficiency as a function of age. *Journal of the Optical Society of America. A, Optics, Image Science, and Vision*, 18(11):2659–67, Nov. 2001. http://dx.doi.org/10.1364/JOSAA.18.002659.

F. S. Said and R. A. Weale. The variation with age of the spectral transmissivity of the living human crystalline lens. *Gerontologia*, 3: 213–231, 1959. http://www.ncbi.nlm.nih.gov/pubmed/14440799.

V. D. Saini and G. H. Cohen. Using color substitution pupil response to expose chromatic mechanisms. *Journal of the Optical Society of America*, 69(7):1029–1035, July 1979. http://dx.doi.org/10.1364/JOSA.69.001029.

K. Sakamoto, C. Liu, and G. Tosini. Classical photoreceptors regulate melanopsin mRNA levels in the rat retina. *J. Neurosci.*, 24(43):9693–9697, Oct. 2004. http://dx.doi.org/10.1523/JNEUROSCI.2556-04.2004.

K. Sakamoto, C. Liu, M. Kasamatsu, N. V. Pozdeyev, P. M. Iuvone, and G. Tosini. Dopamine regulates melanopsin mRNA expression in intrinsically photosensitive retinal ganglion cells. *European Journal of Neuroscience*, 22(12):3129–3136, 2005. http://dx.doi.org/10.1111/j.1460-9568.2005.04512.x.

E. Salcedo, A. Huber, S. Henrich, L. V. Chadwell, W. H. Chou, R. Paulsen, and S. G. Britt. Blue- and green-absorbing visual pigments of drosophila: ectopic expression and physiological characterization of the r8 photoreceptor cell-specific rh5 and rh6 rhodopsins. *The Journal of Neuroscience: The Official Journal of the Society for Neuroscience*, 19(24):10716–10726, Dec. 1999. http://www.ncbi.nlm.nih.gov/pubmed/10594055.

M. Samoilov, S. Plyasunov, and A. P. Arkin. Stochastic amplification and signaling in enzymatic futile cycles through noise-induced bistability with oscillations. *Proceedings of the National Academy of Sciences of the United States of America*, 102(7):2310–2315, Feb. 2005. http://dx.doi.org/10.1073/pnas.0406841102.

P. Sample, F. Esterson, R. Weinreb, and R. Boynton. The aging lens: in vivo assessment of light absorption in 84 human eyes. *Invest. Ophthalmol. Vis. Sci.*, 29(8): 1306–1311, Aug. 1988. http://www.ncbi.nlm.nih.gov/pubmed/3417414.

P. A. Sample, J. S. Quirante, and R. N. Weinreb. Age-related changes in the human lens. *Acta Ophthalmologica*, 69(3):310–314, June 1991. http://dx.doi.org/10.1111/j.1755-3768.1991.tb04820.x.

J. S. San Agustin, H. Skovsgaard, J. P. Hansen, and D. W. Hansen. Low-cost gaze interaction: ready to deliver the promises. pages 4453–4458, Boston, MA, USA, 2009. ACM. http://dx.doi.org/10.1145/1520340.1520682.

J. S. San Agustin, H. Skovsgaard, E. Mollenbach, M. Barret, M. Tall, D. W. Hansen, and J. P. Hansen. Evaluation of a low-cost open-source gaze tracker. pages 77–80, Austin, Texas, 2010. ACM. http://dx.doi.org/10.1145/1743666.1743685.

A. Sandberg and L. Stark. Wiener g-function analysis as an approach to non-linear characteristics of human pupil light reflex. *Brain Research*, 11(1):194–211, Oct. 1968. http://dx.doi.org/10.1016/0006-8993(68)90081-4.

J. Santamaria, P. Artal, and J. Bescós. Determination of the point-spread function of human eyes using a hybrid optical-digital method. *Journal of the Optical Society of America A*, 4(6):1109–1114, June 1987. http://dx.doi.org/10.1364/JOSAA.4.001109.

N. Santhi, H. C. Thorne, D. R. van der Veen, S. Johnsen, S. L. Mills, V. Hommes, L. J. M. Schlangen, S. N. Archer, and D. Dijk. The spectral composition of evening light and individual differences in

the suppression of melatonin and delay of sleep in humans. *Journal of Pineal Research*, ePub, 2011. http://dx.doi.org/10.1111/j.1600-079X.2011.00970.x.

C. B. Saper, J. Lu, T. C. Chou, and J. Gooley. The hypothalamic integrator for circadian rhythms. *Trends in Neurosciences*, 28(3):152–157, Mar. 2005a. http://dx.doi.org/10.1016/j.tins.2004.12.009.

C. B. Saper, T. E. Scammell, and J. Lu. Hypothalamic regulation of sleep and circadian rhythms. *Nature*, 437(7063):1257–1263, Oct. 2005b. http://dx.doi.org/10.1038/nature04284.

A. Sarkar, F. Autrusseau, F. Viénot, P. Le Callet, and L. Blondé. From CIE 2006 physiological model to improved age-dependent and average colorimetric observers. *Journal of the Optical Society of America A*, 28(10):2033–2048, Oct. 2011. http://dx.doi.org/10.1364/JOSAA.28.002033.

A. Sassaroli and S. Fantini. Comment on the modified Beer–Lambert law for scattering media. *Physics in Medicine and Biology*, 49:N255–N257, July 2004. http://dx.doi.org/10.1088/0031-9155/49/14/N07.

A. K. Satoh, H. Xia, L. Yan, C. Liu, R. C. Hardie, and D. F. Ready. Arrestin translocation is stoichiometric to rhodopsin isomerization and accelerated by phototransduction in drosophila photoreceptors. *Neuron*, 67(6):997–1008, Sept. 2010. http://dx.doi.org/10.1016/j.neuron.2010.08.024.

G. L. Savage, C. A. Johnson, and D. L. Howard. A comparison of noninvasive objective and subjective measurements of the optical density of human ocular media. *Optometry and Vision Science: Official Publication of the American Academy of Optometry*, 78(6):386–95, June 2001. http://www.ncbi.nlm.nih.gov/pubmed/11444627.

T. J. Savides, S. Messin, C. Senger, and D. F. Kripke. Natural light exposure of young adults. *Physiology & Behavior*, 38(4):571–574, Oct. 1986. http://dx.doi.org/10.1016/0031-9384(86)90427-0.

A. Savitzky and M. J. E. Golay. Smoothing and differentiation of data by simplified least squares procedures. *Analytical Chemistry*, 36(8):1627–1639, July 1964. http://dx.doi.org/10.1021/ac60214a047.

F. Schaeffel. Test systems for measuring ocular parameters and visual function in mice. *Frontiers in Bioscience: A Journal and Virtual Library*, 13:4904–4911, 2008. http://dx.doi.org/10.2741/3049.

E. Schell, T. Theorell, and H. Saraste. Workplace aesthetics: Impact of environments upon employee health? *Work: A Journal of Prevention, Assessment and Rehabilitation*, 39(3):203–213, Jan. 2011. http://dx.doi.org/10.3233/WOR-2011-1182.

E. S. Schernhammer and K. L. Stone. Light pollution /= light pollution? *Chronobiology International*, 28(4):378–379, May 2011. http://dx.doi.org/10.3109/07420528.2011.565898.

C. Schierz. Lighting for the elderly: physiological basics and their consequences. *Light& Engineering*, 19(2):19–27, 2011.

R. Schmid, B. Wilhelm, and H. Wilhelm. Naso-temporal asymmetry and contraction anisocoria in the pupillomotor system. *Graefe's Archive for Clinical and Experimental Ophthalmology*, 238:123–128, Feb. 2000. http://dx.doi.org/10.1007/PL00007879.

S. Y. Schmidt and R. D. Peisch. Melanin concentration in normal human retinal pigment epithelium. regional variation and age-related reduction. *Investigative Ophthalmology & Visual Science*, 27(7):1063–1067, July 1986. http://www.ncbi.nlm.nih.gov/pubmed/3721785.

T. M. Schmidt and P. Kofuji. Functional and morphological differences among intrinsically photosensitive retinal ganglion cells. *J. Neurosci.*, 29(2):476–482, Jan. 2009. http://dx.doi.org/10.1523/JNEUROSCI.4117-08.2009.

T. M. Schmidt and P. Kofuji. Differential cone pathway influence on intrinsically photosensitive retinal ganglion cell subtypes. *The Journal of Neuroscience*, 30(48):16262–16271, Dec. 2010. http://dx.doi.org/10.1523/JNEUROSCI.3656-10.2010.

T. M. Schmidt and P. Kofuji. An isolated retinal preparation to record light response from genetically labeled retinal ganglion cells. *Journal of Visualized Experiments: JoVE*, (47), 2011a. http://dx.doi.org/10.3791/2367.

T. M. Schmidt and P. Kofuji. Structure and function of bistratified intrinsically photosensitive retinal ganglion cells in the mouse. *The Journal of Comparative Neurology*, 519(8):1492–1504, June 2011b. http://dx.doi.org/10.1002/cne.22579.

T. M. Schmidt, K. Taniguchi, and P. Kofuji. Intrinsic and extrinsic light responses in Melanopsin-Expressing ganglion cells during mouse development. *J Neurophysiol*, 100(1):371–384, July 2008. http://dx.doi.org/10.1152/jn.00062.2008.

T. M. Schmidt, S. Chen, and S. Hattar. Intrinsically photosensitive retinal ganglion cells: many subtypes, diverse functions. *Trends in Neurosciences*, 34(11):572–580, Nov. 2011. http://dx.doi.org/10.1016/j.tins.2011.07.001.

C. Schmoll, C. Tendo, P. Aspinall, and B. Dhillon. Reaction time as a measure of enhanced blue-light mediated cognitive function following cataract surgery. *The British Journal of Ophthalmology*, Sept. 2011. http://dx.doi.org/10.1136/bjophthalmol-2011-300677.

J. Schnakenberg. Amplification and latency in photoreceptors: Integrated or separated phenomena? *Biological Cybernetics*, 60, Apr. 1989. http://dx.doi.org/10.1007/BF00204697.

J. L. Schnapf, B. J. Nunn, M. Meister, and D. A. Baylor. Visual transduction in cones of the monkey macaca fascicularis. *The Journal of Physiology*, 427:681–713, Aug. 1990. http://www.ncbi.nlm.nih.gov/pubmed/2100987/.

D. Schneeweis and J. Schnapf. Photovoltage of rods and cones in the macaque retina. *Science*, 268(5213):1053 –1056, May 1995. http://dx.doi.org/10.1126/science.7754386.

H. A. W. Schober and R. Hilz. Contrast sensitivity of the human eye for Square-Wave gratings. *Journal of the Optical Society of America*, 55(9):1086–1090, 1965. http://dx.doi.org/10.1364/JOSA.55.001086.

P. Schoenenberger, Y. Z. Schärer, and T. G. Oertner. Channelrhodopsin as a tool to investigate synaptic transmission and plasticity. *Experimental Physiology*, 96(1):34 –39, Jan. 2011. http://dx.doi.org/10.1113/expphysiol.2009.051219.

E. Schubert and F. Thoss. Der einfluß verschiedener adaptation auf die schwelle sowie auf die reizstärkeabhängigkeit von latenzzeit und amplitude am konsensuellen pupillenreflex des menschen. *Pflügers Archiv für die Gesamte Physiologie des Menschen und der Tiere*, 294:28–39, 1967. http://dx.doi.org/10.1007/BF00417049.

E. F. Schubert and J. K. Kim. Solid-State light sources getting smart. *Science*, 308(5726): 1274–1278, May 2005. http://dx.doi.org/10.1126/science.1108712.

N. Schweitzer. Threshold measurements on the light reflex of the pupil in the dark adapted eye. *Documenta Ophthalmologica. Proceedings Series*, 10:1–78, 1956. http://dx.doi.org/10.1007/BF00172098.

N. Schweitzer and M. A. Bouman. Differential threshold measurements on the light reflex of the human pupil. *A.M.A. Archives of Ophthalmology*, 59(4):541–550, Apr. 1958. http://www.ncbi.nlm.nih.gov/pubmed/13519976.

J. Schwemer. *Molekulare Grundlagen der Photorezeption bei der Schmeissfliege Calliphora erythrocephala Meig*. Habilitationsschrift, Bochum, 1979.

J. Schwemer. Renewal of visual pigment in photoreceptors of the blowfly. *Journal of Comparative Physiology A*, 154:535–547, 1984. http://dx.doi.org/10.1007/BF00610167.

J. Schwemer. Visual pigments of compound eyes – structure, photochemistry, and regeneration. In D. G. Stavenga and R. C. Hardie, editors, *Facets of vision*, page 112–133. Springer, Berlin, Heidelberg, New York, 1989.

J. Schwemer, I. M. Pepe, R. Paulsen, and C. Cugnoli. Light-induced trans-cis isomerization of retinal by a protein from honeybee retina. *Journal of Comparative Physiology A*, 154:549–554, 1984. http://dx.doi.org/10.1007/BF00610168.

J. Schwiegerling. Theoretical limits to visual performance. *Survey of Ophthalmology*, 45 (2):139–146, Sept. 2000. http://dx.doi.org/10.1016/S0039-6257(00)00145-4.

K. Scott and C. S. Zuker. Assembly of the drosophila phototransduction cascade into a signalling complex shapes elementary responses. *Nature*, 395(6704):805–808, Oct. 1998. http://dx.doi.org/10.1038/27448.

S. Sekaran, G. S. Lall, K. L. Ralphs, A. J. Wolstenholme, R. J. Lucas, R. G. Foster, and M. W. Hankins. 2-Aminoethoxydiphenylborane is an acute inhibitor of directly photosensitive retinal ganglion cell activity in vitro and in vivo. *The Journal of Neuroscience*, 27(15):3981 –3986, Apr. 2007. http://dx.doi.org/10.1523/JNEUROSCI.4716-06.2007.

P. R. Selvin. The renaissance of fluorescence resonance energy transfer. *Nat Struct Mol Biol*, 7(9):730–734, 2000. http://dx.doi.org/10.1038/78948.

J. Semmlow, D. Hansmann, and L. Stark. Variation in pupillomotor responsiveness with mean pupil size. *Vision Research*, 15(1): 85–90, Jan. 1975. http://dx.doi.org/10.1016/0042-6989(75)90064-4.

J. L. Semmlow. *Biosignal and Medical Image Processing*. CRC Press, 2 edition, Oct. 2008.

M. Semo, A. A. Vugler, and G. Jeffery. Paradoxical opsin expressing cells in the inner retina that are augmented following retinal degeneration. *European Journal of Neuroscience*, 25(8):2296–2306, Apr. 2007. http://dx.doi.org/10.1111/j.1460-9568.2007.05461.x.

R. Sessoli, D. Gatteschi, A. Caneschi, and M. A. Novak. Magnetic bistability in a metal-ion cluster. *Nature*, 365(6442):141–143, 1993. http://dx.doi.org/10.1038/365141a0.

T. Sexton, E. Buhr, and R. N. Van Gelder. Melanopsin and mechanisms of non-visual ocular photoreception. *Journal of Biological Chemistry*, 287(3):1649 –1656, Jan. 2012. http://dx.doi.org/10.1074/jbc.R111.301226.

M. Sezgin and B. Sankur. Survey over image thresholding techniques and quantitative performance evaluation. *Journal of Electronic Imaging*, 13:146, 2004. http://dx.doi.org/10.1117/1.1631315.

M. A. Shah, S. M. Shah, S. B. Shah, C. G. Patel, and U. A. Patel. Morphology of traumatic cataract: does it play a role in final visual outcome? *BMJ Open*, 1(1):e000060, Jan. 2011. http://dx.doi.org/10.1136/

bmjopen-2011-000060.

S. Shah and A. Ross. Iris segmentation using geodesic active contours. *IEEE Transactions on Information Forensics and Security*, 4(4): 824–836, Dec. 2009. http://dx.doi.org/10.1109/TIFS.2009.2033225.

L. F. Shampine and M. W. Reichelt. The MATLAB ODE suite. *SIAM Journal on Scientific Computing*, 18(1):1, 1997. http://dx.doi.org/10.1137/S1064827594276424.

A. S. M. Shamsuzzaman, B. J. Gersh, and V. K. Somers. Obstructive sleep apnea: implications for cardiac and vascular disease. *JAMA: The Journal of the American Medical Association*, 290(14):1906–1914, Oct. 2003. http://dx.doi.org/10.1001/jama.290.14.1906.

L. T. Sharpe and A. Stockman. Luminous efficiency functions. In *Visual Transduction and Non-Visual Light Perception*, pages 329–351. 2008. http://dx.doi.org/10.1007/978-1-59745-374-5_15.

L. T. Sharpe, A. Stockman, W. Jagla, and H. Jägle. A luminous efficiency function, v*(lambda), for daylight adaptation. *Journal of Vision*, 5(11):948–68, 2005. http://dx.doi.org/10.1167/5.11.3.

L. T. Sharpe, A. Stockman, W. Jagla, and H. Jägle. A luminous efficiency function, VD65* (?), for daylight adaptation: A correction. *Color Research & Application*, pages n/a–n/a, 2010. http://dx.doi.org/10.1002/col.20602.

C. M. Sherwin and E. F. Glen. Cage colour preferences and effects of home cage colour on anxiety in laboratory mice. *Animal Behaviour*, 66(6):1085–1092, Dec. 2003. http://dx.doi.org/10.1006/anbe.2003.2286.

G. Shi, K. Yau, J. Chen, and V. J. Kefalov. Signaling properties of a Short-Wave cone visual pigment and its role in phototransduction. *The Journal of Neuroscience*, 27(38): 10084 –10093, 2007. http://dx.doi.org/10.1523/?JNEUROSCI.2211-07.2007.

K. Shinomori and J. S. Werner. Impulse response of an s-cone pathway in the aging visual system. *Journal of the Optical Society of America A*, 23(7):1570–1577, July 2006. http://dx.doi.org/10.1364/JOSAA.23.001570.

K. Shinomori and J. S. Werner. The impulse response of S-Cone pathways in detection of increments and decrements. *Visual Neuroscience*, 25(03):341–347, 2008. http://dx.doi.org/10.1017/S0952523808080218.

P. A. Shoemaker. Neural bistability and amplification mediated by NMDA receptors: Analysis of stationary equations. *Neurocomputing*, 74(17):3058–3071, Oct. 2011. http://dx.doi.org/10.1016/j.neucom.2011.04.018.

S. Siegert, B. G. Scherf, K. Del Punta, N. Didkovsky, N. Heintz, and B. Roska. Genetic address book for retinal cell types. *Nat Neurosci*, 12(9):1197–1204, 2009. http://dx.doi.org/10.1038/nn.2370.

G. J. Siegle, E. Granholm, R. E. Ingram, and G. E. Matt. Pupillary and reaction time measures of sustained processing of negative information in depression. *Biological Psychiatry*, 49(7):624–636, Apr. 2001. http://dx.doi.org/10.1016/S0006-3223(00)01024-6.

G. J. Siegle, S. R. Steinhauer, V. A. Stenger, R. Konecky, and C. S. Carter. Use of concurrent pupil dilation assessment to inform interpretation and analysis of fMRI data. *NeuroImage*, 20(1):114–124, Sept. 2003. http://dx.doi.org/10.1016/S1053-8119(03)00298-2.

G. J. Siegle, S. R. Steinhauer, and M. E. Thase. Pupillary assessment and computational modeling of the stroop task in depression. *International Journal of Psychophysiology*, 52 (1):63–76, Mar. 2004. http://dx.doi.org/10.1016/j.ijpsycho.2003.12.010.

P. A. Sieving. *In vivo determination of visual pigment regeneration in humans by measurements of the early receptor potential (ERP)*. PhD thesis, University of Illinois, Chicago, 1981.

E. Sigg and T. Sigg. The modification of the pupillary light reflex by chlorpromazine, diazepam, and pentobarbital. *Brain Research*, 50(1):77–86, Feb. 1973. http://dx.doi.org/10.1016/0006-8993(73)90595-7.

G. A. Silva, J. R. Hetling, and D. R. Pepperberg. Dynamic and steady-state light adaptation of mouse rod photoreceptors in vivo. *The Journal of Physiology*, 534(1):203–216, July 2001. http://dx.doi.org/10.1111/j.1469-7793.2001.00203.x.

R. H. Silverman, F. Kong, H. O. Lloyd, and Y. C. Chen. Fine-resolution photoacoustic imaging of the eye. pages 75640Y–75640Y–8, 2010. http://dx.doi.org/10.1117/12.842471.

E. P. Simoncelli and B. A. Olshausen. Natural image statistics and neural representation. *Annual Review of Neuroscience*, 24: 1193–1216, 2001. http://dx.doi.org/10.1146/annurev.neuro.24.1.1193.

S. Simpson and J. Galbrath. Observations on the normal temperature of the monkey and its diurnal variation, and on the effects of changes in the daily routine on this variation. *Trans R Soc Edinburgh*, 45:65–106, 1906.

C. R. Skoglund. On the influence of alcohol on the pupillary light reflex in man. *Acta Physiologica Scandinavica*, 6(1):94–96, Sept. 1943. http://dx.doi.org/10.1111/j.1748-1716.1943.tb02831.x.

K. Skorkovská, H. Lüdtke, H. Wilhelm, and B. Wilhelm. Pupil campimetry in patients

with retinitis pigmentosa and functional visual field loss. *Graefe's Archive for Clinical and Experimental Ophthalmology*, 247(6): 847–853, Dec. 2008. http://dx.doi.org/10.1007/s00417-008-1015-0.

T. L. Sletten, V. L. Revell, B. Middleton, K. A. Lederle, and D. J. Skene. Age-Related changes in acute and Phase-Advancing responses to monochromatic light. *J Biol Rhythms*, 24(1):73–84, Feb. 2009. http://dx.doi.org/10.1177/0748730408328973.

D. H. Sliney. Measurement of light and the geometry of exposure of the human eye. In J. Marshall, editor, *Visual and visual dysfunction, Vol. 16, The Susceptible Visual Apparatus*, page 23–39. MacMillan, New York, 1991.

D. H. Sliney. Ocular exposure to environmental light and ultraviolet - the impact of lid opening and sky conditions. In K. Sasaki and O. Hockwin, editors, *Cataract Epidemiology*. Karger, Basel, 1997. http://www.ncbi.nlm.nih.gov/pubmed/8969964.

D. H. Sliney. Exposure geometry and spectral environment determine photobiological effects on the human eye. *Photochemistry and Photobiology*, pages 483–489, 2005. http://dx.doi.org/10.1111/j.1751-1097.2005.tb00212.x.

D. H. Sliney. Blue light risk and light therapy. CIE x031:2006, Ottawa, Canada, 2006.

D. H. Sliney. How light reaches the eye and its components. *International Journal of Toxicology*, 21(6):501–9, Nov. 2008. http://dx.doi.org/10.1080/10915810290169927.

L. L. Sloan. The effect of intensity of light, state of adaptation of the eye, and size of photometric field on the visibility curve: a study of the purkinje phenomenon. *Pscyhological Monographs*, 38:1–87, 1928.

M. E. Sloane, C. Owsley, and S. L. Alvarez. Aging, senile miosis and spatial contrast sensitivity at low luminance. *Vision Research*, 28 (11):1235–1246, 1988. http://dx.doi.org/10.1016/0042-6989(88)90039-9.

J. Smakman and D. Stavenga. Spectral sensitivity of blowfly photoreceptors: Dependence on waveguide effects and pigment concentration. *Vision Research*, 26(7):1019–1025, 1986. http://dx.doi.org/10.1016/0042-6989(86)90036-2.

J. G. J. Smakman, J. H. Hateren, and D. G. Stavenga. Angular sensitivity of blowfly photoreceptors: intracellular measurements and wave-optical predictions. *Journal of Comparative Physiology A*, 155:239–247, 1984. http://dx.doi.org/10.1007/BF00612641.

P. M. Smallwood, B. P. Ölveczky, G. L. Williams, G. H. Jacobs, B. E. Reese, M. Meister, and J. Nathans. Genetically engineered mice with an additional class of cone photoreceptors: Implications for the evolution of color vision. *Proceedings of the National Academy of Sciences*, 100(20):11706 – 11711, 2003. http://dx.doi.org/10.1073/pnas.1934712100.

K. Smet, W. R. Ryckaert, M. R. Pointer, G. Deconinck, and P. Hanselaer. Correlation between color quality metric predictions and visual appreciation of light sources. *Optics Express*, 19(9):8151–8166, Apr. 2011. http://dx.doi.org/10.1364/OE.19.008151.

J. D. Smith, L. Y. Ichinose, G. A. Masek, T. Watanabe, and L. Stark. Midbrain single units correlating with pupil response to light. *Science (New York, N.Y.)*, 162(859): 1302–3, Dec. 1968. http://dx.doi.org/10.1126/science.162.3859.1302.

J. S. Smith, D. F. Kripke, J. A. Elliott, and S. D. Youngstedt. Illumination of upper and middle visual fields produces equivalent suppression of melatonin in older volunteers. *Chronobiology International*, 19(5): 883–891, Sept. 2002. http://www.ncbi.nlm.nih.gov/pubmed/12405551.

K. A. Smith, M. W. Schoen, and C. A. Czeisler. Adaptation of human pineal melatonin suppression by recent photic history. *The Journal of Clinical Endocrinology and Metabolism*, 89(7):3610–4, July 2004. http://dx.doi.org/10.1210/jc.2003-032100.

L. Smith. A tutorial on principal component analysis, 2002.

M. Smith. Time to turn off the lights. *Nature*, 457(7225):27, Jan. 2009. http://dx.doi.org/10.1038/457027a.

R. C. Smith and K. S. Baker. Optical properties of the clearest natural waters (200-800 nm). *Applied Optics*, 20(2):177–184, Jan. 1981. http://dx.doi.org/10.1364/AO.20.000177.

S. A. Smith. Factors determining the potency of mydriatic drugs in man. *British Journal of Clinical Pharmacology*, 3(3):503–507, June 1976.

S. A. Smith, C. J. Ellis, and S. E. Smith. Inequality of the direct and consensual light reflexes in normal subjects. *The British Journal of Ophthalmology*, 63(7):523–527, July 1979. http://www.ncbi.nlm.nih.gov/pubmed/465430/.

V. C. Smith and J. Pokorny. Psychophysical estimates of optical density in human cones. *Vision Research*, 13(6):1199–1202, June 1973. http://dx.doi.org/10.1016/0042-6989(73)90156-9.

V. C. Smith and J. Pokorny. The design and use of a cone chromaticity space: A tutorial. *Color Research & Application*, 21 (5):375–383, 1996. http://dx.doi.org/10.1002/(SICI)1520-6378(199610)21:5<375::AID-COL6>3.0.CO;2-V.

E. Snitzer and H. Osterberg. Observed dielectric waveguide modes in the visible spec-

trum. *Journal of the Optical Society of America*, 51(5):499–505, May 1961. http://dx.doi.org/10.1364/JOSA.51.000499.

D. Snodderly, P. Brown, F. Delori, and J. Auran. The macular pigment. i. absorbance spectra, localization, and discrimination from other yellow pigments in primate retinas. *Invest. Ophthalmol. Vis. Sci.*, 25(6):660–673, June 1984. http://www.ncbi.nlm.nih.gov/pubmed/6724836.

A. W. Snyder. Photoreceptor optics : theoretical principles. In A. W. Snyder and R. Menzel, editors, *Photoreceptor optics*, pages 38–55. Springer, New York, 1975.

A. W. Snyder and S. B. Laughlin. Dichroism and absorption by photoreceptors. *Journal of Comparative Physiology A*, 100:101–116, 1975. http://dx.doi.org/10.1007/BF00613963.

A. W. Snyder, S. B. Laughlin, and D. G. Stavenga. Information capacity of eyes. *Vision Research*, 17(10):1163–1175, 1977. http://dx.doi.org/10.1016/0042-6989(77)90151-1.

S. H. Snyder and J. Axelrod. Circadian rhythm in pineal serotonin: Effect of monoamine oxidase inhibition and reserpine. *Science*, 149(3683):542 –543, July 1965. http://dx.doi.org/10.1126/science.149.3683.542.

F. So, J. Kido, and P. Burrows. Organic Light-Emitting devices for Solid-State lighting. *MRS Bulletin*, 33(07):663–669, 2008. http://dx.doi.org/10.1557/mrs2008.137.

P. G. Söderberg, R. Al-Saqry, K. Schulmeister, K. Gallichanin, M. Kronschläger, and Z. Yu. Photochemical effects in the lens from near infrared radiation? *Proceedings of SPIE*, 7163(1):716311, Feb. 2009. http://spiedigitallibrary.org/proceedings/resource/2/psisdg/7163/1/716311_1.

E. Solessio and G. A. Engbretson. Antagonistic chromatic mechanisms in photoreceptors of the parietal eye of lizards. *Nature*, 364(6436):442–445, July 1993. http://dx.doi.org/10.1038/364442a0.

E. Solessio and G. A. Engbretson. Electroretinogram of the parietal eye of lizards: Photoreceptor, glial, and lens cell contributions. *Visual Neuroscience*, 16(05):895–907, 1999. http://www.ncbi.nlm.nih.gov/pubmed/10580725.

S. G. Solomon and P. Lennie. The machinery of colour vision. *Nature Reviews. Neuroscience*, 8(4):276–86, Apr. 2007. http://dx.doi.org/10.1038/nrn2094.

D. E. Somers, P. F. Devlin, and S. A. Kay. Phytochromes and cryptochromes in the entrainment of the arabidopsis circadian clock. *Science*, 282(5393):1488 –1490, Nov. 1998. http://dx.doi.org/10.1126/science.282.5393.1488.

H. Song, T. Y. P. Chui, Z. Zhong, A. E. Elsner, and S. A. Burns. Variation of cone photoreceptor packing density with retinal eccentricity and age. *Investigative Ophthalmology & Visual Science*, 52(10):7376 –7384, 2011. http://dx.doi.org/10.1167/iovs.11-7199.

B. G. Soni and R. G. Foster. A novel and ancient vertebrate opsin. *FEBS Letters*, 406(3):279–283, Apr. 1997. http://dx.doi.org/10.1016/S0014-5793(97)00287-1.

J. M. Sparrow, A. J. Bron, N. A. P. Brown, W. Ayliffe, and A. R. Hill. The oxford clinical cataract classification and grading system. *International Ophthalmology*, 9(4):207–225, Dec. 1986. http://dx.doi.org/10.1007/BF00137534.

H. G. Sperling and R. S. Harwerth. Red-Green cone interactions in the Increment-Threshold spectral sensitivity of primates. *Science*, 172(3979):180 –184, Apr. 1971. http://dx.doi.org/10.1126/science.172.3979.180.

K. H. Spring and W. S. Stiles. Variation of pupil size with change in the angle at which the light stimulus strikes the retina. *The British Journal of Ophthalmology*, 32(6):340–346, June 1948. http://dx.doi.org/10.1136/bjo.32.6.340.

M. V. Srinivasan and S. Zhang. Visual motor computations in insects. *Annual Review of Neuroscience*, 27(1):679–696, 2004. http://dx.doi.org/10.1146/annurev.neuro.27.070203.144343.

V. Srinivasan, D. W. Spence, S. R. Pandi-Perumal, I. Trakht, and D. P. Cardinali. Therapeutic actions of melatonin in cancer: Possible mechanisms. *Integr Cancer Ther*, 7(3):189–203, Sept. 2008. http://dx.doi.org/10.1177/1534735408322846.

V. J. Srinivasan, M. Wojtkowski, J. G. Fujimoto, and J. S. Duker. In vivo measurement of retinal physiology with high-speed ultrahigh-resolution optical coherence tomography. *Optics Letters*, 31(15):2308–2310, 2006. http://dx.doi.org/10.1364/OL.31.002308.

U. Stabell and B. Stabell. Spectral sensitivity of the dark-adapted extrafoveal retina at photopic intensities. *Journal of the Optical Society of America*, 71(7):841–844, July 1981. http://dx.doi.org/10.1364/JOSA.71.000841.

P. A. Stanley and A. K. Davies. The effect of field of view size on steady-state pupil diameter. *Ophthalmic and Physiological Optics*, 15(6):601–603, Nov. 1995. http://dx.doi.org/10.1046/j.1475-1313.1995.9400019v.x.

S. F. Stanten and L. Stark. A statistical analysis of pupil noise. *Biomedical Engineering, IEEE Transactions on*, BME-13(3):140–152, 1966. http://dx.doi.org/10.1109/TBME.1966.4502424.

L. Stark. Stability, oscillations, and noise in the human pupil servomechanism. *Proceedings of the IRE*, 47(11):1925–1939, 1959. http://dx.doi.org/10.1109/JRPROC.1959.287206.

L. Stark. Biological rhythms, noise, and asymmetry in the pupil-retinal control system. *Annals of the New York Academy of Sciences*, 98(4):1096–1108, 1962. http://dx.doi.org/10.1111/j.1749-6632.1962.tb30621.x.

L. Stark and T. N. Cornsweet. Testing a servoanalytic hypothesis for pupil oscillations. *Science (New York, N.Y.)*, 127(3298): 588, Mar. 1958. http://dx.doi.org/10.1126/science.127.3298.588.

L. Stark and P. M. Sherman. A servoanalytic study of consensual pupil reflex to light. *Journal of Neurophysiology*, 20(1):17 –26, Jan. 1957.

L. Stark, F. W. Campbell, and J. Atwood. Pupil unrest: An example of noise in a biological servomechanism. *Nature*, 182(4639):857–858, 1958. http://dx.doi.org/10.1038/182857a0.

L. W. Stark. The pupil as a paradigm for neurological control systems. *Biomedical Engineering, IEEE Transactions on*, BME-31 (12):919–924, 1984. http://dx.doi.org/10.1109/TBME.1984.325259.

W. S. Stark. Spectral selectivity of visual response alterations mediated by interconversions of native and intermediate photopigments in drosophila. *Journal of Comparative Physiology ? A*, 96:343–356, 1975. http://dx.doi.org/10.1007/BF00619224.

W. S. Stark and M. A. Johnson. Microspectrophotometry of drosophila visual pigments: Determinations of conversion efficiency in r1-6 receptors. *Journal of Comparative Physiology ? A*, 140:275–286, 1980. http://dx.doi.org/10.1007/BF00606268.

W. S. Stark and C. F. Thomas. Microscopy of multiple visual receptor types in drosophila. *Molecular Vision*, 10:943–955, Dec. 2004. http://www.ncbi.nlm.nih.gov/pubmed/15616481.

W. S. Stark and W. G. Zitzmann. Isolation of adaptation mechanisms and photopigment spectra by vitamin a deprivation in drosophila. *Journal of Comparative Physiology ? A*, 105:15–27, Feb. 1976. http://dx.doi.org/10.1007/BF01380050.

W. S. Stark, G. S. Pransky, and W. G. Zitzmann. Separation of photopigment from membrane adaptation by vitamin a deprivation in the drosophila retina. *Society of Neuroscience (Abstract)*, 5:112, 1975.

W. S. Stark, A. M. Ivanyshyn, and R. M. Greenberg. Sensitivity and photopigments of r1-6, a two-peaked photoreceptor, in drosophila, calliphora and musca. *Journal of Comparative Physiology ? A*, 121(3):289–305, 1977. http://dx.doi.org/10.1007/BF00613010.

D. Stavenga and H. van Barneveld. On dispersion in visual photoreceptors. *Vision Research*, 15(10):1091–1095, Oct. 1975. http://dx.doi.org/10.1016/0042-6989(75)90006-1.

D. Stavenga, R. Smits, and B. Hoenders. Simple exponential functions describing the absorbance bands of visual pigment spectra. *Vision Research*, 33(8):1011–1017, May 1993. http://dx.doi.org/10.1016/0042-6989(93)90237-Q.

D. Stavenga, J. Oberwinkler, M. Postma, W. D. D.G. Stavenga, and E. Pugh. Modeling primary visual processes in insect photoreceptors. In *Molecular Mechanisms in Visual Transduction*, volume Volume 3, pages 527–574. North-Holland, 2000. http://dx.doi.org/10.1016/S1383-8121(00)80013-5.

D. G. Stavenga. Derivation of photochrome absorption spectra from absorbance difference measurements. *Photochemistry and Photobiology*, 21(2):105–110, 1975. http://dx.doi.org/10.1111/j.1751-1097.1975.tb06636.x.

D. G. Stavenga. Fly visual pigments difference in visual pigments of blowfly and dronefly peripheral retinula cells. *Journal of Comparative Physiology A: Neuroethology, Sensory, Neural, and Behavioral Physiology*, 111(2):137–152, Jan. 1976. http://dx.doi.org/10.1007/BF00605529.

D. G. Stavenga. Visual pigment processes and prolonged pupillary responses in insect photoreceptor cells. *European Biophysics Journal*, 5(2):175–185, June 1979. http://dx.doi.org/10.1007/BF00535446.

D. G. Stavenga. Short wavelength light in invertebrate visual sense cells. pigments, potentials and problems. In H. Senger, editor, *The blue light syndrome*, pages 5–24. Springer, Berlin, Heidelberg, New York, 1980.

D. G. Stavenga. Fluorescence of blowfly metarhodopsin. *Biophysics of Structure and Mechanism*, 9:309–317, 1983. http://dx.doi.org/10.1007/BF00535666.

D. G. Stavenga. Eye regionalization and spectral tuning of retinal pigments in insects. *Trends in Neurosciences*, 15(6):213–218, June 1992. http://dx.doi.org/10.1016/0166-2236(92)90038-A.

D. G. Stavenga. Colour in the eyes of insects. *Journal of Comparative Physiology A: Sensory, Neural, and Behavioral Physiology*, 188:337–348, June 2002. http://dx.doi.org/10.1007/s00359-002-0307-9.

D. G. Stavenga. Angular and spectral sensitivity of fly photoreceptors. II. dependence on facet lens f-number and rhabdomere type in drosophila. *Journal of Comparative Physiology A: Neuroethology, Sensory, Neu-*

ral, and Behavioral Physiology, 189(3):189–202, Mar. 2003. http://dx.doi.org/10.1007/s00359-003-0390-6.

D. G. Stavenga. On visual pigment templates and the spectral shape of invertebrate rhodopsins and metarhodopsins. *Journal of Comparative Physiology. A, Neuroethology, Sensory, Neural, and Behavioral Physiology*, 196(11):869–878, Nov. 2010. http://dx.doi.org/10.1007/s00359-010-0568-7.

D. G. Stavenga and R. C. Hardie. Metarhodopsin control by arrestin, light-filtering screening pigments, and visual pigment turnover in invertebrate microvillar photoreceptors. *Journal of Comparative Physiology A*, 197(3):227–241, Nov. 2010. http://dx.doi.org/10.1007/s00359-010-0604-7.

D. G. Stavenga and J. W. Kuiper. Insect pupil mechanisms. i. on the pigment migration in the retinula cells of hymenoptera (suborder apocrita). *Journal of Comparative Physiology*, 113:55–72, 1977.

D. G. Stavenga and J. H. van Hateren. Focusing by a high-power, low-Fresnel-number lens: the fly facet lens. *Journal of the Optical Society of America A*, 8(1):14–19, Jan. 1991. http://dx.doi.org/10.1364/JOSAA.8.000014.

D. G. Stavenga, J. H. Flokstra, and J. W. Kuiper. Photopigment conversions expressed in pupil mechanism of blowfly visual sense cells. *Nature*, 253(5494):740–742, Feb. 1975. http://dx.doi.org/10.1038/253740a0.

D. G. Stavenga, N. Franceschini, and K. Kirschfeld. Fluorescence of housefly visual pigment. *Photochemistry and Photobiology*, 40(5):653–659, Nov. 1984. http://dx.doi.org/10.1111/j.1751-1097.1984.tb05355.x.

R. A. Steer, R. Ball, W. F. Ranieri, and A. T. Beck. Further evidence for the construct validity of the beck depression Inventory-II with psychiatric outpatients. *Psychological Reports*, 1997. http://www.ncbi.nlm.nih.gov/pubmed/9129364.

D. Steidtmann, R. E. Ingram, and G. J. Siegle. Pupil response to negative emotional information in individuals at risk for depression. *Cognition & Emotion*, 24(3):480, 2010. http://dx.doi.org/10.1080/02699930902738897.

S. R. Steinhauer, G. J. Siegle, R. Condray, and M. Pless. Sympathetic and parasympathetic innervation of pupillary dilation during sustained processing. *International Journal of Psychophysiology*, 52(1):77–86, Mar. 2004. http://dx.doi.org/10.1016/j.ijpsycho.2003.12.005.

F. K. Stephan and I. Zucker. Circadian rhythms in drinking behavior and locomotor activity of rats are eliminated by hypothalamic lesions. *Proceedings of the National Academy of Sciences of the United States of America*, 69(6):1583–1586, June 1972. http://www.ncbi.nlm.nih.gov/pubmed/4556464.

K. M. Stephenson, C. M. Schroder, G. Bertschy, and P. Bourgin. Complex interaction of circadian and non-circadian effects of light on mood: Shedding new light on an old story. *Sleep Medicine Reviews*, Epub, Jan. 2012. http://dx.doi.org/10.1016/j.smrv.2011.09.002.

R. S. Stephenson and W. L. Pak. Heterogenic components of a fast electrical potential in drosophila compound eye and their relation to visual pigment photoconversion. *The Journal of General Physiology*, 75(4):353–379, Apr. 1980. http://www.ncbi.nlm.nih.gov/pubmed/7381424.

R. G. Stevens, D. E. Blask, G. C. Brainard, J. Hansen, S. W. Lockley, I. Provencio, M. S. Rea, and L. Reinlib. Meeting report: The role of environmental lighting and circadian disruption in cancer and other diseases. *Environmental Health Perspectives*, Aug. 2007. http://dx.doi.org/10.1289/ehp.10200.

B. E. Stewart and R. S. L. Young. Pupillary response: an index of visual threshold. *Applied Optics*, 28(6):1122–1127, Mar. 1989. http://dx.doi.org/10.1364/AO.28.001122.

W. S. Stiles. Increment thresholds & the mechanisms of colour vision. *Documenta Ophthalmologica*, 3:138–165, 1949a. http://dx.doi.org/10.1007/BF00162601.

W. S. Stiles. Investigations of the scotopic and trichromatic mechanisms of vision by the two-colour threshold technique. *Archives D'ophtalmologie Et Revue Générale D'ophtalmologie*, 28(4):215–237, Apr. 1949b. http://www.ncbi.nlm.nih.gov/pubmed/18130116.

W. S. Stiles and B. H. Crawford. Equivalent adaptational levels in localized retinal areas. In *Report of Joint Discussion on Vision, Physical Society of London*. Cambridge University Press, Cambridge, UK, 1932.

W. S. Stiles and B. H. Crawford. The luminous efficiency of rays entering the eye pupil at different points. *Proceedings of the Royal Society of London. Series B, Containing Papers of a Biological Character (1905-1934)*, 112(778):428–450, Mar. 1933. http://dx.doi.org/10.1098/rspb.1933.0020.

A. Stockman and L. Sharpe. CVRL color & vision database. http://cvision.ucsd.edu/, Sept. 2007. http://cvision.ucsd.edu/.

A. Stockman and L. T. Sharpe. Into the twilight zone: the complexities of mesopic vision and luminous efficiency. *Ophthalmic and Physiological Optics*, 26(3):225–239, 2006. http://dx.doi.org/10.1111/j.1475-1313.2006.00325.x.

A. Stockman, D. I. MacLeod, and D. D. DePriest. The temporal properties of the human short-wave photoreceptors and their associated pathways. *Vision Research*, 31 (2):189–208, 1991. http://dx.doi.org/10.1016/0042-6989(91)90111-H.

A. Stockman, L. T. Sharpe, and C. Fach. The spectral sensitivity of the human short-wavelength sensitive cones derived from thresholds and color matches. *Vision Research*, 39(17):2901–2927, Aug. 1999. http://dx.doi.org/10.1016/S0042-6989(98)00225-9.

A. Stockman, D. J. Plummer, and E. D. Montag. Spectrally opponent inputs to the human luminance pathway: slow +M and -L cone inputs revealed by intense long-wavelength adaptation. *The Journal of Physiology*, 566(Pt 1):61–76, July 2005. http://dx.doi.org/10.1113/jphysiol.2005.084046.

A. Stockman, L. Sharpe, R. H. Masland, P. Dallos, D. Oertel, S. Firestein, G. K. Beauchamp, M. C. Bushnell, J. H. Kaas, E. Gardner, A. I. Basbaum, A. Kaneko, G. M. Shepherd, G. Westheimer, and T. D. Albright. Spectral sensitivity. In *The Senses: A Comprehensive Reference*, pages 87–100. Academic Press, New York, 2008. http://dx.doi.org/10.1016/B978-012370880-9.00300-5.

E. C. Stokes, N. Gayeski, and M. Andersen. Estimating spectral information of complex fenestration systems in a video-goniophotometer. *Lighting Research and Technology*, 40(4):269–285, Dec. 2008. http://dx.doi.org/10.1177/1477153508092003.

N. J. Stone. Environmental view and color for a simulated telemarketing task. *Journal of Environmental Psychology*, 23(1):63–78, Mar. 2003. http://dx.doi.org/10.1016/S0272-4944(02)00107-X.

S. Stowe. Rapid synthesis of photoreceptor membrane and assembly of new microvilli in a crab at dusk. *Cell and Tissue Research*, 211, Oct. 1980. http://dx.doi.org/10.1007/BF00234397.

W. P. Stratten and T. E. Ogden. Spectral sensitivity of the barnacle, balanus amphitrite. *The Journal of General Physiology*, 57(4):435–447, Apr. 1971. http://www.ncbi.nlm.nih.gov/pubmed/4323488.

R. H. Straub, U. Thies, A. Jeron, K. D. Palitzsch, and J. Schölmerich. Valid parameters for investigation of the pupillary light reflex in normal and diabetic subjects shown by factor analysis and partial correlation. *Diabetologia*, 37(4):414–419, Apr. 1994. http://dx.doi.org/10.1007/BF00408480.

S. H. Strogatz, R. E. Kronauer, and C. A. Czeisler. Circadian pacemaker interferes with sleep onset at specific times each day: role in insomnia. *The American Journal of Physiology*, 253(1 Pt 2):R172–178, July 1987. http://www.ncbi.nlm.nih.gov/pubmed/3605382.

J. Strong and J. Lisman. Initiation of light adaptation in barnacle photoreceptors. *Science*, 200(4349):1485 –1487, June 1978. http://dx.doi.org/10.1126/science.663629.

J. F. Sturr, L. Zhang, H. A. Taub, D. J. Hannon, and M. M. Jackowski. Psychophysical evidence for losses in rod sensitivity in the aging visual system. *Vision Research*, 37(4): 475–481, Feb. 1997. http://dx.doi.org/10.1016/S0042-6989(96)00196-4.

C. Su, D. Luo, A. Terakita, Y. Shichida, H. Liao, M. A. Kazmi, T. P. Sakmar, and K. Yau. Parietal-Eye phototransduction components and their potential evolutionary implications. *Science*, 311(5767):1617 –1621, Mar. 2006. http://dx.doi.org/10.1126/science.1123802.

J. Su and C. Lu. Color temperature tunable white light emitting diodes packaged with an omni-directional reflector. *Optics Express*, 17(24):21408–21413, Nov. 2009. http://dx.doi.org/10.1364/OE.17.021408.

S. Su, J. D. McArthur, R. J. Truscott, and J. A. Aquilina. Truncation, cross-linking and interaction of crystallins and intermediate filament proteins in the aging human lens. *Biochimica et Biophysica Acta (BBA) - Proteins & Proteomics*, 1814(5):647–656, May 2011. http://dx.doi.org/10.1016/j.bbapap.2011.03.014.

F. Sun and L. Stark. Pupillary escape intensified by large pupillary size. *Vision Research*, 23(6):611–615, 1983. http://dx.doi.org/10.1016/0042-6989(83)90066-4.

F. Sun, X. Zhau, S. Dai, H. Liu, and R. Yan. Dynamic characteristics of the pupillary control system: measurement and mathematical model. *Acta Automatica Sinica*, 5:130–135, 1979.

F. Sun, W. C. Krenz, and L. W. Stark. A systems model for the pupil size effect: I transient data. *Biological Cybernetics*, 48(2):101–108, 1983. http://dx.doi.org/10.1007/BF00344393.

F. C. Sun, H. K. Liu, and Y. M. Liu. Dynamic pupillary response to positive differential of light stimulus. *Scientia Sinica*, 24(6):872–884, June 1981. http://www.ncbi.nlm.nih.gov/pubmed/7256255.

Y. Sun, C. Wang, and J. Dai. Biophotons as neural communication signals demonstrated by in situ biophoton autography. *Photochemical & Photobiological Sciences*, 9(3): 315, 2010. http://dx.doi.org/10.1039/B9PP00125E.

C. H. Sung, C. M. Davenport, J. C. Hennessey, I. H. Maumenee, S. G. Jacobson, J. R. Heckenlively, R. Nowakowski, G. Fishman, P. Gouras, and J. Nathans. Rhodopsin mutations in autosomal dominant retini-

tis pigmentosa. *Proceedings of the National Academy of Sciences of the United States of America*, 88(15):6481–6485, Aug. 1991. http://www.ncbi.nlm.nih.gov/pubmed/1862076.

J. Surakka, J. Ruutiainen, A. Romberg, P. Puukka, E. Kronholm, and H. Karanko. Pupillary function in early multiple sclerosis. *Clinical Autonomic Research*, 18(3):150–154, May 2008. http://dx.doi.org/10.1007/s10286-008-0471-2.

R. Suryakumar, D. Kwok, S. Fernandez, and W. R. Bobier. Dynamic photorefraction system: An offline application for the dynamic analysis of ocular focus and pupil size from photorefraction images. *Computers in Biology and Medicine*, 39(3):195–205, Mar. 2009. http://dx.doi.org/10.1016/j.compbiomed.2008.12.006.

T. Suzuki, K. Uji, and Y. Kito. Studies on cephalopod rhodopsin: Photoisomerization of the chromophore. *Biochimica et Biophysica Acta (BBA) - General Subjects*, 428(2):321–338, Apr. 1976. http://dx.doi.org/10.1016/0304-4165(76)90040-4.

W. H. Swanson and G. E. Fish. Age-related changes in the Color-match–Area effect. *Vision Research*, 36(14):2079–2085, July 1996. http://dx.doi.org/10.1016/0042-6989(95)00280-4.

A. M. Sweeney, C. A. Boch, S. Johnsen, and D. E. Morse. Twilight spectral dynamics and the coral reef invertebrate spawning response. *Journal of Experimental Biology*, 214 (5):770 –777, Mar. 2011. http://dx.doi.org/10.1242/jeb.043406.

Z. Szabo, Z. Tokaji, J. Kalman, L. Oroszi, A. Pestenacz, and Z. Janka. The effect of bright light exposure on pupillary fluctuations in healthy subjects. *Journal of Affective Disorders*, 78(2):153–156, Feb. 2004. http://dx.doi.org/10.1016/S0165-0327(02)00241-0.

W. Szczepanowska-Nowak, A. Hachol, and H. Kasprzak. System for measurement of the consensual pupil light reflex. *Optica Applicata*, XXXIV(4), 2004.

I. Szundi, J. Epps, J. W. Lewis, and D. S. Kliger. Temperature dependence of the lumirhodopsin i-lumirhodopsin II equilibrium. *Biochemistry*, 49(28):5852–5858, July 2010. http://dx.doi.org/10.1021/bi100566r.

J. Tabernero, A. Benito, V. Nourrit, and P. Artal. Instrument for measuring the misalignments of ocular surfaces. *Optics Express*, 14(22):10945–10956, Oct. 2006. http://dx.doi.org/10.1364/OE.14.010945.

T. Takahashi, R. Y. Cho, T. Murata, T. Mizuno, M. Kikuchi, K. Mizukami, H. Kosaka, K. Takahashi, and Y. Wada. Age-related variation in EEG complexity to photic stimulation: A multiscale entropy analysis. *Clinical Neurophysiology*, 120(3):476–483, Mar. 2009. http://dx.doi.org/10.1016/j.clinph.2008.12.043.

Y. Takahashi, T. Katsuura, Y. Shimomura, and K. Iwanaga. Prediction model of light-induced melatonin suppression. *Journal of Light & Visual Environment*, 35(2):123–135, 2011. http://dx.doi.org/10.2150/jlve.35.123.

J. Takalo, I. Ignatova, M. Weckström, and M. Vähäsöyrinki. A novel estimator for the rate of information transfer by continuous signals. *PLoS ONE*, 6(4):e18792, Apr. 2011. http://dx.doi.org/10.1371/journal.pone.0018792.

A. Talukder, J. Morookian, S. Monacos, R. Lam, C. LeBaw, and J. L. Lambert. Eye-tracking architecture for biometrics and remote monitoring. *Applied Optics*, 44(5):693–700, Feb. 2005. http://dx.doi.org/10.1364/AO.44.000693.

H. Tamura and T. Iwata. Field investigation on the exposed illuminance and the activity in daily life. *Proceeding of Annual Conference of The Illuminating Engineering Institute of Japan*, 34:204–205, 2001.

K. Tan. *Vision in the ultraviolet*. PhD thesis, Utrecht, 1971.

X. Tao and S. Y. Hui. Dynamic photo-electrothermal theory for Light-Emitting diode systems. *IEEE Transactions on Industrial Electronics*, 59(4):1751–1759, Apr. 2012. http://dx.doi.org/10.1109/TIE.2011.2109341.

E. E. Tarttelin, J. Bellingham, M. W. Hankins, R. G. Foster, and R. J. Lucas. Neuropsin (Opn5): a novel opsin identified in mammalian neural tissue. *FEBS Letters*, 554(3):410–416, Nov. 2003. http://dx.doi.org/10.1016/S0014-5793(03)01212-2.

P. Tassi and A. Muzet. Sleep inertia. *Sleep Medicine Reviews*, 4(4):341–353, Aug. 2000. http://dx.doi.org/10.1053/smrv.2000.0098.

P. Tassi, N. Pellerin, M. Moessinger, R. Eschenlauer, and A. Muzet. Variation of visual detection over the 24-hour period in humans. *Chronobiology International*, 17(6):795–805, Nov. 2000a. http://dx.doi.org/10.1081/CBI-100102115.

P. Tassi, N. Pellerin, M. Moessinger, A. Hoeft, and A. Muzet. Visual resolution in humans fluctuates over the 24h period. *Chronobiology International*, 17(2):187–95, Mar. 2000b. http://dx.doi.org/10.1081/CBI-100101042.

H. R. Taylor, S. K. West, F. S. Rosenthal, B. Muñoz, H. S. Newland, H. Abbey, and E. A. Emmett. Effect of ultraviolet radiation on cataract formation. *The New England Journal of Medicine*, 319(22):1429–1433, Dec. 1988. http://dx.doi.org/10.1056/NEJM198812013192201.

C. TC6-62. Action spectra and dosimetric quantities for circadian and related neurobiological effects. chair: Howard m. cooper. http://www.cie.co.at/div6/tcs.htm.

P. Teikari. *Biological effects of light*. M.Sc. thesis, Helsinki University of Technology, Espoo, Finland, 2006a.

P. Teikari. Circadian field photometry. Course project work on measurement science and technology, Dec. 2006b.

P. Teikari. Automated pupillometry. Course project work on measurement science and technology, 2007a.

P. Teikari. Light pollution: Definition, legislation, measurement, modeling and environmental effects. Special assignment on illumination engineering, Barcelona, Spain, 2007b.

P. Teikari and E. Rautkylä. Optical performance: Characterization of a pupillometric camera. Postgradute seminar work on illumination engineering, 2008.

J. ten Doesschate and M. Alpern. Effect of photoexcitation of the two retinas on pupil size. *Journal of Neurophysiology*, 30(3):562 –576, May 1967. http://www.ncbi.nlm.nih.gov/pubmed/6037594.

A. Terakita, H. Tsukamoto, M. Koyanagi, M. Sugahara, T. Yamashita, and Y. Shichida. Expression and comparative characterization of gq-coupled invertebrate visual pigments and melanopsin. *Journal of Neurochemistry*, 105(3):883–90, May 2008. http://dx.doi.org/10.1111/j.1471-4159.2007.05184.x.

A. Terakita, E. Kawano-Yamashita, and M. Koyanagi. Evolution and diversity of opsins. *Wiley Interdisciplinary Reviews: Membrane Transport and Signaling*, 1(1):104–111, Jan. 2012. http://dx.doi.org/10.1002/wmts.6.

K. Thapan, J. Arendt, and D. J. Skene. An action spectrum for melatonin suppression: evidence for a novel non-rod, non-cone photoreceptor system in humans. *The Journal of Physiology*, 535(1):261–267, 2001. http://dx.doi.org/10.1111/j.1469-7793.2001.t01-1-00261.x.

M. M. Thomas and T. D. Lamb. Light adaptation and dark adaptation of human rod photoreceptors measured from the a-wave of the electroretinogram. *The Journal of Physiology*, 518(2):479–496, 1999. http://dx.doi.org/10.1111/j.1469-7793.1999.0479p.x.

Y. G. Thomas, I. Szundi, J. W. Lewis, and D. S. Kliger. Microsecond time-resolved circular dichroism of rhodopsin photointermediates. *Biochemistry*, 48(51):12283–12289, Dec. 2009. http://dx.doi.org/10.1021/bi901657b.

C. L. Thompson, W. S. Blaner, R. N. Van Gelder, K. Lai, L. Quadro, V. Colantuoni, M. E. Gottesman, and A. Sancar. Preservation of light signaling to the suprachiasmatic nucleus in vitamin a-deficient mice. *Proceedings of the National Academy of Sciences*, 98(20):11708 –11713, 2001. http://dx.doi.org/10.1073/pnas.201301498.

H. Thompson. Pupil. In W. Hart, editor, *Adler's Physiology of the Eye: Clinical Application*. Mosby Year Book, St. Louis, 9 edition, 1992.

H. S. Thompson and R. H. Kardon. The argyll robertson pupil. *Journal of Neuro-Ophthalmology: The Official Journal of the North American Neuro-Ophthalmology Society*, 26(2):134–8, June 2006. http://www.ncbi.nlm.nih.gov/pubmed/16845316.

S. Thompson, R. G. Foster, E. M. Stone, V. C. Sheffield, and N. Mrosovsky. Classical and melanopsin photoreception in irradiance detection: Negative masking of locomotor activity by light. *European Journal of Neuroscience*, 27(8):1973–1979, Apr. 2008. http://dx.doi.org/10.1111/j.1460-9568.2008.06168.x.

S. Thompson, S. F. Stasheff, J. Hernandez, E. Nylen, J. S. East, R. H. Kardon, L. H. Pinto, R. F. Mullins, and E. M. Stone. Different inner retinal pathways mediate Rod-Cone input in irradiance detection for the pupillary light reflex and regulation of behavioral state in mice. *Investigative Ophthalmology & Visual Science*, 52(1):618 –623, Jan. 2011. http://dx.doi.org/10.1167/iovs.10-6146.

L. C. Thomson. Binocular summation within the nervous path ways of the pupillary light reflex. *The Journal of Physiology*, 106(1):59–65, Mar. 1947. http://www.ncbi.nlm.nih.gov/pubmed/20241958.

T. E. Thorgeirsson, J. W. Lewis, S. E. Wallace-Williams, and D. S. Kliger. Effects of temperature on rhodopsin photointermediates from lumirhodopsin to metarhodopsin II. *Biochemistry*, 32(50):13861–13872, 1993. http://dx.doi.org/10.1021/bi00213a015.

L. Thorington. Temperature dependence of the emission of an improved Manganese-Activated magnesium germanate phosphor. *Journal of the Optical Society of America*, 40(9):579–583, 1950. http://dx.doi.org/10.1364/JOSA.40.000579.

H. C. Thorne, K. H. Jones, S. P. Peters, S. N. Archer, and D. Dijk. Daily and seasonal variation in the spectral composition of light exposure in humans. *Chronobiology International: The Journal of Biological and Medical Rhythm Research*, 26(5):854, 2009. http://dx.doi.org/10.1080/07420520903044315.

J. Thornton and E. Pugh. Red/Green color opponency at detection threshold. *Science*, 219(4581):191 –193, Jan. 1983. http://dx.

doi.org/10.1126/science.6849131.

S. Thyagarajan, M. van Wyk, K. Lehmann, S. Löwel, G. Feng, and H. Wässle. Visual function in mice with photoreceptor degeneration and transgenic expression of channelrhodopsin 2 in ganglion cells. *The Journal of Neuroscience: The Official Journal of the Society for Neuroscience*, 30(26):8745–8758, June 2010. http://dx.doi.org/10.1523/JNEUROSCI.4417-09.2010.

B. Thylefors, J. Chylack, L T, K. Konyama, K. Sasaki, R. Sperduto, H. R. Taylor, and S. West. A simplified cataract grading system. *Ophthalmic Epidemiology*, 9(2):83–95, Apr. 2002. http://www.ncbi.nlm.nih.gov/pubmed/11821974.

N. Tiedt. Die 24 Stunden-Rhythmik der kinetik des lichtreflexes der menschlichen pupille. *Pflügers Archiv für die Gesamte Physiologie des Menschen und der Tiere*, 277 (4):458–472, 1963. http://dx.doi.org/10.1007/BF00363260.

C. Tilmant, L. Sarry, G. Gindre, and J. Boire. Monitoring and modeling of pupillary dynamics. volume 1, pages 678–681, 2003. http://dx.doi.org/10.1109/IEMBS.2003.1279854.

M. Timonen, J. Nissilä, H. Jurvelin, A. Liettu, J. Jokelainen, A. Aunio, P. Räsänen, and T. Takala. Transcranial brain targeted light treatment via ear canals in seasonal affective disorder (SAD) – a pilot study, 2011.

T. To and N. Maheshri. Noise can induce bimodality in positive transcriptional feedback loops without bistability. *Science*, 327 (5969):1142 –1145, Feb. 2010. http://dx.doi.org/10.1126/science.1178962.

Y. Toh and T. H. Waterman. Diurnal changes in compound eye fine structure in the blue crab callinectes. *Journal of Ultrastructure Research*, 78(1):40–59, Jan. 1982. http://dx.doi.org/10.1016/S0022-5320(82)80012-9.

H. Tomita, E. Sugano, H. Isago, T. Hiroi, Z. Wang, E. Ohta, and M. Tamai. Channelrhodopsin-2 gene transduced into retinal ganglion cells restores functional vision in genetically blind rats. *Experimental Eye Research*, 90(3):429–436, Mar. 2010. http://dx.doi.org/10.1016/j.exer.2009.12.006.

G. Toraldo di Francia. Retina cones as dielectric antennas. *Journal of the Optical Society of America*, 39(4):324, Apr. 1949. http://dx.doi.org/10.1364/JOSA.39.000324.

M. Torii, D. Kojima, T. Okano, A. Nakamura, A. Terakita, Y. Shichida, A. Wada, and Y. Fukada. Two isoforms of chicken melanopsins show blue light sensitivity. *FEBS Letters*, 581(27):5327–5331, Nov. 2007. http://dx.doi.org/10.1016/j.febslet.2007.10.019.

G. J. Tortora and B. H. Derrickson. *Principles of Anatomy and Physiology*. Wiley, 12 edition, Apr. 2008.

G. Tosini and C. Fukuhara. The mammalian retina as a clock. *Cell and Tissue Research*, 309:119–126, July 2002. http://dx.doi.org/10.1007/s00441-002-0578-z.

G. Tosini, S. Doyle, M. Geusz, and M. Menaker. Induction of photosensitivity in neonatal rat pineal gland. *Proceedings of the National Academy of Sciences*, 97(21):11540 – 11544, Oct. 2000. http://dx.doi.org/10.1073/pnas.210248297.

G. H. Travis, J. Kaylor, and Q. Yuan. Analysis of the retinoid isomerase activities in the retinal pigment epithelium and retina. In H. Sun and G. H. Travis, editors, *Retinoids*, volume 652, pages 329–339. Humana Press, Totowa, NJ, 2010. http://dx.doi.org/10.1007/978-1-60327-325-1_19.

L. J. Trejo and C. M. Cicerone. Retinal sensitivity measured by the pupillary light reflex in RCS and albino rats. *Vision Research*, 22 (9):1163–1171, 1982. http://dx.doi.org/10.1016/0042-6989(82)90081-5.

P. D. Trevor-Roper. *The Eye and Its Disorders*, volume 3. Blackwell Science Ltd, Jan. 1984.

H. W. Trissl. On the rise time of the r1-component of the "Early receptor potential...: Evidence for a fast light-induced charge separation in rhodopsin. *Biophysics of Structure and Mechanism*, 8(3):213–230, 1982. http://dx.doi.org/10.1007/BF00535460.

A. Troelstra. Detection of Time-Varying light signals as measured by the pupillary response. *Journal of the Optical Society of America*, 58(5):685–690, May 1968. http://dx.doi.org/10.1364/JOSA.58.000685.

D. Troxler. Über das verschwinden gegebener gegenstände unnerhalb unseres gesichtskreises. In J. Himly and J. Schmidt, editors, *Ophtalmologische Bibliothek*. Fromann, Jena, 1804.

W. W. Tryon. Pupillometry: A survey of sources of variation. *Psychophysiology*, 12 (1):90–93, Jan. 1975. http://dx.doi.org/10.1111/j.1469-8986.1975.tb03068.x.

J. W. Tsai, J. Hannibal, G. Hagiwara, D. Colas, E. Ruppert, N. F. Ruby, H. C. Heller, P. Franken, and P. Bourgin. Melanopsin as a sleep modulator: Circadian gating of the direct effects of light on sleep and altered sleep homeostasis in opn4-/- mice. *PLoS Biol*, 7(6):e1000125, June 2009. http://dx.doi.org/10.1371/journal.pbio.1000125.

J. Tsao, M. Coltrin, M. Crawford, and J. Simmons. Solid-State lighting: An integrated human factors, technology, and economic perspective. *Proceedings of the IEEE*, 98(7): 1162–1179, 2010. http://dx.doi.org/10.1109/JPROC.2009.2031669.

S. Tsujimura, J. S. Wolffsohn, and B. Gilmartin. A linear chromatic mechanism drives the pupillary response. *Proceedings. Biological Sciences / The Royal Society*, 268(1482):2203–2209, Nov. 2001. http://dx.doi.org/10.1098/rspb.2001.1775.

S.-i. Tsujimura and Y. Tokuda. Delayed response of human melanopsin retinal ganglion cells on the pupillary light reflex. *Ophthalmic and Physiological Optics*, in press, 2011. http://dx.doi.org/10.1111/j.1475-1313.2011.00846.x.

S.-i. Tsujimura, J. S. Wolffsohn, and B. Gilmartin. Pupil response to color signals in Cone-Contrast space. *Current Eye Research*, 31:401–408, Jan. 2006. http://dx.doi.org/10.1080/02713680600681327.

S. i. Tsujimura, K. Ukai, D. Ohama, A. Nuruki, and K. Yunokuchi. Contribution of human melanopsin retinal ganglion cells to steady-state pupil responses. *Proceedings of the Royal Society B: Biological Sciences*, Apr. 2010. http://dx.doi.org/10.1098/rspb.2010.0330.

Y. Tsukahara and G. A. Horridge. Visual pigment spectra from sensitivity measurements after chromatic adaptation of single dronefly retinula cells. *Journal of Comparative Physiology ? A*, 114(3):233–251, 1977. http://dx.doi.org/10.1007/BF00657321.

H. Tsukamoto and A. Terakita. Diversity and functional properties of bistable pigments. *Photochemical & Photobiological Sciences: Official Journal of the European Photochemistry Association and the European Society for Photobiology*, 9(11):1435–1443, Nov. 2010. http://dx.doi.org/10.1039/c0pp00168f.

D. C. Tu, M. L. Batten, K. Palczewski, and R. N. Van Gelder. Nonvisual photoreception in the chick iris. *Science*, 306(5693):129–131, Oct. 2004. http://dx.doi.org/10.1126/science.1101484.

D. C. Tu, D. Zhang, J. Demas, E. B. Slutsky, I. Provencio, T. E. Holy, and R. N. V. Gelder. Physiologic diversity and development of intrinsically photosensitive retinal ganglion cells. *Neuron*, 48(6):987–999, Dec. 2005. http://dx.doi.org/10.1016/j.neuron.2005.09.031.

P. L. Turner, E. J. Van Someren, and M. A. Mainster. The role of environmental light in sleep and health: Effects of ocular aging and cataract surgery. *Sleep Medicine Reviews*, 14(4):269–280, Aug. 2010. http://dx.doi.org/10.1016/j.smrv.2009.11.002.

A. Tuunainen, D. F. Kripke, A. C. Cress, and S. D. Youngstedt. Retinal circadian rhythms in humans. *Chronobiology International*, 18(6):957–971, Nov. 2001. http://dx.doi.org/10.1081/CBI-100107971.

C. W. Tyler. Two processes control variations in flicker sensitivity over the life span. *Journal of the Optical Society of America A*, 6(4):481–490, Apr. 1989. http://dx.doi.org/10.1364/JOSAA.6.000481.

J. K. Udupa, V. R. LeBlanc, Y. Zhuge, C. Imielinska, H. Schmidt, L. M. Currie, B. E. Hirsch, and J. Woodburn. A framework for evaluating image segmentation algorithms. *Computerized Medical Imaging and Graphics*, 30(2):75–87, Mar. 2006. http://dx.doi.org/10.1016/j.compmedimag.2005.12.001.

R. Uhl, R. Wagner, and N. Ryba. Watching g proteins at work. *Trends in Neurosciences*, 13(2):64–70, Feb. 1990. http://dx.doi.org/10.1016/0166-2236(90)90070-Q.

K. Ukai, K. Tsuchiya, and S. Ishikawa. Induced pupillary hippus following near vision: increased occurrence in visual display unit workers. *Ergonomics*, 40(11):1201–1211, Nov. 1997. http://www.ncbi.nlm.nih.gov/pubmed/9375534.

S. Usui. *Functional organization of the human pupillary light reflex system*. PhD thesis, University of California, Berkeley, CA, USA, 1974.

S. Usui and Y. Hirata. Estimation of autonomic nervous activity using the inverse dynamic model of the pupil muscle plant. *Annals of Biomedical Engineering*, 23(4):375–387, July 1995. http://dx.doi.org/10.1007/BF02584438.

S. Usui and L. Stark. Sensory and motor mechanisms interact to control amplitude of pupil noise. *Vision Research*, 18(4):505–507, 1978. http://www.ncbi.nlm.nih.gov/pubmed/664330.

S. Usui and L. Stark. A model for nonlinear stochastic behavior of the pupil. *Biological Cybernetics*, 45(1):13–21, 1982. http://dx.doi.org/10.1007/BF00387209.

G. Vakkur and P. Bishop. The schematic eye in the cat. *Vision Research*, 3(7-8):357–381, Aug. 1963. http://dx.doi.org/10.1016/0042-6989(63)90009-9.

J. Valeton and D. van Norren. Light adaptation of primate cones: An analysis based on extracellular data. *Vision Research*, 23(12):1539–1547, 1983. http://dx.doi.org/10.1016/0042-6989(83)90167-0.

J. M. Valeton and D. v. Norren. Retinal site of transient tritanopia. *Nature*, 280(5722):488–490, 1979. http://dx.doi.org/10.1038/280488a0.

J. A. Van Best and E. V. Kuppens. Summary of studies on the blue-green autofluorescence and light transmission of the ocular lens. *Journal of Biomedical Optics*, 1(3):243, 1996. http://link.aip.org/link/JBOPFO/v1/i3/p243/s1&Agg=doi.

W. J. van Bommel. Non-visual biological effect of lighting and the practical meaning for lighting for work. *Applied Ergonomics*, 37(4):461–466, July 2006. http://dx.doi.org/10.1016/j.apergo.2006.04.009.

E. Van Cauter, R. Leproult, and D. J. Kupfer. Effects of gender and age on the levels and circadian rhythmicity of plasma cortisol. *Journal of Clinical Endocrinology & Metabolism*, 81(7):2468 –2473, July 1996. http://dx.doi.org/10.1210/jc.81.7.2468.

H. van de Hulst. *Light Scattering by Small Particles*. Dover, 1957.

J. van de Kraats and D. van Norren. Optical density of the aging human ocular media in the visible and the UV. *Journal of the Optical Society of America. A, Optics, Image Science, and Vision*, 24(7):1842–57, July 2007a. http://dx.doi.org/10.1364/JOSAA.24.001842.

J. van de Kraats and D. van Norren. Sharp cutoff filters in intraocular lenses optimize the balance between light reception and light protection. *Journal of Cataract & Refractive Surgery*, 33(5):879–887, May 2007b. http://dx.doi.org/10.1016/j.jcrs.2007.02.020.

J. van de Kraats and D. van Norren. Directional and nondirectional spectral reflection from the human fovea. *Journal of Biomedical Optics*, 13(2):024010–13, Mar. 2008. http://dx.doi.org/10.1117/1.2899151.

M. Van De Werken, M. C. Giménez, B. De Vries, D. G. M. Beersma, E. J. W. Van Someren, and M. C. M. Gordijn. Effects of artificial dawn on sleep inertia, skin temperature, and the awakening cortisol response. *Journal of Sleep Research*, 19(3):425–435, Sept. 2010. http://dx.doi.org/10.1111/j.1365-2869.2010.00828.x.

T. J. van den Berg. Quantal and visual efficiency of fluorescence in the lens of the human eye. *Investigative Ophthalmology & Visual Science*, 34(13):3566 –3573, Dec. 1993. http://www.ncbi.nlm.nih.gov/pubmed/8258514.

T. J. van den Berg, L. (René) van Rijn, R. Kaper-Bongers, D. Vonhoff, H. Völker-Dieben, G. Grabner, C. Nischler, M. Emesz, H. Wilhelm, D. Gamer, A. Schuster, L. Franssen, G. de Wit, and J. Coppens. Disability glare in the aging eye. assessment and impact on driving. *Journal of Optometry*, 2(3):112–118, 2009a. http://dx.doi.org/10.3921/joptom.2009.112.

T. J. T. P. van den Berg and H. Spekreijse. Near infrared light absorption in the human eye media. *Vision Research*, 37(2):249–253, Jan. 1997. http://dx.doi.org/10.1016/S0042-6989(96)00120-4.

T. J. T. P. van den Berg and K. Tan. Light transmittance of the human cornea from 320 to 700 nm for different ages. *Vision Research*, 34(11):1453–1456, June 1994. http://dx.doi.org/10.1016/0042-6989(94)90146-5.

T. J. T. P. van den Berg, J. K. Ijspeert, P. W. T. Waard, and F. Meire. Functional quantification of diaphany. *Documenta Ophthalmologica*, 75:239–246, Oct. 1990. http://dx.doi.org/10.1007/BF00164837.

T. J. T. P. van den Berg, J. Ijspeert, and P. de Waard. Dependence of intraocular straylight on pigmentation and light transmission through the ocular wall. *Vision Research*, 31(7-8):1361–1367, 1991. http://dx.doi.org/10.1016/0042-6989(91)90057-C.

T. J. T. P. van den Berg, L. Franssen, and J. E. Coppens. Straylight in the human eye: testing objectivity and optical character of the psychophysical measurement. *Ophthalmic and Physiological Optics*, 29(3):345–350, May 2009b. http://dx.doi.org/10.1111/j.1475-1313.2009.00638.x.

B. van der Pol. The nonlinear theory of electric oscillations. *Proceedings of the Institute of Radio Engineers*, 22(9):1051–1086, Sept. 1934. http://dx.doi.org/10.1109/JRPROC.1934.226781.

J. van Derlofske, A. Bierman, M. S. Rea, J. Ramanath, and J. D. Bullough. Design and optimization of a retinal flux density meter. *Measurement Science and Technology*, 13(6):821–828, June 2002. http://dx.doi.org/10.1088/0957-0233/13/6/301.

R. N. Van Gelder. Non-visual ocular photoreception. *Ophthalmic Genetics*, 22:195–205, Jan. 2001. http://dx.doi.org/10.1076/opge.22.4.195.2215.

R. N. Van Gelder. Non-Visual photoreception: Sensing light without sight. *Current Biology*, 18(1):R38–R39, Jan. 2008. http://dx.doi.org/10.1016/j.cub.2007.11.027.

R. N. Van Gelder and K. Mawad. Illuminating the mysteries of melanopsin and circadian photoreception. *Journal of Biological Rhythms*, 23(5):394–5, Oct. 2008. http://dx.doi.org/10.1177/0748730408323066.

R. N. Van Gelder, R. Wee, J. A. Lee, and D. C. Tu. Reduced pupillary light responses in mice lacking cryptochromes. *Science*, 299 (5604):222, Jan. 2003. http://dx.doi.org/10.1126/science.1079536.

M. M. van Genderen, M. M. Bijveld, Y. B. Claassen, R. J. Florijn, J. N. Pearring, F. M. Meire, M. A. McCall, F. C. Riemslag, R. G. Gregg, A. A. Bergen, and M. Kamermans. Mutations in TRPM1 are a common cause of complete congenital stationary night blindness. *The American Journal of Human Genetics*, 85(5):730–736, Nov. 2009. http://dx.doi.org/10.1016/j.ajhg.2009.10.012.

J. van Hateren. Photoreceptor optics, theory and practice. In D. G. Stavenga and R. C. Hardie, editors, *Facets of vision*, pages 74–89. Springer, Berlin, Heidelberg, New York, 1989.

J. H. van Hateren. Processing of natural time series of intensities by the visual system of the blowfly. *Vision Research*, 37(23):3407–

3416, Dec. 1997. http://dx.doi.org/10.1016/S0042-6989(97)00105-3.

J. van Hoof, A. Schoutens, and M. Aarts. High colour temperature lighting for institutionalised older people with dementia. *Building and Environment*, 44(9):1959–1969, Sept. 2009. http://dx.doi.org/10.1016/j.buildenv.2009.01.009.

M. J. Van Hook, K. Y. Wong, and D. M. Berson. Dopaminergic modulation of ganglion-cell photoreceptors in rat. *The European Journal of Neuroscience*, Feb. 2012. http://dx.doi.org/10.1111/j.1460-9568.2011.07975.x.

J. A. J. Van Loo and J. M. Enoch. The scotopic Stiles-Crawford effect. *Vision Research*, 15 (8-9):1005–1009, 1975. http://dx.doi.org/10.1016/0042-6989(75)90243-6.

F. L. Van Nes and M. A. Bouman. Spatial modulation transfer in the human eye. *Journal of the Optical Society of America*, 57(3):401–406, Mar. 1967. http://dx.doi.org/10.1364/JOSA.57.000401.

D. van Norren and T. G. M. Gorgels. The action spectrum of photochemical damage to the retina: A review of monochromatic threshold data. *Photochemistry and Photobiology*, 2011. http://dx.doi.org/10.1111/j.1751-1097.2011.00921.x.

D. van Norren and J. van de Kraats. Spectral transmission of intraocular lenses expressed as a virtual age. *British Journal of Ophthalmology*, 91(10):1374 –1375, Oct. 2007. http://dx.doi.org/10.1136/bjo.2007.117903.

D. van Norren and J. J. Vos. Spectral transmission of the human ocular media. *Vision Research*, 14(11):1237–1244, Nov. 1974. http://dx.doi.org/10.1016/0042-6989(74)90222-3.

E. J. Van Someren and E. Nagtegaal. Improving melatonin circadian phase estimates. *Sleep Medicine*, 8(6):590–601, Sept. 2007. http://dx.doi.org/10.1016/j.sleep.2007.03.012.

G. Vandewalle, E. Balteau, C. Phillips, C. Degueldre, V. Moreau, V. Sterpenich, G. Albouy, A. Darsaud, M. Desseilles, T. T. Dang-Vu, P. Peigneux, A. Luxen, D. Dijk, and P. Maquet. Daytime light exposure dynamically enhances brain responses. *Current Biology*, 16:1616–1621, Aug. 2006. http://dx.doi.org/10.1016/j.cub.2006.06.031.

G. Vandewalle, S. Gais, M. Schabus, E. Balteau, J. Carrier, A. Darsaud, V. Sterpenich, G. Albouy, D. J. Dijk, and P. Maquet. Wavelength-Dependent modulation of brain responses to a working memory task by daytime light exposure. *Cerebral Cortex*, 17(12):2788 –2795, Dec. 2007a. http://dx.doi.org/10.1093/cercor/bhm007.

G. Vandewalle, C. Schmidt, G. Albouy, V. Sterpenich, A. Darsaud, G. Rauchs, P. Berken, E. Balteau, C. Degueldre, A. Luxen, P. Maquet, and D. Dijk. Brain responses to violet, blue, and green monochromatic light exposures in humans: Prominent role of blue light and the brainstem. *PLoS ONE*, 2(11): e1247, Nov. 2007b. http://dx.plos.org/10.1371/journal.pone.0001247.

G. Vandewalle, P. Maquet, and D. Dijk. Light as a modulator of cognitive brain function. 13(10):429–438, Oct. 2009. http://dx.doi.org/10.1016/j.tics.2009.07.004.

G. Vandewalle, S. Schwartz, D. Grandjean, C. Wuillaume, E. Balteau, C. Degueldre, M. Schabus, C. Phillips, A. Luxen, D. J. Dijk, and P. Maquet. Spectral quality of light modulates emotional brain responses in humans. *Proceedings of the National Academy of Sciences*, 107(45):19549 –19554, Nov. 2010. http://dx.doi.org/10.1073/pnas.1010180107.

G. Vandewalle, S. N. Archer, C. Wuillaume, E. Balteau, C. Degueldre, A. Luxen, D. Dijk, and P. Maquet. Effects of light on cognitive brain responses depend on circadian phase and sleep homeostasis. *Journal of Biological Rhythms*, 26(3):249 –259, June 2011. http://dx.doi.org/10.1177/0748730411401736.

D. Varjú. Pupillenreaktionen auf sinusförmige leuchtdichteänderungen. *Biological Cybernetics*, 2(3):124, 1964.

D. K. Vaughan, J. L. Nemke, S. J. Fliesler, R. M. Darrow, and D. T. Organisciak. Evidence for a circadian rhythm of susceptibility to retinal light damage. *Photochemistry and Photobiology*, 75(5):547–53, May 2002. http://www.ncbi.nlm.nih.gov/pubmed/12017483.

J. A. Veitch. Psychological processes influencing lighting quality. *Journal of the Illuminating Engineering Society*, 30(1):124, Apr. 2001.

J. A. Veitch. Investigating and influencing how buildings affect health: Interdisciplinary endeavours. *Canadian Psychology/Psychologie canadienne*, 49(4):281–288, 2008. http://dx.doi.org/10.1037/a0013567.

F. A. Vera-Díaz and N. Doble. Adaptive optics confocal scanning laser ophthalmoscope. In R. K. Tyson, editor, *Topics in Adaptive Optics*. InTech, Jan. 2012.

M. Verbeek. *A Guide to Modern Econometrics*. John Wiley & Sons, June 2000.

W. Verdon and P. A. Howarth. The pupil's response to short wavelength cone stimulation. *Vision Research*, 28(10):1119–1128, 1988. http://dx.doi.org/10.1016/0042-6989(88)90138-1.

D. M. Verra, M. A. Contín, D. Hicks, and M. E. Guido. Early onset and differential Temporo-Spatial expression of melanopsin isoforms in the developing chicken retina. *Investigative Ophthalmology & Visual Science*, June 2011. http://dx.doi.org/10.1167/iovs.11-75301.

C. Vetter, M. Juda, D. Lang, A. Wojtysiak, and T. Roenneberg. Blue-enriched office light competes with natural light as a zeitgeber. *Scandinavian Journal of Work, Environment & Health*, 37(5):437–445, Sept. 2011. http://dx.doi.org/10.5271/sjweh.3144.

F. Viénot, M. Durand, and E. Mahler. Kruithof's rule revisited using LED illumination. *Journal of Modern Optics*, 56(13): 1433–1446, 2009. [ishi2003preferred].

F. Viénot, S. Bailacq, and J. L. Rohellec. The effect of controlled photopigment excitations on pupil aperture. *Ophthalmic and Physiological Optics*, 30(5):484–491, 2010. http://dx.doi.org/10.1111/j.1475-1313.2010.00754.x.

F. Viénot, H. Brettel, T. Dang, and J. Le Rohellec. Domain of metamers exciting intrinsically photosensitive retinal ganglion cells (ipRGCs) and rods. *Journal of the Optical Society of America A*, 29(2):A366–A376, Feb. 2012. http://dx.doi.org/10.1364/JOSAA.29.00A366.

A. Villanueva, R. Cabeza, and S. Porta. Eye tracking: Pupil orientation geometrical modeling. *Image and Vision Computing*, 24(7):663–679, July 2006. http://dx.doi.org/10.1016/j.imavis.2005.06.001.

T. J. Viney, K. Balint, D. Hillier, S. Siegert, Z. Boldogkoi, L. W. Enquist, M. Meister, C. L. Cepko, and B. Roska. Local retinal circuits of Melanopsin-Containing ganglion cells identified by transsynaptic viral tracing. *Current Biology*, 17(11):981–988, June 2007. http://dx.doi.org/10.1016/j.cub.2007.04.058.

J. Vinós, K. Jalink, R. W. Hardy, S. G. Britt, and C. S. Zuker. A g Protein-Coupled receptor phosphatase required for rhodopsin function. *Science*, 277(5326):687–690, 1997. http://dx.doi.org/10.1126/science.277.5326.687.

A. U. Viola, L. M. James, L. J. M. Schlangen, and D. Dijk. Blue-enriched white light in the workplace improves self-reported alertness, performance and sleep quality. *Scandinavian Journal of Work, Environment & Health*, 34(4):297–306, Aug. 2008. http://www.ncbi.nlm.nih.gov/pubmed/18815716.

E. K. Visser, D. G. M. Beersma, and S. Daan. Melatonin suppression by light in humans is maximal when the nasal part of the retina is illuminated. *Journal of Biological Rhythms*, 14(2):116 –121, Apr. 1999. http://dx.doi.org/10.1177/074873099129000498.

P. M. Vissers, P. H. Bovee-Geurts, M. D. Portier, C. H. Klaassen, and W. J. Degrip. Large-scale production and purification of the human green cone pigment: characterization of late photo-intermediates. *Biochemical Journal*, 330(Pt 3):1201–1208, Mar. 1998. http://www.ncbi.nlm.nih.gov/pubmed/9494086.

R. Vogel, F. Siebert, G. Mathias, P. Tavan, G. Fan, and M. Sheves. Deactivation of rhodopsin in the transition from the signaling state meta II to meta III involves a thermal isomerization of the retinal chromophore CN double bond†. *Biochemistry*, 42(33):9863–9874, 2003. http://dx.doi.org/10.1021/bi034684+.

K. Vogt and K. Kirschfeld. Sensitizing pigment in the fly. *Biophysics of Structure and Mechanism*, 9:319–328, 1983. http://dx.doi.org/10.1007/BF00535667.

K. Vogt, K. Kirschfeld, and D. G. Stavenga. Spectral effects of the pupil in fly photoreceptors. *Journal of Comparative Physiology ? A*, 146(2):145–152, 1982. http://dx.doi.org/10.1007/BF00610232.

B. Vohnsen. Photoreceptor waveguides and effective retinal image quality. *Journal of the Optical Society of America A*, 24(3):597–607, Mar. 2007. http://dx.doi.org/10.1364/JOSAA.24.000597.

B. Vohnsen and D. Rativa. Absence of an integrated Stiles–Crawford function for coherent light. *Journal of Vision*, 11(1), Jan. 2011a. http://dx.doi.org/10.1167/11.1.19.

B. Vohnsen and D. Rativa. Ultrasmall spot size scanning laser ophthalmoscopy. *Biomedical Optics Express*, 2(6):1597–1609, June 2011b. http://dx.doi.org/10.1364/BOE.2.001597.

J. von Lintig, P. D. Kiser, M. Golczak, and K. Palczewski. The biochemical and structural basis for trans-to-cis isomerization of retinoids in the chemistry of vision. *Trends in Biochemical Sciences*, 35(7):400–410, July 2010. http://dx.doi.org/10.1016/j.tibs.2010.01.005.

J. J. Vos. *On mechanisms of glare*. Doctoral thesis, University of Utrecht, 1963.

B. W. Vought, E. Salcedo, L. V. Chadwell, S. G. Britt, R. R. Birge, and B. E. Knox. Characterization of the primary photointermediates of drosophila rhodopsin. *Biochemistry*, 39(46):14128–14137, 2000. http://dx.doi.org/10.1021/bi001135k.

G. F. J. M. Vrensen. Early cortical lens opacities: a short overview. *Acta Ophthalmologica*, 87(6):602–610, Sept. 2009. http://dx.doi.org/10.1111/j.1755-3768.2009.01674.x.

A. A. Vugler, P. Redgrave, M. Semo, J. Lawrence, J. Greenwood, and P. J. Coffey. Dopamine neurones form a discrete plexus with melanopsin cells in normal and degenerating retina. *Experimental Neurology*, 205(1):26–35, May 2007. http://dx.doi.org/10.1016/j.expneurol.2007.01.032.

T. M. Vuong, M. Chabre, and L. Stryer. Millisecond activation of transducin in the cyclic nucleotide cascade of vision. *Nature*, 311(5987):659–661, Oct. 1984. http://dx.doi.org/10.1038/311659a0.

P. D. Wade, J. Taylor, and P. Siekevitz. Mammalian cerebral cortical tissue responds to low-intensity visible light. *Proceedings of the National Academy of Sciences*, 85(23):9322–9326, Dec. 1988. http://www.ncbi.nlm.nih.gov/pubmed/3194426.

I. H. Wagman and J. E. Gullberg. The relationship between monochromatic light and pupil diameter. the low intensity visibility curve as measured by pupillary measurements. *American Journal of Physiology – Legacy Content*, 137(4):769–778, Nov. 1942.

I. H. Wagman and L. M. Nathanson. Influence of intensity of white light upon pupil diameter of the human and of the rabbit. *Proceedings of the Society for Experimental Biology and Medicine. Society for Experimental Biology and Medicine (New York, N.Y.)*, 49(3):466–470, Mar. 1942. http://dx.doi.org/10.3181/00379727-49-13598.

G. Wagner and R. M. Boynton. Comparison of four methods of heterochromatic photometry. *Journal of the Optical Society of America*, 62(12):1508–1515, Dec. 1972. http://dx.doi.org/10.1364/JOSA.62.001508.

K. Wakamatsu, D. Hu, S. A. McCormick, and S. Ito. Characterization of melanin in human iridal and choroidal melanocytes from eyes with various colored irides. *Pigment Cell & Melanoma Research*, 21(1):97–105, Feb. 2008. http://dx.doi.org/10.1111/j.1755-148X.2007.00415.x.

G. Wald. The photochemistry of vision. *Documenta Ophthalmologica*, 3(1):94–137, 1949. http://dx.doi.org/10.1007/BF00162600.

G. Wald. The receptors of human color vision. *Science*, 145(3636):1007–1016, 1964. http://dx.doi.org/10.1126/science.145.3636.1007.

G. Wald. The molecular basis of visual excitation. *Nature*, 219(5156):800–807, 1968. http://dx.doi.org/10.1038/219800a0.

G. Wald and P. K. Brown. The molar extinction of rhodopsin. *The Journal of General Physiology*, 37(2):189–200, Nov. 1953. http://www.ncbi.nlm.nih.gov/pubmed/13109155.

G. Wald and P. K. Brown. Human rhodopsin. *Science*, 127(3292):222–249, 1958. http://dx.doi.org/10.1126/science.127.3292.222.

M. T. Walker. *Characterization of the light activated properties of the novel photopigment melanopsin*. PhD thesis, University of Maryland, Baltimore, USA, 2008.

M. T. Walker, R. L. Brown, T. W. Cronin, and P. R. Robinson. Photochemistry of retinal chromophore in mouse melanopsin. *Proceedings of the National Academy of Sciences of the United States of America*, 105(26):8861–5, July 2008. http://dx.doi.org/10.1073/pnas.0711397105.

P. Walraven. CIE report. Technical Report TC 1-36 Draft 7, 2003.

G. Walsh. The effect of mydriasis on the pupillary centration of the human eye. *Ophthalmic and Physiological Optics*, 8(2):178–182, 1988. http://dx.doi.org/10.1111/j.1475-1313.1988.tb01034.x.

G. Walther and K. A. Hellner. Early receptor potential recordings for clinical routine. *Documenta Ophthalmologica*, 62(1):31–39, Jan. 1986. http://dx.doi.org/10.1007/BF00140544.

B. Wang and K. J. Ciuffreda. Depth-of-Focus of the human eye: Theory and clinical implications. *Survey of Ophthalmology*, 51(1):75–85, 2006. http://dx.doi.org/10.1016/j.survophthal.2005.11.003.

J. Wang and V. J. Kefalov. The cone-specific visual cycle. *Progress in Retinal and Eye Research*, 30(2):115–128, Mar. 2011. http://dx.doi.org/10.1016/j.preteyeres.2010.11.001.

X. Wang, T. Wang, Y. Jiao, J. von Lintig, and C. Montell. Requirement for an enzymatic visual cycle in drosophila. *Current Biology*, 20(2):93–102, Jan. 2010. http://dx.doi.org/10.1016/j.cub.2009.12.022.

X. Wang, T. Wang, J. D. Ni, J. Von Lintig, and C. Montell. The drosophila visual cycle and de novo chromophore synthesis depends on rdhB. *The Journal of Neuroscience*, 32(10):3485–3491, Mar. 2012. http://dx.doi.org/10.1523/JNEUROSCI.5350-11.2012.

R. Want. When cell phones become computers. *IEEE Pervasive Computing*, 8(2):2–5, June 2009. http://dx.doi.org/10.1109/MPRV.2009.40.

M. Warga, H. Lüdtke, H. Wilhelm, and B. Wilhelm. How do spontaneous pupillary oscillations in light relate to light intensity? *Vision Research*, 49(3):295–300, Feb. 2009. http://dx.doi.org/10.1016/j.visres.2008.09.019.

E. J. Warrant and D. Nilsson. Absorption of white light in photoreceptors. *Vision Research*, 38(2):195–207, Jan. 1998. dx.doi.org/10.1016/S0042-6989(97)00151-X.

E. J. Warren, C. N. Allen, R. L. Brown, and D. W. Robinson. Intrinsic light responses of retinal ganglion cells projecting to the circadian system. *European Journal of Neuroscience*, 17(9):1727–1735, May 2003. http://dx.doi.org/10.1046/j.1460-9568.2003.02594.x.

E. J. Warren, C. N. Allen, R. L. Brown, and D. W. Robinson. The light-activated signaling pathway in SCN-projecting rat retinal ganglion cells. *European Journal of Neuroscience*, 23(9):2477–2487, May 2006. http://dx.doi.org/10.1111/j.1460-9568.2006.04777.x.

H. Wässle. Parallel processing in the mammalian retina. *Nat Rev Neurosci*, 5(10):747–757, Oct. 2004. http://dx.doi.org/10.1038/nrn1497.

M. Watanabe and S. K. Nayar. Telecentric optics for computational vision. In *Proceedings of the 4th European Conference on Computer Vision-Volume II - Volume II*, ECCV '96, page 439–451, London, UK, 1996. Springer-Verlag.

T. Watanabe, N. Mori, and F. Nakamura. A new superbright LED stimulator: Photodiode-feedback design for linearizing and stabilizing emitted light. *Vision Research*, 32(5):953–961, May 1992. http://dx.doi.org/10.1016/0042-6989(92)90038-K.

R. A. Weale. On an early stage of rhodopsin regeneration in man. *Vision Research*, 7(11-12):819–827, Nov. 1967. http://dx.doi.org/10.1016/0042-6989(67)90002-8.

R. A. Weale. Human lenticular fluorescence and transmissivity, and their effects on vision. *Experimental Eye Research*, 41(4):457–473, Oct. 1985. http://dx.doi.org/10.1016/S0014-4835(85)80004-X.

R. A. Weale. Age and the transmittance of the human crystalline lens. *The Journal of Physiology*, 395:577–587, Jan. 1988. http://www.ncbi.nlm.nih.gov/pubmed/3411488.

R. A. Weale. A theoretical link between lenticular absorbance and fluorescence. *Proceedings. Biological Sciences / The Royal Society*, 263(1374):1111–1116, Sept. 1996. http://dx.doi.org/10.1098/rspb.1996.0163.

M. Weber, K. Schulmeister, and E. Schernhammer. Temporal and radiometrical aspects of light induced melatonin suppression studies. CIE x027:2004, pages 116–128, Vienna, Austria, 2004.

J. G. Webster. Pupillary light reflex: Development of teaching models. *Biomedical Engineering, IEEE Transactions on*, BME-18 (3):187–194, 1971. http://dx.doi.org/10.1109/TBME.1971.4502830.

J. G. Webster, G. A. Cohen, and R. M. Boynton. Optimizing the use of the criterion response for the pupil light reflex. *Journal of the Optical Society of America*, 58(3):419–424, Mar. 1968. http://dx.doi.org/10.1364/JOSA.58.000419.

M. A. Webster, K. Halen, A. J. Meyers, P. Winkler, and J. S. Werner. Colour appearance and compensation in the near periphery. *Proceedings of the Royal Society B: Biological Sciences*, 277(1689):1817 –1825, June 2010. http://dx.doi.org/10.1007/BF02442326.

M. Weckström, R. C. Hardie, and S. B. Laughlin. Voltage-activated potassium channels in blowfly photoreceptors and their role in light adaptation. *The Journal of Physiology*, 440(1):635 –657, Jan. 1991. http://www.ncbi.nlm.nih.gov/pubmed/1804980.

A. Wegener and H. Laser-Junga. Photography of the anterior eye segment according to scheimpflug's principle: options and limitations – a review. *Clinical & Experimental Ophthalmology*, 37(1):144–154, Jan. 2009. http://dx.doi.org/10.1111/j.1442-9071.2009.02018.x.

A. Wegener, H. Laser, M. Ahrend, O. Breck, E. Bjerkås, C. Glöckner, P. Midtlyng, and W. Breipohl. Light scattering in normal and cataractous lenses of farmed atlantic salmon (Salmo salar): A slit lamp and scheimpflug photographic study. *Ophthalmic Research*, 33(5):264–270, 2001. http://content.karger.com/produktedb/produkte.asp?DOI=55679&typ=pdf.

A. Wegner and R. Khoramnia. Cataract is a self-defence reaction to protect the retina from oxidative damage. *Medical Hypotheses*, 76(5):741–744, May 2011. http://dx.doi.org/10.1016/j.mehy.2011.02.013.

G. W. Weinstein, R. R. Hobson, and J. E. Dowling. Light and dark adaptation in the isolated rat retina. *Nature*, 215(5097):134–138, July 1967. http://dx.doi.org/10.1038/215134a0.

J. M. Weinstein, J. C. Van Gilder, and H. S. Thompson. Pupil cycle time in optic nerve compression. *American Journal of Ophthalmology*, 89(2):263–267, Feb. 1980. http://www.ncbi.nlm.nih.gov/pubmed/6892589.

S. Weiss, J. Kremers, and J. Maurer. Interaction between rod and cone signals in responses of lateral geniculate neurons in dichromatic marmosets (Callithrix jacchus). *Visual Neuroscience*, 15(5):931–943, Oct. 1998. http://www.ncbi.nlm.nih.gov/pubmed/9764535.

J. J. Weiter, F. C. Delori, G. L. Wing, and K. A. Fitch. Relationship of senile macular degeneration to ocular pigmentation. *American Journal of Ophthalmology*, 99(2):185–187, Feb. 1985. http://www.ncbi.nlm.nih.gov/pubmed/3970124.

D. L. Wells, C. L. McDonald, and J. E. Ringland. Color preferences in gorillas (Gorilla gorilla gorilla) and chimpanzees (Pan troglodytes). *Journal of Comparative Psychology*, 122(2):213–219, 2008. http://dx.doi.org/10.1037/0735-7036.122.2.213.

S. Weng, K. Y. Wong, and D. M. Berson. Circadian modulation of Melanopsin-Driven light response in rat Ganglion-Cell photoreceptors. *J Biol Rhythms*, 24(5):391–402, Oct. 2009. http://dx.doi.org/10.1177/0748730409343767.

A. Wenzel, V. Oberhauser, E. N. Pugh, T. D. Lamb, C. Grimm, M. Samardzija, E. Fahl, M. W. Seeliger, C. E. Remé, and J. von Lintig. The retinal g protein-coupled receptor (RGR) enhances isomerohydrolase activity independent of light. *Journal of Biological Chemistry*, 280(33):29874 –29884,

2005. http://dx.doi.org/10.1074/jbc.M503603200.

A. Werner, A. Bayer, G. Schwarz, E. Zrenner, and W. Paulus. Effects of ageing on postreceptoral short-wavelength gain control: Transient tritanopia increases with age. *Vision Research*, 50(17):1641–1648, Aug. 2010. http://dx.doi.org/10.1016/j.visres.2010.05.004.

J. S. Werner. Development of scotopic sensitivity and the absorption spectrum of the human ocular media. *Journal of the Optical Society of America*, 72(2):247–258, Feb. 1982. http://dx.doi.org/10.1364/JOSA.72.000247.

J. S. Werner, S. K. Donnelly, and R. Kliegl. Aging and human macular pigment density. *Vision Research*, 27(2):257–268, 1987. http://dx.doi.org/10.1016/0042-6989(87)90188-X.

K. E. West, M. R. Jablonski, B. Warfield, K. S. Cecil, M. James, M. A. Ayers, J. Maida, C. Bowen, D. H. Sliney, M. D. Rollag, J. P. Hanifin, and G. C. Brainard. Blue light from light-emitting diodes elicits a dose-dependent suppression of melatonin in humans. *Journal of Applied Physiology*, 110(3):619 –626, Mar. 2011. http://dx.doi.org/10.?1152/?japplphysiol.?01413.?2009.

G. Westheimer. Pupil size and visual resolution. *Vision Research*, 4(1-2):39–45, May 1964. http://dx.doi.org/10.1016/0042-6989(64)90030-6.

G. Westheimer. Directional sensitivity of the retina: 75 years of Stiles–Crawford effect. *Proceedings of the Royal Society B: Biological Sciences*, 275(1653):2777–2786, Dec. 2008. http://dx.doi.org/10.1098/rspb.2008.0712.

G. Westheimer. Visual acuity: Information theory, retinal image structure and resolution thresholds. *Progress in Retinal and Eye Research*, 28(3):178–186, May 2009. http://dx.doi.org/10.1016/j.preteyeres.2009.04.001.

C. Westphal. Über einen fall von chronischer progressiver lähmung der augenmuskeln (Ophthalmoplegia externa) nebst beschreibung von ganglienzellengruppen im bereiche des oculomotoriuskerns. *Archiv für Psychiatrie und Nervenkrankheiten*, 18:846–871, Oct. 1887. http://dx.doi.org/10.1007/BF02037688.

N. Wiener. *Cybernetics: or the Control and Communication in the Animal and the Machine: Or Control and Communication in the Animal and the Machine*. MIT Press, 1947.

B. Wilhelm, H. Giedke, H. Lüdtke, E. Bittner, A. Hofmann, and H. Wilhelm. Daytime variations in central nervous system activation measured by a pupillographic sleepiness test. *Journal of sleep research*, 10(1):1–7, Mar. 2001. http://dx.doi.org/10.1046/j.1365-2869.2001.00239.x.

B. Wilhelm, P. Weckerle, W. Durst, C. Fahr, and R. Röck. Increased illuminance at the workplace: Does it have advantages for daytime shifts? *Lighting Research and Technology*, 43(2):185 –199, June 2011. http://dx.doi.org/10.1177/1477153510380879.

A. Wilkins, J. Veitch, and B. Lehman. LED lighting flicker and potential health concerns: IEEE standard PAR1789 update. In *Energy Conversion Congress and Exposition (ECCE), 2010 IEEE*, pages 171–178, 2010. http://dx.doi.org/10.1109/ECCE.2010.5618050.

P. S. J. Williams. *The Politics of Sleep: Governing (Un)consciousness in the Late Modern Age*. Palgrave Macmillan, Mar. 2011.

S. B. Williams and R. K. Poole. A circadian timing mechanism in the cyanobacteria. In *Advances in Microbial Physiology*, volume Volume 52, pages 229–296. Academic Press, 2006. http://dx.doi.org/10.1016/S0065-2911(06)52004-1.

T. P. Williams. Photoreversal of rhodopsin bleaching. *The Journal of General Physiology*, 47(4):679 –689, Mar. 1964. http://dx.doi.org/10.1085/jgp.47.4.679.

T. P. Williams. Limitations on the use of the concept of quantum efficiency in rhodopsin bleaching. *Nature*, 209(5030):1350–1351, Mar. 1966. http://dx.doi.org/10.1038/2091350a0.

T. P. Williams. An isochromic change in the bleaching of rhodopsin. *Vision Research*, 10(7):525–533, July 1970. http://dx.doi.org/10.1016/0042-6989(70)90046-5.

T. P. Williams. Upper limits to the bleaching of rhodopsin by high intensity flashes. *Vision Research*, 14(8):603–607, Aug. 1974. http://dx.doi.org/10.1016/0042-6989(74)90053-4.

T. P. Williams and J. P. P. Webbers. Photometer for measuring intensity and rhodopsin distributions in intact eyes. *Applied Optics*, 34(25):5720–5724, 1995. http://dx.doi.org/10.1364/AO.34.005720.

E. O. Wilson. *Biophilia*. Harvard University Press, Jan. 1984.

M. Wilson, M. Campbell, and P. Simonet. Change of pupil centration with change of illumination and pupil size. *Optometry and Vision Science*, 69(2):129–136, 1992. http://dx.doi.org/10.1089/ham.2008.1026.

M. H. Wilson, M. Edsell, C. Imray, and A. Wright. Changes in pupil dynamics at high altitude–an observational study using a handheld pupillometer. *High Altitude Medicine & Biology*, 9(4):319–325, 2008. http://dx.doi.org/10.1089/ham.2008.1026.

L. Wind and W. W. Szymanski. Quantification of scattering corrections to the Beer-Lambert law for transmittance measurements in turbid media. *Measure-*

ment Science and Technology, 13(3):270–275, Mar. 2002. http://dx.doi.org/10.1088/0957-0233/13/3/306.

B. Winn, D. Whitaker, D. Elliott, and N. Phillips. Factors affecting light-adapted pupil size in normal human subjects. *Invest. Ophthalmol. Vis. Sci.*, 35(3):1132–1137, Mar. 1994. http://www.ncbi.nlm.nih.gov/pubmed/8125724.

A. Wirz-Justice. How to measure circadian rhythms in humans. *Medicographia*, 29(1): 84–90, 2007.

A. Wirz-Justice. *Chronotherapeutics for Affective Disorders: A Clinician's Manual for Light and Wake Therapy*. S. Karger AG (Switzerland), 1 edition, Mar. 2009.

J. J. Wisowaty. An action spectrum for the production of transient tritanopia. *Vision Research*, 23(8):769–774, 1983. http://dx.doi.org/10.1016/0042-6989(83)90199-2.

B. Wong. Color blindness. *Nat Meth*, 8(6):441, June 2011. http://dx.doi.org/10.1038/nmeth.1618.

K. Y. Wong, F. A. Dunn, and D. M. Berson. Photoreceptor adaptation in intrinsically photosensitive retinal ganglion cells. *Neuron*, 48(6):1001–1010, Dec. 2005. http://dx.doi.org/10.1016/j.neuron.2005.11.016.

K. Y. Wong, F. A. Dunn, D. M. Graham, and D. M. Berson. Synaptic influences on rat ganglion-cell photoreceptors. *The Journal of Physiology*, 582(1):279–296, July 2007. http://dx.doi.org/10.1113/jphysiol.2007.133751.

K. Y. Wong, M. P. Flannery, A. M. Lynch, and B. H. Kim. Prolonged light stimulation of intrinsically photosensitive retinal ganglion cells (ipRGCs) reveals novel properties of melanopsin phototransduction. *ARVO Meeting Abstracts*, 52(6):5286, Apr. 2011.

J. P. M. Wood, G. Chidlow, T. Tran, J. G. Crowston, and R. J. Casson. A comparison of differentiation protocols for RGC-5 cells. *Investigative Ophthalmology & Visual Science*, 51(7):3774 –3783, July 2010. http://dx.doi.org/10.1167/iovs.09-4305.

J. Woodhouse. The effect of pupil size on grating detection at various contrast levels. *Vision Research*, 15(6):645–648, June 1975. http://dx.doi.org/10.1016/0042-6989(75)90278-3.

J. Woodhouse and F. Campbell. The role of the pupil light reflex in aiding adaptation to the dark. *Vision Research*, 15(6):649–653, June 1975. http://dx.doi.org/10.1016/0042-6989(75)90279-5.

B. R. Wooten, B. R. Hammond, R. I. Land, and D. M. Snodderly. A practical method for measuring macular pigment optical density. *Invest. Ophthalmol. Vis. Sci.*, 40(11): 2481–2489, Oct. 1999. http://www.iovs.org/cgi/content/abstract/40/11/2481.

B. R. Wooten, B. R. Hammond, and L. M. Renzi. Using scotopic and photopic flicker to measure lens optical density. *Ophthalmic & Physiological Optics*, 27(4):321–328, July 2007. http://dx.doi.org/10.1111/j.1475-1313.2007.00489.x.

R. Wright and D. Cosens. Blue-adaptation and orange-adaptation in white-eyed drosophila: Evidence that the prolonged afterpotential is correlated with the amount of m580 in r1-6. *Journal of Comparative Physiology ? A*, 113:105–128, 1977. http://dx.doi.org/10.1007/BF00610456.

W. Wright. The visual sensitivity of normal and aphakic observers in the ultra-violet. *Ann. Psychol*, 50:169–177, 1951.

W. D. Wright. The breakdown of a colour match with high intensities of adaptation. *The Journal of Physiology*, 87(1):23–33, June 1936. http://www.ncbi.nlm.nih.gov/pubmed/16994773.

C. F. Wu and W. L. Pak. Light-induced voltage noise in the photoreceptor of drosophila melanogaster. *The Journal of General Physiology*, 71(3):249–268, Mar. 1978. http://www.ncbi.nlm.nih.gov/pubmed/418142.

J. Wu, S. Seregard, and P. V. Algvere. Photochemical damage of the retina. *Survey of Ophthalmology*, 51(5):461–481, 2006. http://dx.doi.org/10.1016/j.survophthal.2006.06.009.

J. Wu, R. T. Dauchy, P. C. Tirrell, S. S. Wu, D. T. Lynch, P. Jitawatanarat, C. M. Burrington, E. M. Dauchy, D. E. Blask, and M. W. Greene. Light at night activates IGF-1R/PDK1 signaling and accelerates tumor growth in human breast cancer xenografts. *Cancer Research*, 71(7):2622 –2631, Apr. 2011. http://dx.doi.org/10.1158/0008-5472.CAN-10-3837.

Z. Wu, N. E. Huang, S. R. Long, and C. Peng. On the trend, detrending, and variability of nonlinear and nonstationary time series. *Proceedings of the National Academy of Sciences*, 104(38):14889 –14894, 2007. http://dx.doi.org/10.1073/pnas.0701020104.

H. J. Wyatt. The form of the human pupil. *Vision Research*, 35(14):2021–2036, July 1995. http://dx.doi.org/10.1016/0042-6989(94)00268-Q.

H. J. Wyatt. The human pupil and the use of video-based eyetrackers. *Vision Research*, 50 (19):1982–1988, Sept. 2010. http://dx.doi.org/10.1016/j.visres.2010.07.008.

H. J. Wyatt and J. F. Musselman. Pupillary light reflex in humans: Evidence for an unbalanced pathway from nasal retina, and for signal cancellation in brainstem. *Vision Research*, 21(4):513–525, 1981. http://dx.doi.org/10.1016/0042-6989(81)90097-3.

K. C. Wybar. The ocular manifestations of disseminated sclerosis. *Proceedings of the Royal Society of Medicine*, 45(5):315–320,

May 1952. http://www.ncbi.nlm.nih.gov/pubmed/14941838.

G. Wyszecki and W. S. Stiles. *Colour science: concepts and methods, quantitative data and formulae*. Wiley, New York, 1st edition, 1967.

W. Xu and W. J. van Bommel. Inferior verso superior: Inferior retinal light exposure is more effective in pupil contraction in humans. *Light& Engineering*, 19(2):14–18, 2011.

L. Xue, D. R. Gollapalli, P. Maiti, W. J. Jahng, and R. R. Rando. A palmitoylation switch mechanism in the regulation of the visual cycle. *Cell*, 117(6):761–771, June 2004. http://dx.doi.org/10.1016/j.cell.2004.05.016.

T. Xue, M. T. H. Do, A. Riccio, Z. Jiang, J. Hsieh, H. C. Wang, S. L. Merbs, D. S. Welsbie, T. Yoshioka, P. Weissgerber, S. Stolz, V. Flockerzi, M. Freichel, M. I. Simon, D. E. Clapham, and K. Yau. Melanopsin signalling in mammalian iris and retina. *Nature*, 479(7371):67–73, Nov. 2011. http://dx.doi.org/10.1038/nature10567.

S. Yamaguchi, C. Desplan, and M. Heisenberg. Contribution of photoreceptor subtypes to spectral wavelength preference in drosophila. *Proceedings of the National Academy of Sciences*, 107(12):5634 –5639, Mar. 2010. dx.doi.org/10.1073/pnas.0809398107.

K. Yamaji, Y. Hirata, and S. Usui. Improvement of the method for monitoring autonomic nervous activity by pupillary flash response. *Systems and Computers in Japan*, 32(13):23–30, 2001. http://dx.doi.org/10.1002/scj.1082.

K. Yamaji, Y. Hirata, and S. Usui. Evaluation of the autonomic nervous activity during parabolic flight by pupillary flash response. *Electronics and Communications in Japan (Part III: Fundamental Electronic Science)*, 85(11):56–64, Nov. 2002. http://dx.doi.org/10.1002/ecjc.10054.

K. Yamaji, H. Sakai, Y. Okumura, and S. Usui. Customizable neuroinformatics database system: XooNIps and its application to the pupil platform. *Computers in Biology and Medicine*, 37(7):1036–1041, July 2007. http://dx.doi.org/10.1016/j.compbiomed.2006.09.003.

T. Yamashita, H. Ohuchi, S. Tomonari, K. Ikeda, K. Sakai, and Y. Shichida. Opn5 is a UV-sensitive bistable pigment that couples with gi subtype of g protein. *Proceedings of the National Academy of Sciences*, 107(51):22084 –22089, Dec. 2010. http://dx.doi.org/10.1073/pnas.1012498107.

Q. Yang, D. W. Arathorn, P. Tiruveedhula, C. R. Vogel, and A. Roorda. Design of an integrated hardware interface for AOSLO image capture and cone-targeted stimulus delivery. *Optics Express*, 18(17):17841–17858, 2010. http://dx.doi.org/10.1364/OE.18.017841.

X. Yao, A. Yamauchi, B. Perry, and J. S. George. Rapid optical coherence tomography and recording functional scattering changes from activated frog retina. *Applied Optics*, 44(11):2019–2023, Apr. 2005. http://dx.doi.org/10.1364/AO.44.002019.

A. Yarbus. *Eye movements and vision*. Plenum press, 1967.

A. Yasukouchi and K. Ishibashi. Non-visual effects of the color temperature of fluorescent lamps on physiological aspects in humans. *Journal of Physiological Anthropology and Applied Human Science*, 24(1):41–43, 2005. http://dx.doi.org/10.2114/jpa.24.41.

A. Yasukouchi, Y. Yasukouchi, and K. Ishibashi. Effects of color temperature of fluorescent lamps on body temperature regulation in a moderately cold environment. *Journal of PHYSIOLOGICAL ANTHROPOLOGY and Applied Human Science*, 19(3):125–134, 2000. http://dx.doi.org/10.2114/jpa.19.125.

K. Yau and R. C. Hardie. Phototransduction motifs and variations. *Cell*, 139(2):246–264, Oct. 2009. http://dx.doi.org/10.1016/j.cell.2009.09.029.

H. Ye, M. D. Baba, R. Peng, and M. Fussenegger. A synthetic optogenetic transcription device enhances Blood-Glucose homeostasis in mice. *Science*, 332(6037):1565 –1568, June 2011. http://dx.doi.org/10.1126/science.1203535.

T. Yeh, B. B. Lee, J. Kremers, J. A. Cowing, D. M. Hunt, P. R. Martin, and J. B. Troy. Visual responses in the lateral geniculate nucleus of dichromatic and trichromatic marmosets (Callithrix jacchus). *The Journal of Neuroscience: The Official Journal of the Society for Neuroscience*, 15(12):7892–7904, Dec. 1995. http://www.ncbi.nlm.nih.gov/pubmed/8613728.

H. Yoshida, K. Yana, F. Okuyama, and T. Tokoro. Time-varying properties of respiratory fluctuations in pupil diameter of human eyes. *Methods of Information in Medicine*, 33(1):46–48, Mar. 1994. http://www.ncbi.nlm.nih.gov/pubmed/8177078.

M. Young and R. Lund. The anatomical substrates subserving the pupillary light reflex in rats: Origin of the consensual pupillary response. *Neuroscience*, 62(2):481–496, Sept. 1994. http://10.1016/0306-4522(94)90381-6.

R. S. Young and J. Kennish. Transient and sustained components of the pupil response evoked by achromatic spatial patterns. *Vision Research*, 33(16):2239–52, Nov. 1993. http://dx.doi.org/10.1016/0042-6989(93)90103-4.

R. S. Young and E. Kimura. Pupillary correlates of light-evoked melanopsin activity in humans. *Vision Research*, 48(7):862–871, Mar. 2008. http://dx.doi.org/10.1016/j.visres.2007.12.016.

R. S. Young, B. Han, and P. Wu. Transient and sustained components of the pupillary responses evoked by luminance and color. *Vision Research*, 33(4):437–446, Mar. 1993. http://dx.doi.org/10.1016/0042-6989(93)90251-Q.

R. S. L. Young and M. Alpern. Pupil responses to foveal exchange of monochromatic lights. *Journal of the Optical Society of America*, 70(6):697–706, June 1980. http://dx.doi.org/10.1364/JOSA.70.000697.

M. Yu, M. A. Kautz, M. L. Thomas, D. Johnson, E. R. Hotchkiss, and M. B. Russo. Operational implications of varying ambient light levels and time-of-day effects on saccadic velocity and pupillary light reflex. *Ophthalmic & physiological optics : the journal of the British College of Ophthalmic Opticians (Optometrists)*, 27(2):130–41, Mar. 2007. http://dx.doi.org/10.1111/j.1475-1313.2006.00450.x.

N. T. Yu, M. Bando, and J. Kuck, J F. Fluorescence/Raman intensity ratio for monitoring the pathologic state of human lens. *Investigative Ophthalmology & Visual Science*, 26(1):97–101, Jan. 1985. http://www.ncbi.nlm.nih.gov/pubmed/3967960.

N. P. A. Zagers and D. van Norren. Absorption of the eye lens and macular pigment derived from the reflectance of cone photoreceptors. *Journal of the Optical Society of America A*, 21(12):2257–2268, Dec. 2004. http://dx.doi.org/10.1364/JOSAA.21.002257.

F. H. Zaidi, J. T. Hull, S. N. Peirson, K. Wulff, D. Aeschbach, J. J. Gooley, G. C. Brainard, K. Gregory-Evans, J. F. Rizzo, C. A. Czeisler, R. G. Foster, M. J. Moseley, and S. W. Lockley. Short-Wavelength light sensitivity of circadian, pupillary, and visual awareness in humans lacking an outer retina. *Current Biology*, 17:2122–2128, Dec. 2007. http://dx.doi.org/10.1016/j.cub.2007.11.034.

A. Zajonc. *Catching the Light: The Entwined History of Light and Mind*. Oxford University Press, USA, Apr. 1995.

A. Zanen and J. Debecker. Wavelength sensitivity of the two components of the early receptor potential (ERP) of the human eye. *Vision Research*, 15(1):107–112, Jan. 1975. http://dx.doi.org/10.1016/0042-6989(75)90067-X.

W. H. Zangemeister, T. Gronow, and U. Grzyska. Pupillary responses to single and sinusoidal light stimuli in diabetic patients. 1(1), Nov. 2009. http://dx.doi.org/10.4081/ni.2009.e19.

J. M. Zeitzer, N. F. Ruby, R. A. Fisicaro, and H. C. Heller. Response of the human circadian system to millisecond flashes of light. *PLoS ONE*, 6(7):e22078, July 2011. http://dx.doi.org/10.1371/journal.pone.0022078.

A. J. Zele, B. Feigl, S. S. Smith, and E. L. Markwell. The circadian response of intrinsically photosensitive retinal ganglion cells. *PLoS ONE*, 6(3):e17860, Mar. 2011. http://dx.doi.org/10.1371/journal.pone.0017860.

D. Zhang, K. Y. Wong, P. J. Sollars, D. M. Berson, G. E. Pickard, and D. G. McMahon. Intraretinal signaling by ganglion cell photoreceptors to dopaminergic amacrine neurons. *Proceedings of the National Academy of Sciences*, 105(37):14181 –14186, 2008. http://dx.doi.org/10.1073/pnas.0803893105.

G. Zhang. Abnormal noise detection method based on wavelet filter and K-L information. In *Computer Science and Information Engineering, 2009 WRI World Congress on*, volume 7, pages 24–29, 2009. http://dx.doi.org/10.1109/CSIE.2009.162.

Y. Zhu, D. C. Tu, D. Denner, T. Shane, C. M. Fitzgerald, and R. N. Van Gelder. Melanopsin-Dependent persistence and photopotentiation of murine pupillary light responses. *Invest. Ophthalmol. Vis. Sci.*, 48(3):1268–1275, Mar. 2007. http://dx.doi.org/10.1167/iovs.06-0925.

P. Zieliński. Opengazer: open-source gaze tracker for ordinary webcams. Technical report, 2007.

M. Zuckerman. Physiological measures of sexual arousal in the human. *Psychological Bulletin*, 75(5):297–329, 1971. http://dx.doi.org/10.1037/h0030923.

J. A. Zuclich, R. D. Glickman, and A. R. Menendez. In situ measurements of lens fluorescence and its interference with visual function. *Investigative Ophthalmology & Visual Science*, 33(2):410–415, Feb. 1992. http://www.ncbi.nlm.nih.gov/pubmed/1740373.

J. C. Zwinkels, E. Ikonen, N. P. Fox, G. Ulm, and M. L. Rastello. Photometry, radiometry and 'the candela': evolution in the classical and quantum world. *Metrologia*, 47(5):R15–R32, Oct. 2010. http://dx.doi.org/10.1088/0026-1394/47/5/R01.